CONF-830466--

DE84 014058

PROCEEDINGS OF THE WORKSHOP ON

COPPER AND COPPER ALLOYS for FUSION REACTOR APPLICATIONS

DOE FORRESTAL BUILDING
Washington, DC
April 14-15, 1983

Published: June 1984

Compiled and Edited by:

F. W. WIFFEN
Metals and Ceramics Division
Oak Ridge National Laboratory

R. E. Gold
Advanced Energy Systems Division
Westinghouse Electric Corporation

Published for
U.S. DEPARTMENT OF ENERGY
OFFICE OF ENERGY RESEARCH
OFFICE OF FUSION ENERGY
by OAK RIDGE NATIONAL LABORATORY
Operated by MARTIN MARIETTA ENERGY SYSTEMS, INC.
Contract Number DC-AC05-840R21400

CONTENTS

SUMMARY AND RECOMMENDATIONS

SUMMARY AND RECOMMENDATIONS OF THE COPPER AND COPPER ALLOYS WORKSHOP

F. W. Wiffen,* T. C. Reuther,† and R. E. Gold‡

Recent analyses of the probable operating requirements of both near-term experimental and longer term power-producing fusion reactors have underscored the need to use copper and copper-base alloys in certain critical applications. These applications can generally be assigned to one of three categories:

- High Heat Flux Components. These include limiter and/or divertor collector plates, beam dumps, direct energy convertors, first walls of high energy density reactors, and protective armor.
- High Thermal/Electrical Conductivity Components. These include rf system components, highly conductive first walls, special sector connectors, and possible diagnostic/instrumentation applications.
- Magnet Components. These applications include leads and stabilizers in superconducting magnets and conductors in various normal magnets where super-conductors cannot easily be used due, for example, to maintainability, field requirements, or shielding limitations.

In conceptual and engineering design of these components, fusion designers are often frustrated by the lack of specific property data, particularly for some of the newer, higher strength alloys. Additional complexities are introduced for some applications where operation at elevated temperatures and/or in a neutron radiation environment is required.

A workshop was convened under the auspices of the Office of Fusion Energy, U.S. Department of Energy, to assess and to calibrate the various aspects of the materials and data needs for copper and copper alloys for fusion applications.

---

*Metals and Ceramics Division, Oak Ridge National Laboratory, Martin Marietta Energy Systems, Inc., under contract DE-AC05-840R21400 with the Office of Fusion Energy, U.S. Department of Energy.

†Reactor Technologies Branch, OFE, Department of Energy.

‡Advanced Energy Systems, Westinghouse Electric Corporation.

Goals of the workshop were: To provide in-depth descriptions of the requirements presently perceived for copper and copper alloys in fusion applications; to review the known properties, characteristics, and radiation response of commercial and developmental copper alloys; and to review the objectives and current status of existing fusion-relevant experiments and programs focused on these materials. Presentations were made by representatives of the fusion design community, copper and copper alloy manufacturers, and materials specialists from universities, the national laboratories, and industry.

Specific issues which were addressed by the presenters included: temperature limits for copper and copper alloys, temperature-property data (limits of availability), the potential for developing improved alloys, the effects and limitations of welding/brazing operations, the effects of neutron radiation, and currently available product forms and sizes.

The intention of the workshop was to develop recommendations for the effort needed to assure that qualified copper and copper alloys would be available when they are needed for fusion applications. To this purpose, following presentation of the technical information, Working Groups were convened and charged with developing specific summaries and recommendations in each of the following four areas:

A. Fusion Design Requirements,
B. Status of the Current Data Base,
C. Directions for Alloy Development,
D. Fusion Needs: Experimental Programs.

A brief synopsis of the efforts of each of these Working Groups is presented below.

FUSION DESIGN REQUIREMENTS

Design requirements were developed for four general areas of application: high heat flux components, rf system components, magnet components, and the first wall. For each application, specific parameter ranges of interest and key (or limiting) materials properties were defined. Finally, a prioritized ranking was developed to express the relative importance of the major thermal, physical, mechanical, and radiation-response properties for each class of components.

STATUS OF THE CURRENT DATA BASE

Attention was given to three segments of the data base available for copper and copper alloys: thermophysical properties, mechanical properties, and manufacturing-related information. In each of these areas the Working Group defined the specific properties of interest, the ranges of important variables (e.g., temperature, magnetic field, joining technology) which are of concern, and provided a listing of possible data sources for each type of property. In addition, specific (albeit qualitative) estimates were provided regarding the perceived adequacy of the data base for each category.

DIRECTIONS FOR ALLOY DEVELOPMENT

This Working Group discussed briefly the metallurgical basis that exists for the potential development and production of high-strength, high-conductivity, high-temperature copper alloys. Separate discussion was offered on each of three types of copper alloys: oxide dispersion-stabilized alloys; low solid solubility, age-hardened alloys containing Cr, Zr, Mg, or similar low solubility alloying elements; and age-hardened alloys such as the Cu-Ti or Cu-Be alloys which undergo coherent aging reactions.

The approximate tensile, stress-rupture, and electrical properties of representatives of each of these alloy groups were compared and additional comments were provided regarding other important characteristics such as joining, fabrication (size) limits, and water corrosion. An outline of a program logic for the development and qualification of copper alloys for fusion reactor applications was provided.

FUSION NEEDS: EXPERIMENTAL PROGRAMS

Consideration of the experimental program needs for fusion applications was separated into needs perceived to be appropriate to near-term (e.g., the present to 1986) and long-term (1987 and beyond) applications. Near-term applications include heat sinks, beam dumps, limiters/divertors, and normal magnet components of interest for such devices as TFTR, MFTF, and the next stage of fusion experimental devices.

Longer term applications would generally parallel those of the short term but would emphasize effects believed or observed to be neutron fluence- or time-dependent. For each time frame of interest, programs associated with irradiation response were considered separate from those where neutron radiation response was not considered important. No attempt was made to specifically prioritize or rank the various program needs.

SUMMARY OF WORKING GROUP RECOMMENDATIONS

The greatest data void for the application of copper and copper alloys to fusion reactor service is for irradiation effects information. The need is for data over the temperature range 20°C to an upper limit dependent on the properties of each alloy class, perhaps only 300°C for some alloys but well above 450°C for the oxide dispersion-stabilized alloys. The fluence range of interest depends on the application, and ranges from less than 1 dpa to more than 100 dpa. Irradiation programs must provide adequate simulation of neutron spectrum effects, since solid transmutation products have a strong effect on conductivity. Property measurements that must be included in an irradiation program are electrical, thermal, and mechanical properties.

Future work on copper alloys should use material from a central stock of representative alloys. A possible set of alloys might include:

Unalloyed copper (e.g., C10100),
An alloy with Cr, Zr, Mg (e.g., C15000 or AMAX-MZC),
A Be-Ni alloy (e.g., C17510),
An oxide-dispersed alloy (e.g., C15715).

Better and more complete characterization of alloy properties is needed, to develop the processing and heat treatments that will optimize specific properties of a given alloy. Should existing alloys prove inadequate for intended applications, alloy development methods exist to optimize compositions within current alloy specification ranges or to develop new copper-base alloys. Possible new systems that indicate promise include Cu-Ti, Cu-Mo, and Cu-V alloys.

WORKING GROUP REPORTS

WORKING GROUP A:

DESIGN REQUIREMENTS FOR USE OF COPPER IN FUSION REACTOR COMPONENTS

Chairman: J. W. Davis, MDAC

Participants: R. L. Hagenson, TI/LANL
B. L. Hunter, FEDC/GE
L. J. Perkins, University of Wisconsin
W. A. Rinehart, MDAC
S. N. Rosenwasser, INESCO, Inc.

DESIGN REQUIREMENTS FOR USE OF COPPER IN FUSION REACTOR COMPONENTS

INTRODUCTION

As part of the copper workshop a working group was created to examine the requirements for various components used in a fusion reactor. The working group took this charter to mean an approximate identification of the operating environment, factors that enter into the design, and key material properties that have to be considered in designing or determining component lifetimes. For convenience the components were divided into four groups: high heat flux components, RF components, first wall, and magnets. The specific requirements for the various components are discussed in the appropriate sections. If the requirements are unique to a specific concept or machine (compacts, mirrors, or tokamaks) they are identified, otherwise they are assumed to be generic.

HIGH HEAT FLUX COMPONENTS

The high heat flux components consist of limiters, divertors, neutral beam target plates, first wall armor, and beam dumps. Their primary function is to protect the first wall from the high particle fluxes emitted from the plasma during normal and off-normal operation of a power reactor. The working group examined only the design and operating requirements for limiters, beam dumps, and divertors since these components will need to be capable of removing large quantities of heat and, as a result are prime candidates for fabrication from copper alloys. The factors that must be considered in designing these components are presented in Table A1. Also listed in this table are the key material properties that are used or must be considered in designing the component. Since these components will interface directly with the plasma they will experience higher heat fluxes than the first wall. These heat fluxes can be many times that encountered by the first wall, depending upon the radiation versus particle flux from the plasma. Typically this flux can range from 2–10 MW/m^2 for a limiter to 20–50 MW/m^2 for a beam dump. To accommodate these heat fluxes will require that these components be actively cooled. As a result the

Table A1. Design requirements for limiters/divertors

Requirement	Parameter	Key material property
Accommodation of high heat fluxes	2–50 MW/m^2	Thermal conductivity
Compatibility with coolant	T = 100–400°C	Corrosion rates
Acceptable component lifetime	T = 100–400°C $\leq 10^6$ cycles	Thermal expansion Tensile strength Modulus of elasticity Strain controlled fatigue
Accommodates plasma disruptions	$\leq 10^3$ cycles	Electrical resistivity Tensile strength Strain rate effects
Minimum impact on plasma performance		Sputtering yield Compatibility with low Z coating
Radiation resistance	≤40 dpa	Swelling Ductility
Fabricability		Formability Weldability

material selected will require not only good thermal conductivity but must also have low erosion/corrosion rates with the selected coolant.

It was not clear to the working group, from the information presented, what an acceptable life of these components should be. However, it was felt that if these components could not be readily replaced, to minimize down time, they should be designed to achieve 1–2 years of operation. Factors that influence component lifetime include thermal stresses, mechanical loads, and disruption loads. Since cyclic thermal stresses can produce fatigue or flaw growth failures it is desirable to minimize their magnitude. This can be accomplished by using materials with low coefficients of thermal expansion, low modulus of elasticity, and high thermal conductivity. By careful design and materials selection, it is possible to reduce the magnitude of thermal stresses; they cannot, however, be entirely eliminated except by going to steady state operation.

Plasma disruptions produce a rapid increase in the surface temperature of the component as well as a rapid increase in mechanical loads caused by induced eddy currents. The rapid increase in surface temperature in some designs can produce melting or vaporization of the material while the eddy current forces may be sufficient to cause tensile failures or deformation. The number of disruptions and their frequency is unknown since they vary from machine to machine. Important material properties that are used in designing these components are electrical resistivity, tensile strength, toughness, and stress-strain data. The desire to use a material with both high thermal conductivity and high electrical resistivity is a conflict in terms since materials with high thermal conductivity tend to have low electrical resistivity. Since thermal conductivity is a more important property, design innovation such as segmenting the limiter or use of electrical breaks may be required to break up the eddy current effects. To accommodate the rapid increase in tensile loads, materials with low strain rate sensitivity and high yield points are preferred.

The impact of high Z materials on plasma performance is well known. What is not well known is the flux of particles from the plasma and their energy when they impact the surface of the target. In addition it is not clear how the sputtered particles will be transported from the surface of the material to the plasma and the depth to which they will penetrate it. In general, for plasmas with low to medium edge temperatures (<200 eV) materials with high sputtering energy thresholds are preferred (these tend to be high Z metals such as tungsten) while for plasmas with high edge temperatures low Z materials such as beryllium are preferred. The information available on copper indicates that it does not fall in either category and as a result will have to be protected with a coating.

Radiation damage information has not been used in designing these components primarily because of greater concerns regarding erosion of the components. Assuming that these components can be designed to survive the plasma bombardment then radiation resistance will become an important criterion in design. Specific failure modes have not been identified for these components; however, they are likely to be deformation, fracture, or coolant leakage. Deformation is of concern because of the potential for

increased heating if the part deforms into the plasma. Key material properties are the swelling rate and irradiation creep rate as well as thermal creep rate. Fracture may occur as a result of plasma disruptions. Of concern in this case is embrittlement. Key material properties are ductility and change in tensile strength as a result of helium and dpa's. Leaks would occur as a result of cyclic loads. Key material data needs include the effects of irradiation on crack growth rate, fatigue, and creep rupture.

RADIO FREQUENCY (RF) COMPONENTS

In the design of an RF system the launcher will present the greatest challenges in both material selection and design since it is the interface between the high power transmission line and the plasma. The actual design of the launcher and the severity of the operating environment will depend upon the particular RF approach pursued. For example with ICRH the launcher would consist of an electrically insulated conductor covered by a Faraday shield. The function of the Faraday shield is to prevent the plasma particles and heat flux from entering the internal region of the launcher which could lead to arcing the conductor. In order to locate the launcher as close to the plasma as possible to maximize coupling, the Faraday shield will be required to operate in an environment similar to that of a limiter with roughly the same particle fluxes. For LHH and ECRH a Faraday shield would not be required since these heating regimes employ frequencies in which electrostatic coupling would not be a problem. As a result the launcher could consist of a waveguide or a parabolic mirror recessed in the shield cavity away from the plasma particles and in a lower radiation field. In this case the design requirements with respect to heat loads would not be as severe as for ICRH but would essentially be the same regardless of the RF approach considered. A comparison of the design requirements for an ICRH and an ECRH launcher is shown in Table A?. On this table the ECRH launcher is a parabolic mirror which is proposed for use on a mirror reactor. The function of the parabolic mirror is to reflect and focus the RF wave from a series of gyrotrons which are

Table A2. Materials design requirements for RF systems

Requirement	Parameter	Key material property
	ICRH	
Key components: Antenna, Faraday shield		
• High transmission efficiency	>80% IACS	Electrical resistivity
• High heat flux capability	1–15 MW/m^2	Thermal conductivity
• Minimum impact on plasma performance		Sputtering yield Compatibility with low Z coating
• Radiation resistance	≤40 dpa	Swelling Ductility
	ECRH (Quasi-Optical launcher systems only)	
Key component: Parabolic mirrors		
• High transmission efficiency	~99% IACS	Electrical resistivity
• Dimensional stability	±0.1 mm	Thermal conductivity
• Radiation resistance	≤20 dpa	Swelling

recessed in the blanket away from the plasma. For this design, dimensional tolerances are important since changes in the shape of the mirrors could alter their focus.

The objective of both ICRH and ECRH is to transmit power to the plasma. Since power loss is directly proportional to electrical resistivity it is desirable to use materials with as low an electrical resistivity as possible. For ICRH, electrical conductivities need to be greater than 80% IACS while for ECRH the electrical resistivities need to be 99% IACS. Decreases in the electrical conductivity or increases in the resistivity result in heating of the component. This heating for ICRH is in addition to the heat load produced by the plasma particles. While the heating of the Faraday shield will not be as great as that of a limiter,

because limiters can be positioned to protect the Faraday shield, it will be sufficiently high to require materials with good thermal conductivity.

Distortion is of particular concern with the ECRH mirror concept since dimensional changes in the range of 1% have the potential for altering the focus of the mirror and reducing the effectiveness of the heating. For ICRH the dimensional stability is not as severe unless the Faraday shield moves from the shadow of the limiter and begins to act itself as a limiter. The influence of radiation damage on RF performance has not been assessed. In general the working group was most concerned about the influence of transmuted elements on the electrical conductivity, followed by swelling as it relates to dimensional stability. Ductility and changes in ductility produced by neutron irradiation are more of a concern with ICRH since it will operate in an environment almost as severe as a limiter and will have to meet the same design criteria.

FIRST WALL

In general, the working group felt that the design criteria developed for the first wall in previous studies would be applicable to reactors using copper first walls. The primary difference is that devices that use copper first walls do so because the designers want to take advantage of the higher thermal conductivity of copper which permits higher wall loadings. A comparison of the wall loadings and operating environment for the various reactors or experimental machines that have proposed the use of copper first walls is shown in Table A3. This table shows that compact devices including the Riggatron will put the greatest stress on material selection and design if credible component lifetimes are to be achieved.

The design requirements for a first wall are based around four modes of failure. These modes of failure are:

- Leaks — in which the coolant penetrates the vacuum chamber and can then enter the plasma. This is of concern in closed confinement systems such as tokamaks but is of slightly less concern in mirrors. Key material properties needed in design are crack growth rate, fatigue, and creep-rupture.

Table A3. Operating conditions in designs with copper first walls

System	Surface heat flux (MW/m^2)	Neutron wall loading (MW/m^2)	Operating temperature (°C)	Limiter/divertor
Tokamak	0.3	1.2	125	Limiter
Mirror	0.1	5.0	Not copper	Natural divertor
Compact reactors	3–5	10–20	350–400	either (?)
Riggatron	12 (20)[a]	48–68	350–400	either (?)

[a]Commercial machine.

- Fracture — or gross rupture of the wall which can lead to interruption of coolant flow, loss of vacuum, or flow of coolant into adjacent areas. In general, fracture is most likely to occur during an off-normal situation such as plasma disruption which produces high loads in fractions of a second. The same concerns for limiters also apply in this situation; as a result of copper's low electrical resistivity segmented structures or electrical breaks will likely be required. The key material properties that would have to be considered in designing structures resistant to fracture are tensile and shear strength, ductility and fracture toughness, creep-rupture, and stress-strain information.
- Deformation — that occurs when the total allowable strain, as defined by structural symmetry or by a design code such as the ASME Boiler and Pressure Vessel Code, is exceeded. The key material properties are those that determine thermal stress (thermal conductivity, coefficient of expansion, and modulus of elasticity) as well as thermal creep, irradiation creep and swelling. However, the amount of thermal creep or irradiation creep that can be tolerated without causing problems is design dependent and criteria have not been established.
- Instability — or buckling of structural components, local buckling, or wrinkling of structural members. Instability can usually be avoided in design by providing adequate stiffness. However, large

amounts of plastic deformation or swelling can lead to buckling. The key properties that are used in design are the modulus of elasticity and the shear modulus (rigidity).

Implicit in this discussion of the modes of failure and the properties that are used to design against these failures is the effect of radiation damage. Radiation damage is more of a concern for the first wall than for other components because the performance of the first wall directly affects the production of electricity. Therefore in design it is desirable to maximize first wall life time so as to minimize downtime. Since a number of properties are used in designing these structures any changes in these properties as a result of radiation will have to be factored into the design.

MAGNETS

In examining the requirements for magnets the working group essentially limited themselves to applications requiring normal copper magnets since this is an area in which the use of high strength, low resistance copper alloys offer an advantage. A comparison of the operating/design requirements for normal magnets is shown in Table A4. The tokamak referred to in this table is an FED-R type machine. In general, the philosophy used to design magnets is the same as that used for a pressure vessel and the stress allowables conform to the ASME Boiler and Pressure Vessel Code. The type of failure a magnet designer is concerned with is gross overloading or growth of an undetected flaw. Key mechanical properties used in design are the tensile strength, modulus (tension and compression), fatigue strength, and fatigue-crack growth information. While changes in these properties as a result of radiation damage can be factored into design, the major concern expressed by the working group was in the change in electrical resistivity and swelling of the copper. Changes in resistivity decrease the efficiency of the magnet and increase the heating as a result of resistive power dissipation. This added heating, when coupled with nuclear heating, will cause an increase in cooling requirements if a constant magnet temperature is to be maintained. Since the cooling channels in a magnet are small, swelling has the potential for reducing coolant flow by restricting or closing off coolant channels.

Table A4. Magnet operational/design requirements

System	Design field strength (T)	Operating temperature (°C)	End of life damage level (dpa)	Strength		Elongation (%)	Electrical conductivity (% IACS)
				UTS (ksi)	TYS (ksi)		
Tokamak	9	100	1–10	80	60		>85
Mirror	18 (24)	150	1 to 100	133	100		>85
Compact reactors	8	100	5				>85
Riggatron	16	150	0.001 to 100	130–150	90–100	10	>85

SUMMARY

After examining the design requirements of the various systems or components the working group tried to prioritize the various material properties. The results of this comparison are shown in Table A5. In this examination the working group rated each material property on a scale of 1 to 10, with 10 being most critical and 1 least critical. This table reveals that for the first wall, RF, and high heat flux components, thermal conductivity and changes in thermal conductivity as a result of irradiation are most important followed by tensile strength (first wall and high heat flux) and electrical resistivity (RF). For magnets, electrical resistivity and changes in electrical resistivity due to irradiation are most important followed by irradiation creep, swelling, tensile, and fatigue strength.

Table A5. Relative importance of material property in design[a]

Property	First wall	Magnets	RF	High heat flux
Electrical resistivity	2	10 (8)[b]	8 (10 ECRH)	2
Thermal conductivity	9	1	8	10
Tensile strength	7	4 (10)	6	8
Fatigue crack growth	7	1	6	6
Creep rupture	3	2	1	3
Swelling	4	8	8	3–4
Irradiation creep	2	1	8	4
Change in resistivity	2	8 (8)	10 (ECRH)	1
Change in thermal conductivity	10	2	2	9

[a]10 = most critical need.

[b]Numbers in parenthesis refer to Riggatron.

WORKING GROUP B:

STATUS OF THE CURRENT DATA BASE

Chairman: E. N. C. Dalder, LLNL

Participants: F. R. Fickett, NBS
J. J. Holmes, HEDL
L. M. Schetky, INCRA
B. Weggel, MIT
C. I. Whitman, SCM Corp.

STATUS OF THE CURRENT DATA BASE

Current available data bases vary from "adequate" to "good," in the areas of thermophysical properties, to "non-existent" in the areas of the effects of radiation on mechanical properties of copper and its alloys of interest to MFE design efforts. The Working Group on Data Bases chose to divide the types of properties to be considered into three classes: (1) thermophysical; (2) mechanical; and (3) manufacturing related.

Considering first the status of data bases for thermophysical properties, the properties of interest include thermal conductivity and diffusivity, electrical conductivity, specific heat, thermal expansion, elastic constants, and total emissivity. Table B1 identifies the physical-variable fields over which each property is of importance, as well as existing sources of data. Table B2 rates each property in terms of relative amount of information ("OK", "fair", or "none") and relative importance of obtaining such information ("critical" where little to no data exists to "nil" where sufficient data is thought to be available).

Considering next the status of data bases for mechanical properties, the properties of interest are: (1) uniaxial tensile properties; (2) unnotched fatigue properties; (3) fatigue-crack growth, fracture toughness (J_{IC}); and (4) creep and stress-rupture properties. Table B3 identifies the physical-variable fields of interest, as well as existing data bases. Table B4 rates each property in terms of relative amounts of information and the importance of obtaining additional information.

Considering last the important, but often over-looked category of manufacturing-related properties, these are (1) joinability (fusion welding, resistance welding, solid-state bonding, brazing, soldering, adhesive bonding, and mechanical fastening); (2) hot-formability; (3) cold-formability; (4) castability; (5) machinability; and (6) powder-metallurgy (P.M.) processing. Table B5 lists these properties in terms of the class of alloy to which they might be applied, and lists available data sources. Table B6 attempts to assess the relative amount of information available for each of these properties, ranging from "high" where much information is felt to be available, to "fair" where it was felt that information is available on only 1 or 2 alloys.

Table B1. Comments on thermophysical properties data bases

Property	Important ranges of variables	Possible data sources
Thermal conductivity and diffusivity Electrical conductivity Specific heat Elastic constants[a] Thermal expansion Total emissivity	Temperature: 1.8 to 800 K Magnetic Field: Earth's to 32 Tesla Fluence (14.1 MeV neutrons) $\leq$10 MW-yr/m^2 ($\sim$120 dpa) Material: Complete chemical composition and processing history	Purdue University Thermo-Physical Properties Research Center National Bureau of Standards International Copper Research Association British Non-Ferrous Research Association Metallgesellschaft (W. Germany) American Society For Testing & Materials Special Technical Publications General Electric Co. Materials Data Center

[a]Any two of Elastic Modulus, Shear Modulus, and Poisson's Ratio.

Table B2. Qualitative evaluation of adequacy and needed expansion of thermophysical properties data bases

Property	Temperature	Magnetic field	Neutron fluence	Composition and processing
Relative amount of present information as a function of				
Thermal conductivity and diffusivity	OK	OK	None	OK
Electrical conductivity	OK	OK to 8 T, None beyond 8 T	None	OK
Specific heat	OK	*a*	*a*	OK
Elastic constants	Some	*a*	None	Some
Thermal expansion	OK	*a*	*a*	OK
Total emissivity	Some	*a*	*a*	OK
Relative importance of obtaining additional information as a function of				
Thermal conductivity and diffusivity	Nil	Nil	Critical	Nil
Electrical conductivity	Nil	Critical beyond 8 T	Critical	Nil
Specific heat	Nil	Nil	Nil	Nil
Elastic constants	Moderate	Nil	Critical	Moderate
Thermal expansion	Nil	Nil	Nil	Nil
Total emissivity	Some	Nil	Nil	Nil

[a]Property is not sensitive to this variable.

Table B3. Comments on mechanical properties data bases

Property	Important ranges of variables	Possible data sources
Uniaxial tensile properties: yield strength, ultimate strength, uniform elongation, total elongation, reduction in area	1. Temperature: 1.8–800 K 2. Fluence: 0–10 MW-yr/m^2 (~120 dpa) 3. Time of testing: dynamic (10^{-5} h) to static (10^{-1} h) 4. Environment: high-purity H_2O, energetic H and H_2, vacuum, liquid metals (Na, Li, $Li_{17}Pb_{83}$) 5. Composition range for commercially produced alloys 6. Thermomechanical processing (TMP)[a]	1. ASM "Metals Handbook" 2. International Copper Research Association reports 3. General Electric Co. Materials Data Center 4. Manufacturers of electrical machinery (G.E., Westinghouse, Siemens, Hitachi, Toshiba, etc.) 5. American Society For Testing and Materials Special Technical Publications
Unnotched fatigue (both load-controlled and strain-controlled), fatigue crack growth	1. As above 2. As above 3. Cycling rate: 10^{-5} to 10^{6} per minute 4. As above 5. As above 6. As above 7. Number of cycles: 10^{1} to 10^{7}	6. British Non-Ferrous Research Association 7. DOE Basic Energy Sciences Programs 8. National Bureau of Standards Monographs 9. U.S. Copper Development Association "Extracts" 10. Various open literature publications
Entire strain-time curve in creep loading (constant load); stress rupture	1. Temperature: 500–800 K 2. As above 3. Time of loading: Static to 10^{5} hr 4. As above 5. As above 6. As above	11. Alloy Digest 12. Materials suppliers literature
Fracture toughness (probably J_{IC} converted to K_{IC})	1. Temperature: 1.8–800 K 2. As above 3. Time of loading: as for "tensile properties" 4. Environment: as above 5. As above 6. As above	

[a]Thermomechanical Processing (TMP) – Important factors include (a) melting and casting practices; (b) primary ingot breakdown methods, times at temperatures, temperatures, critical cooling and/or heating rates; (c) secondary working methods used to convert slab, billet, or bloom into final product forms, i.e., types of mechanical working, times at temperatures, temperatures, critical cooling and/or heating rates; (d) testing variables such as section shape and size, specimen orientations relative to primary directions of working; (e) sequencing of TMP operations; and (f) characterization of as-tested microstructures as to grain size and occurrence, distribution, and sizes of minor phases.

Table B4. Qualitative evaluation of adequacy of mechanical property data bases

Property	Temperature	Neutron fluence	Loading time	Cycling rate	Environment	Composition	Thermomechanical processing
			Relative amount of present information as a function of				
Uniaxial tensile properties	Good	Nil	Fair	Fair	Nil	Fair	Fair
Unnotched fatigue (load-controlled and strain-controlled)	Good <300 K Poor >300 K	Nil	Fair	Fair	Nil	Fair	Fair
Fatigue crack growth, fracture toughness	Good <300 K Poor >300 K	Nil	Fair	Fair	Nil	Fair	Fair
Entire strain-time curve in creep, stress rupture	Fair	Nil	Fair $<10^3$ h Poor $>10^3$ h	Not applicable	Air: Good Others: Nil	Fair	Fair
			Relative importance of obtaining additional information as a function of				
Uniaxial tensile properties	Nil	Critical	Moderate	Moderate	Critical in first wall and blanket environments	Moderate	Moderate
Unnotched fatigue (load-controlled and strain-controlled)	Nil <300 K Critical >300 K	Critical	Moderate	Moderate	Critical in first wall and blanket environments	Moderate	Moderate
Fatigue crack growth, fracture toughness	Nil <300 K Critical >300 K	Critical	Moderate	Moderate	Critical in first wall and blanket environments	Moderate	Moderate
Entire strain-time curve in creep, stress rupture	Moderate	Critical	Moderate to 10^3 h Critical $>10^3$ h	Not applicable	Critical in environments other than air	Moderate	Moderate

Table B5. Comments on manufacturing-related data bases

Property	Type material-based variable	Possible data sources
Joinability: fusion welding resistance welding brazing soldering solid state bonding adhesive bonding mechanical fastening Hot formability Cold formability Castability Machinability Powder processing	Method(s) of strengthening used in alloy a. "Pure" copper, i.e., no intentional strengthening additions b. Strengthening by additions of substitutional solid-solution alloying elements c. Strengthening by TMP below the recrystallization range, i.e., "cold work" d. Strengthening by addition of alloying elements that convey precipitation-hardening or spinodal-decomposition hardening e. Strengthening by addition of inert compounds that form a strengthening dispersion f. Sequencing of TMP operations	1–12. Same as for "Mechanical Properties" 13. American Welding Society "Welding Handbook"

Table B6. Evaluation of adequacy of manufacturing-related data bases

Property	Relative amount of information	Need for obtaining additional information
Joinability	Fair, unless a new alloy is considered	High for users
Hot formability	Good	Moderate for material suppliers
Cold formability	Fair	High for users
Castability	High	Moderate for material suppliers
Machinability	Fair	High for users
Powder processing	Fair, unless a new alloy is considered	High for suppliers of new alloys

Table B7 summarizes the Working Group's recommendations for data generation. First, and most important, is the need for systematic studies of thermophysical and mechanical properties as functions of neutron fluences and temperatures representative of planned power-producing fusion devices for four to six representative copper alloys. Second is accumulation of electrical-conductivity data at magnetic fields beyond 8–10 T at temperatures from 1.8 K to room temperature. Third, but not last, is the assembly of more complete information on manufacturing processes and their impact on physical and mechanical properties of representative alloys.

Table B7. Generic areas for additional work

1. Physical and mechanical properties as functions of temperature and neutron fluence relevant to fusion reactor designs.
2. Electrical conductivity at magnetic fields greater than 8 T from 1.8 to 300 K.
3. More complete information on manufacturing processes: for alloys for specific components, effects on mechanical properties, and effects on electrical conductivity.

WORKING GROUP C:

DIRECTIONS FOR ALLOY DEVELOPMENT

Chairman: N. J. Grant, MIT

Participants: T. C. Reuther, DOE
D. L. Smith, ANL
W. D. Speigelberg, Brush Wellman
P. W. Taubenblat, AMAX

THE DEVELOPMENT OF HIGH-STRENGTH, HIGH-CONDUCTIVITY HIGH-TEMPERATURE COPPER-BASE ALLOYS

The development and production of high-strength, high-conductivity, high-temperature copper or copper-base alloys require highly selective alloying, control of impurities and tramp elements, and careful thermomechanical processing to optimize, in particular, the conductivity. Achieving all three aims is not a simple task since certain aspects of alloying and strengthening are contrary to those which enhance conductivity.

Classically, oxide dispersed (OD), or oxide dispersion stabilized (ODS) copper provides all three property aims in excellent proportions because pure copper is the base and there is no alloying between the copper and the stable, refractory oxide dispersoid. Table C1 shows the useful combination of low- and high-temperature strength, with thermal conductivities in excess of 90% IACS.

A second class of alloys depends on the addition of very low solid solubility alloying elements, singly or in combination. The resultant alloys are not as stable at high temperatures as the OD-Cu alloys, but are able to generate higher strengths at low temperatures (below, say, 350–400°C) with conductivity values greater than about 80% IACS. The more common alloying elements are Cr (which tends to precipitate elementally, and has significant aging response), Zr (which forms the relatively insoluble phase Cu_4Zr, contributing a dispersion strengthening effect) and combinations of Cr, Zr, Mg, and others. Other elements offering similar strengthening patterns are Hf, Mo, W, V, Ta, Nb, but have not been used extensively because of higher costs, greater melting and casting problems, etc.

A third class of alloys is the age-hardening group, typified by the elements Ti and Be. Coherently aged alloys, including spinodal alloys, result in very high tensile strength levels, in excess of 180,000 psi, depending on composition and thermomechanical treatments. Ductility and conductivity suffer at the very high strength levels, and care must be exercised to process the alloys to optimize specific properties or combinations of properties. These same Cu-Be and Cu-Ti alloys frequently

Table C1. Mechanical properties of oxide dispersed Cu-Al_2O_3

Alloy	Condition	Stress for 100 h life (psi)	Elongation (%)	Reduction of area (%)
	Stress-rupture at 450°C (in air)			
Cu-0.4 vol % Al_2O_3	As extruded	17,000	2	14
Cu-1.1 vol % Al_2O_3	As extruded	31,000	2	6
Cu-3.5 vol % Al_2O_3	As extruded	38,000	2	10
	Stress-rupture at 650°C (in air)			
Cu-0.4 vol % Al_2O_3	As extruded	7,500	1	4
Cu-1.1 vol % Al_2O_3	As extruded	16,000	2	8
Cu-3.5 vol % Al_2O_3	As extruded	21,000	3	8
304 SS (Ingot)[a]	Annealed	22,000	8	15
	Stress-rupture at 850°C (in nitrogen)			
Cu-0.4 vol % Al_2O_3	As extruded	2,200	1	2
Cu-1.1 vol % Al_2O_3	As extruded	6,000	1	1
Cu-3.5 vol % Al_2O_3	As extruded	8,000	1	1
304 SS (Ingot)	Annealed	4,000	12	20
	Tensile properties at 20°C			
		YS	UTS	
Cu-0.4 vol % Al_2O_3	As extruded	41,500	52,300	18	44
Cu-1.1 vol % Al_2O_3	As extruded	54,000	65,400	14	30
Cu-3.5 vol % Al_2O_3	As extruded	59,200	71,400	12	13
304 SS (Ingot)	Annealed	35,000	87,000	72	80
316 SS (Path A-1, RS-PM)[b]	62% CW	157,000	160,000	15	40

[a]Type 304 stainless steel prepared by conventional wrought product ingot metallurgy.

[b]RS-PM is rapidly solidified, powder metallurgy product.

have other elements added to enhance specific properties, for example, Cu-Be-Co, Cu-Be-Ni, Cu-Ni-Ti. Properly selected compositions can be useful for improved thermal conductivity.

Processing is a critical feature of the combinations of properties these various alloys will achieve. The usual methods, ingot casting and shape casting, lead to slow solidification rates (from 10^{-2} to 10^{0} K/s); this promotes segregation, separation of phases, and coarse structures, both grain size and precipitated phases. These structures make hot and cold working more difficult, lead to poor yields of product, increased costs, and decreased properties. The amount of alloying is sharply restricted because of solidification faults; typically Cr additions are about 0.6% or less, and Zr additions are 0.2 to 0.4, usually nearer to 0.2.

The recent development of rapid solidification techniques (RST) (solidification rates of 10^{2} to 10^{7} K/s) has permitted major changes in compositions, conversion methods, and processing techniques. (Application to beryllium containing alloys is restricted, due to concern over health problems in the production and handling of fine powders or flakes, foils, and ribbons. This may be a temporary situation however.) At the high solidification rates associated with RST, segregation is sharply minimized and formation of coarse phases is limited; instead totally different sizes, shapes, and dispersions of excess phases occur. The grain size of the resultant alloys is very fine, typically 1–5 μm, and can be made finer if desired. Hot and cold working are very much improved, mechanical properties are enhanced, ductility is very significantly increased over similar ingot products, and conductivity values are uniformly higher for all the alloyed coppers.

Alloying potential is also sharply increased by RST. There is no problem in adding several percent of elements such as Cr and Zr where strength increases at low and high temperatures are desired. In fact one of the advantages of RST is the potential for developing either more highly alloyed coppers or of developing new alloy systems, for example, Cu-Mo or Cu-V alloys. Such highly successful alloy development programs are particularly well documented for Al-base alloys, stainless steels,

high-speed tool steels, and Co-base and Ni-base superalloys. The developments with Cu-base alloys are equally positive but are based on less work and fewer alloy systems, leaving open the attractive issues of significant further improvements in a broad range of properties.

Table C2 lists approximate levels of tensile properties and conductivity for the several classes of alloys discussed above. In many instances the values listed are for experimental alloys, or alloys with different thermomechanical processing than those which are found in handbooks and commercial literature. Alloy processing, including starting ingot or slab size, final product section size, and specific thermomechanical processing will cause important differences in the properties, particularly conductivity, which is sensitive to small structural and compositional changes.

Table C2. Current status of tensile properties and conductivity achieved in advanced copper alloys

Material[a]	Condition[b]	Yield stress (psi)	Ultimate tensile strength (psi)	Elongation (%)	Conductivity (% IACS)
OFHC	Ann	8,000	40,000	30–40	~100
	20% CW	30,000	50,000	20–30	96
	50% CW	50,000	70,000	10–15	92
OD-Cu	CW	60,000	75,000	10–15	85–90
Amzirc	FHT	50,000	70,000	20	85–90
MZC	FHT	85,000	95,000	20	80–90
CuNiTi	FHT	90,000	95,000	20	50
MZC	OD Mod	90,000	100,000	20	60–70
CuNiTi	OD Mod	105,000	130,000	20	50
CuTi		100,000–180,000	160,000–210,000	5–3	10
Cu-1.8Be-0.2Co	FHT	100,000–180,000	170,000–220,000	10–3	10–25
Cu-0.4Be-1.8Ni	FHT	100,000–120,000	120,000–150,000	10–5	45–60

[a]Classes of alloys and useful preparation methods
(1) Pure coppers: Ingot metallurgy (IM)
(2) Age hardened -- with and without cold work: IM, PM, Flake
(3) Spinodal: IM, PM, Flake
(4) OD Alloys — simple and complex: PM, Flake

[b]Ann = fully annealed, CW = cold worked, FHT = fully heat treated, OD Mod = powder metallurgy preparation from rapidly solidified flake.

Table C3 summarizes a spectrum of items of interest associated with possible applications of the three classes of alloys being discussed. Some of the listed issues are untested or are poorly known, and represent areas where additional work must be undertaken. For example; weldability, high-temperature brazing, radiation stability and response are largely unknown areas for these alloys.

Table C3. Status of copper alloy development

Alloys	Pure copper	Precipitation hardened alloys[a]	Oxide dispersion stabilized alloys (ODS)
Electrical and thermal conductivity[b]	Excellent	Good/fair	Excellent/good
High-temperature strength	Poor	Fair	Good
Low-temperature strength	Fair	Good	Fair
Weldability	Fair	Fair	Poor
High-temperature brazing	Fair	Fair	Good
Water corrosion	Good	Good	Good
Radiation stability	?	?	?
Fabrication			
Sheet	Good	Good	Development required
Strip	Good	Good	Fair
Plate	Fair	Development required	Development required
Manufacturing Technology:			
Ingot metallurgy	Yes	Yes	No
Powder metallurgy	Yes	Yes	Yes

[a]Spinodal alloys are included in this classification but are not rated for lack of adequate data.

[b]Excellent, >95% IACS; Good, 50–90%; Fair, <50%.

Finally, Table C4 lists recommended research, development and testing programs to develop the desired alloys, determine processing parameters and establish the levels of properties for the numerous fusion reactor applications contemplated for copper-base alloys.

Table C4. Elements recommended for inclusion in copper alloy developmental programs

1.	Optimization of properties through alloy development
2.	Optimization of properties through thermomechanical processing
3.	Coatings, cladding, and surface treatments
4.	Studies of effects of irradiation on phase transformation, metastable phase formation, strength, ductility, corrosion, erosion, and other relevant properties
5.	Study of the potential for spinodal alloys: Cu-Ti and others
6.	Studies of fiber-reinforced composite alloys
7.	Production of large section sizes for all alloys except the pure coppers
8.	Alloy performance at high temperatures and long term exposure: creep and stress-rupture testing
9.	Joining studies, to include a broad range of techniques: welding, high-temperature brazing, diffusion bonding

WORKING GROUP D:

EXPERIMENTAL PROGRAM NEEDS FOR COPPER AND COPPER-BASE ALLOYS

Chairman: R. E. Gold, Westinghouse

Participants: F. W. Clinard, LANL
M. W. Guinan, LLNL
O. K. Harling, MIT
S. N. Rosenwasser, INESCO
J. M. Vitek, ORNL
J. B. Whitley, SNL-A

EXPERIMENTAL PROGRAM NEEDS FOR COPPER AND COPPER-BASE ALLOYS

This portion of the Workshop Proceedings presents a summary of discussions which occurred at a Working Group meeting convened to assess the needs and priorities which could be assigned to experimental programs relevant to Cu and Cu-base alloys for fusion reactor applications. There is unavoidably some overlap between the areas discussed by this Working Group and others convened at this Workshop — e.g., the "Requirements" and "Data Base" Working Groups. Hence, implementation or detailed evaluation of the deliberations provided here must be integrated into a uniform and consistent framework.

ASSUMPTIONS, GROUNDRULES, AND RECOMMENDATIONS

- Program needs should be separated, for planning purposes, into near-term and long-term needs. The time frames and applications of interest to each of these categories are identified later.
- Attention is recommended to three "types" of copper/copper alloys:
  - Unalloyed/Solid Solution, e.g. oxygen-free Cu
  - Precipitation strengthened, CuMgZr, CuBe(Ni)
  - Oxide dispersion stabilized, e.g. mechanically alloyed, or RST product

  Each of these types have certain properties or groups of properties which recommend them for specific applications.
- If a testing program is to be conducted, it is imperative that the Office of Fusion Energy establish a controlled inventory of "optimally prepared" and uniformly characterized materials. Emphasis must be on the material product forms of interest, e.g. sheet, bar, and rod.

NEAR TERM ACTIVITIES (1983–86)

This time frame is considered most appropriate for the needs of such devices as TFTR, MFTF, and perhaps, experimental phases of compact fusion devices.

Applications

- Heat sinks and heat dumps, including coated components.
- First wall and near-first wall components, including limiters and divertors.
- Nonsuperconducting magnets.

Program Needs — Unirradiated

The major needs in this category, particularly for the near term devices, are primarily associated with better characterization of thermal, electrical, and mechanical properties of these materials. Specific data needs include:

- Time/temperature effects on thermal and electrical properties.
- Time/temperature effects on mechanical properties, with particular attention to fatigue and possibly flaw growth behavior.
- Data regarding the performance and survivability of copper alloy/coating pairs under extreme thermal loads, including the effects of cycling on bond integrity.
- Charged particle sputtering data (emphasis on angle of incidence effects and use of appropriate incident particle energies) for "bare" metal applications.
- Surface erosion information for coated components.

Program Needs — Irradiated

Scoping neutron irradiations (e.g. to ~10 dpa) should be performed for the purposes of:

— early discrimination between candidate materials/alloys on the basis of microstructural stability, mechanical property response, etc.

— examination of substrate/coating response to neutron radiation-induced damage.

In addition to the preceding scoping experiments, which could be carried out in fission test reactors, value was cited for RTNS-based in situ measurements of the electrical resistivity during 14 MeV neutron irradiation.

Other Near Term Issues

In view of their importance to the application of copper and copper alloys for fusion reactors, the Working Group felt that, even in the near term, information is needed in the areas of:

- significance of corrosion and/or erosion in high pressure, high temperature water, and
- significance of hydrogen (tritium) effects.

LONG TERM ACTIVITIES (1987+)

Obviously, the pace of long-term activities may differ considerably from those focused on near-term data needs. The effort would still be a "scoping effort" with emphasis on the most promising candidate compositions.

Applications

In general, the applications would remain the same as those identified previously for near-term activities. The emphasis, however, would shift to those effects known or believed to be fluence or time-dependent.

Program Needs — Irradiated

The emphasis here would likely be on the irradiated materials performance/properties since, presumably, the unirradiated property evaluations would have been sufficiently scoped in the near-term programs. Because of the costs and time associated with an extensive neutron radiation testing program, this effort should await the results of the scoping evaluations of the mechanical, thermal, electrical, and corrosion properties of candidate alloys.

Irradiation experiments would then focus on the evaluation of the effects of neutron radiation on:

- Mechanical properties
- Irradiation creep
- Microstructural stability
- Thermal and electrical properties (postirradiation)

Radiations could be performed in test reactors such as ORR and HFIR, and should cover the temperature range from 50 to 450°C. The maximum temperature might have to be lowered pending early scoping evaluations.

WORKSHOP PRESENTATIONS

INTRODUCTION

F. W. Wiffen

Fusion Engineering Design Center
and
Oak Ridge National Laboratory

WORKSHOP ON

COPPER AND COPPER ALLOYS FOR FUSION REACTOR APPLICATIONS

SCOPE

The need for copper or copper-base alloys in a number of fusion reactor applications has been defined by design studies and analysis of component operating requirements. In addition to the stabilizers in the superconducting magnets, copper may be required in other, quite demanding applications. These applications generally fall into three categories:

1. Normally conducting magnets; ranging from trim coils through full TF or PF coils to very high field coils that must operate in high neutron flux regions.

2. High heat flux components; including beam dumps, divertor, limiter, and armor. These may require bimaterial combinations.

3. First walls, with specialized requirements on electrical or thermal conductivity.

Copper alloyed with beryllium or zirconium has been specified to meet some of these needs; unalloyed copper is adequate for other applications. Well-defined limits are set by thermal, electrical and strength properties; less well-defined limitations may be set by joining technology and the effects of neutron irradiation.

The purpose of this workshop is to bring together representatives of the fusion reactor design teams, the fusion materials experimentalists, and the copper industry. This group will examine the range of requirements for copper alloy reactor components, and will briefly discuss the available data on these materials. They will then formulate recommendations to OFE/DOE for experimental program needs, to assure that the appropriate alloys and a data base covering their response to fusion applications conditions will be available.

COPPER WORKSHOP

GOAL

DEVELOP RECOMMENDATIONS TO OFE/DOE

OF WORK NEEDED ON COPPER ALLOYS,

BASED ON EXAMINATION OF SYSTEM

REQUIREMENTS AND OF AVAILABLE

COPPER DATA.

QUESTIONS ON USE OF COPPER ALLOYS

TEMPERATURE LIMITS FOR COPPER ALLOYS

TEMPERATURE-PROPERTY DATA

POTENTIAL FOR DEVELOPING IMPROVED ALLOYS

WELD/BRAZE EFFECTS ON PROPERTIES:

- LOSS OF STRENGTH
- INCREASE IN RESISTIVITY

AVAILABLE SIZE AND PRODUCT FORMS

POTENTIAL APPLICATIONS OF COPPER ALLOYS IN FUSION REACTORS

A. MAGNET APPLICATIONS

1. STABILIZERS in S/C MAGNETS
2. CONDUCTORS IN NORMAL MAGNETS, INCLUDING
   - VERY HIGH-FIELD MAGNETS
   - COIL INSERTS TO AUGMENT FIELD
   - FIELD CORRECTION COILS
3. HIGH-STRENGTH, HIGH-CONDUCTIVITY JOINTS
4. LEADS AND BUS BARS

B. HIGH-HEAT FLUX COMPONENTS

5. LIMITER/DIVERTOR COLLECTOR PLATES
6. BEAM DUMPS
7. DIRECT CONVERTORS
8. FIRST WALL OF COMPACT REACTORS (AND ADVANCED REACTORS)

C. HIGH CONDUCTIVITY COMPONENTS

9. CONDUCTIVE FIRST WALL
10. rf SYSTEM COMPONENTS
11. CONNECTORS BETWEEN SECTORS

April 11, 1983

AGENDA FOR THE WORKSHOP ON

COPPER AND COPPER ALLOYS FOR FUSION REACTOR APPLICATIONS

Thursday, April 14, 1983

9:00–9:30 a.m. Session 1 – Introduction

T. C. Reuther	.....	Welcome and Appreciation DOE Expectations of Meeting
F. W. Wiffen	.....	Workshop Purpose, Organization, Agenda and Assignments

9:30–12:00 Session 2 – Fusion Applications of Copper

B. L. Hunter	.....	Unique Requirements in Resistive Magnets
F. W. Wiffen	.....	Electrically Conducting First Wall for Tokamaks
D. L. Smith	.....	Copper in Impurity Control Systems, INTOR and Power Reactors
J. W. Davis	.....	Copper Components of rf Systems
R. L. Hagenson	.....	First Wall, Limiters, and Magnet Coils in Compact Concepts

1:00–5:30 p.m. Session 3 – Properties of Copper Alloys

P. Taubenblatt	.....	Specialty Copper Alloys, Especially the Cu-Zr Alloys
W. D. Spiegelberg	.....	The Cu-Be Alloy Family
C. I. Whitman	.....	Dispersion Strengthened Copper
L. M. Schetky	.....	Low Alloyed Copper
L. J. Perkins	.....	Radiation Effects Limitations on Copper in Normal Conducting Magnets
M. W. Guinan	.....	Radiation Effects Limits on Copper in Superconducting Magnets
E.N.C. Dalder	.....	Processing, Properties and Microstructures of High-Strength, High-Conductivity Copper Alloys

Friday, April 15, 1983

8:30–12:00 a.m. Session 4 – Experiments and Programs in Place

S. N. Rosenwasser	.....	Copper Alloys for Riggatron Applications
N. J. Grant	.....	The Development of High Strength/High Temperature Copper Alloys
F. W. Clinard, Jr.	.....	Copper Alloy Irradiation Studies in Support of CRFPR First Wall
O. K. Harling	.....	The MIT/INCRA Radiation Effects Studies
J. B. Whitley	.....	The High Heat Flux Components Program
W. A. Rinehart	.....	Fabrication of Copper Alloy Beam Dumps

1:00–4:00 Session 5 – Tentative Working Groups and Discussion Leaders

A. Statement of Requirements ..... John Davis
B. Adequacy of Existing Data Base..... Ed Dalder
C. Directions for Required Alloy Development..... Nick Grant
D. Needs and Priorities for Experimental Programs.. Bob Gold

4:00–5:00 Session 6 – Summary

Review of working group discussions. Discussion leaders hand in preliminary writeup of summary and recommendations.

TENTATIVE ASSIGNMENTS FOR WORKING SESSIONS

A. Requirements

John Davis, Leader
D. G. Doran
G. M. Haas
R. L. Hagenson
B. L. Hunter
W. A. Rinehart
S. N. Rosenwasser

B. Data Base

Ed Dalder, Leader
M. M. Cohen
F. R. Fickett
J. J. Holmes
L. M. Schetky
B. Weggel
C. I. Whitman

C. Alloy Development

Nick Grant, Leader
T. C. Reuther
D. L. Smith
W. D. Speigelberg
P. W. Taubenblatt

D. Experimental Program Needs

Bob Gold, Leader
F. W. Clinard
M. W. Guinan
O. K. Harling
L. J. Perkins
J. M. Vitek
J. B. Whitley

FUSION APPLICATIONS OF COPPER: UNIQUE REQUIREMENTS IN RESISTIVE MAGNETS

Brook Hunter

Fusion Engineering Design Center
and
General Electric Company

The Fusion Engineering Design Center (FEDC) is focusing FY 1983 activities on evaluating upgrade alternatives for the major fusion device now being completed. FEDC resources are divided equally between tokamak applications, in support of TFTR upgrade, and tandem mirror applications, supporting upgrade of the MFTF-B facility. In the course of magnet system design studies related to these activities, several needs for water cooled copper coils are presently perceived. The applications discussed in this paper are the high field choke coils (tandem mirror) and toroidal field coils or coil inserts (tokamaks). In these applications, the important properties are low electrical resistance, high mechanical strength and tolerance to neutron fluence.

Poloidal field ring coils internal to the bore of toroidal field coils in a tokamak may also be constructed of copper. The poloidal field ring coil application will not be discussed, since the presently available grades of copper provide material properties adequate for this application.

This paper will also not address the application of copper as a stabilizer in superconductors.

The current favorite among candidate upgrades of the MFTF-B machine now under construction is designated as the MFTF-α+T upgrade. The MFTF-α+T machine incorporates new end plugs to improve performance and a D-T axicell inserted into the MFTF-B center cell. Two high field solenoidal coil sets, a pair of 12T choke coils in the D-T axicell and an 18T barrier coil at each end of the central cell are required in the MFTF-α+T design. Design parameters for the high field coils in the MFTF-α+T concept are listed in Table 1.

Table 1. MFTF-α+T High Field Coil Design Parameters

	Choke Coil	Barrier Coil
Number of coils	2	2
Field, Tesla	12	18
Current Density, A/cm^2	2900	2900
Inside Radius, m	0.17	0.28
Outside Radius, m	0.47	1.13
Megamp turns	23	19
Stress, Mpa	163	598
Resistive Power Loss per Coil, MW	39	73

The design of these high field coils is driven by system configuration considerations. In order to fit into the machine without interference, these coils are designed to be made very compact. Therefore, a high current density, about 2900 A/cm^2, was chosen. The stress reported is a crude estimate of general stress level computed from the formula $\sigma = BjR$, the hoop membrane stress in an unsupported conductor due to the magnetic dilational forces. The estimates are conservative in that they are based on maximum field and maximum radius.

The FEDC has adopted magnet structural design criteria which limit primary membrane stress to 2/3 yield or 1/3 ultimate, whichever is less. For these limits, the strength required is 244 MPa yield and 500 MPa ultimate for the 12T choke coil and 900 MPa yield and 1800 MPa ultimate for the 18T barrier coil. The strength requirements for the 12T coil can be met using the AMAX-MZC alloy, 40% cold worked (450 MPa yield and 500 MPa ultimate). The required strength for the 18T barrier is not

attainable in copper or copper alloys. Consequently, it will be necessary to provide structural support for the conductor in the form of a case around the winding or steel support channels co-wound with the conductor.

The MFTF-α+T application is near term; it will be necessary to order long lead-time material in 1986 and complete construction by 1993. However, reactor relevant design studies also include similar high field axicell coils. The MARS study, for example, includes a 24T choke coil.

The FED-R is a recently completed tokamak design study based on near term technology. It uses large rectangular resistive toroidal field (TF) coils, approximately 11 m by 7 m. The FED-R study illustrates some of the design problems encountered with resistive TF coils or coil inserts. One of the major considerations in FED-R was the power loss in the coils, and the design objective was to limit resistive loss to 275 MW. By choosing a very modest nominal current density of 415 A/cm^2, with a maximum of 810 A/cm^2 in the nose region, resistive loss was limited to 22.2 MW for each of the 12 coils for a total of 266 MW. Bending stresses in the corners of the coils necessitated the incorporation of one meter corner radii.

A key feature of the FED-R TF coils is the demountable joint design. The purpose of these joints is to permit easy disassembly of coils in order to permit removal of torus sectors during the operating life of the device. The design of the demountable joint required the use of a high strength copper alloy, CDA-175, for insert fingers.

The Fusion Engineering Design Center (FEDC) is focusing FY 1983 effort on evaluating upgrade alternatives for the next fusion device

- support of Lawrence Livermore National Laboratory (LLNL), evaluating upgrades of MFTF-B (tandem mirrors)

- support of Princeton Plasma Physics Laboratory (PPPL), evaluating upgrades of TFTR (tokamaks)

We presently perceive several potential applications of copper coils to magnetic systems for fusion devices

- Tandem Mirror Machines
  - choke and barrier coils
- Tokamaks
  - toroidal field coils (or coil inserts)
  - poloidal field ring coils

In all of these applications, our material needs may be summarized as:

- low resistivity
- high strength
- tolerance to neutron irradiation

The recommended mirror upgrade is designated MFTF-Alpha+T

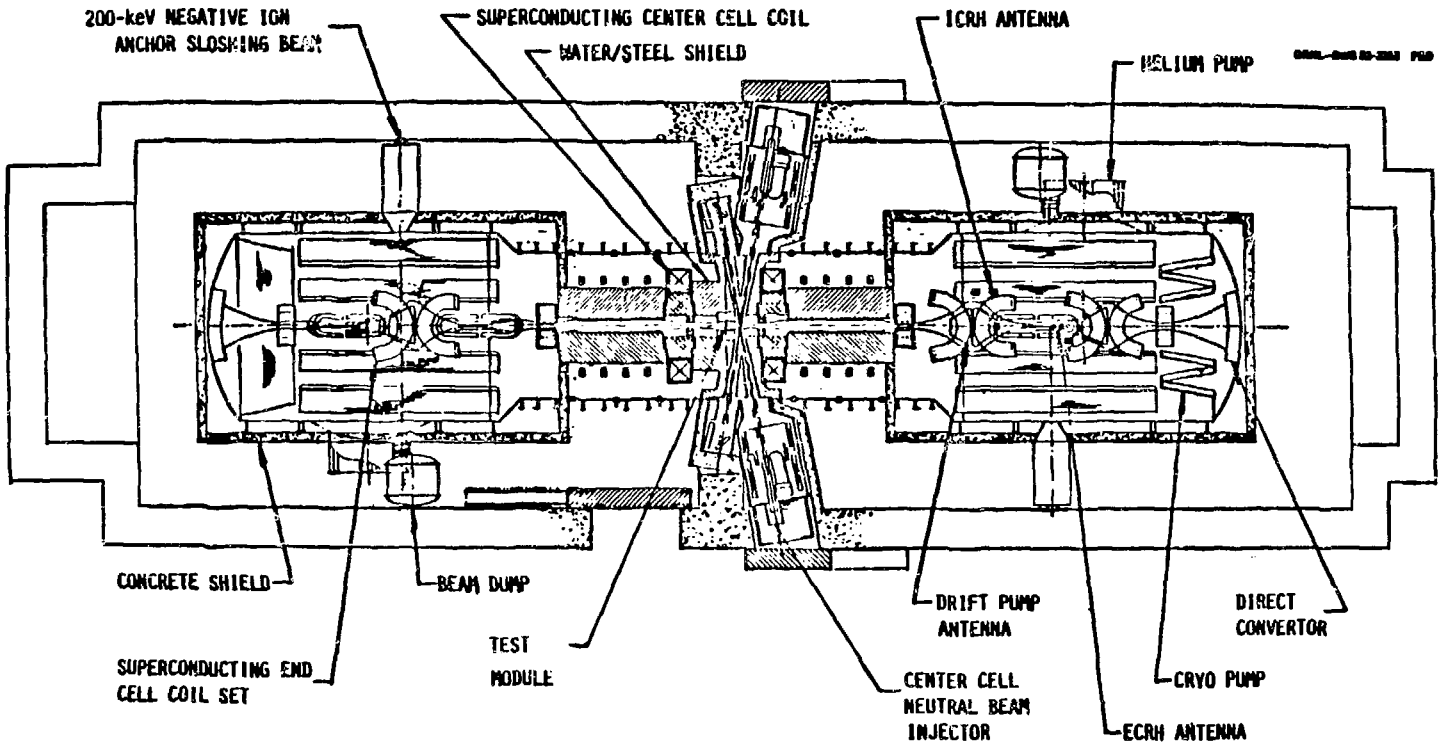

Present concepts include two resistive (copper) coils in the Alpha+T machine, a 12 T choke coil and an 18 T barrier coil.

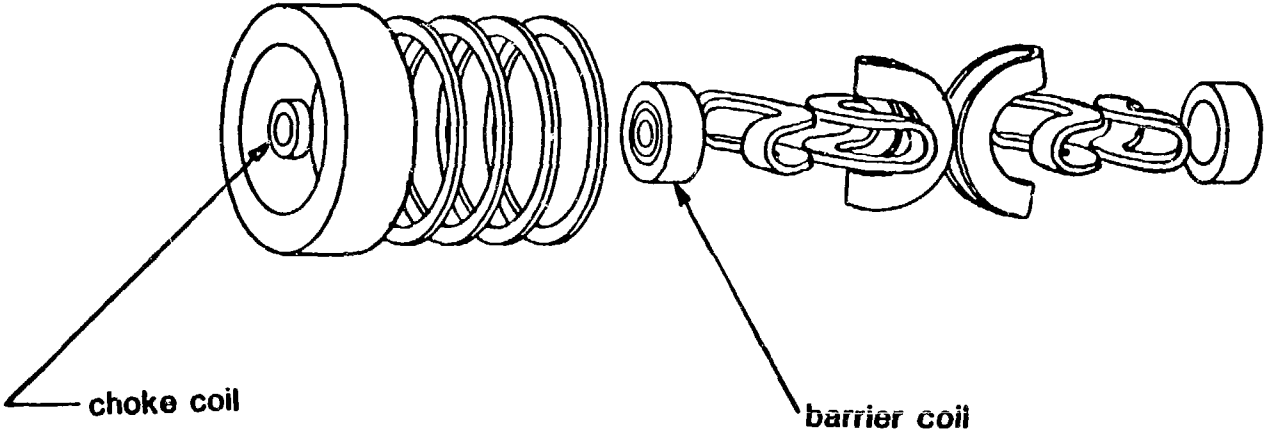

Three conductor concepts are being seriously considered for copper coils:

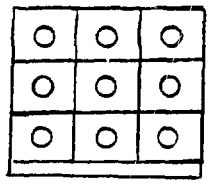

● Internally Cooled Cable

● Externally Cooled Cable

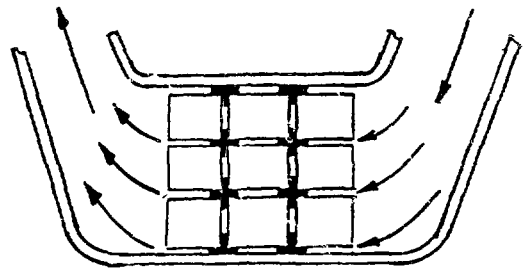

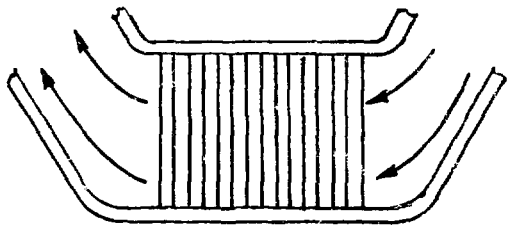

● Bitter (Plate)

EXTERNALLY H_2O COOLED POLYHELIX IS OUR SELECTED BASELINE CONCEPT FOR THE TDF CHOKE COIL

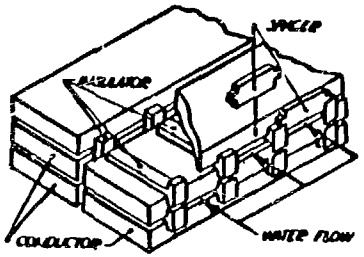

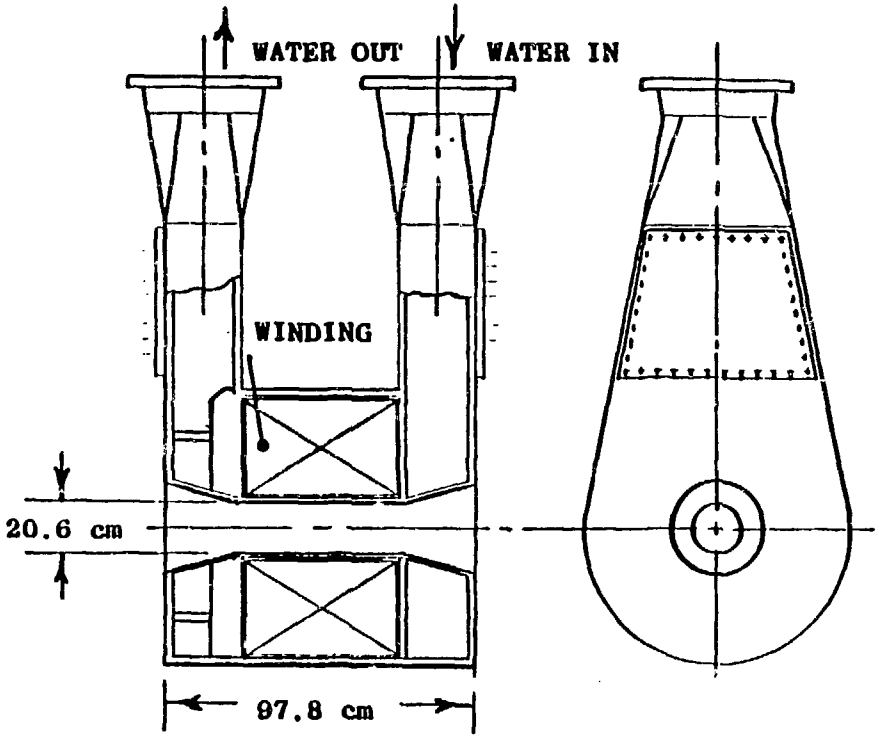

CONFIGURATION

- AXIALLY COOLED
- CONDUCTOR - ZIRCONIUM COPPER or MAGNESIUM-ZIRCONIUM-CHROMIUM COPPER
- SPINEL CERAMIC INSULATION
- 304L SS CASE

KEY FEATURES

- CENTRAL FIELD - 12.0T (15.0T w/BACKGROUND)
- CURRENT DENSITY - 4800 A/cm^2
- POWER CONSUMPTION 25.9 MW
- WATER FLOW RATE 2,450 GPM
- WEIGHT 6500 POUNDS

The magnetic running load (force per unit length) on a current carrying conductor in a magnetic field is the product of the current I times the flux density $B_\perp$ perpendicular to the current and is mutually orthogonal to I and $B_\perp$

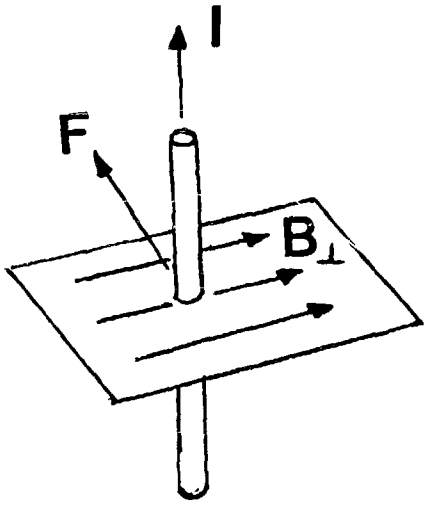

$$F \text{ (Newtons/meter)} = I \text{ (Amps)} \times B_\perp \text{ (Tesla)}$$

The magnetic running load in a solenoid is dilational in character,

producing hoop tensile stress of amplitude

$$\sigma = j\ B\ R$$

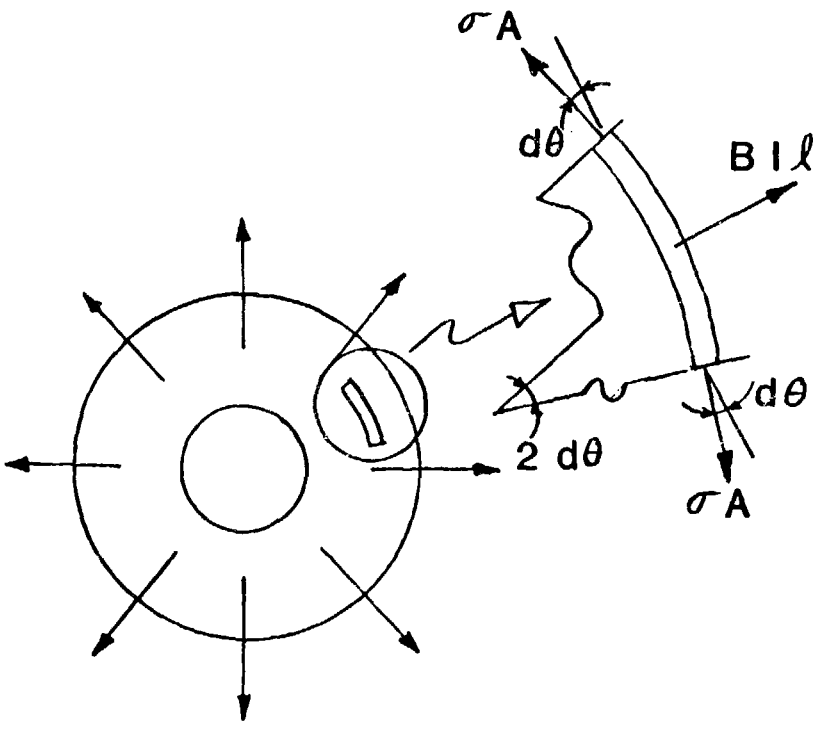

$$2\sigma A \sin d\theta = B\ I\ (2\ R\ d\theta)$$

$$\sin d\theta \simeq d\theta$$

$$\sigma = (I/A)\ B\ R = j\ B\ R$$

FEDC Magnet Structural Design Criteria

- PRIMARY STRESS LIMITS

  Limits are defined as multiples of S_m, defined as follows:

  Metals S_m = the lesser of 2/3 yield strength or 1/3 ultimate strength at operating temperature

  Nonmetallics S_m - 1/3 ultimate strength at operating temperature

  - Normal operating conditions

    Primary membrane stress intensity $\leq S_m$

    Primary membrane plus bending stress intensity $\leq 1.5\ S_m$

    Average shear stress $\leq 0.6\ S_m$ (metals)

  - Abnormal operating conditions

    Each of the above limits is multiplied by 1.5

  - If buckling is a potential failure mode, a margin of 5 against elastic buckling is required

- FATIGUE AND FRACTURE MECHANICS LIMITS

  An allowable peak tensile stress is derived from the Paris crack growth law and from fundamental fracture mechanics principles

  For 304 stainless steel (similar to the Nitronic 33 used in FED-R), the combination of 6000 Stage I pulses plus 3300 Stage II pulses results in an allowable peak tensile stress of 69 ksi for Stage II operation and 44 ksi for Stage I operation

The power dissipated in the coil by resistive heating is also proportional to current density

$$P = I^2(\rho L/A) = I^2(\rho/A)\,(2\pi R\,N)$$

$$= 2\pi(NI)\,R\rho j$$

in which NI and R are determined by system considerations.

For the Alpha+T choke coil

- B = 12 T
- R_i = 0.17 m
- R_o = 0.47 m
- j = 2882 A/cm^2
- NI = 22.6 MAT
- T = 100°C(200°C)

from which it follows that

σ = 163 MPa (23.6 ksi)

$\Longrightarrow$ $S_y > 244$ MPa (35.4 ksi) $S_{ult} > 488$ MPa (70.8 ksi)

Use AMAX-MZC 40% CW S_y = 450 MPa S_{ult} = 500MPa

P = 39.3 MW per coil (ρ = 3μohm-cm)

Neutron environment is

5.9 x 10^{21} n/cm^2 per MW yr/m^2

7.5 dpa per MW yr/m^2

GOAL Life = 1.3 MW/m^2 (10 yr)(0.01) = 0.13 MW yr/m^2

For the Alpha+T barrier coil

- B = 18 T
- R_i = 0.28 m
- R_o = 1.13 m
- j = 2941 A/cm^2
- NI = 18.8 MAT
- T = 100°C(200°C)

from which it follows that

σ = 598 MPa $\Longrightarrow$ S_y > 897 MPa S_{ult} > 1795 MPa

Will require a supporting case or cowound stiffeners

P = 73 MW per coil

The Alpha+T application is near term (order long-lead material FY86, complete construction FY93)

HOWEVER.....

long term, reactor relevant concepts (e.g., MARS) incorporate high field (24 T) barrier coils.

FED-R is a recently completed study of a tokamak based on near term technology.

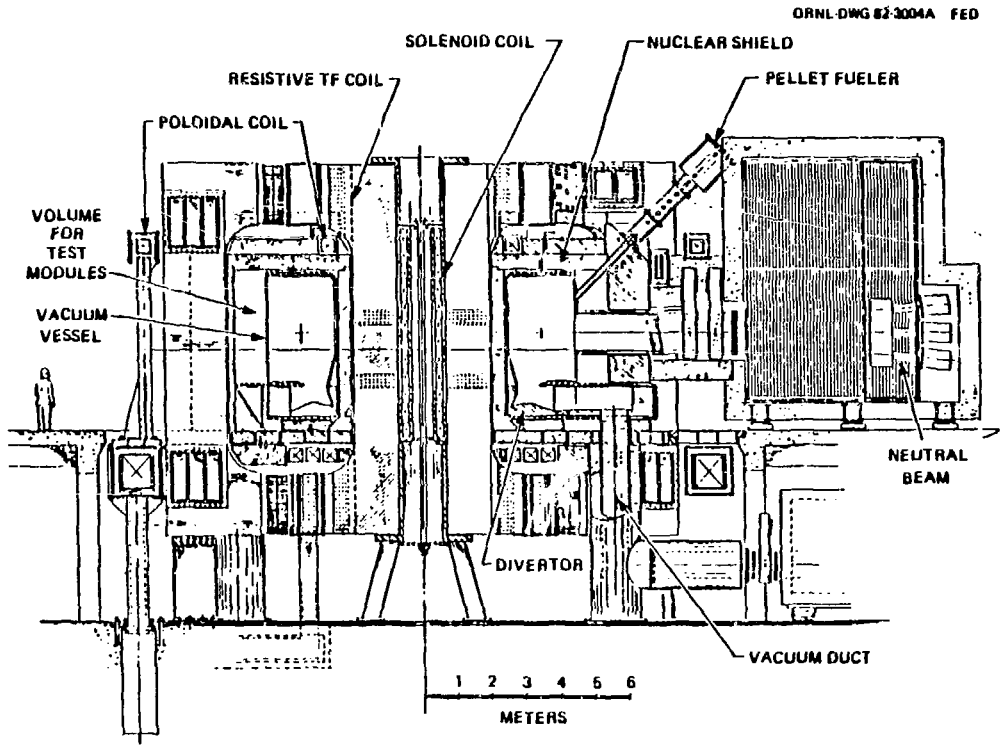

For the FED-R TF coils, current density is fairly low to limit power to 275 MW.

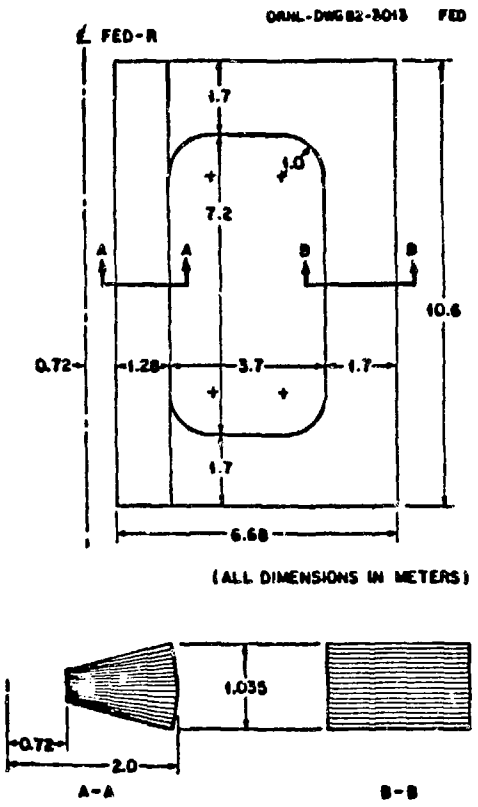

- B = 8.8 T
- j = $\begin{cases} 810\ A/cm^2, \text{ inboard} \\ 415\ A/cm^2, \text{ elsewhere} \end{cases}$
- NI = 7.3 MAT
- P = 22.2 MW per coil
  ($\rho = 2\mu$ohm-cm)
- T = 100°C

Even with low current density, structural design is challenging because of high bending stress.

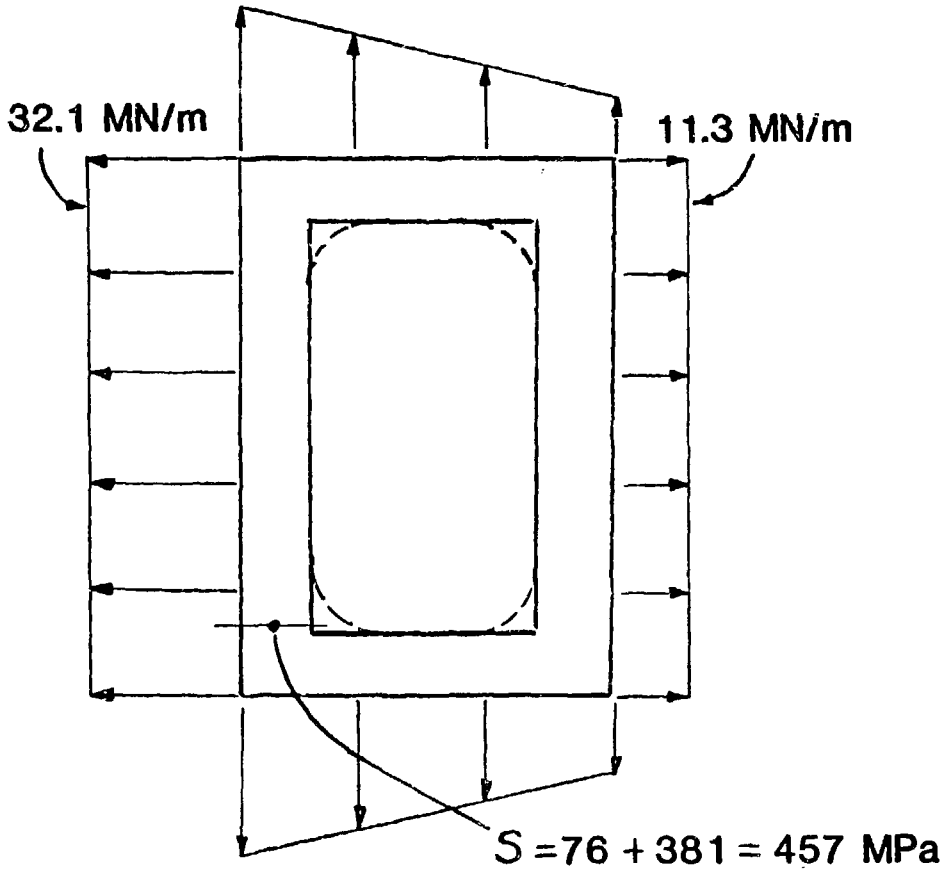

- Required S_y is 457 MPa
- Actual S_y is 128 MPa
- Add 1-m corner radii

FED-R TF coils feature three kinds of mechanical joints

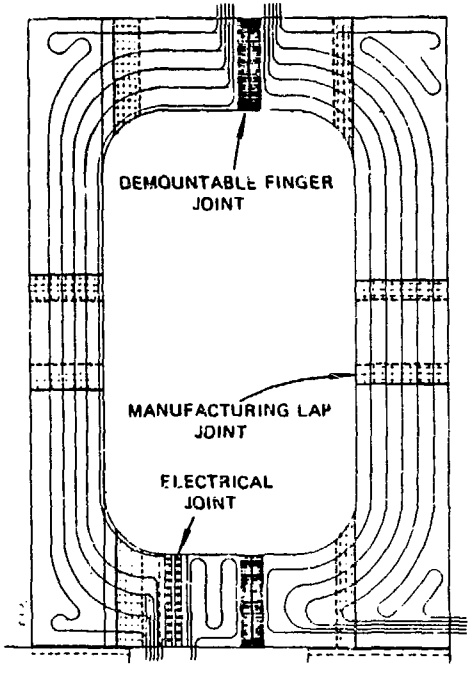

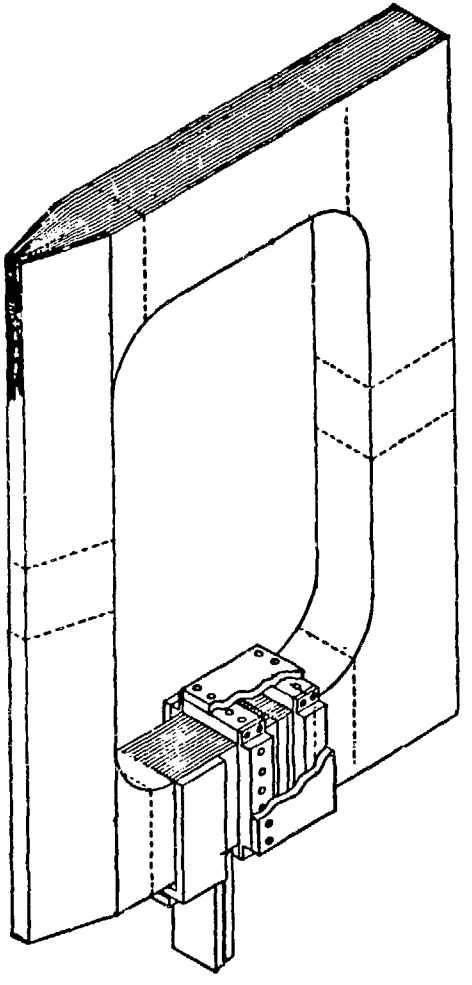

The demountable joint was patterned after a similar joint used in Doublet III, and high strength insert bars are required to transmit load across the joint.

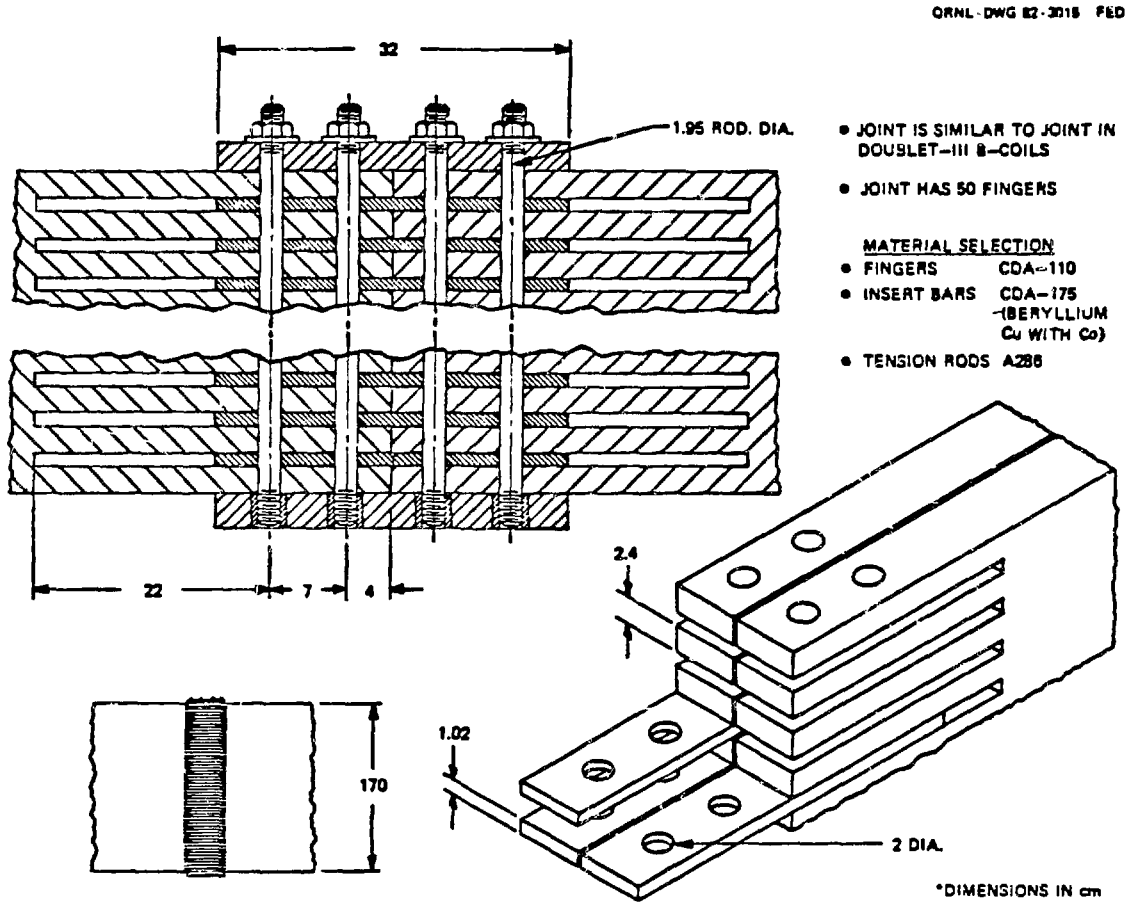

All applications of copper TF coils may be regarded as near term (FY86-FY93).

A SUMMARY OF REQUIREMENTS FOR APPLICATION OF COPPER TO FUSION MAGNET SYSTEMS IS:

APPLICATION	POWER* MW	RESISTIVITY μOHM-CM	MAGNET STRESS MPA(KSI)	DESIRED YIELD** MPA(KSI)
CHOKE COIL	79	3	163(23.6)	244(35.4)
BARRIER COIL	146	3	598(86.7)	897(130)
TF COIL	265	2	457(66.3)	457(66.3)
TF INSERTS	?	4	191(27.7)	286(41.6)

*TOTAL FOR THE MACHINE

**AT MAXIMUM OPERATING TEMPERATURE, 200°C

POWER CONSUMPTION RESULTS IN SIGNIFICANT OPERATING COST

PACIFIC GAS & ELECTRIC CO. CHARGES

$1.35/KW/MONTH	DEMAND CHARGE
$ .078/KWH	USAGE CHARGE

SO FOR A 100 MW LOAD,

DUTY FACTOR	MONTHLY DEMAND CHARGE	MONTHLY USAGE CHARGE	TOTAL MONTHLY CHARGE
0.01	$135 K	$ 56 K	$ 191 K
0.1	$135 K	$ 562 K	$ 697 K
0.5	$135 K	$2808 K	$2943 K

A COPPER ALLOY CONDUCTING FIRST WALL FOR THE FED-A TOKAMAK

F. W. Wiffen

Fusion Engineering Design Center
and
Oak Ridge National Laboratory

A COPPER ALLOY CONDUCTING FIRST WALL FOR THE FED-A TOKAMAK

F. W. Wiffen
Fusion Engineering Design Center
and
Oak Ridge National Laboratory

The first wall of the tokamak FED-A device was designed to satisfy two conflicting requirements. They are a low electrical resistance to give a long eddy-current decay time and a high neutron transparency to give a favorable tritium breeding ratio. The tradeoff between these conflicting requirements resulted in a copper alloy first wall that satisfied the specific goals for FED-A, i.e., a minimum eddy-current decay time of 0.5 sec and a tritium breeding ratio of at least 1.2. Aluminum alloys come close to meeting the requirements and would also probably work. Stainless steel will not work in this application because shells thin enough to satisfy temperature and stress limits are not thick enough to give a long eddy-current decay time and to avoid disruption induced melting.

The baseline first wall design is a rib-stiffened, double-wall construction. The total wall thickness is 1.5 cm, including a water coolant thickness of 0.5 cm. The first wall is divided into twelve 30-degree sectors. Flange rings at the ends of each sector are bolted together to form the torus. Structural support is provided at the top center of each sector.

OBJECTIVES:

- DEVELOP A FIRST WALL DESIGN WITH A LONG (≥0.5 s) TOROIDAL EDDY-CURRENT DECAY TIME. REDUCED PLASMA DISRUPTION DAMAGE.
- MAXIMIZE THE FIRST WALL NEUTRON TRANSPARENCY TO ACHIEVE BREEDING BLANKET PERFORMANCE.

APPROACH:

- COMPARE STAINLESS STEEL, COPPER, AND ALUMINUM ALLOYS FOR THIS APPLICATION.
- SELECT BASELINE MATERIAL FOR BEST COMBINATION OF TOROIDAL EDDY-CURRENT DECAY TIME AND BLANKET BREEDING PERFORMANCE.
- ESTABLISH DESIGN APPROACHES FOR SECTOR TO SECTOR ATTACHMENT.

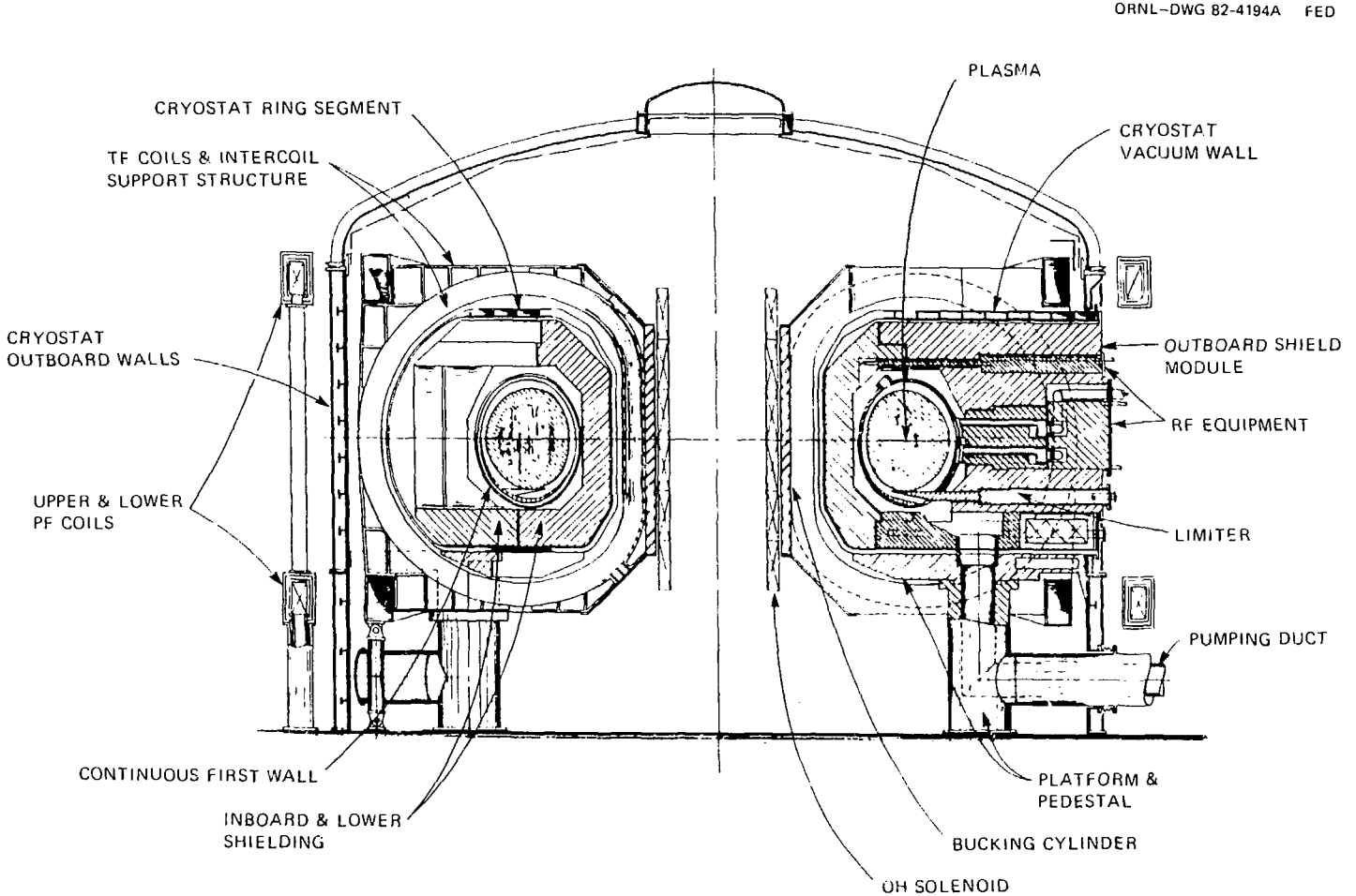
ORNL-DWG 82-4194A FED
PLASMA
CRYOSTAT RING SEGMENT
CRYOSTAT VACUUM WALL
TF COILS & INTERCOIL SUPPORT STRUCTURE
CRYOSTAT OUTBOARD WALLS
OUTBOARD SHIELD MODULE
RF EQUIPMENT
UPPER & LOWER PF COILS
LIMITER
PUMPING DUCT
CONTINUOUS FIRST WALL
INBOARD & LOWER SHIELDING
PLATFORM & PEDESTAL
BUCKING CYLINDER
OH SOLENOID

Table 1. Reference parameters for FED-A

Description	Unit	Value
Major radius, R	m	4.22
Plasma radius, a	m	0.92
Plasma elongation, κ	m	1.2
Aspect ratio, A		4.59
Scrape-off layer	m	0.15
Burn time, t_{burn}	s	100 to 1000
Fusion power, P_{DT}	MW	255
No. of full-field current pulses/lifetime		3×10^4
Avg. no. of burn pulses in each current pulse		10
Avg. neutron wall load at first wall	MW/m^2	1.2

TARGET Life ~ at least 1 MW-y/m^2

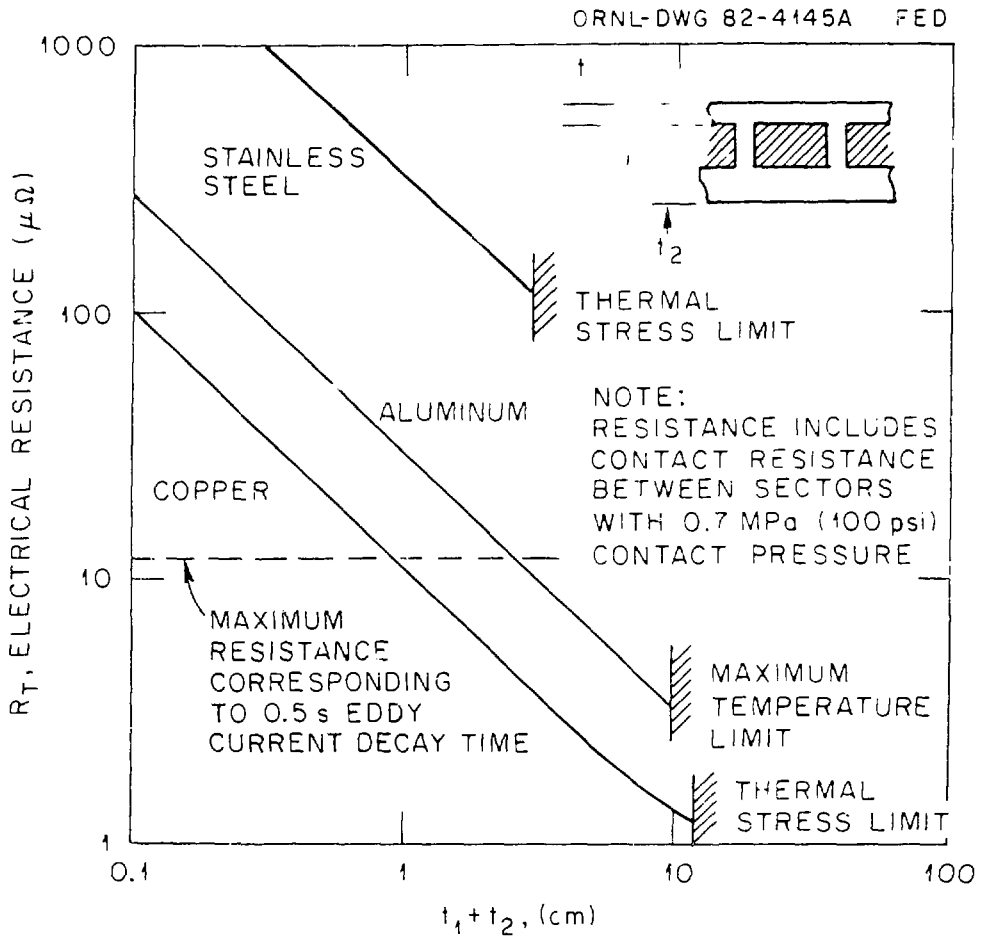
ORNL-DWG 82-4145A FED
1000
100
10
1
0.1
1
10
100
R_T, ELECTRICAL RESISTANCE ($\mu\Omega$)
$t_1 + t_2$, (cm)
t
t_2
STAINLESS STEEL
ALUMINUM
COPPER
THERMAL STRESS LIMIT
MAXIMUM TEMPERATURE LIMIT
THERMAL STRESS LIMIT
NOTE:
RESISTANCE INCLUDES CONTACT RESISTANCE BETWEEN SECTORS WITH 0.7 MPa (100 psi) CONTACT PRESSURE
MAXIMUM RESISTANCE CORRESPONDING TO 0.5 s EDDY CURRENT DECAY TIME

Table 2. Material properties for alloys considered for conducting first wall

Property	316 SS (250°C)[a]	5083 Al (100°C)[a]	AMAX-MZC Cu (200°C)[a]
Density (Mg/m^3)	7.9	2.7	8.9
Thermal conductivity (W/m-k)	17.8	170	310
Specific heat (J/kg-K)	534	900	400
Thermal expansion coefficient (K^{-1})	17×10^{-6}	24×10^{-6}	18×10^{-6}
Electrical resistivity (μΩ-cm)	90	8.3	3.5
Elastic modulus (GPa)	190	69	138
Yield strength (MPa)	140	130	97 (360)[b]
Ultimate strength (MPa)	430	270	200 (400)[b]
Allowable design stress (MPa)	93	87	55

[a]For fully annealed condition.

[b]For worked and aged material.

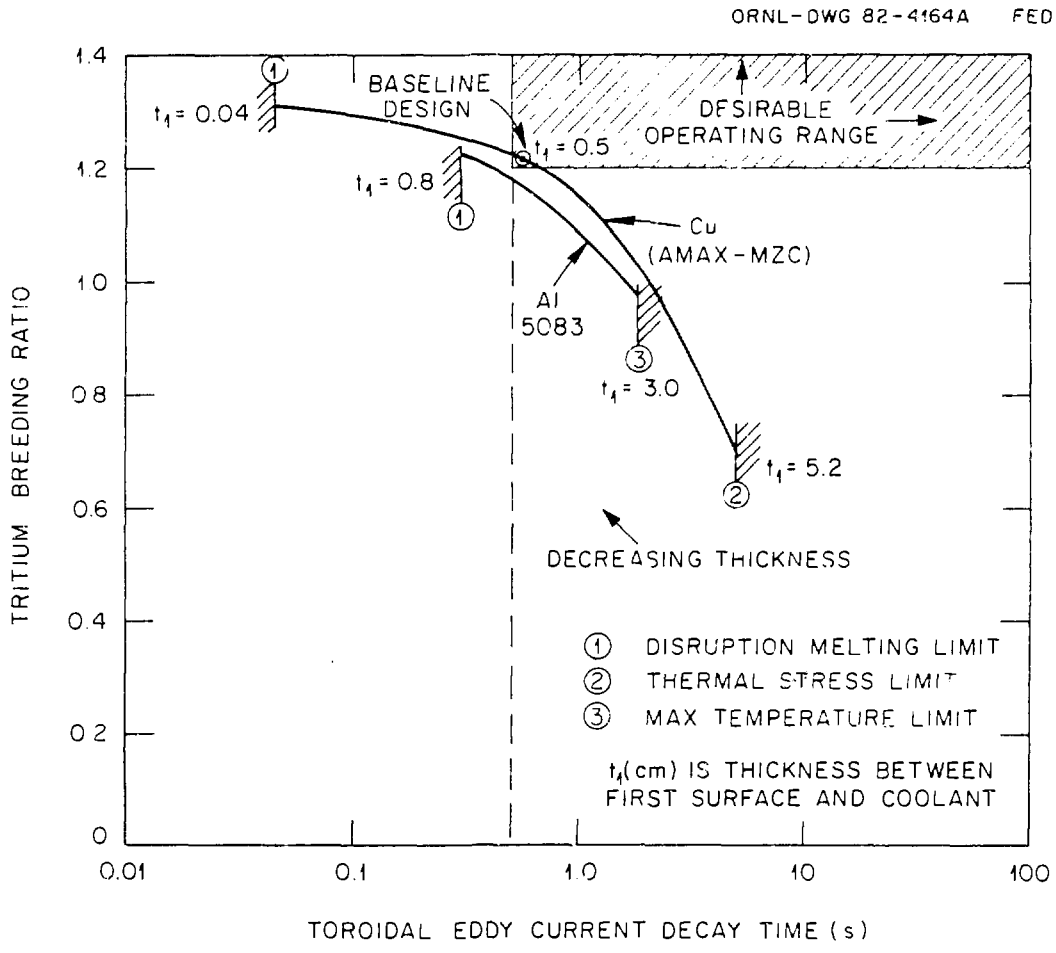
ORNL-DWG 82-4164A FED
TRITIUM BREEDING RATIO
1.4
1.2
1.0
0.8
0.6
0.4
0.2
0
0.01
0.1
1.0
10
100
TOROIDAL EDDY CURRENT DECAY TIME (s)
BASELINE DESIGN
DESIRABLE OPERATING RANGE
t_1 = 0.04
t_1 = 0.5
t_1 = 0.8
t_1 = 3.0
t_1 = 5.2
Cu (AMAX-MZC)
Al 5083
DECREASING THICKNESS
① DISRUPTION MELTING LIMIT
② THERMAL STRESS LIMIT
③ MAX TEMPERATURE LIMIT
t_1(cm) IS THICKNESS BETWEEN FIRST SURFACE AND COOLANT

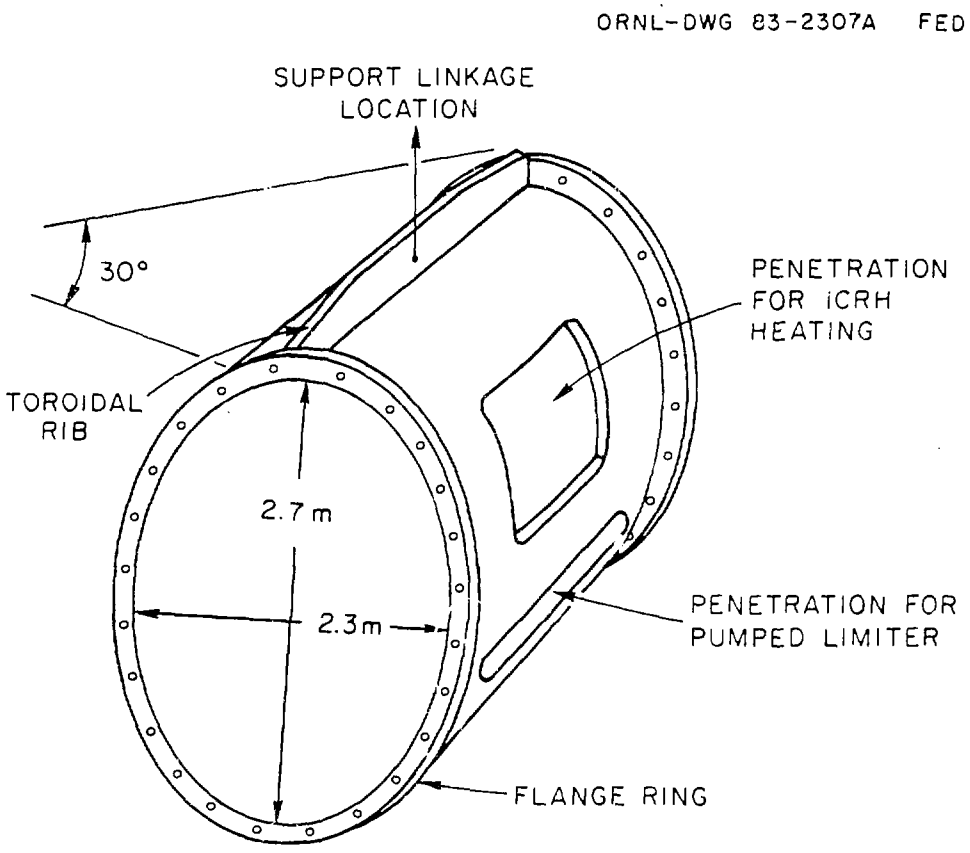
ORNL-DWG 83-2307A FED
SUPPORT LINKAGE LOCATION
30°
TOROIDAL RIB
PENETRATION FOR ICRH HEATING
2.7 m
2.3m
PENETRATION FOR PUMPED LIMITER
FLANGE RING

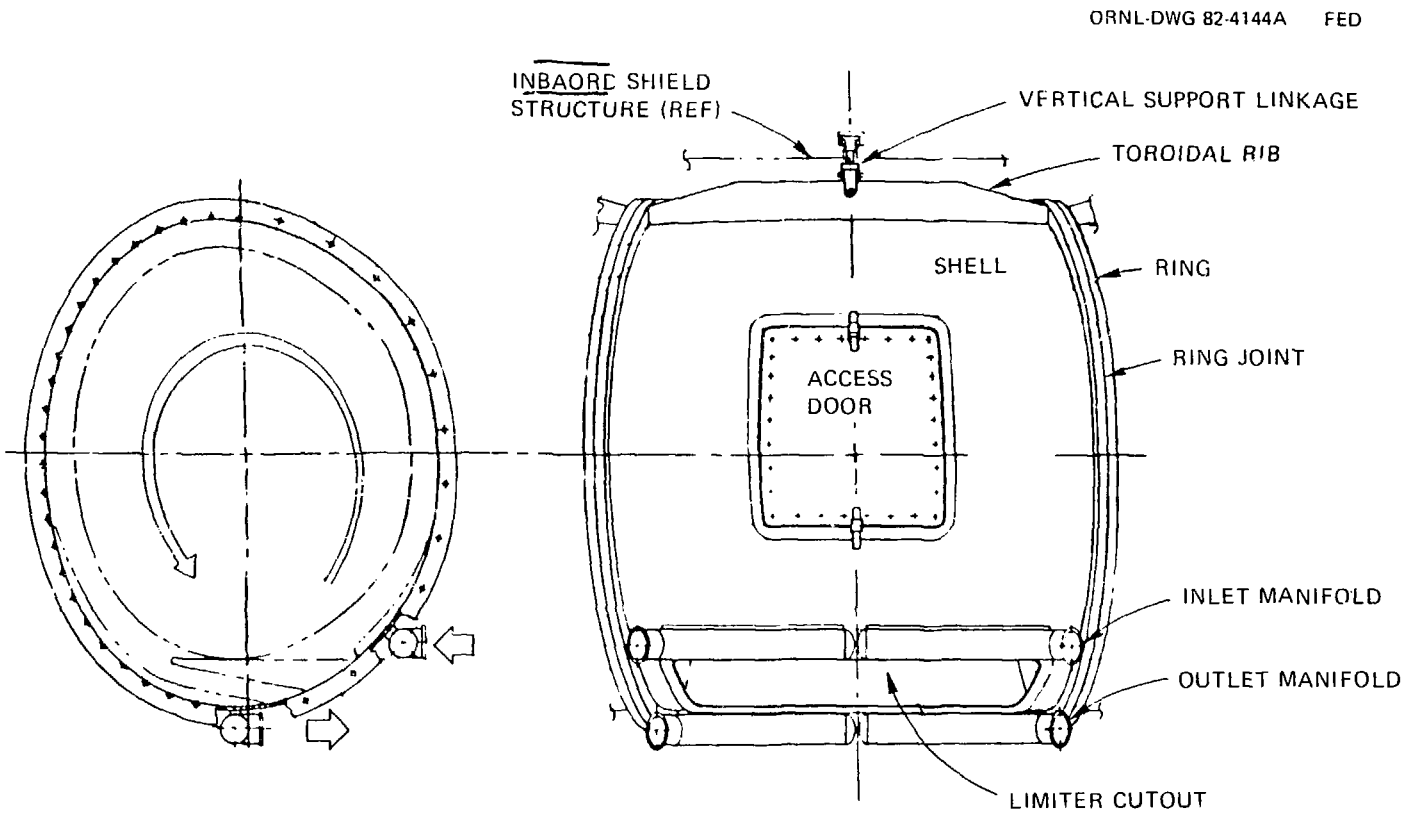
ORNL-DWG 82-4144A FED
INBAORD SHIELD STRUCTURE (REF)
VERTICAL SUPPORT LINKAGE
TOROIDAL RIB
SHELL
RING
RING JOINT
ACCESS DOOR
INLET MANIFOLD
OUTLET MANIFOLD
LIMITER CUTOUT

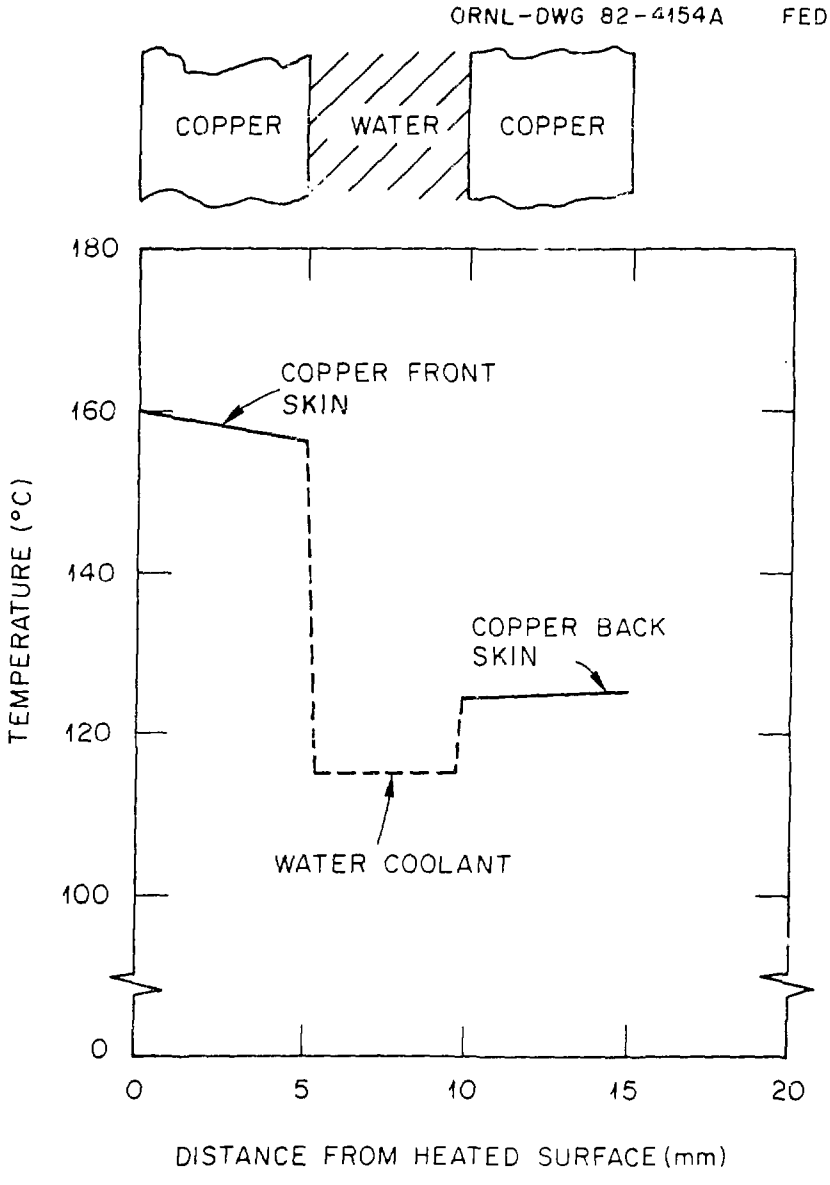
ORNL-DWG 82-4154A FED
COPPER
WATER
COPPER
180
160
140
120
100
0
TEMPERATURE (°C)
COPPER FRONT SKIN
COPPER BACK SKIN
WATER COOLANT
0
5
10
15
20
DISTANCE FROM HEATED SURFACE (mm)

ORNL–DWG 82-4155A FED

INLET TEMPERATURE (°C)	60
OUTLET TEMPERATURE (°C)	115
INLET PRESSURE (MPa)	0.69
PRESSURE DROP (kPa)	4.2
MASS FLOW RATE (kg/s)	360
PUMPING POWER (kW)	1.6

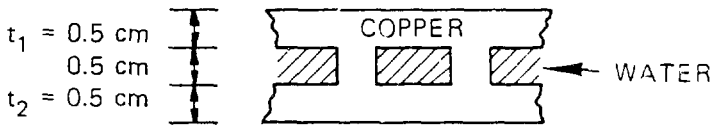

CONCLUSIONS:

- COPPER ALLOYS MEET THE PERFORMANCE REQUIREMENTS. (BASELINE MATERIAL)
- ALUMINUM ALLOYS COME CLOSE TO MEETING THE REQUIREMENTS. (COULD ALSO BE USED)
- STAINLESS STEEL WILL NOT WORK IN THIS APPLICATION.
- A BOLTED FLANGE IS THE MOST RELIABLE APPROACH FOR SECTOR TO SECTOR ATTACHMENT.

APPLICATIONS OF COPPER IN IMPURITY CONTROL SYSTEMS FOR FUSION POWER REACTORS

D. L. Smith and R. F. Mattas

Argonne National Laboratory

Applications of Copper in Impurity Control Systems for Fusion Power Reactors

D. L. Smith and R. F. Mattas
Argonne National Laboratory

Summary

The potential of copper and high conductivity (thermal) copper alloys have been evaluated as candidate structural materials for the limiter/divertor of a fusion power reactor. This work has been conducted as part of the FED/INTOR Phase 2A and ANL DEMO studies. The reader is referred to these references for more detailed information. Both devices are the tokamak configuration with relatively modest neutron wall loadings, duty factors, and operating lifetimes compared to anticipated commercial power reactors.

Limiter and divertor configurations considered in these studies are shown in the attached figures. In general, two types of alloys have been considered for these applications. Selected copper alloys are attractive because of their high thermal conductivities, which are beneficial for minimizing thermal gradients and thermal stress in walls exposed to high heat fluxes. A major problem relates to the relatively low strength of copper at elevated temperatures. Alloying tends to improve the elevated temperature strength, usually at the expense of reduced thermal conductivity. A primary trade-off is this increased strength versus the loss in conductivity. The Group V refractory metals are considered to be the primary alternative materials to copper. A vanadium alloy (V-15Cr-5Ti) was selected for comparison purposes. These materials provide higher temperature capability. Their considerably lower thermal conductivity is partially balanced by lower thermal expansion coefficients.

Copper does not have properties favorable for use in direct contact with the plasma, e.g., low sputtering yields and low-Z. A coating or cladding is necessary for the plasma interface. Design problems associated with candidate coating/cladding materials on copper are summarized in the attached figures. The relatively high thermal expansion coefficient of copper produces high interfacial stresses for most duplex combinations of interest.

The favorable characteristics and the major limitations associated with the use of copper alloys as a limiter/divertor structural material are summarized in the final chart.

APPLICATIONS OF COPPER IN IMPURITY CONTROL SYSTEMS FOR FUSION POWER REACTORS

- Information Based Primarily on Work in Support of FED/INTOR Phase 2A and ANL DEMO Study

- Focused Primarily on Limiter and Divertor for a Tokamak Reactor

- Operating Conditions Considered:
  - Heat Flux: ≤ 5 MW/m^2
  - Neutron Wall Loading: 1-2 MW/m^2
  - Radiation Lifetime: $\sim$ 20 DPA
  - Coolant: H_2O @ T $\leq 100^\circ$C
  - Operating Temperature: 100-300°C
  - Thermal-Cycle Lifetime: $\leq 10^5$ Cycles
  - Cladding for Plasma Interface

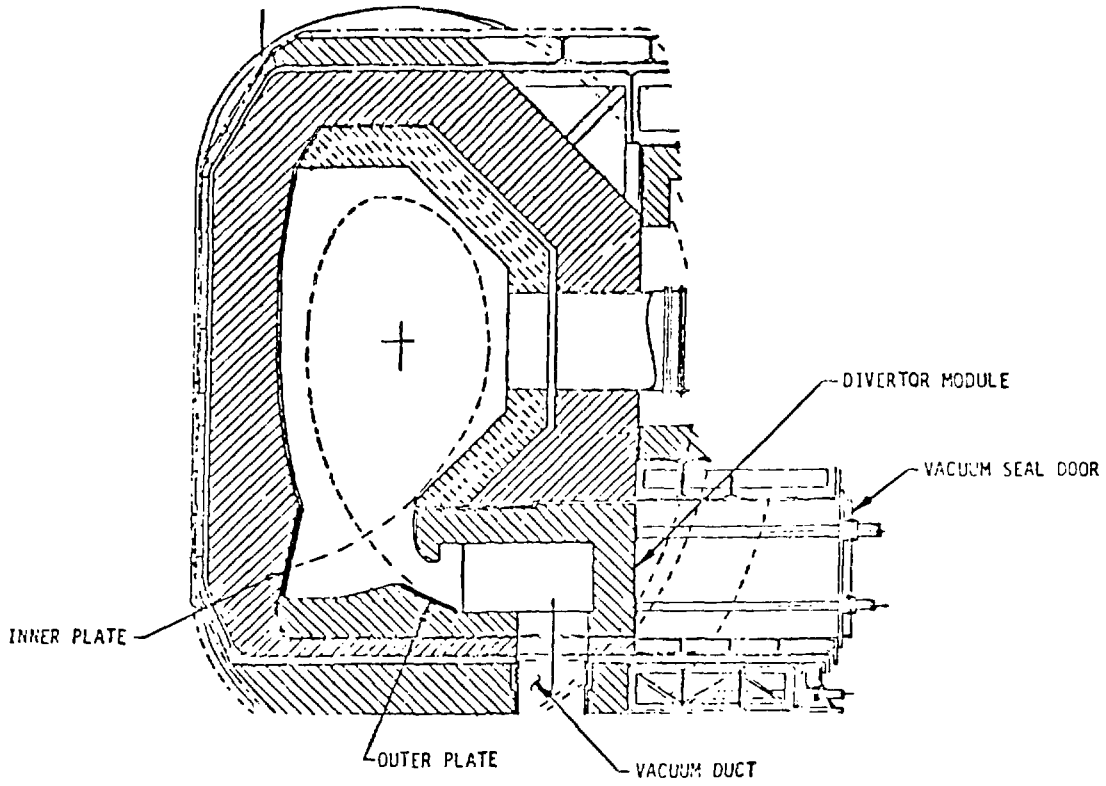

FIG. VII.1-1. Divertor configuration.

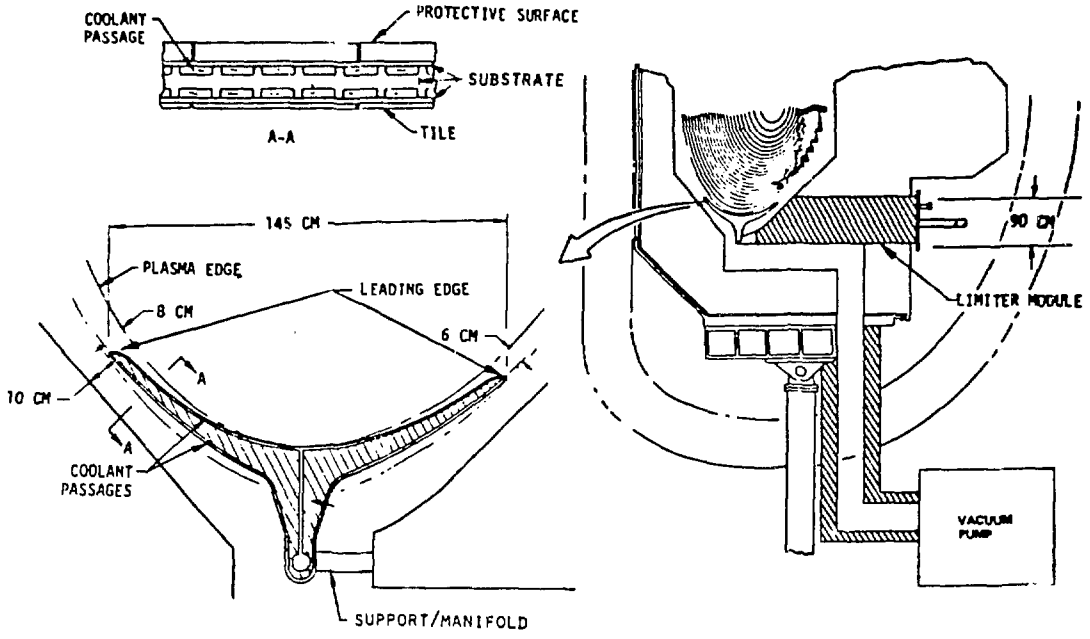

FIG. VII.3-9. Limiter configuration (reference design).

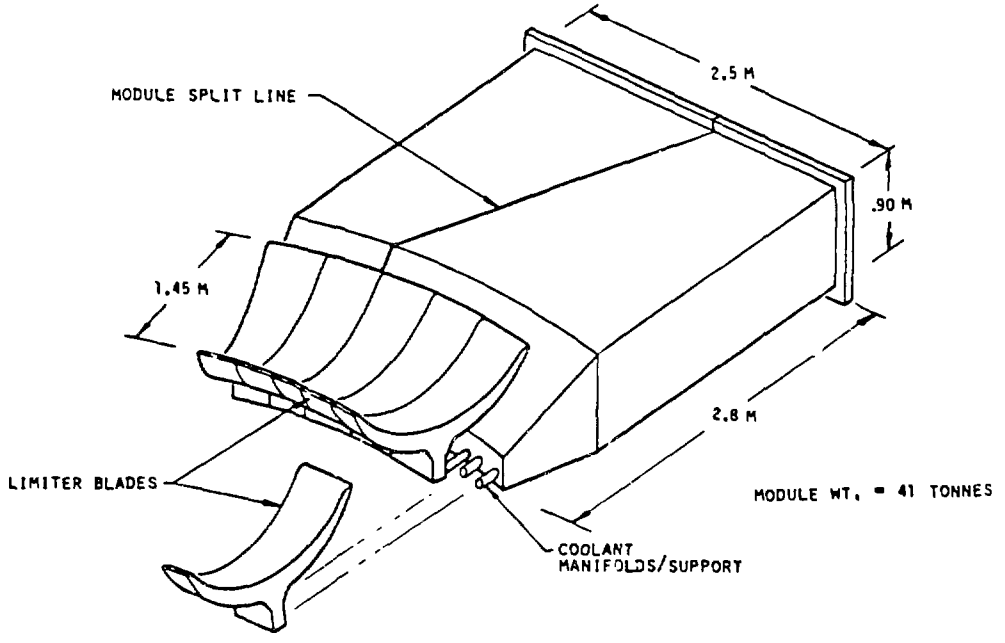

FIG. VII.3-10. Shaped, double-edged, bottom limiter.

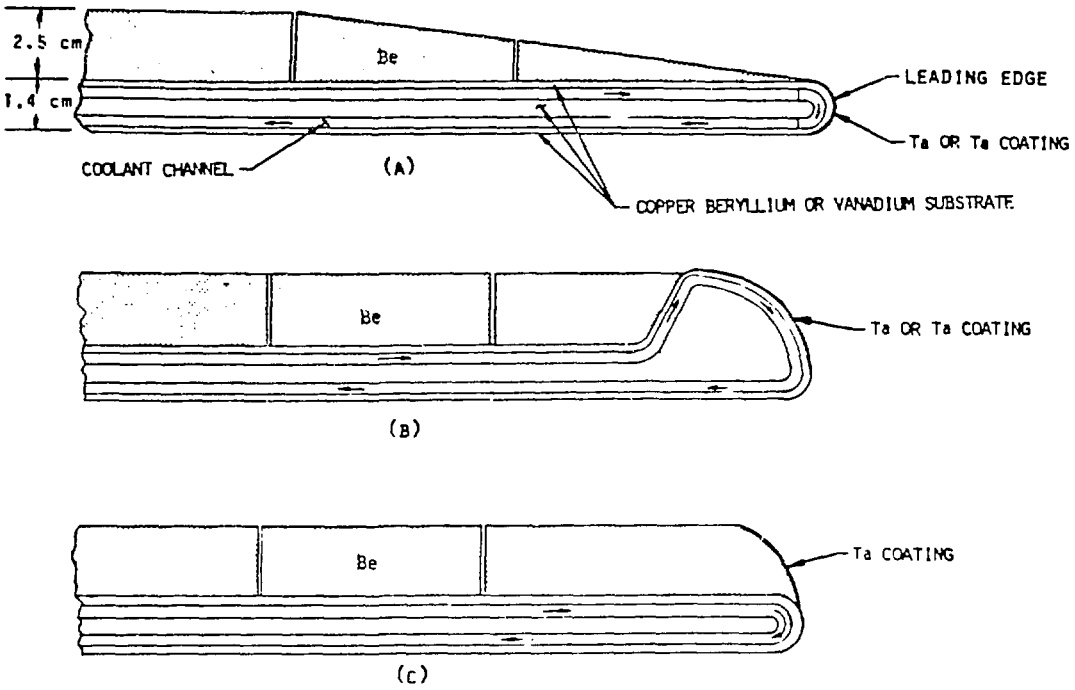

FIG. VII.3-11. Limiter leading edge design concepts.

- Materials Requirements/Considerations
  - Withstand High Heat Fluxes (Cyclic) (Temperature Limits)
  - Provide Structural Support
  - Withstand Electromagnetic Forces
  - Coolant Containment
  - Radiation Damage Resistance
  - Availability/Fabricability
- Desired Materials Properties
  - High Thermal Conductivity
  - Low Thermal Expansion
  - Acceptable Fatigue/Crack Growth Properties
  - Compatibility with Coolant
  - High Strength (Irradiation)
  - Adequate Ductility (Irradiation)
  - Radiation Creep Resistance
  - Low Swelling
  - Compatibility with Plasma/Cladding

CANDIDATE MATERIALS

- Copper Alloys (High Thermal Conductivity)
  - OFHC Copper
  - AM-ZIRC (0.2 Zr)
  - ANSIL (0.05 Ag)
  - AMAX-MZC (0.1 Zr, 0.6 Cr, 0.05 Mg)
  - Cu-Be Alloy 25 (1.85 Be, 0.25 Co or Ni)
  - Cu-Be Alloy 10 (0.50 Be, 2.5 Co or Ni)

Primary Trade-Off Is Increased Strength Vs. Reduced Thermal Conductivity

- Refractory Metal Alloys (Reference Case V-15Cr-5Ti)
  - Lower Thermal Expansion
  - Lower Thermal Conductivity
  - Better Strength at Higher Temperatures
  - Better Radiation Damage Resistance

Major Question is Compatibility with Coolant

COPPER LIMITER/DIVERTOR

- Must Be Protected from Plasma by Coating/Cladding, Etc.
  - Relatively High D-T Sputtering Yields
  - Self-Sputtering > 1 at Low E
  - High-Z Impurity
  - Relatively High Vaporization/Melting during Disruption
- Relatively High Thermal Expansion Coefficient of Copper Contributes to Large Interfacial Stresses for Most Candidate Coating/Cladding Materials (Be, W)

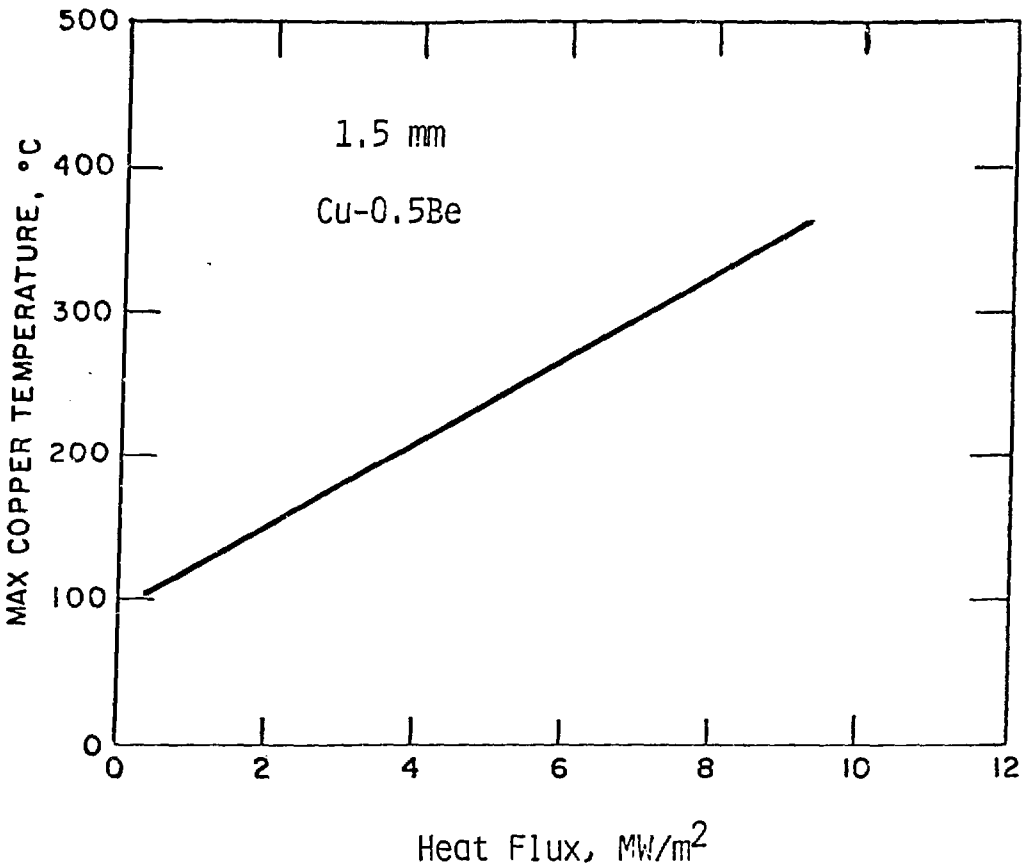
500
400
300
200
100
0
MAX COPPER TEMPERATURE, °C
1.5 mm
Cu-0.5Be
0
2
4
6
8
10
12
Heat Flux, MW/m2

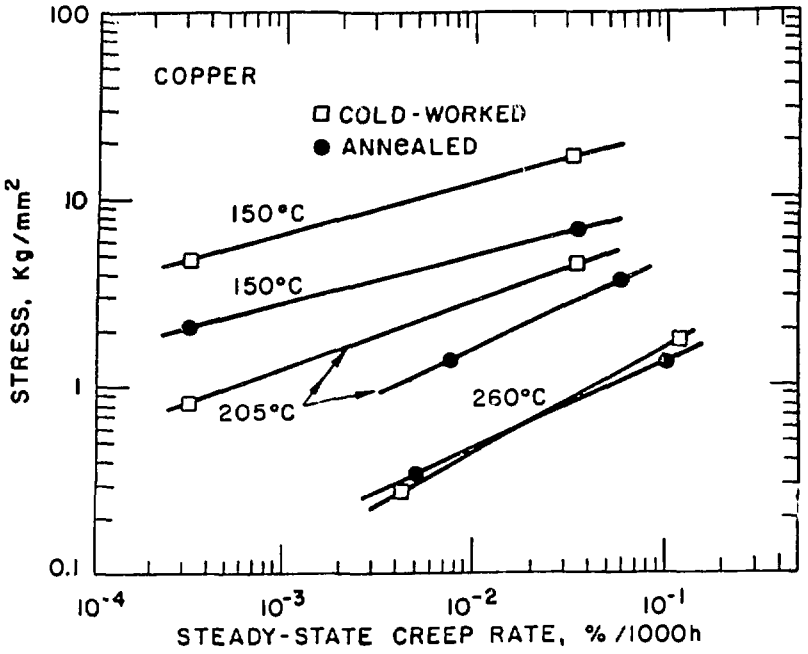

FIG. A.2.2.2-2. Steady-state creep rate of annealed and cold-worked copper.

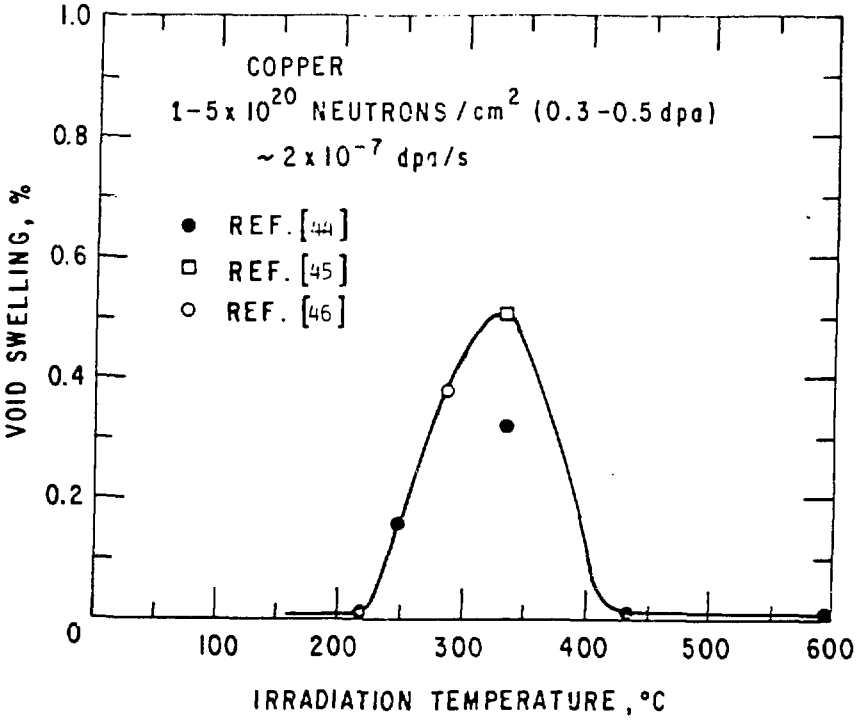

FIG. A.2.2.3-1. Dependence of void swelling of neutron-irradiated copper on temperature.

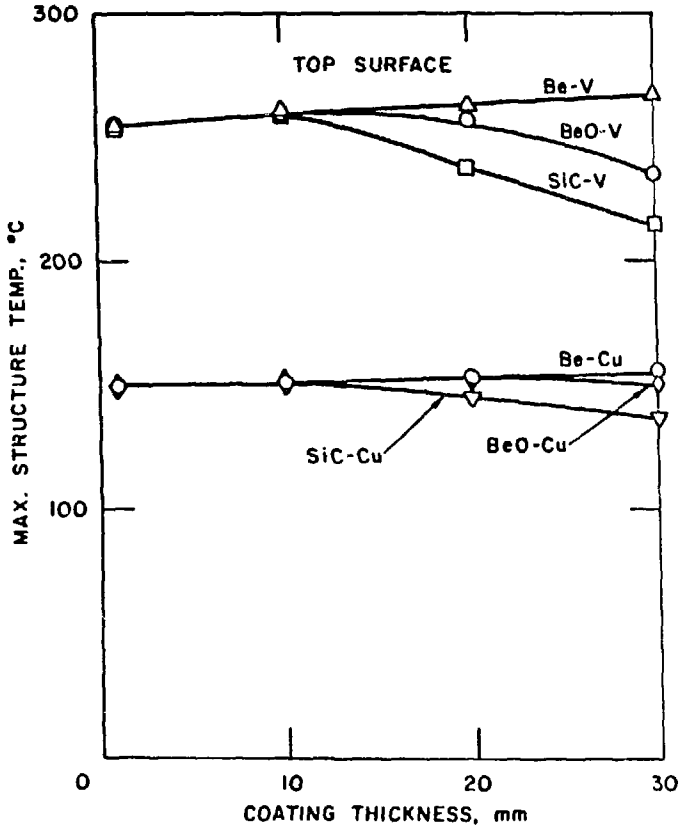

FIG. VII.6-15. Maximum heat sink temperatures as a function of surface coating thickness.

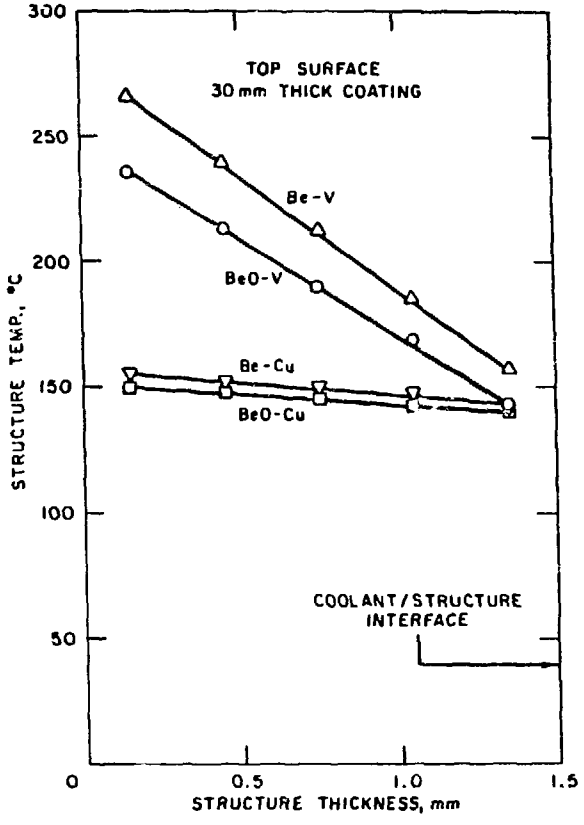

FIG. VII.6-16. Temperature profile through the heat sink material with a 30 mm thick coating of either Be or BeO.

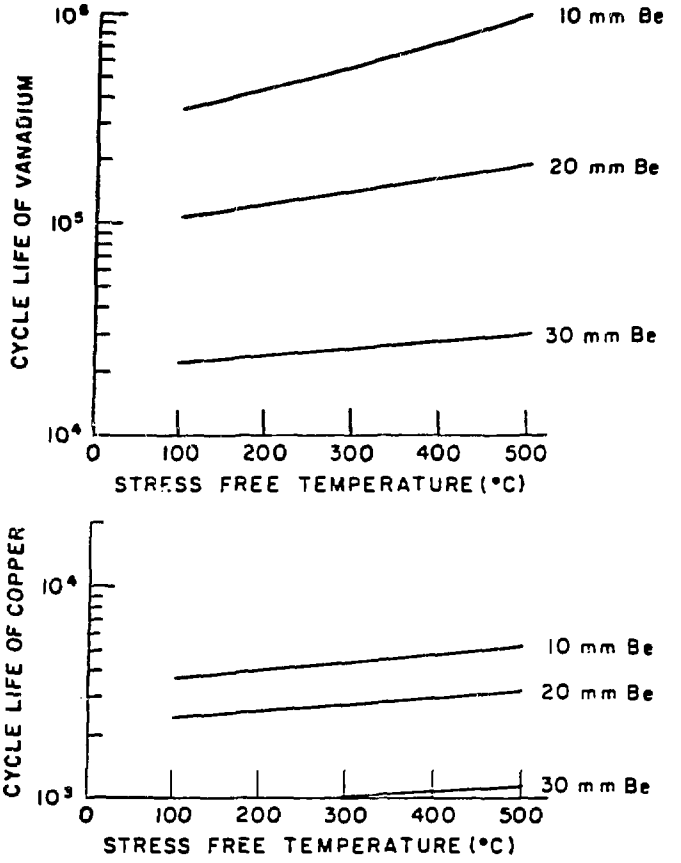

FIG. VII.6-29. Variation of fatigue life of heat sink materials as a function of the surface material/heat sink stress free temperature.

SUMMARY AND CONCLUSIONS

- Copper Is a Leading Candidate for a Limiter/Divertor Structural Material (Particularly for Near-Term Devices)
- Good Availability, Fabricability and Technology
- High Thermal Conductivity Provides:
  - High Heat Flux Capability
  - Low ΔT_W at High Heat Flux
  - Low Thermal Stresses
  - Low Temperature Coating/Cladding
- Compatible with Low Temperature Water Coolant
- Operating Temperature Limited to < 250-300°C
  - Loss of Strength
  - Radiation Swelling (?)
  - High Pressure of Water Coolant
- Limited Radiation Data Base
  - Swelling
  - Ductility
  - Creep

SUMMARY AND CONCLUSIONS

(continued)

- Must Be Protected from Plasma
  - High-Z
  - High Sputtering Yield
- High Thermal Expansion Coefficient Leads to High Interfacial Cladding Stresses
- Only Fair Fatigue Properties
- Copper Is Not Compatible with Other Coolants
  - He (Temperature Limit)
  - Li (Corrosion)
- High Electrical Conductivity Tends to Increase Induced Electromagnetic Forces
- Copper Yields Relatively Long-Term Activation Products (Similar to Ni)
- Since Surface Erosion May Limit Limiter/Divertor Lifetime and Frequent (1-2 Years) Changeout May Be Acceptable/Necessary, Long Lifetime (Radiation, Fatigue, Etc.) Does Not Appear to be a Requirement.

USE OF COPPER IN RF HEATING SYSTEMS

J. W. Davis

McDonnell Douglas Corporation

USE OF COPPER ALLOYS IN RF HEATING SYSTEMS

J. W. DAVIS
MCDONNELL DOUGLAS ASTRONAUTICS CO.
ST. LOUIS

Radio frequency (RF) waves or neutral beams or a combination of the two will be needed to raise the temperature of the plasma to the point at which the D-T reaction can occur. Currently these are three types of RF being investigated. They are ion cyclotron resonance heating (ICRH), which operates in the mega-Hertz frequency range; electron cyclotron resonance heating (ECRH), which operates in the giga-Hertz frequency range; and lower hybrid heating (LLH), which operates in the range between ICRH and ECRH. Traditionally ECRH has been used in plasma start-up, LLH for plasma current drive, and ICRH for high temperature plasma heating, above the temperatures achievable with ohmic heating. However, as more reliable high frequency power supplies become available, this situation may change.

A typical RF system essentially consists of a transmitter or wave generator, a tuning network and a launching structure. While there a number of material challenges in this system the greatest challenge and the area where radiation resistant copper alloys will be needed is in the launcher. The present form of this launcher for ICRH consists of an electrically insulated conductor covered by a Faraday Shield. The Faraday shield is used to protect the conductor from plasma particle bombardment which may lead to arcing. To maximize the RF power coupled to the plasma, both the conductor and the Faraday shield will have to be fabricated out of material with good electrical and thermal conductivity. In the enclosed figures the relative power loss which is proportional to the electrical resistivity and inversely to the thermal conductivity, is shown for various materials. In both properties copper or a copper alloy is preferred with beryllium or aluminum as possible alternates. However, if the machine is pulsed then thermal stresses will be of a concern. In examining the thermal stress figure of merit there is a distinct stress advantage in the use of copper alloys over aluminum or beryllium but not if pure copper is used. Since the Faraday shield directly faces the plasma sputtering will be a concern particularly if copper atoms are allowed to enter the plasma. In examining the figure showing the relative radiation plasma power loss it

can be seen that because of copper's high sputtering yield and atomic number the impact of copper atoms on a plasma is almost 60 times more damaging than titanium carbide atoms and 100 times worse than beryllium. Therefore the copper will have to be coated with a material of lower sputtering yield and atomic number but in selecting a coating consideration will have to be given to the relative thermal mismatch between the coating and copper due to the differences in the coefficient of expansion.

For LLH and ECRH the material requirements are not quite as severe as for ICRH primarily because they operate at a frequency where electrostatic coupling is not a problem and as a result do not need a Faraday shield. The higher operating frequency allows the use of a wave guide and vacuum window which can be recessed in the blanket structure away from the plasma particles thus reducing the thermal loads and eliminating the surface erosion. In future experiments it may also become feasible to eliminate the Faraday shield for ICRH. The criteria for the selection of material for use in the waveguide is the same as in ICRH conductor. In essence the material should have low electrical resistivity, good dimensional stability, and good mechanical and thermal properties. The primary difference is that the waveguide can use a thin copper coating over a more radiation resistant substrate. This can also be done on the Faraday shield but is more difficult because of the higher heat loads caused by the plasma particles. For ECRH, an alternate to the waveguide is the use of parabolic mirrors which has been proposed by Perkins of the University of Wisconsin for an RF injection system in MARS. This concept uses a series of hyperbolic and parabolic mirrors which are arranged so that they can reflect and focus the RF wave from a series of gyrotrons which are recessed in the blanket away from the plasma. While the design is different from previous concepts the criteria for material selection are the same: low electrical resistivity, good dimensional stability, good thermal properties and tensile strength and creep resistance at elevated temperatures.

In summary irrespective of the particular RF technique the primary concern for the conductor, mirror, and Faraday shield is electrical resistivity. Ideally one would like a material with the resistivity of oxygen free copper since it would radiate the bulk of the RF energy into the plasma with a minimum of absorption. Changes in resistivity through radiation damage either as a result of radiation hardening or transmutation will reduce the performance of the RF and lead to increased heating in the conductor. The magnitude of the change in resistivity that can be tolerated will depend upon the specific design and the RF technique selected.

20 kW ICRH EBT-S ANTENNA

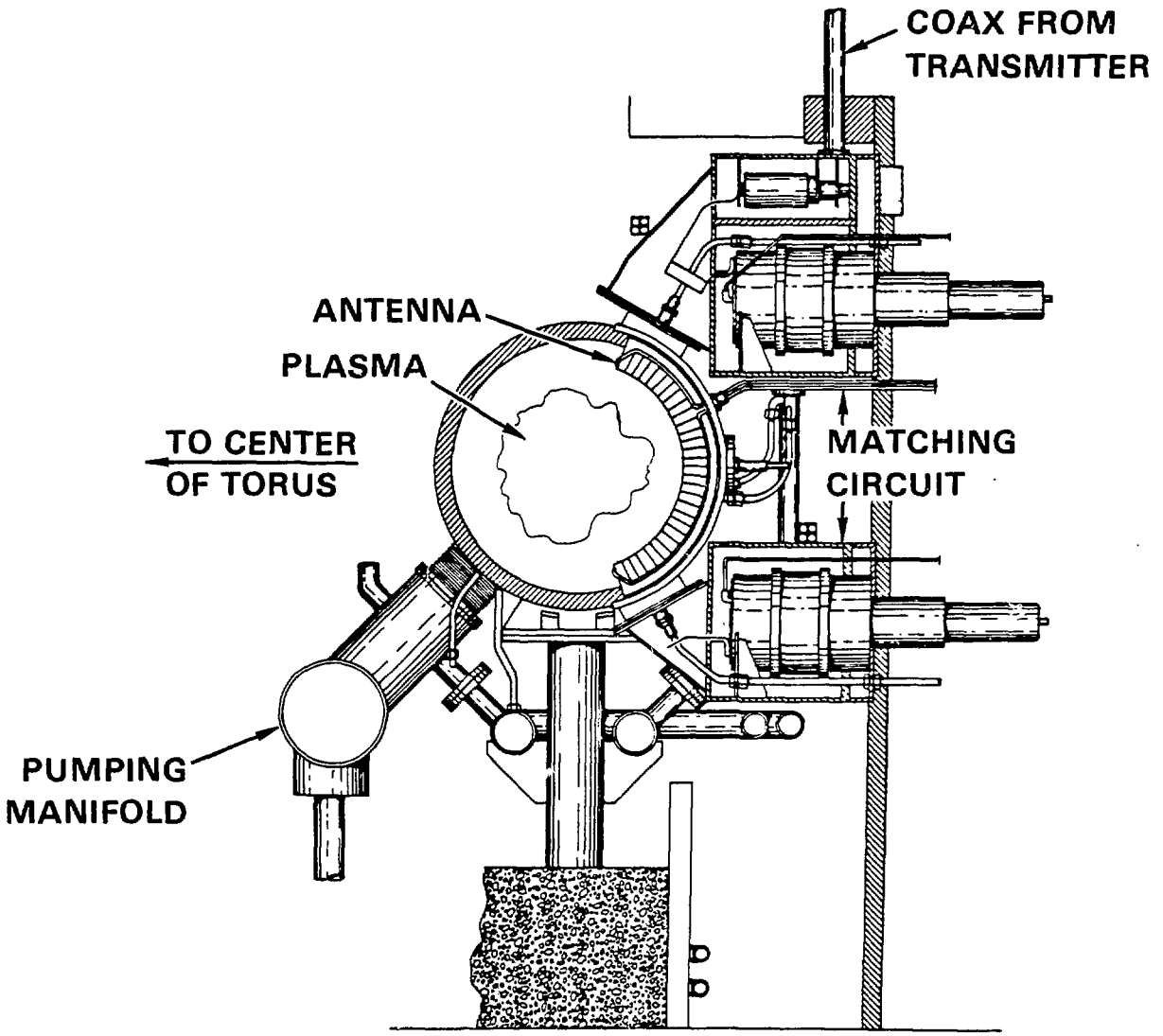

TYPICAL CONSTRUCTION OF ICRH ANTENNA

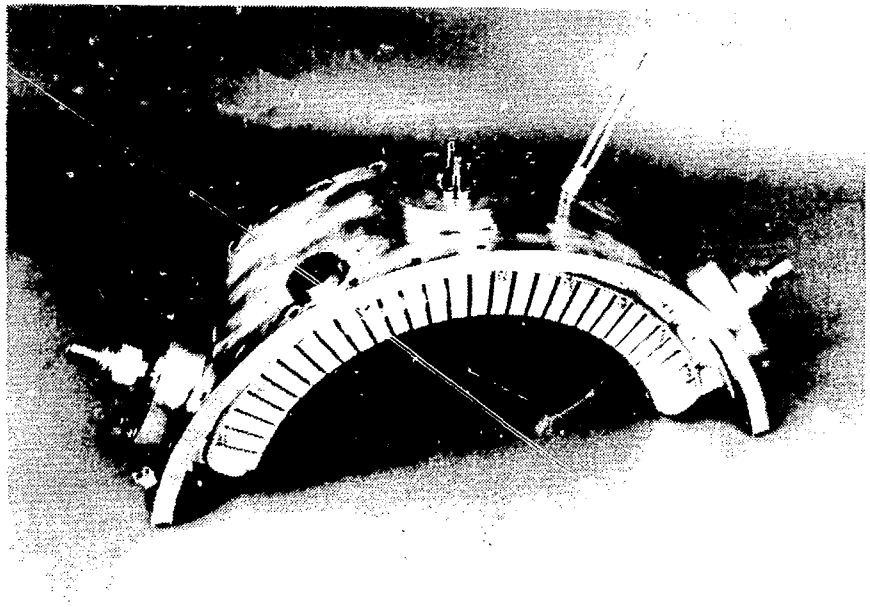

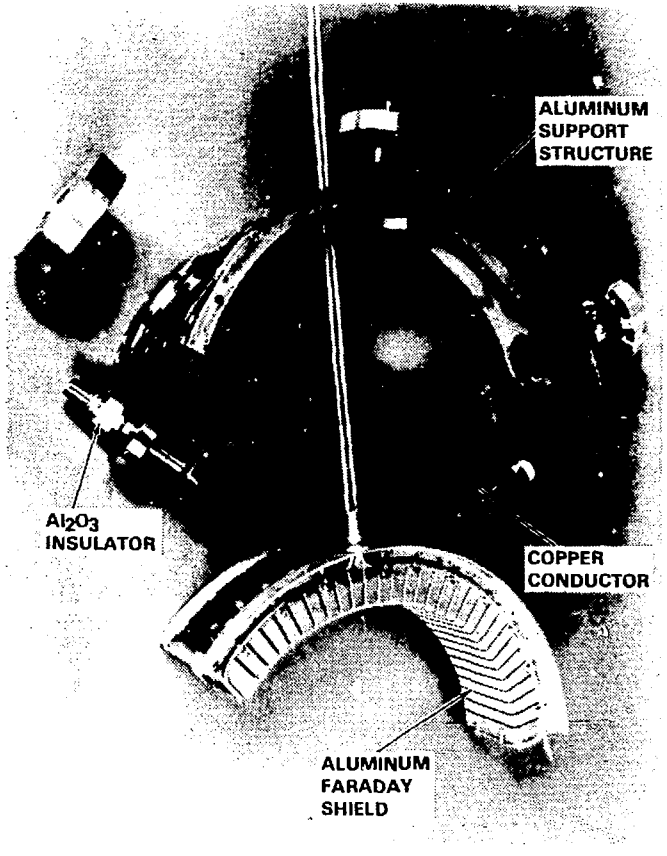

OPERATIONAL REQUIREMENTS

- LOW ELECTRICAL RESISTIVITY
- GOOD THERMAL CONDUCTIVITY
- ADEQUATE MECHANICAL PROPERTIES
- LOW EROSION RATE
- COMPATABILITY WITH COATINGS

RELATIVE RF POWER LOSS FOR VARIOUS MATERIALS

$$P = I^2R$$

$$R = \frac{\rho C_L}{A} \qquad A = L\left(\frac{2\rho}{\omega\mu_o}\right)^{1/2}$$

$$P \approx \rho^{1/2}$$

GRAPHITE	16
SiC	6.6
TiC	4.5
TITANIUM (6Al-4V)	7.3
NICKEL (INCONEL 625)	6.3
STAINLESS STEEL (316)	5.2
VANADIUM (V-20Ti)	3.2
NIOBIUM (Nb-1Zr)	3.0
MOLYBDENUM (TZM)	2.3
BERYLLIUM	1.73
ALUMINUM (2024-T4)	1.33
COPPER (MZC)	1.04
COPPER (OHFC)	1

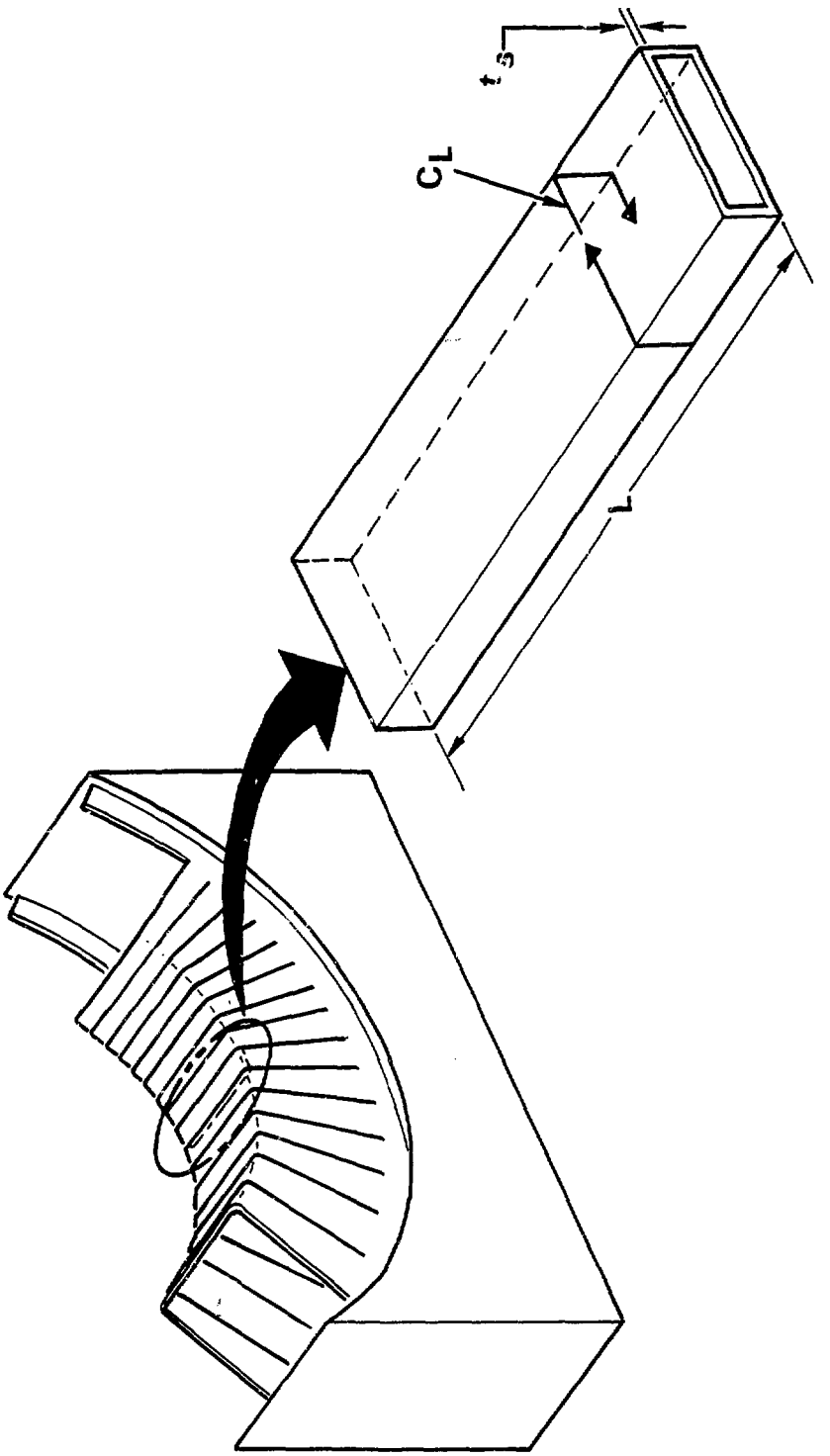
t_s
C_L
L

FARADAY SHIELD LIMITER DESIGN

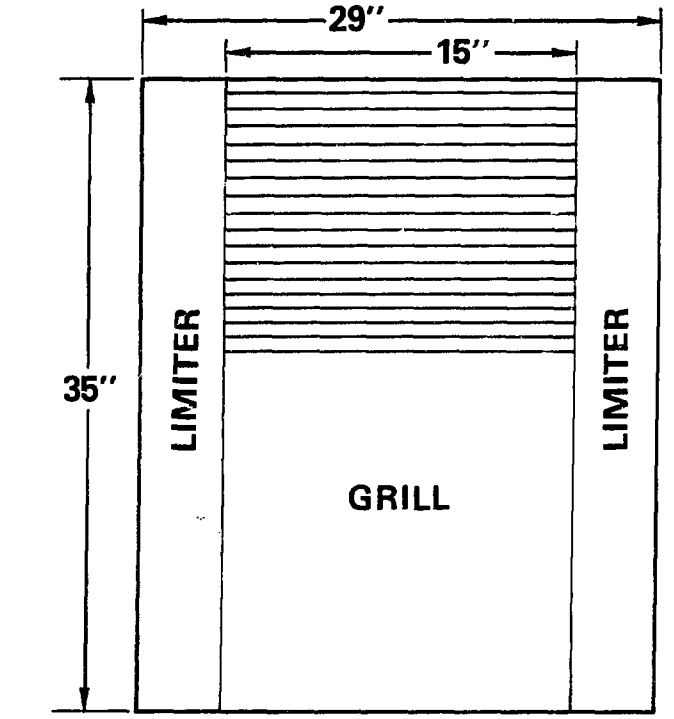

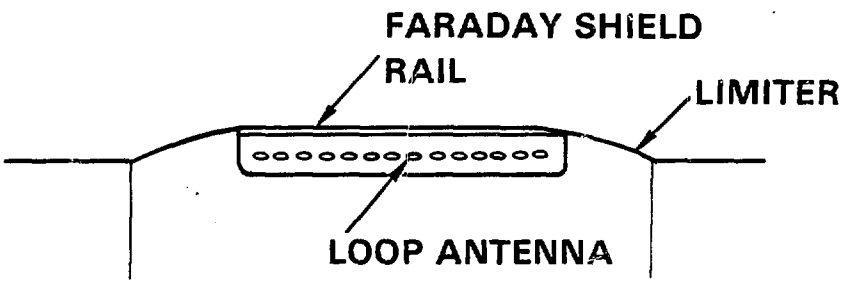

FARADAY SHIELD POWER LOSSES FOR VARIOUS STRUCTURAL MATERIALS

- 1 OHM PLASMA RESISTANCE
- FARADAY SHIELD-LIMITER DESIGN (15" SHIELD)
- 5MW TRANSMITTED POWER
- 75 MH_z FREQUENCY

MATERIAL	ELECTRICAL RESISTIVITY ($\mu\Omega$-m)	SKIN DEPTH (cm)	RAIL RESISTANCE (Ω)	POWER LOSS IN RAIL (WATTS)	RMS ELECTRICAL HEAT LOAD (W/cm^2)	PEAK ELECTRICAL HEAT LOAD (W/cm^2)	TOTAL POWER LOSS (MW)
GRAPHITE (AXF-5Q)	8.68	0.17	54,500	5.34×10^5	174	232	3.1
COPPER	0.037	0.0011	3,600	3.53×10^4	11.5	15.3	0.2
ALUMINUM	0.06	0.0014	4,600	4.5×10^4	14.7	19.6	0.26
BERYLLIUM	0.102	0.0018	6,000	5.9×10^4	19.2	25.6	0.35
STAINLESS STEEL	0.925	0.0056	17,750	1.7×10^5	56.8	75.7	1.02

THERMAL CONDUCTIVITY AT 250 °C

MATERIAL	λ (W/M . K)
GRAPHITE (AXF-5Q)	111
TITANIUM CARBIDE	33
SILICON CARBIDE	100
TITANIUM (6Al-4V)	10
NICKEL (INCONEL 625)	13
STAINLESS STEEL (316)	20
VANADIUM	22
NIOBIUM	45
MOLYBDENUM	109
BERYLLIUM	126
ALUMINUM (2024-T4)	189
COPPER (MZC)	~ 300
COPPER (OFHC)	356

TMX COPPER ICRH ANTENNA AND TUNER

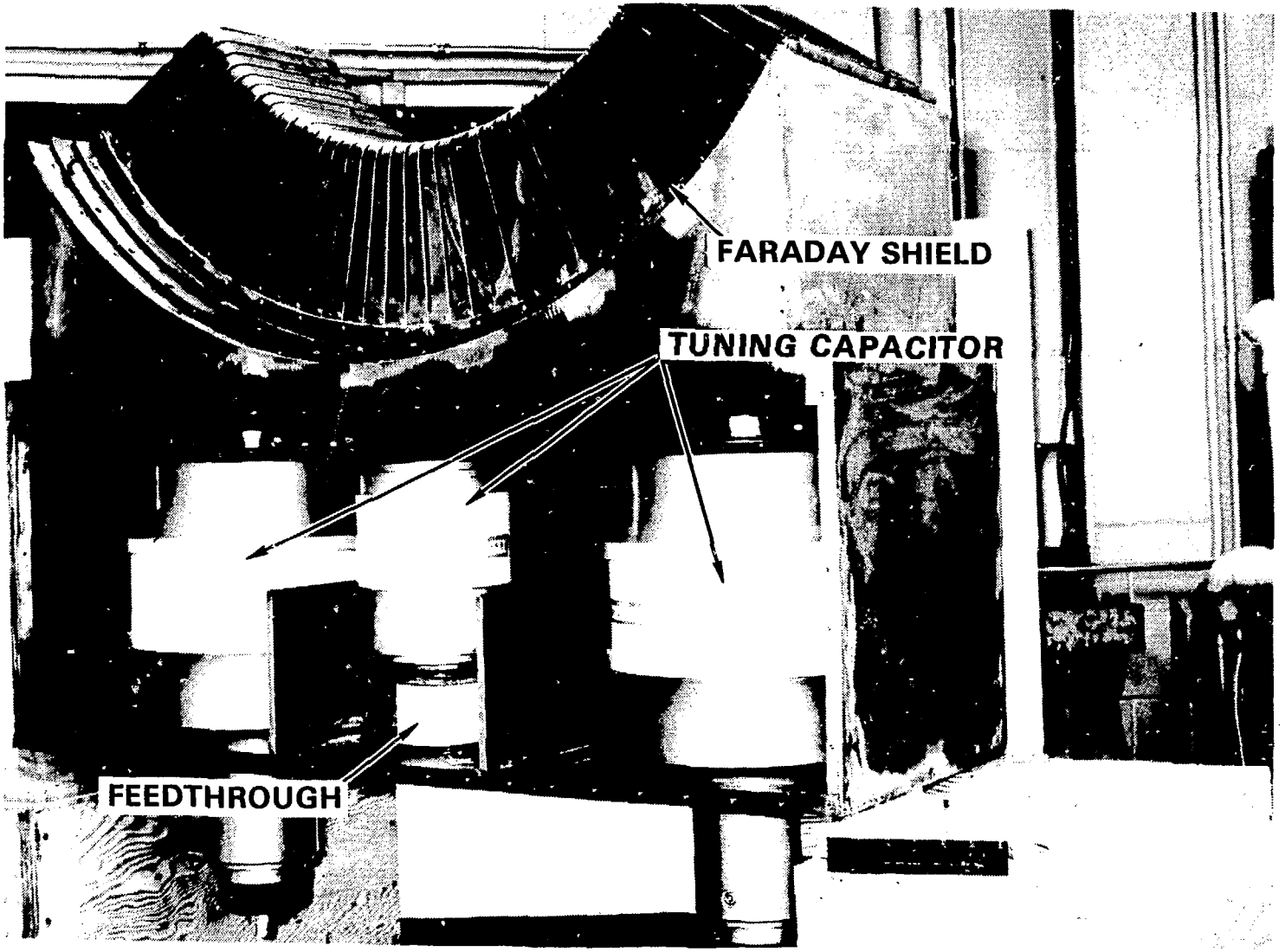

TMX COPPER FARADAY SHIELD DURING FABRICATION

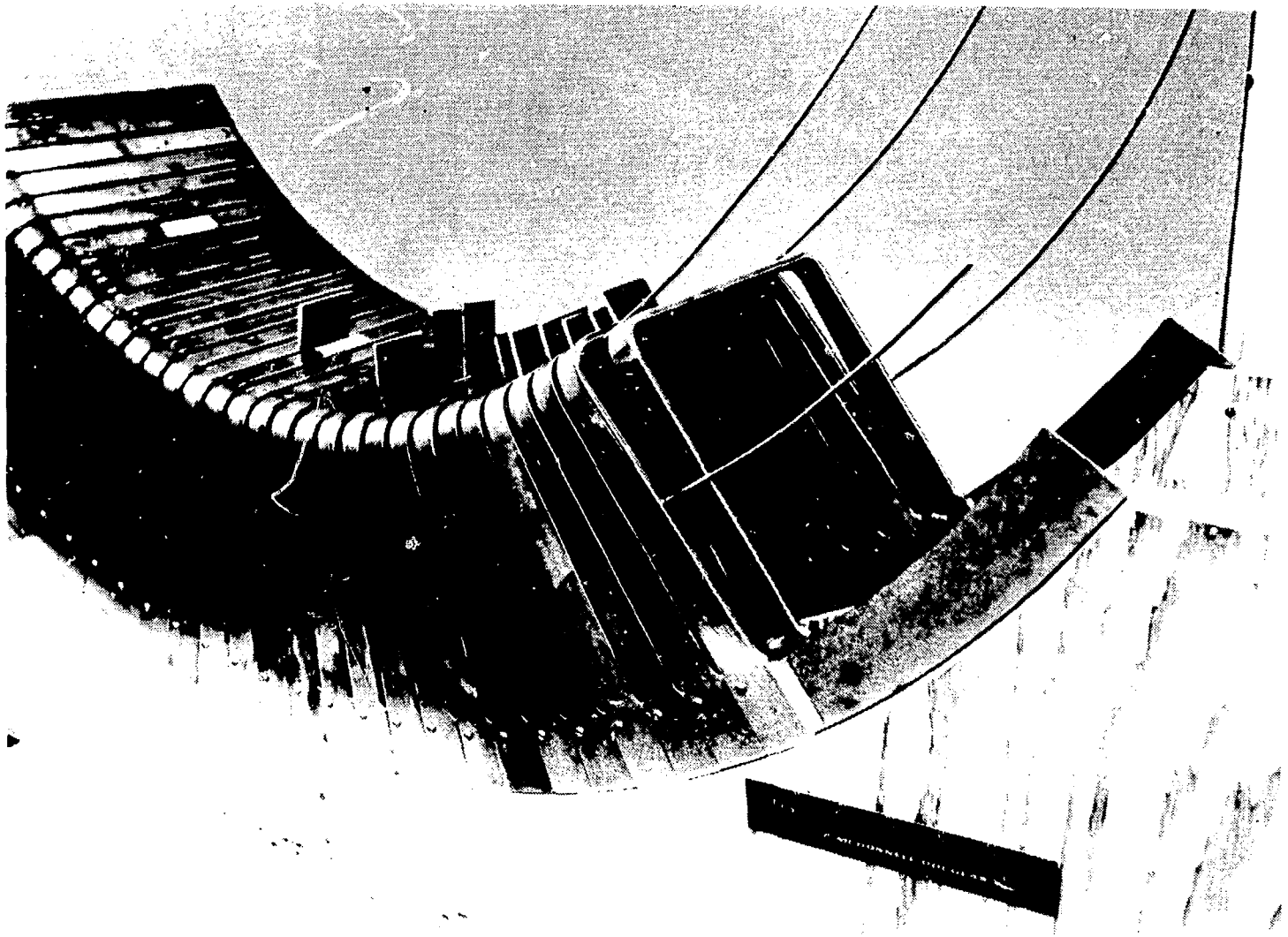

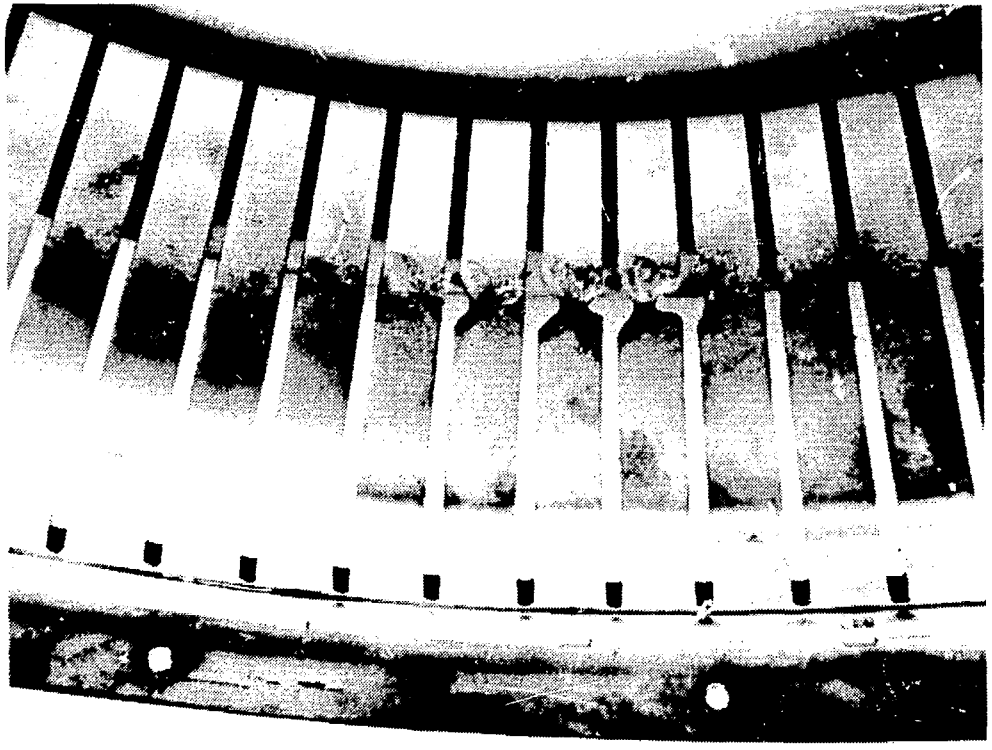

EBT-S FARADAY SHIELD AFTER 25kW-ICRH AND 175kW-ECRH

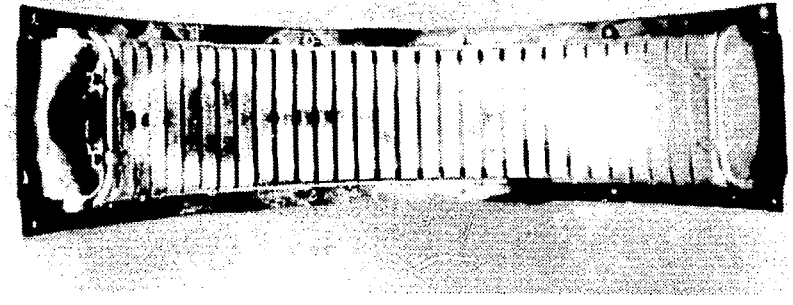

RELATIVE RADIATIVE PLASMA POWER LOSS FOR VARIOUS MATERIALS

$P_R \propto S_Z Z^2$

MATERIAL	E_p = 200 eV	1 keV
Be	0.64	0.16
C	0.74	0.22
Al	6.12	2.76
Ti	9.20	5.53
V	9.03	5.51
Fe	13.7	8.89
Cu	59.5	48.3
Nb	13.15	11.23
Mo	15.36	13.06
SiC	2.17	0.85
B_4C	0.62	0.18
TiC	1	1

FARADAY SHIELD DESIGN

13-6039

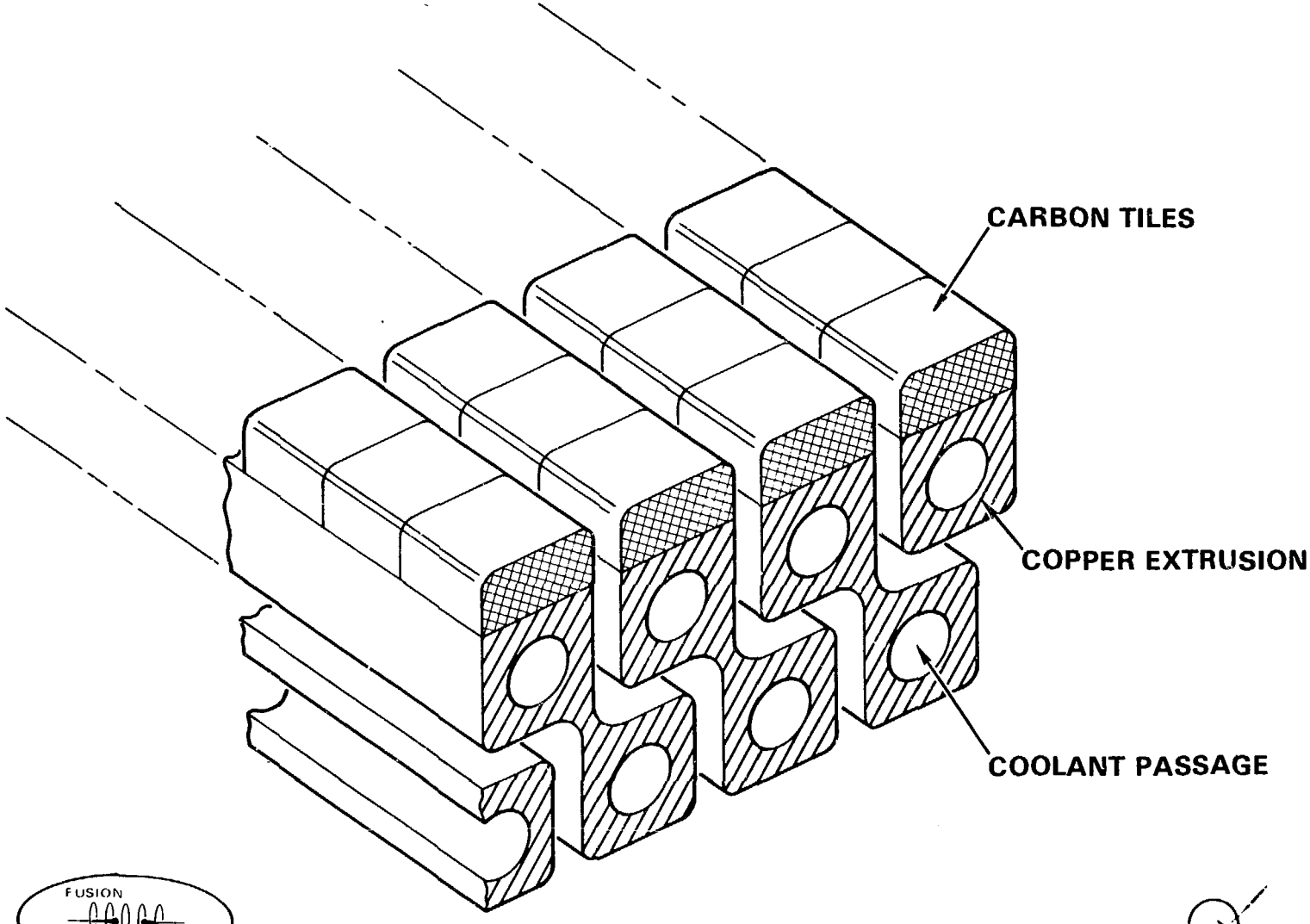

FUSION ENERGY

MCDONNELL DOUGLAS CORPORATION

PPPL FARADAY SHIELD DESIGN THERMAL RESPONSE

13-5877

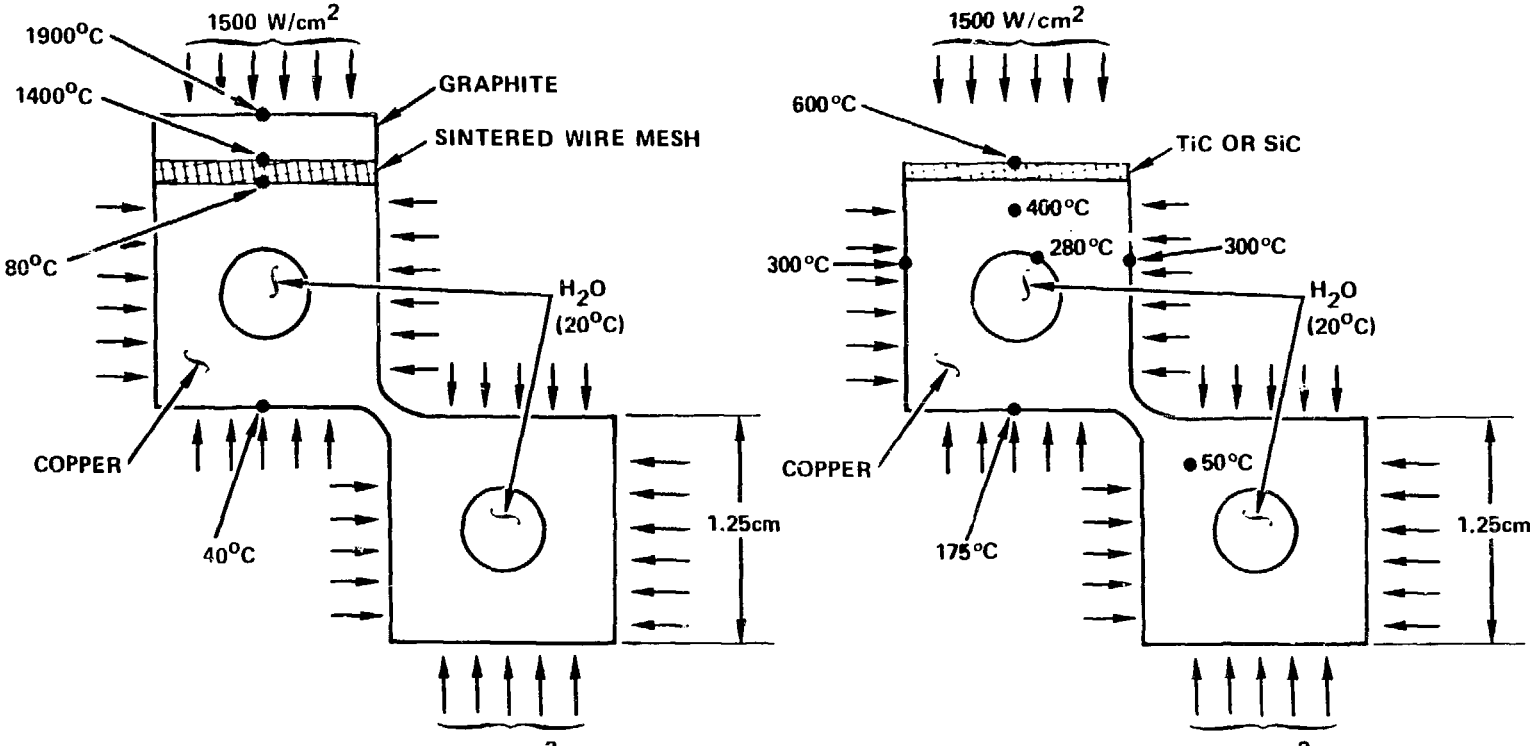

HEATING PROFILE

1500 W/cm^2 PLASMA, 0–1 SEC
30 W/cm^2 RF LOSS, 0.5–1 SEC

FUSION ENERGY

MCDONNELL DOUGLAS CORPORATION

THERMAL STRESS FIGURE OF MERIT AT 250 °C

$$M = \frac{2\sigma yk\,(1-\nu)}{\alpha E}$$

ALLOY	(W/M) x 10^{-3}
TITANIUM (6-4)	13
NIOBIUM (Nb-1 Zr)	19.4
MOLYBDENUM (TZM)	65.3
VANADIUM (V-20 Ti)	12.2
BERYLLIUM	9.7
ALUMINUM (2024-T4)	19.5
COPPER (MZC)	88.4
COPPER (OFHC)	8
NICKEL (INCONEL 625)	2
GRAPHITE	196

RELATIVE THERMAL MISMATCH IN COATING AND SUBSTRATE UP TO 250°C

13–6070

	TiC/M	SiC/M	B_4C/M	Al/M
GRAPHITE (AXF-5Q)	1.5	0.92	0.92	5.2
TITANIUM (6Al-4V)	0.75	0.45	0.45	2.6
NICKEL (625)	0.38	0.23	0.23	1.3
STAINLESS STEEL (316)	0.41	0.25	0.25	1.4
VANADIUM (V-20Ti)	0.71	0.47	0.47	2.7
NIOBIUM (Nb-1Zr)	1	0.60	0.60	3.4
MOLYBDENUM	1.28	0.77	0.77	4.4
BERYLLIUM	0.93	0.56	0.56	3.2
ALUMINUM (2024)	0.28	0.17	0.17	—
COPPER (MZC)	0.37	0.22	0.22	1.3
COPPER ((OFHC)	0.41	0.24	0.24	1.38

CONCLUSION

- A COPPER ALLOY APPEARS TO BE A VIABLE MATERIAL FOR FARADAY SHIELD
- HIGH EROSION RATES WILL NECESSITATE COATINGS
- RADIATION DAMAGE MAYBE A PROBLEM PARTICULARLY WITH RESPECT TO SWELLING AND CHANGES IN ELECTRICAL CONDUCTIVITY
- PROPERTIES OF IMPORTANCE IN MATERIAL SELECTION ARE
  - LOW ELECTRICAL RESISTANCE
  - HIGH THERMAL CONDUCTIVITY
  - ELEVATED TEMPERATURE STRENGTH
  - COMPATABILITY WITH COATINGS

FUSION ENERGY

MCDONNELL DOUGLAS CORPORATION

FIRST WALL, LIMITER, AND MAGNETIC COILS IN COMPACT CONCEPTS

R. L. Hagenson
Technology International, Inc.

R. A. Krakowski
Los Alamos National Laboratory

VIEWGRAPH SUMMARY

Concern over the dominance in mass and cost of the fusion power core (FPC, i.e., first-wall/ blanket/ shield/ coils) for many large, low-powered density MFE approaches has led recently to serious consideration of the compact option. Power densities within the FPC approaching those of light-water fission reactors (i.e., 10-30 times greater than for superconducting MFE systems); projected costs relatively insensitive to large changes in unit costs ($/Kg) used to estimate FPC and associated reactor plant equipment (RPE) costs, as well as uncertainties in the associated physics and technology; considerably reduced size and mass of the FPC with potential for "block" (single or few-piece) installation and maintenance; and the potential for rapid, minimum-cost development are general characteristics being sought through the compact reactor options.

Several devices are potentially compact[1] with the major emphasis to date including the Compact Reversed-Field Pinch Reactor (CRFPR), the reactor embodiment of the Ohmically-Heated Toroidal Experiment (OHTE), high-field tokamaks (Riggatron™) and certain subelements of compact toroids (CT). The CT configurations of primary interest[2] are steady-state spheromaks and translating configurations based upon the field-reversed theta pinch.

The compact option for fusion power will require the extension of existing technologies to accommodate higher heat flux, higher power density and (in some instances) higher magnetic fields required to operate FPCs with system power densities (thermal power/FPC volume) in the 10-15 MWt/m^3

range rather than in the 0.3-0.5 MWt/m^3 range being predicted for low-power density (superconducting) MFE approaches. The major engineering technology issues include

- High-heat flux first walls (2-5 MWt/m^2) and limiters similar to other MFE requirements, sputtering/ erosion and particle control being the main concern.
- High-power density (30 MWt/m^3 average) breeding blankets may preclude solid breeders.
- High-radiation-flux resistive magnets positioned outside a thin (0.5-0.6 m) tritium-breeding/ heat-recovering blanket.

The following presentation details the devices under study having the most promising compact reactor embodiments. Engineering requirements are presented where available, with particular emphasis on the probable need for copper as a heat transfer medium and/or electrical conductor.

REFERENCES

(1) R.A. Krakowski and R.L. Hagenson, "Compact Fusion Reactors," Fifth ANS Topical Meeting on the Technology of Fusion Energy, Knoxville, TN (April 26-28, 1983).

(2) R.L. Hagenson, "Reactor Scenarios for Compact Toroids," Fifth Symposium on Physics and Technology of Compact Toroids, Bellevue, WA (1982).

CONFINEMENT SYSTEMS THAT COULD CONTRIBUTE TO THE COMPACT REACTOR OPTION

- COMPACT RFP REACTOR (CRFPR)
- OHTE REACTOR
- HIGH-FIELD TOKAMAK REACTOR (RIGGATRON, HFCTR)
- HELIACS(?)
- COMPACT TOROIDS (FPCs OR SPHEROMAKS)
  - TRACT
  - LINUS
  - FIELD-REVERSED MIRROR REACTOR (MRFRMR)
  - FIELD-REVERSED THETA PINCH (CTOR)
  - SPHEROMAK
- FAST-PULSED DENSE SYSTEMS
  - DENSE Z-PINCH REACTOR (DZPR)
  - FAST-LINER REACTOR (FLR)
  - WALL-CONFINED FUSION REACTOR

CHARACTERISTICS SOUGHT FOR COMPACT REACTOR OPTION

	CONVENTIONAL	COMPACT
High system power density (MWt/m^3)	0.3–0.5	10–15
Acceptable total power (MWt)	$\gtrsim$ 4000	< 4000
Low FPC mass utilization (tonne/MWt)	4–10	0.3–1.0
High fusion neutron first wall loading (MW/m^2)	1–5	10–20
High blanket power density (MW/m^3)	1–5	> 100
Low FPC cost sensitivity RPE/TDC	0.50–0.75	< 0.3
Little or no passive magnet shield	SC	N
Acceptable recirculating power fraction	< 0.15	< 0.1

CHARACTERISTICS SOUGHT FOR COMPACT REACTOR OPTION (contd-2)

- Competitive COE based on conservative costing assumptions
  - first-of-a-kind rather than 10th-of-a-kind costs
  - reduced construction time
  - batch versus patch maintenance
  - economic plant availability
- Reduced development time and dollars using extensions of existing technology rather than development of new technology
  - Ohmic versus rf on NB heating
  - N versus SC coils
  - reduced front end costs

RECENT MFE REACTOR CONCEPTS

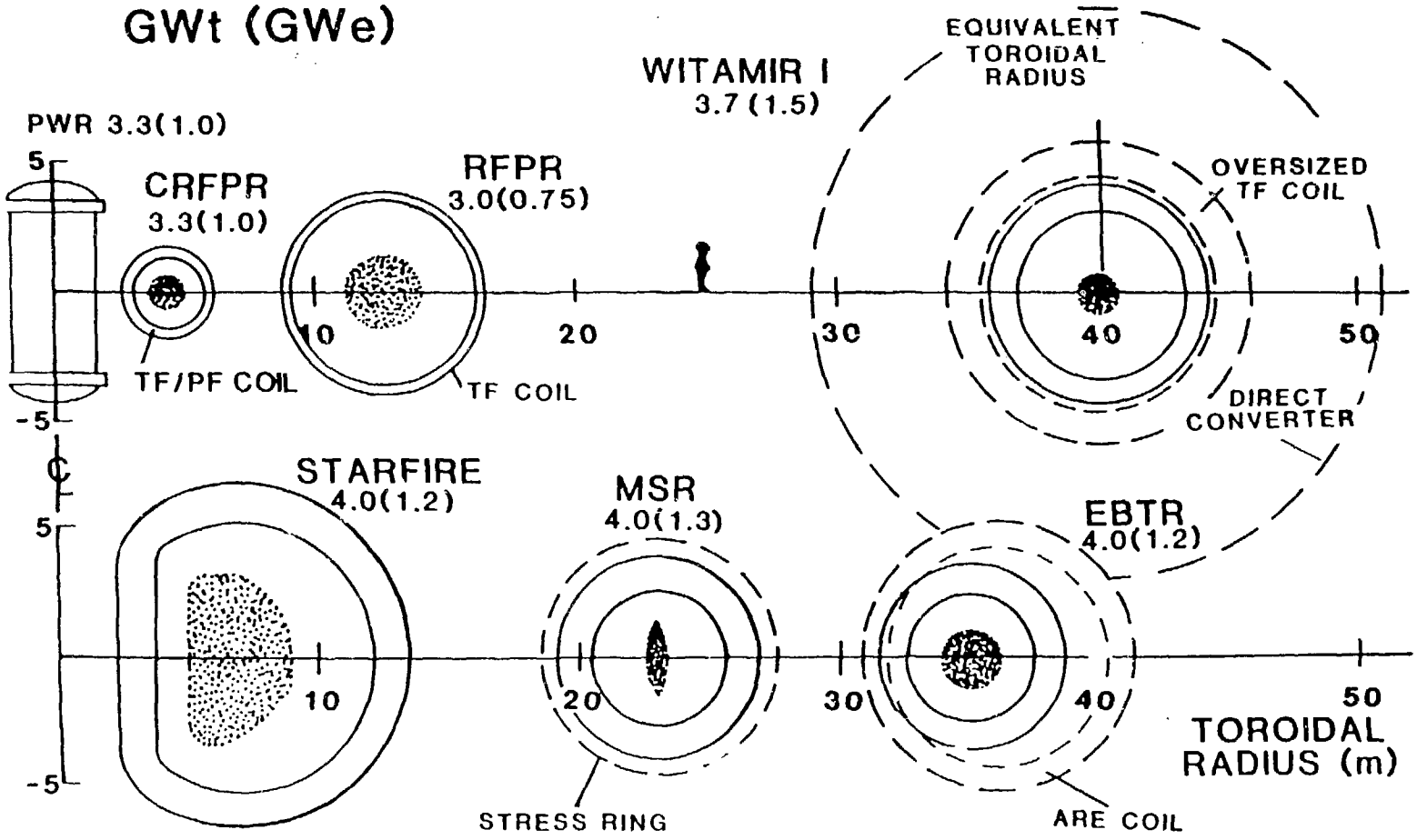

KEY ISSUES EFFECTING THE RELIABILITY/AVAILABILITY OF COMPACT REACTORS

•FIRST WALL

- Heat fluxes, PCASS not possible, high-strength copper alloy desirable
- Radiation-induced strength degradation and swelling
- Electrical resistivity degradation
- First-wall erosion*
- Dense, cold gas blanket
- Magnetic divertors
- FW geometry, energy partition, FW versus B temperature, overall plant efficiency

•BLANKET POWER DENSITY

- Solid breeder probably precluded by high local power density
- Liquid-metal breeder/coolant well suited to power density envisaged, containment and chemical compatability
- Compatability with water-cooled high-heat-flux first walls
- FW versus B power split

*For same plasma edge physics, sputtering rate per se is not only a compact reactor issue.

KEY ISSUES EFFECTING THE RELIABILITY/AVAILABILITY OF COMPACT REACTORS (cont-2)

- MAGNETS (water-cooled copper conductor, inorganic insulator)
  - High-field magnets located at/near first wall
    - -- system power balance
    - -- tritium breeding
    - -- magnet life
  - Radiation-induced strength degradation and swelling
  - Electrical resistivity degradation
- MAINTAINABILITY
  - Rapidity and reliability of block maintenance
  - Dominance of coolant and vacuum ducting relative to high-power-density FPC
  - Potentially higher mass usage and associated O&M costs

SUMMARY OF KEY PARAMETERS FOR COMPACT HIGH-POWER-DENSITY TOROIDAL FUSION REACTORS

	STARFIRE	CRFPR	OHTE	RIGGATRON
Plasma radius (m)	2.38	0.71	0.67	0.32
Major radius (m)	7.0	4.3	5.91	0.80
Plasma volume (m^3)	781.	42.7	52.1	2.0
Average density ($10^{20}/m^3$)	0.8	3.4	12.0	20-30
Temperature (keV)	22	20	5-6	12-20
Average beta	0.067	0.20	0.43	0.20
Plasma power density (MW/m^3)	4.5	72.4	64.0	500.
Plasma current (MA)	10.1	18.5	12.4	3-4
Plasma current density (MA/m^2)	0.57	11.7	8.8	7.2-9.6
Magnetic field (T)	5.8	3.3	11.2	10.-16.
Neutron current (MW/m^2)	3.6	19.5	19.5	68.4
Thermal power (MWt)	4033.	3350.	2740.	1325.
Net power (MWe)	1200.	1000.	904.	355.
System power density (MWt/m^3)	0.30	15.0	3.2	5.2
Mass utilization (tonne/MWt)	3.9	0.37	1.45	0.28
Thermal conversion efficiency	0.35	0.35	0.40	0.41
Recirculating power fraction	0.167	0.15	0.35	0.33
Net plant efficiency	0.30	0.30	0.24	0.27

SUMMARY OF PARAMETERS USED TO ASSESS TECHNOLOGY R&D NEEDS FOR COMPACT REACTORS RELATIVE TO STARFIRE

	CONVENTIONAL	COMPACT		
	STARFIRE	CRFPR	OHTE	Riggatron
Plasma Engineering Systems				
• Average density ($10^{20}/m^3$)	0.8	3.4	10.0	20-30
• Plasma current (MA)	10.1	18.5	12.4	3-4
• Plasma current density (MA/m^2)	0.5	11.7	8.8	7.2-9.6
Nuclear Systems				
• Limiters (MW/m^2)	5.0	NR	NR	NR
• First-wall thermal loading (MW/m^2)	0.9	4-5	5	20-50
• Blanket				
- Average/peak power density (MW/m^3)	9.5/60.	27/255	27/120	3/18
- Breeder	solid	liquid	liquid	liquid
Magnet Systems				
• TF coil (T)	11.1(SC)	3.3(N)	4(N)	10-16(N)
• OH coil (T)	8(SC)	2.6(N)	11.2(N)	30(N)
• Energy storage (GJ)	61(11)	1.65	9	0.6
Remote Maintenance				
• mass of unit replaced (tonne)	65	435	164	25
• Annual mass usage (tonne/y)	260	276	492	900
Safety				
• afterheat (MW/m^3)	2	12	10	--

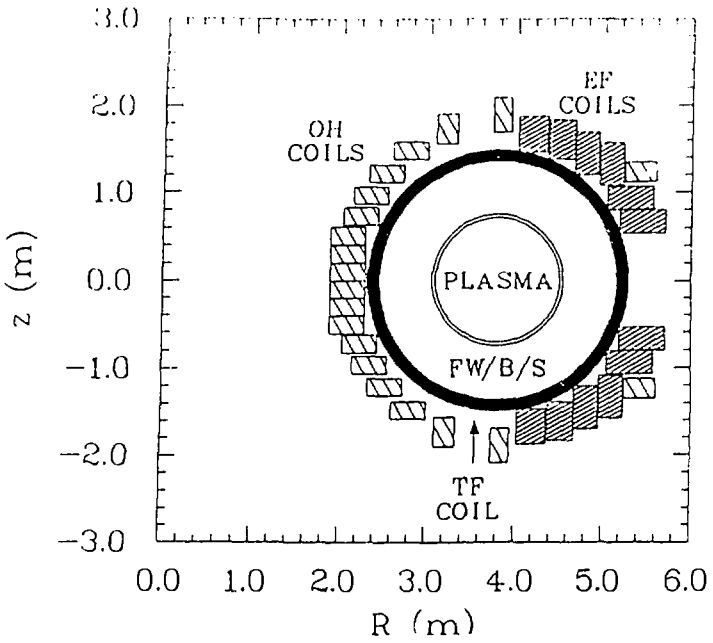
3.0
2.0
1.0
0.0
−1.0
−2.0
−3.0
z (m)
0.0
1.0
2.0
3.0
4.0
5.0
6.0
R (m)
EF
COILS
OH
COILS
PLASMA
FW/B/S
TF
COIL

CRFPR

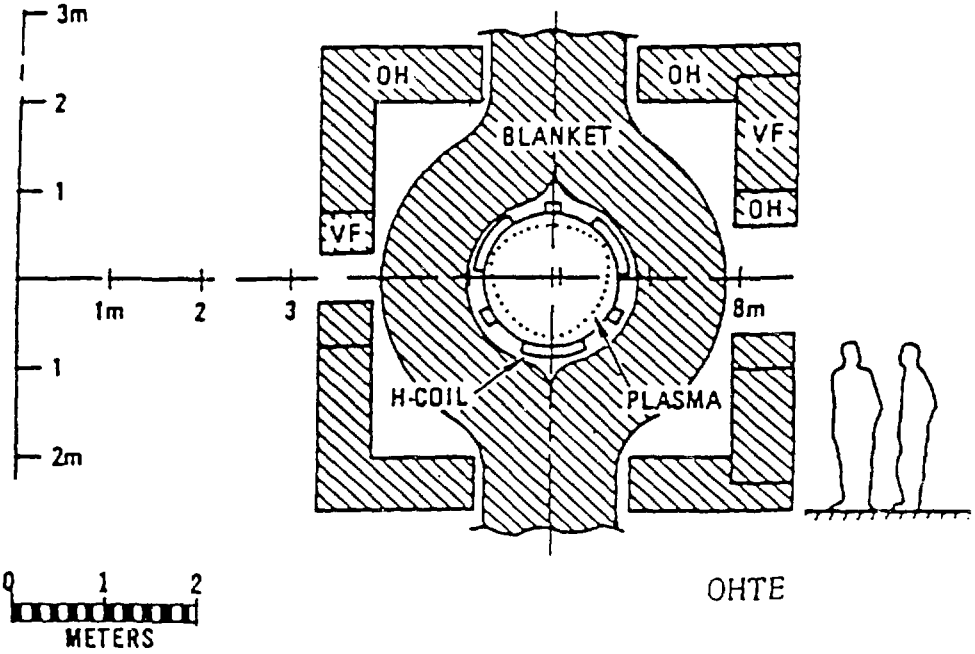
3m
2
1
1
2m
1m
2
3
8m
OH
OH
BLANKET
VF
OH
VF
H-COIL
PLASMA
0
1
2
METERS

OHTE

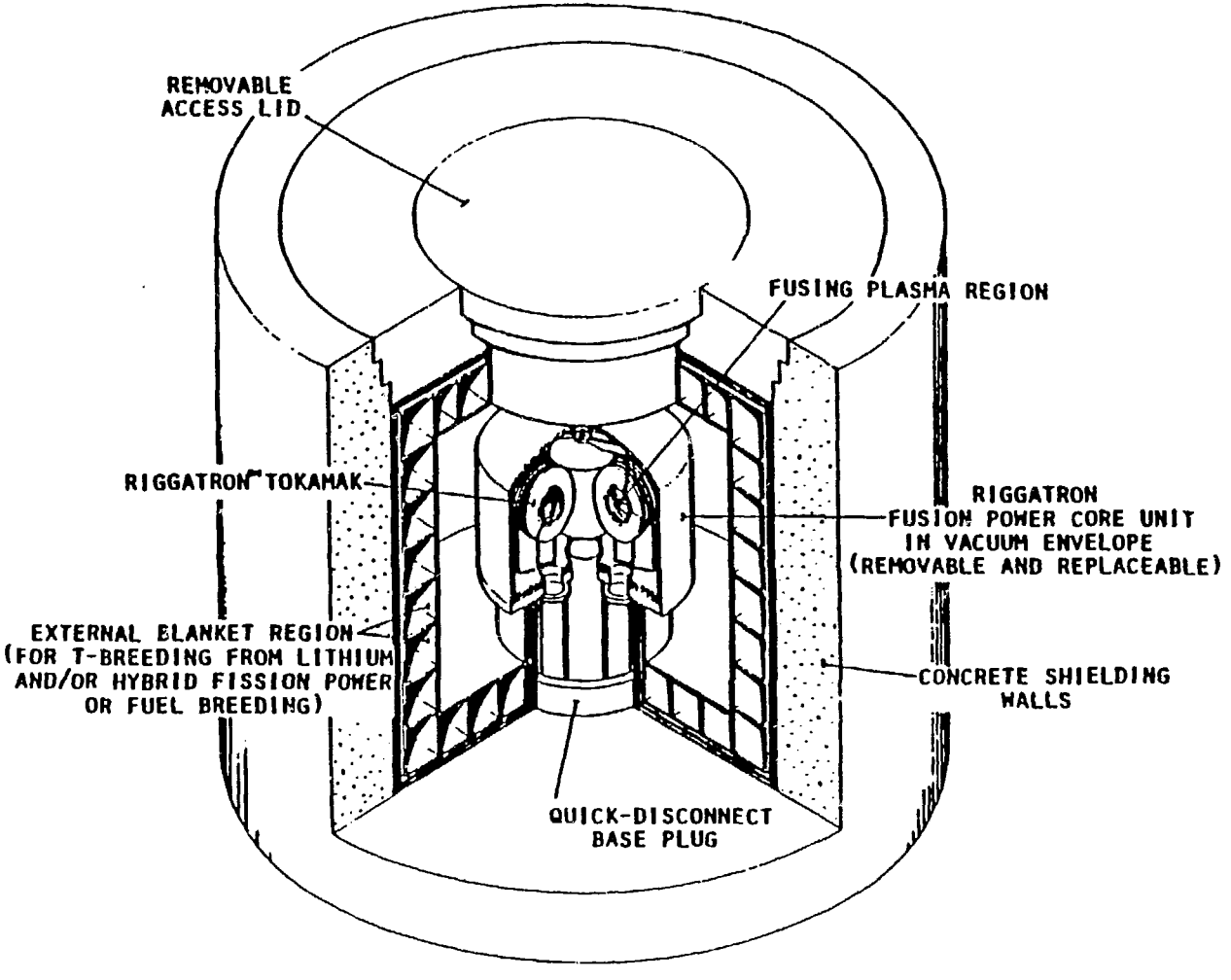

RIGGATRON™ FUSION SYSTEM

TOKAMAK VERSUS REVERSED-FIELD PINCH

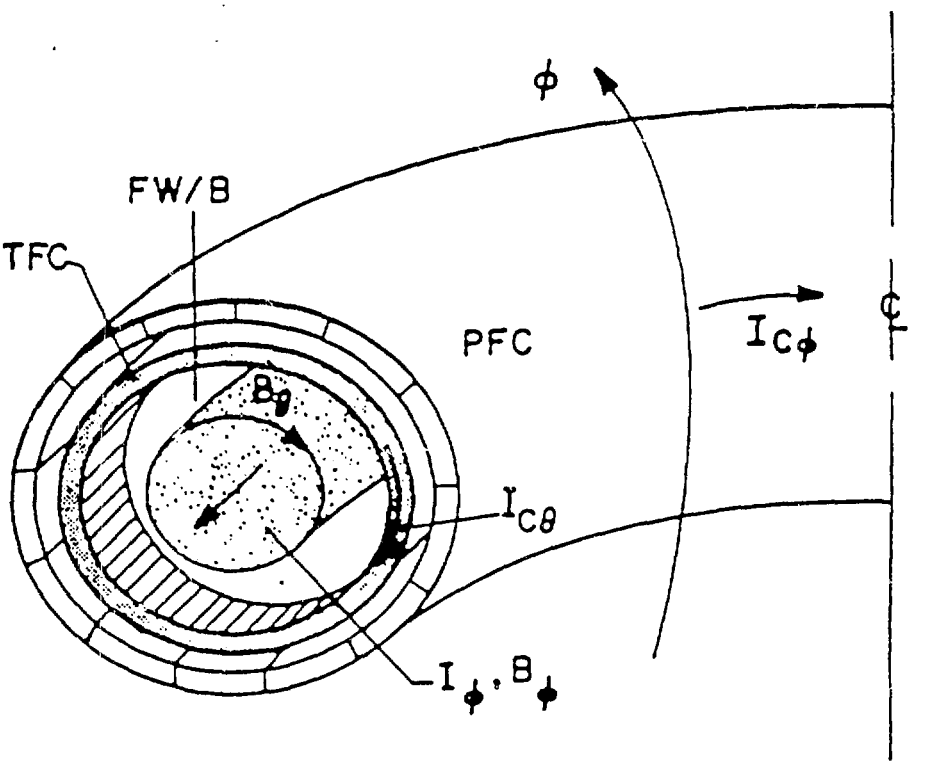

RFP($B_\theta \simeq B_\Phi$)

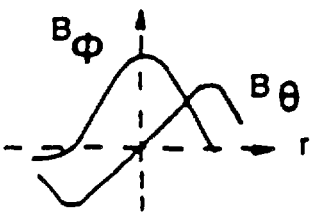

TOKAMAK($B_\theta \ll B_\Phi$)

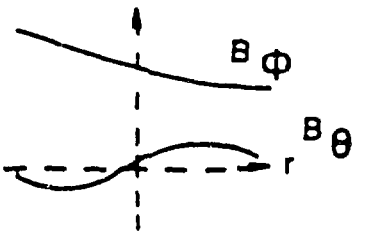

KEY PARAMETERS FOR MAJOR DEVICES REQUIRED TO DEVELOP RFP TO COMMERCIAL DEMONSTRATION OF FUSION POWER

DEVICE	ZT-40	ZT-40 UPGRADE STAGE I	ZT-40 UPGRADE STAGE II	ITR/ETR	DEMO
PARAMETER	PRESENT/DESIGN	A/B	DT/DD	DT/DD	DT/DD
r_w(m)	0.2	0.4/0.25	0.35/0.25	0.55/0.42	0.75/0.6
R_T(m)	1.14	2.4	2.4	3.2	4.3
I_ϕ(MA)	0.2/0.6	2.0	4.0	10.0/12.5	18.5/25.0
j_ϕ(MA/m^2)	1.6/4.8	4/10	10/20	10.5/22.5	10.5/22.5
E_{STOR}(GJ)	0.0011/0.005	0.2/0.25	0.25	0.3/0.55	1.6/5.0
I_w(MW/m^2)	-	-	-	3.5/0.55	19.5/3.0
I_s(MW/m^2)	1-2/1.5-5	1/5	2/5	0.87	4.8
P_{TH}(MWt)	-	-	-	350/80	3350/1000
T_i(keV)	0.3/0.8-1.0	1-2	4-6	10-20/20-30	10-20/20-30
β_θ	0.1-0.2	0.1-0.2	0.1-0.2	0.2	0.2
$n\tau_E$(10^{20} s/m^3)	$5(10)^{-5}$/2-8$(10)^{-4}$	0.01-0.4	0.07-0.2	1.0/10.0	1.0/10.0

REVERSED-FIELD PINCH PROGRAM TECHNOLOGY REQUIREMENTS

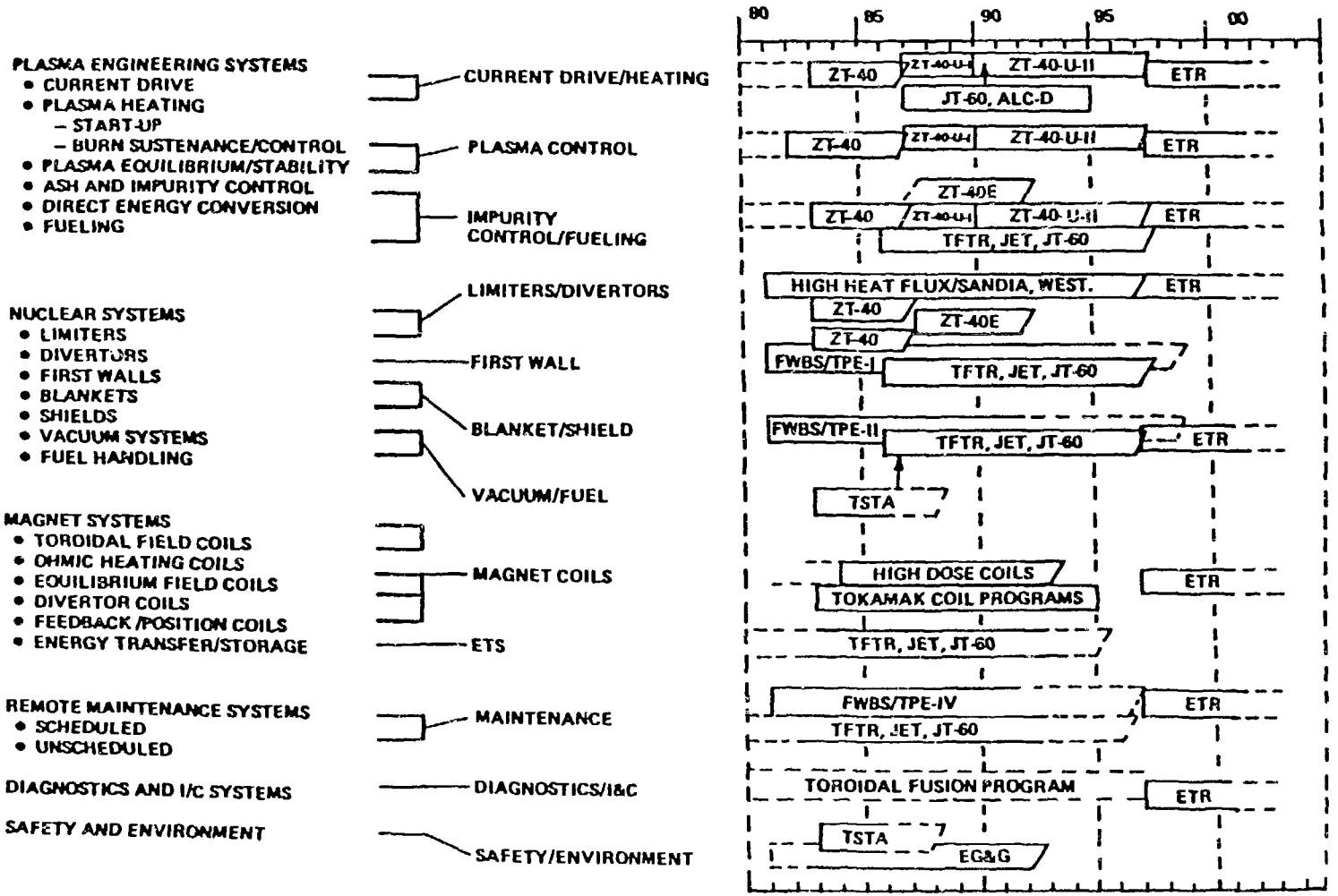

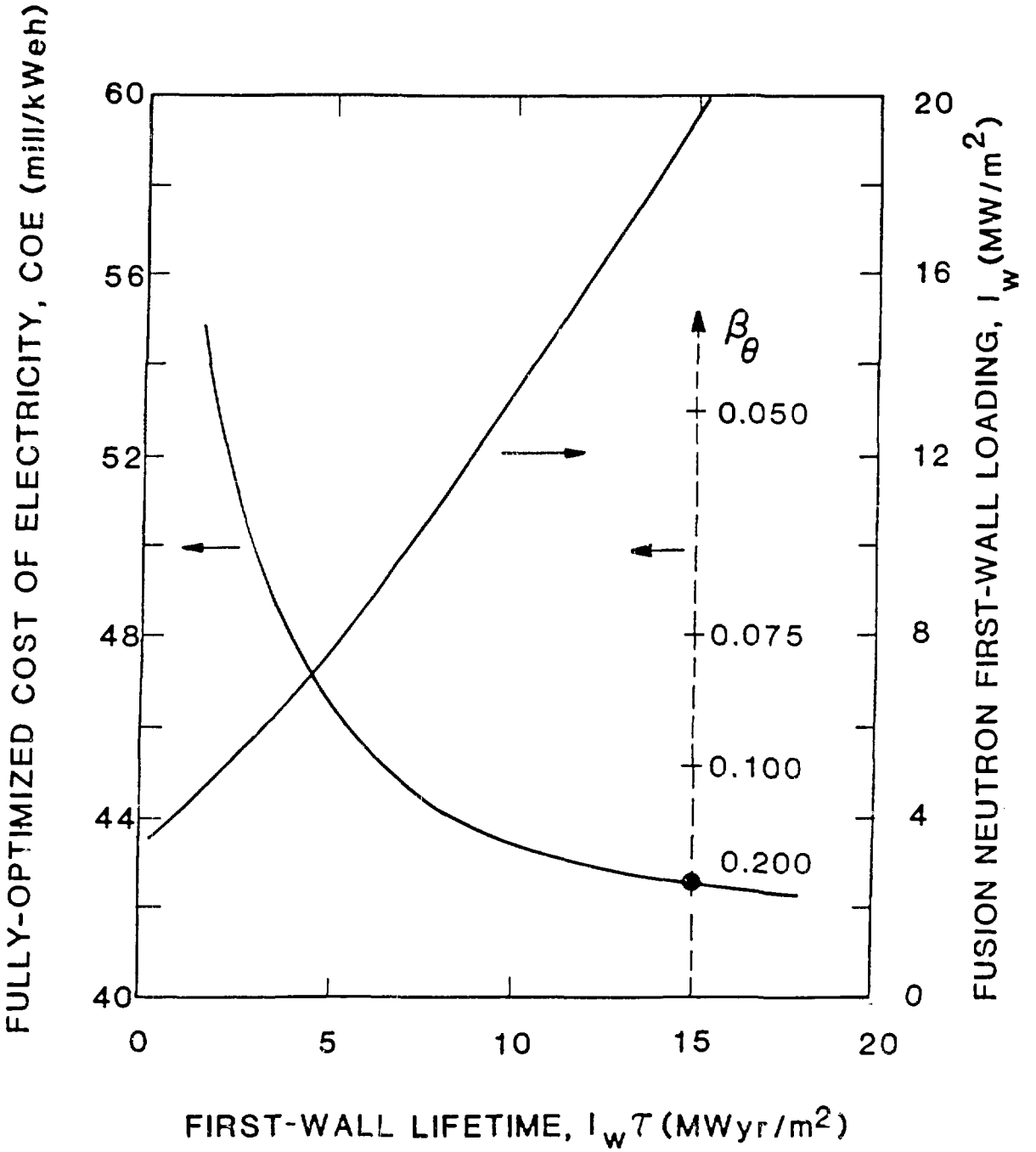
FULLY-OPTIMIZED COST OF ELECTRICITY, COE (mill/kWeh)
FUSION NEUTRON FIRST-WALL LOADING, I_w(MW/m^2)
FIRST-WALL LIFETIME, $I_w\tau$ (MWyr/m^2)
60
56
52
48
44
40
20
16
12
8
4
0
0
5
10
15
20
β_θ
0.050
0.075
0.100
0.200

SUMMARY OF MFE HEAT FLUXES

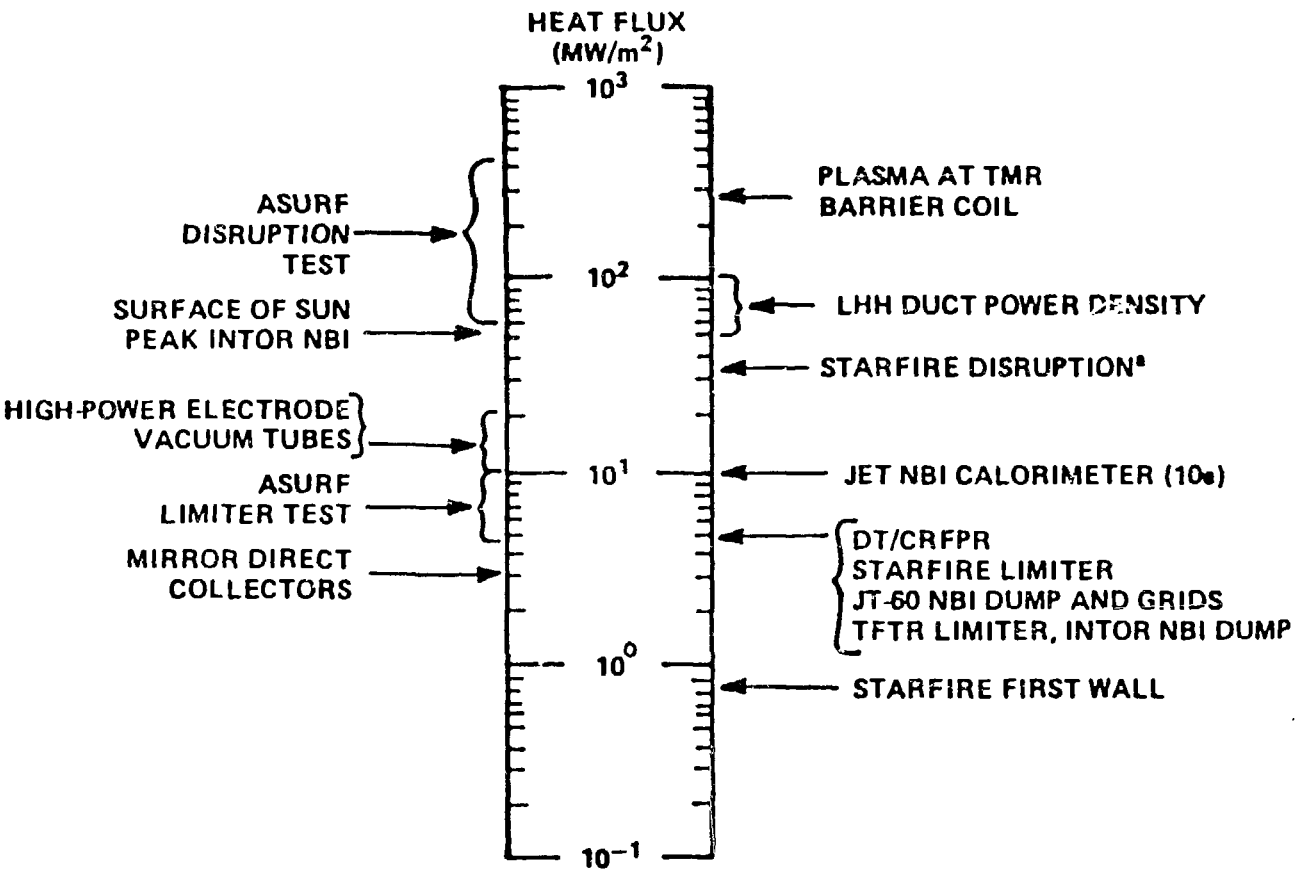

[a]920 MJ deposited in 100 ms over 30% of the 800-m^2 (total) surface area

CRFPR NEUTRONICS MODEL

REGION ID	PLASMA (VOID)	VOID	FIRST WALL	SECOND WALL	BLANKET	THIRD WALL	TOROIDAL COIL	POLOIDAL COIL
MESH POINTS	5	2	5	2	30	2	25	25
CUMULATIVE MESH	5	7	12	14	44	46	71	96
RADIAL THICKNESS (m)	0.73	0.02	0.02	0.005	Δb(VARIED)	0.005	0.10	0.37
RADIUS (m)	0.73	0.75	0.77	0.775	0.775 + Δb	0.78 + Δb	0.88 + Δb	1.25 + Δb
COMPOSITION	VOID	VOID	60% Cu 29% H_2O	60% PCASS 29% H_2O	90% Pb-Li 10% PCASS	90% PCASS 7.3% H_2O	80% Cu 10% PCASS 10% H_2O	80% Cu 10% PCASS 10% H_2O

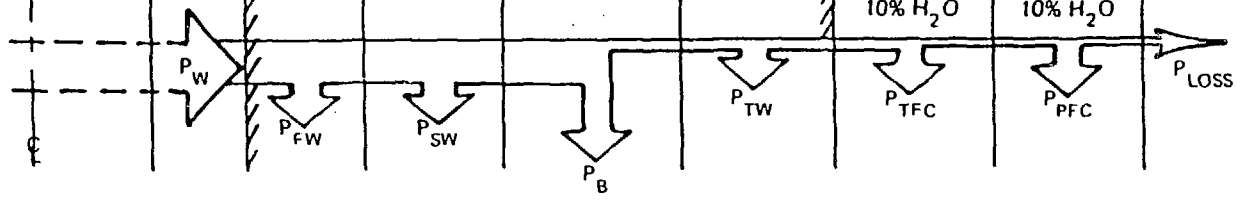

BLANKET ENERGY MULTIPLICATION, $M_N = (P_{FW} + P_{SW} + P_B + P_{TW})/P_W$

BLANKET EFFICIENCY, $\epsilon_B = M_N P_W/(M_N P_W + P_{TFC} + P_{PFC} + P_{LOSS})$

TRITIUM BREEDING RATIO, BR

$I_W = 19.5\ MW/m^2$, $P_W = 91.89\ MW/m$

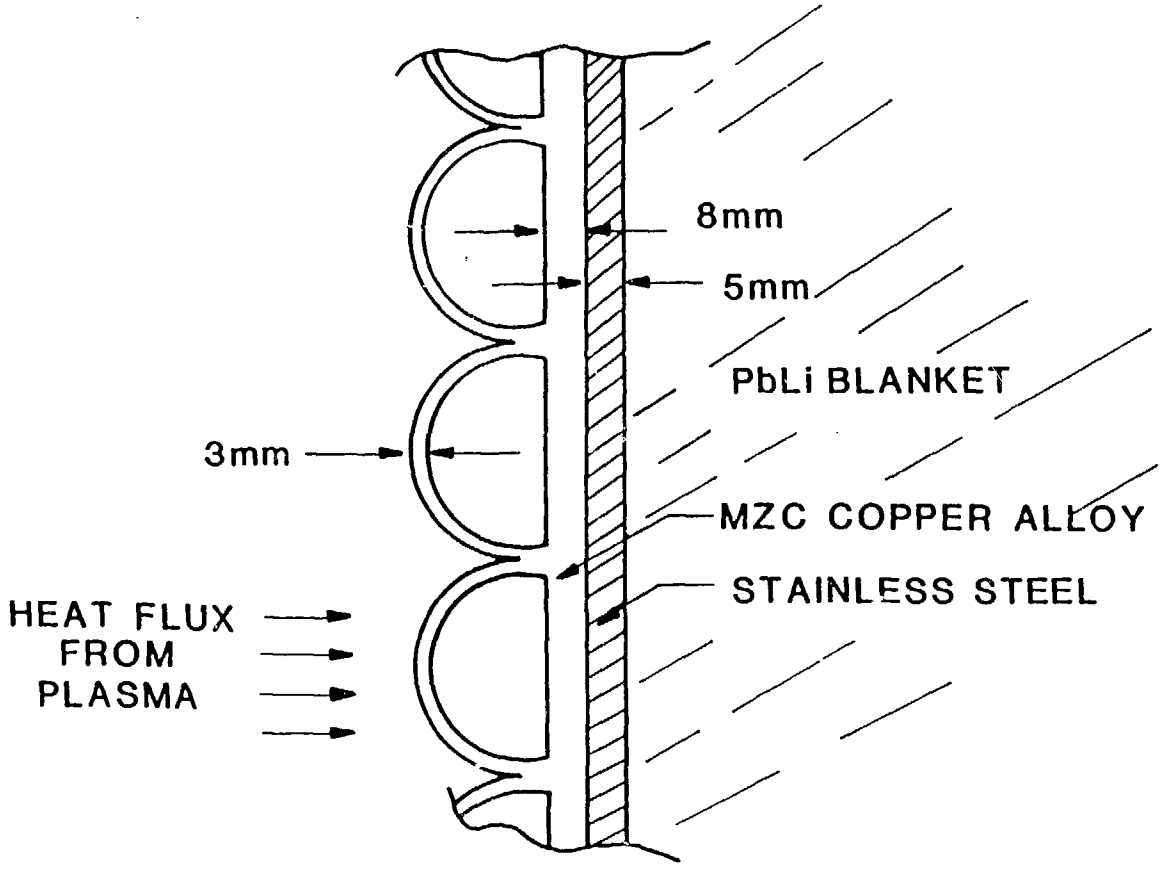
8mm
5mm
PbLi BLANKET
3mm
MZC COPPER ALLOY
STAINLESS STEEL
HEAT FLUX
FROM
PLASMA

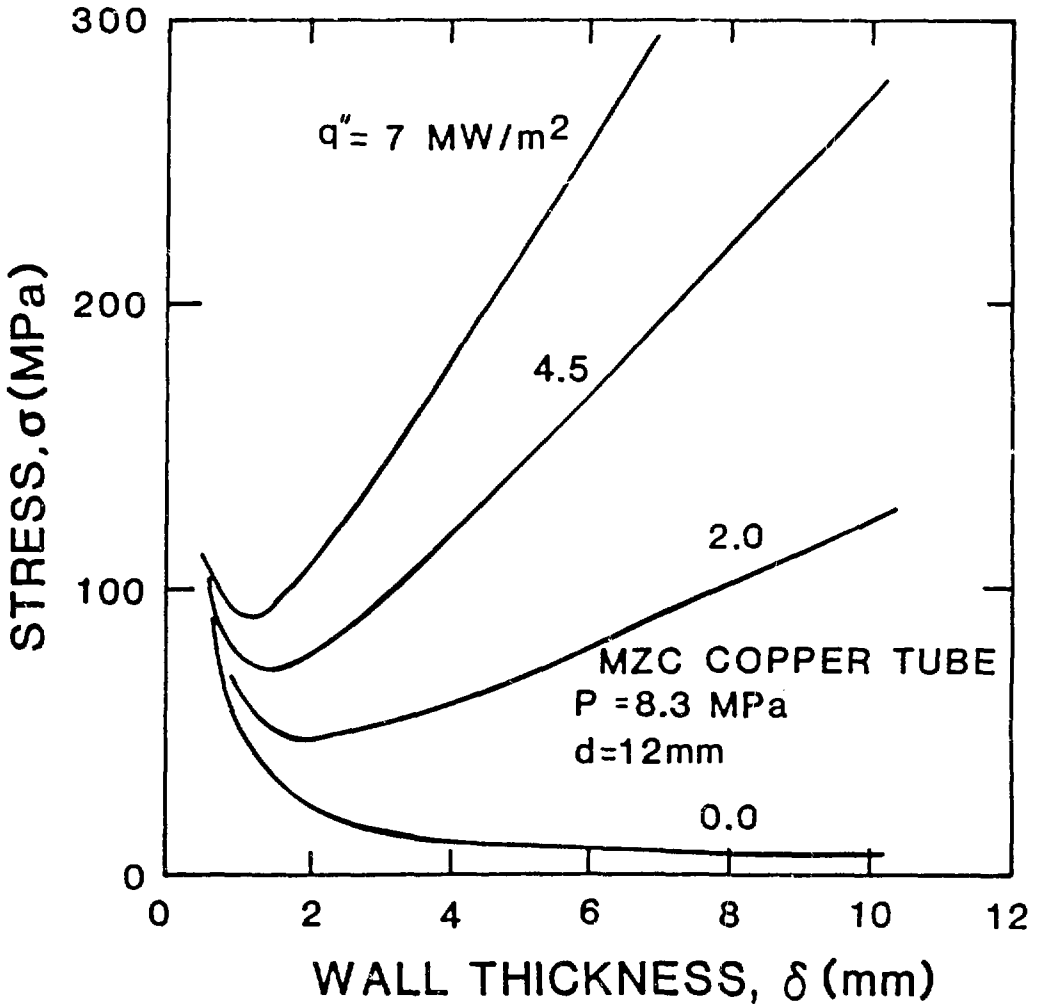
300
200
100
0
STRESS, σ (MPa)
q"= 7 MW/m2
4.5
2.0
0.0
MZC COPPER TUBE
P =8.3 MPa
d=12mm
0
2
4
6
8
10
12
WALL THICKNESS, δ (mm)

FIRST WALL

Composition: 60 v/o AMAX Cu(MZC, 0.06% Mn, 0.15% Zr, 0.4% Cr by weight)

40 v/o H_2O (Coolant)

Overall thickness (mm)	20
Total first-wall mass (tonne)	31
Number of coolant tubes facing plasma	774
Tube length/diameter/wall thickness (mm)	243/24.3/3.0
Subcooled water pressure (MPa/psia)	8.27/1200
Coolant velocity (m/s)	10.3
Inlet/outlet/maximum wall temperature (K)	423/503/590
Average/maximum design surface heat flux (MW/m^2)	5.0/9.0
Average power density (MW/m^3)	200.0
Maximum dpa/yr	220.0
Average transmutation rates Ni/Zn (%/yr)	2.6/2.2
Electrical resistivity increase (%/yr)	100-200

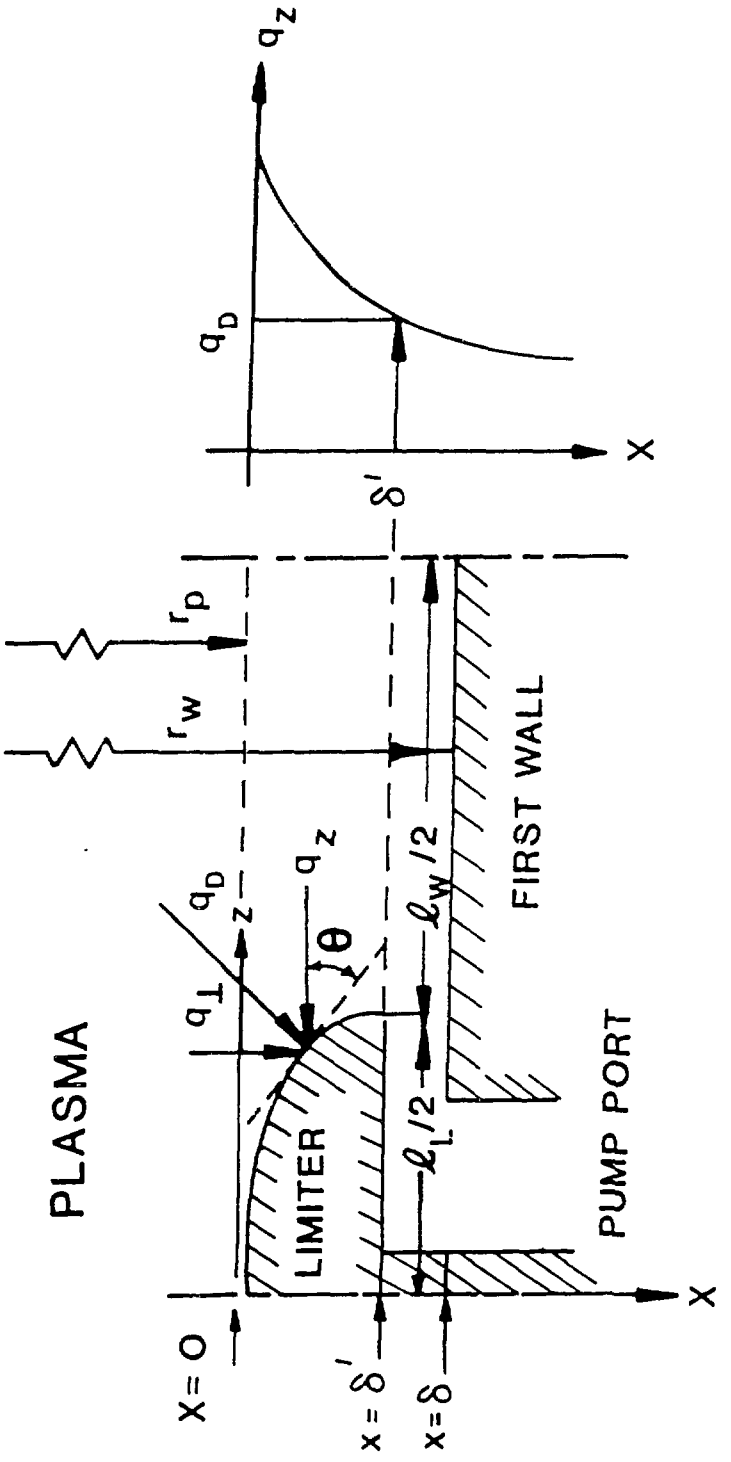
q_z
q_D
X
δ'
r_p
r_w
FIRST WALL
q_z
q_D
z
θ
$q_\perp$
$\ell_w/2$
PLASMA
LIMITER
$\ell_L/2$
PUMP PORT
X
X= O
x= δ'
x= δ

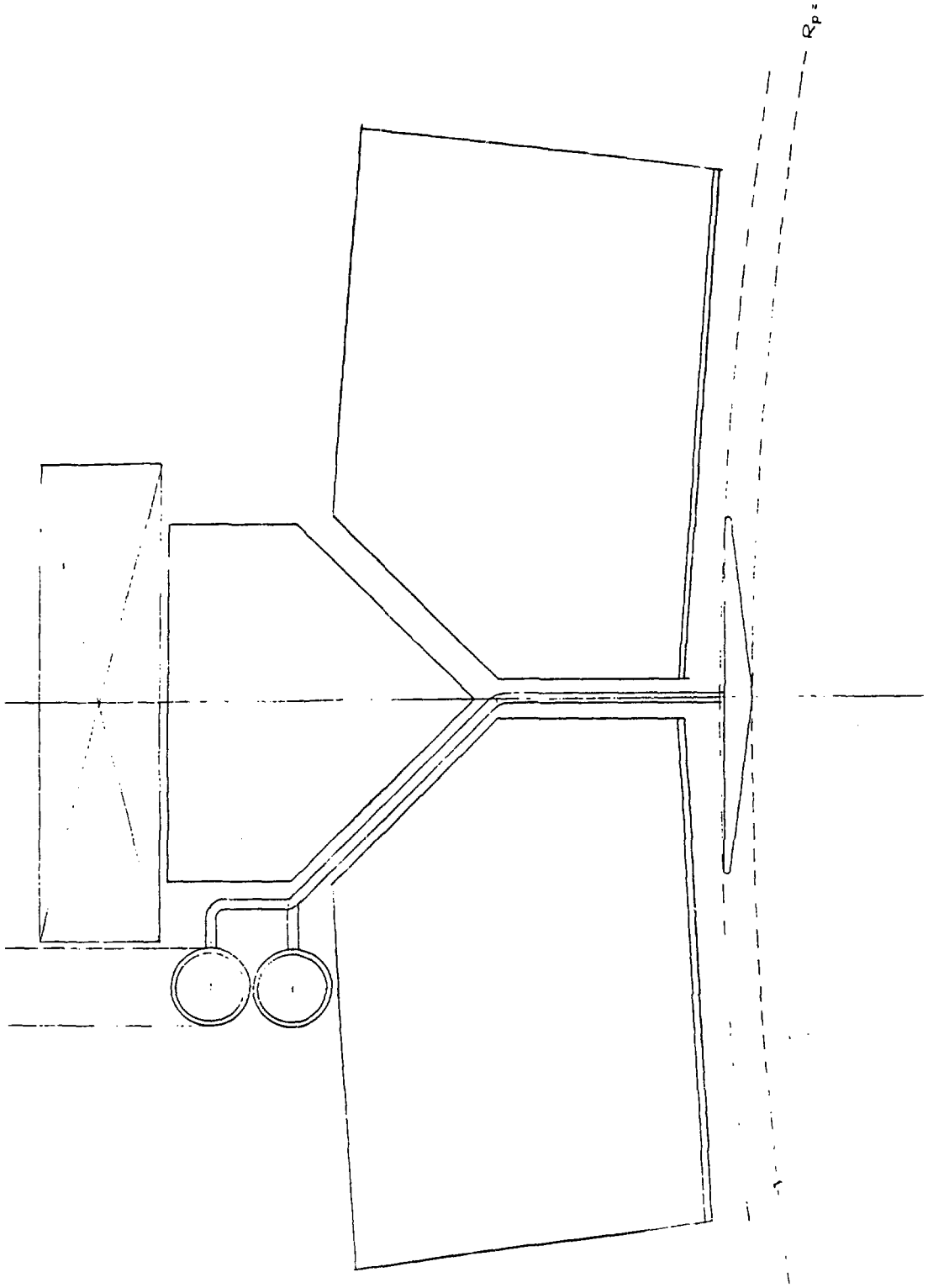
$R_{p=}$

PUMPED-LIMITER PARAMETERS

Configuration	Poloidal
Number of limiters, N	24
Edge-plasma recycle, R_L^*	0.95
Fraction plasma energy loss radiated, f_{RAD}	0.90
Design heat flux onto limiter, q_D (MW/m^2)	6.0
Limiter coverage fraction, $\ell_L/(\ell_L + \ell_w)$	0.31
Toroidal extent of limiter, ℓ_L (m)	0.35
Fraction particles under limiter, f_p	0.21
Fraction energy under limiter, f_E	0.13

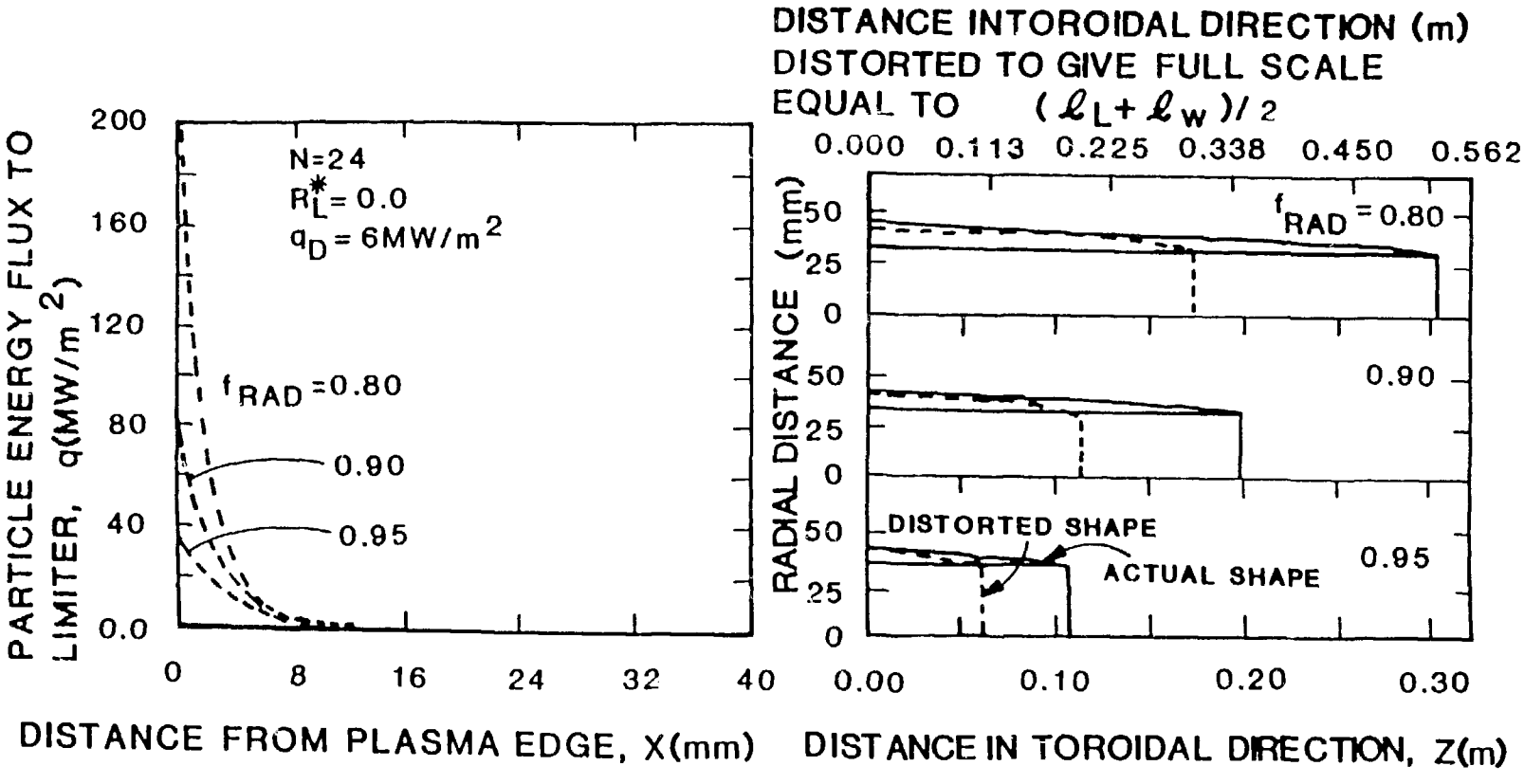
PARTICLE ENERGY FLUX TO LIMITER, q(MW/m^2)
200
160
120
80
40
0.0
N=24
R_L^* = 0.0
q_D = 6MW/m^2
f_{RAD} =0.80
0.90
0.95
0
8
16
24
32
40
DISTANCE FROM PLASMA EDGE, X(mm)
DISTANCE INTOROIDAL DIRECTION (m)
DISTORTED TO GIVE FULL SCALE
EQUAL TO $(\ell_L + \ell_W)/2$
0.000 0.113 0.225 0.338 0.450 0.562
RADIAL DISTANCE (mm)
50
25
0
f_{RAD} = 0.80
0.90
DISTORTED SHAPE
ACTUAL SHAPE
0.95
0.00
0.10
0.20
0.30
DISTANCE IN TOROIDAL DIRECTION, Z(m)

BLANKET/THIRD WALL

Composition:

Blanket:	95 v/o PbLi, 5 v/o PCASS
Third wall:	80 v/o B_4C, 10 v/o PCASS, 10 v/o PbLi
(Alternating Layers)	80 v/o W, 10 v/o PCASS, 10 v/o PbLi
Blanket thickness (m)	0.5
Third wall thickness (m)	0.1
Total blanket mass, without coolant (tonne)	223
Neutron multiplication, M_N	1.295
Tritium breeding ratio, BR	1.11
Thermal energy recovery efficiency, ε_B	0.985
PbLi flow rate (kg/s)	69,500
Inlet/outlet/maximum wall temperature (k)	573/773/774
Pump work (MW/%)	16.7/1.7
Peak power density (in LiPb coolant, MW/m^3)	260
Average power density (MW/m^3)	28

TOROIDAL-FIELD COILS

Composition: 70 v/o Cu, 20 v/o PCASS, 10 v/o H_2O

Number, N	24
Coil radius/width/length (m)	1.43/0.15/0.6
Mass per coil (tonne)	5.9
Average toroidal field (on-axis/at conductor, T)	0.68/0.90
Total stored energy (MJ)	30
Total current per coil (MA)	0.54
Toroidal current density (MA/m^2)	6.06
Ohmic dissipation during burn (MW)	17.9
Maximum dpa/yr	1.22
Peak resistivity increase (%/yr)	0.7-1.4

POLOIDAL-FIELD COILS

Composition: 70 v/o Cu, 20 v/o PCASS, 10 v/o H_2O

OHC/EFC total mass (tonne)	393/405
OHC/EFC total current during burn (MA)	17.9/11.1
OHC/EFC current density (MA/m^2)	6.8/6.2
OHC/EFC dissipated power during burn (MWe)	51.6/55.4
PFC maximum stored energy (GJ)	1.45
Maximum dpa/yr	0.208
Peak resistivity increase (%/yr)	~ 0.1-0.2

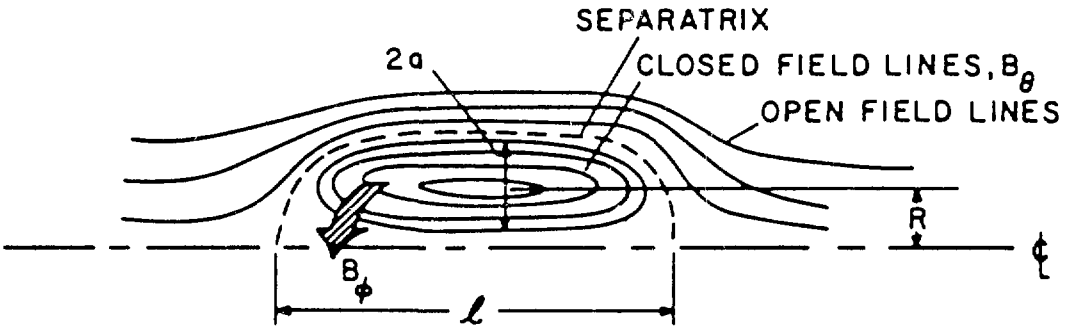

POLOIDAL (B_θ) vs TOROIDAL (B_ϕ) FIELD	LARMOR RADIUS << a (MHD-LIKE)	LARMOR RADIUS >> a (ORBIT-LIKE)
$B_\theta >> B_\phi \sim 0$	• FIELD-REVERSED MIRROR (FRM) • FIELD-REVERSED THETA PINCH (FRθP) (HIGH BETA)	• ASTRON-LIKE ION COMPRESSORS • e-LAYERS • p-LAYERS • REB-INJECTED TOROIDS
$B_\theta \cong B_\phi$	• SPHEROMAK • B_ϕ (a) = 0 REVERSED-FIELD Z-PINCH (RFP) (LOW BETA)	

COMPACT TOROID REACTORS

CONFIGURATION	TRANSLATING	STATIONARY
FIELD-REVERSED THETA-PINCH (FRθP)	CTOR (LANL)	TRACT (MSNW) LINUS (NRL, LANL) FRM (LLL, UI)
SPHEROMAK	KARIN - I (JAPAN) SPH (PPPL, UI)	SPH (PPPL)
HIGH-ENERGY RING	IRC (COR)	
HYBRID	MOVING - RING (PG & E, LLL)	

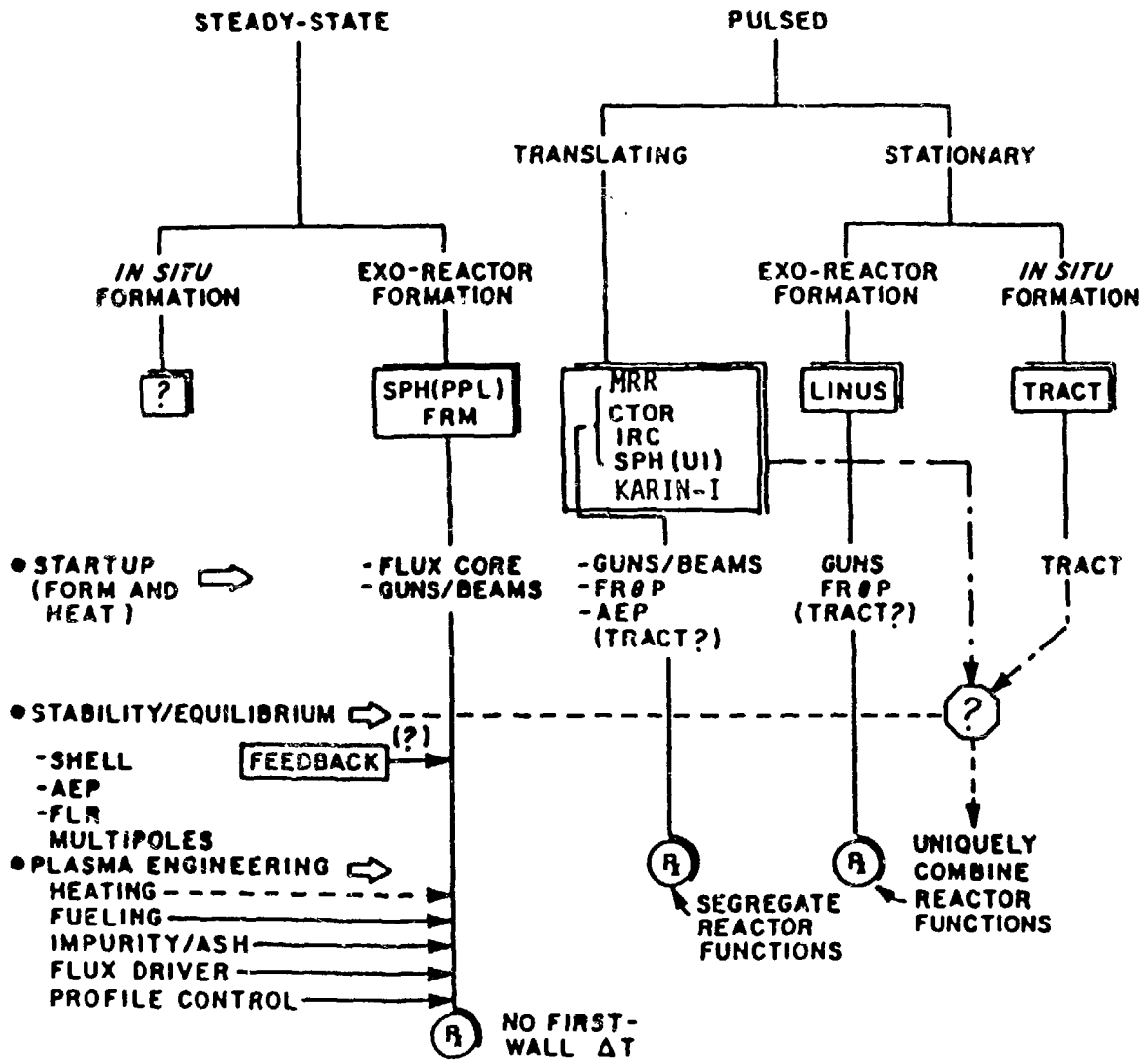
STEADY-STATE
PULSED
TRANSLATING
STATIONARY
IN SITU FORMATION
EXO-REACTOR FORMATION
EXO-REACTOR FORMATION
IN SITU FORMATION
?
SPH(PPL) FRM
MRR
CTOR
IRC
SPH (UI)
KARIN-I
LINUS
TRACT
• STARTUP (FORM AND HEAT)
- FLUX CORE
- GUNS/BEAMS
-GUNS/BEAMS
-FRθP
-AEP
(TRACT?)
GUNS
FRθP
(TRACT?)
TRACT
• STABILITY/EQUILIBRIUM
?
(?)
FEEDBACK
-SHELL
-AEP
-FLR
MULTIPOLES
• PLASMA ENGINEERING
HEATING
FUELING
IMPURITY/ASH
FLUX DRIVER
PROFILE CONTROL
R
NO FIRST-WALL ΔT
R
SEGREGATE REACTOR FUNCTIONS
R
UNIQUELY COMBINE REACTOR FUNCTIONS

CT DESIGN COMPARISON

	(FRθP) TRACT (INIT-FINAL)	CTOR (INLET-OUTLET)	FRM (STEADY STATE)	LINUS (INIT-COMP)
FIRST-WALL RADIUS (m)	0.68	1.2-1.6	0.73	1.4-0.11
BURNER LENGTH (m)	10	40	22	10
SHELL RADIUS (m)	0.7(?)	1.7-2.1	---	1.4-0.11
SEPARATRIX RADIUS (m)	0.39-0.55	0.85-1.05	0.21	1.4
PLASMOID LENGTH (m)	2.3-3.0	5.0-8.0	0.42	10.0
BURN/DWELL TIME (s)	0.9/0.2	2.0/5.8	---	0.001/0.5
PLASMA DENSITY ($10^{20}/m^3$)	20	25-5	6.5	8.2-1900
PLASMA TEMP (keV) (PRECOMP/COMP/FINAL)	4.4/12/37	1.5/8/12	96	0.5/20/20
ENERGY CONF. TIME (s)	∿0.9	∿0.1	∿0.5	∿0.001
BURN MAGNETIC FIELD (T)	4.7	4.1-2.0	4.1	0.6-60
RING SPEED (m/s)	---	38-10	---	---
FIRST-WALL LOAD (MW/m^2) (AVE/PEAK)	7.48/38	2.0/5.8	1.8	?/260
PEAK SURFACE FLUX (MW/m^2)	1.3	∿0.4	---	---
BURN-SECTION POWER DENSITY (MWt/m^3)	1	0.5	0.4	∿20
NET/GROSS POWER	0.88	0.85	0.54	0.78
NET ELECTRIC (MWe)	99	310	74	900

A Compact-Toroid Fusion Reactor Based on the Field-Reversed Theta Pinch

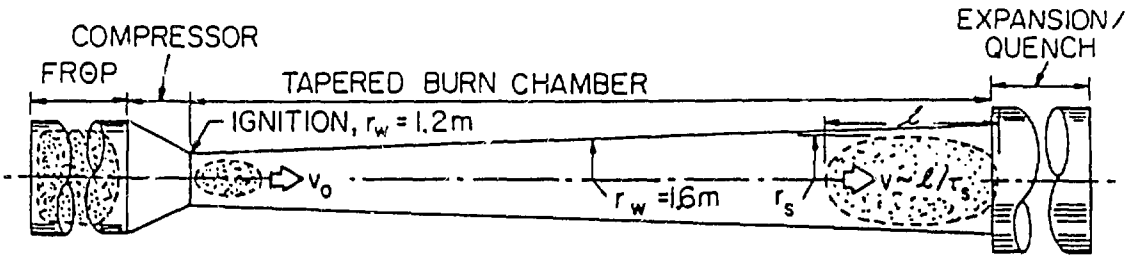

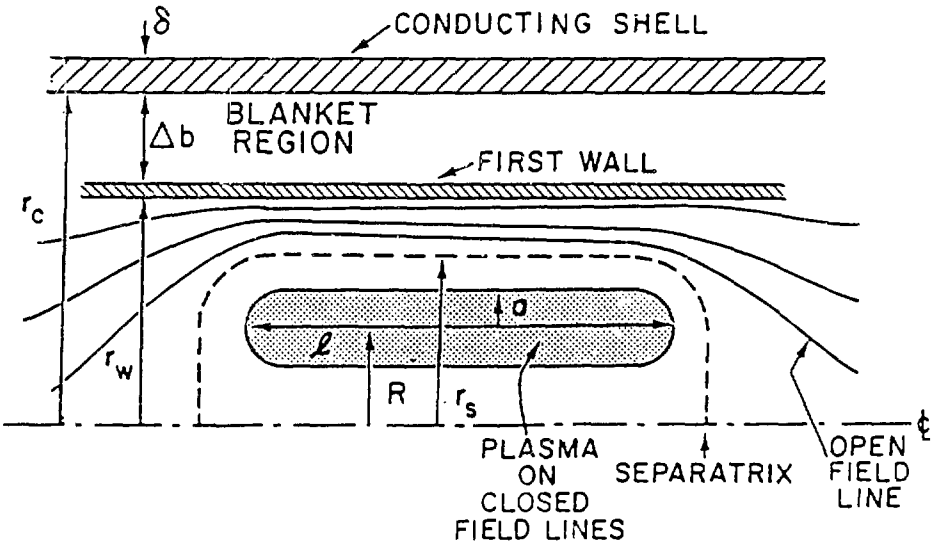

CT DESIGN COMPARISON

SPHEROMAKS

	SPH (PPPL) (STATIONARY)	SPH (UI) (TRANSLATING)	KARIN-I
FIRST-WALL RADIUS (m)	3.2	1.4	2.0
BURNER LENGTH (m)	6	8.5	50
SHELL RADIUS (m)	3.2	1.4 (?)	2.0 (?)
SEPARATRIX RADIUS (m)	3	1.05	2.0
PLASMOID LENGTH (m)	3	0.7	1.0
BURN/DWELL TIME (s)	---	~8.5/5	10/1
PLASMA DENSITY ($10^{20}/m^3$)	2.1	~3	4.8
PLASMA TEMP (keV) (PRECOMP/COMP/FINAL)	15	15	1.6/9.3/9.3
ENERGY CONF. TIME (s)	1.4	~1.0	~1.0
BURN MAGNETIC FIELD (T)	4.0	5.0	2.88
RING SPEED (m/s)	---	~1	5
FIRST-WALL LOAD (MW/m^2) (AVE/PEAK)	4.0/	7.8/	2.4/
PEAK SURFACE FLUX (MW/m^2)	?	?	?
BURN-SECTION POWER DENSITY (MWt/m^3)	1.3	~1	0.7
NET/GROSS POWER	---	~0.75	0.74
NET ELECTRIC (MWe)	1000 (thermal)	200	647

STATIONARY SPHEROMAK (PPPL)

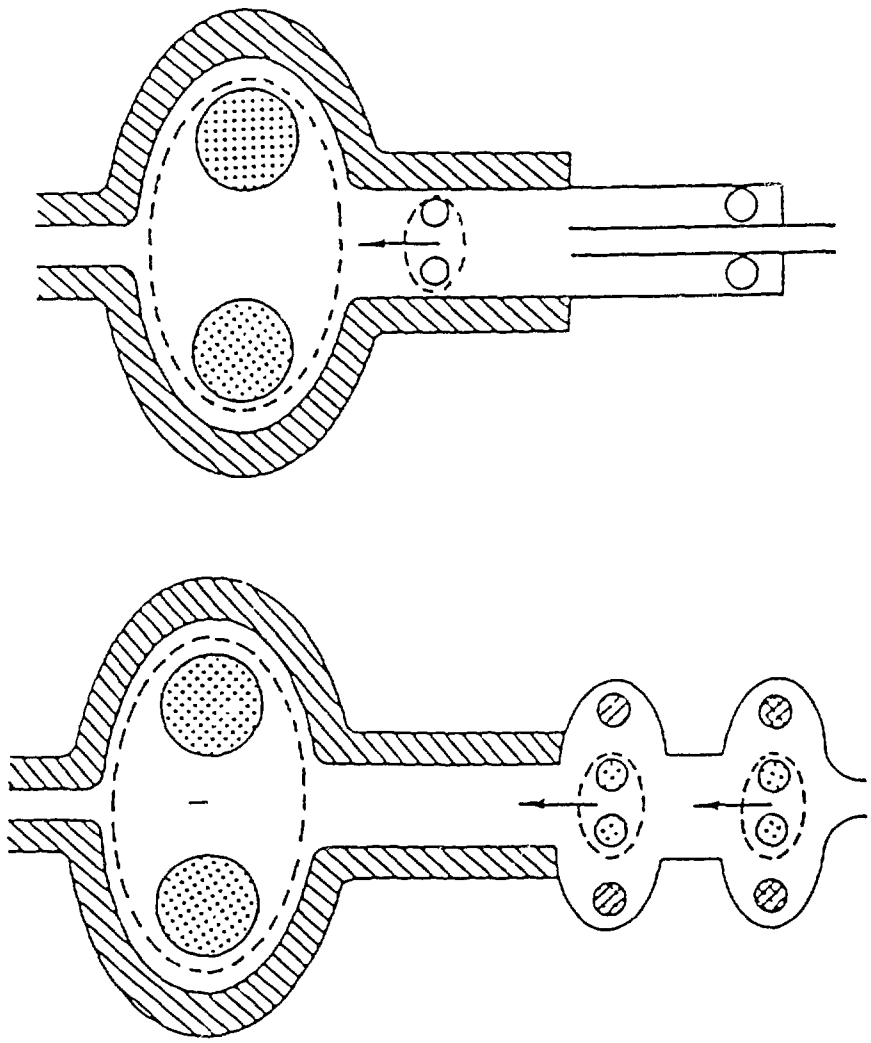

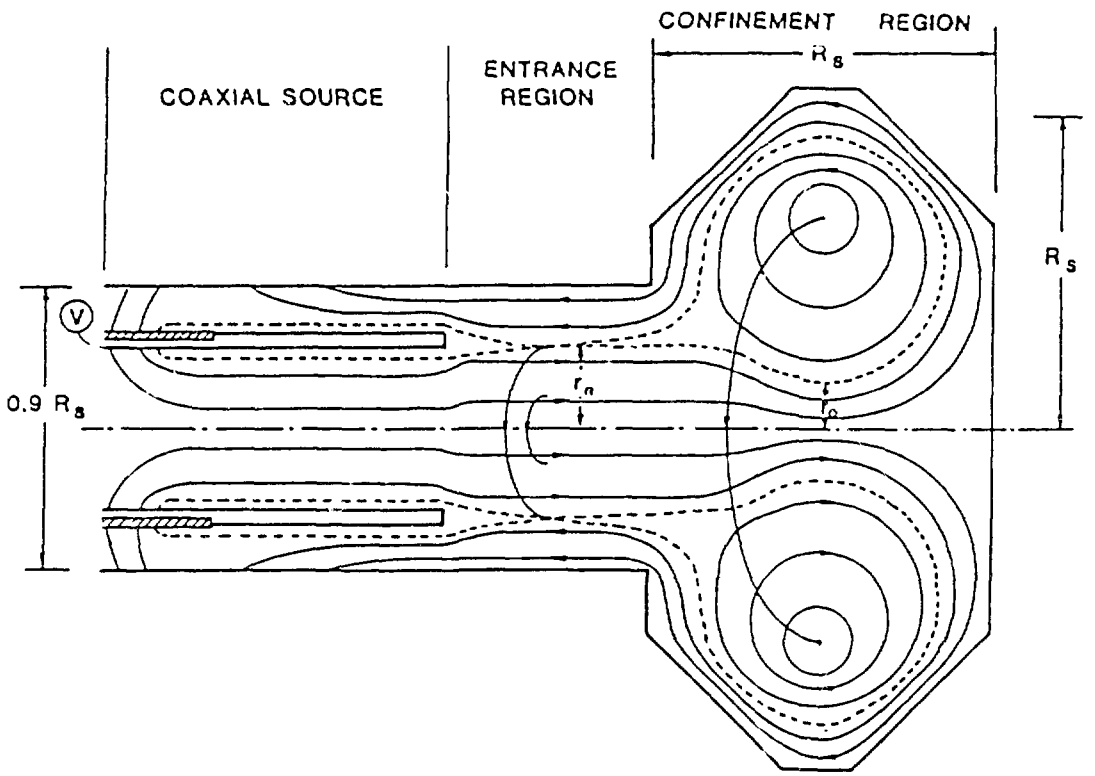
CONFINEMENT REGION
R_s
COAXIAL SOURCE
ENTRANCE REGION
R_s
V
0.9 R_s
r_a
r_o

FUTURE ENGINEERING NEEDS OF BOTH MAINLINE AND COMPACT APPROACHES

- Plasma engineering (auxiliary and/or startup heating, impurity/ash/fuel control, current drive versus long-pulsed operation).
- First-wall/limiter systems (transient thermal effects, sputtering, radiation effects, tritium permeation/ retention/recycle, end-of-life mechanism(s) and lifetime, maximum operating temperature and overall plant efficiency).
- Blanket/shield (materials compatibility, radiation damage, solid-breeder properties versus liquid-metal breeder containment).
- Magnets (thermomechanical/electromechanical properties, radiation effects to conductors and insulators, reliability, maximum fields and hybrid magnets, size/modularity).
- Remote maintenance (better definition of maintenance scheme and downtime, need for less massive modules, quantify relative merits of block versus patch maintenance FPC reliability analysis).

SUMMARY OF COMPACT REACTOR TECHNOLOGY REQUIREMENTS

Plasma Engineering Systems

- Operate with high toroidal current density ($\geq$ 10 MA/m^2) in a dense plasma to achieve DT ignition by Ohmic heating alone, possibly with auxiliary-heating boost or plasma preconditioning in order to minimize volt-second consumption while attaining ignition.

- Understand means to provide fueling, impurity/ash control, and steady-state current drive in dense plasma.

- Plasma edge control, dense gas blanket, isolation of plasma from FW.

- Examine potential of compact options for confinement systems that operate with currentless plasma.

SUMMARY OF COMPACT REACTOR TECHNOLOGY REQUIREMENTS (cont-2)

Nuclear Systems

- High heat-flux (3-5 MW/m^2) FW and high-power-density breeding blanket (100 MWt/m^3 peak, 50 MWt/m^3 average) precludes use of PCASS at the FW and solid tritium breeders within the blanket.

- Control/understand FW sputter erosion through use of magnetic divertor, dense gas blankets, and/or tailoring of plasma edge conditions.

- Interrelationship between FW temperature, FW life-limiting mechanisms, maximum blanket temperature, blanket thickness, and overall plant efficiency needs better resolution.

- Single/few-piece FW/B/S construction for purposes of block maintenance requires careful resolution, particularly with respect to coolant and vacuum ducting.

- Better resolve tradeoff between reduced inner coil shield thickness and with increased biological and exo-FPC equipment radiation shielding.

- Better resolve interrelationships between overall system stress, reliability, and availability.

SUMMARY OF COMPACT REACTOR TECHNOLOGY REQUIREMENTS (cont-3)

Magnet Systems

- Very high-field (30 T) first-wall resistive OH coils required by Ohmically-heated compact tokamak reactor (Riggatron).
- Most compact systems require resistive coils to operate in high radiation field.
- Need exists to understand response of such coils (conductor and insulation) and life-limiting mechanisms (swelling, resistivity change, structural integrity, etc.).
- Certain compact options successfully trade off higher recirculating power and BOP cost for reduced shield and coil costs; this tradeoff requires additional study.

SUMMARY OF COMPACT REACTOR TECHNOLOGY REQUIREMENTS (cont-4)

Remote Maintenance

- The basic maintenance approach differs considerably from the conventional mainline and AFC concepts; total block maintenance of the FW/B/S (200-400 tonne) is proposed. The merits of block versus patch maintenance require further examination.

- The topology of coolant and vacuum ducts, the size of which should not change for a given total power output, and the FPC, which is decreased in volume by a factor of 10-30, must be resolved and reconciled with the "block" maintenance approach.

HIGH STRENGTH-HIGH CONDUCTIVITY AMZIRC COPPER AND AMAX-MZC ALLOY

P. W. Taubenblat

AMAX Base Metals R&D, Inc.

ABSTRACT

AMZIRC copper (Cu-0.15Zr) and AMAX-MZC alloy (Cu-0.03Mg-0.1Zr-0.6Cr) are two copper base materials which offer combinations of strength, high softening temperature and good electrical and thermal conductivity. By varying fabrication sequences, mechanical properties can be modified to meet a variety of electronic and electrical needs in military and commercial applications. AMAX-MZC copper alloy, in the form of 30 AWG wire, attains a strength level of 85 ksi and an electrical conductivity of 80% IACS. AMZIRC copper's strength is slightly less, but compensates with better conductivity. Relatively high softening temperatures, between 425 and 500 C, are characteristic of the two materials with AMAX-MZC alloy having the better resistance to softening.

INTRODUCTION

AMZIRC and AMAX-MZC are materials that provide excellent room temperature mechanical properties, good electrical conductivity and retention of strength at elevated temperatures. The nominal composition of the two alloys are shown in Table I.

Table I

Chemical Composition of AMZIRC Copper and AMAX-MZC Alloy

	Nominal Composition, Wt %			
	Zr	Mg	Cr	Cu
AMZIRC	0.15	-	-	Bal
AMAX-MZC	0.1	0.03	0.6	Bal

Figure 1 is an equilibrium phase diagram of copper-zirconium in the region of the AMZIRC composition. It is a typical precipitation hardening system, with the solubility of the second phase a function of the

temperature. At 950 C (1740 F), for example, about 0.13% zirconium is soluble in copper and this amount is retained on quenching from this temperature. A subsequent aging treatment at 400 to 500 C (750 to 930 F) causes precipitation of Cu_5Zr finely dispersed in the copper matrix. Because of the relatively small amount of precipitated phase, AMZIRC copper develops its strength through cold working and relies on precipitation to prevent recrystallization thus imparting high temperature strength and high conductivity.

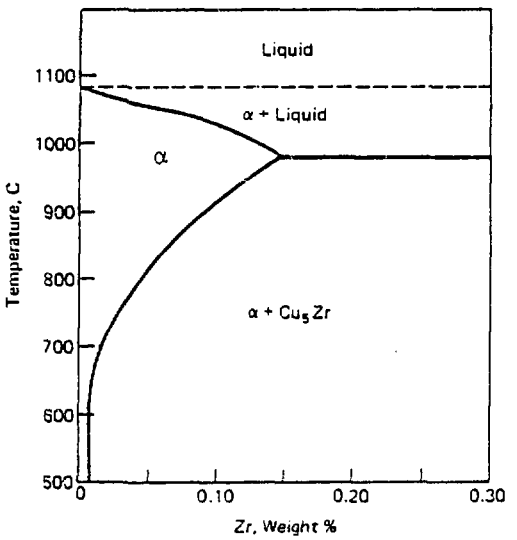

Figure 1 - Copper-Zirconium Equilibrium Phase Diagram

AMAX-MZC alloy differs from AMZIRC copper in that there are considerably more second phase precipitates in the former, consequently there is appreciable strengthening and hardening during aging by impediment to dislocation motion. Quenching AMAX-MZC alloy from hot work is, in most cases, enough to keep the alloying elements in solution. This is possible because magnesium in this alloy makes the precipitation of the second phase more sluggish than for most other age-hardenable alloys. Nevertheless, solution annealing of AMAX-MZC may be desirable to increase the homogenity and achieve additional improvement in mechanical properties. While the basic mechanical properties of AMAX-MZC alloy are developed by cold work, subsequent aging improves not only the electrical conductivity and ductility but also the strength.

Casting Procedures

AMZIRC and AMAX-MZC are members of a family of copper alloys produced with an oxygen-free copper base. Consequently, the small quantities of reactive elements needed to develop optimum properties can be added to the copper without loss by oxidation. Furthermore, melting and casting is done under a protective atmosphere to further prevent oxidation and permit the production of compositions within closely controlled limits. All materials are semi-continuously cast to assure more uniform and sound products. A typical cast structure of the AMAX-MZC alloy is shown in Figure 2.

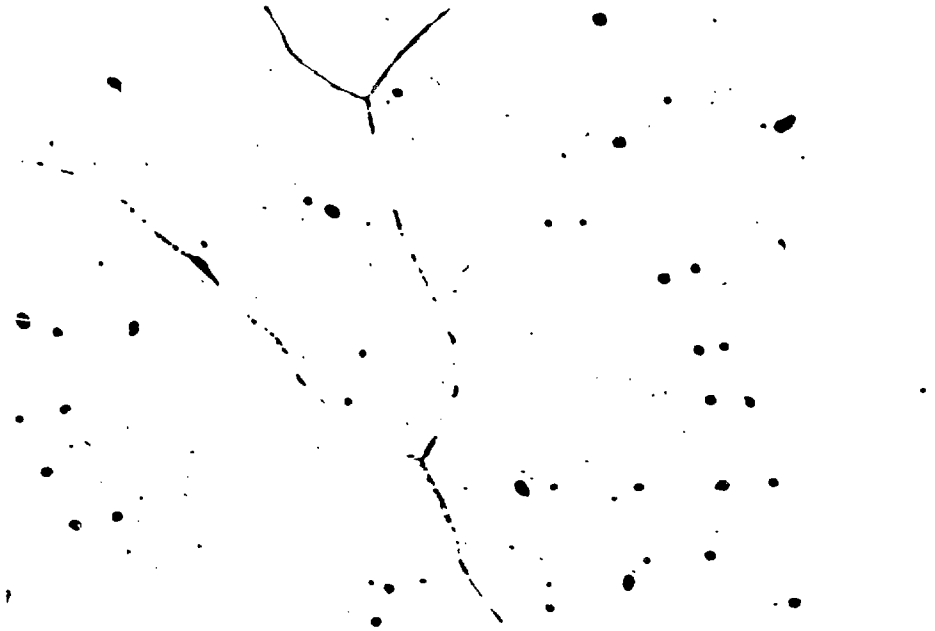

Figure 2 - Cast Structure of AMAX-MZC Alloy Showing Distribution of Second Phase (200X).

Both AMZIRC and AMAX-MZC are available as billets and cakes in the sizes shown in Table II.

Table II

	Diameter in.	Cross-Section in.	Weight lb/in. of length
Billets	8	-	16
	12	-	36
	14	-	49
	22	-	121
Cakes	-	6x17	33
Cakes	-	8x25	65
Wirebars	-	4x4	5

Production of Wire

An outline of the temperatures recommended for fabrication of AMZIRC or AMAX-MZC wire is given in Table III. Billets are usually hot extruded to rod and, depending on the finished product size, the rod is solution heat treated at 900 to 975 C (1650 to 1790 F), quenched, drawn and aged at the temperatures indicated in the table to develop optimum properties.

Table III

Recommended Temperatures for Production of Wire

1. Hot Working	:	790 to 900 C (1450 to 1650 F)
2. Solution Annealing	:	900 to 975 C (1650 to 1790 F)
3. Aging		
AMZIRC	:	400 to 450 C (750 to 840 F)
AMAX-MZC	:	450 to 500 C (840 to 930 F)

Figure 3 shows a typical cold worked and aged structure of AMAX-MZC alloy. Cold working after aging can be used to improve the strength but there is some reduction in electrical conductivity if this procedure is followed. However, as will be shown later, some of the electrical conductivity can be restored by an additional aging step without undue loss of strength.

Figure 3 - Structure of Cold Worked and Aged AMAX-MZC Alloy (150X).

Mechanical Properties

Room Temperature

Typical room temperature properties of the two materials in the form of wire are shown in Table IV. These data indicate that the tensile strength of solution annealed AMAX-MZC alloy is more than doubled by cold work of at least 90% followed by aging and that the electrical conductivity after aging increases from 52 to 80% IACS. AMZIRC copper follows a similar pattern.

Table IV

Typical Room Temperature Properties of AMZIRC Copper and AMAX-MZC Alloy

	Wire Dia in.	Wire Gage	Treatment	Tensile Strength ksi	Yield Strength 0.1% Offset ksi	Elongation in 10 in. %	Electrical Conductivity % IACS
AMZIRC	0.128	8	SA, Quenched	34	5	26	68
	0.08	12	SA, CW 61%, Aged 1 hr at 425 C (800 F)	64	53	6	88
	0.051	16	SA, CW 84% Aged 1 hr at 425 C (800 F)	67	58	6	86
AMAX-MZC	0.128*	8	SA, Quenched	37	-	26	52
	0.08	12	SA, CW 61% Aged 1/2 hr at 475 C (885 F)	75	68	11**	76
	0.08	12	SA, CW 90% Aged 1 hr at 450 C (840 F)	85	75	13**	80
	0.04	24	CW 60%, Aged 1/2 hr at 450 C (840 F), CW 93%	102	98	4.3**	67
	0.004	37	SA, CW 99%	105	85	1.9	74

* Data on AMAX-MZC courtesy of Hudson Wire Company
** Values in 2 in.

The strength of AMAX-MZC alloy can be modified substantially by initial solution heat treating at different temperatures as indicated in Figure 4.

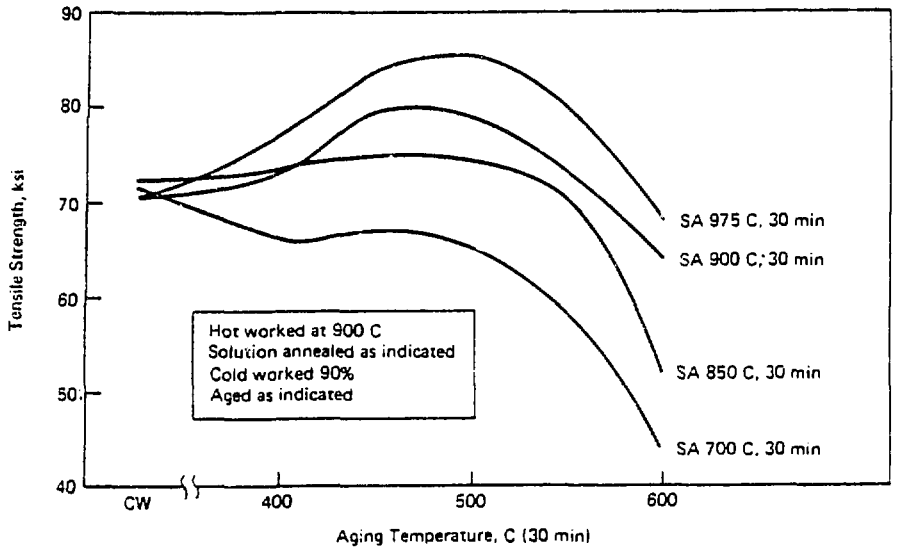

Figure 4 - Effect of Aging on Tensile Strength of AMAX-MZC Solution Annealed at Various Temperatures.

Electrical conductivity is also affected by the initial solution annealing temperature but that change is less pronounced, as shown in Figure 5.

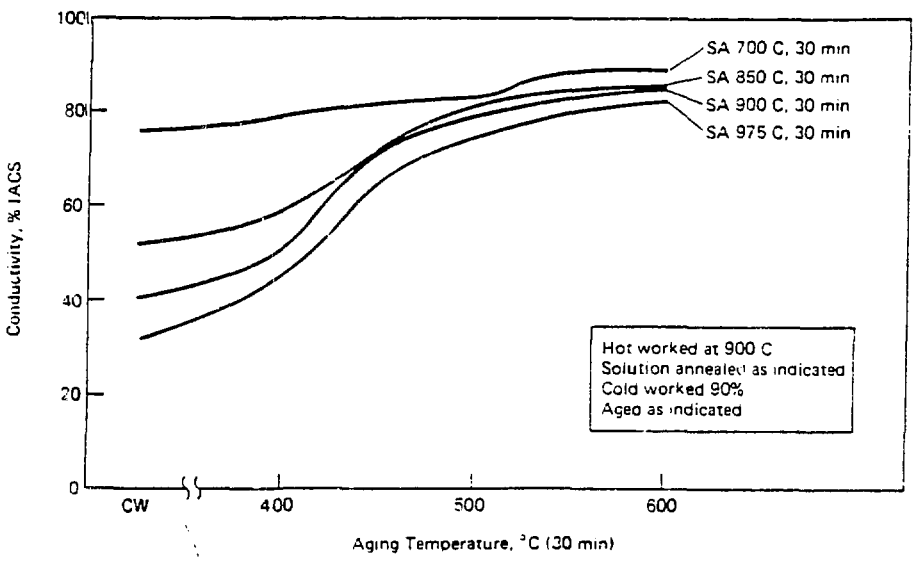

Figure 5 - Effect of Aging on the Electrical Conductivity of AMAX-MZC Solution Annealed at Various Temperatures.

Figure 6 shows how the degree of cold work affects the hardness of the solution annealed materials. The modification of electrical conductivity for both alloys by selective aging of the 90% cold worked alloys is indicated in Figure 7. The conductivity rises with aging temperature due to increased precipitation of the second phase from the supersaturated copper matrix.

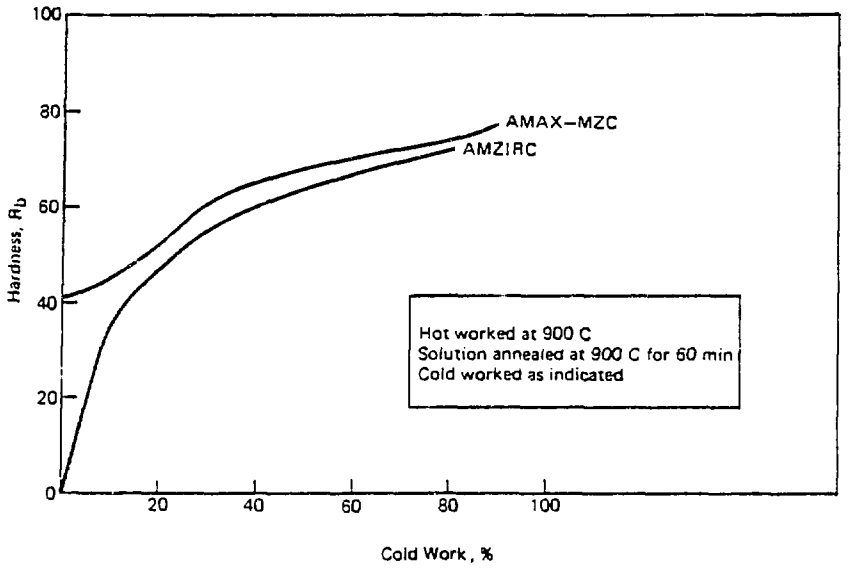

Figure 6 - Effect of Cold Work on Hardness of Solution Annealed AMZIRC and AMAX-MZC.

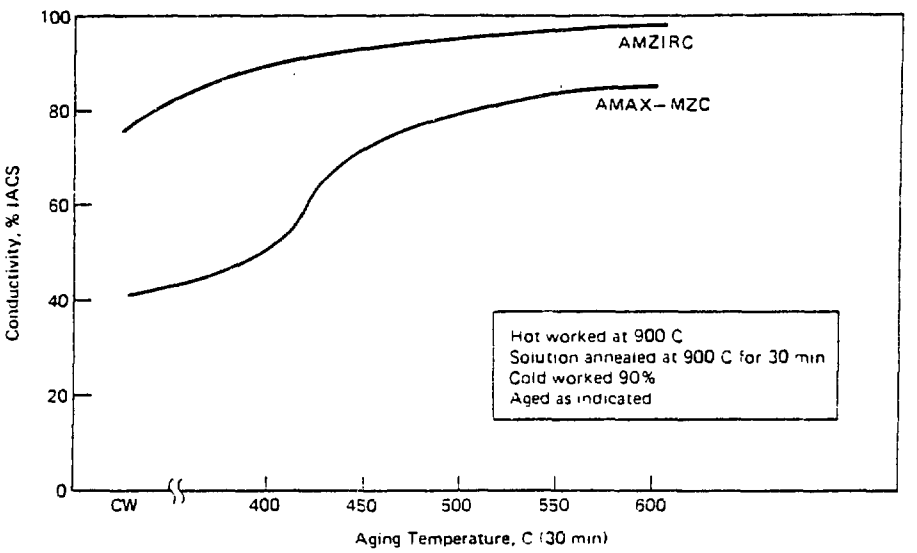

Figure 7 - Effect of Aging Tempeature on the Electrical Conductivity of AMZIRC and AMAX-MZC.

Secondary cold work after aging of AMAX-MZC alloy raises its strength as noted earlier but reduces the conductivity. The extent of the effect is illustrated in Figure 8. However, as indicated in Figure 9, re-aging can restore much of the conductivity without significant sacrifice of strength. Moreover, elongation is appreciably improved, rising from about 5 to over 11% as a result of such re-aging.

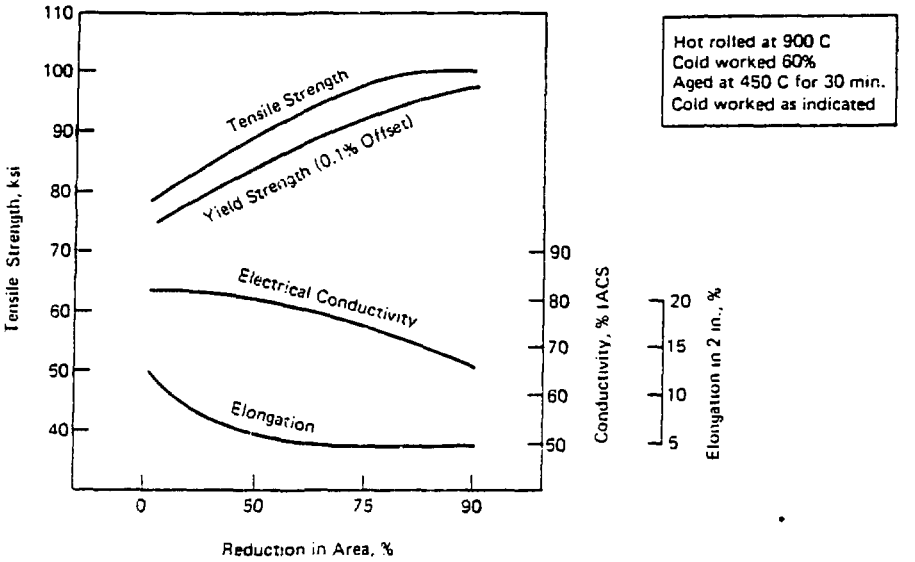

Figure 8 - Effect of Cold Work After Aging on the Mechanical Properties and Electrical Conductivity of AMAX-MZC.

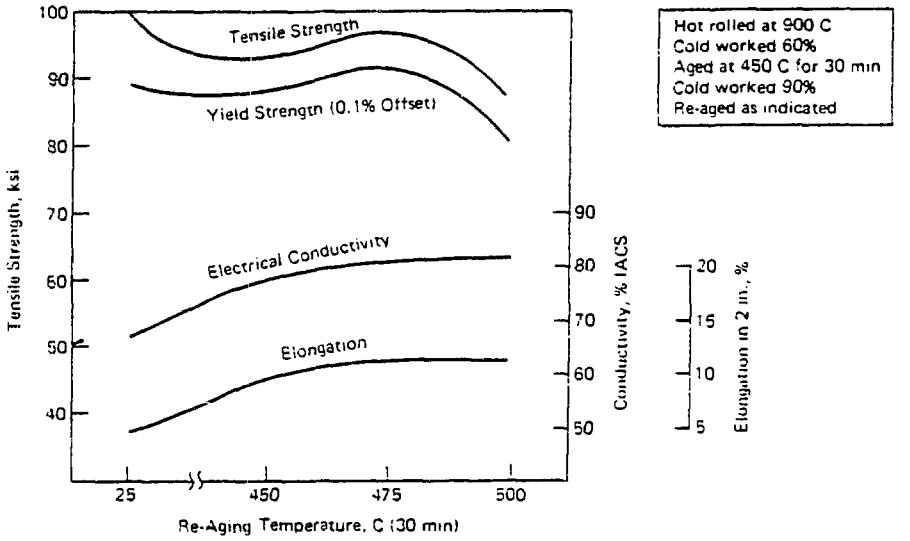

Figure 9 - Effect of Re-Aging Temperature on the Mechanical Properties and Electrical Conductivity of AMAX-MZC.

In all deformation processes ductility is of prime importance. One measure of such ductility can be obtained by a simple torsion or twist test. Figure 10 shows the effect of aging on the ductility of AMZIRC copper and AMAX-MZC alloy as measured by such a twist test. The number of twists reached 74 after aging at 450 C (840 F). By comparison, tough pitch copper, after annealing, survived only 60 twists before failure.

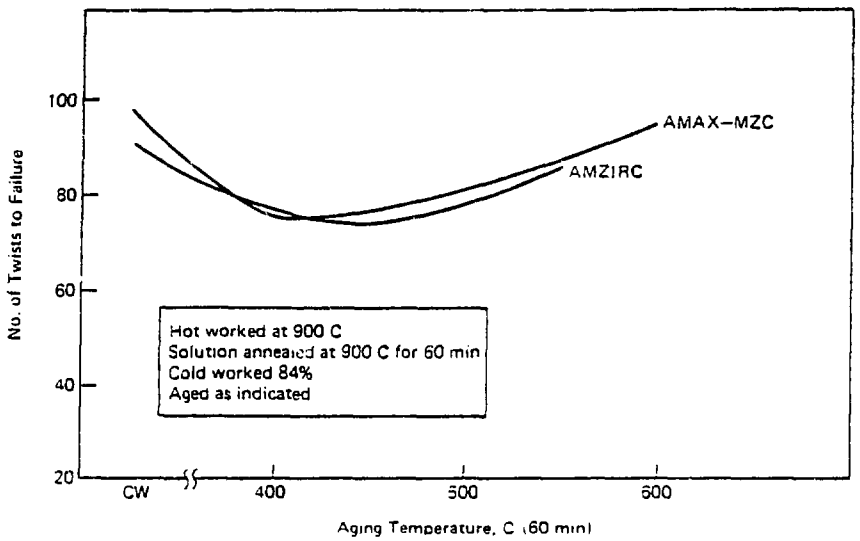

Figure 10 - Effect of Aging Temperature on Number of Twists to Failure for 84% Cold Worked AMZIRC and AMAX-MZC.

Elevated Temperature Properties

Elevated temperature properties are becoming increasingly important in the selection of materials for use in the aircraft industry, high-speed electric motors and continuous-casting molds. In these applications, sudden temperature increases reaching several hundred degrees are not uncommon. For this kind of use both AMZIRC and AMAX-MZC alloy have demonstrated their excellent short-time elevated temperature tensile properties which are noted in Table V with related creep properties shown in Table VI. Both materials have good resistance to creep formation at temperatures as high as 400 C (750 F).

Table V

Short Time Elevated Temperature Tensile Properties of AMZIRC Copper & AMAX-MZC Alloy After Cold Working 84% & Aging

	Test Temperature C	Test Temperature F	Tensile Strength ksi	Yield Strength 0.2% Offset ksi	Elongation in 2 in. %
AMZIRC	300	570	54	-	10
	400	750	52	44	8
AMAX-MZC	200	390	59	53	13
	300	570	57	54	13
	400	750	57	-	13

Table VI

Creep Properties of AMZIRC Copper & AMAX-MZC Alloy After Cold Working 84% and Aging

	Test Temperature C	Test Temperature F	Stress for Creep of: 0.00001%/hr ksi	0.0001%/hr ksi	0.001%/hr ksi
AMZIRC	300	570	35	39	44
	400	750	19	23	26
AMAX-MZC	300	570	40	45	50
	400	750	21	26	33

The electrical conductivity of copper and copper-base materials characteristically decreases with increasing temperature. As shown in Figure 11, the conductivity of AMZIRC copper falls from approximately 90% IACS at room temperature to about 40% at 400 C (750 F) and AMAX-MZC alloy follows a similar trend.

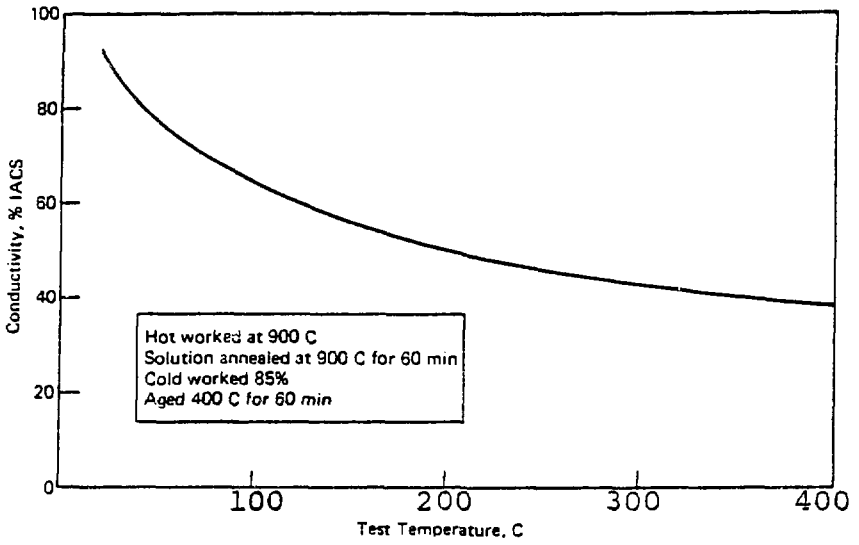

Figure 11 - Effect of Temperature on the Electrical Conductivity of Cold Worked and Aged AMZIRC.

Applications

The excellent electrical conductivities and elevated temperature mechanical properties of AMZIRC copper and AMAX-MZC alloy have led to a number of applications in electrical and electronic components such as commutators, electrical switches, solderless wrapped connectors, stud bases and resistance welding tips and wheels. Other applications have included high temperature magnet wire, canned motor windings, rotor wedges, electrical clamps, oxygen lance tips, and pistons for plastics presses as well as molds for continuous casting machines. A more detailed description of some of these applications follows.

Aircraft and Missile Wire

For wire use in aircraft or missiles, materials must exhibit a combination of high temperature strength retention, high electrical conductivity and good elongation in the finished product. After appropriate processing treatment, AMAX-MZC alloy can meet the performance criteria specified below:

Ultimate Tensile Strength	65-75 ksi
Electrical Conductivity	85% IACS min
Elongation (in 10 in.)	8% min

Commutators

Both materials offer superior strength and toughness in addition to excellent conductivity, which makes them suitable for use in commutator assemblies. Such assemblies produced with AMZIRC copper have been operated at 330 C (625 F) without failure. Because of AMZIRC copper's thermal stability, the alloy has twice the permissible power rating of comparable silver-bearing copper in commutator use.

Electrical Switches

A combination of good electrical conductivity and high tensile strength makes these materials desirable for switch-jaws, current-carrying springs and similar parts. Silver-bearing copper tends to soften under the heat generated by arcing at contact points of the switch-jaws and steel back-up springs are required for satisfactory service. No steel back-up springs are required when AMZIRC alloy is used because of its superior elevated temperature strength retention properties.

Solderless Wrapped Connectors

To be reliable solderless wrapped connections must maintain a constant contact force with the post over which they are wound for long periods of time. In some applications, relaxation could occur as a result of vibration and exposure to moderately elevated temperatures. Accelerated tests have indicated that AMZIRC copper in this application may retain 70% of its initial yield strength even after 40 years service at 150 C (300 F). Under the same conditions, silver-bearing copper would be unsuitable for service.

Stud Bases

Ductility and high thermal conductivity are required to meet manufacturing and operating conditions in which thin sections designed as heat carriers are also subject to torque stresses. Flat bottom stud bases for power rectifiers and diodes are examples of parts that require high resistance to torque to permit tight mounting for maximum heat transfer.

Improved performance has been achieved by using AMZIRC copper for such mounting studs. This copper withstands a 150% higher installation torque than the materials used previously and maintains adequate heat conductivity in the face of vibration.

Resistance Welding Tips and Wheels

Both AMZIRC copper and AMAX-MZC alloy rods can be produced to meet the Resistance Welding Manufacturers Association Specifications for Group A, Class I materials. In addition, as both materials retain most of their strength up to a temperature of 450 C (840 F), they make excellent materials for resistance welding electrode tips. By varying mill practice, both materials can be processed to meet the requirements of RWMA Group A, Class II materials which is used for welding wheels.

Wheel Molds for Continuous Casting

With the increasing use of continuous casting systems using wheel-type molds, there has been a rising demand for improved mold materials. Both tough pitch copper and steel molds were found to be lacking in either strength retention at elevated temperature or the necessary heat transfer properties. Silver-bearing and chrome copper could not withstand the thermal stresses and, in addition, chrome copper was found to be notch sensitive. In this application, AMAX-MZC alloy has shown itself to be able to provide the necessary heat transfer with better strength retention than silver-bearing or chrome copper and better resistance to thermal stress as well as less susceptibility to cracking.

PWT:rf

PROPERTIES OF BERYLLIUM COPPER ALLOY C17510

by

Amitava Guha
Brush Wellman Inc.
17876 St. Clair Ave.
Cleveland, Ohio 44110

ABSTRACT

This paper reviews the properties of beryllium copper Alloy C17510 employed in the manufacture of current-carrying springs in relays used for low-voltage, high-current applications. Specific data are given which compare the thermal, mechanical and electrical properties of this alloy at room temperature, and after elevated temperature exposure. In order to provide the designer with a comprehensive view of the alloy's performance, the paper also discusses the fabrication characteristics, bending fatigue strength and stress relaxation. Metallurgical characteristics that have led to the optimization of the alloy's performance are discussed.

INTRODUCTION

Due to the growing concern for product reliability, today's electronic components require materials that provide greater electrical and thermal conductivity, higher mechanical strength and improved resistance to stress relaxation in service. The trend toward miniaturization in the electronics industry has prompted the use of high strength copper alloys as the primary material for meeting design requirements for reliable mechanical properties. In addition, the need for a material with greater electrical and thermal conductivity particularly for high current applications has also become apparent. With the increase in the current carrying capacity of the switches, relays and electric terminals, temperature rise problems are encountered with materials possessing low electrical and thermal conductivity. Temperature rise has a deleterious effect on the spring contact performance for two reasons: first, it affects stress relaxation, which is strongly dependent upon the service temperature; second, the increase in the temperature causes the material to oxidize, thus altering the surface characteristics and increasing the contact resistance of the material.

Beryllium Copper Alloy C17510, developed by Brush Wellman to be an economical, high conductivity, moderately high strength copper alloy, offers the designer a high performance material. Development of Alloy C17510 was made possible through Brush Wellman's research effort to substitute less critical alloying elements as strengthening additions in high conductivity beryllium copper. In particular, the critical element most affected is cobalt which has been replaced by nickel in C17510.

To examine the properties in perspective, Table I compares the nominal mechanical, electrical and thermal properties of this alloy with other commercial copper alloy spring materials available in strip form. As shown in this Table, the most important feature of C17510 is that it combines reasonably high strength with superior electrical and thermal conductivity. This paper characterizes the alloy in detail for applications in switches and relays for high current circuits requiring high conductivity and high strength. Comparisons have been made with the cobalt-containing alloy C17500, a beryllium copper alloy of the same strength/conductivity regime of Alloy C17510.

TABLE I Comparison of C17510 with Copper Alloy Current-Carrying Spring Materials

Copper Alloy Number	Alloy Condition	Tensile Strength ksi	Yield Strength 0.2% Offset ksi	Elongation % in 2 in.	Modulus of Elasticity in Tension psi	Electrical Conductivity % IACS	Thermal Conductivity BTU/ft.hr°F
C17510	**Cold Rolled and Aged**	**120**	**110**	**12**	**20 x 10^6**	**50**	**144**
C17200	Cold Rolled and Aged	200	180	2	19 x 10^6	22	60
C17500	Cold Rolled and Aged	120	110	12	20 x 10^6	50	115
C19400	Spring	73	70.5	2	17 x 10^6	65	150
C19500	Spring	93	90	4	17 x 10^6	50	115
C51000	Spring	100	80	4	16 x 10^6	15	40
C63800	Spring	128	110	4	17 x 10^6	10	23
C64400	Cold Rolled Extra Spring and Aged	160	155	1	17 x 10^6	13	36
C65400	Spring	129	118	2	17 x 10^6	7	21
C68800	Spring	129	110	2	17 x 10^6	18	23
C72500	Spring	91	90	1	20 x 10^6	11	31

NOTE: Data compiled from published literature and/or Standards Handbook, Wrought Copper and Copper Alloy Mill Products, Alloy Data, Part 2, Copper Development Association, Inc., New York, NY, 1973.

HEAT TREATMENT AND METALLURGICAL CONSIDERATIONS

Alloy C17510 is a precipitation hardenable beryllium copper alloy containing nickel. This ternary alloy contains beryllium in the range of 0.2 to 0.6 weight percent, and nickel in the range of 1.4 to 2.2 weight percent. The high electrical and thermal conductivity of the alloy in conjunction with reasonably high mechanical strength are achieved through a two-stage heat treatment. This comprises solution annealing in the temperature range of 1650-1700 F (900-927 C) to ensure solid solution of the alloying elements, beryllium and nickel, followed by a rapid quench to retain this condition at room temperature. The alloy in this state is subjected to a precipitation hardening treatment in the temperature range of 850-900 F (455-482 C) to precipitate finely dispersed particles which strengthen the matrix and increase the conductivity as the alloying elements are effectively removed from the solid solution.

Heat treatment for C17510 can be designed to develop optimum combinations of strength and electrical conductivity. The yield strength normally reaches a peak value during the aging cycle, after which it diminishes as a result of overaging. Electrical conductivity, on the other hand, increases with increasing time and/or temperature during aging. Figure 1 shows typical aging response of C17510 strip, cold worked 21 percent prior to aging, and aged for 8 hours at temperatures ranging from 850-1050 F (454-566 C). This plot demonstates that depending on the choice of aging temperature, a wide range of strength and electrical conductivity with reasonable tensile elongation can be attained in C17510 in the precipitation hardened condition.

To provide the high strength and hardness along with maximum electrical and thermal conductivity the composition of Alloy C17510 is selected to optimize weight ratios between the alloying elements, nickel and beryllium. The ratio of nickel to beryllium is related to the stoichiometric amount necessary to form nickel beryllide (NiBe) such that during precipitation hardening, the precipitation reaction removes nickel and beryllium from the solid solution to provide high conductivity and a fine precipitate dispersion in the copper matrix.

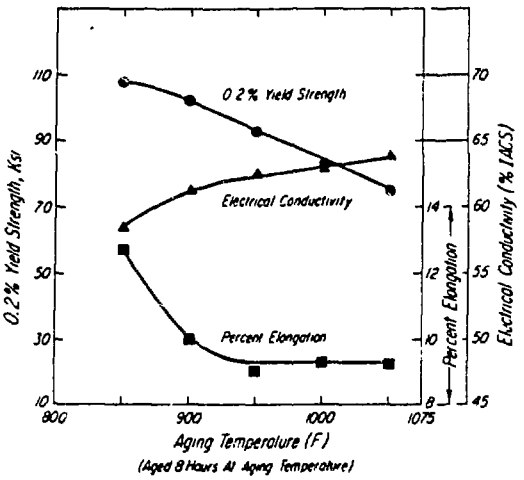

Figure 1 - Aging Response Curves for Alloy C17510 Strip (0.38 Be, 1.60 Ni, balance Cu), 0.016" thick, Cold Worked 21% Prior to Aging.

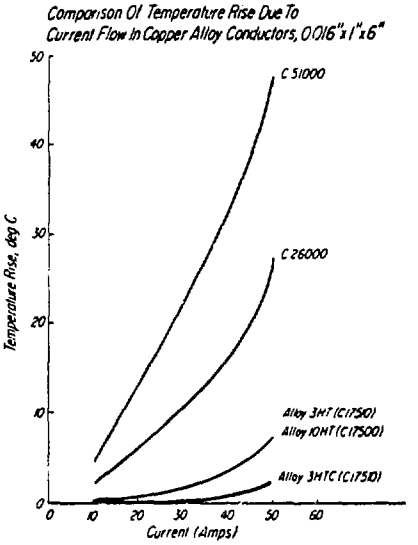

Figure 2 - Comparison of Temperature Rise due to Current Flow in Copper Alloy Conductors, 0.016" x 1" x 6".

PROPERTIES

Specific mechanical and physical properties of Alloy C17510 described in this section are intended to aid the designer with the selection of an optimum high conductivity, high strength alloy based upon performance. Other pertinent characteristics of this alloy are available from the trade literature[1] published by Brush Wellman. Applicable ASTM Standards were followed for the test procedures used to determine the special properties of this alloy.

Electrical and Thermal Conductivity

The electrical conductivity of a connector material has a direct influence on the temperature change of a current carrying conductor. Materials with the highest electrical conductivities yield the lowest temperature in a terminal while carrying a steady flow of current. To measure the temperature rise due to heat generated during the passage of current, tests were performed at various current levels for C17510 in ambient laboratory air. Comparison was made with C17500, and with other copper alloy spring materials, such as phosphor bronze and brass. Figure 2 plots the data indicating the temperature change due to current flow. For C17510 and C17500 in the HT (TH01) condition, the temperature change is not considered sufficient to cause any significant change in the spring properties of the material. The change in the temperature is even less for C17510 in the HTC condition[1], which combines high electrical conductivity (60% IACS minimum) with reasonable strength and good formability. On the other hand, the rise in the temperature in C51000 and C26000 should be sufficient to limit the current carrying capacity of these materials.

The electrical conductivity is inversely proportional to resistivity and is expressed as percent of the International Annealed Copper Standard or % IACS. The change in the resistivity of a conductor with rising temperature can be important in design of current carrying components. Figure 3 is a plot of the thermal conductivity and electrical resistivity of Alloy C17510 versus temperature in both the AT (TF00) and the HT (TH01) condition. There is a linear relationship with resistivity, i.e., the electrical conductivity diminishes with increasing temperature. The average temperature coefficient of resistance of C17510 in both the AT and the HT conditions defined as the rate of change in the resistivity per degree of temperature rise, generally expressed as ohms per ohm per degree Celsius[2], can be estimated to be 0.00202 at a reference temperature of 20 C (68 F). For copper of 100% conductivity the temperature coefficient of resistance is 0.00393[2].

The thermal conductivity of this alloy increases slowly and nonlinearly with rising temperature and is less dependent upon temperature than is the electrical conductivity. The excellent thermal conductivity of this alloy facilitates rapid heat transfer, which makes it ideal for applications as a precious metal contact support member in relays.

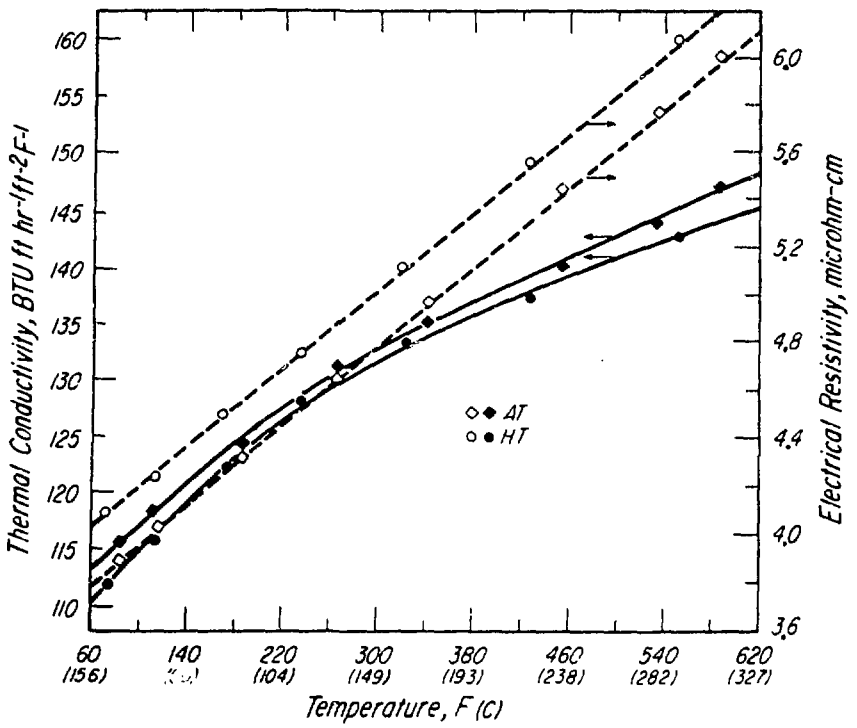

Figure 3 - Variation of the Thermal Conductivity and the Electrical Resistivity of Alloy C17510 with Temperature.

Mechanical Properties

Table II compares the mechanical properties of C17510 and C17500 in the precipitation hardened AT (TF00) condition at room temperature and at 300 F (149 C). The tensile properties of the two alloys are similar; the mechanical properties determined at 300 F (149 C) indicate excellent short term load carrying ability of the two alloys at higher operating temperatures.

TABLE II

Comparison of the Tensile Properties* of Alloy C17510 (0.38 Be, 1.53 Ni, balance Cu) and Alloy C17500 (0.54 Be, 2.51 Co, balance Cu) Strip in the AT (TF00) Condition.

Alloy	Test Temperature F(C)**	Tensile Strength ksi	Yield Strength 0.2% Offset ksi	Elongation % in 2 in.
C17510	70 (21)	121	94	15
	300 (149)			
C17500	70 (21)	116	89	16
	300 (149)	109	85	16

*Average of duplicate tests, longitudinal orientation.
**Tested in air after 10 min., exposure at temperature.

Stress Relaxation

Due to the importance of stress relaxation in current carrying springs, a detailed investigation has been conducted on the subject. The stress relaxation behavior of Alloy C17510 was studied by a method previously described[3]. Figure 4 plots the stress relaxation behavior of Alloy C17510 in strip form as a function of exposure time at temperatures 350 F (177 C), 450 F (232 C) and 600 F (316 C). Comparisons have been made with Alloy C17500 possessing tensile properties equivalent to Alloy C17510. The data were plotted as loss in stress, expressed as a percentage of the initial stress vs. the log of time. Assuming the permissible loss in stress as 25 percent of the initial value, both Alloys C17500 and C17510 appear to have adequate resistance to stress relaxation for temperatures as high as 350 F (177 C). The superiority of the nickel-containing version is evident from Figure 4. For example, as much as a 7 percent advantage is obtained after 100 hours at an operating temperature of 450 F. These alloys are used as current carrying springs where high operating temperatures up to 350 F (177 C) are expected.

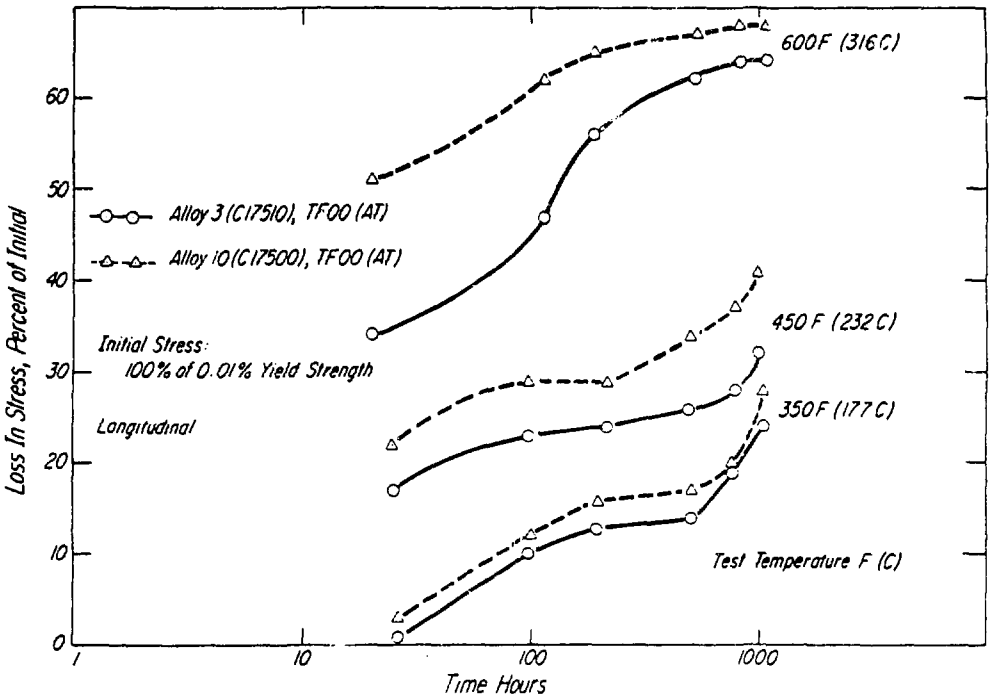

Figure 4 - Stress Relaxation Characteristics of Alloy C17510 Strip Compared to Alloy C17500 in AT Condition.

Fatigue

Fatigue properties of Alloy C17510 were evaluated in fully reversed bending to assess the performance of this alloy in sensitive switches and relays requiring repeated cyclical operations. Comparison has been made with the fatigue characteristics of C17500 strip at equivalent tensile properties. Figure 5 shows the results plotted as maximum bending stress versus the number of cycles of reversed fatigue loading. The data represent the first comparative investigation of the fatigue characteristics of the two alloys. At present, tests on additional heats and processing lots are underway to provide a statistically significant comparison of the fatigue life of the two alloys. The fatigue strength of C17510 is exceeded only by the high strength beryllium copper (C17200) noted for its outstanding fatigue strength[4]. Based on approximately equivalent yield strengths at 0.2% offset, C17510 compares favorably well with the other commercially available fatigue resistant copper alloy strip such as phosphor bronze (C51000), aluminum brass (C68800) and aluminum bronze (C63800). The high fatigue strength of C17510 strip recommends it is material for cyclical operation such as in environments subjected to vibration.

Reverse Bending (R=-1) Fatigue Data of Alloy 3 (C17510) and Alloy 10 (C17500), HT Strip, 0.020" Thick, at Room Temperature (Run at 26 Hz in Model VSS-40 H Fatigue Testing Machine)

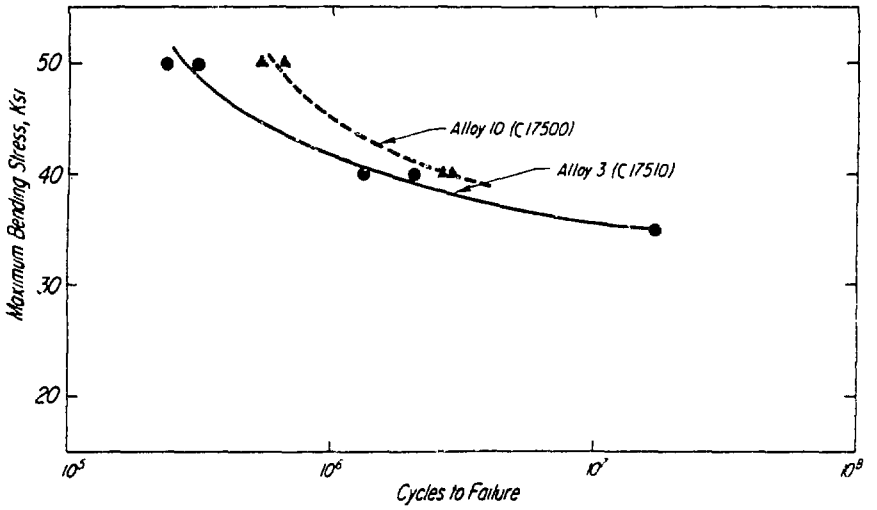

Figure 5 - Fatigue Curve of Alloy C17510 Compared to Alloy C17500 in Bending.

Fabrication

Finished parts or components can be easily formed from C17510 by most conventional metalforming processes. Table III compares the relative formability of this alloy in strip form with the C17500. Samples were bent 180° around pins with successively smaller radii until cracking occured on the tensile surface of the bend. The minimum bend radius, taken as the smallest radius which can be used without cracking, was expressed in multiples of strip thickness. The low directionality of the alloy permits design freedom and assures the most economical use of the material. No differences were observed in the formability of the two alloys.

Alloy C17510 can be joined by conventional techniques. Surface preparation, as with all copper based alloys, is critical for consistent production of high quality joints. The joining characteristics of 0.0114" C17510 strip in the AT (TF00) condition were evaluated and compared to C17500, in the same condition using brazing and soldering. Precleaning and fluxing prior to joining were employed to insure good wetting of the filler metal. Brazed joints were produced using silver-brazing alloys normally used with other copper alloys. The suitability of joining by soldering was evaluated using a 5% Sn-50 Pb filler metal. In both instances spreading of the filler metals was found to be uniform between the joints.

TABLE III

Results of Formability Test*

Alloy and Temper	Yield Strength, 0.2% Offset, ksi	Minimum Bend Radius, 180° Bend (multiples of strip thickness, t)
C17510 AT (TF00)	88	1.0 t
C17510 HT (TH01)	107	1.4 t
C17500 AT (TF00)	91	1.0 t
C17500 HT (TH01)	105	1.4 t

*Directions of bending normal to the rolling direction, average of tests from two heats.

APPLICATIONS

The advantages of beryllium copper Alloy C17510 include excellent electrical and thermal conductivity, high strength and improved resistance to stress relaxation at ambient temperatures ranging from room temperature to 300 F (149 C). This material, therefore, is extensively used in electrical switches and relays designed for high current applications.

CONCLUSIONS

Alloy C17510 offers the designer a high performance material that provides a unique combination of relatively high electrical and thermal conductivity and high strength. Conductive springs used in switches and relays made from this alloy can be upgraded because of the excellent electrical and thermal properties. Because of the high strength, components may be further miniaturized. High fatigue strength, resistance to stress relaxation and good forming characteristics make this alloy particularly suitable for many electrical applications. This material was originally developed to replace Alloy C17500 because of cobalt's critical situation. Comparative data presented in this paper demonstrate that Alloy C17510 can be used as a fully interchangeable, and less expensive, substitute for Alloy C17500. In the case of stress relaxation a clear superiority of C17510 is demonstrated.

REFERENCES

1. "Brush Wellman Beryllium Copper Alloy 3", Data Sheet, June, 1979.

2. Annual Book of ASTM Standards, Part 6, Copper and Copper Alloys, American Society for Testing and Materials, Philadelphia, PA, 1979, pp. 396.

3. J. C. Harkness and C. S. Lorenz, "Stress Relaxation of Beryllium Copper in Bending", Twelfth Annual Connector Symposium Proceedings, pp. 38-52, October, 1979.

4. Standards Handbook, Wrought Copper and Copper Alloy Mill Products, Alloy Data, Part 2, Copper Development Association, Inc., New York, NY, 1973.

BIOGRAPHY

Dr. Amitava Guha is Senior Research Metallurgist in the Alloy Research and Development Department, Brush Wellman Inc., where he is engaged in materials development and the physical metallurgy of copper-base alloys. His MS and PhD degrees, both in Metallurgy, are from Carnegie-Mellon University and the University of Pittsburgh, respectively. Dr. Guha is a member of the ASTM Committee E28.10 on Standard Methods of Bend Testing for Spring Applications.

DISPERSION STRENGTHENED COPPER

C.I. Whitman, A. Nadkarni and J. Synk

SCM Metal Products

DISPERSION STRENGTHENED COPPER

by Anil Nadkarni & James Synk
SCM Metal Products

INTRODUCTION:

Copper is a major industrial metal. It is widely used because of its high electrical and thermal conductivities, outstanding resistance to corrosion, and ease of fabrication. In its pure form copper has relatively low yield strength and fatigue resistance. A wide variety of copper alloys is commercially available. These alloys generally offer higher strength levels but with much reduced electrical and thermal conductivities and varying degrees of corrosion resistance in different environments. A special group among these is precipitation hardened alloys. These alloys offer high strength and high electrical and thermal conductivities. However, the strength and conductivity are drastically reduced upon prolonged heating to temperatures above that of the initial precipitation heat treatment which is generally in the range of 1/3 to 1/2 the melting point of the copper matrix. Dispersion strengthened (DS) copper overcomes some of the shortcomings of these copper alloys.

Since 1973 a family of dispersion strengthened (DS) copper materials has been commercially available in the U.S. These materials offer a unique combination of high strength and high electrical and thermal conductivities, and couple it with the ability to retain a large portion of these important properties even after prolonged exposure to temperatures approaching the melting point of the copper matrix. Thus, these materials extend the useful temperature range of copper alloys considerably. They enable fabrication of parts by high temperature joining processes such as brazing without losing their strength. They can also be used in applications where high operating temperatures are encountered.

The properties of this family of DS coppers arise from a fine and uniform dispersion of aluminum oxide (Al_2O_3) particles in the copper matrix. These particles range in size from about 30 Å to 120 Å with an interparticle spacing between about 300 Å to 1000 Å. The Al_2O_3 particles are hard and thermally stable at high temperatures. They retain their original particle size and interparticle spacing even at temperatures approaching the melting point of copper, hence the superior high temperature properties of DS copper. The quality of the dispersion depends heavily on the method of manufacture.

MANUFACTURE OF DS COPPER:

DS copper can be made by any of the techniques mentioned previously in the general introduction to DS materials. However, the best product is made by internal oxidation because it produces the finest dispersoid particles and the most uniform distribution. Copper matrix is well suited for internal oxidation because oxygen can diffuse rapidly in it. For effective internal oxidation, oxygen must diffuse in the matrix several orders of magnitude faster than the solute element, such as aluminum, does. Since internal oxidation depends on the diffusion of oxygen into the matrix, the reaction time is proportional to the square of the distance through which the oxygen must diffuse to complete the reaction. Therefore in order to hold the reaction times within practical limits the diffusion distance must be small. In wrought form internal oxidation can only be practical in thin wire or strip and this can severely limit the use of DS materials. Powder metallurgy offers a unique solution to this problem in that powder particles can be internally oxidized in short times and the powders can then be consolidated into almost any shape. The DS coppers mentioned above use internal oxidation of powder.

The process involves melting a dilute solid solution alloy of aluminum in copper and atomizing the melt by high pressure gas such as nitrogen. The resulting powder is blended with an oxidant comprising fine copper oxide powder. The blend is heated to a high temperature at which the copper oxide dissociates and the oxygen thus produced diffuses into the particles of solid solution copper-aluminum alloy. As aluminum is a stronger oxide former than copper, the aluminum in the alloy gets preferentially oxidized to Al_2O_3. Any excess oxygen left in the powder, after complete oxidation of all the aluminum, is reduced by heating the powder in hydrogen or dissociated ammonia atmosphere.

Full theoretical density is essential to realize the full potential properties of DS copper. The powder is fabricated into fully dense shapes by various techniques. Mill forms, such as rod and bar, are made by canning the powder in a suitable metal container, generally copper, and hot extruding it to the desired size. Wire is made by cold drawing coils of rod. Strip is made either by rolling coils of extruded rectangular bar or by directly rolling powder with or without a metal container. Large shapes which cannot be made by hot extrusion are made by hot isostatic pressing of canned powder. Alternatively, such shapes can be made by hot forging canned powder or partially dense compacted preforms. Properties of consolidated material depend upon the deformation introduced into the powder particles. Consequently, low deformation processes such as hot isostatic pressing, and to a lesser extent hot forging, develop lower strengths and ductilities than extrusion. Finished parts can be made from consolidated shapes by further operations such as machining, brazing, soldering, etc. Fusion welding is not recommended because this causes the Al_2O_3 to segregate from the liquid copper matrix and thus results in loss of dispersion strengthening. However, flash welding

wherein the liquid metal is squeezed out of the weld joint or electron beam welding with a minimal heat affected zone has been successfully used.

PROPERTIES OF DS COPPER:

DS copper offers a unique combination of high strength and high electrical and thermal conductivities. More importantly it retains a larger portion of these properties at and after exposure to elevated temperatures than any other copper alloy.

TAILORED PROPERTIES:

The properties of DS copper can be tailored to meet a wide range of design requirements in physical and mechanical properties by varying its Al_2O_3 content and/or amount of cold work. Figure-I shows the ranges in tensile strength, elongation, hardness, and electrical conductivity obtained by varying Al/Al_2O_3 contents. These properties are for rodstock in hot extruded condition. Cold work can be used to further broaden the ranges in tensile strength, elongation, and hardness while its effect on electrical conductivity is minimal. The effects of cold work on mechanical properties are shown later.

Two grades of DS copper are offered commercially. They are designated as C15760 and C15715*; the latter is a new grade replacing C15720 with the * denoting designation pending approval by Copper Development Association. The nominal compositions of the two grades are given in Table-1 and shown by verticle lines in Figure-I at respective Al_2O_3 contents. Other grades can be easily produced if the property requirements justify.

FIG. 1 . "TAILORED PROPERTIES OF D.S. COPPER"

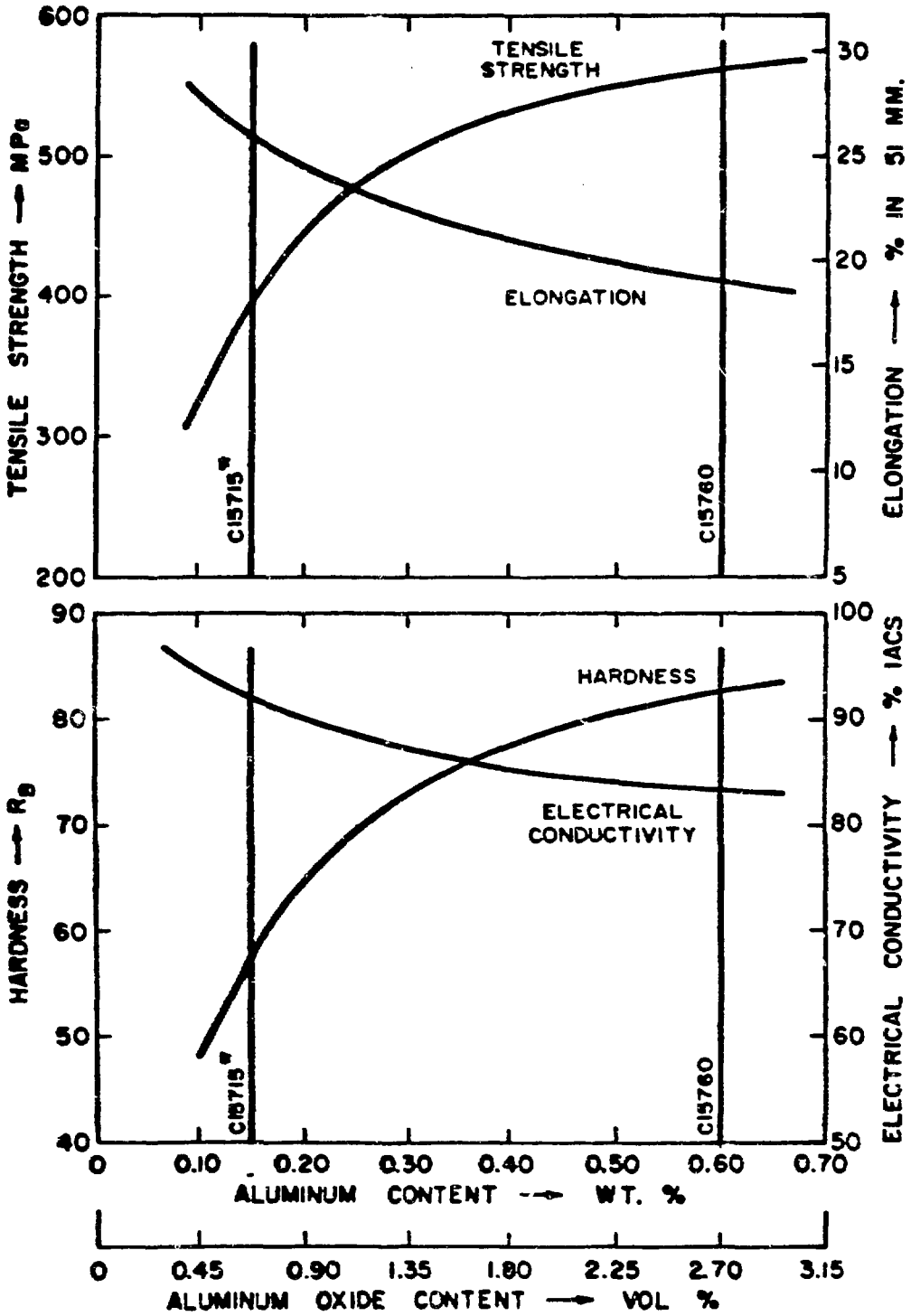

Table-1

Chemical Compositions of DS Coppers

Grade	Copper		Al_2O_3	
	wt. %	vol. %	wt. %	vol. %
C15715*	99.7	99.3	0.3	0.7
C15760	98.9	97.3	1.1	2.7

Not shown in Table-1 is the free or reducible oxygen content, generally about .02-.05 wt. %, which is present in the form of dissolved oxygen and cuprous oxide. To this extent these alloys are prone to hydrogen embrittlement at high temperatures. Oxygen-free (OF) compositions are available in both the commercial grades wherein the reducible oxygen is converted to non-reducible oxides. These are therefore immune to hydrogen embrittlement and must be specified for applications in which the components are likely to be subjected to reducing atmospheres during their manufacture or use.

PHYSICAL PROPERTIES:

As DS copper contains small amounts of Al_2O_3 as discrete particles in an essentially pure copper matrix, its physical properties closely resemble those of pure copper. Table-2 shows physical properties of the two commercial DS coppers along with properties of OF copper for comparison. The melting point is essentially the same as for copper because the matrix melts and the Al_2O_3 separates from the melt. Density, modulus of elasticity, and coefficient of thermal expansion are very similar to those for pure copper. The coefficient of thermal expansion reported in the table is an average value over the temperature range of 20-1000°C, and the variations within narrow segments

of this range are negligible.

High electrical and thermal conductivities are of particular interest to design engineers in electrical and electronic industries. At room temperature these range from 78 to 92% of those for pure copper. When coupled with the high strengths of these materials they open up opportunities for increased current-carrying or heat dissipation capabilities for a given section size and structural strength of the component. Alternatively they enable reduction of section sizes for miniaturization of components without sacrificing structural strength or the current and heat-carrying capabilities. At elevated temperatures the electrical and thermal conductivities of DS coppers closely parallel those of pure copper as shown in Figure-II.

MECHANICAL PROPERTIES:

ROOM TEMPERATURE PROPERTIES:

Room temperature mechanical properties of DS coppers in the various available mill forms are given in Tables 3-8. The tables cover a wide range of sizes typified by various amounts of cold work by drawing, rolling, etc. Alos shown are properties obtained after annealing the material at elevated temperatures.

Some noteworthy characteristics of DS copper that are evident from the tables are as follows:

a) DS copper has strength comparable to many steels, but it has conductivity comparable to copper.

b) It has a large capacity for being cold worked. For example, C15715* material can be drawn from an extruded size of 28.6mm to a wire of 0.25mm without any intermediate annealing treatments. This is unlike most copper alloys and is due to the slow work hardening rate of DS copper. Although both commercial grades of DS copper can be cold worked readily, C15715* is generally recommended for applications requiring a lot of cold work.

Table-2

Physical Properties of DS Coppers & OF Copper

Property	C15715*	C15760	OF Copper
Melting Point:			
^{o}C	1083	1083	1083
^{o}F	1981	1981	1981
Density:			
at 20°C, Mg/m^3	8.84	8.81	8.94
at 68°F, lb/in^3	.319	.318	.323
Electrical Resistivity:			
at 20°C, nΩ • m	18.6	22.1	17.1
at 68°F, Ω • circular mil./ft.	11.19	13.29	10.28
Electrical Conductivity:			
at 20°C 1/nΩ • m	.054	.045	.058
at 68°F, % IACS	92	78	101
Thermal Conductivity:			
at 20°C, W/m • °K	365	322	391
at 68°F, $Btu/ft^2/ft/hr/^{o}F$	211	186	226
Coefficient of Thermal Expansion:			
(20-1000°C), m/m/°C	16.6×10^{-6}	16.6×10^{-6}	17.7×10^{-6}
(68-1832°F), in/in/°F	9.2×10^{-6}	9.2×10^{-6}	9.8×10^{-6}
Modulus of Elasticity:			
at 20°C, GPa	115	115	115
at 68°F, psi	17×10^{6}	17×10^{6}	17×10^{6}

FIG. II: "ELEVATED TEMPERATURE ELECTRICAL AND THERMAL CONDUCTIVITIES"

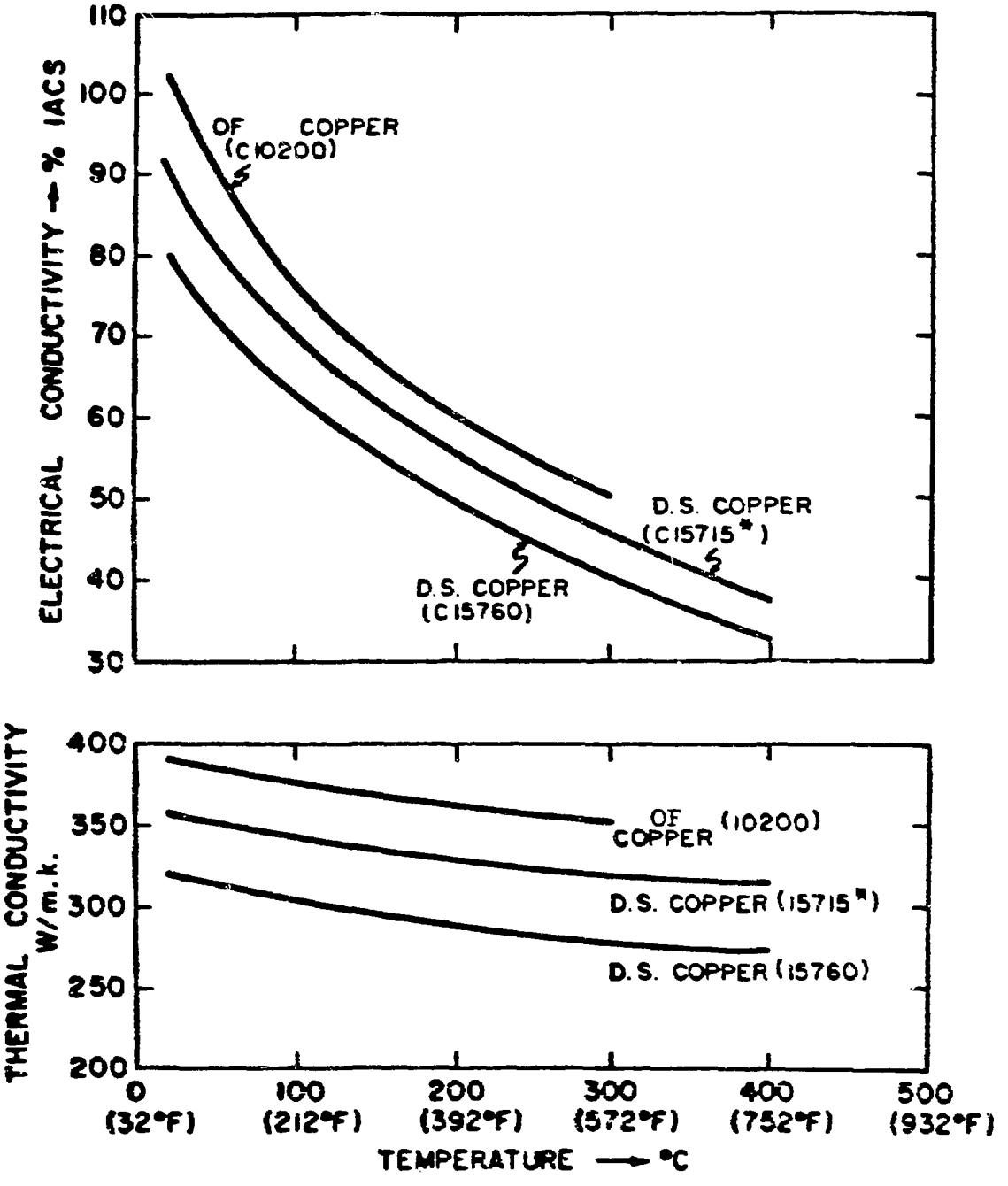

c) DS copper exhibits a high yield strength/ultimate tensile strength (YS/UTS) ratio and retains much of it even after annealing. This ratio is generally high for copper and its alloys in highly cold worked condition, but it drops drastically when the alloys are annealed.

d) DS copper also exhibits a high yield strength retention ratio which may be defined as (yield strength in annealed condition)/(yield strength in work hardened condition). High values of this ratio at annealing temperatures close to the melting point of the copper matrix are indicative of its ability to resist weakening or softening.

e) Like most materials, annealing enhances the ductility (or formability) of DS copper. Due to its high YS retention ratio DS copper offers the highest yield strength for a given amount of ductility among the high conductivity copper alloys.

DS copper has excellent fatigue resistance. It exhibits a high fatigue ratio (endurance limit/tensile strength). The fatigue properties of the two commercial DS coppers are shown in Figure-III. The tests were conducted at room temperature in a Krause cantilever bending-rotating beam mode at a frequency of 10 000 cycles/minute. It should be noted that the C15715* rod used in the test had 94% cold work while the C15760 rod had 14% cold work. At comparable cold work levels C15760 would be expected to have significantly higher fatigue strength than C15715*.

ELEVATED TEMPERATURE PROPERTIES:

DS copper has excellent strength at elevated temperatures. Figure-IV shows the 100 hour stress rupture strengths the two DS coppers at temperatures up to 870°C. Various other high conductivity copper based materials are also shown for comparison. Starting with pure copper on the low end to the precipitation hardened alloys on the high end there is a sharp drop in stress rupture strengths in the 200°C to 450°C temperature range. Above about 400°C the DS coppers are significantly superior to any of the alloys shown. Above 600°C the DS coppers have rupture strengths comparable or superior to some stainless steels. The log stress-log rupture life plots have extremely flat

Table-3

Room Temperature Mechanical Properties of C15715* Rod/Bar

Rod Dia. (mm)	Cold Work (%)	Condition (Anneal Temp)** (^{o}C)	UTS (MPa)	UTS (KSI)	0.2% YS (MPa)	0.2% YS (KSI)	Elong. 0.64" gage length (%)	Red. in Area (%)	YS/UTS (%)	YS Retention Ratio $\frac{\text{YS (Annealed)}}{\text{YS (Drawn)}}$ (%)	Hardness (R_B)
28.6	0	As Extruded	393	57	324	47	27	68	82	---	57
		315	393	57	324	47	27	70	82	100	57
		650	393	57	324	47	28	70	82	100	56
		980	386	56	317	46	29	73	82	98	55
19.1	55	As Drawn	428	62	407	59	24	67	95	---	63
		315	428	62	399	58	24	69	94	98	62
		650	393	57	345	50	27	69	88	85	60
		980	393	57	331	48	27	72	85	81	56
12.7	80	As Drawn	455	66	434	63	21	66	95	---	67
		315	448	65	421	61	21	68	94	97	64
		650	399	58	352	51	25	69	88	81	62
		980	393	57	331	48	27	70	85	76	59
7.0	94	As Drawn	496	72	469	68	19	65	95	---	68
		315	462	67	434	63	19	65	94	93	67
		650	407	59	359	52	24	66	88	76	63
		980	393	57	331	48	27	69	85	71	60

**Annealing in nitrogen for 1 hour.

Copper cladding machined off prior to testing.

Table-4

Room Temperature Mechanical Properties of C15715* Wire

Wire Dia. (mm)	Cold Work (%)	Condition (Anneal Temp)** (°C)	UTS (MPa)	UTS (KSI)	0.2% YS (MPa)	0.2% YS (KSI)	Elong. 10" gage length (%)	YS/UTS (%)	YS Retention Ratio YS (Annealed) / YS (Drawn) (%)
2.54	99.2	As Drawn	496	72	469	68	2	95	--
		315	448	65	421	61	3	94	90
		650	386	56	338	49	11	88	72
		980	338	49	290	42	12	85	62
1.27	99.8	As Drawn	524	76	496	72	2	95	--
		315	445	66	428	62	3	94	86
		650	399	58	352	51	10	88	71
		980	358	52	303	44	11	85	61
0.51	99.9	As Drawn	600	87	572	83	2	95	--
		315	483	70	455	66	3	94	80
		650	407	59	359	52	9	88	63
		980	352	51	296	43	10	85	52
0.36	99.9	As Drawn	607	88	579	84	1	95	--
		315	503	73	476	69	3	94	82
		650	407	59	359	52	8	88	62
		980	365	53	310	45	9	85	54

** Annealing in nitrogen for 1 hour.

Table-5

Room Temperature Mechanical Properties of C15715* Strip

Strip Thickness (mm)	Cold Work (%)	Condition (Anneal Temp)** (°C)	UTS (MPa)	UTS (KSI)	0.2% YS (MPa)	0.2% YS (KSI)	Elong. 2" gage length (%)	YS/UTS (%)	YS Retention Ratio YS Annealed) / YS (Rolled) (%)
6.35	0	As Extruded	379	55	317	46	6	82	--
		315	372	54	310	45	26	83	98
		650	372	54	296	43	28	80	93
		980	359	52	283	41	30	78	89
2.29	64	As Rolled	483	70	455	66	7	95	--
		315	448	65	393	57	13	88	86
		650	421	61	359	52	21	86	79
		980	365	53	290	42	22	79	64
1.27	80	As Rolled	503	73	476	69	6	95	--
		315	476	69	421	61	11	88	88
		650	421	61	358	52	20	86	75
		980	358	52	283	41	22	79	59
0.76	88	As Rolled	510	74	483	70	6	95	--
		315	476	69	421	61	11	88	87
		650	434	63	372	54	20	86	77
		980	358	52	283	41	21	79	59
0.25	96	As Rolled	607	88	579	84	4	95	--
		315	483	70	428	62	8	88	74
		650	441	64	379	55	16	86	65
		980	358	52	283	41	18	79	49

**Annealing in nitrogen for 1 hour.

Table-6

Bend Test Data for C15715* Strip

Strip Thickness (mm)	Bend Radius (mm)	Condition (Anneal Temp)** (°C)	No. Bends*** Longitudinal	No. Bends*** Transverse	Minimum Bend Radius+ Longitudinal (mm)	Minimum Bend Radius+ Transverse (mm)
2.29	2.29 (1T)	As Rolled	1	0		
		315	3	2		
		650	4	3		
		815	5	4		
		980	6	5		
	4.57 (2T)	As Rolled	3	1	1.27	3.81
		315	6	4	0.76	2.29
		650	9	7	0.51	1.27
		815	10	8	0.25	0.76
		980	12	9	0.25	0.76
	6.86 (3T)	As Rolled	5	2		
		315	10	8		
		650	12	10		
		815	15	13		
		980	18	17		
1.27	1.27 (1T)	As Rolled	2	0		
		315	3	2		
		650	5	3		
		815	6	4		
		980	7	5		
	2.54 (2T)	As Rolled	2	0	.76	3.81
		315	6	3	0.51	1.27
		650	8	6	0.51	0.51
		815	10	8	0.25	0.25
		980	12	9	<0.25	0.25
	3.81 (3T)	As Rolled	4	1		
		315	8	6		
		650	10	8		
		815	15	12		
		980	18	15		

**Annealing in nitrogen for 1 hour.

***1 bend defined as a 90° fold over radius and back to original upright position without cracking. All bends identical.

+Minimum bend radius is smallest radius that allows one bend.

Table-6 (contd.)

Bend Test Data for C15715* Strip

Strip Thickness (mm)	Bend Radius (mm)	Condition (Anneal Temp)** (°C)	No. Bends*** Longitudinal	No. Bends*** Transverse	Minimum Bend Radius+ Longitudinal (mm)	Transverse (mm)
0.76	0.76 (1T)	As Rolled	1	0		
		315	3	2		
		650	5	4		
		815	8	6		
		980	9	6		
	1.52 (2T)	As Rolled	3	0	0.25	2.54
		315	5	3	0.25	0.51
		650	9	8	<0.25	<0.25
		815	11	10	<0.25	<0.25
		980	12	10	<0.25	<0.25
	2.29 (3T)	As Rolled	6	0		
		315	11	6		
		650	13	12		
		815	16	15		
		980	18	15		
0.25	0.25 (1T)	As Rolled	2	0		
		315	6	4		
		650	7	6		
		815	8	7		
		980	9	8		
	0.51 (2T)	As Rolled	3	0	<0.25	0.76
		315	8	6	<0.25	<0.25
		650	9	8	<0.25	<0.25
		815	10	8	<0.25	<0.25
		980	11	9	<0.25	<0.25
	0.76 (3T)	As Rolled	4	1		
		315	10	7		
		650	11	9		
		815	15	13		
		980	18	15		

**Annealing in nitrogen for 1 hour.

***1 bend defined as 90° fold over radius and back to original upright position without cracking. All bends identical.

+ Minimum bend radius is smallest radius that allows one bend.

Table-7

Room Temperature Mechanical Properties of C15760 Rod/Bar

Rod Dia. (mm)	Cold Work (%)	Condition (Anneal Temp)* (°C)	UTS (MPa)	UTS (KSI)	0.2% YS (MPa)	0.2% YS (KSI)	Elong. 0.64" gage length (%)	Red. in Area (%)	YS/UTS (%)	YS Retention Ratio YS (Annealed) / YS (Drawn) (%)	Hardness (R_B)
12.7	14	As Drawn	572	83	545	79	16	56	95	--	83
		315	565	82	538	78	18	57	95	99	81
		650	524	76	496	72	22	59	94	92	78
		980	496	72	455	66	22	45	92	84	75
7.0	74	As Drawn	621	90	600	87	14	50	97	--	86
		315	614	89	586	85	16	51	96	98	84
		650	579	84	545	79	18	53	94	91	80
		980	524	76	490	71	18	40	93	82	77

*Annealing in nitrogen for 1 hour.

Copper cladding machined off prior to testing.

Table-8

Room Temperature Mechanical Properties of Ci5760 Wire

Wire Dia. (mm)	Cold Work (%)	Condition (Anneal Temp)** (°C)	UTS (MPa)	UTS (KSI)	0.2% YS (MPa)	0.2% YS (KSI)	Elong. 10" gage length (%)	YS/UTS (%)	YS Retention Ratio YS (Annealed) / YS (Drawn) (%)
2.54	96.6	As Drawn	627	91	607	88	4	97	--
		315	579	84	558	81	4	96	92
		650	552	80	517	75	7	94	85
		980	496	72	462	67	7	93	76
1.27	99.1	As Drawn	655	95	634	92	3	97	--
		315	641	93	614	89	4	96	97
		650	593	86	558	81	5	94	88
		980	503	73	469	68	5	93	74
0.51	99.9	As Drawn	710	103	690	100	2	97	--
		315	648	94	621	90	3	96	90
		650	621	90	586	85	4	94	85
		980	531	77	496	72	4	93	72

*Annealing in nitrogen for 1 hour.

FIG. III: "FATIGUE RESISTANCE OF D.S. COPPER"

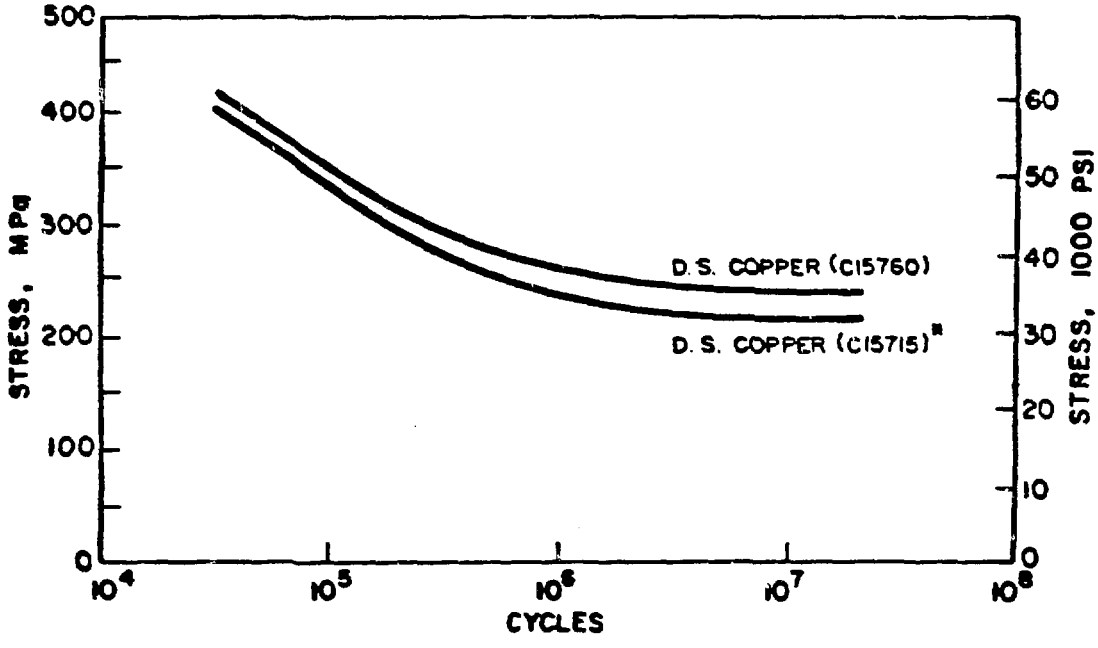

D.S. COPPER C15760 COLD WORKED 14% PRIOR TO TEST

D.S. COPPER C15715* COLD WORKED 94% PRIOR TO TEST

* DESIGNATION PENDING

slopes for DS coppers and therefore the rupture strengths for 1000 hour and longer lives are not much different from 1000 hour rupture strengths. For example at 650°C a C15760 rod having 100 hour rupture strength of 200 MPa (29 000 psi) would have an extrapolated 1000 hour rupture strength of 186 MPa (27 000 psi), and a 10 000 hour rupture strength of 172 MPa (25 000 psi). This shows the excellent thermal stability of DS copper at high temperatures which arises because the Al_2O_3 particles retain their original particle size and distribution even after prolonged heating and do not allow recrystallization of the matrix.

Cold work enhances the stress rupture properties of DS copper dramatically and the higher the temperature the greater the enhancement. This is illustrated in Table-9.

Table-9

Effect of Cold Work on Stress Rupture Properties of C15715*

Cold Work (%)	Test Temperature (°C)	100 Hour Stress Rupture Strength (MPa)	(KSI)
0	425	124	28
	650	55	8
	870	14	2
94	425	241	35
	650	145	21
	870	76	11

DS copper thus offers the best combination of strength, electrical and thermal conductivities, fatigue resistance, and resistance to softening at elevated temperatures among all the copper based materials. The strengths

FIG. IX: "STRESS RUPTURE PROPERTIES OF D. S. COPPER*

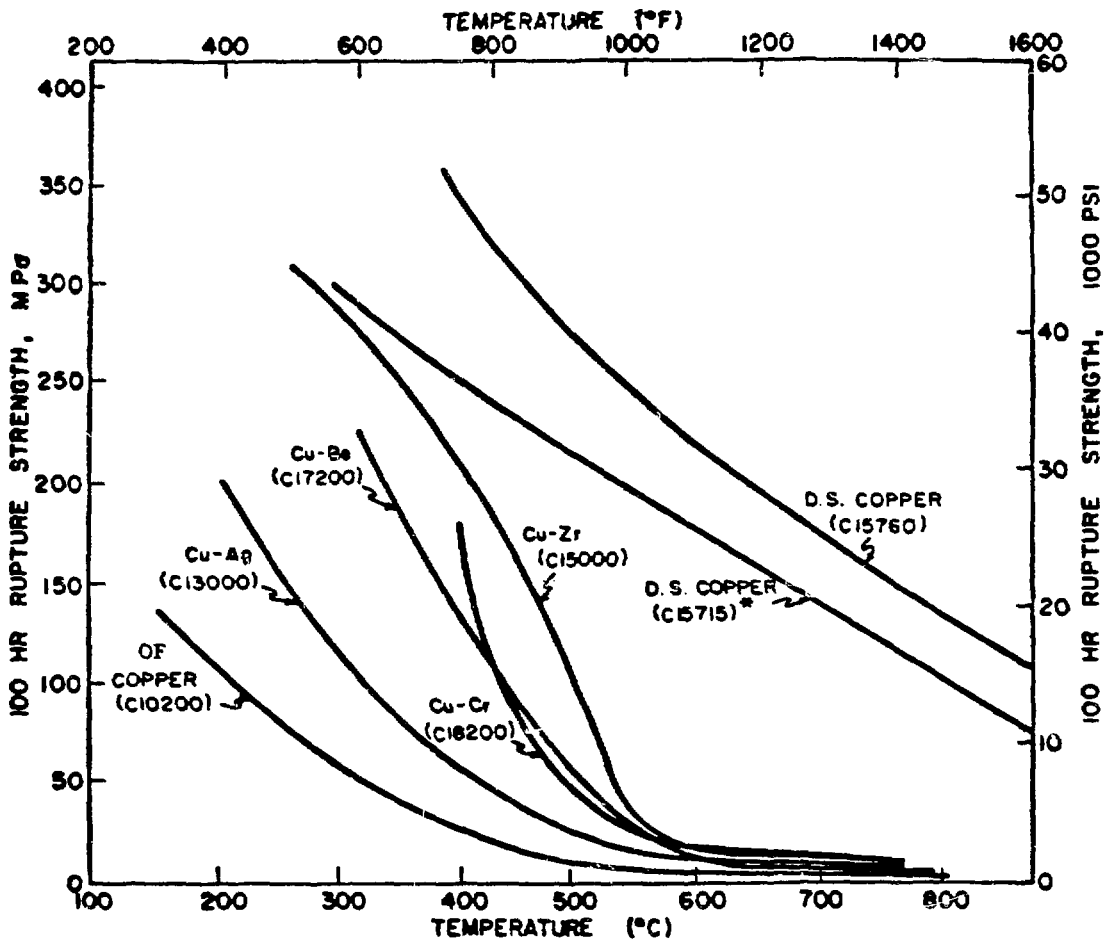

* DESIGNATION PENDING

of DS copper at room and elevated temperatures are comparable to some steels with electrical and thermal conductivities comparable to copper.

APPLICATIONS:

Since its inception, DS copper has received wide market acceptance in several applications and design engineers are continually developing new applications. The major present and potential applications are as follows:

RESISTANCE WELDING ELECTRODES:

DS copper electrodes are used in RWMA Class II and some Class III welding applications, mainly in automotive and appliance industries. They last 4-10 times as long as conventional Class II (Cu-Cr) electrodes. Due to their slow mushrooming rates and non-sticking characteristics against galvanized steel, they minimize down times associated with electrode dressing and changing operations. This is particularly important in automatic press and robot welding applications in the high volume assembly lines. With increasing usage of galvanized steel in automobiles and emphasis on automation, the DS copper electrodes are finding wider usage in this industry. The slow mushrooming rate also allows less frequent current step ups during welding and leads to substantial energy savings.

LEAD WIRES:

DS copper wire is used in leads for incandescent lamps. Its high temperature strength retention capability enables the glass stem pressing operation without undue softening of the leads. This in turn eliminates the need for expensive molybdenum support wires without sacrificing the lead stiffness. Because of the superior strength of the leads, the diameter can be reduced to conserve valuable material. Thinner leadwires also minimize heat loss from the filament and enable the lamp to provide higher light

output at lower wattage and hence lower energy consumption.

DS copper wire is also expected to find usage in leads for discrete electronic components such as diodes. Here, important advantages are high temperature strength retention during hermetic sealing operation and wire stiffness which enable multiple insertions in the circuit boards.

COMMUTATORS:

DS copper has been used in commutators for helicopter starter motors where high strength is required to combat the high deformation stresses associated with high rotational speeds. It is also finding usage in commutators for submerged fuel pumps in automobiles equipped with fuel injection systems. In this case resistance to both wear and corrosion in "sour" gasoline are of particular interest.

RELAY BLADES AND CONTACT SUPPORTS:

DS copper strip is used in relay blades and contact supports. Strength retention capability of DS copper after exposure to elevated temperatures allows brazing of contacts to the blade without appreciable loss in strength. Because of higher electrical conductivity, DS copper has replaced conventional copper alloys such as phosphor bronze and beryllium copper in some relays. These relays were upgraded to higher current carrying capacity without changing the design of the package.

OTHER APPLICATIONS:

Other potential applications for DS copper include continuous casting molds, side dam blocks for Hazelett casting machines, MIG welding tips, seam welding wheels, high current welding cables, microwave tube components, electrical connectors, etc. In most applications DS copper must be designed in to demonstrate cost effectiveness and exploit its full capabilities. Imaginative design engineering in the future will surely unfold even more applications for this valuable engineering material.

MANUFACTURE OF DS COPPER

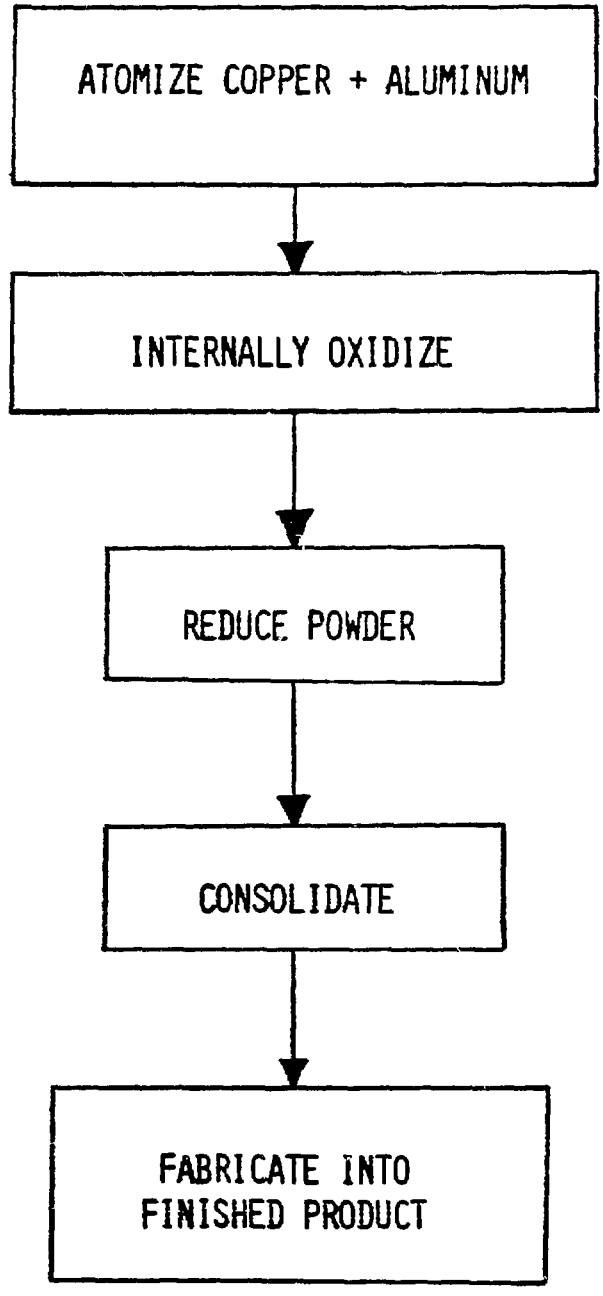

SCM METAL PRODUCTS

DISPERSION STRENGTHENED COPPER

WHAT DSC OFFERS

- HIGH YIELD STRENGTH WITH GOOD DUCTILITY
- THERMAL AND ELECTRICAL CONDUCTIVITY
- FATIGUE RESISTANCE
- STRESS RELAXATION RESISTANCE
- HIGH TEMP STRENGTH
- FABRICABILITY
- FLEXIBILITY OF PRODUCT DESIGN

LOW ALLOY COPPER AND INCRA COPPER RELATED RESEARCH

L. M. Schetky

International Copper Research
Association, Inc.

DISCUSSION OF LOW ALLOY COPPER AND INCRA COPPER RELATED RESEARCH:

The International Copper Research Association, Inc. has for many years sponsored studies of various phases of copper alloy development, mechanical property research, and processing developments. A summary of two current programs were presented by Prof. Grant and Prof. Harling. The other current program which will be described relates to the synergistic effect of elements added to copper at the ppm level. During the past year and a half the understanding of the interactions which take place in the Cu-Mn-Se and Cu-Mn-Te can be summarized as follows:

1) The softening characteristics of a series of Cu-Mn-Se alloys containing less than 100 ppm Mn+Se were determined and indicated softening temperature increases of over 200°C relative to pure (99.999%) copper. The activation energies for softening were evaluated from a study of the kinetics of recrystallization.

2) The surface tensions of several liquid binary Cu-Mn and dilute Cu-Mn-Se alloys were measured as a function of Mn and Se employing the sessile-drop technique. The results indicated the strong surface activity of Se and a synergistic interaction between Se and Mn which enhances the adsorption or segregation of Se to copper surfaces.

3) Residual electrical resistivity ratio measurements (at 4°K and 77.3°K) were performed on solution-treated and aged Cu-Mn-Se alloys. The resultant increase in resistivity ratio with aging time reflected a decrease in impurity scattering caused by precipitation phenomena.

4) A brief survey was made of the softening behavior of a number of other dilute ternary copper alloys containing either Se or Te. The results indicated a qualitative correlation between softening temperature and the enthalpy of formation of the metal selenide or telluride.

The research has thus far primarily yielded <u>indirect</u> information on the behavior of the solute additions largely through macroscopic measurements. Attempts to directly observe the effects of solutes in the transmission electron microscope have not yet yielded conclusive results. Nevertheless, the indirect experimental evidence supports a model in which the strongly active surface specie (Se or Te) segregates at grain boundaries in the form of a compound with the second alloying element.

This approach to developing improved elevated temperature behavior with minimum effect on conductivity may lead to alloys of interest where the strength requirements are not as high as those requiring the Cu-Be family of alloys.

A list of INCRA project reports relating to improved copper alloys and mechanical behavior is attached.

TITLES AND RESEARCH FACILITIES

Project No. 29 - "Determination of Solid Solubility Limits And Precipitation Hardening Characteristics of Copper-Rare Earth Systems"
Denver Research Institute
Denver, Colorado

Project No. 50 - "Low Temperature Mechanical Properties Of Copper And Selected Copper Alloys"
National Bureau of Standards
Boulder, Colorado

Project No. 127 - "Avoidance Of Softening In Dilute Alloys Of Copper Containing Hexagonal Solute Additions"
University of Kentucky
Lexington, Kentucky

Project No. 128 - "Powder Methods For Production Of Wrought High Strength, High Conductivity, Thermally Stable Copper-Base Alloys"
Massachusetts Institute of Technology
Cambridge, Massachusetts

Project No. 186 - "A Preliminary Investigation Of The Behavior Of High Purity Copper In High Magnetic Fields"
National Bureau of Standards
Cryogenic Division
Boulder, Colorado

Data on low temperature resistivity of copper in magnetic fields. Also determined the effect of iron impurities and internal oxidation procedures on the resistivity.

Project No. 207 - "Stress Relaxation In Copper-Base Alloys"
Polytechnic Institute of New York
Brooklyn, New York

Includes a five-page summary report plus a thesis, "Microsturcture and Properties of Dilute Copper-Age Hardening Alloys".

Project No. 228 - "The Cyclic Stress Response Of Copper Alloys At 100-500°C"
University of Waterloo
Waterloo, Canada

Examines the relationship between the low cycle fatigue response at moderately elevated temperatures and microstructure in high strength, high conductivity copper alloys.

continued.....

Project No. 237 - "Grain Boundary Segregation In Copper And Copper Alloys"
National Bureau of Standards
Cryogenics Division
Boulder, Colorado

This localized intense segregation is caused by impurity redistribution during recrystallization.

Project No. 255 - "Investigation Of A Practical Superconductor With A Copper Matrix"
National Bureau of Standards
Thermophysical Properties Division
Boulder, Colorado

This project had made considerable progress in developing a single melt, niobium-in-copper, superconducting wire for practical applications in motors, generators and the windings of magnets.

Project No. 311 - "Structure-Property Relationships In High-Temperature, High Strength, High Conductivity Copper-Base Alloys"
Massachusetts Institute of Technology
Cambridge, Massachusetts

A study of two copper alloy systems which show great promise in such demanding new applications as the core of water-cooled gas turbines. Includes the powder metallurgy refinement of these alloys.

Project No. 312 - "Creep At Cryogenic Temperatures"
Westinghouse R&D Development Center
Pittsburgh, Pennsylvania
and
Columbia University
New York, New York

Project No. 327 - "Fatigue Mechanism Maps For Industrial Copper Alloys"
University of Waterloo
Waterloo, Canada

Project No. 337 - "The Development Of P/M MZC Copper Alloy Water-Cooled Gas Turbine Applications"
General Electric Company
Gas Turbine Division
Schenectady, New York

Project No. 344 - "Solute Effects In Very Dilute Ternary Alloys"
Stevens Institute of Technology
Hoboken, New Jersey

Project No. 347 - "Critical Survey Of Available High Temperature Mechanical Property Data For Copper And Copper Alloys"
BNF Metals Technology Centre
Grove Laboratories
Oxfordshire, England

RADIATION EFFECTS AND LIFETIME CONSIDERATIONS FOR THE HIGHLY-IRRADIATED COPPER MAGNETS IN THE MARS TANDEM MIRROR REACTOR

L. John Perkins

University of Wisconsin

INTRODUCTION

The Mirror Advanced Reactor Study[3] (MARS) is a major two year conceptual design study of a 1200 MWe commercial tandem mirror reactor. MARS employs a magnetic choke coil at each end of the long central cell region with a requirement for an on-axis magnetic field of 24 T (2.4×10^5 Gauss). Production of this very high field necessitates the use of hybrid solenoids where outer superconducting coils provide ~ 14 T of the required axial field while inner concentric normal-conducting copper coils supply the balance.

Figure 1 is a schematic of one of the 24 T choke coils for MARS, while Fig. 2 shows contours of constant magnetic field in the hybrid coil system. Note that the maximum field in the normal-conducting coil is ~ 24 T. Table 1 lists the key operating parameters for the normal insert coil.

For economic reasons, the water-cooled normal-conducting insert coils are operated with no intervening shielding between the first wall and their inner windings. In view of the fact that the peak neutron wall load here is 4.5 MWm^{-2}, these magnets will be operating in a severe neutron and gamma radiation environment. It is important, therefore, to recognize potential radiation-induced failure mechanisms so that coil lifetimes can be reasonably predicted. Accordingly, four potential radiation problem areas were identified as follows:

- Resistivity degradations in the ceramic insulation under instantaneous neutron and gamma absorbed dose-rates.
- Mechanical and structural degradations in the ceramic insulation under long-term neutron fluences.
- Radiolytic dissociation of the coolant water leading to corrosion product formation.
- Resistivity increases in the MZC copper conductor due to radiation damage and neutron-induced transmutations.

It will be seen below that cognizance of these various effects had a considerable impact on the evolution of the coil design.

DOSE-RATE RESISTIVITY DEGRADATION IN CERAMIC INSULATION

Under neutron and gamma dose-rates typical of fusion reactor first wall conditions, common ceramic insulators such as Al_2O_3, MgO, $MgAl_2O_4$, etc., exhibit a significant and instantaneous decrease in their DC resistivity.[1,2] Ceramics in the form of a compacted powder typically show a greater effect than those in solid form.[2] Unlike long term fluence effects, this phenomenon is dependent on the instantaneous neutron and gamma dose-rate and is, therefore, a potential problem as soon as the fusion plasma reaches operating power.

The extent to which the performance of a normal-conducting magnet is degraded due to this effect depends rather critically on magnet design and power supply voltage.[2] In particular, for internally cooled magnets of the extruded winding design (i.e., inner conductor and outer grounded-case separated by compacted powdered insulation), the resulting dose-rate-induced leakage currents flowing across the insulation are potentially capable of Joule heating rates sufficient to lead to insulator destruction via thermal runaway effects. In view of this phenomenon and the large peak dose-rates of ~ 1.4×10^4 Gy/s (1.4×10^6 rads/s) absorbed in the ceramic insulation in the inner layers of the coils, it was decided not to employ magnets of the extruded winding design in MARS. Instead, a magnet design with windings having turn-to-turn solid insulation rather than turn-to-ground powdered insulation was specified.[2] Such designs do not suffer the same deleterious heating effects when their ceramic resistivity degrades.[2]

STRUCTURAL DEGRADATION IN CERAMIC INSULATION

To assess the mechanical and structural degradations in the ceramic insulation under elevated neutron fluences, it is necessary to consider two physical characteristics of the material:

- Is the insulator a polycrystalline solid or a compacted powder?
- If the insulator is a solid, does it have a cubic or non-cubic crystal structure?

For compacted powder ceramics, neutron damage has no effect on the strength of the material since each grain is affected individually. Accordingly, the fluence limit is set only by the swelling limit of the bulk material. Since compacted powder ceramics have typical void fractions of at least 30%, the lifetime of this insulation is not usually the limiting factor in irradiated normal-conducting magnets.

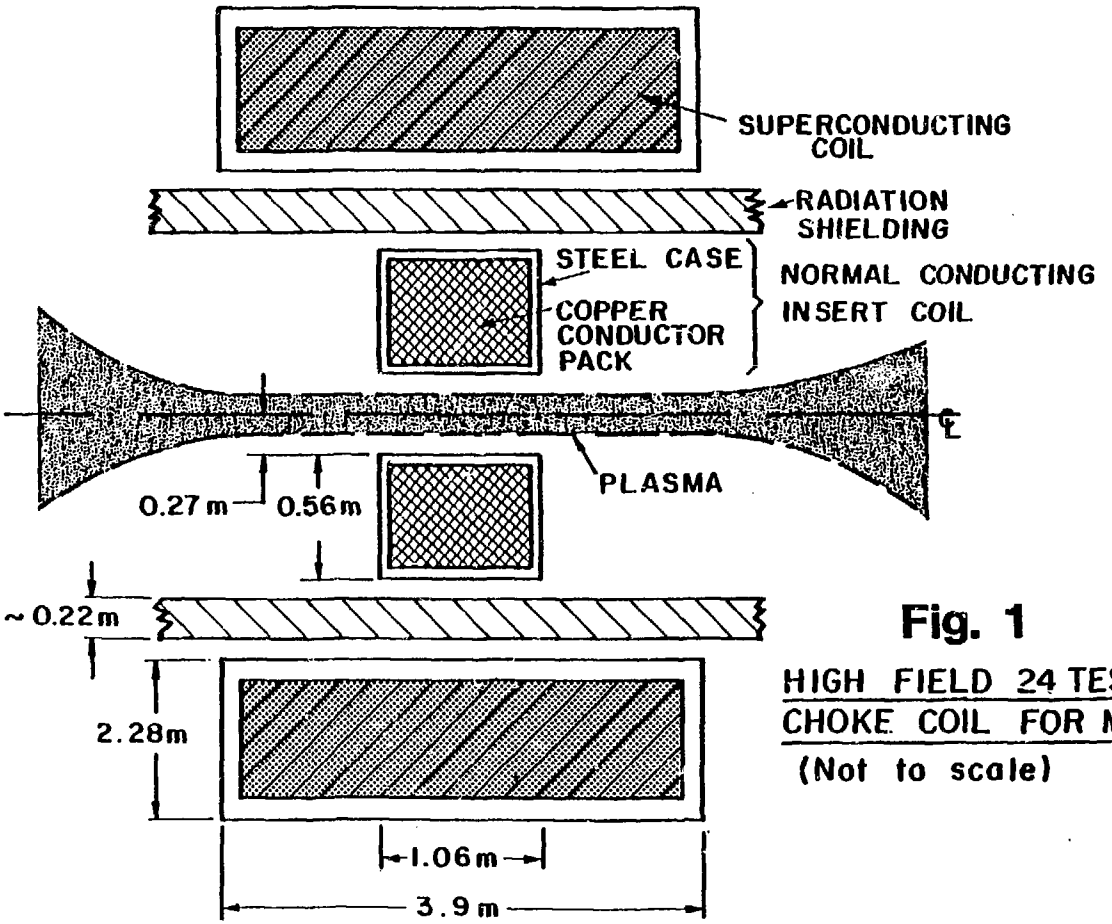

Fig. 1

HIGH FIELD 24 TESLA CHOKE COIL FOR MARS

(Not to scale)

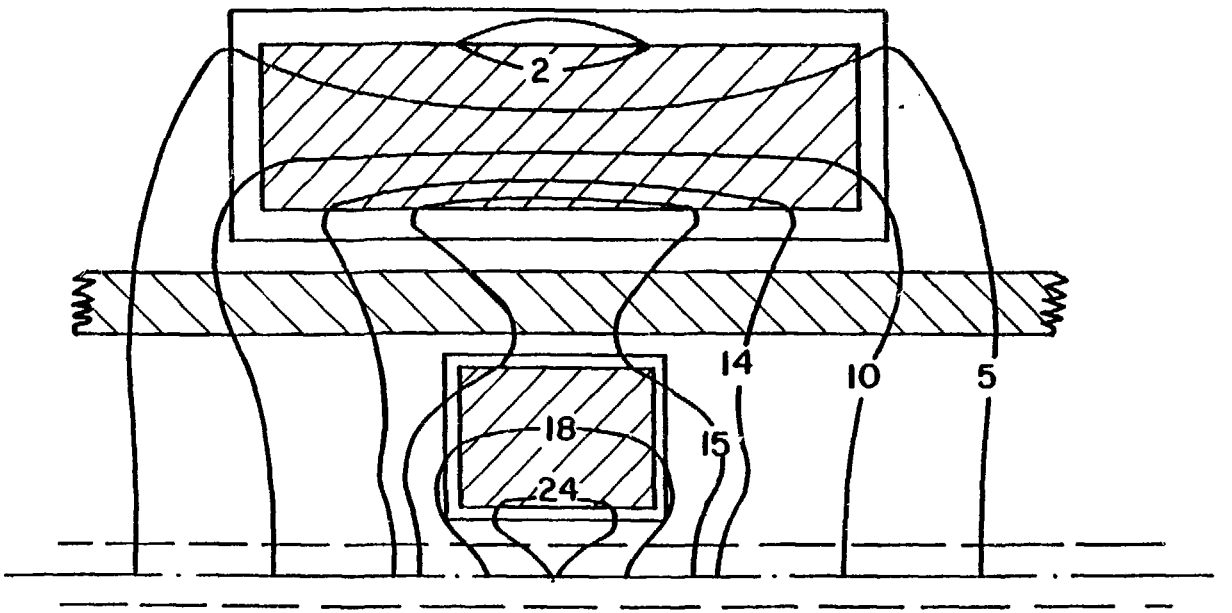

Fig. 2 CONTOURS OF CONSTANT MAGNETIC FIELD (TESLAS) FOR THE MARS 24T CHOKE COIL.

TABLE 1

MARS CHOKE COIL REQUIREMENTS

COPPER ALLOY	MZC (Mg, Zr, Cr)
INSULATOR	SPINEL ($Mg\ Al_2O_4$)
COOLANT	DEIONIZED WATER
MAX. CONDUCTOR TEMP.	140°C
MAX. FIELD IN MAGNET	24 T
CONDUCTOR DESIGN / YIELD STRESS	357 / 570 MPa (50/80) ksi
MAXIMUM NEUTRON WALL LOAD	4·5 MW / m^2
ELEC. POWER AT t=0	41 MW / COIL

In the case of cubic materials (e.g. MgO or $MgAl_2O_4$), swelling is isotropic under neutron irradiation.[4] In fact, the fracture toughness of these materials actually increases under elevated fluences. For example, for a fluence of ~ 2.1 x 10^{22} ncm^{-2} (E_n > 0.2 MeV), $MgAl_2O_4$ exhibits swelling of ~0.8 v/o and a strength increase of ~ 20%. Similarly, MgO exhibits swelling of ~ 2.6-3 v/o and a strength increase of ~ 12-24%.[4] The fluence limit for cubic ceramics is, therefore, determined only by the maximum swelling limit which a particular magnet design can tolerate. However, for non-cubic materials (e.g. Al_2O_3), swelling proceeds anisotropically which leads to the onset of structural microcracking even at modest fluences.[1] These factors dictated the choice of spinel ($MgAl_2O_4$) for the insulation in the normal conducting coils. A reasonable experimental database on swelling exists for this material[4] and, to date, appears to offer the lowest degree of swelling among its class of cubic ceramic insulators.

The peak neutron wall loading at the normal magnet is ~ 4.5 MWm^{-2}. From the 1-D transport calculations, this results in a peak neutron fluence to the spinel of 3.26 x 10^{22} ncm^{-2} (E_n > 0.1 MeV) per full power year of operation. The reported neutron swelling data for this material has been for fast fission irradiation and includes < 0.5 v/o swelling for fluences in the range 2.8 x 10^{21} ncm^{-2} to 1.2 x 10^{22} ncm^{-2} (E_n > 0.1 MeV) at temperatures of ~ 1000 K, and 0.8 v/o swelling for irradiation to 2.1 x 10^{22} ncm^{-2} (E_n > 0.2 MeV) at T = 430 K.[4] For the particular magnet design under consideration here, 3 v/o swelling of the insulation was stipulated as a reasonable design limit. Therefore, with the rather conservative asumption that the harder fusion spectrum will enhance the swelling rate by a factor of two over fast fission irradiation, the fluence limit to the spinel insulation was taken to be ~ 2.1 x 10^{22} x (3/0.8) x (1/2) = 3.94 x 10^{22} ncm^{-2}.

WATER RADIOLYSIS AND CORROSION PRODUCT FORMATION

Even in the absence of a radiation field, water-cooled copper magnets can undergo failure due to conductor-coolant interactions,[5] e.g.: water oxidation of mechanical joints, growth of CuO filaments in the water, erosion and redeposition of copper, etc. The corrosion rate of copper varies with the resistivity of the water and is minimized[5] at ~ 0.013 mm/year for water of resistivity ~ 10^4 Ωm. Under irradiation, radiolysis of the water will occur resulting in new mechanisms of corrosion. Water molecules are split to form H^+ and OH^- radicals which can recombine as H_2, O_2 and H_2O_2.[5] Radiolytic corrosion via H_2O_2 might be expected to erode ~ 0.33 mm of copper per full power year of operation of the magnet.

The original design of the normal conducting insert coil employed an externally-cooled conductor where bulk water flow was directed across the conductor layers. Since each layer is at a different electrical potential, it was expected that the buildup of radiolytic corrosion products could lead to arcing or shorting. Accordingly, in view of these electrochemical failure mechanisms, the coil was reconfigured with an internally-cooled winding design with water flowing entirely within the conductor. The disadvantages of the internally-cooled coil, i.e., its lower current density and separate water passages, are more than compensated by its increased electrical reliability and lifetime.

RESISTIVITY INCREASES IN THE COPPER CONDUCTOR

Resistivity of the copper conductor will increase under neutron irradiation due to two mechanisms, namely:

- Neutron damage via the production of defects and dislocations.
- Production of neutron-induced transmutations leading to the buildup of impurity elements.

The vast majority of work on the effects of neutron damage on copper resistivity has been performed at liquid helium temperatures and stems from interest in copper stabilizers for superconducting magnets. However, two factors combine here to suggest that resistivity effects due to damage are probably small compared with those due to transmutations. First, a large fraction of the defect-induced resistivity which would be encountered at 4.2 K is expected to be self-annealed at the operating temperature (~ 400 K) of the n/c coils[6]; defect resistivity is therefore likely to be small relative to the intrinsic resistivity at this temperature. Second, defect-induced resistivity increases approximately as the square root of the accumulated fluence and lends to a saturation limit at moderately high fluences.[6] In view of the fact that transmutation-induced resistivity scales linearly with fluence, we conclude that defect-induced resistivity is probably only a second-order consideration relative to transmutation effects.

Neutron reactions with the two stable isotopes of copper, ^{63}Cu and ^{65}Cu, give rise to transmutation products. The reactions of interest are (n,p), (n,α), (n,2n) and (n,γ), the latter resulting in unstable isotopes of coper which subsequently decay to other elements. At any instant of time, neutron transmutations of copper will have produced a mixture of radioactive Co, Ni and Cu isotopes and stable Ni, Zn and Cu isotopes.

A calculation of the number densities of impurity nuclides as a function of radial distance through the normal-conducting coil was performed as follows. First a 1-D transport calculation of the neutron spectra through the coil was made with the ANISN discrete-ordinates code. The resulting fluxes were then fed to the DKR code[7] which computes time-dependent inventories of radioactive nuclides. Subsidiary calculations were made of stable impurity nuclide inventories using the results from DKR. Figure 3 shows the concentration of the neutron-induced impurities Co, Ni and Zn, as a function of radial distance through the n/c coil after two full power years of operation. Note that the ordinate is normalized to 1 MWm^{-2} of neutron wall loading. Maximum concentrations at the inner winding are seen to be $\gtrsim$ 1750 ppm Ni, 971 ppm Zn and 33 ppm Co per MWm^{-2}. Figure 4 shows the resulting resistivity increase in the conductor as a function of radial distance due to these impurities. Again, these are after two full power years for a wall loading of 1 MWm^{-2}. Also indicated in Fig. 4 for reference are the unradiated resistivities of pure copper and a typical Zirconium-copper alloy (e.g. AMZIRC). From Fig. 4, we see that the maximum resistivity change in the inner winding is ~ 3.23×10^{-9} $\Omega m/MWm^{-2}$ after 2 FPY. Given our peak wall load of ~ 4.5 MWm^{-2} at the coil, we would expect a maximum resistivity change in the inner Zr-Cu winding of ~ 1.55 at an operating temperature of 100°C. Due to the attenuation of the neutron flux with distance through the coil, the resistivity changes are seen to fall off approximately exponentially with a factor of only ~ 1.005 at the outer winding. The average resistivity change through the coil after 2 FPY is ~ 1.12.

Increasing resistivity with time means increasing power dissipation P in the coil according to $P(t) = I^2R(t)$; note that I must be kept constant to preserve the required ampere-turn conditions. Coil lifetime due to transmutations is, therefore, dependent on the maximum reserve capacity of the magnet power supply (see below).

STRUCTURAL AND MECHANICAL DEGRADATIONS OF THE COPPER CONDUCTOR

One other aspect of neutron damage in the copper conductor should be mentioned here. The conductor in the normal magnet has to satisfy two rather conflicting requirements, namely high yield strength against hoop stresses and high electrical conductivity. For these reasons, a number of high strength copper alloys were considered[3], including MZC (Mg, Zr, Cr, Cu) and AMZIRC (Zr, Cu).

Figure 5 illustrates two potential neutron damage mechanisms as a function of radial distance through the coil, namely the number of displacements per atom from neutron impact and the helium production rate from (n,α) reactions. Both parameters are normalized to an incident neutron wall loading of 1 MW m^{-2} and are for 1 FPY of operation. Although we have assessed the effect of neutron fluence on conductor resistivity, the effects of the damage mechanisms in Fig. 5 on conductor strength and swelling-rate is not clear. According to Blewitt[8], there should be no significant loss of ductility in pure copper (or any other FCC material) up to a (fission) fluence of 10^{20} ncm^{-2}. However, these recommendations may not necessarily extrapolate to high strength copper alloys at (fusion) fluences of $>10^{22}$ ncm^{-2} encountered here.

Therefore, the following questions will require answers:

- From the dimension stability standpoint:
  - Will voids form in the copper?
  - If so, what magnitude of swelling should be expected?
  - Will the helium generated by the fusion neutrons have any effect on bubble or void formation?
- From the mechanical property standpoint:
  - How much will the yield properties be altered (up or down) by the fusion neutrons?
  - What effect will helium and/or precipitates have on the ductility of the coil during start up or shut down?

CONCLUSIONS - COIL LIFETIME

Of the four radiation mechanisms likely to degrade the performance of the n/c insert coils, only two are seen as lifetime limiting for this particular coil design, namely swelling of the spinel ceramic insulation and neutron-induced transmutations leading to resistivity increases in the conductor. Fluence degradation of the

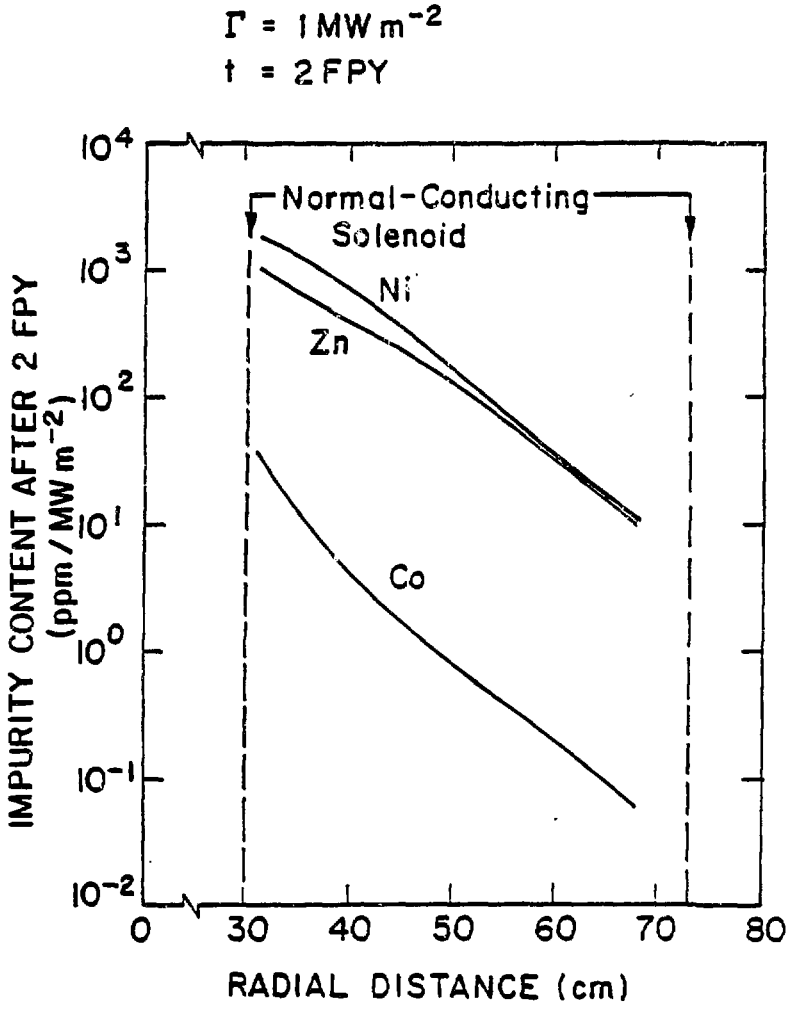
Γ = 1 MW m⁻²
t = 2 FPY
Normal-Conducting Solenoid
Ni
Zn
Co
IMPURITY CONTENT AFTER 2 FPY (ppm / MW m⁻²)
RADIAL DISTANCE (cm)
10⁴
10³
10²
10¹
10⁰
10⁻¹
10⁻²
0
30
40
50
60
70
80

Fig. 3

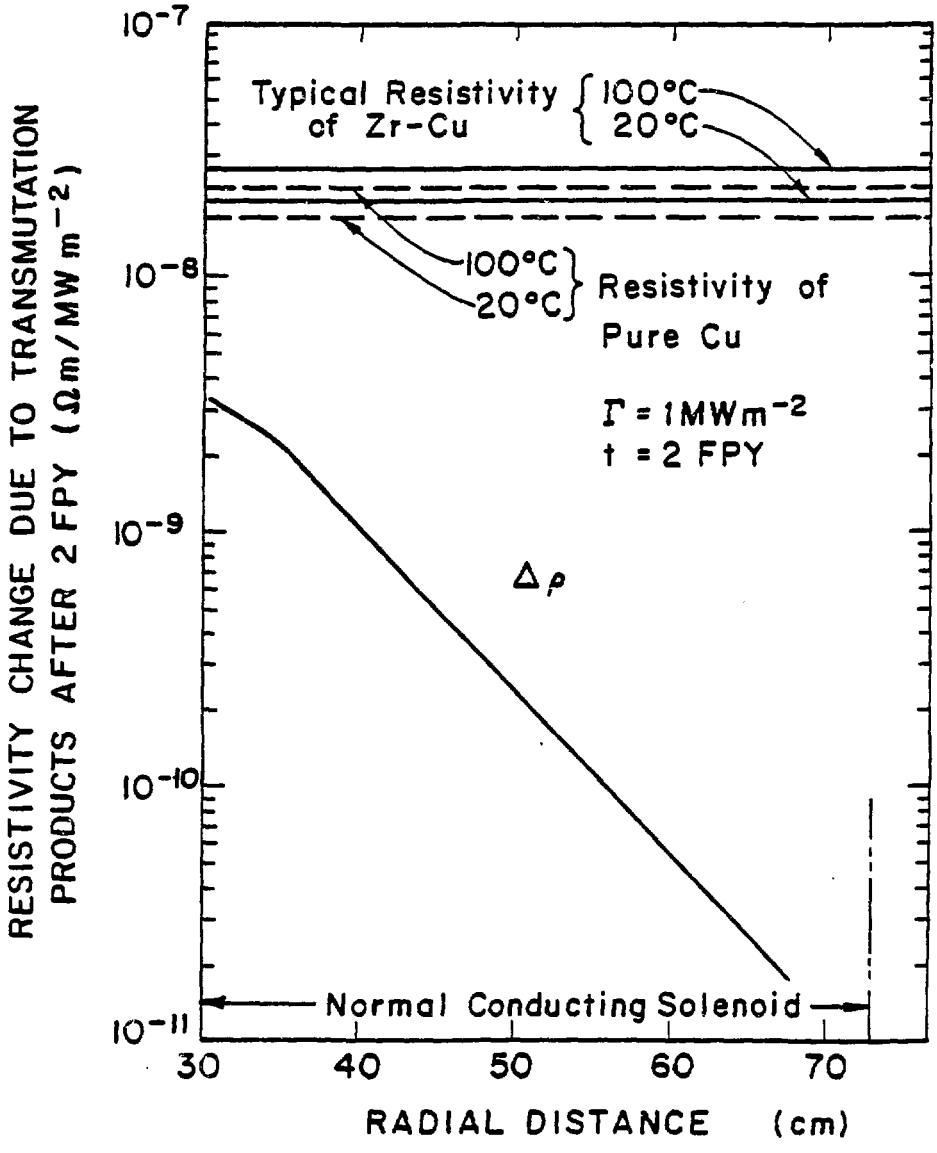
RESISTIVITY CHANGE DUE TO TRANSMUTATION PRODUCTS AFTER 2 FPY (Ωm/MW m⁻²)
10⁻⁷
10⁻⁸
10⁻⁹
10⁻¹⁰
10⁻¹¹
Typical Resistivity of Zr-Cu
100°C
20°C
100°C
20°C
Resistivity of Pure Cu
Γ = 1MWm⁻²
t = 2 FPY
Δρ
Normal Conducting Solenoid
30
40
50
60
70
RADIAL DISTANCE (cm)

Fig. 4

Fig. 5

VARIATION OF RADIATION DAMAGE IN MARS COPPER CHOKE COIL

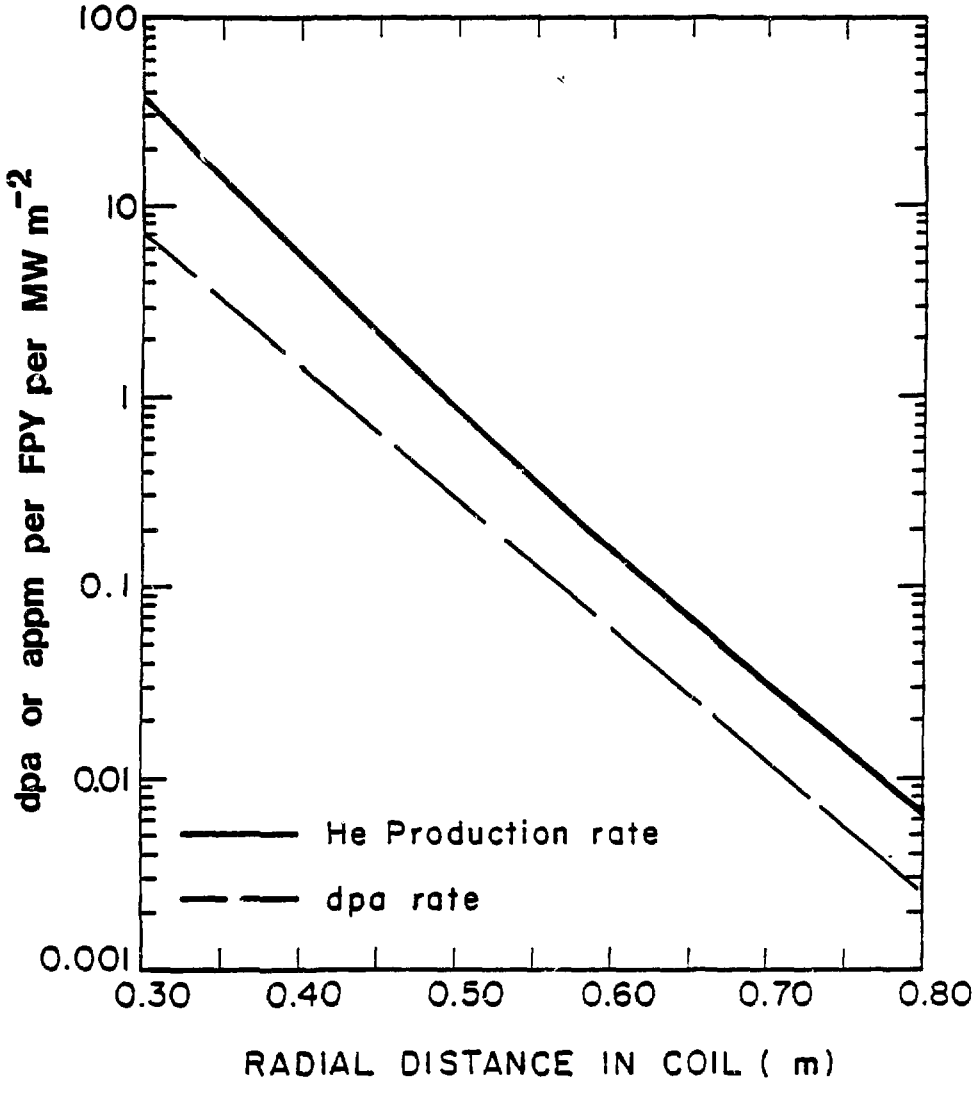

strength of the conductor may be an additional factor.

The fluence limit to the spinel insulation was seen to be ~ 3.94 x 10^{22} ncm^{-2} for the swelling design limit of 3 v/o. In addition, for a first wall load of 4.5 MWm^{-2}, the peak fluence in the spinel was shown to be ~ 3.26 x 10^{22} ncm^{-2}. Therefore, a lifetime of ~ 1.21 full power years of operation is indicated.

The coil lifetime from a transmutation viewpoint is determined rather critically by the way in which power is supplied to the magnet. The baseline design of the coil is a set of ~ 30 concentric winding layers, each powered by a separate supply.[3] In this case, the lifetime would be limited by the reserve margin of the supply feeding the inner winding. Eg, for a supply with a 50% reserve margin, the coil would require replacement every 1.82 FPY since the resistivity of the inner winding was seen to increase by a factor of 1.55 after 2 FPY. However, at this time a design change is contemplated in which the whole winding length would be powered by one supply. In this case, the power supply margin after two full power years would only need to compensate for the average increase in resistivity of the coil, i.e. ~ 12%. Therefore, providing the increased Joule heating in the inner windings can be accommodated, this latter design should ensure long coil life with regard to conductor resistivity increases.

However, one other important feature of increasing coil resistivity is the asociated increasing operating costs. Depending on the particular coil design under consideration, the normal Joule heating losses are ~ 41 MW per coil at start of life.[3] Assuming that the resistivity datum point at 2 FPY can be scaled linearly with operating life (a reasonable assumption provided the number density of transmuted products remains below ~ 1% of the copper atomic density), the curves in Fig. 6 result. Here is shown the additional power requirements due to resistivity increases and the corresponding increase in integrated operating costs as a function of the coil operating life. Note that if both coils in the reactor were to be operated for 20 years this would result in an extra 200 M$ in operating costs! There is thus a strong economic incentive to changeout the coils after only a few FPY of operation.

At present, therefore, the lifetime of this highly irradiated coil appears to be limited by swelling of the spinel insulation to ~ 1.21 full power years. In view of the deleterious effect of frequent coil changeout on the downtime of the machine and, therefore, on the cost of generated electricity, it would seem expedient to increase this lifetime, either by providing some relatively thin intervening shielding or by designing for a greater than 3 v/o swelling in the inner windings. Coil lifetimes of 2 FPY or more would seem to be a desirable goal.

REFERENCES

1. F.W. Clinard, "Ceramics for Applications in Fusion Systems," J. Nucl. Mater., 85, 86, 393 (1979).

2. L.J. Perkins, "Radiation Dose-Rate Resistivity Degradation in Ceramic Insulators and Assessment of the Consequences in Fusion Reactor Applications," UWFDM-469, University of Wisconsin Fusion Engineering Program Report (1982).

3. "Mirror Advanced Reactor Study (MARS) - Interim Report," UCRL-53333, Lawrence Livermore National Laboratory (to be published 1983).

4. G.F. Hurley, J.C. Kennedy and F.W Clinard, "Structural Properties of MgO and $MgAl_2O_4$ after Fission Neutron Irradiation Near Room Temperature," LA-UR 81-2078, Los Alamos Scientific Laboratory (1981).

5. J.H. Schultz, "Design Practice and Operational Experience of Highly Irradiated High Performance Normal Magnets" PFC/RR-82-25, MIT Plasma Fusion Center (1982).

6. J.M. Williams, C.E. Klabunde, J.K Redman, R.R. Coltman and R.L. Chaplin, "The Effects of Irradiation on the Copper Normal Metal of a Composite Superconductor," IEEE Trans. Mag., MAG-15, 731, (1979).

7. T.Y. Sung and W.F. Vogelsang, "DKR: A Radioactivity Calculation Code for Fusion Reactors," UWFDM-170, University of Wisconsin Fusion Engineering Program Report (1976).

8. See Reference 5, p. 27.

Fig. 6

ECONOMIC CONSEQUENCES OF RADIATION-INDUCED RESISTIVITY INCREASES IN THE MARS NORMAL INSERT COIL

(Graph is for one coil. Multiply by 2 for total costs.)

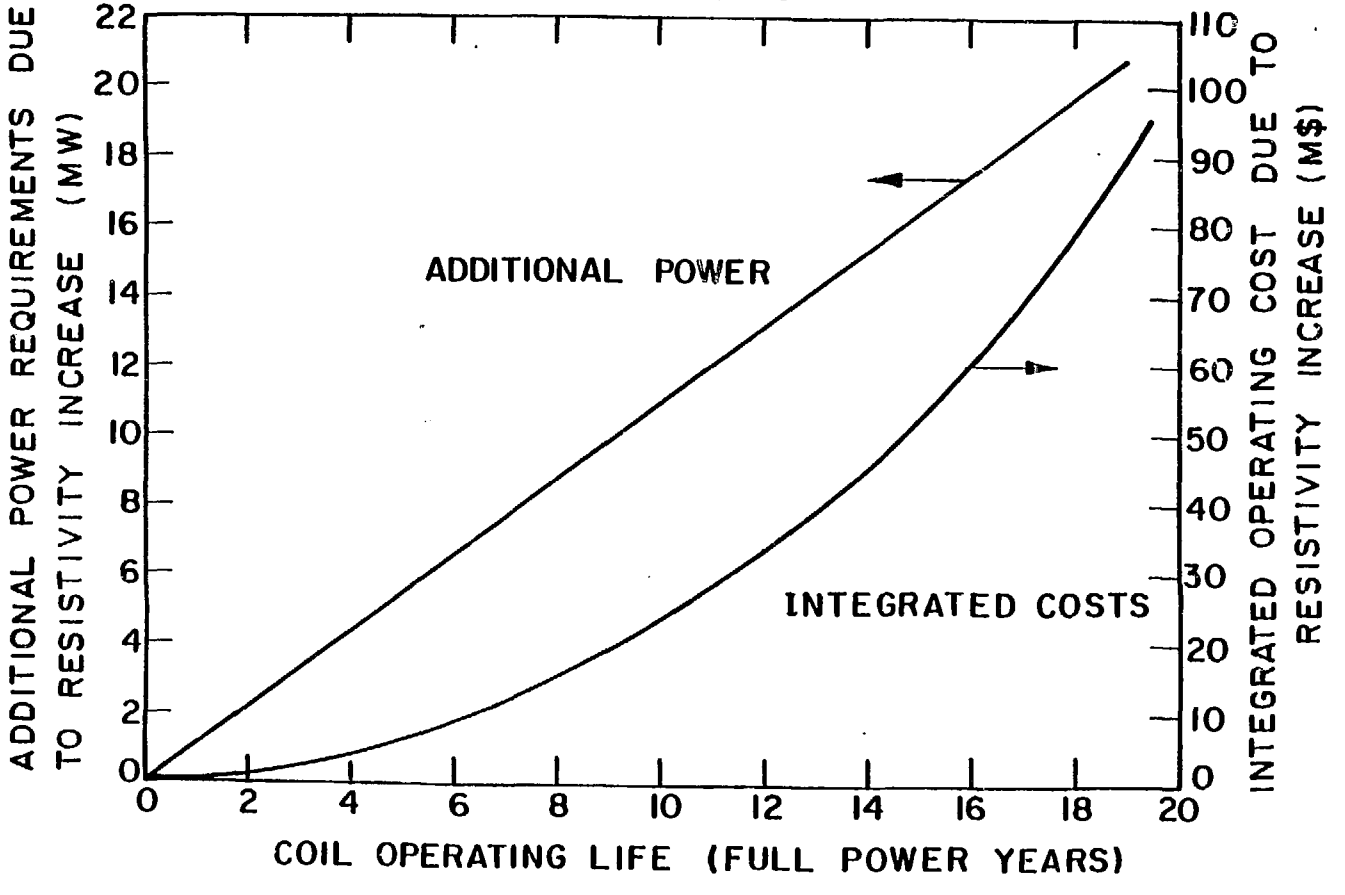

RADIATION EFFECTS AND LIFETIME CONSIDERATIONS FOR THE HIGHLY IRRADIATED COPPER MAGNETS IN THE MARS TANDEM MIRROR REACTOR

L. John Perkins
University of Wisconsin

April 1983

Requirements for High Field Hybrid Magnets in Mirror Fusion Devices

- **MARS – Mirror Advanced Reactor Study (~2020)**
  24 Tesla (240 kG)*

- **TASKA – Joint University of Wisconsin/Karlsruhe Tandem Mirror Study (1990s)**
  20 Tesla (200 kG)*

- **MFTF-B Upgrade – DT Burning MFTF-B (1980s)**
  12 and 18 Tesla (120 and 180 kG)**

*** Outer Nb_3Sn solenoid; inner normal–conducting copper coil**

**** Outer NbTi solenoids; inner normal–conducting copper coils.**

MARS REACTOR CONFIGURATION

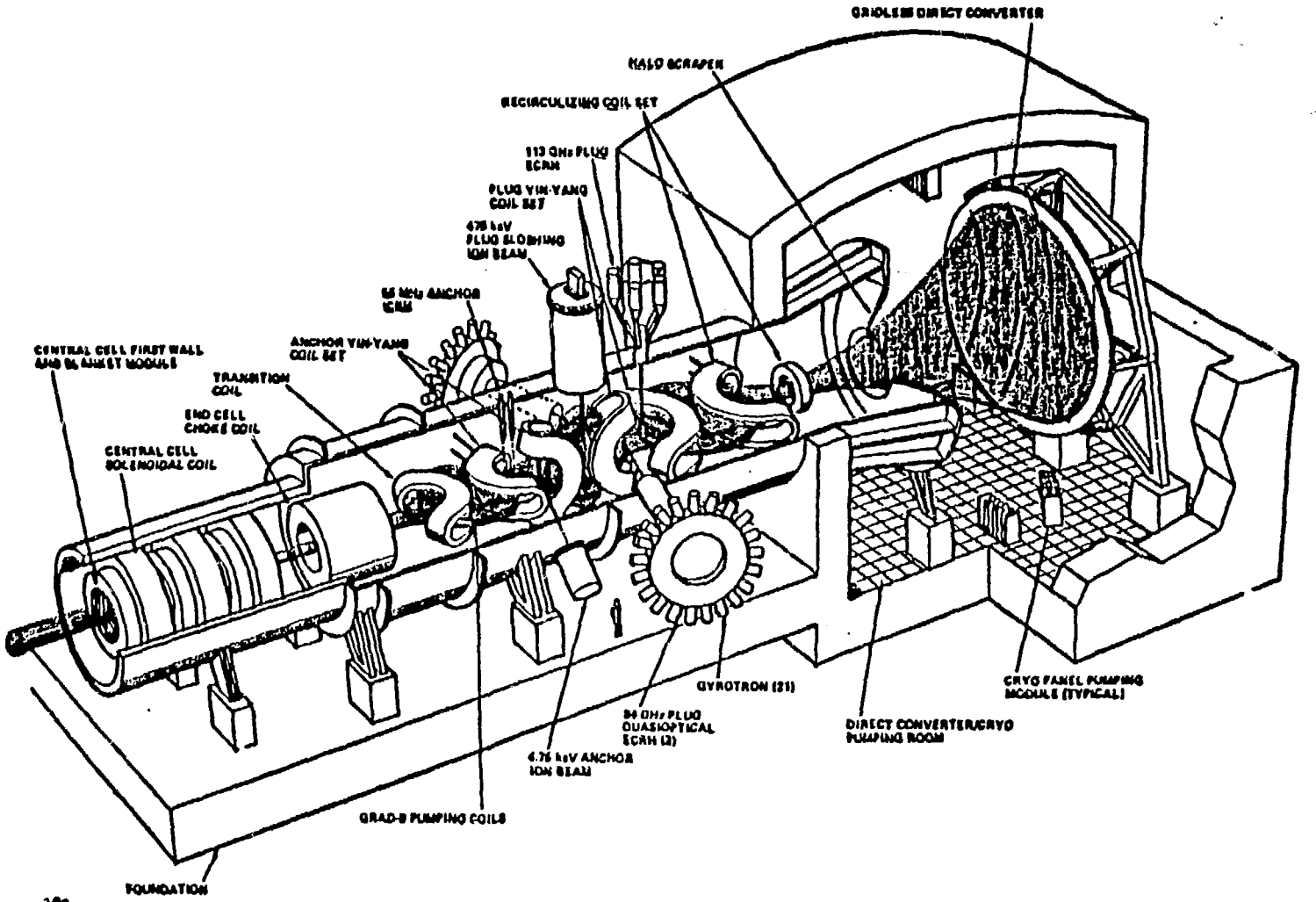

TASKA CENTRAL CELL LAYOUT

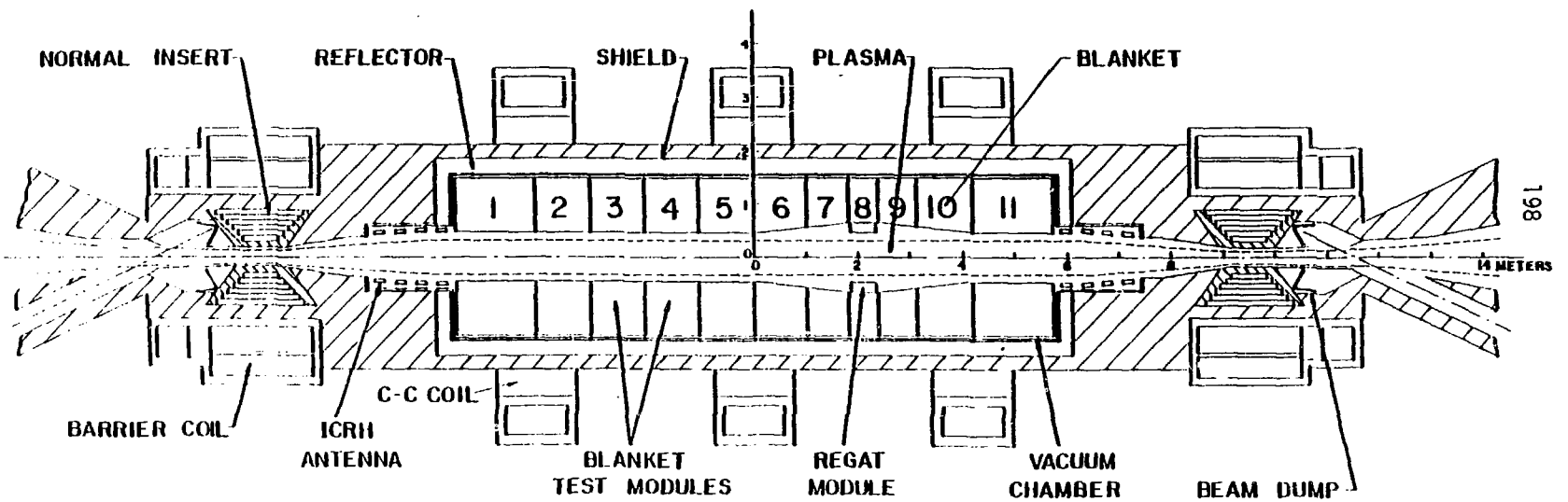

Radiation Problem Areas for The MARS Normal–Conducting Insert Coils

- **Resistivity degradations in ceramic insulation under instantaneous neutron and gamma absorbed dose–rates.**
- **Radiolytic dissociation of coolant water leading to conductor corrosion product formation.**
- **Mechanical and structural degradations in the ceramic insulation under long–term neutron fluence.**
- **Resitivity increases in the MZC copper conductor due to radiation damage and neutron–induced transmutations.**
- **Mechanical and structural degradations in the MZC copper conductor under long–term neutron fluence??**

AXIAL VIEW OF RESISTIVE INSERT

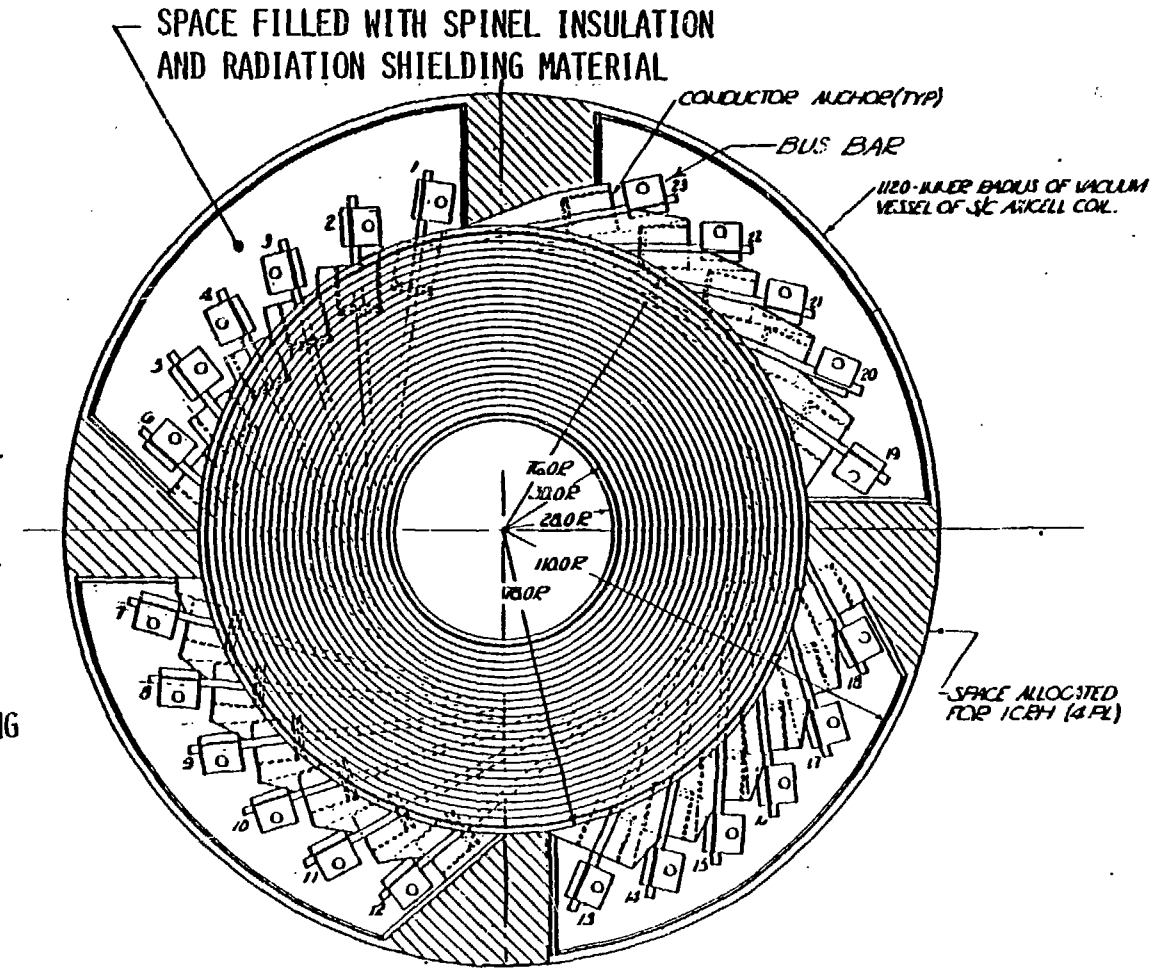

- LEADS ARE INDIVIDUALLY ANCHORED TO END PLATES THAT PROVIDE STRUCTURAL SUPPORT.
- COIL LEADS CONFIGURATION LEAVES SPACE FOR ICRH COMPONENTS AND RADIATION SHIELDING MATERIAL.

DIMENSIONS IN CENTIMETERS

WE HAVE DEVELOPED A MACHINED-DISC RESISTIVE COIL CONCEPT

KEY FEATURES —

- PANCAKE WINDING - 4 TURNS/PANCAKE, 38 PANCAKES
- TWO PANCAKES MACHINED FROM A DISC
- CONDUCTORS SPIRALLY MACHINED, CONDUCTOR DEPTH INCREASES WITH RADIUS
- PANCAKES CONNECTED ELECTRICALLY IN SERIES
- WATER FLOW COOLS DOUBLE PANCAKES IN PARALLEL

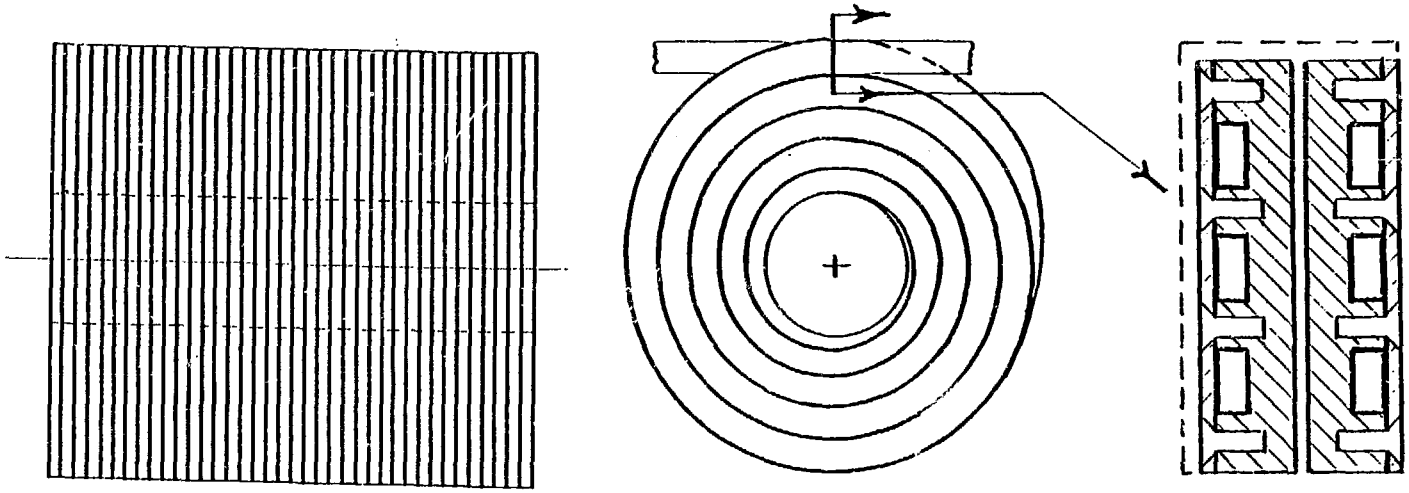

THE CONDUCTOR HEIGHT VARIES

KEY FEATURES

- MZC MATERIAL
- WATER CARRIED IN THIN-WALLED TUBES SOLDERED INTO MACHINED GROOVES
- HEIGHT VARIED TO KEEP STRESS CONSTANT
- MAXIMUM WATER TEMPERATURE 125°C
- MAXIMUM COPPER TEMPERATURE 140°C

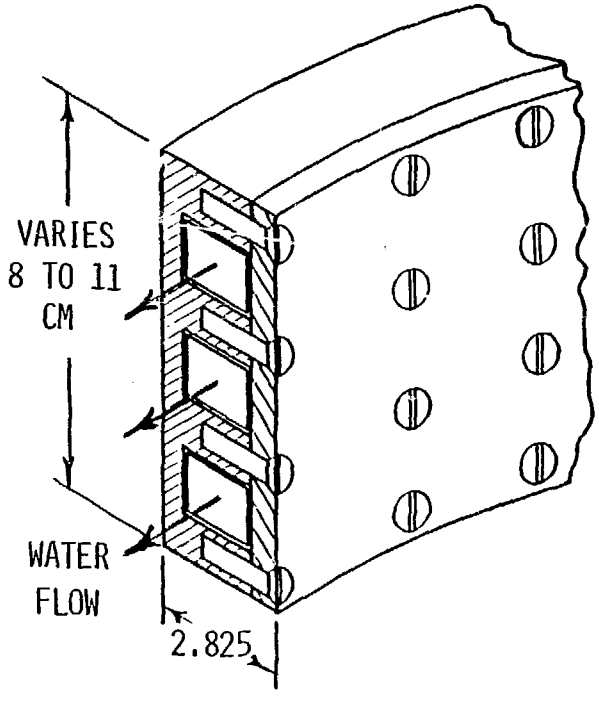

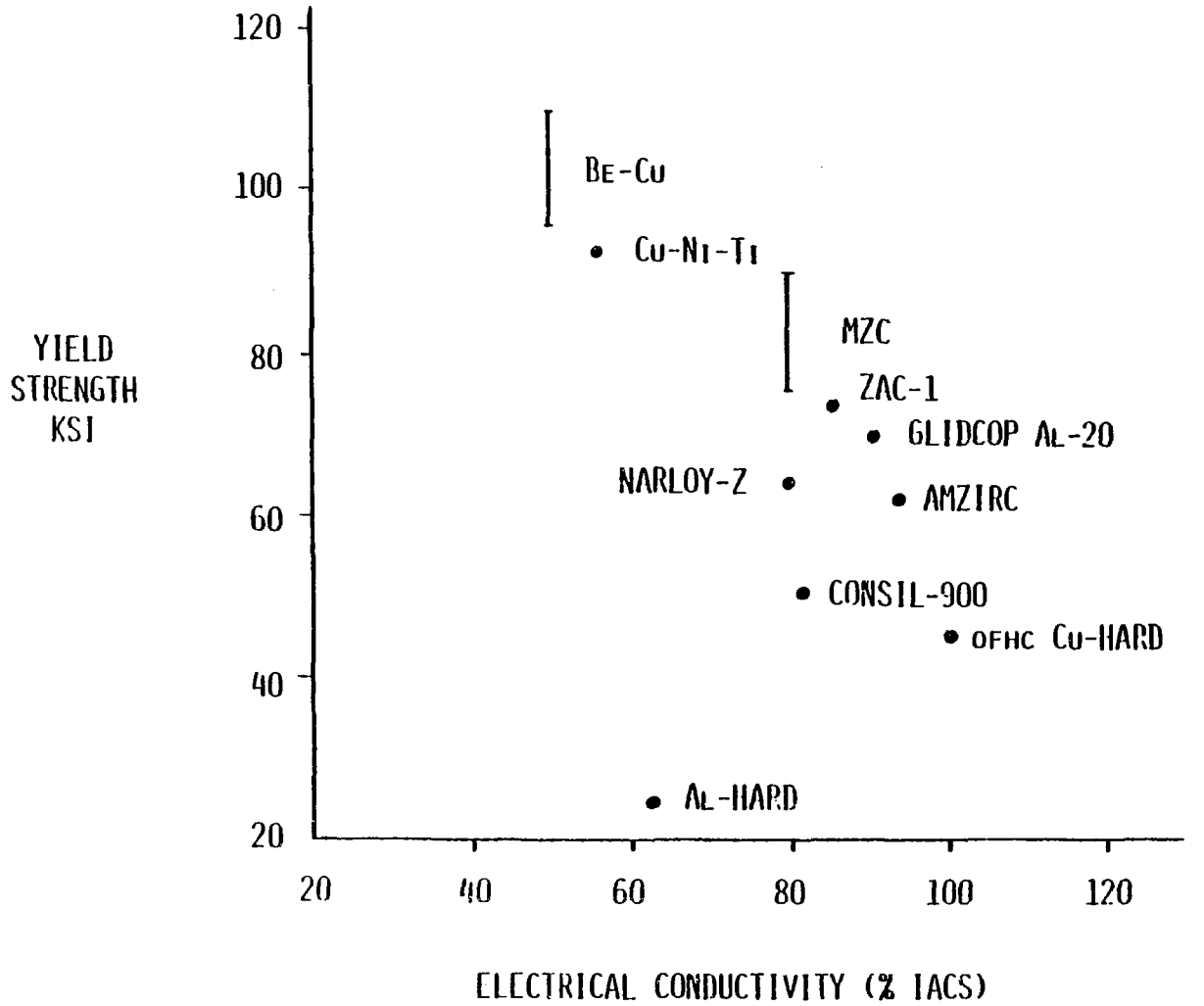

Alloy Properties for Resistive Coils

RESISTIVITY INCREASE IN NORMAL CONDUCTING SOLENOID DUE TO NEUTRON–INDUCED TRANSMUTATIONS OF COPPER

- **Neutron reactions with ^{63}Cu (0.69 a/o) resulting in transmuted products are:**

$^{63}Cu(n,\gamma)^{64}Cu(\beta^-, \beta^+, EC, 12.7\ h)\ ^{64}Zn, ^{64}Ni$

$^{63}Cu(n,2n)^{62}Cu(\beta^+, 9.7\ m)^{62}Ni$

$^{63}Cu(n,p)^{63}Ni(\beta^-, 100\ y)^{63}Cu$

$^{63}Cu(n,\alpha)^{60}Co(\beta^-, 52.7\ y)^{60}Ni$

- **Neutron reactions with ^{65}Cu (0.31 a/o) resulting in transmuted products are:**

$^{65}Cu(n,\gamma)^{66}Cu(\beta^-, 5.1\ m)^{66}Zn$

$^{65}Cu(n,2n)^{64}Cu(\beta^-, \beta^+, EC, 12.7\ h)^{64}Zn, ^{64}Ni$

$^{65}Cu(n,p)^{65}Ni(\beta^-, 2.52\ h)^{65}Cu$

$^{65}Cu(n,\alpha)^{62}Co(\beta^-, 1.5\ m)^{62}Ni$

- **After 2 FPY, result is a mixture of radioactive Co, Ni and Cu and stable Ni, Zn and Cu isotopes**

Calculation of Resistivity Changes in MZC due to Transmutations

- **Perform 1–D neutron transport calculations to obtain neutron fluxes as a function of radial distance through coil (codes: ANISN, ONEDANT, etc.).**

- **Incorporate fluxes in DKR radioactivity code to obtain radioactive transmuted products.**

- **Compute stable transmuted products from DKR results.**

- **Use prescription of Seitz* to relate resistivity changes to impurity product concentrations.**

- **After 2 FPY of operation, maximum concentrations of impurities at inner windings are 1750 ppm Ni, 971 ppm Zn and 33 ppm Co per MWm^{-2} wall loading.**

- **For typical Zr–Cu at 100°C, $\Delta\rho/\rho = 12\%$ per MWm^{-2} at inner windings and 2.7% per MWm^{-2} volume–averaged, after 2 FPY operation.**

---

*F. Seitz, "The Modern Theory of Solids", McGraw Hill (1940).

Design Questions for Irradiated Copper Conductors

1) From the dimension stability standpoint;

- **Will voids form in the copper?**
- **If so, what magnitude of swelling should be expected?**
- **Will the helium generated by the fusion neutrons have any effect on bubble or void formation?**

2) From the physical property standpoint;
How much will the electrical resistivity change as transmutations are produced and precipitates are dissolved?

3) From the mechanical property standpoint;

- **How much will the yield properties be altered (up or down) by the fusion neutrons?**
- **What effect will helium and/or precipitates have on the ductility of the coil during startup or shutdown?**

4) From the operations viewpoint;

- **When will the magnet have to be replaced?**
- **Can we trade longer life (by shielding the magnet) against higher operating costs (higher R)?**

Conclusions

- **Lifetime of MARS normal insert coil is presently limited to ~1.2 FPY due to swelling in the spinel ceramic insulation.**

- **Resistivity changes due to transmutations in the MZC conductor after 2 FPY are**

–Inner winding, peak $\Delta\rho/\rho$ = 55%.

–Overall magnet, vol.–averaged $\Delta\rho/\rho$ = 12 %.

- **Increase in resistivity due to damage can probably be neglected compared with that due to transmutations.**

- **Effect of neutron damage on strength of Zr–Cu alloys needs to be investigated. By how much does the 80 ksi yield strength increase/decrease per MW-year/m^2 of neutron wall load?**

- **Effect of conductor swelling under elevated neutron fluences needs investigation. Maximum swelling tolerance of MARS conductor is a design constraint for the coil.**

LEFT BLANK INTENTIONALLY

RADIATION EFFECTS LIMITS ON COPPER IN SUPERCONDUCTING MAGNETS

M. W. Guinan

Lawrence Livermore National Laboratory

RADIATION EFFECTS LIMITS ON COPPER IN SUPERCONDUCTING MAGNETS

M. W. Guinan
Lawrence Livermore National Laboratory

SUMMARY

The determination of the response of copper stabilizers to neutron irradiation in fusion reactor superconducting magnets requires information in four areas.

1. Neutron flux and spectrum determination are a major factor in the accuracy with which stabilizer response can be predicted. Since magnet stability depends on the "weakest link", calculations must be made in sufficient detail to fully account for steep flux gradients and local pertubations from penetrations.

2. Resistivity changes at zero field in magnet spectra are generally calculated from the damage energy cross-section or the equivalent displacement (dpa) rate. While such scaling is valid for hard (high energy spectra), it underestimates the resistivity changes in typical magnet spectra by as much as 20%. Furthermore, misapplication of dpa scaling can lead to errors of a factor of two. Methods to standardize the calculation of resistivity changes are presented.

3. Resistivity changes at field for conceptual designs are generally determined from the changes predicted at zero field by the use of a Kohler plot. This can lead to a significant uncertainty (25% or more) in the resistance at field since Kohler plots for all copper samples are not identical. It has been observed, however, that a Kohler plot determined on a conductor solely by varying the field can also be used to describe the variation of the magnetoresistance

as a result of cold-work, neutron irradiation and subsequent annealing. This greatly simplifies the task of predicting the response of the magnetoresistance of actual conductors to changes resulting from fabrication of magnets and use in fusion reactors. It does, however, require that initial measurements be made on the actual conductor.

4. The cyclic irradiation and annealing, expected to be characteristic of fusion reactor magnet operation, is presently the largest source of uncertainty in determining the limits of neutron exposure for copper stabilizers. As a result of a joint ORNL/LLNL effort to study cyclic effects with both 14.8 MeV neutrons at RTNS-II and in a very soft spectrum at BSR, limits to the expected behavior have been obtained. Planned work by ORNL at the Intense Pulsed Neutron Source (IPNS) at Argonne in a spectrum much closer to that expected for magnets will further refine uncertainties.

Applications of our current understanding of the limits of copper stabilizers in fusion reactor designs are explored in two examples. Recommendations for future additions to the data base are discussed.

INFORMATION REQUIREMENTS FOR THE ASSESSMENT OF RADIATION EFFECTS LIMITS

- NEUTRON FLUX AND SPECTRUM
- RESISTIVITY CHANGE AT ZERO FIELD $[\Delta\rho(0)]$ AS A FUNCTION OF SPECTRUM AND FLUENCE
- RESISTIVITY CHANGE AT FIELD $[\Delta\rho(H)]$ AS A FUNCTION OF $\Delta\rho(0)$
- RECOVERY DURING CYCLIC ANNEALING

Neutron Flux and Spectrum

- FLUX GRADIENTS
- PENETRATIONS
- GROUP STRUCTURE
- CROSS-SECTION FILES

ABDOU - TEPR
ENGHOLM - ETF
U. WI[illegible] - MARS

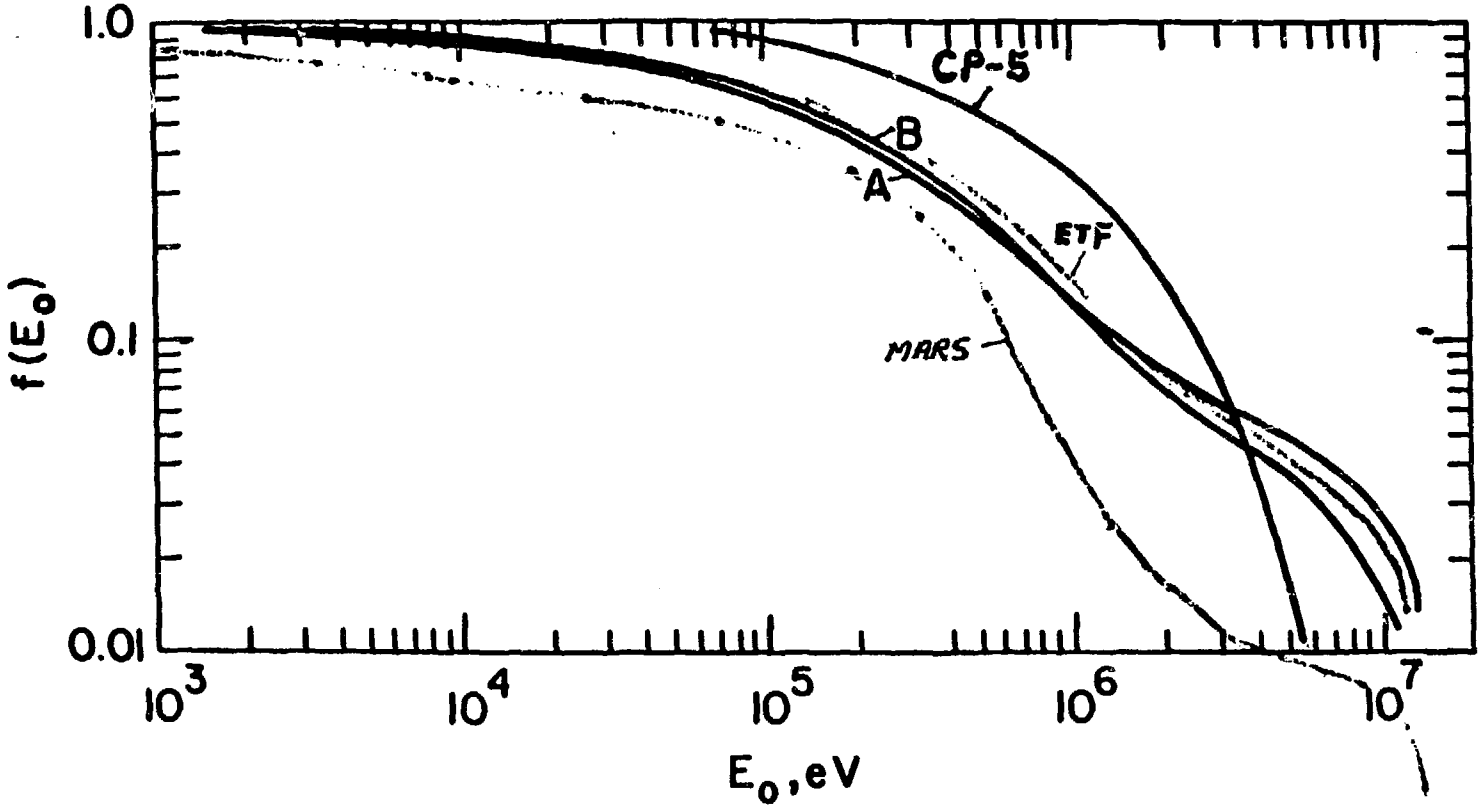

The Fraction, $f(E_0)$, of the Total Neutron Flux with Neutron Energies above E_0, as a Function of E_0. Curves A and B are for the Flux Outside a SS-B_4C Blanket/Shield of Thickness 60 and 100 cm, Respectively. Curve C is for the Flux in ANL Low Temperature Facility.

Resistivity Damage Rate ($\Delta\rho/\Delta\phi t$) at Zero Field

- Definitions
- Pitfalls
- Damage energy (DPA) scaling
- $\Delta\rho/\Delta\phi t$ vs neutron energy

DEFINITIONS

the number of displacements produced by a recoiling atom of energy T is

MODIFIED KINCHIN-PEASE $$\nu(T) = K \frac{T - T_e}{2T_A} = K \frac{T_{DE}}{2T_A}$$

where T_{DE} is called the damage energy

integrating over all recoils produced by an irradiating particle or spectrum of particles we can write

$$\underline{dpa} = K \frac{\sigma_{DE} \Delta\phi t}{2T_A} \quad (K = 0.8 \text{ is "STANDARD"})$$

the copper resistivity change in a magnet neutron spectrum is thus calculated from

$$\Delta\rho_{CALC} = \eta \rho_f \underline{dpa}$$

where ρ_f is the Frenkel pair resistivity and η is determined from experiment (in general in a different spectrum) as

$$\eta = \left(\frac{\Delta\rho}{\Delta\phi t}\right)_{EXP} \frac{2T_A}{0.8 \rho_f \sigma_{DE}}$$

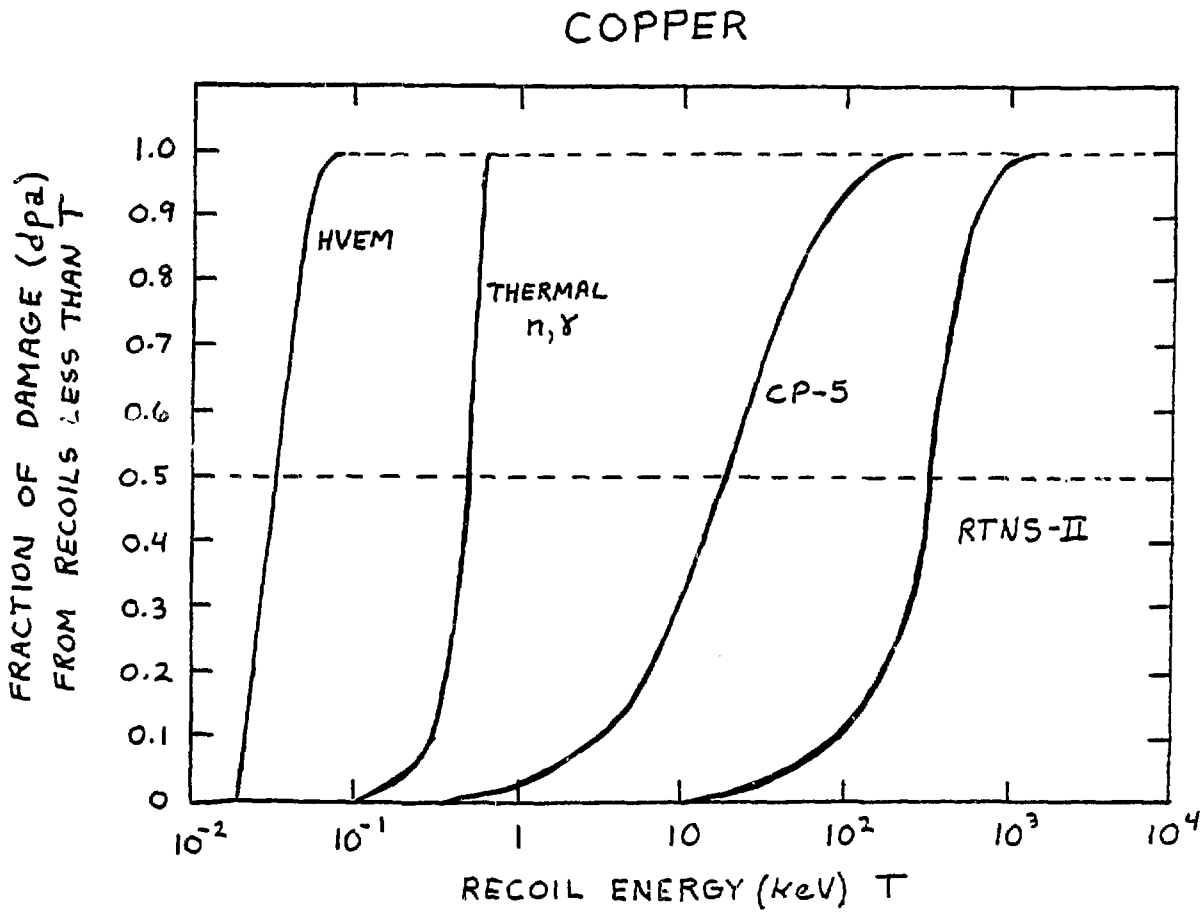

INTEGRAL DAMAGE ENERGY (dpa)
FOR VARIOUS SOURCES

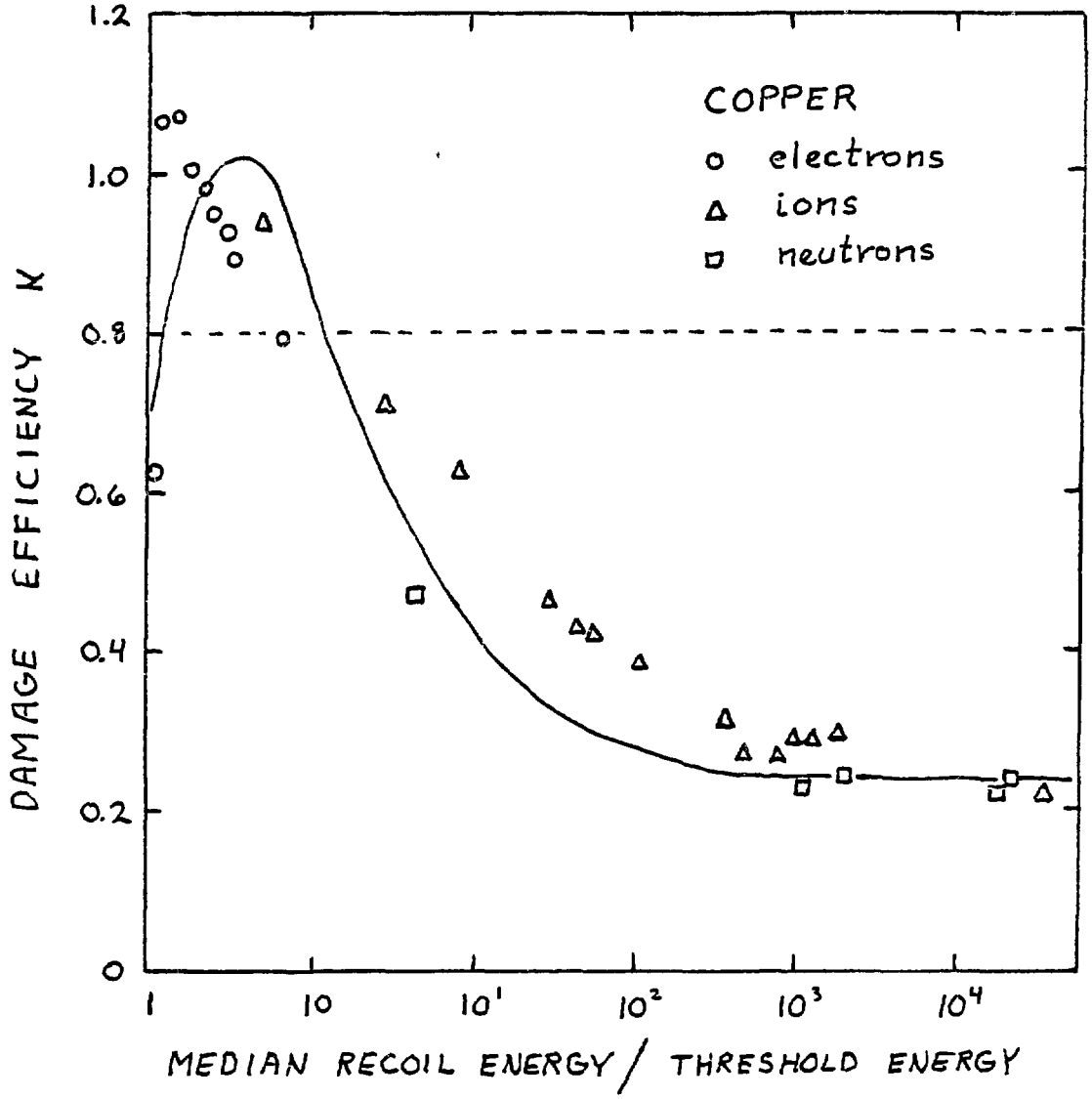

EXPERIMENTAL DEFECT PRODUCTION

DAMAGE RATES IN MAGNET SPECTRA

SPECTRUM	DAMAGE ENERGY CROSS-SECTION (b-keV)	RELATIVE σ_{DE}	RELATIVE $\partial\varrho/\partial\phi t$
TEPR (A)	36.4	0.448	0.535
ETF	39.1	0.481	0.556
STARFIRE	37.8	0.465	0.542
MARS			
"PURE FISSION"	81.3	1.00	1.00†
RTNS-II	288.0	3.54	3.43†

† from experiment

TABLE II

Copper Resistivity Damage Rates by Neutron Groups

Upper Bound Neutron Energy (MeV)	$\delta\rho/\delta\phi^*$ (10^{-25} Ω-cm/n/cm^2)
2.500 E00	0.755
1.988 E00	0.655
1.581 E00	0.584
1.257 E00	0.556
1.000 E00	0.499
8.409 E-01	0.462
7.071 E-01	0.422
5.946 E-01	0.379
5.000 E-01	0.327
2.236 E-01	0.259
1.000 E-01	0.171
1.261 E-02	0.073
1.590 E-03	0.009
2.000 E-04	0.001
2.520 E-05	0.001
3.180 E-06	0.003
4.000 E-07	0.019
1.000 E-10	

For comparison:

Pure Fission Spectrum	0.723×10^{-25} Ω-cm/n/cm^2
14.8 MeV (RTNS-II)	2.42×10^{-25} Ω-cm/n/cm^2

*At zero field

Resistivity Changes at Field

- Kohler plots
- sources of variations
- conductor characterization

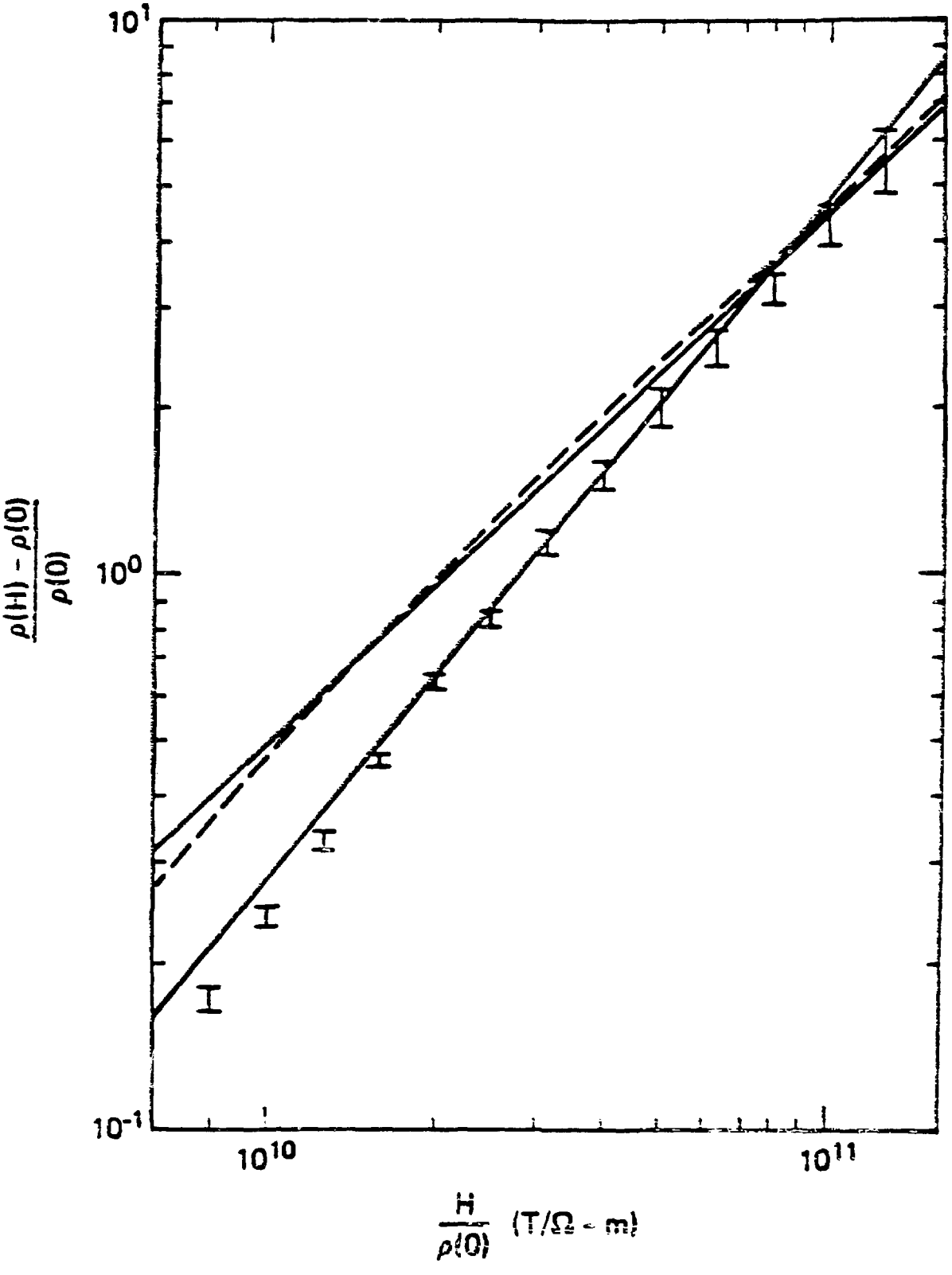
10^1
10^0
10^{-1}
10^{10}
10^{11}
$\frac{\rho(H) - \rho(0)}{\rho(0)}$
$\frac{H}{\rho(0)}$ (T/Ω - m)

MAGNETORESISTANCE

$$[\rho(H)-\rho(0)]/\rho_0 = f(H/\rho(0))$$

KOHLERS RULE

WILLIAMS ET AL (ORNL)

NEUTRON IRRADIATED COPPER

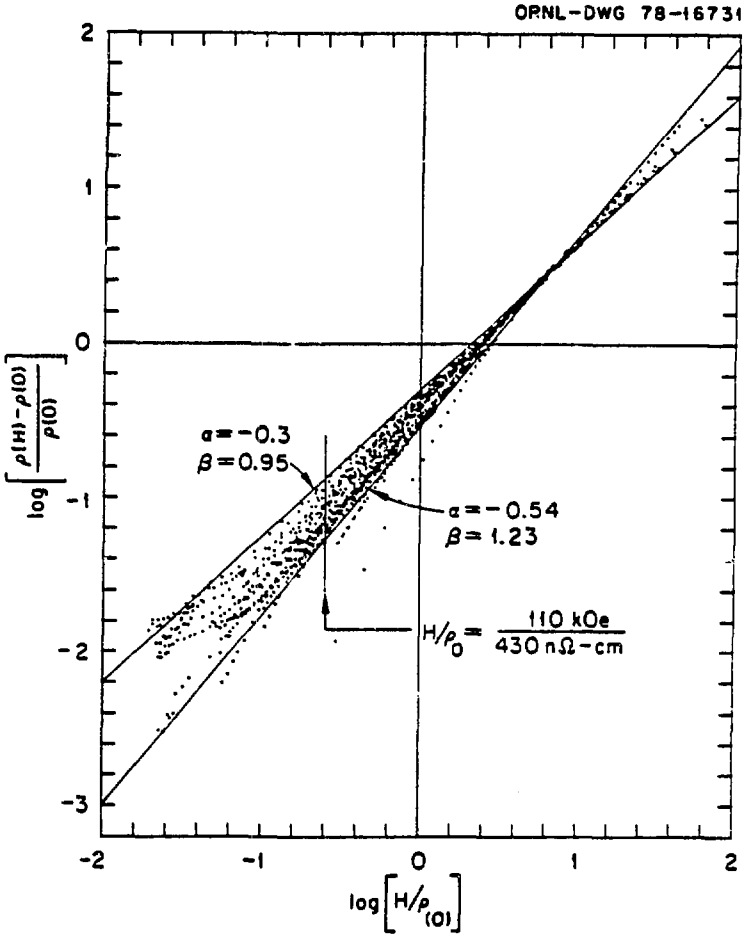

DEVIATIONS FROM A SINGLE KOHLER PLOT CAN BE VERY SIGNIFICANT

IRRADIATION OF COPPER FROM THE LARGE COIL PROGRAM

- JOINT ORNL/LLNL PROGRAM
- VARIOUS AMOUNTS OF COLD WORK
- CYCLIC IRRADIATION AND ANNEAL

FACILITY	MAXIMUM FIELD	STATUS
BSR (ORNL)	3.8 T	COMPLETE
IPNS (ANL)	4.6 T	EARLY FY82
RTNS-II (LLNL)	13.0 T	~~LATE FY82~~ COMPLETE

Table 3.4.1. Sample Specifications

Sample	Treatment	Diameter (mm)	Gauge Length (mm)	ρ^d(4.2K)	RRR[e]
CUUN0[a]	Recrystallized	.1259	11.0	4.74	363
CUUN1[a]	7.5% cold-worked	.1261	11.1	11.27	153
CUUN2[a]	14.3% cold-worked	.1261	10.1	19.10	91
CUOX0[b]	Recrystallized	.1260	7.9	2.77	621
CUOX1[b]	7.5% cold-worked	.1263	9.1	9.35	185
CUOX2[b]	14.3% cold-worked	.1261	10.0	16.15	107
CUHP0[c]	Recrystallized	.1262	9.3	0.37	4621
CUHP2[c]	14.3% cold-worked	.1260	8.1	9.59	180

[a] OFHC copper Intermagnetics General Corp. CDA-101.

[b] Same as [a] with an oxidizing anneal.

[c] 99.999% Asarco copper with an oxidizing anneal.

[d] Corrected for size effect. Resistivity in $10^{-11}\Omega$-m.

[e] Ratio of resistance at 293 K to that at 4.2 K.

Pre-irradiation values of the resistivity as a function of field for all eight samples are given below in Table 3.4.2. The field and resistivity values shown are averages of measurements made in stepping the field up to and down from 11.783 T.

Table 3.4.2. Pre-Irradiation Resistivities[a]

Field[b]	0	1.816	3.827	5.791	7.694	9.767	11.783
Sample							
CUUN0	4.99	12.39	22.43	31.96	40.50	49.39	57.60
CUUN1	11.14	17.54	26.84	36.51	45.98	56.12	65.83
CUUN2	17.04	23.31	31.86	40.93	50.08	60.13	69.83
CUOX0	3.09	10.93	20.40	28.39	35.88	43.42	50.49
CUOX1	8.46	15.05	24.58	33.97	42.92	52.39	61.32
CUOX2	14.72	21.26	29.96	38.96	47.85	57.46	66.60
CUHF0	0.82	8.29	16.25	23.64	30.83	38.78	47.01
CUHP2	9.25	17.34	26.18	34.67	43.01	51.80	60.22

[a] Size effect corrected. Values in units (±.05) of $10^{-11}\Omega m$

[b] Values in tesla (±.005)

In order to make comparisons with the work of Coltman and Klabunde on these materials as precise as possible, the values of A/ℓ for conversion of resistance measurements to resistivities were inferred from resistance measurements near room temperature, rather than from measured values of area (A) and gauge length (ℓ). The standard thermal resistivity (ρ_{th}) adopted[7] for this purpose was $1.7860 \times 10^{-8}\Omega m$ at a temperature of 36.1°C. Because of the small diameter of the wires and the high purity of some of the samples, corrections for size effects are important. These were made from the tables published by Dworschak et al.[8] using a value[9] for the product of the bulk resistivity and electron mean free path in copper ($\rho_b \ell$) of $7 \times 10^{-16}\Omega m^2$.

Sample CUUN1 was used as a monitor during the irradiation-anneal cycles with the objective of reaching the same resistivity at 12 T at the conclusion of each irradiation. A raw data plot of sample resistance at zero field vs. proton recoil counts is shown in Fig. 3.4.1. The number of recoil counts is approximately proportional to the neutron fluence on the sample. This relationship is not exact because of small variations in the deuteron beam size and position. However, combining the five irradiation legs, this assumption is sufficiently accurate to derive a value for the saturation resistivity, ρ_{∞}, of $165 \pm 15 \times 10^{-11} \Omega m$ for this sample.

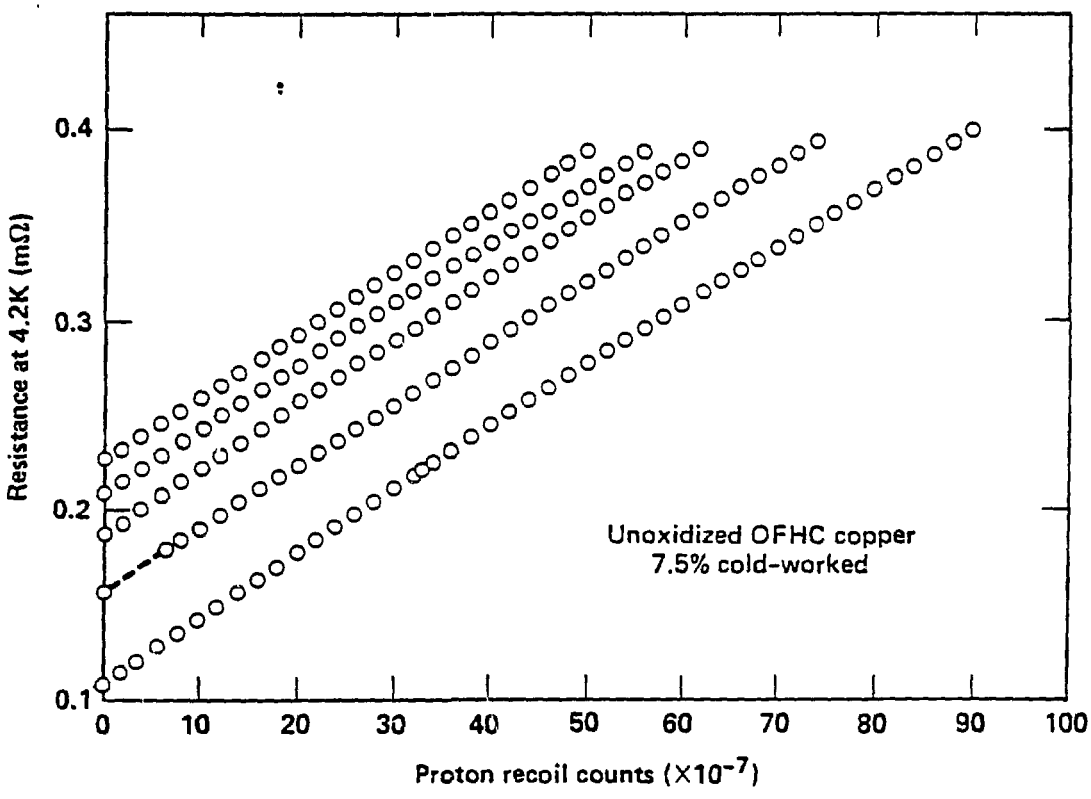

Fig. 3.4.1 Resistance of sample CUUN1 as a function of fluence (proton recoil counts) during 14.8 MeV neutron irradiation at 4.2K. The sample was annealed at 307K between each irradiation leg.

As noted earlier, the magnetoresistivities measured as a function of field before irradiation have been tabulated in Table 3.4.2. We have interpolated the measurements on the three unoxidized OFHC samples to produce magnetoresistivity values for them at 10.00 ± .01 T in the following states: before irradiation, after the first irradiation, after the first irradiation-anneal cycle, and after the fifth irradiation-anneal cycle. These values are tabulated in Table 3.4.4, and they span the full range of values of zero-field resistivity encountered with these samples.

Table 3.4.4. Resistivities at 0 and 10.00±.01 tesla (expressed in $10^{-11}\Omega m$)

	Before Irradiation		After Cycle 1 Irradiation		After Cycle 1 Anneal		After Cycle 5 Anneal	
Sample	ρ(0)	ρ(10)	ρ(0)	ρ(10)	ρ(0)	ρ(10)	ρ(0)	ρ(10)
CUUN0	5.01	50.34	35.33	76.43	11.01	58.24	20.20	65.49
CUUN1	11.14	57.23	42.49	81.26	16.55	61.67	25.35	69.08
CUUN2	17.03	61.25	48.05	85.51	21.59	65.23	29.55	72.41

The results above involving the variation of zero field resistivity by cold work, irradiation, and repeated irradiation and anneal cycles, all fall on a single Kohler line[16] to within ±2%. This plot is compared to that obtained from the pre-irradiation variation with field in Figs 3.4.3&.4. Here the points are again all within ±2% of a single line covering 1-1/2 orders of magnitude. For comparison, the Kohler plot obtained by Fickett[17] on pure copper samples when purity, temperature, and field were varied is also shown. At high values of H/ρ(0) the magnetoresistances are comparable, but at low values, corresponding to increasing ρ(0) at constant field, the curves diverge.

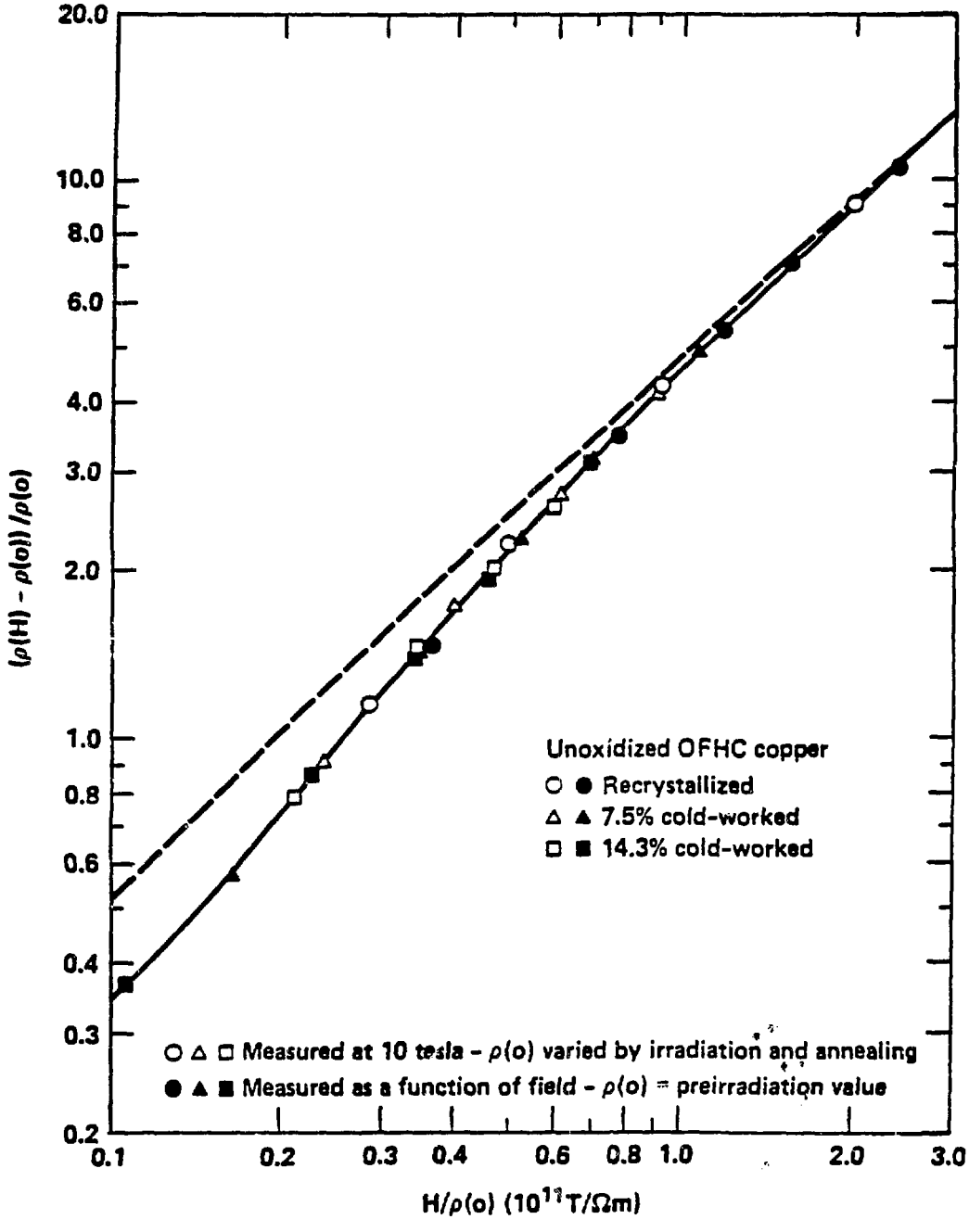

Fig. 3.4.3 Kohler plot for unoxidized OFHC copper. Data points were taken from Tables 3.4.2 (filled symbols) and 3.4.4 (open symbols). Dashed line is from Fickett.[17]

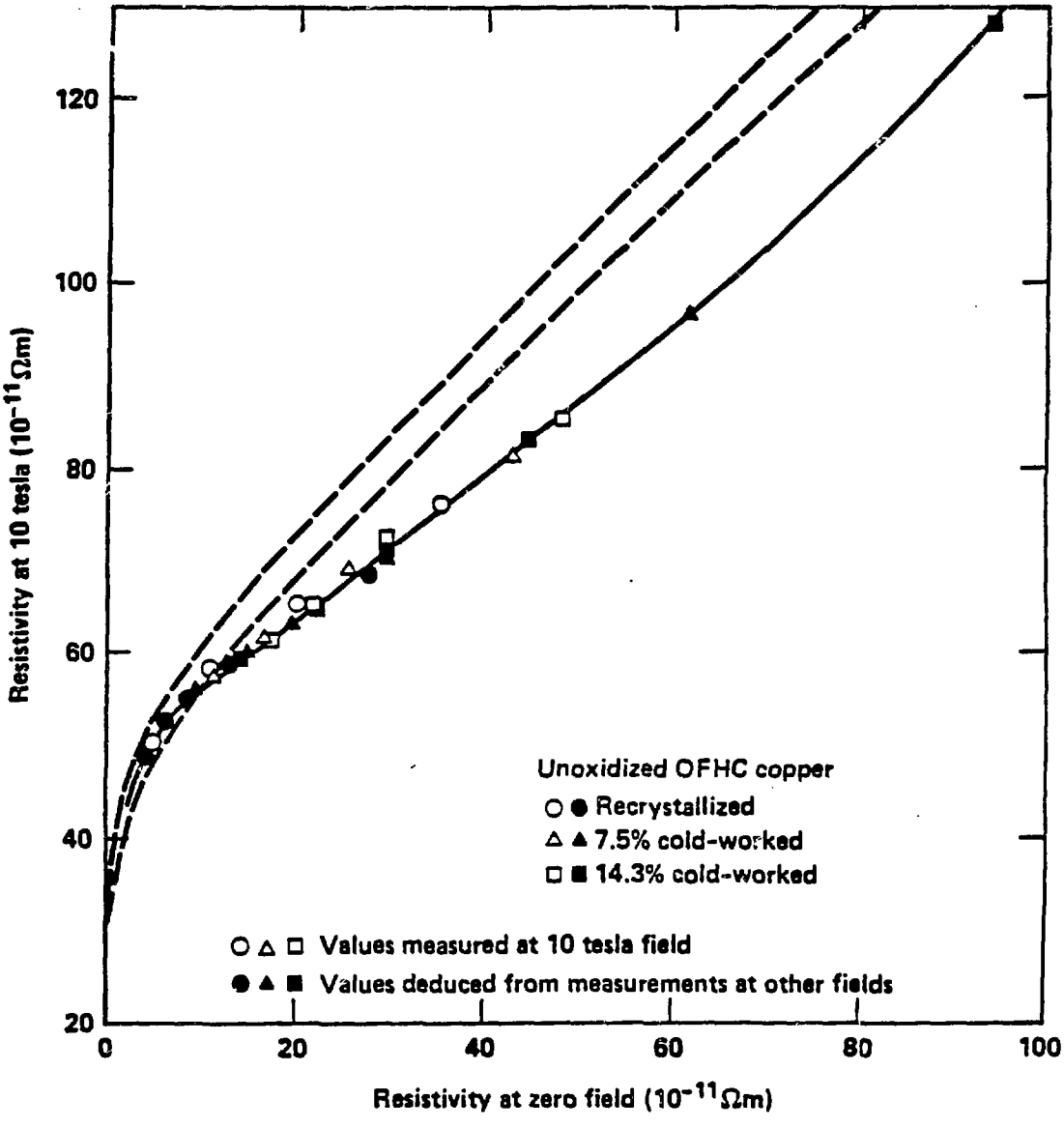

Fig. 3.4.4 Resistivity at 10 tesla as a function of resistivity at zero field for unoxidized OFHC copper. The open symbols are measurements taken at 10 tesla. The closed symbols are values deduced from the Kohler plot of Fig. 3.4.3. The dashed lines correspond to Fickett's Kohler plot ±5%.

Recovery During Irradiation-Anneal Cycles

- RECOVERY AS A FUNCTION OF TEMPERATURE
- RECOVERY AS A FUNCTION OF FLUENCE
- CYCLIC ANNEALING

ANNEALING OF NEUTRON RADIATION DAMAGE

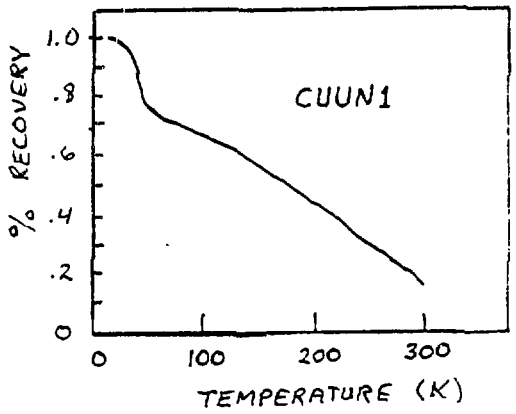

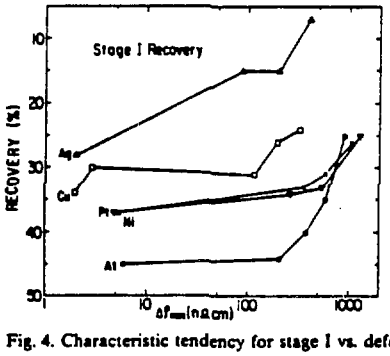

Fig. 4. Characteristic tendency for stage I vs. defect concentration (after Nakagawa et al. [7]).

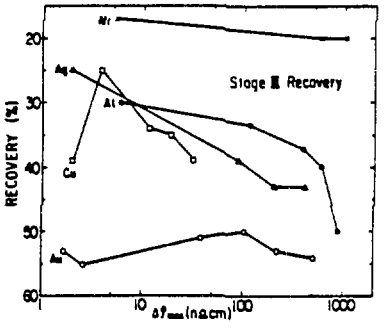

Fig. 5. Characteristic tendency for stage III vs. defect concentration (after Nakagawa et al. [7]).

It is evident from Fig. 3.4.1 that a higher percentage of damage recovers in later cycles compared to that recovered in the first cycle. This is illustrated in Fig. 3.4.2 for all three OFHC samples. Here we have plotted the percentage of the accumulated resistivity change retained after 30 minute anneals at 307 K as a function of the total damage resistivity change produced at 4.2 K. For all three samples the percentage of retained damage decreases with increasing damage. As cold work is increased the damage retained decreases significantly. For example, at an accumulated damage resistivity of 100 × $10^{-11}\Omega m$, the recrystallized sample retains 14.5 × $10^{-11}\Omega m$, while the 7.5% and 14.3% cold-worked samples retain 13.2 and 11.7 × $10^{-11}\Omega m$, respectively.

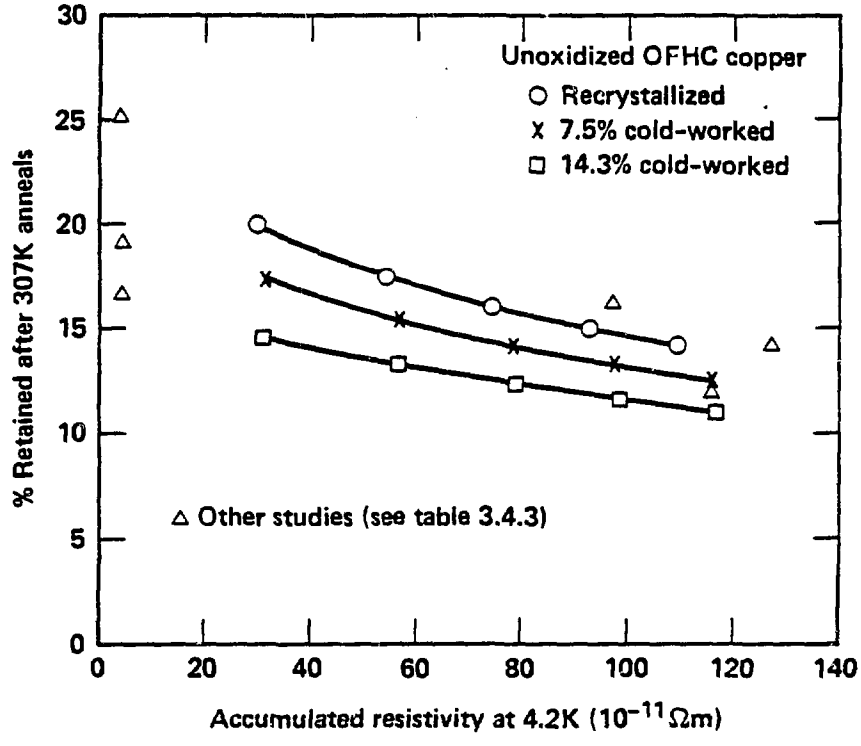

Fig. 3.4.2 The percentage of the total accumulated resistivity change at 4.2K retained after annealing at 307K as a function of the total resistivity change accumulated at 4.2K during neutron irradiation.

For comparison, we have also plotted the results of six other annealing studies following low temperature neutron irradiation. The three data points at low damage resistivities are from Takamura et al.,[10] and they also illustrate the effects of increasing amounts of cold work. The three points at the damage resistivities comparable to the maximum accumulated values attained here, in order of increasing damage, are from Burger et al.,[11] Horak and Blewitt,[12] and Brown et al.[13] Table 3.4.3 shows the initial sample resistivities, damage resistivities, and retained damage.

Table 3.4.3. Results of Isochronal Annealing Studies to 307 K

Neutron Source	Ref.	Neutron Spectrum	Initial ρ^a at 4.2 K	Damage ρ^a at 4.2 K	Annealing time (min)	Damage ρ^a retained after 307 K anneal	% Retained
JRR-3 (LHTL)[b]	10	Fast	1.5	2.9	6	0.75	25.8
"	10	"	5.8[e]	3.2	6	0.63	19.7
"	10	"	9.2[f]	3.2	6	0.55	17.2
FRM (LTIF)[c]	11	Reactor	-	94.3	3	15.8	16.8
CP-5 (VT53)[d]	12	Fast	0.82	116.2	5	14.5	12.5
CP-5 (VT53)[d]	13	Fast	3.80	127.0	5	18.5	14.6
RTNS-II	-	14.8 MeV	5.01	30.32	30	6.00	19.8
"	-	"	11.14[g]	31.35	30	5.41	17.3
"	-	"	17.03[h]	31.02	30	4.56	14.7

[a] Resistivities in units of 10^{-11} Ωm

[b] Liquid Helium Temperature Loop at the JRR-3 Reactor at Jaeri (Tokai-Mura)

[c] Low Temperature Irradiation Facility at the FRM Reactor at Munich

[d] VT53 facility in CP-5 Reactor at Argonne National Laboratory

[e] Sample cold-worked by twisting 53%

[f] Sample cold-worked by twisting 106%

[g] Sample drawn to 7.5% reduction of area

[h] Sample drawn to 14.3% reduction of area

Applications to Fusion Reactor Designs

- ETF lifetime
- Mars anchor and plug

From the point of view of stabilizer materials for superconducting magnets, the results given above are significant in two respects: 1) A Kohler plot determined on a conductor solely by varying the field can also be used to describe the variation of the magnetoresistance as a result of cold work, high energy neutron irradiation and subsequent annealing. This greatly simplifies the task of predicting the response of the magnetoresistance of actual conductors to changes resulting from fabrication of magnets and use in fusion reactors. 2) The fraction of accumulated damage remaining at 4.2 K after several irradiation-anneal cycles is nearly a factor of two lower than that previously estimated from studies of the annealing of lower-dose neutron damage.[18] The consequences of these facts are explored in the following two examples.

1) The present results significantly increase estimated lifetimes for copper stabilizers. Table 3.4.5 presents past and present estimates of lifetimes for the stabilizer of the inboard leg of the toroidal field coil in the Engineering Test Facility (ETF) design. (This example is used because a detailed neutron spectrum was available for this design.) Also shown is an estimate based only on data available in 1978. For each entry, the year of the estimate, the allowed change in resistivity at zero field to increase the resistance at 8 and 12 T by 25%, the lifetime and the estimated accuracy are shown.

Table 3.4.5. Lifetime of the copper stabilizer in ETF

Year	$\Delta\rho^a(0)$ to increase $\rho(8T)$ by 25%	$\Delta\rho^a(0)$ to increase $\rho(12T)$ by 25%	Lifetime[b] MWy/m^2 8T	12T	Uncertainty (%)
1978	5.2	7.1	10	13	+100 - 50
1980	9.8	13.3	18	24	+100 - 50
1981	14.5	21.6	23	33	± 40
1983	16.3	18.9	38	44	+ 30 - 10

[a] Resistivities in units of $10^{-11}\rho m$

[b] Assuming 10 annealing cycles

In early 1978, there were no studies available of magnetoresistance following neutron irradiation. There were, however, the extensive magnetoresistance measurements of Fickett[17] and a large body of data[10-13] from reactor irradiations at 4-15 K. The various data available from reactor irradiations gave values of the change of resistivity at zero field per displacement per atom (dpa) which differed from each other by as much as a factor of 2. Although codes for calculating neutron-induced displacements were highly developed and the dpa calculations were probably accurate to within ±25%, the neutron spectra in most facilities were seriously in error as a result of flux and spectrum determinations based on much older neutron cross-section data. By 1979, in part because of the growing interest in neutron spectral effects in the fusion program many facilities had been recharacterized and discrepancies in dρ/d(dpa) were reduced to ±25%.[20] At present we believe the uncertainty in this parameter is within ±10% as a result of improved neutronics calculations and careful experiments[9,21] involving neutrons, ions and electrons.

Over the same time period magnetoresistance measurements after neutron irradiation at 4.2 K[21,5] were refining our ability to predict changes in resistivity at field from changes at zero field. Most recently cyclic annealing experiments have been carried out in both a very soft spectrum[2] and here (at RTNS-II) in a very hard spectrum. Planned cyclic irradiations by Coltman et al. in a spectrum closer to that expected in fusion reactor magnets will complete these refinements. From the results which they have already in hand we expect that our results from the hard spectrum over-estimate the fraction which will be retained after annealing with a fusion reactor spectrum. Hence, we expect that the lifetime estimates in Table 3.4.5 will increase further.

2) Application of the present results to an advanced superconductor design shows that the stabilizer is not the determining factor for the lifetime of LHe-II-cooled (1.8 K) magnets. G. Carlson has prepared a preliminary design of the conductor pack to be used in the anchor and plug yin-yang coils for the Mirror Advanced Reactor Study (MARS).[22] These coils present the most critical shielding problems in MARS because of local peaks in neutron source strength and limited space for shielding. In this design the determining factor for shield thickness was an assumed dose limit of 100 MGy to the aluminized polyimide thermal insulation separating the cryocooled magnet case from the shield.

The conductor used for the MARS design is similar to that already in use in the MFTF-B yin-yang coils, but in MARS it would operate at 1.8 K and 10 T. Under these conditions the conductor would have a cryostability limit on stabilizer resistivity of $120 \times 10^{-11} \Omega m$, assuming a heat transfer limit of 1 W/cm^2 of area wetted by the LHe-II. A design safe-limit of 80% of this value would most likely be employed. (We note that the design operating limit for the MFTF-B yin-yang coils was 70% of the cryostability limit, and for the final MFTF-B choke coil it was 80% of the cryostability limit.) To estimate the response of the copper resistivity to irradiation it would receive with the MARS shield design, the calculated values of copper dpa per full power year (FPY) (cited by Carlson from the work of Maynard and El-Guebaly) were converted to $\Delta\rho(0)$ by the following equation: $\Delta\rho(0) = 300 \times 10^{-11} \Omega m \ (1 - e^{-360 dpa})$. This equation takes into account the high damage efficiency of the low energy neutrons in this spectrum.[19] Using the annealing results and the observed field dependence for sample CUUN1 we calculated the time history of the resistivity at field. The results are shown in Fig. 3.4.5. As can be seen, only two annealing cycles are required to reach the design lifetime of 24 FPY.

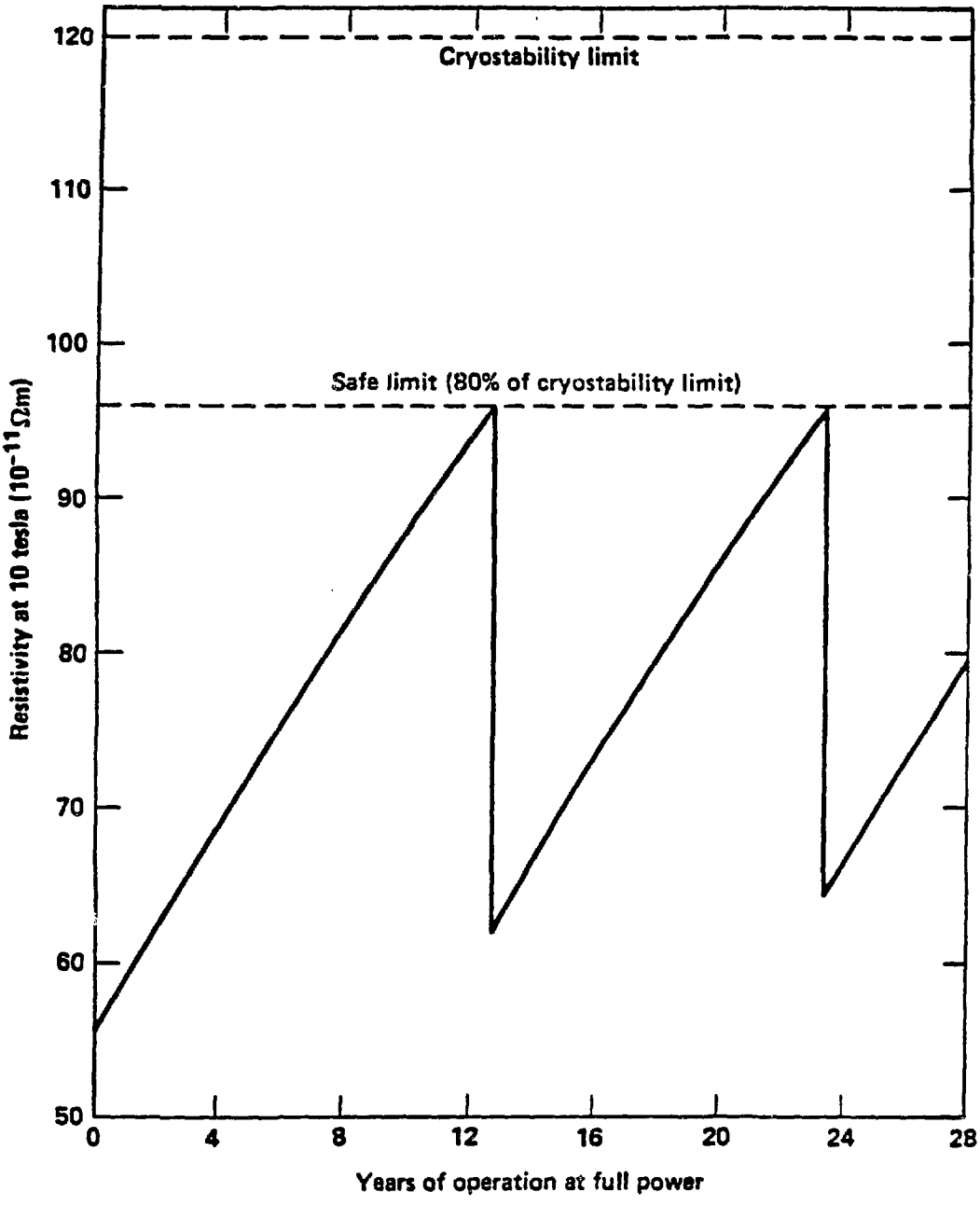

Fig. 3.4.5 Resistivity at 10 tesla of the copper stabilizer in the anchor and plug yin-yang coils of a MARS design as a function of time at full power.

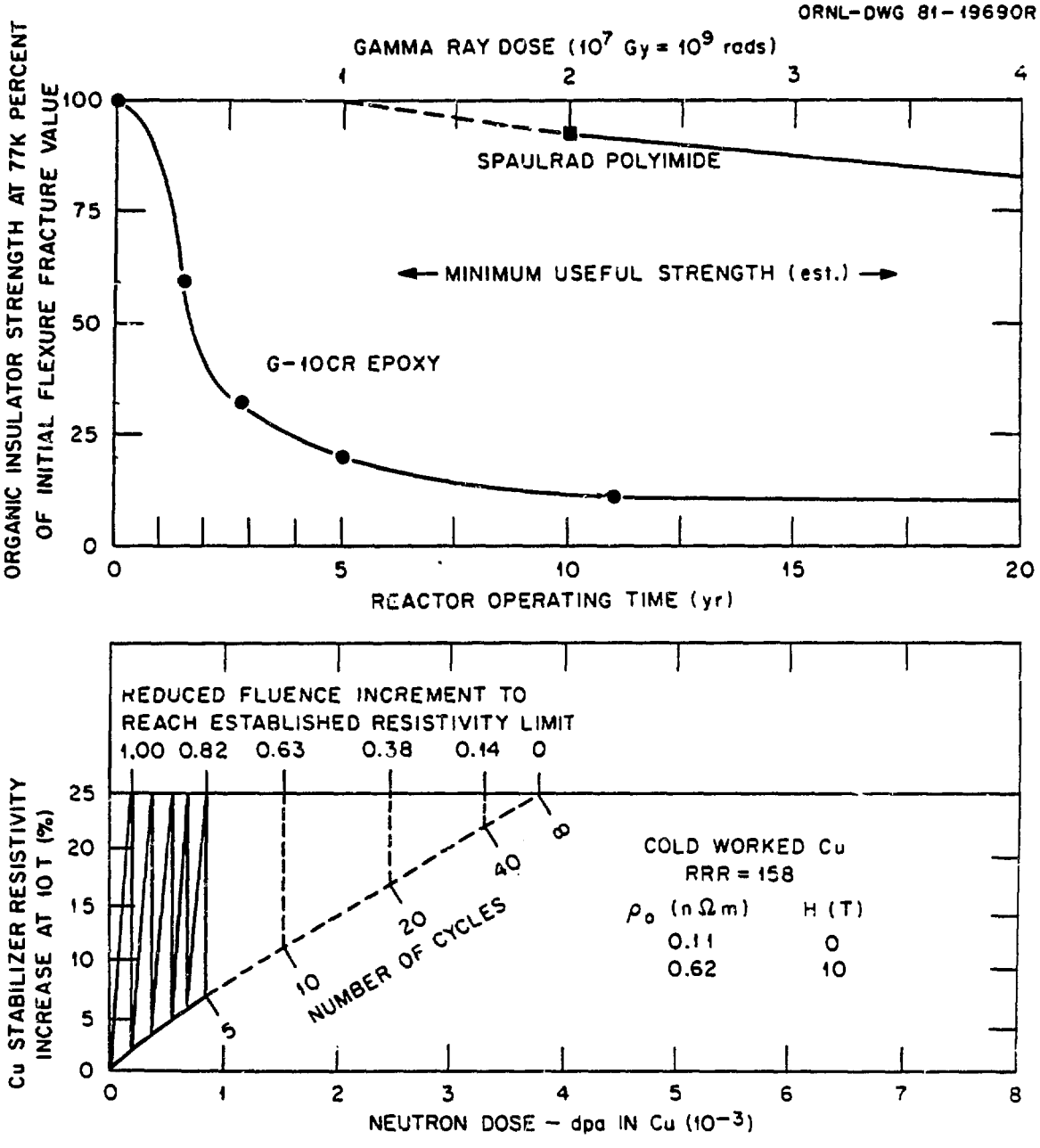
ORNL-DWG 81-19690R
GAMMA RAY DOSE (10^7 Gy = 10^9 rads)
1
2
3
4
ORGANIC INSULATOR STRENGTH AT 77K PERCENT OF INITIAL FLEXURE FRACTURE VALUE
100
75
50
25
0
SPAULRAD POLYIMIDE
MINIMUM USEFUL STRENGTH (est.)
G-10CR EPOXY
0
5
10
15
20
REACTOR OPERATING TIME (yr)
REDUCED FLUENCE INCREMENT TO
REACH ESTABLISHED RESISTIVITY LIMIT
1.00 0.82 0.63 0.38 0.14 0
Cu STABILIZER RESISTIVITY INCREASE AT 10 T (%)
25
20
15
10
5
0
5
10
20
40
80
NUMBER OF CYCLES
COLD WORKED Cu
RRR = 158
ρ_o (n Ω m)
H (T)
0.11
0
0.62
10
0
1
2
3
4
5
6
7
8
NEUTRON DOSE – dpa IN Cu (10^{-3})

CONCLUSIONS FROM JOINT STUDY

- A Kohler plot determined by varying only the magnetic field on a sample was adequate to describe the effects on the magnetoresistivity of subsequent variations in $\rho(0)$ due to cold work, irradiation, and annealing.

- The fraction of irradiation-produced zero-field resistivity which remained after successive irradiation-anneal cycles decreased as the total amount of damage resistivity produced at 4.2 K was increased. This held true up to the maximum accumulated 4.2 K damage resistivity studied, which was $120 \times 10^{-11} \Omega m$.

- From consideration of these data and a preliminary design of a LHeII-cooled magnet system (1.8 K), it appears that the magnetoresistivity of the stabilizer will not be the determining factor for shielding requirements in systems of this type which utilize polyimide thermal insulation.

- Upon the completion of planned experiments at the Intense Pulsed Neutron Source by Coltman and Klabunde of ORNL using the same sample materials as used here, it will be possible, from all the data, to make accurate predictions of the magnetoresistive behavior of copper stabilizers under expected fusion reactor conditions.

THERMAL STABILITY OF FOUR HIGH-STRENGTH, HIGH-CONDUCTIVITY COPPER SHEET ALLOYS

E.N.C. Dalder, W. Ludemann and B. Schumacher

Lawrence Livermore National Laboratory

THERMAL STABILITY OF FOUR HIGH-STRENGTH, HIGH-CONDUCTIVITY COPPER SHEET ALLOYS

E. N. C. Dalder, W. Ludemann, and B. Schumacher
Lawrence Livermore National Laboratory, University of California
Livermore, California 94550

OBJECT

The object is to determine the effects of the thermal treatments used during diffusion bonding, forming, and tritiding 50-cm-dia. RTNS-II targets on the room-temperature tensile properties of Amzirc, MZC, Elbrodur RS, and Glid-Cop copper alloy sheets of 0.04-in. thickness.

BACKGROUND

Three of these alloys, Amzirc, MZC, and Elbrodur RS, obtain their high room-temperature yield and tensile strengths by a controlled sequence of heat treatment (at approximately 900 °C), quenching, and cold working (40-90%), followed by aging (one-half to one hour at 370 to 510 °C).[1,2] The first heat treatment takes the strengthening phase, Cu_3Zr for Amzirc, a complex Mg-Zr-Cr-Cu intermetallic compound for MZC, and a complex Zr-Cr-P-Cu intermetallic compound for Elbrodur RS into a solid solution. Rapid cooling to room temperature maintains these elements in solid solution. Cold-working serves mainly to increase the density of nucleation sites, such as dislocation tangles and subgrain boundaries, upon which the strengthening phases precipitate during the final heat treatment. The fourth alloy, Glid-Cop, contains a finely dispersed oxide, Al_2O_3, which is inert to thermal treatments below the melting point of the matrix copper. Glid-Cop derives its strength soley from dislocation-dispersion interactions that occur during mechanical working. Chemical-analysis results obtained to date for Amzirc and MZC are given in Table 1.

Diffusion bonding of copper-base alloys should be done at as high a temperature as possible, typically in the range of 0.5 T_m to 0.7 T_m, where T_m is the melting point in K.[3] For copper, this translates into a preferred diffusion-bonding temperature range of about 400 °C to 677 °C. This range of temperature is in or above the final heat-treatment temperature range for both Amzirc and MZC. It is mandatory that a minimum room-temperature yield strength of 50 ksi be retained after thermal processing associated with target production. To determine these properties, Amzirc, MZC, and Elbrodur RS were subjected to thermal treatments in the temperature range of 350 °C to 650 °C, while Glid-Cop was subjected to thermal treatments in the temperature range of 500 °C to 900 °C, as shown in Table 2.

PROCEDURE

Thermal Stability Study

Strip tensile specimens, oriented at 0° and 90° to the final rolling direction, were prepared from two sheets of Amzirc, two sheets of MZC, a piece of

experimental Elbrodur RS strip, and one sheet of Glid-Cop and were exposed in flowing Ar to the temperature-time treatments shown in Table 2. Specimens were then tensile tested at room temperature by standard methods and the following quantities were recorded: ultimate tensile strength, 0.2% offset yield strength, and elongation to failure in a 2-in. length. Superficial Rockwell hardness measurements were taken on the shoulders of all specimens before tensile testing. Specimens were removed from the shoulders and gauge lengths of failed tensile samples for metallographic examination and prepared by standard methods. Samples were prepared by swab-etching with a mixture of HCL, HNO_3, NH_4Cl, and H_2O_2 for various times. Photographs were taken on an Axiomat metallograph at magnifications ranging from 100 to 1650, and scanning-electron-microscopy (SEM) examination of selected specimens was conducted on a JEOL-35 instrument.

Solution Heat-Treatment Study

Pieces of MZC alloy, 1 in. x 2 in. x 0.04 in., with the 1 in. dimension parallel to the rolling direction, were heat treated in flowing Ar for 0.5 hours at 913 °C, 927 °C, 954 °C, 982 °C, 1010 °C, or 1038 °C, followed by quenching in water to room temperature. Specimens were prepared for metallographic examination, as previously described.

Electrical-Conductivity Study

The room-temperature electrical conductivity of 0.04 in. MZC and Amzirc sheet was measured by passing a known current through 0.04 in. x 0.5 in. x 24 in. strips of the subject materials and measuring the voltage drop between two points, 18 in. apart, using a precision voltmeter. Similar measurements were made on 0.04 in. Amzirc sheet, made by Amax Specialty Metals, as a comparison. Measurements in Elbrodur RS and Glid-Cop sheet are being done, but are not yet available.

RESULTS

Results are presented in Figs. 1-3 for the tensile tests, Figs. 4-23 and 26-48 for the metallographic examinations, and Figs. 24-25 for the electrical-conductivity study.

Tensile Test Results

Room-temperature ultimate tensile strength, yield strength, and elongation values after various times at the indicated exposure temperatures are presented in Figs. 1, 2, and 3, respectively. Considering the yield strength-exposure conditions behavior of Amzirc, this alloy compares favorably with vendor data in that the highest temperature at which the 50-ksi room-temperature yield strength was retained was about 400 °C for 0.5 hours, as was seen for the vendor data. However, the situation was just the opposite for the MZC sheet, which barely maintained 50-ksi yield strength for temperature-time treatments no greater than 400 °C for one hour. Vendor data indicates that treatments of 593 °C for 0.5 hours should result in retention of the desired yield-strength levels. Note also that in the temperature range of 400-500 °C, the decrease in yield strength is much more rapid for MZC than for Amzirc, the opposite of what is expected on the basis of vendor information. Above 482 °C, the yield strength for Amzirc and MZC becomes much

less dependent on temperature of prior thermal exposure. The yield strength of MZC decreased from about 23 ksi after 500 °C exposure to about 15 ksi after 650 °C exposure, while the yield strength of Amzirc decreased from about 10 ksi after 500 °C exposure to 8 ksi after 650 °C exposure.

The yield strength-exposure conditions behavior for Elbrodur RS parallels that for Amzirc and MZC, but with one important difference, the decrease in yield strength for Elbrodur RS to below 50 ksi occurs at about 520 °C, which is 120 °C higher than for either Amzirc or MZC. Even at temperatures as high as 650 °C, the yield strength of the Elbrodur RS has not reached a minimum level, as had been seen for both Amzirc and MZC at lower temperatures.

The yield strength-exposure conditions behavior for Glid-Cop was relatively insensitive to increasing temperature of exposure, in that while the 50-ksi yield-strength requirement was reached at about 475 °C, the decrease in post-exposure yield strength with increasing exposure temperature was rather gradual. The minimum yield strength of about 42.5 ksi after a 900 °C exposure was only 15% less than the minimum yield strength of 50 ksi at about 475 °C.

The tensile strength-exposure condition results presented in Fig. 1 parallel the previously reported yield-strength trends, in that both Amzirc and MZC undergo rapid decreases in ultimate tensile strength with exposures in the temperature range of 350-500 °C, while the analogous decrease for Elbrodur RS did not occur until the temperature range of 500-600 °C. Again, the relative insensitivity of Glid-Cop's ultimate tensile strength with increasing exposure temperature is seen, with the minimum, ultimate, tensile-strength value of 53 ksi after the 900 °C exposure being only 19.8% less than the minimum, ultimate, tensile-strength value of 63.5 ksi prior to any thermal exposure.

Figure 3 summarizes the subsequent room-temperature total elongation behavior as a function of various exposure times and temperatures. Previous experience has shown that 10% total elongation is a measure of adequate formability when hydroforming the targets into the required hemispherical dome shape. This value is achieved in Amzirc with any treatment at or above 450 °C and in MZC with any treatment at or above 400 °C. Unfortunately, these treatments result in yield-strength values below 50 ksi. Both Elbrodur RS and Glid-Cop have minimum elongations above 10% after any thermal exposure used.

Metallographic Results

Metallographic results are available for as-received material and for material having received the thermal treatments described in the "Procedure" section of this report.

As-Received Material

Microstructures of all four alloys is shown in Figs. 4-7 for Amzirc, MZC, Elbrodur RS, and Glid-Cop, respectively. All materials' microstructures are typical of highly cold-worked materials. The Amzirc (Fig. 4) and Elbrodur RS (Fig. 6) show evidence of a coarse, randomly-dispersed precipitate, while the MZC shows evidence of a fine, randomly-dispersed, general precipitate (Fig. 5). No dispersed second phase was visible in the Glid-Cop (Fig. 7). Similar microstructures were evident in material from sheets other than those shown in Figs. 4-7.

Amzirc After Various Thermal Treatments

Representative microstructures are shown in Figs. 8-9 and 16-17. Little or no apparent changes in microstructure occurred after exposure at 400 °C for times up to 10 hours (Figs. 16a, 16b, and 17). Note that after one hour at 450 °C (Figs. 8a and 9a), extensive recrystallization has occurred; compare Figs. 4a and 8a, 4b and 9b. After one hour at 500 °C, recrystallization is almost complete and grain growth is just beginning; compare Figs. 4a and 8b. No apparent change in the size or distribution of the coarse, randomly-dispersed second phase observed in the as-received material (Figs. 4a and 4b) was seen as a result of these thermal treatments.

MZC After Various Thermal Treatments

Microstructures are shown in Fig. 10-15 and 18-23. After 0.5 to 10 hours at 400 °C (Figs. 14-15) or 1 hour at 450 °C (Figs. 10a and 11), recrystallization is well underway; compare Figs. 5a and 10a and 5b and 11b. Note the occurrence of abnormal grain growth (Figs. 11a and 11b) after one hour at 450 °C or ten hours at 400 °C (Fig. 15b). Note that the fine, general precipitate seen in the as-received material (Figs. 5a and b) appears to be unaffected by thermal exposures in the 400-1038 °C range (Figs. 10-15 and 18-23). After one hour at 500 °C, recrystallization appears to be nearly complete (Figs. 10b and 12a). Exposure at 650 °C for one hour and above appears to have resulted in the formation of an elongated second phase (Figs. 12, 13a, and 13b), as well as some grain growth. These two precipitates may be a chromium-rich oxide and zirconium-rich oxide (Fig. 23).

Elbrodur RS After Various Thermal Treatments

Microstructures are shown in Figs. 26-39. After 500 °C exposures, the material still retains its heavily cold-worked microstructure (compare Figs. 26-27 and 30-33 with Fig. 6), consisting of grains elongated in the longitudinal and long-transverse directions. Two types of finely dispersed, minor phases are seen (Figs. 26-27 and 30-33). One of these minor phases appears to be approximately spherical in shape and is rich in Cr and Cu (Fig. 29a). The other minor phase appears to be cubic to retangular in shape and is rich in Zr, less so in Cr, and contains some Cu (Fig. 29b). The Elbrodur RS matrix contains both Zr and Cr in solid solution (Fig. 28). As the exposure temperature is increased to 550 °C, the first evidence of recrystallization, in the form of the development of equiaxed grains, some of which contain annealing twins, is seen (Fig. 34). As either the exposure time at 550 °C is increased (Figs. 34-36) or the temperature of exposure is increased to 600 °C, the fraction of equiaxed grains increases (Figs. 37-39).

Glid Cop After Various Thermal Treatments

Microstructures are shown in Figs. 40-48. After all exposure conditions, the microstructure consisted of heavily cold-worked, elongated grains (compare Figs. 40-48 with Fig. 7) and a fine dispersion of irregularly shaped particles whose EDAX spectrum was rich in Al (Fig. 41). An EDAX spectrum of the matrix (Fig. 44) showed only Cu lines, with no evidence of any substitutional alloying addition. Comparison of the microstructure of the 500 °C, 0.5-hour exposure (Fig. 40) with that of the 900 °C, 1-hour exposure (Fig. 48) showed few differences.

Results of Electrical-Conductivity Measurements

Material	Conductivity (1% IACS for Copper)
Amzirc	87.5%
MZC	79.5%
Amzirc (Amax data)	72.3%

The LLNL specification required that both the Amzirc and MZC sheet be solution heat treated and cold worked to 60%. Amzirc processed in this manner is expected to have a room-temperature electrical conductivity of 70-75%, as shown in Fig. 24. The Amzirc vendor data falls within this range, but the LLNL Amzirc sheet appeared to have been given an aging treatment equivalent to 400 °C for an hour (Fig. 25). The MZC conductivity of 79.5% is about maximum for the material and could have been produced by aging at 475-500 °C (Fig. 25).

Discussion

The decrease in thermal stability of the Amzirc and MZC is associated with the onset of appreciable recrystallization at temperatures as low as 400-500 °C, as confirmed by the decreases in ultimate tensile strength (Fig. 1) and yield strength (Fig. 2) and changes in microstructure (Figs. 8, 9, 10a and b, 11a, and 14-16). What is not apparent is why, relative to vendor data, the Amzirc performed as well as it did and why the MZC performed as poorly as it did.

Considering first the "poor performance" of MZC, it is possible that the fine, general precipitate seen throughout all conditions of MZC examined (Figs. 5, 10-15, and 18-23) may be the main precipitation-strengthening phase and that it was never put into solution by a proper solution-treatment by the fabricator. If so, the main increment of strengthening in this batch of MZC is due to cold work, which will be removed by prolonged heat treatment in the temperature range of 0.4-0.5 T_m or 271-404 °C. Such appears to be the case, as is born out by the effect of thermal treatment on the ultimate tensile strength (Fig. 1) and the yield strength (Fig. 2). The possibly inert, fine, general precipitate may contribute a small additional strenghtening increment due to interaction with dislocations (dispersion strengthening) and/or grain boundaries (grain-refinement strengthening). However, the failure of either of these precipitates to be dissolved by solution heat treatments as high as 1038 °C (Figs. 18-22), together with the possibility that these precipitates are composed of a single, heavy metal, rather than the complex Mg-Zr-Cr-Cu-strengthening phase, raises the possibility that the alloy additions of zirconium and chromium have been converted to oxides during processing and that these oxides are incapable of being taken into solution and behaving as classical precipitation-hardening phases on subsequent precipitation heat treatment.

Considering the Amzirc next, its behavior is comparable to vendor data. Amzirc owes its high yield strength primarily to cold work done between the solution treatment and aging treatments, with the main purpose of the aging treatment being to remove Zr from solid solution in the form of a noncoherent Cu_3Zr precipitate. This results in high matrix electrical and thermal conductivities and a small increment in dispersion strengthening due to the presence of the noncoherent Cu_3Zr precipitate. This latter effect is confirmed, at least indirectly, by the yield strength of fully-recrystallized Amzirc (after thermal

treatments in the range of 500-650 °C) being about 7.5 to 10.0 ksi, relative to 3 to 5 ksi for fully annealed OFHC copper.[1]

Consider next the Elbrodur RS alloy. It contains two types of dispersed, second phase: one rich in Cr and Cu (possibly alpha Cu-Cr solid solution) and the other richest in Zr, but containing appreciable amounts of Cr and some Cu. Due to outgassing of the microscopy specimens during SEM examination, it was not possible to determine if either or both second phases are present as oxides or intermetallic compounds. Additional work is planned to further resolve these points.

Considering last the Glid-Cop alloy, it appears that the fine Al_2O_3 dispersion remained inert to very high temperatures, with the gradual drop in ultimate tensile and yield strengths being associated with recovery effects in the copper matrix.

CONCLUSIONS

1. The MZC sheet supplied to LLNL appears to have been improperly manufactured. In particular, the precipitation-strengthening second phase appears not to have been taken into solution by a properly applied solution treatment. The premature softening of the alloy is due to the onset of recrystallization at temperatures as low as 400 °C. The possibility of the zirconium and chromium being present as inert, non-strengthening oxides would also explain the premature recrystallization of this material.

2. The Amzirc sheet supplied to LLNL appears to have thermal-stability properties comparable to those exhibited by the Amax-processed product. The most likely explanation for the observed loss of strength is recrystallization.

3. Elbrodur RS, supplied as experimental strip, softens at 120 °C higher than either Amzirc or MZC. Whether this is due to differences in thermomechanical processing, precipitation phenomena, or both, relative to Amzirc and MZC, is yet to be established.

4. Glid-Cop sheet exhibited excellent thermal stability, most likely due to the effectiveness of the inert Al_2O_3 dispersion in inhibiting recrystallization.

RECOMMENDATIONS

1. Identify the secondary phases in Amzirc, MZC, and Elbrodur RS to determine whether they are inert oxides or intermetallic second phases with a potential for precipitation strengthening.

2. Setup and perform a hot-forging and warm-rolling study on Amzirc and MZC ingot to develop and optimize thermomechanical processing variables that will yield a 0.04-in. sheet with useful properties.

3. Obtain 0.04-in. x 24-in. x 24-in. Elbrodur RS sheet, and verify the enhanced thermal stability shown by the experimental strip.

4. Determine the commercial availability of a 0.04-in. x 24-in. x 24-in. Glid-Cop sheet

ACKNOWLEDGMENTS

The authors gratefully acknowledge the support and stimulating technical discussions with C. M. Logan, J. W. Dini, and R. Kershaw, as well as the excellent editorial assistance of J. Matthews and V. Zuppan. Work was performed under the auspices of the U.S. Department of Energy by the Lawrence Livermore National Laboratory under contract number W-7405-ENG-48.

REFERENCES

1. Anon., "Amzirc High-Conductivity Zirconium-Copper with High Strength at Elevated Temperatures," Amax Copper, Inc. (1966).

2. Anon., "Preliminary Data - Amax MZC," Amax Copper, Inc. (1974).

3. S. A. Westgate, "Diffusion Bonding: Practical Considerations," in Diffusion Bonding as a Production Process, p. 6, The Welding Institute (1979).

TABLE 1. CHEMICAL COMPOSITIONS OF COPPER ALLOYS

ALLOY	PRODUCT FORM	COMPOSITION (%) Mg	Zr	Cr	Ag
Amzirc	Cake	---	0.18	---	0.01
	Sheet 1015	---	0.18	---	0.01
	Sheet 1016	---	0.16	---	0.01
	Specification	---	0.20 0.13	---	0.10 0.02
MZC	Cake	0.05	0.18	0.70	---
	Sheet 3002	0.07	0.10	1.15	---
	Sheet D3	0.05	0.19	1.08	---
	Specification	0.10 0.02	---	0.50 0.30	---

TABLE 2. SUMMARY OF THERMAL EXPOSURE CONDITIONS

ALLOY	TEMPERATURE (C)	TIME (HOURS)		
Amzirc, MZC, Elbrodur RS	350	0.5	1.0	10.0
	400	0.5	1.0	10.0
	450		1.0	10.0
	500		1.0	10.0
	550	0.5	1.0	10.0
	600	0.5	1.0	10.0
	650	0.5	1.0	10.0
Glid-Cop	500	0.5	1.0	10.0
	550	0.5	1.0	10.0
	750		1.0	
	800		1.0	
	850		1.0	
	900		1.0	

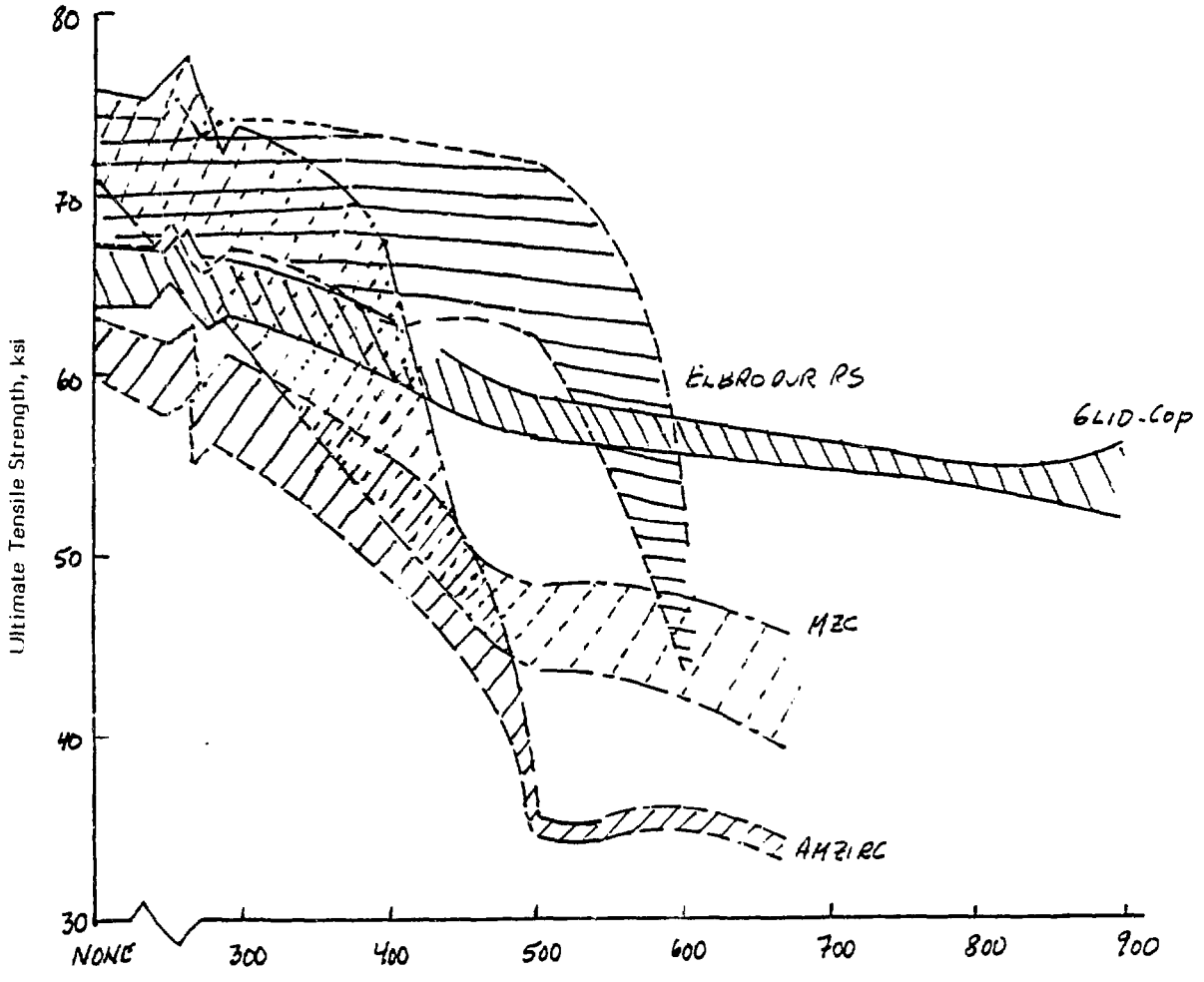

Fig. 1. Ultimate tensile strength at 20 °C after exposure at the indicated temperature.

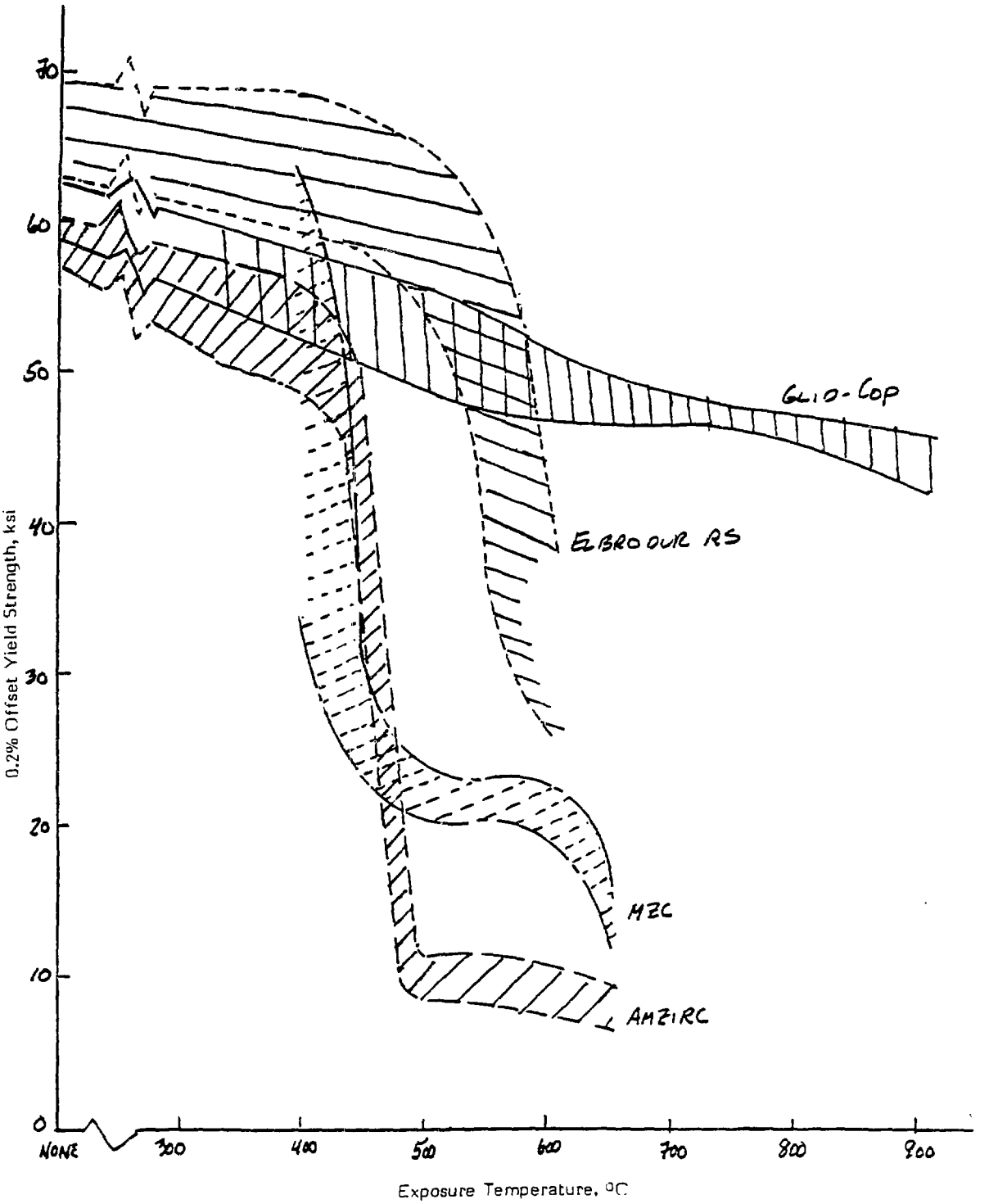

Fig. 2. Yield strength at 20 °C after exposure at the indicated temperature.

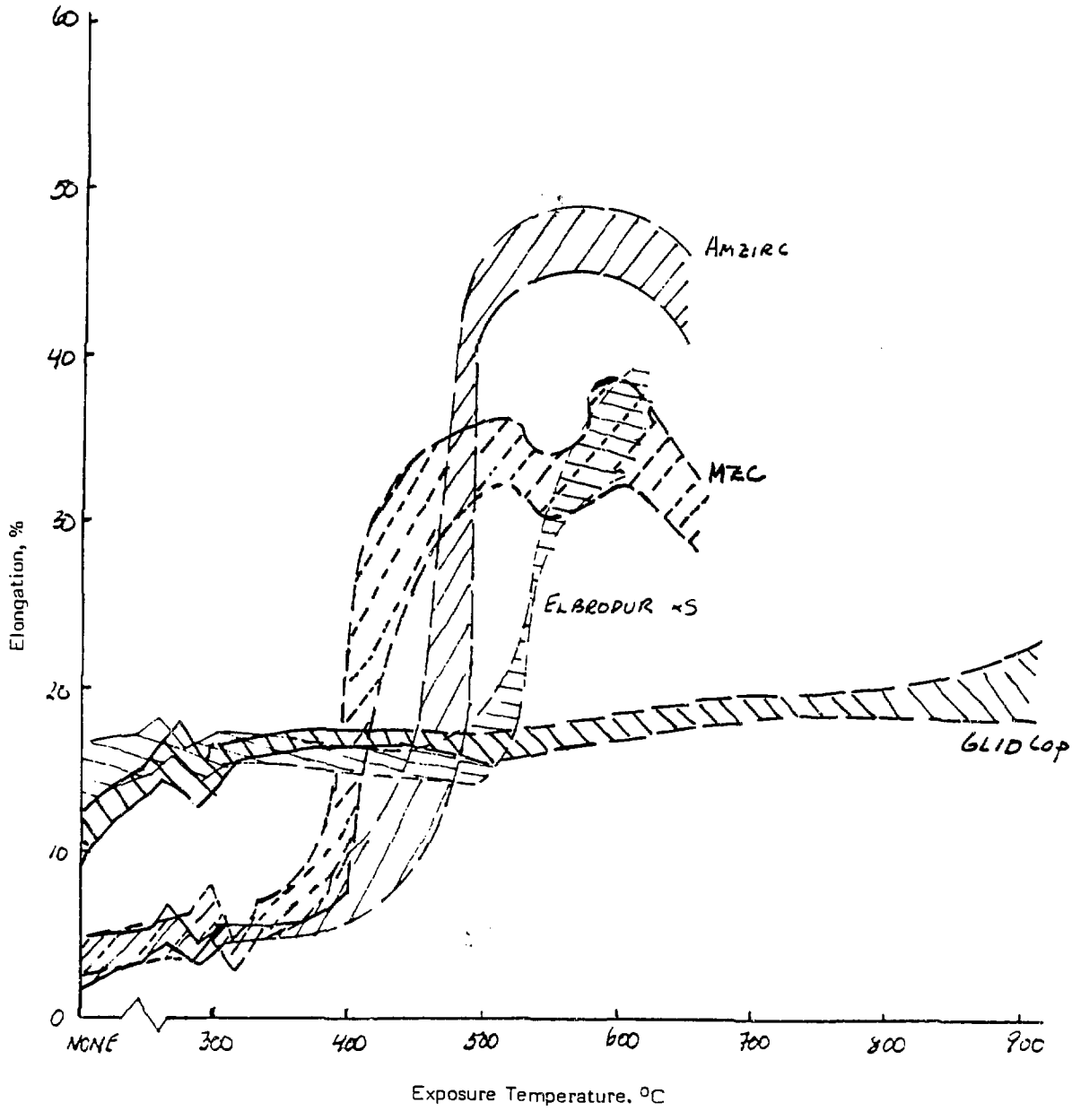

Fig. 3. Total elongation at 20 °C after exposure at the indicated temperature.

CONF-830466--3

CONF-830466--3

DE83 012558

FUSION APPLICATIONS OF COPPER: MASTER

UNIQUE REQUIREMENTS IN RESISTIVE MAGNETS

presented by

Brook Hunter

FEDC/GE

to the

Workshop on

Copper and Copper Alloys for Fusion Reactor Applications

14-15 April 1983

* Research sponsored by the Office of Fusion Energy, U.S. Department of Energy, under contract W-7405-eng-26 with the Union Carbide Corporation.

The Fusion Engineering Design Center (FEDC) is focusing FY 1983 activities on evaluating upgrade alternatives for the major fusion device now being completed. FEDC resources are divided equally between tokamak applications, in support of TFTR upgrade, and tandem mirror applications, supporting upgrade of the MFTF-B facility. In the course of magnet system design studies related to these activities, several needs for water cooled copper coils are presently perceived. The applications discussed in this paper are the high field choke coils (tandem mirror) and toroidal field coils or coil inserts (tokamaks). In these applications, the important properties are low electrical resistance, high mechanical strength and tolerance to neutron fluence.

Poloidal field ring coils internal to the bore of toroidal field coils in a tokamak may also be constructed of copper. The poloidal field ring coil application will not be discussed, since the presently available grades of copper provide material properties adequate for this application.

This paper will also not address the application of copper as a stabilizer in superconductors.

The current favorite among candidate upgrades of the MFTF-B machine now under construction is designated as the MFTF-α+T upgrade. The MFTF-α+T machine incorporates new end plugs to improve performance and a D-T axicell inserted into the MFTF-B center cell. Two high field solenoidal coil sets, a pair of 12T choke coils in the D-T axicell and an 18T barrier coil at each end of the central cell are required in the MFTF-α+T design. Design parameters for the high field coils in the MFTF-α+T concept are listed in Table 1.

Table 1. MFTF-α+T High Field Coil Design Parameters

	Choke Coil	Barrier Coil
Number of coils	2	2
Field, Tesla	12	18
Current Density, A/cm^2	2900	2900
Inside Radius, m	0.17	0.28
Outside Radius, m	0.47	1.13
Megamp turns	23	19
Stress, Mpa	163	598
Resistive Power Loss per Coil, MW	39	73

The design of these high field coils is driven by system configuration considerations. In order to fit into the machine without interference, these coils are designed to be made very compact. Therefore, a high current density, about 2900 A/cm^2, was chosen. The stress reported is a crude estimate of general stress level computed from the formula $\sigma = BjR$, the hoop membrane stress in an unsupported conductor due to the magnetic dilational forces. The estimates are conservative in that they are based on maximum field and maximum radius.

The FEDC has adopted magnet structural design criteria which limit primary membrane stress to 2/3 yield or 1/3 ultimate, whichever is less. For these limits, the strength required is 244 MPa yield and 500 MPa ultimate for the 12T choke coil and 900 MPa yield and 1800 MPa ultimate for the 18T barrier coil. The strength requirements for the 12T coil can be met using the AMAX-MZC alloy, 40% cold worked (450 MPa yield and 500 MPa ultimate). The required strength for the 18T barrier is not

attainable in copper or copper alloys. Consequently, it will be necessary to provide structural support for the conductor in the form of a case around the winding or steel support channels co-wound with the conductor.

The MFTF-α+T application is near term; it will be necessary to order long lead-time material in 1986 and complete construction by 1993. However, reactor relevant design studies also include similar high field axicell coils. The MARS study, for example, includes a 24T choke coil.

The FED-R is a recently completed tokamak design study based on near term technology. It uses large rectangular resistive toroidal field (TF) coils, approximately 11 m by 7 m. The FED-R study illustrates some of the design problems encountered with resistive TF coils or coil inserts. One of the major considerations in FED-R was the power loss in the coils, and the design objective was to limit resistive loss to 275 MW. By choosing a very modest nominal current density of 415 A/cm^2, with a maximum of 810 A/cm^2 in the nose region, resistive loss was limited to 22.2 MW for each of the 12 coils for a total of 266 MW. Bending stresses in the corners of the coils necessitated the incorporation of one meter corner radii.

A key feature of the FED-R TF coils is the demountable joint design. The purpose of these joints is to permit easy disassembly of coils in order to permit removal of torus sectors during the operating life of the device. The design of the demountable joint required the use of a high strength copper alloy, CDA-175, for insert fingers.

The Fusion Engineering Design Center (FEDC) is focusing FY 1983 effort on evaluating upgrade alternatives for the next fusion device

- support of Lawrence Livermore National Laboratory (LLNL), evaluating upgrades of MFTF-B (tandem mirrors)

- support of Princeton Plasma Physics Laboratory (PPPL), evaluating upgrades of TFTR (tokamaks)

We presently perceive several potential applications of copper coils to magnetic systems for fusion devices

- Tandem Mirror Machines
  - choke and barrier coils
- Tokamaks
  - toroidal field coils (or coil inserts)
  - poloidal field ring coils

In all of these applications, our material needs may be summarized as:

- low resistivity
- high strength
- tolerance to neutron irradiation

The recommended mirror upgrade is designated MFTF-Alpha+T

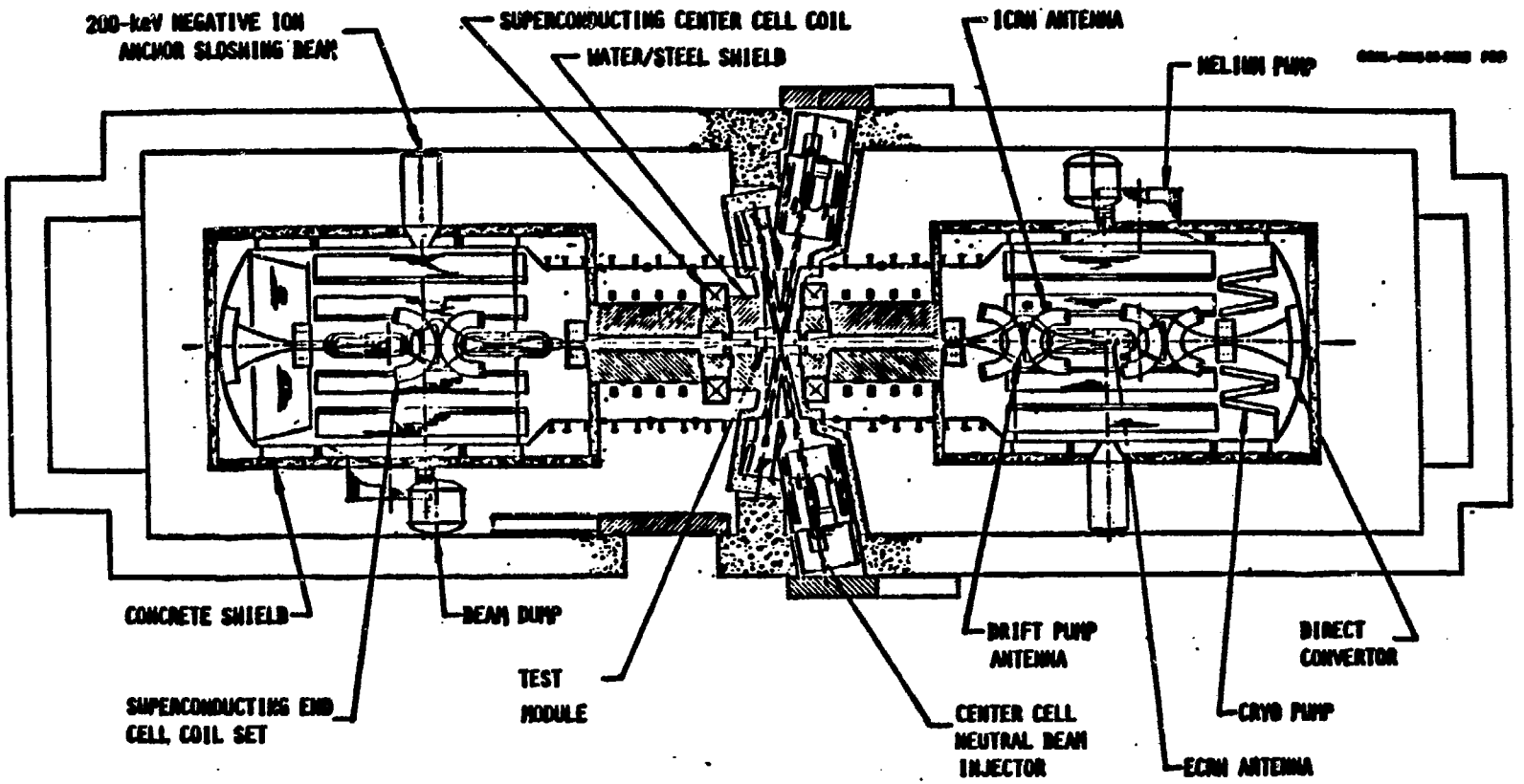

Present concepts include two resistive (copper) coils in the Alpha+T machine, a 12 T choke coil and an 18 T barrier coil.

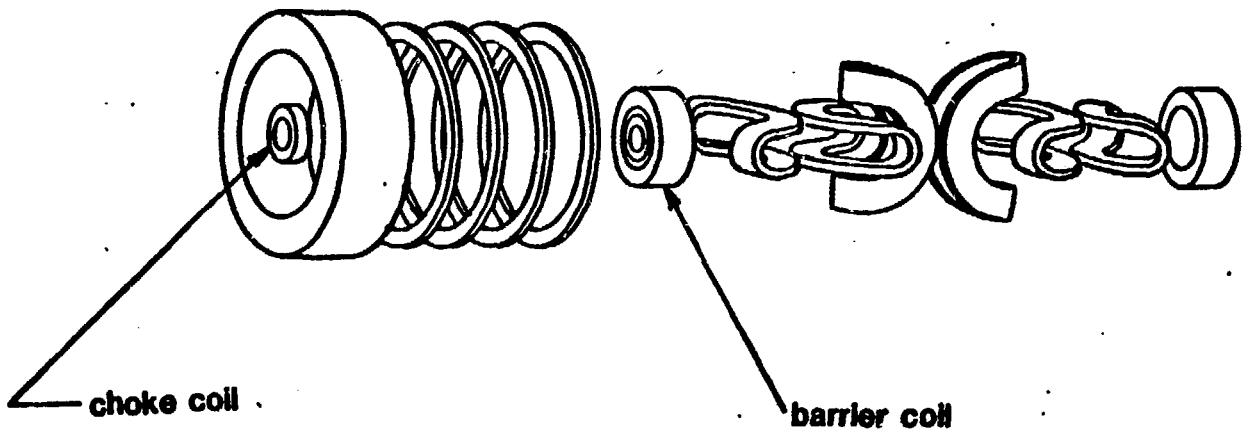

Three conductor concepts are being seriously considered for copper coils:

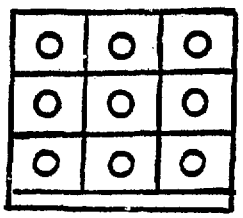

● Internally Cooled Cable

● Externally Cooled Cable

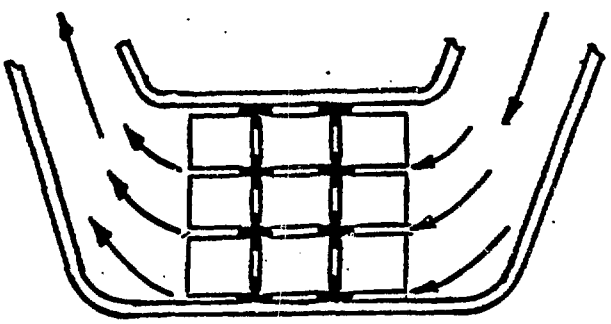

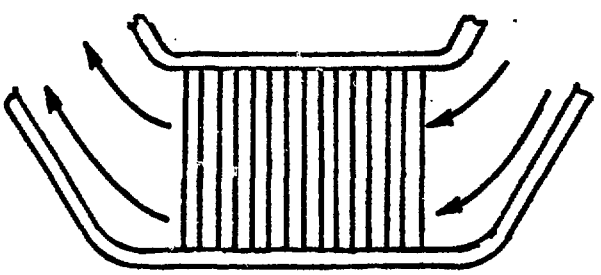

● Bitter (Plate)

EXTERNALLY H_2O COOLED POLYHELIX IS OUR SELECTED BASELINE CONCEPT FOR THE TDF CHOKE COIL

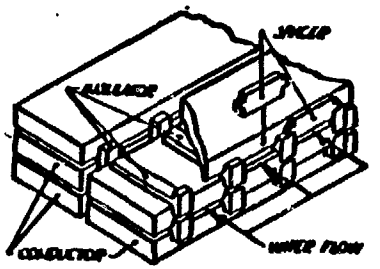

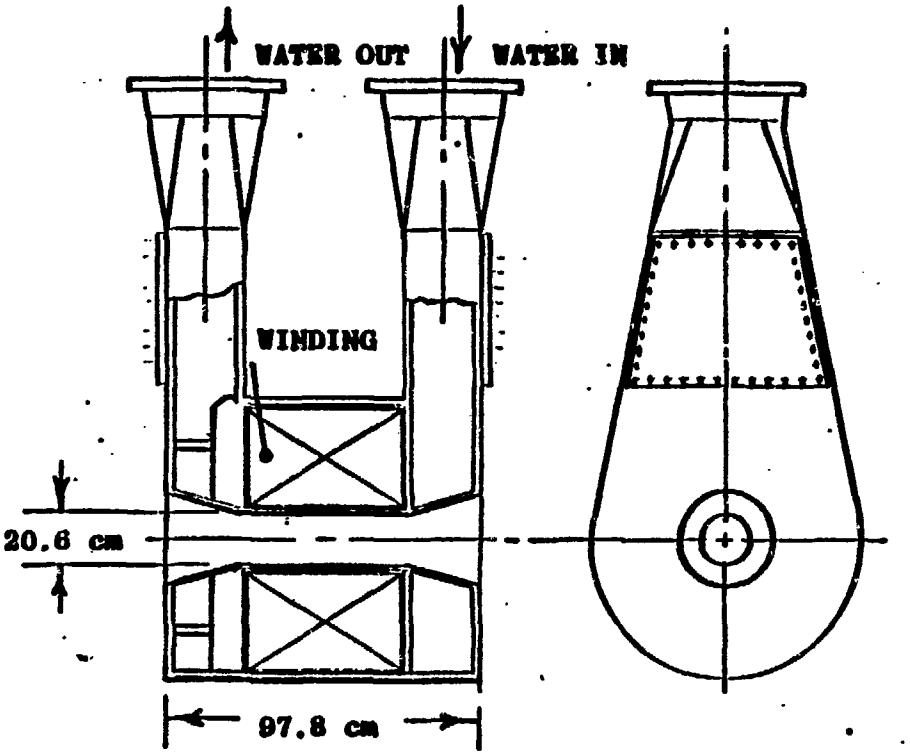

CONFIGURATION

- AXIALLY COOLED
- CONDUCTOR - ZIRCONIUM COPPER or MAGNESIUM-ZIRCONIUM-CHROMIUM COPPER
- SPINEL CERAMIC INSULATION
- 304L SS CASE

KEY FEATURES

- CENTRAL FIELD - 12.0T (15.0T w/BACKGROUND)
- CURRENT DENSITY - 4800 A/cm^2
- POWER CONSUMPTION 25.9 MW
- WATER FLOW RATE 2,450 GPM
- WEIGHT 6500 POUNDS

The magnetic running load (force per unit length) on a current carrying conductor in a magnetic field is the product of the current I times the flux density $B_\perp$ perpendicular to the current and is mutually orthogonal to I and $B_\perp$

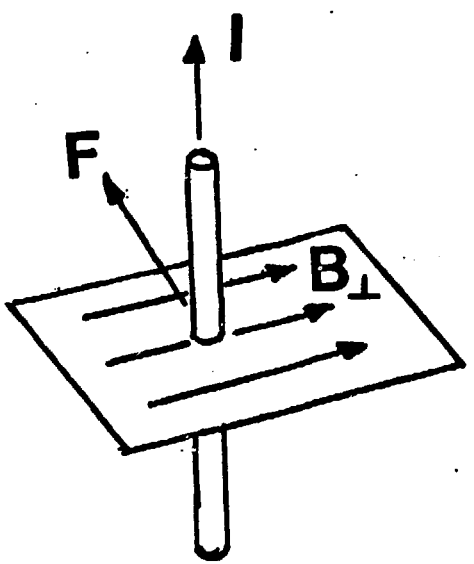

F (Newtons/meter) =

I (Amps) x $B_\perp$ (Tesla)

The magnetic running load in a solenoid is dilational in character,

producing hoop tensile stress of amplitude

$$\sigma = j\ B\ R$$

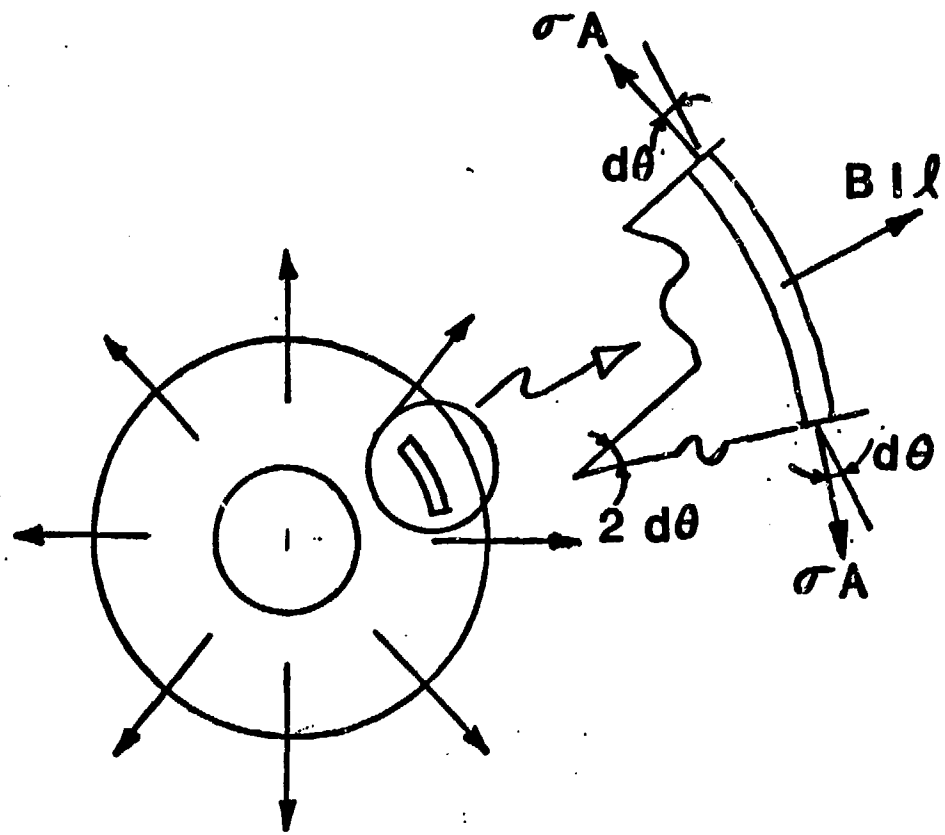

$$2\sigma A \sin d\theta = B\ I\ (2\ R\ d\theta)$$

$$\sin d\theta \simeq d\theta$$

$$\sigma = (I/A)\ B\ R = j\ B\ R$$

FEDC Magnet Structural Design Criteria

- PRIMARY STRESS LIMITS

  Limits are defined as multiples of S_m, defined as follows:

  Metals S_m = the lesser of 2/3 yield strength or 1/3 ultimate strength at operating temperature

  Nonmetallics S_m - 1/3 ultimate strength at operating temperature

  - Normal operating conditions

    Primary membrane stress intensity $\leq S_m$

    Primary membrane plus bending stress intensity $\leq 1.5\ S_m$

    Average shear stress $\leq 0.6\ S_m$ (metals)

  - Abnormal operating conditions

    Each of the above limits is multiplied by 1.5

  - If buckling is a potential failure mode, a margin of 5 against elastic buckling is required

- FATIGUE AND FRACTURE MECHANICS LIMITS

  An allowable peak tensile stress is derived from the Paris crack growth law and from fundamental fracture mechanics principles

  For 304 stainless steel (similar to the Nitronic 33 used in FED-R), the combination of 6000 Stage I pulses plus 3300 Stage II pulses results in an allowable peak tensile stress of 69 ksi for Stage II operation and 44 ksi for Stage I operation

The power dissipated in the coil by resistive heating is also proportional to current density

$$P = I^2(\rho L/A) = I^2(\rho/A)(2\pi R\, N)$$

$$= 2\pi(NI)\, R\rho j$$

in which NI and R are determined by system considerations.

For the Alpha+T choke coil

- B = 12 T
- R_i = 0.17 m
- R_o = 0.47 m
- j = 2882 A/cm^2
- Ni = 22.6 MAT
- T = 100°C(200°C)

from which it follows that

σ = 163 MPa (23.6 ksi)

$\Longrightarrow$ $S_y > 244$ MPa (35.4 ksi) $S_{ult} > 488$ MPa (70.8 ksi)

Use AMAX-MZC 40% CW S_y = 450 MPa S_{ult} = 500MPa

P = 39.3 MW per coil (ρ = 3μohm-cm)

Neutron environment is

5.9×10^{21} n/cm^2 per MW yr/m^2

7.5 dpa per MW yr/m^2

Life = 1.3 MW/m^2 (10 yr)(0.01) = 0.13 MW yr/m^2

For the Alpha+T barrier coil

- B = 18 T
- R_i = 0.28 m
- R_o = 1.13 m
- j = 2941 A/cm^2
- NI = 18.8 MAT
- T = 100°C(200°C)

from which it follows that

σ = 598 MPa $\Longrightarrow$ S_y > 897 MPa S_{ult} > 1795 MPa

Will require a supporting case or cowound stiffeners

P = 73 MW per coil

The Alpha+T application is near term (order long-lead material FY86, complete construction FY93)

HOWEVER.....

long term, reactor relevant concepts (e.g., MARS) incorporate high field (24 T) barrier coils.

FED-R is a recently completed study of a tokamak based on near term technology.

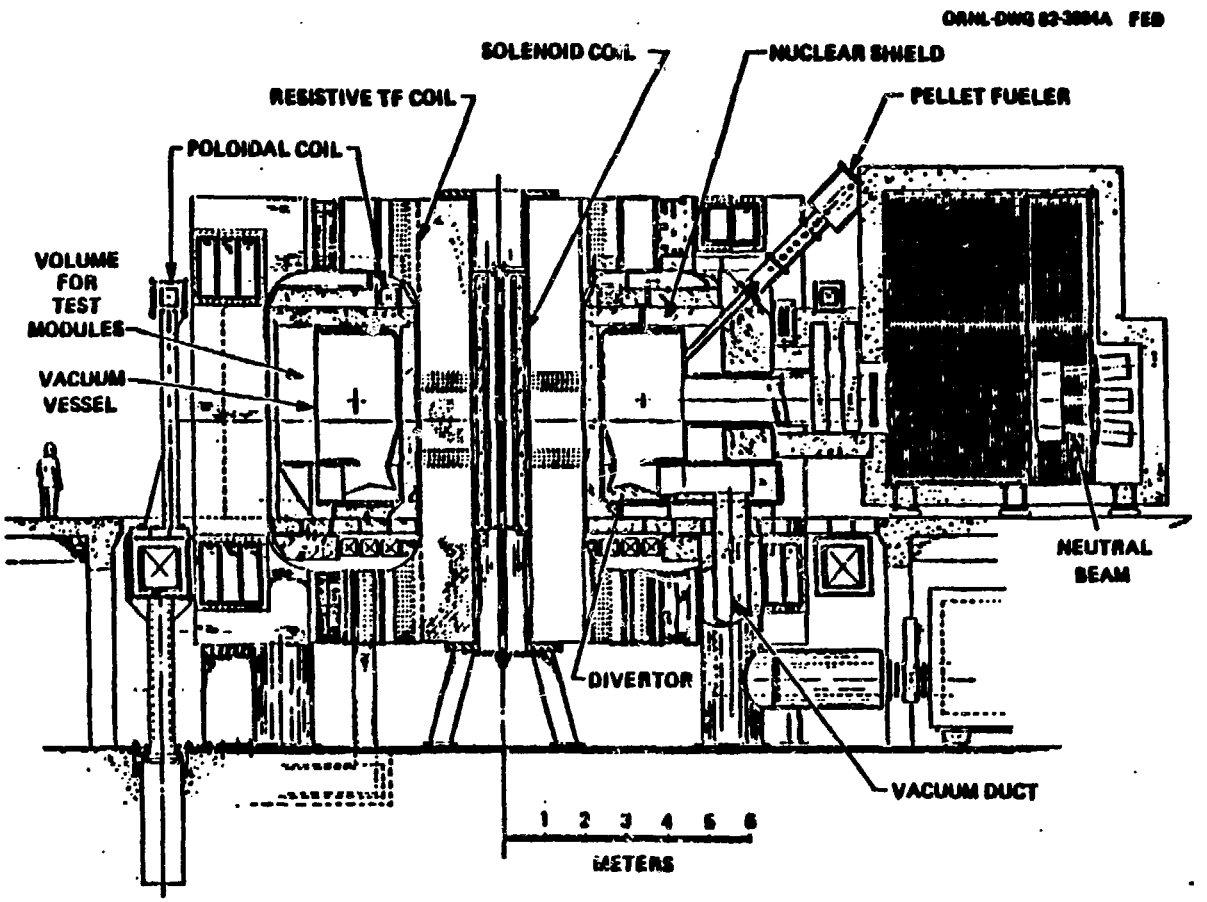

For the FED-R TF coils, current density is fairly low to limit power to 275 MW.

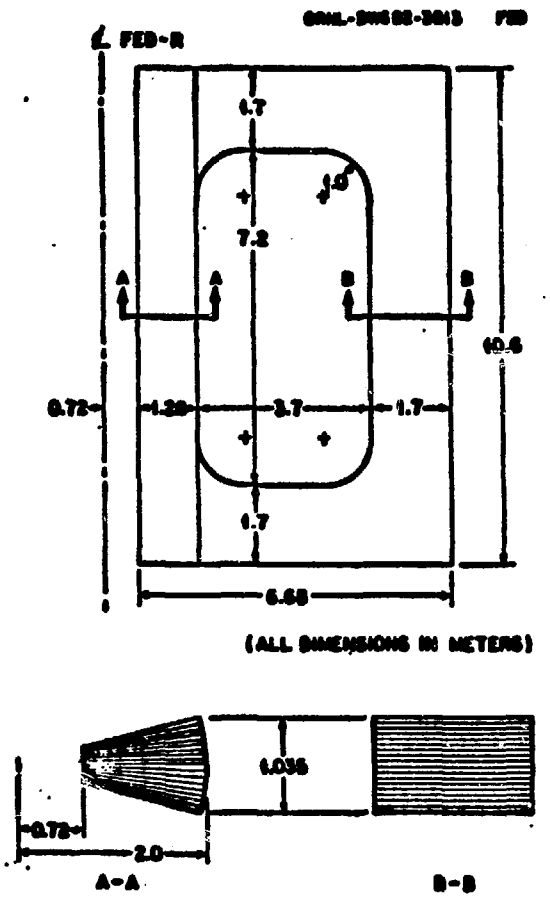

- B = 8.8 T
- $j = \begin{cases} 810\ A/cm^2, \text{ inboard} \\ 415\ A/cm^2, \text{ elsewhere} \end{cases}$
- NI = 7.3 MAT
- P = 22.2 MW per coil

  ($\rho = 2\ \mu$ohm-cm)
- T = 100°C

Even with low current density, structural design is challenging because of high bending stress.

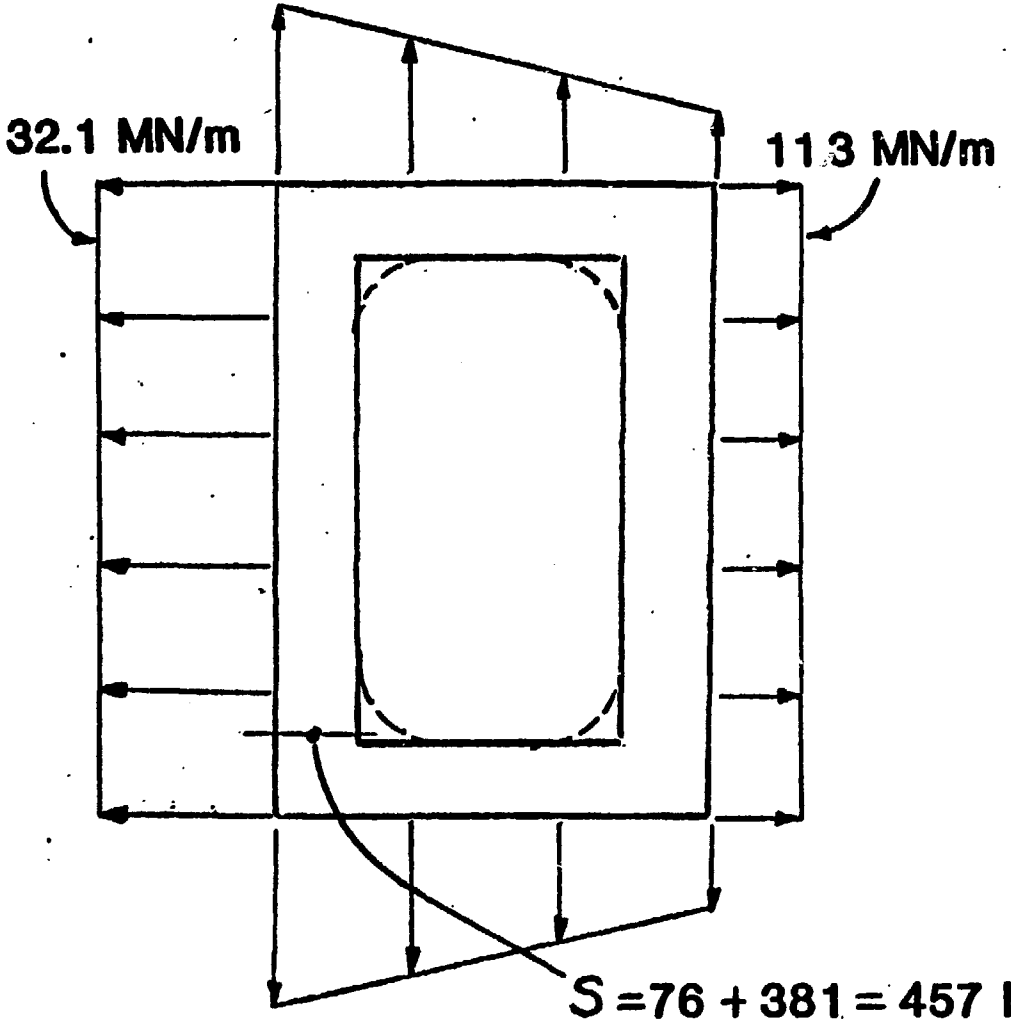

- Required S_y is 457 MPa
- Actual S_y is 128 MPa
- Add 1-m corner radii

FED–R TF coils feature three kinds of mechanical joints

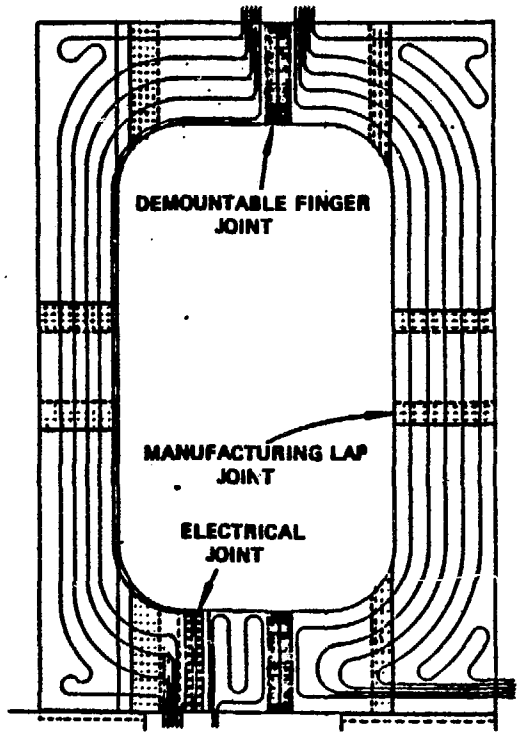

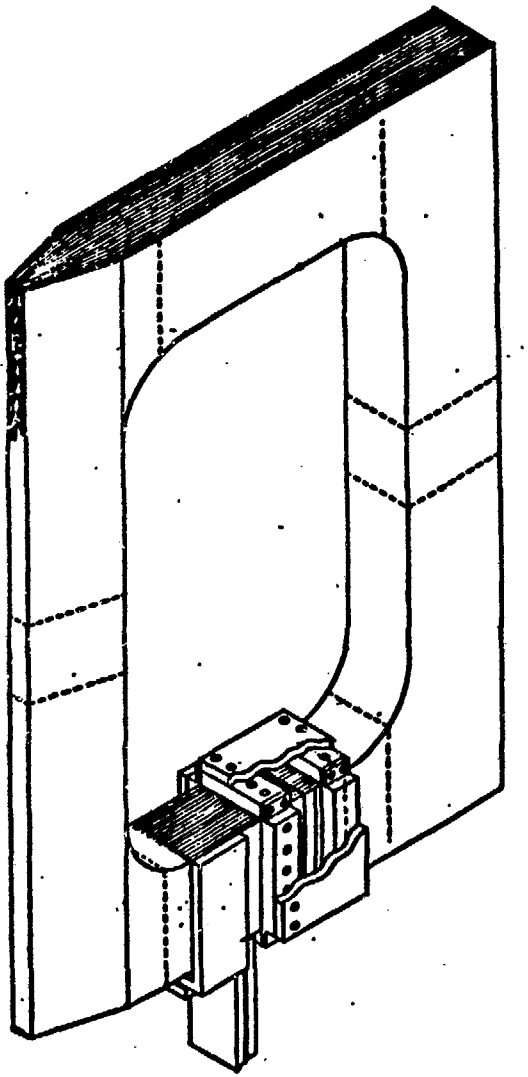

The demountable joint was patterned after a similar joint used in Doublet III, and high strength insert bars are required to transmit load across the joint.

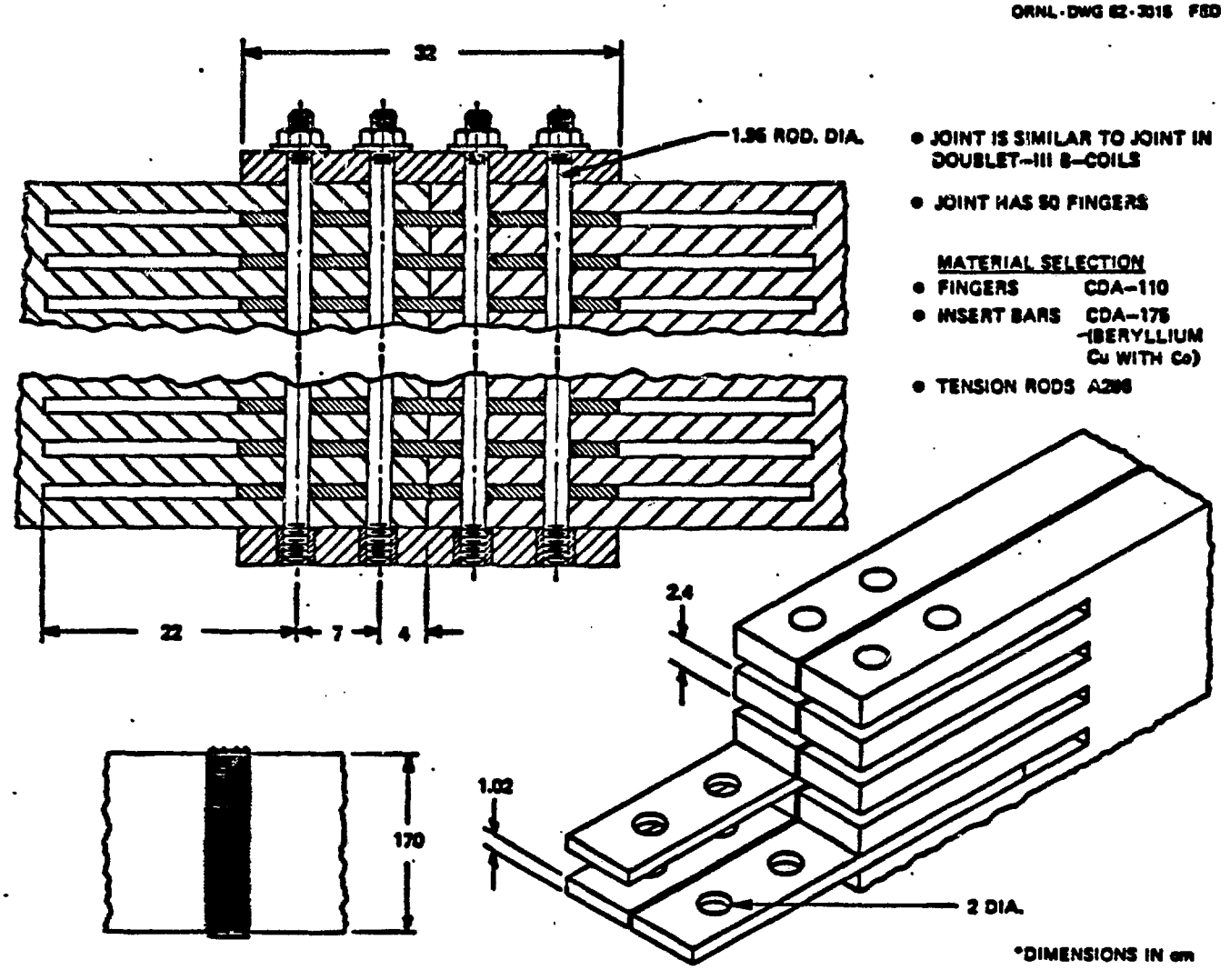

All applications of copper TF coils may be regarded as near term (FY86-FY93).

A SUMMARY OF REQUIREMENTS FOR APPLICATION OF COPPER TO FUSION MAGNET SYSTEMS IS:

APPLICATION	POWER* MW	RESISTIVITY μOHM-CM	MAGNET STRESS MPA(KSI)	DESIRED YIELD** MPA(KSI)
CHOKE COIL	79	3	163(23.6)	244(35.4)
BARRIER COIL	146	3	598(86.7)	897(130)
TF COIL	265	2	457(66.3)	457(66.3)
TF INSERTS	?	4	191(27.7)	286(41.6)

*TOTAL FOR THE MACHINE

**AT MAXIMUM OPERATING TEMPERATURE, 200°C

POWER CONSUMPTION RESULTS IN SIGNIFICANT OPERATING COST

PACIFIC GAS & ELECTRIC CO. CHARGES

$1.35/KW/MONTH	DEMAND CHARGE
$ .078/KWH	USAGE CHARGE

SO FOR A 100 MW LOAD,

DUTY FACTOR	MONTHLY DEMAND CHARGE	MONTHLY USAGE CHARGE	TOTAL MONTHLY CHARGE
0.01	$135 K	$ 56 K	$ 191 K
0.1	$135 K	$ 562 K	$ 697 K
0.5	$135 K	$2808 K	$2943 K

- END -

DATE FILMED

06 / 24 / 83

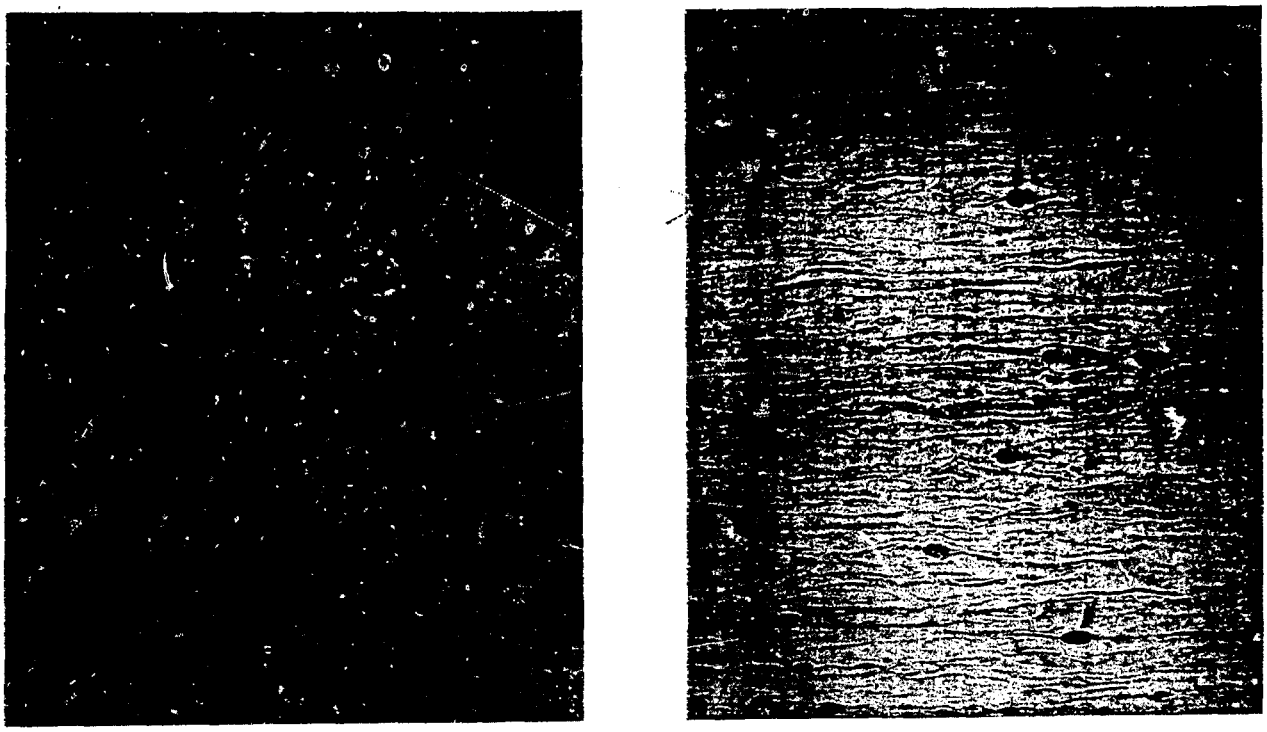

(a) P/N 2-1

(b) P/N 3-1

Mag: 500 X

Fig. 4. Microstructure of Amzirc (Sheet 1015), showing (a) longitudinal, and (b) transverse structures. Material is in as-received condition. Note the presence of a coarse, randomly dispersed precipitate (arrows).

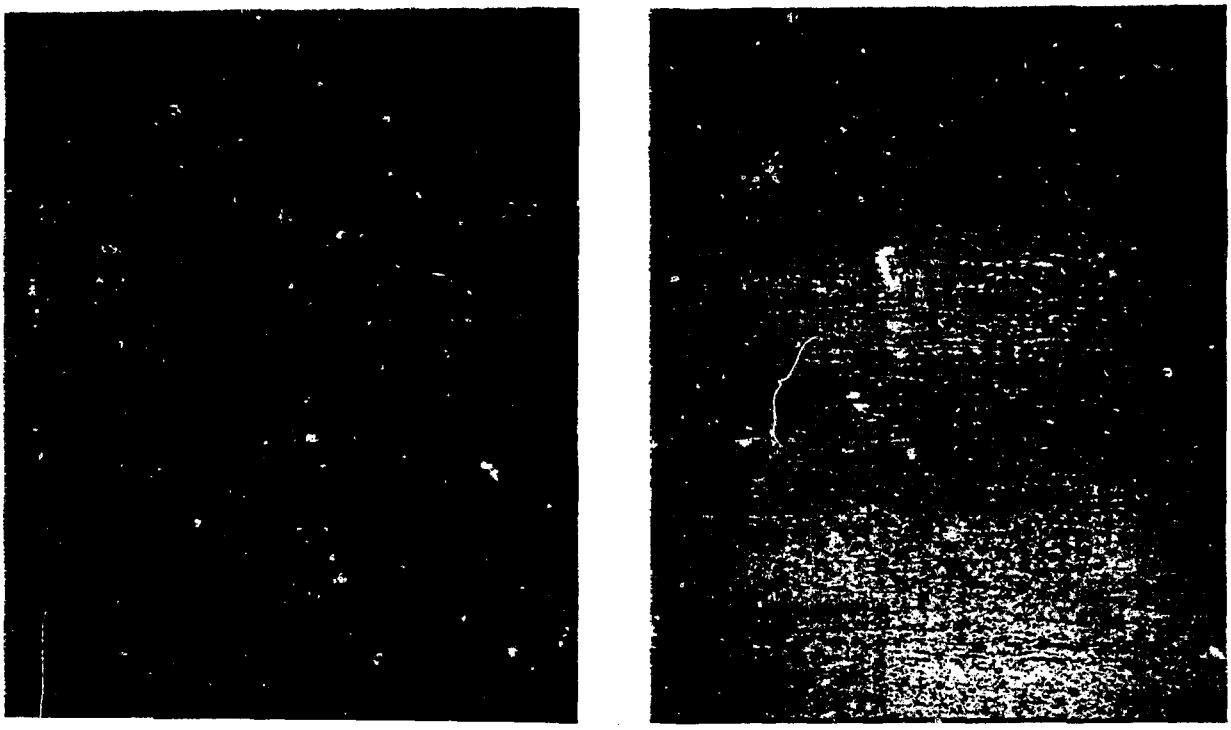

(a) P/N 6-1

(b) P/N 8-1

Mag: 500 X

Fig. 5. Microstructure of MZC (Sheet 3003), showing longitudinal (a) and transverse (b) structures. Material is in as-received condition. Note the presence of a finely dispersed, general precipitate (arrows).

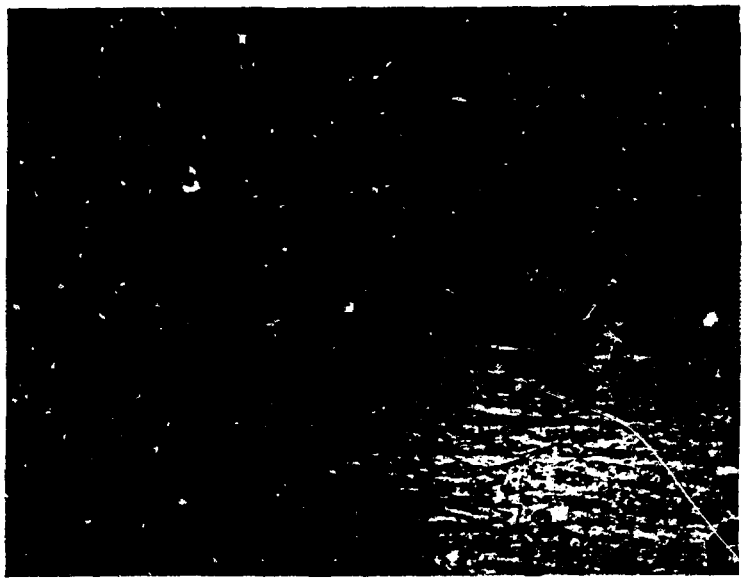

3228-1 Mag: 1000 X

(a) Longitudinal

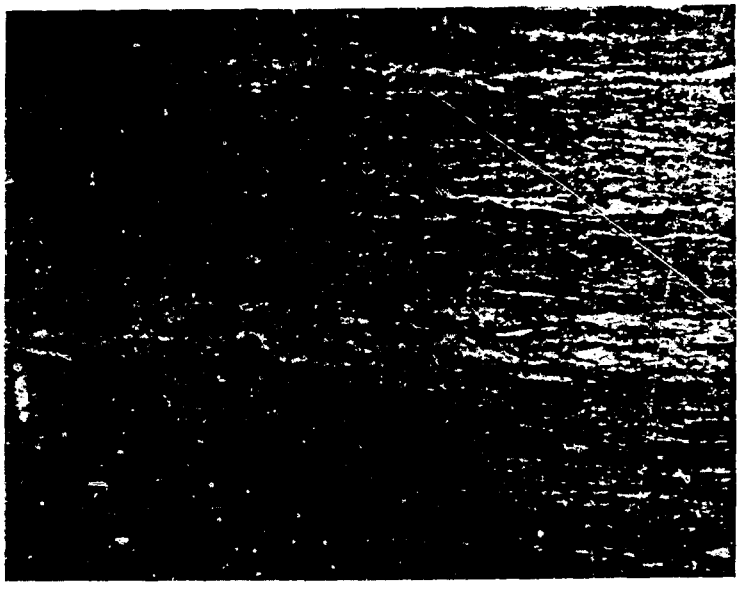

3228-11 Mag: 1000 X

(b) Transverse

Fig. 6. Microstructure of Elbrodur R/S strip, showing highly elongated, cold-worked microstructure (horizontal).

3229-7 Mag: 1000 X

(a) Longitudinal

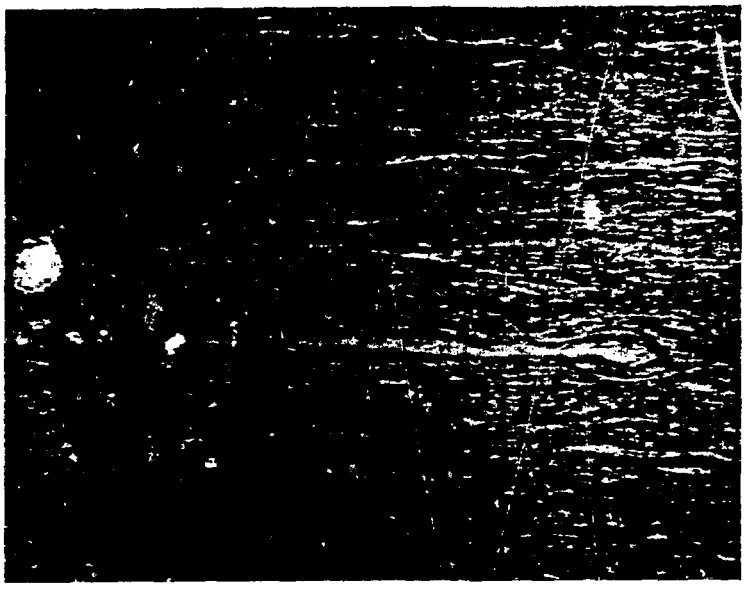

3229-1 Mag: 1000 X

(b) Transverse

Fig. 7. Microstructure of Glid Cop sheet, showing highly elongated, cold-worked microstructure (horizontal).

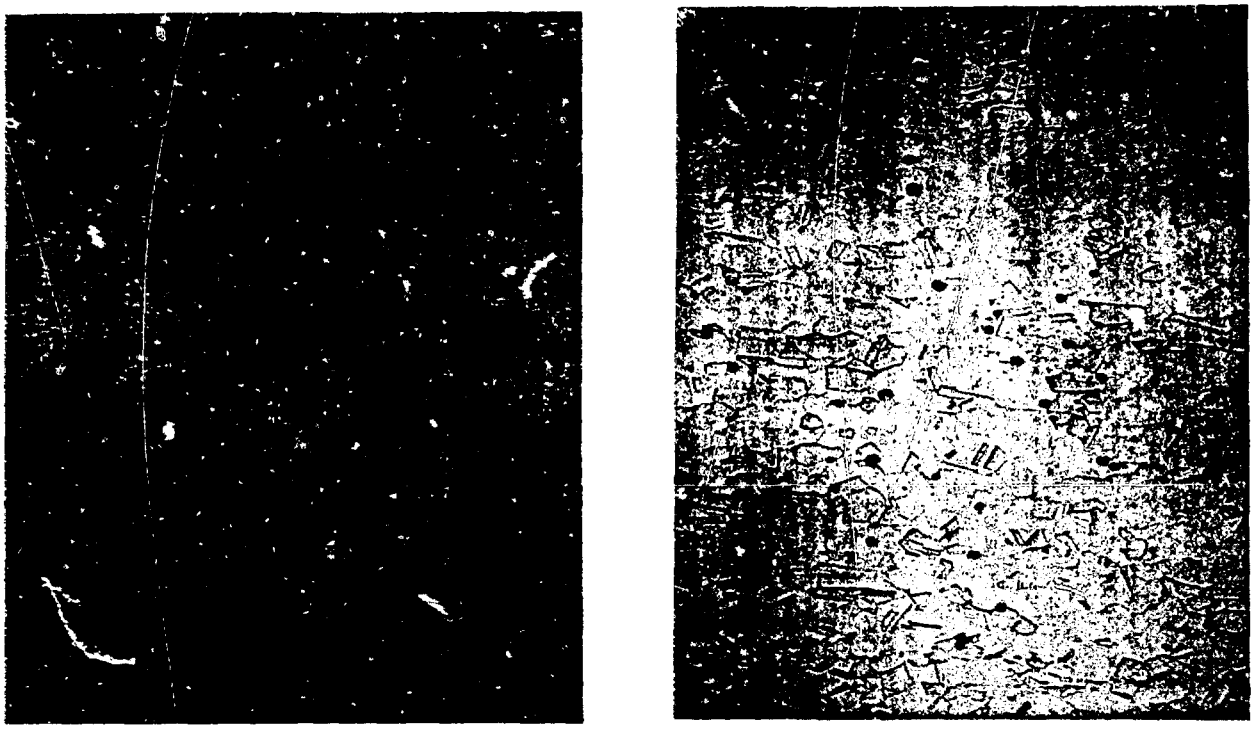

(a) P/N 9-1

(b) P/N 10-1

Mag: 500 X

Fig. 8. Microstructure of Amzirc (Sheet 1015 - longitudinal) after one hour at 840 °F (a) or 930 °F (b). Note partial recrystallization in (a) and almost complete recrystallization in (b).

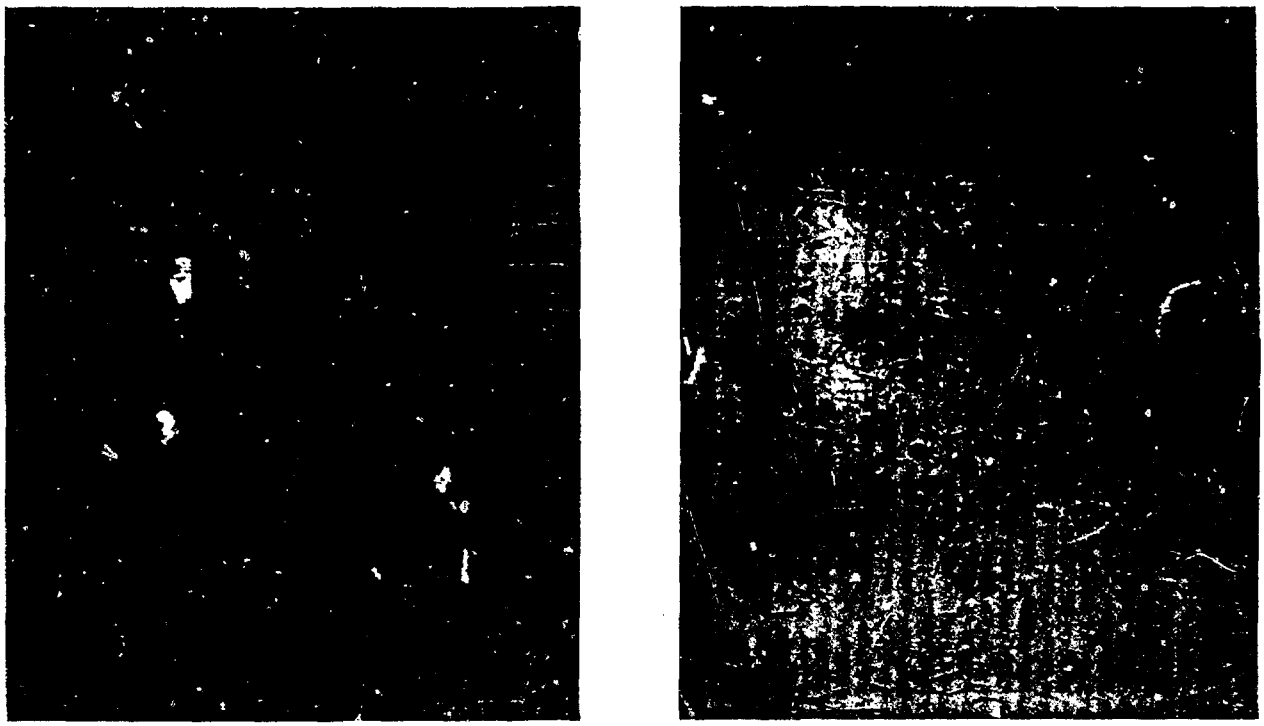

(a) P/N 11-1

(b) P/N 12-1

Mag: 500 X

Fig. 9. Microstructure of Amzirc (Sheet 1015 - transverse) after one hour at 840 °F (a) or 930 °F (b). Note partial recrystallization in (a), and almost complete recrystallization in (b).

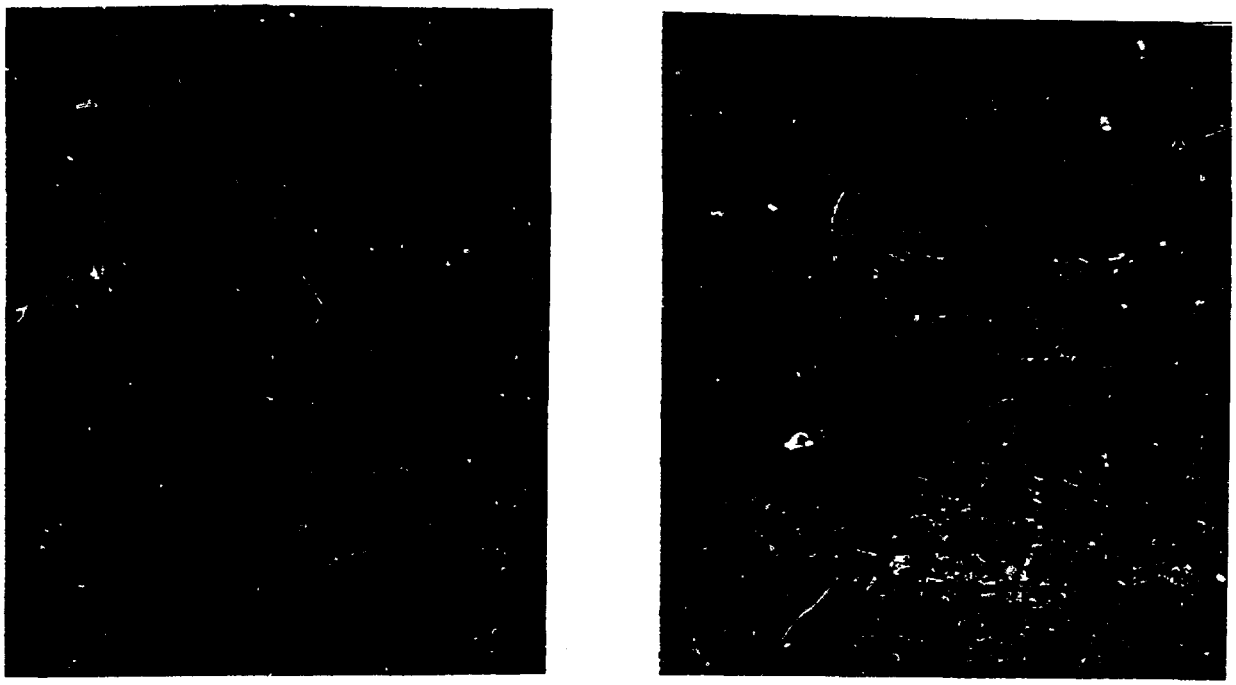

(a) P/N 13-1

(b) P/N 14-1

Mag: 500 X

Fig. 10. Microstructure of MZC (Sheet 3002 - longitudinal) after one hour at 840 °F (450 °C) (a) or 930 °F (500 °C) (b). Note progress of recrystallization, a fine general precipitate (arrows a), and stringers of an elongated precipitate (arrows b).

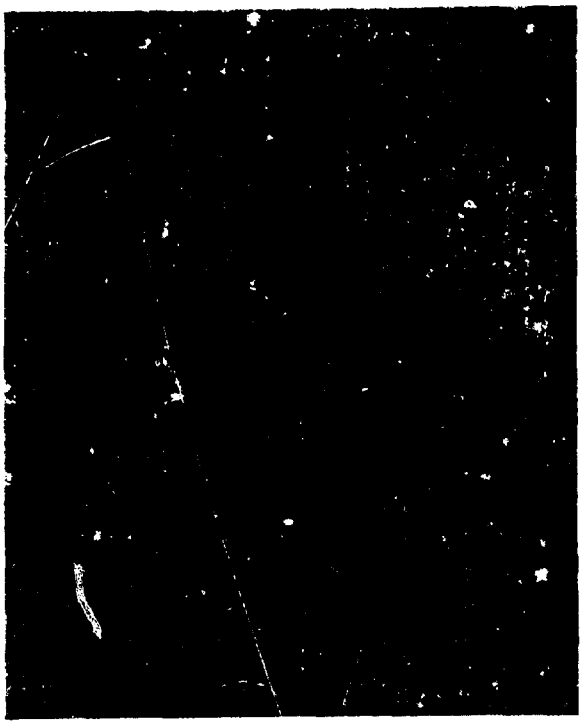

(a) P/N 15-1, 100 X

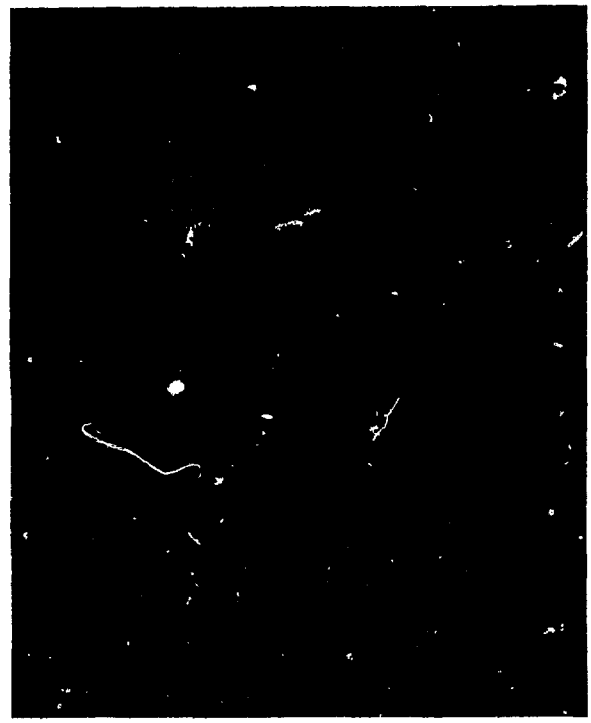

(b) P/N 15-2, 500 X

Fig. 11. Microstructure of MZC (Sheet 3002 - transverse) after one hour at 840 °F. Note abnormal grain growth (arrows) in (a) and (b), the mostly recrystallized microstructure evident in (b), and the presence of a finely dispersed precipitate in (b) (arrows b).

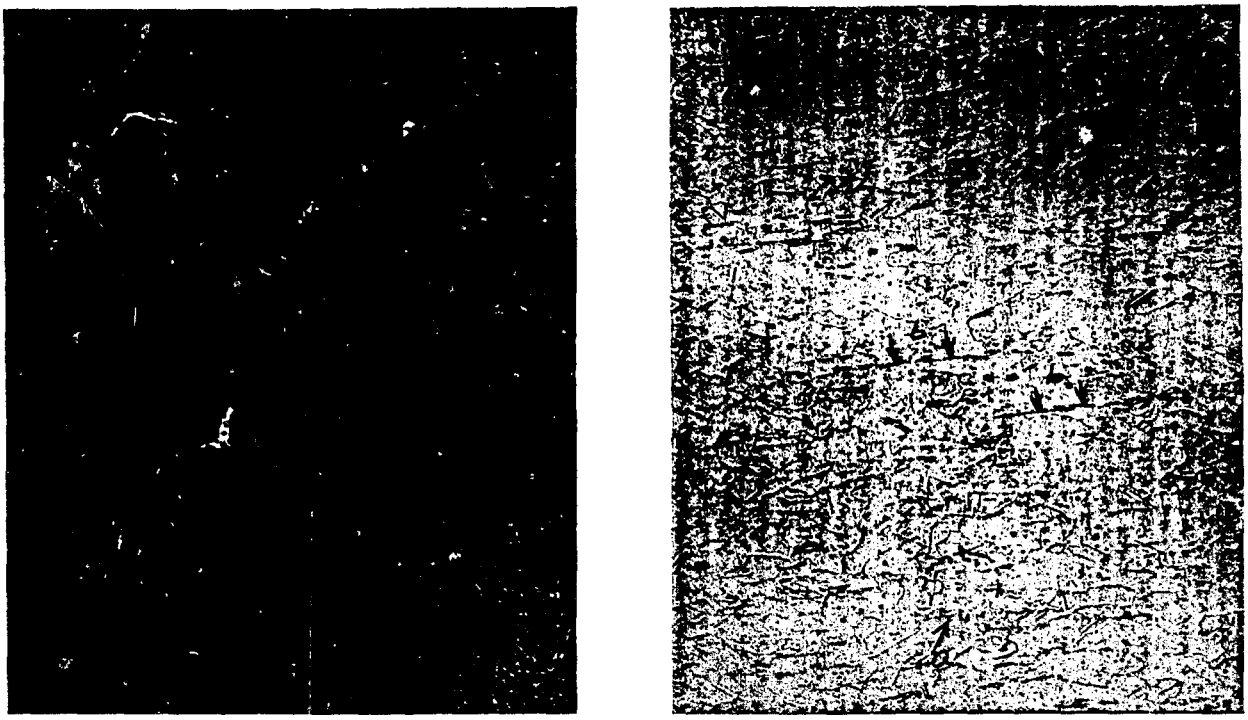

(a) P/N 16-1

(b) P/N 17-1

Mag: 500 X

Fig. 12. Microstructure of MZC (Sheet 3002) after one hour at 930 °F (a - transverse) or 1200 °F (b - transverse) showing recrystallized microstructure, a fine general precipitate (arrows a), and stringers of an elongated precipitate (arrows b).

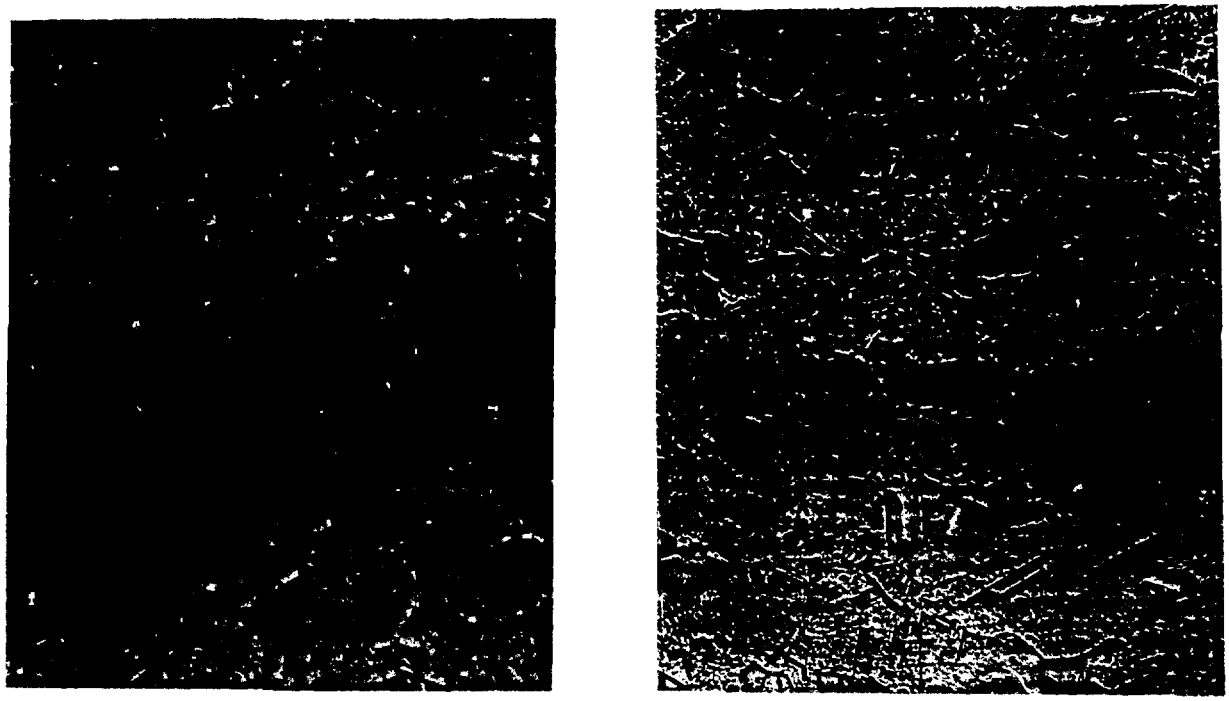

(a) P/N 17-2, 1000 X

(b) P/N 17-3, 1250 X

Fig. 13. Microstructure of MZC (Sheet 3002 - longitudinal) after one hour at 1200 °F (650 °C). Note fine general precipitate (arrows a) and stringers of an elongated precipitate (arrows b).

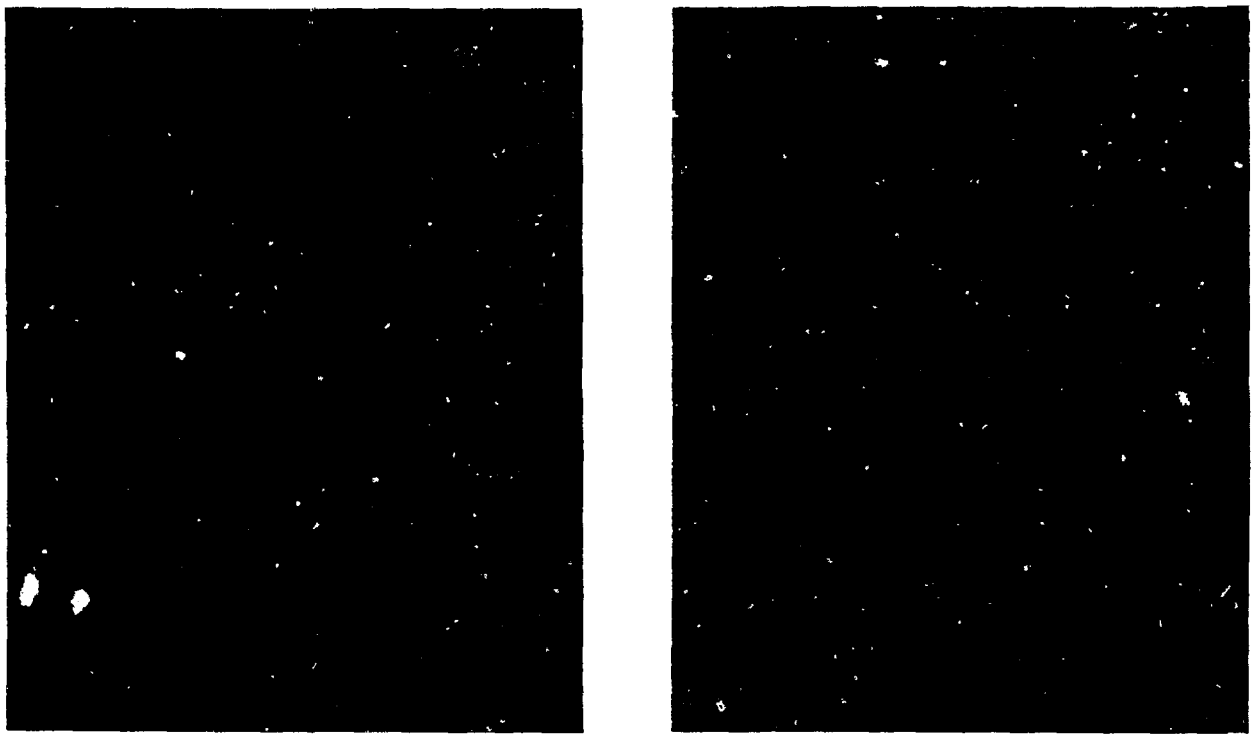

(a) P/N 25-1

(b) P/N 56-1

Mag: 500 X

Fig. 14. Microstructure of MZC sheet (longitudinal) after 0.5 hours (a) or 1.0 hours (b) at 750 °F (399 °C). Note onset of recrystallization, as shown by occurrence of equiaxed grains (arrows 1), and increase in the number of these grains as the time at 750 °F increases. Note also the occurrence of abnormally large grains (arrows 2), a very fine general precipitate (arrows 3), and a coarser precipitate (arrows 4).

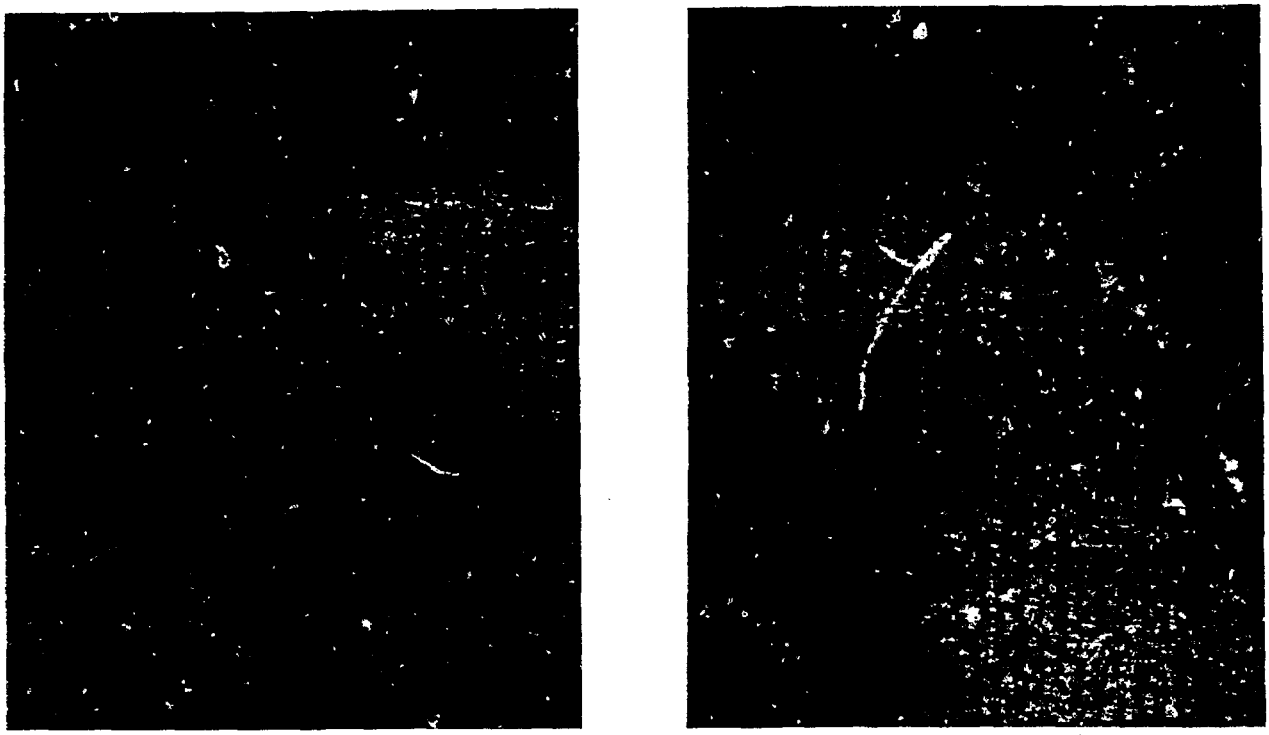

(a) P/N 55-2

(b) P/N 55-1

Mag: 500 X

Fig. 15. Microstructure of MZC sheet (longitudinal) after 70 hours at 750 °F (399 °C). Note progress of recrystallization as shown by occurrence of equiaxed grains (arrows 1), abnormally large grains (arrows 2), a very fine general precipitate (arrows 3), and a coarser precipitate (arrows 4).

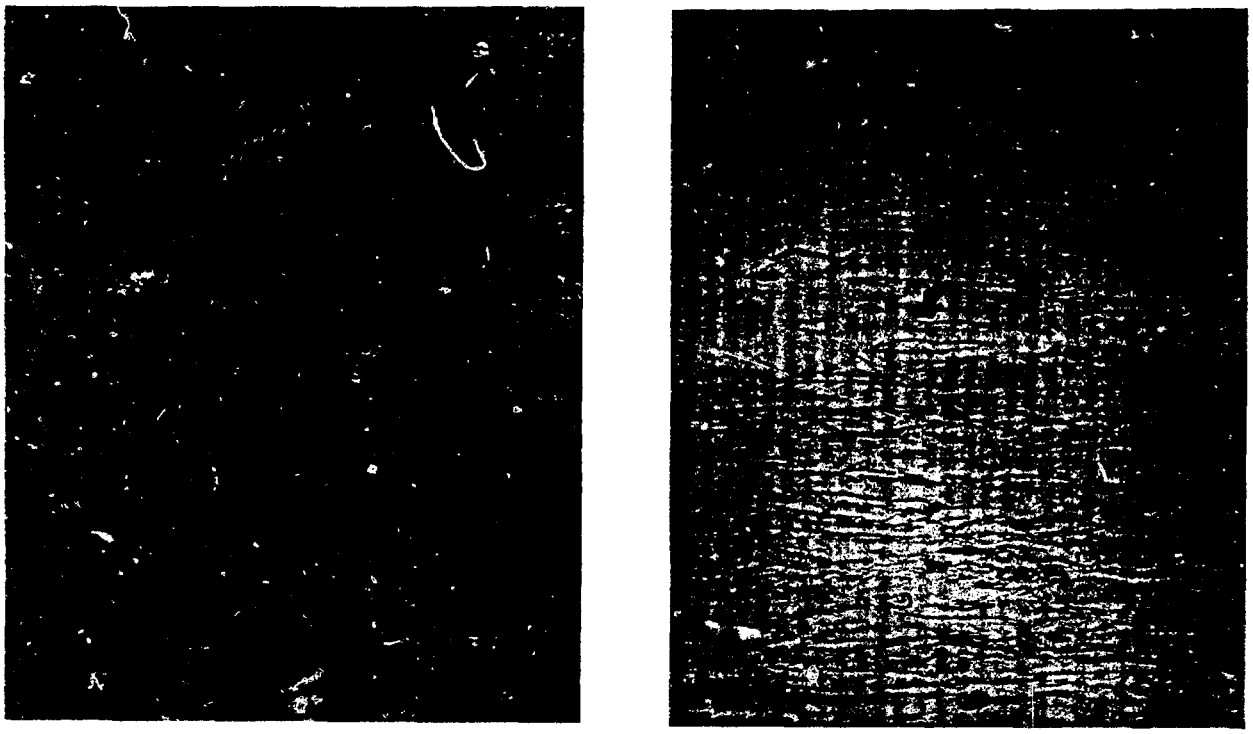

(a) P/N 181-1

(b) P/N 182-1

Mag: 500 X

Fig. 16. Microstructure of Amzirc sheet (longitudinal) after 0.5 hours (a) or 1.0 hours (b) at 750 °F (399 °C). Note cold-worked microstructure and a coarse precipitate (arrows 1).

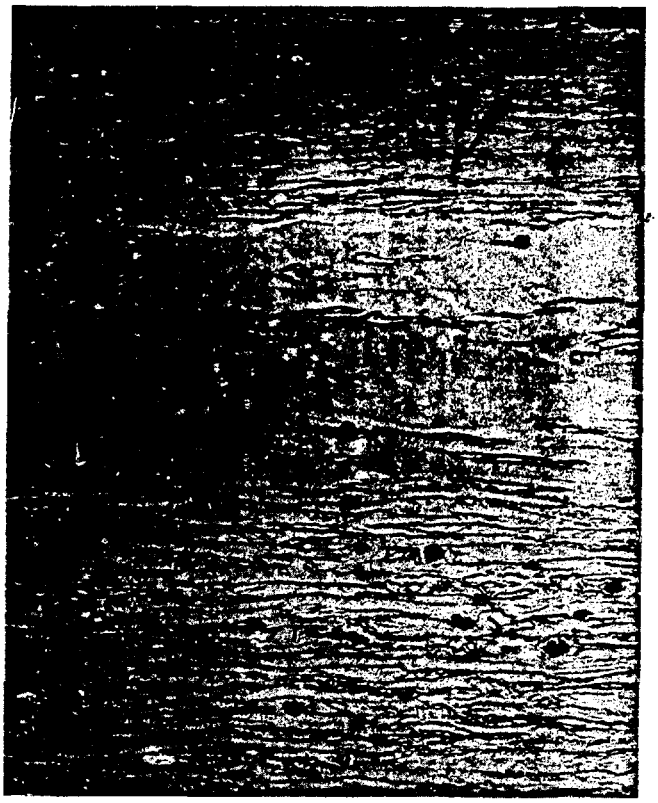

P/N 183-1

Mag: 500 X

Fig. 17. Microstructure of Amzirc sheet (longitudinal) after 10 hours at 750 ^{o}F (399 ^{o}C) showing cold-worked microstructure and a coarse precipitate (arrows 1).

P/N 80-1

Mag: 500 X

Fig. 18. Microstructure MZC sheet (longitudinal) after a solution treatment of 1675 ^{o}F (0.5 hours) and a water quench to room temperature. Note the large grain size, a very fine general precipitate (arrows 1), and a coarse precipitate (arrows 2).

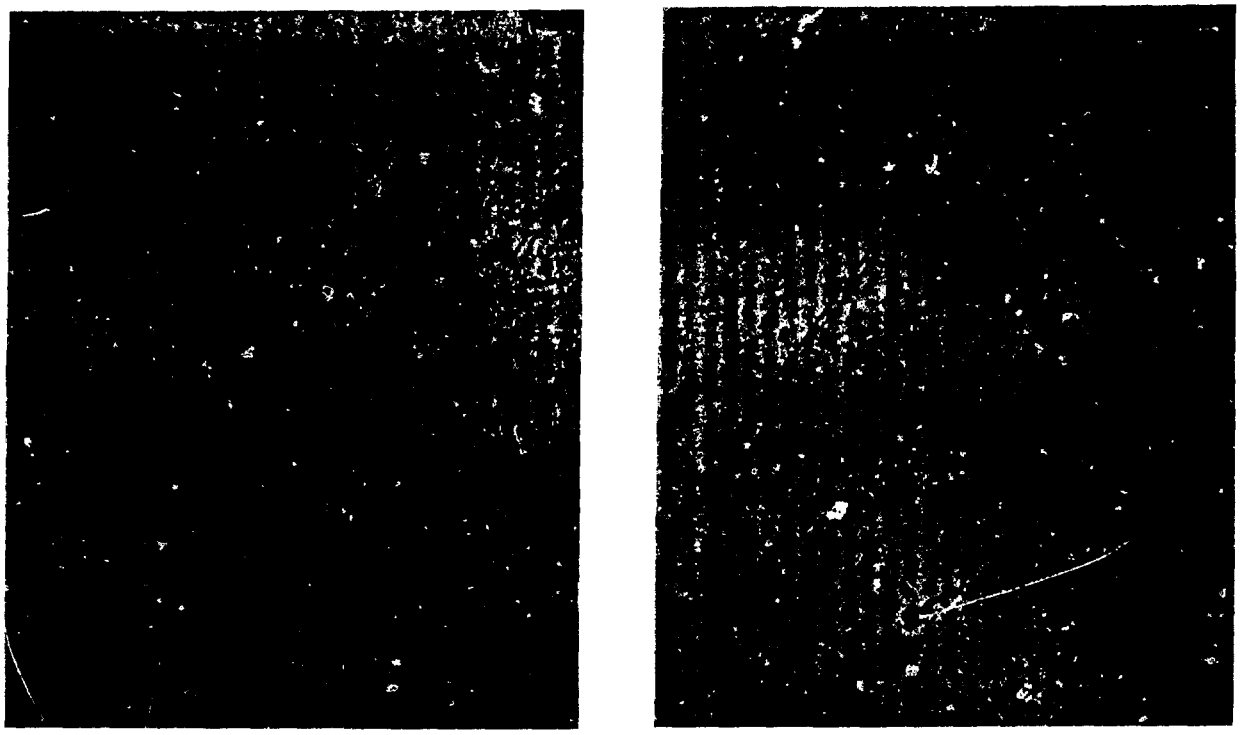

(a) P/N 80-2

(b) P/N 80-3

Mag: 1000 X

Fig. 19. Microstructure of MZC sheet (longitudinal) after a solution treatment of 1675 °F (0.5 hours) and a water quench to room temperature. Note the very fine general precipitate (arrows 1) and a coarse precipitate (arrows 2).

(a) P/N 1700-1

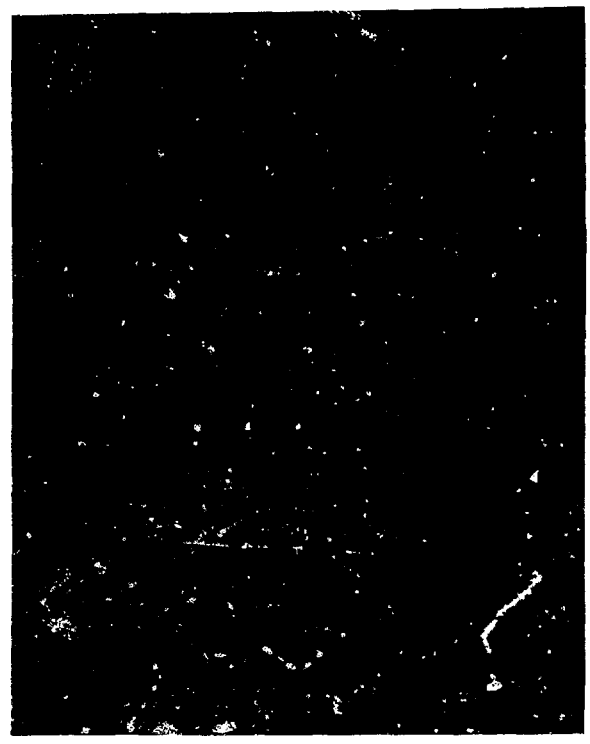

(b) P/N 1750-1

Mag: 500 X

Fig. 20. Transverse sections through MZC alloy sheet after heat treatments of 1700 °F (0.5 hours), water quench (Fig. a) or 1750 °F (0.5 hours), water quench (Fig. b). Note coarse (c) and fine (d) precipitates.

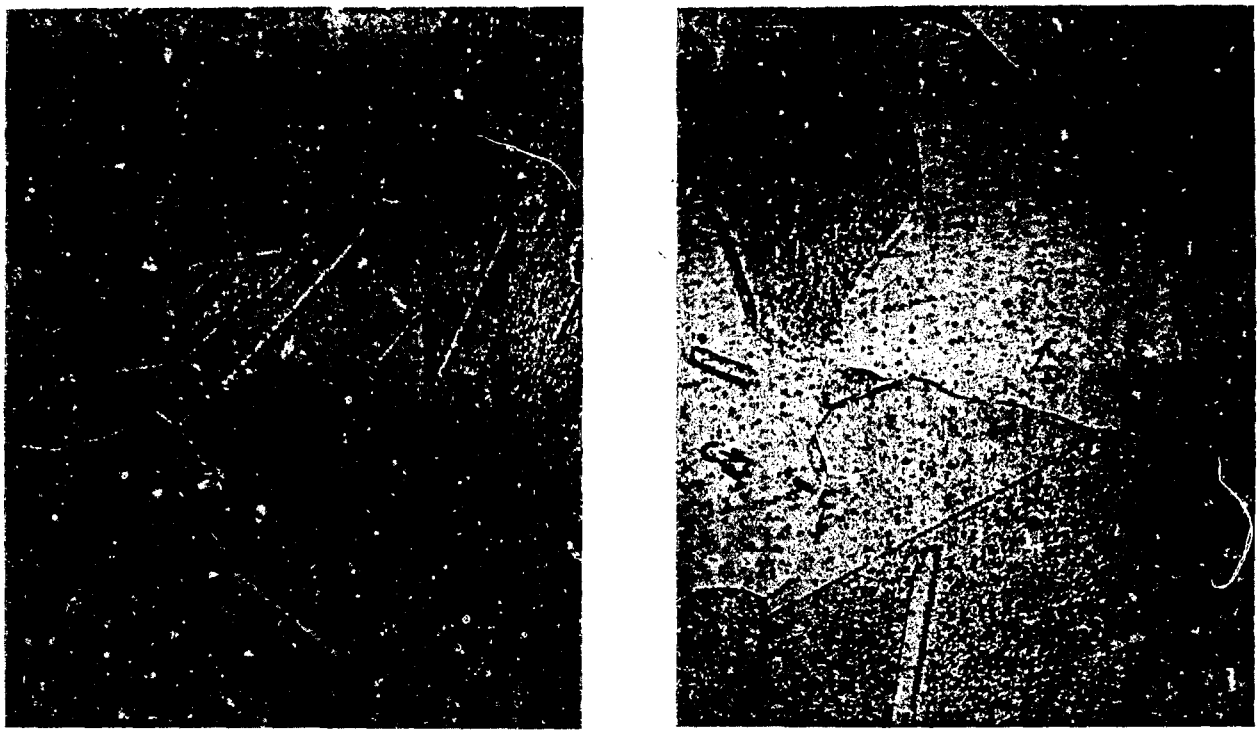

(a) P/N 1800-1

(b) P/N 1850-1

Mag: 500 X

Fig. 21. Transverse sections through MZC alloy sheet after heat treatments of 1800 °F (0.5 hours), water quench (Fig. a) or 1850 °F (0.5 hours), water quench (Fig. b). Note coarse (c) and fine (d) precipitates.

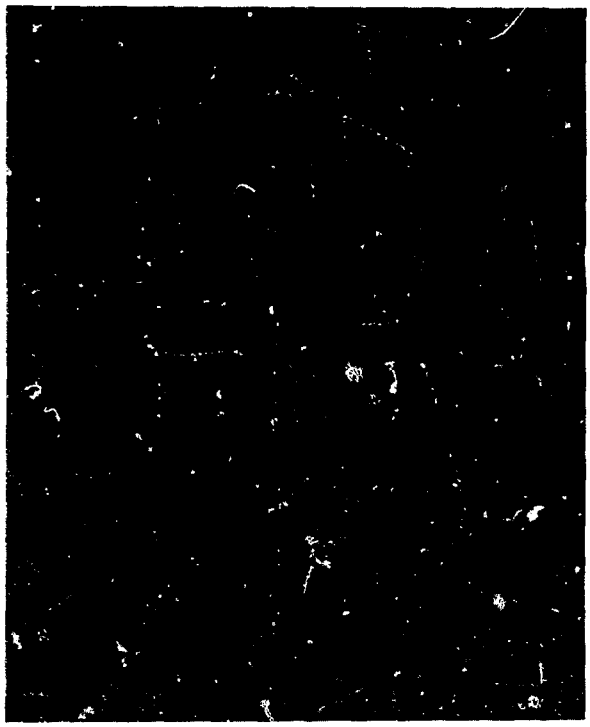

(a) P/N 1900-1, Mag: 500 X

(b) P/N 1900-2, Mag: 1000 X

Fig. 22. A transverse section through MZC alloy sheet after a heat treatment of 1900 ^{0}F (0.5 hours), water quench. Note coarse (c) and fine (d) precipitates.

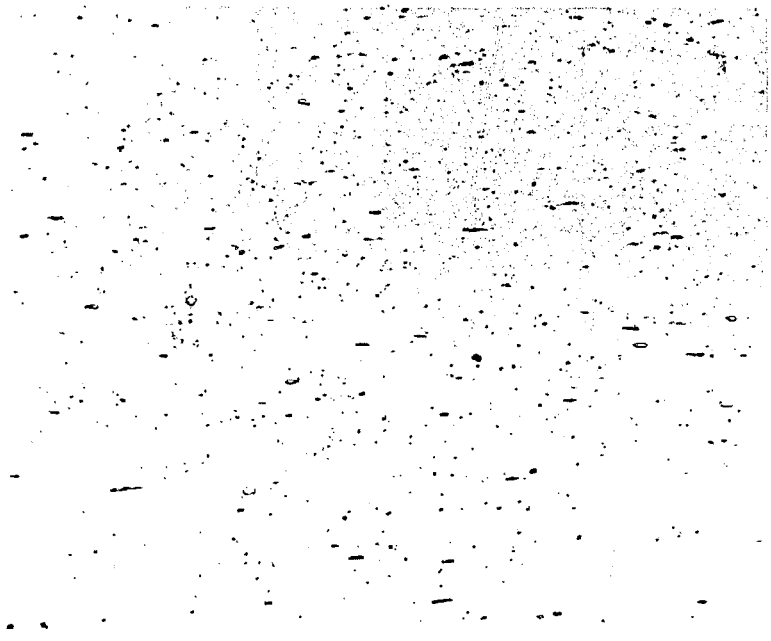

(a) MZC (800 X). Processed into sheet, then annealed eight hours, 550 °C.

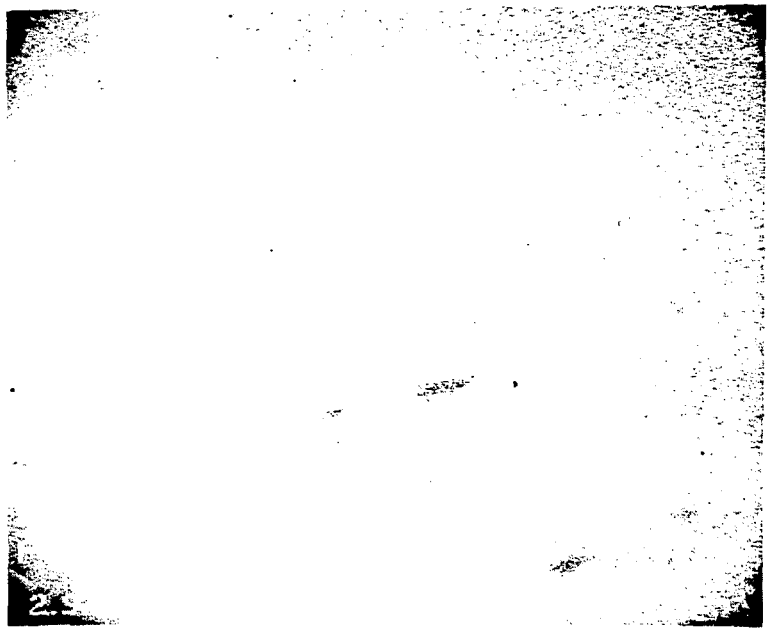

(b) Same sample as above, on SEM with back scattered electrons (approx. 3600 X). Light areas are high zirconium; dark areas are high chromium.

Fig. 23.
Unetched condition.

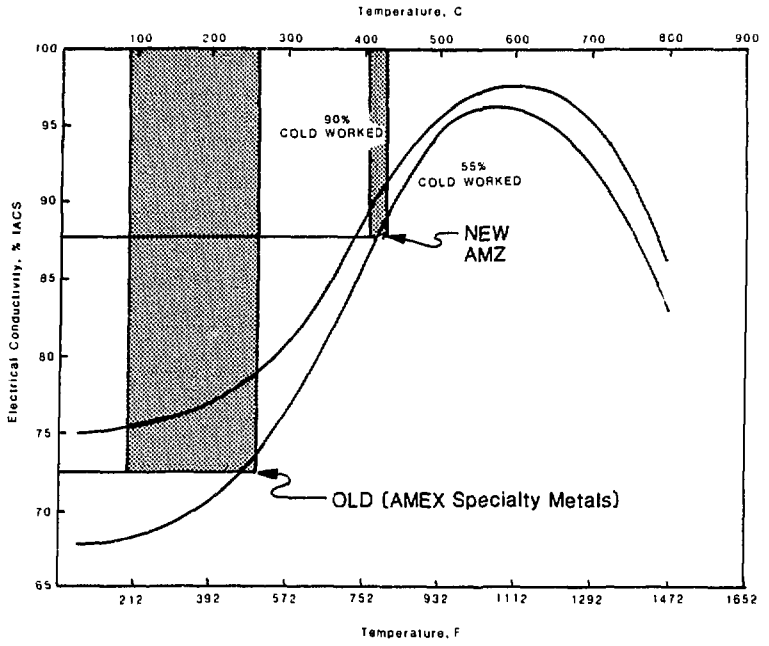

Fig. 24. Effect of aging on electrical conductivity at room temperature. Condition: solution heat treated 1650 °F (900 °C), 1/2 hour, quenched, cold worked and aged (1 hour) as indicated.

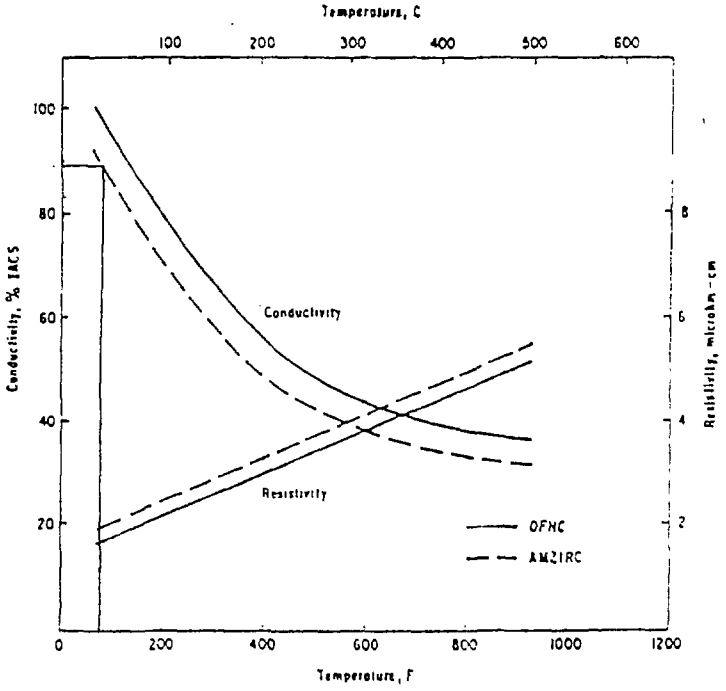

Fig. 25. Elevated temperature electrical conductivity and resistivity. Condition: solution heat treated 1650 °F (900 °C), 1 hour, quenched, cold worked 75%, aged 750 °F (400 °C), 1 hour.

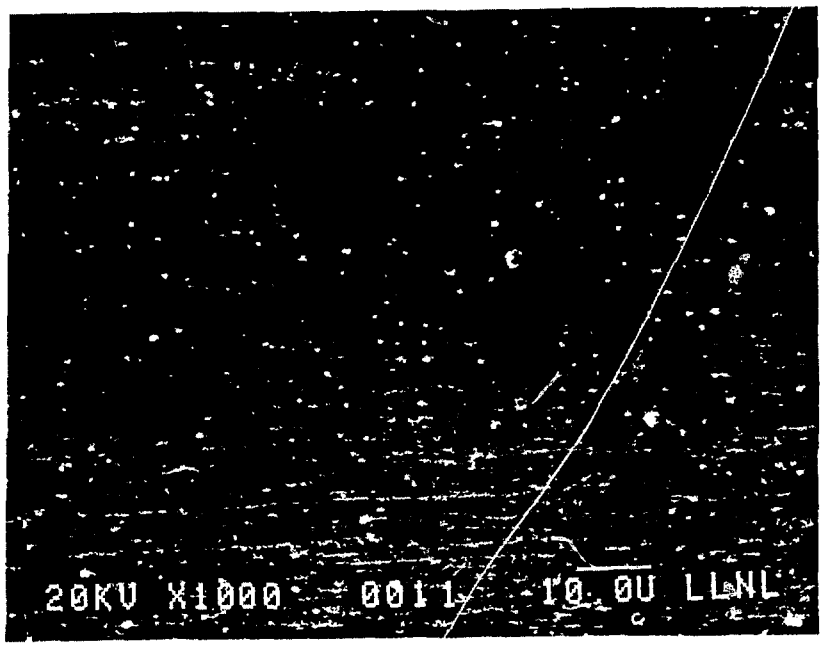

EL40 500 °C, 0.5 hours

(a) Longitudinal

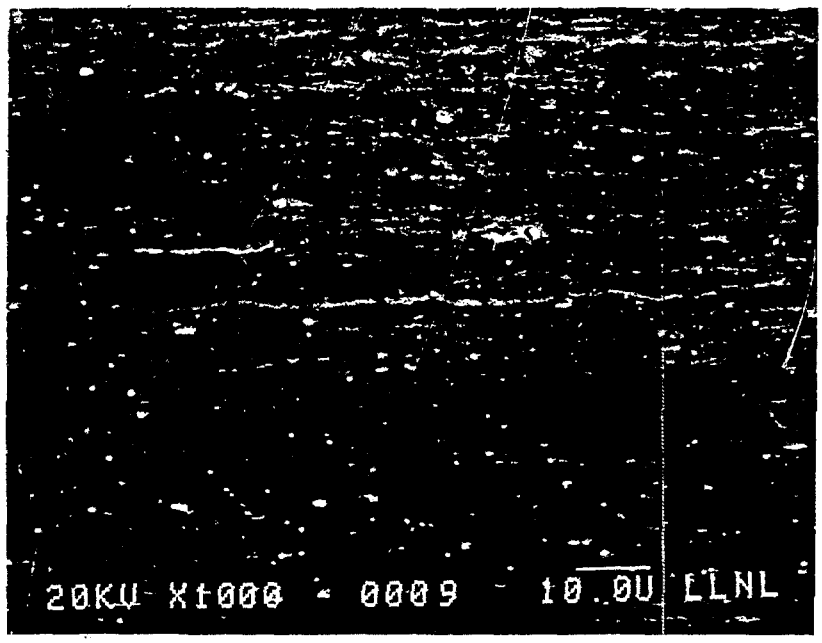

ET10 500 °C, 0.5 hours

(b) Transverse

Fig. 26. Microstructure of Elbrodur RS sheet after a 500 °C, 0.5 hour exposure. Note elongated grain structure (horizontal), a spherical precipitate (a), and a rectangular precipitate (b).

EL40 500 °C, 0.5 hours

(a) Longitudinal

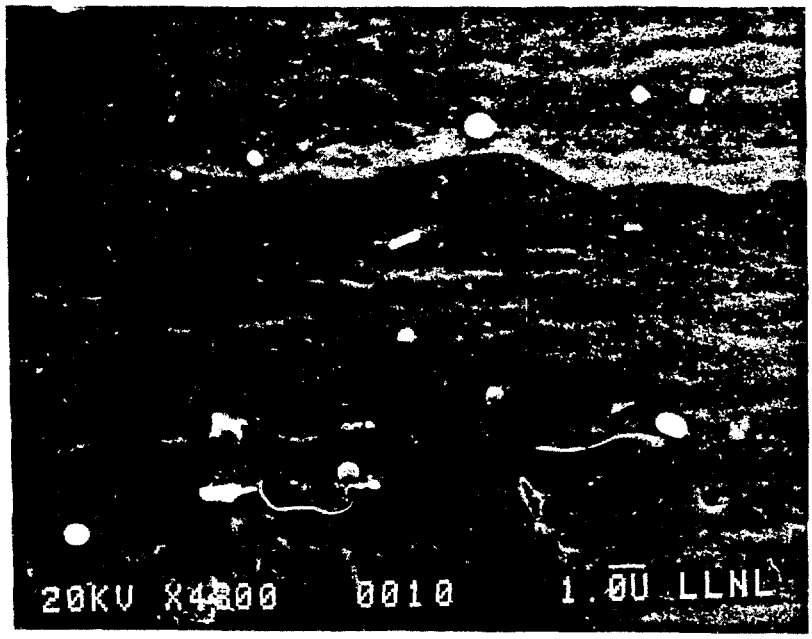

ET10 500 °C, 0.5 hours

(b) Transverse

Fig. 27. Microstructure of Elbrodur RS sheet after a 500 °C, 0.5 hour exposure. Note a spherical precipitate (a) and a rectangular precipitate (b).

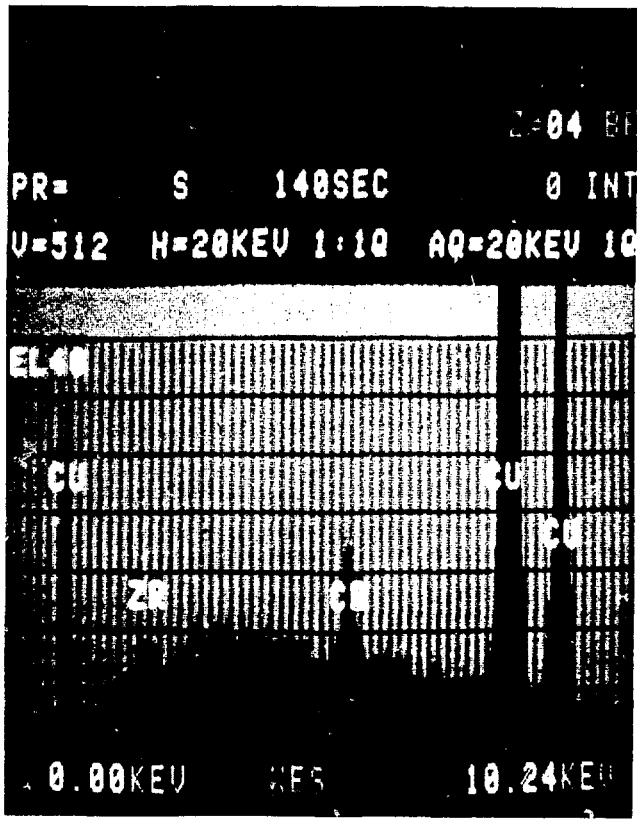

EL40 - 500 °C, 0.5 hour - Matrix

Fig. 28. Edax spectrum from matrix of Elbrodur RS sheet after a 500 °C, 0.5 hour exposure. Note presence of Zr and Cr in solid solution.

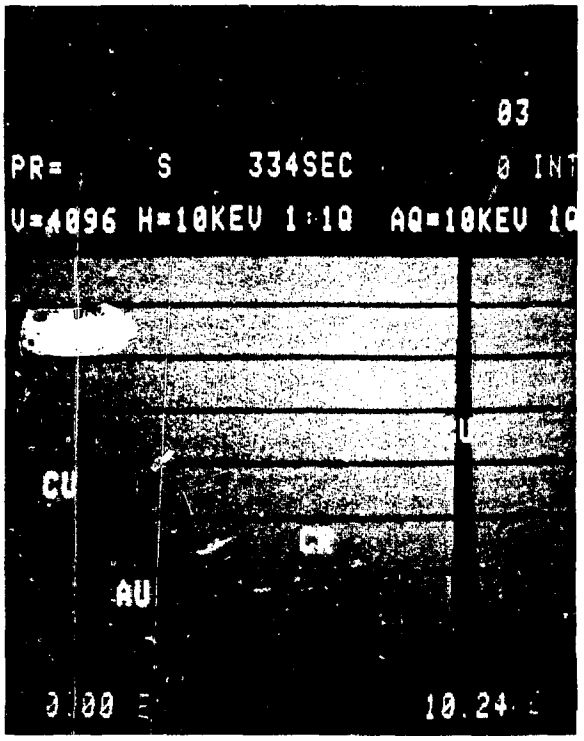

(a) EL40 - 500 °C, 0.5 hr, round particle

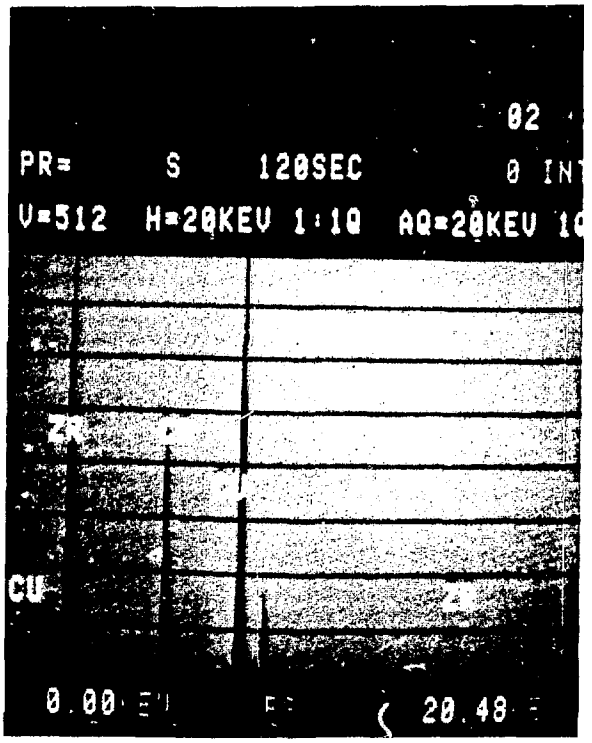

(b) EL40/500 °C, 0.5 hr, cubic particle

Fig. 29. Edax spectra from round particle (a) and rectangular particle (b) found in Elbrodur RS sheet after a 500 °C, 0.5 hour exposure. Note presence of Cr and absence of Zr in round particles (a). Note presence of both Zr and Cr in rectangular particles (b).

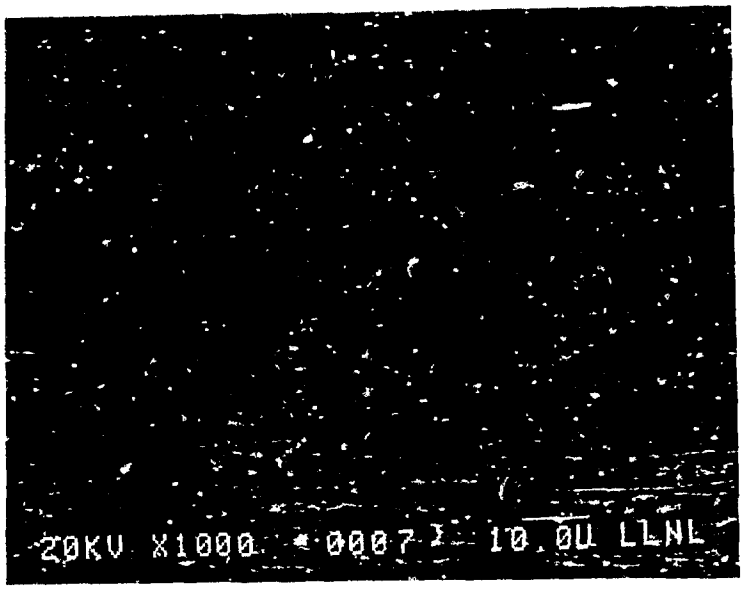

EL41 500 °C, 1.0 hour

(a) Longitudinal

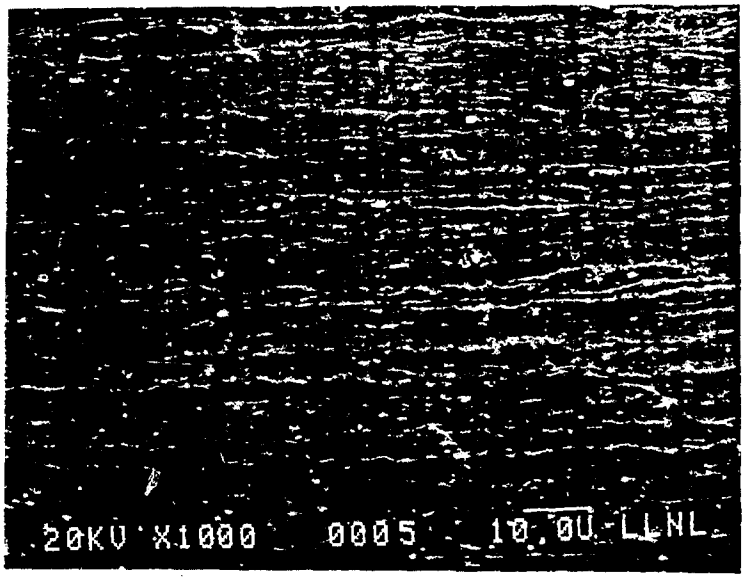

ET11 500 °C, 1.0 hour

(b) Transverse

Fig. 30. Microstructure of Elbrodur RS sheet after a 500 °C, 1.0 hour exposure. Note elongated grain structure (horizontal), a spherical precipitate (a), and a rectangular precipitate (b).

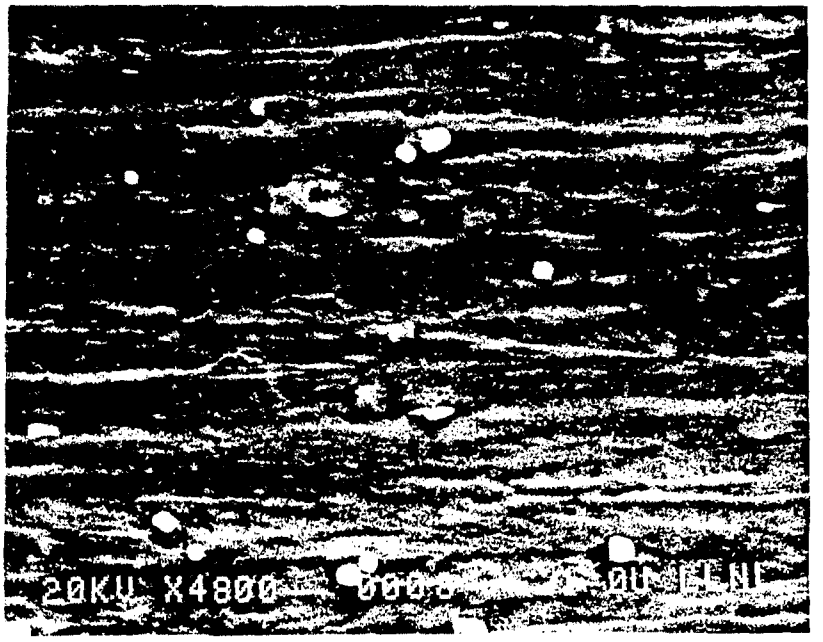

EL41 500 °C, 1.0 hour

(a) Longitudinal

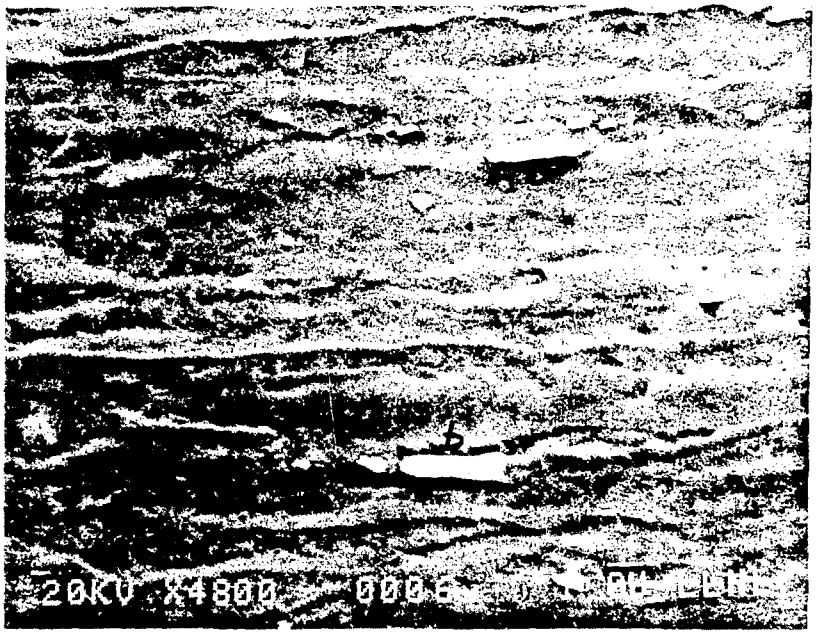

ET11 500 °C, 1.0 hour

(b) Transverse

Fig. 31. Microstructure of Elbrodur RS sheet after a 500 °C: 1.0 hour exposure. Note elongated grain structure (horizontal), a spherical precipitate (a), and a rectangular precipitate (b).

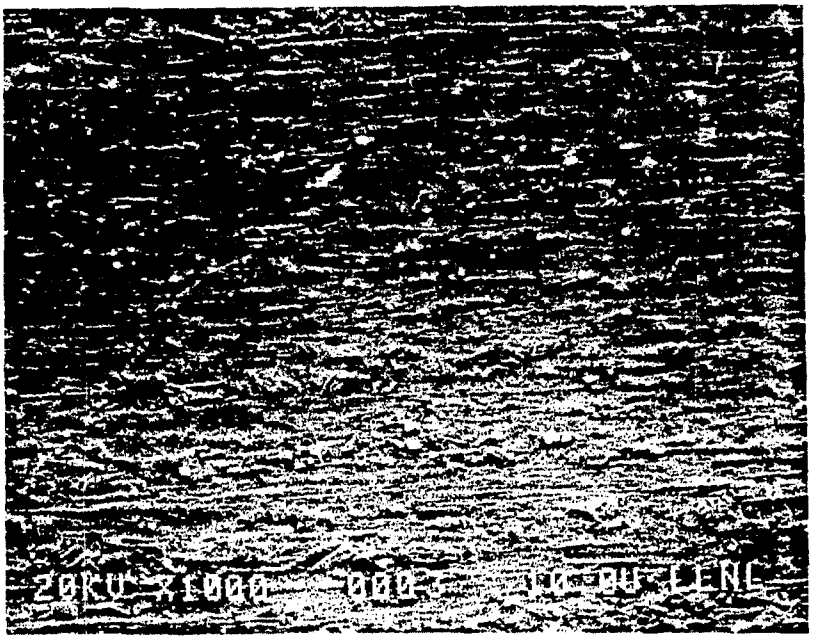

EL42 500 °C, 10.0 hours

(a) Longitudinal

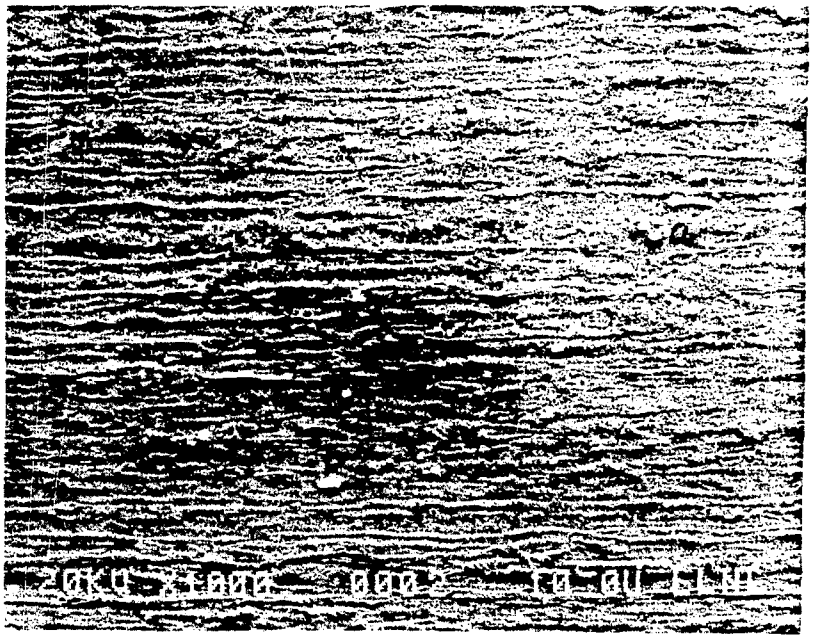

ET12 500 °C, 10.0 hours

(b) Transverse

Fig. 32. Microstructure of Elbrodur RS sheet after a 500 °C, 10.0 hour exposure. Note elongated grain structure (horizontal), a spherical precipitate (a), and a rectangular precipitate (b).

EL42 500 °C, 10.0 hours

(a) Longitudinal

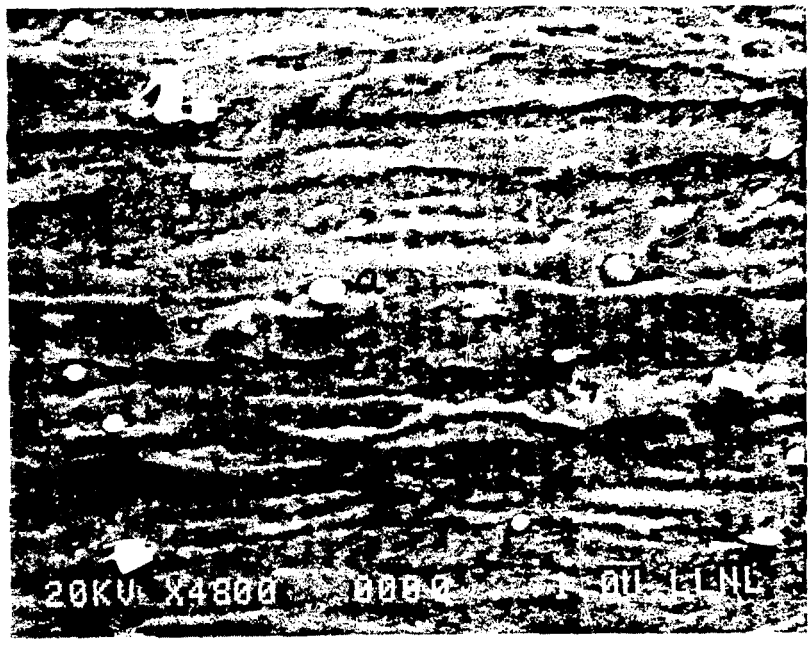

ET12 500 °C, 10.0 hours

(b) Transverse

Fig. 33. Microstructure of Elbrodur RS sheet after a 500 °C, 10.0 hour exposure. Note elongated grain structure (horizontal), a spherical precipitate (a), and a rectangular precipitate (b).

EL45-1, 500 X

Longitudinal

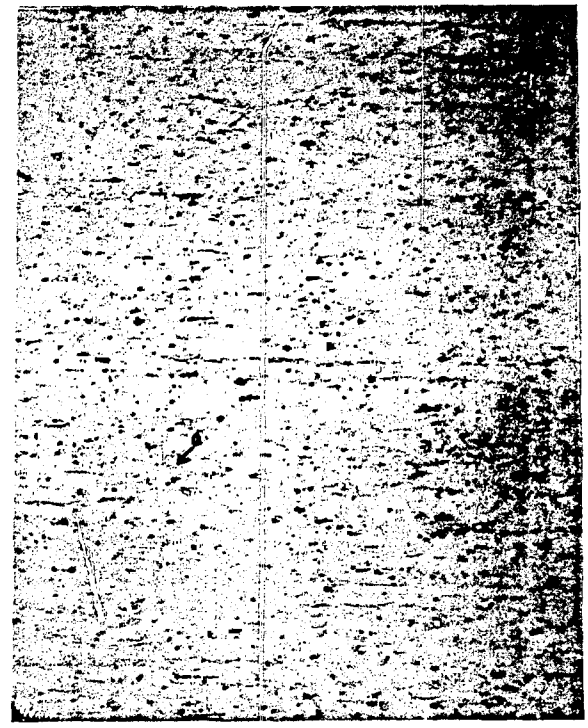

ET15-1, 500 X

Transverse

Fig. 34. Microstructure of Elbrodur RS sheet after a 550 ^{o}C, 0.5 hour exposure. Note equiaxed grains (a), possible twining (b), and a fine precipitate (c).

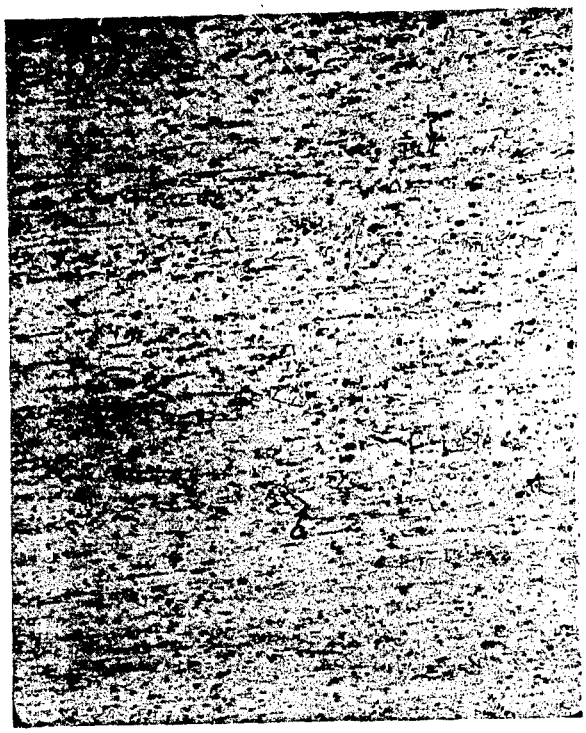

EL46-1, 500 X

Longitudinal

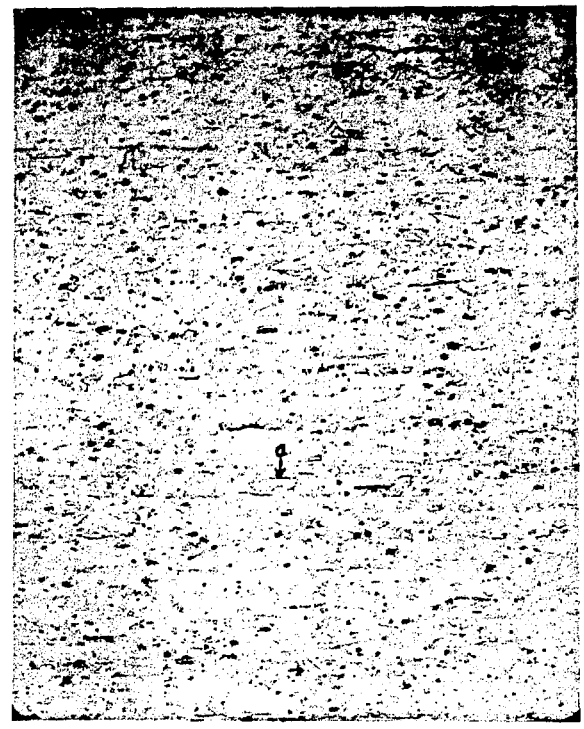

ET16-1, 500 X

Transverse

Fig. 35. Microstructure of Elbrodur RS sheet after a 550 °C, 1 hour exposure. Note equiaxed grains (a), possible twining (b), and a fine precipitate (c).

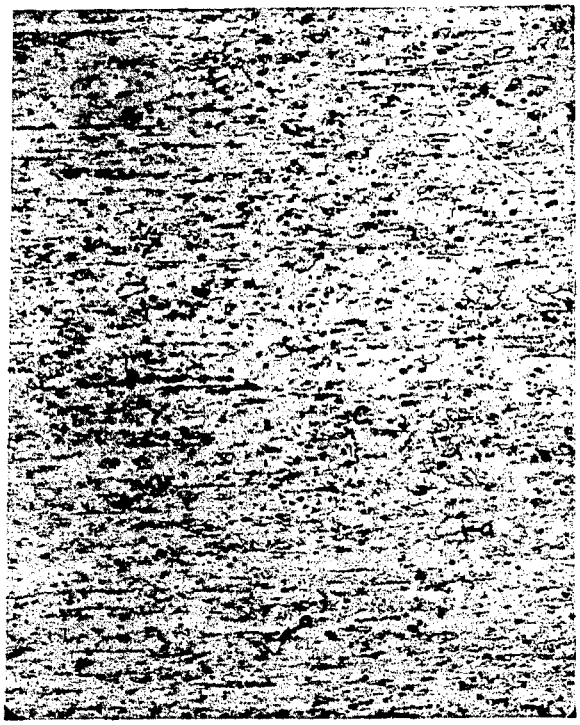

EL47-1, 500 X

Longitudinal

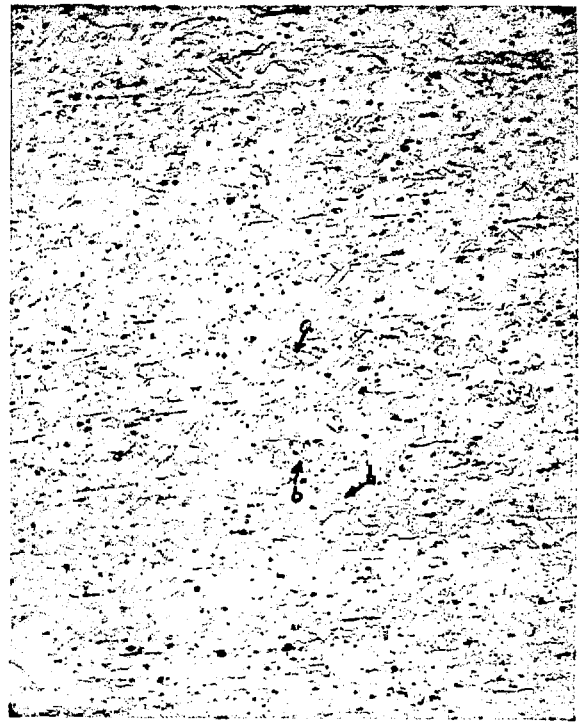

ET17-1, 500 X

Transverse

Fig. 36. Microstructure of Elbrodur RS sheet after a 550 °C, 10 hour exposure. Note equiaxed grains (a), possible twining (b), and a fine precipitate (c).

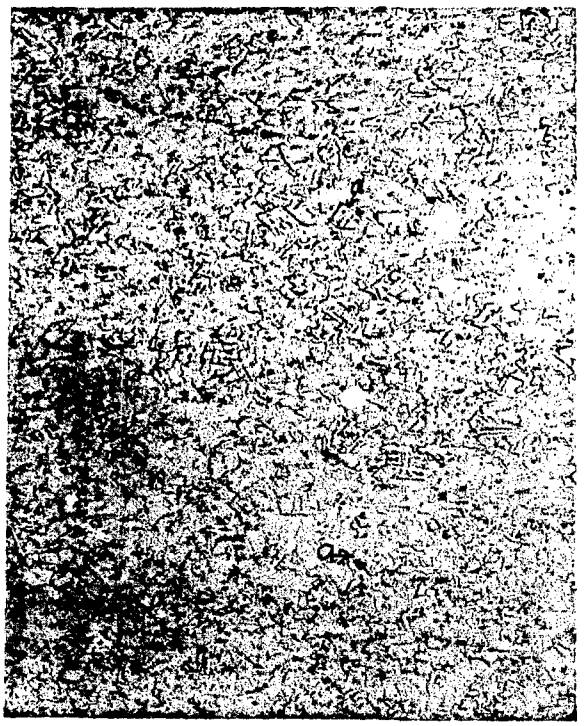

EL48-1, 500 X

Longitudinal

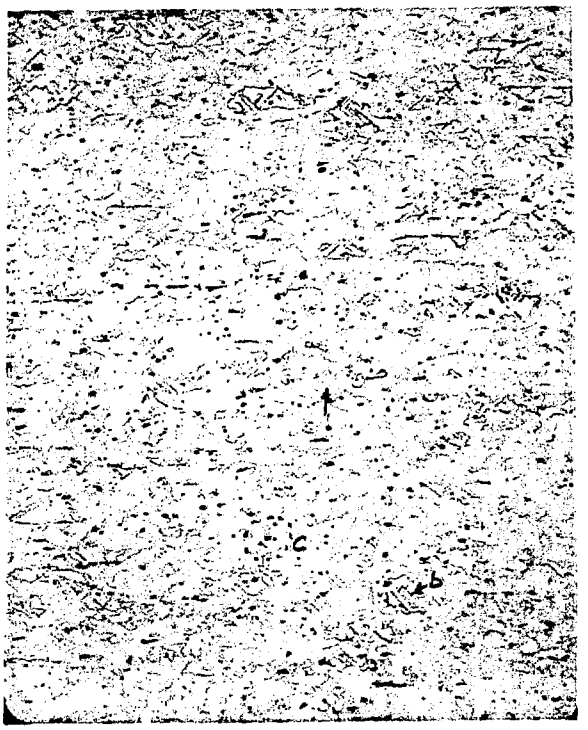

ET18-1, 500 X

Transverse

Fig. 37. Microstructure of Elbrodur RS sheet after a 600 °C, 0.5 hour exposure. Note equiaxed grains (a), possible twining (b), and a fine precipitate (c).

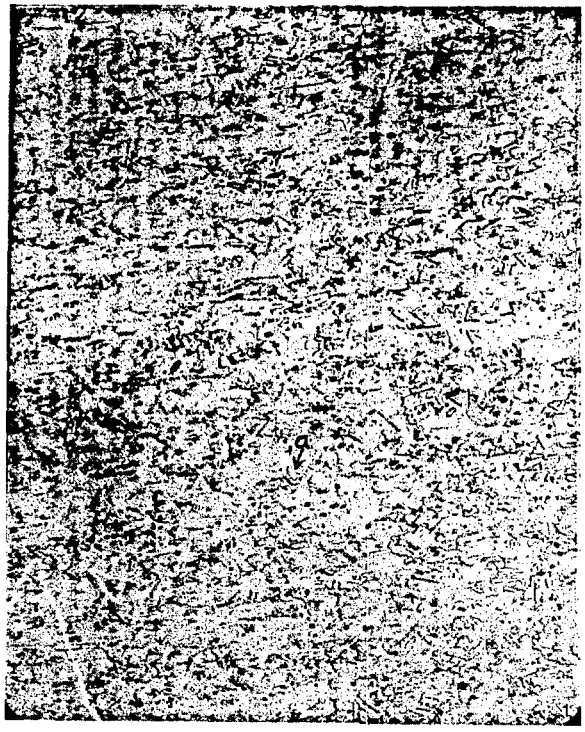

EL49-1, 500 X

Longitudinal

ET19-1, 500 X

Transverse

Fig. 38. Microstructure of Elbrodur RS sheet after a 600 ^{o}C, 1 hour exposure. Note equiaxed grains (a), possible twining (b), and a fine precipitate (c).

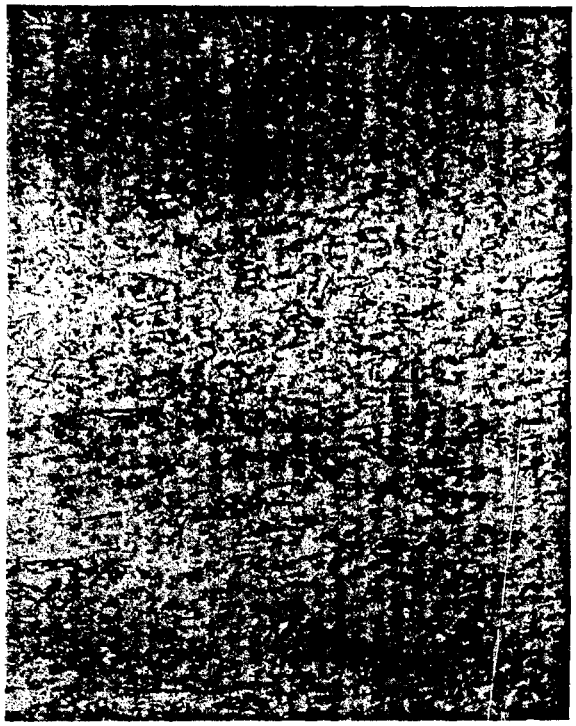

EL50-1, 500 X

Longitudinal

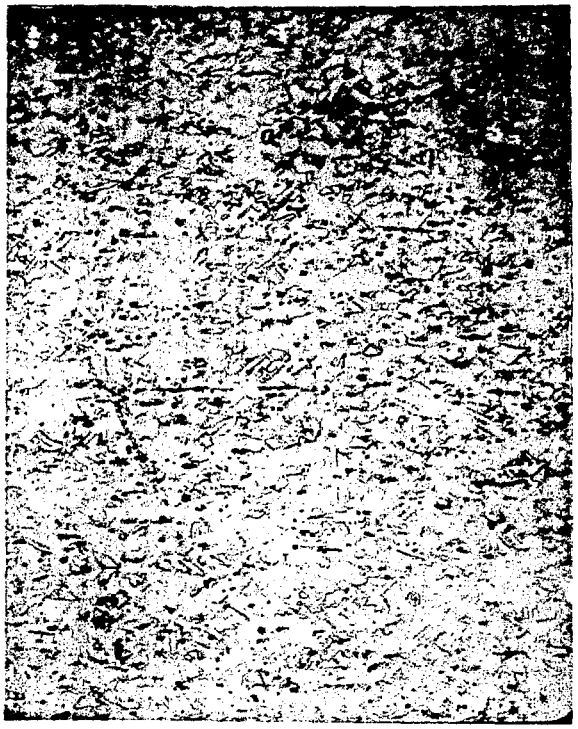

ET20-1, 500 X

Transverse

Fig. 39. Microstructure of Elbrodur RS sheet after a 600 ^{o}C: 10 hour exposure. Note equiaxed grains (a), possible twining (b), and a fine precipitate (c).

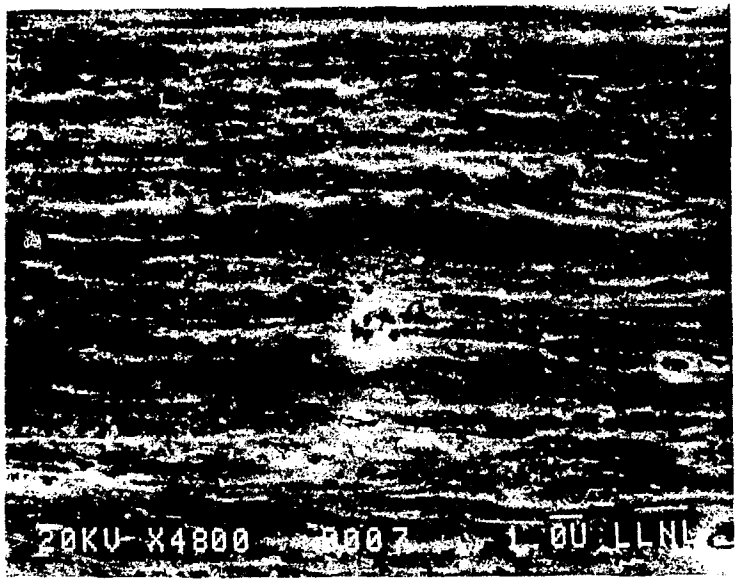

GL104 Longitudinal

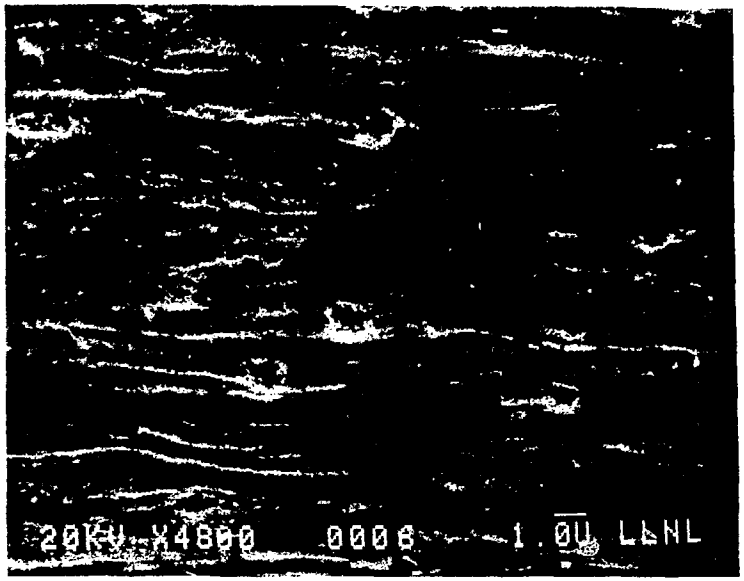

GT64 Transverse

GL104 Longitudinal

Fig. 40. Microstructure of Glid-Cop sheet after a 500 °C, 0.5 hr. exposure. Note elongated grain structure (horizontal) and a fine particle dispersion (a).

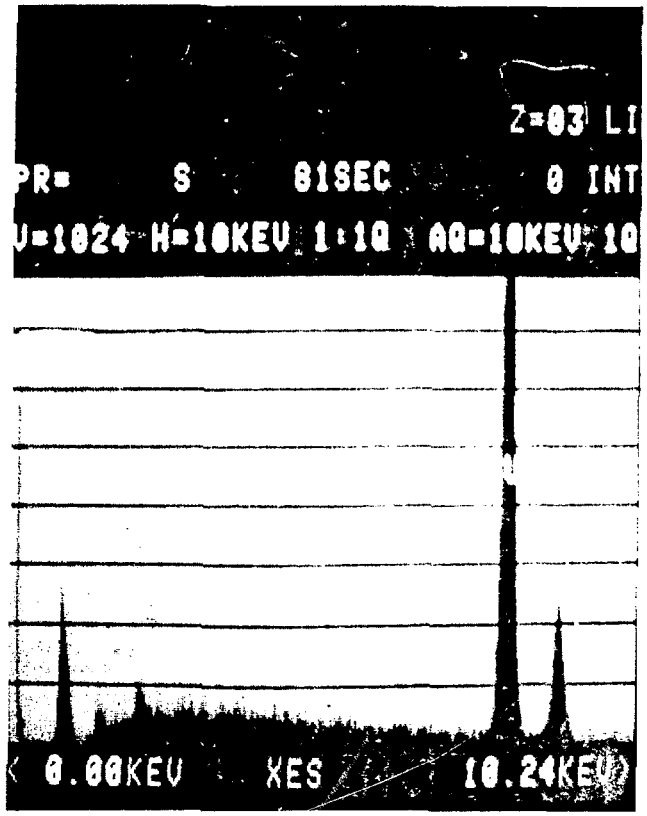

GL104, Particle

Fig. 41. Edax spectrum of dispersed particle in Glid-Cop sheet exposed at 500 °C for 0.5 hours. Note Al peak, indicative of particle being Al_2O_3.

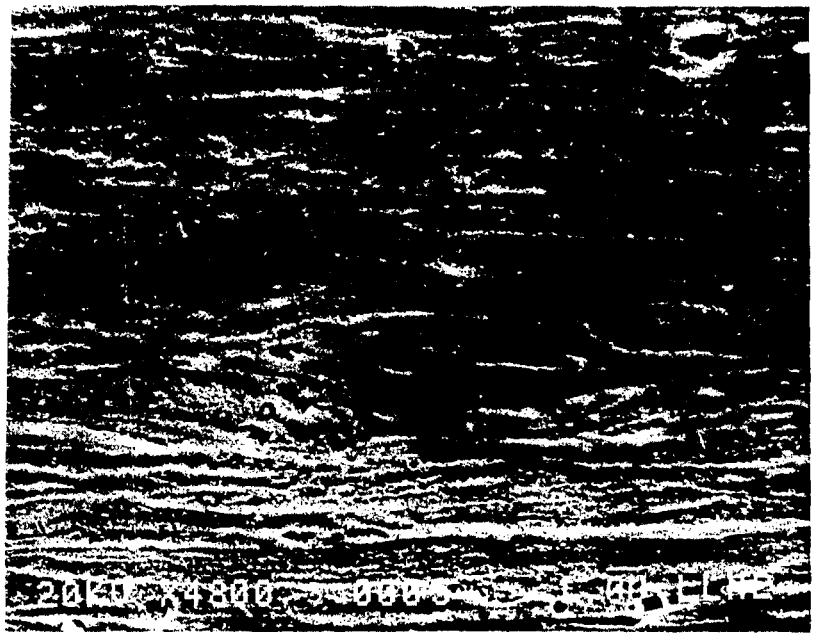

GL105

(a) Longitudinal

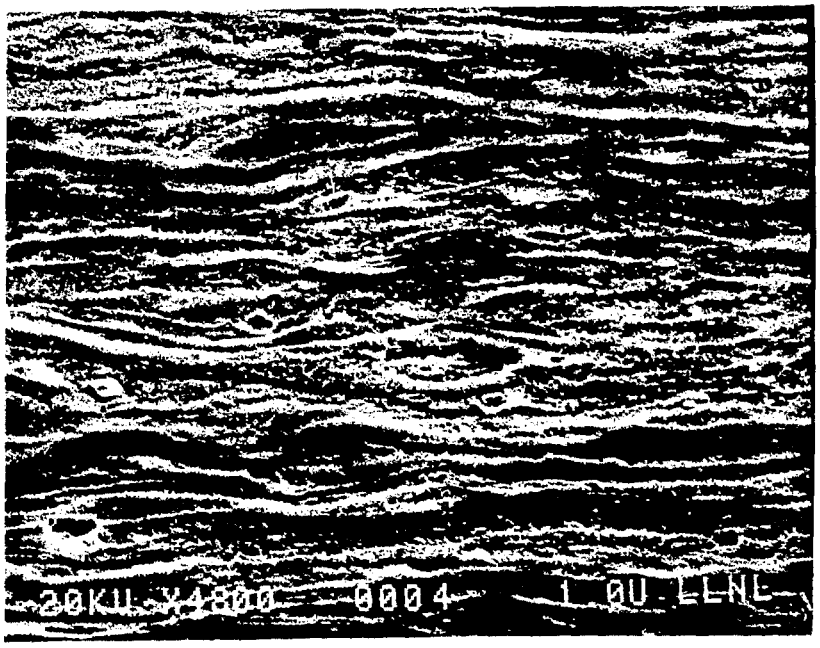

GT65

(b) Transverse

Fig. 42. Microstructure of Glid-Cop sheet given an exposure of 500 °C, 1.0 hour. Note elongated grain structure (horizontal) and a fine dispersion (a).

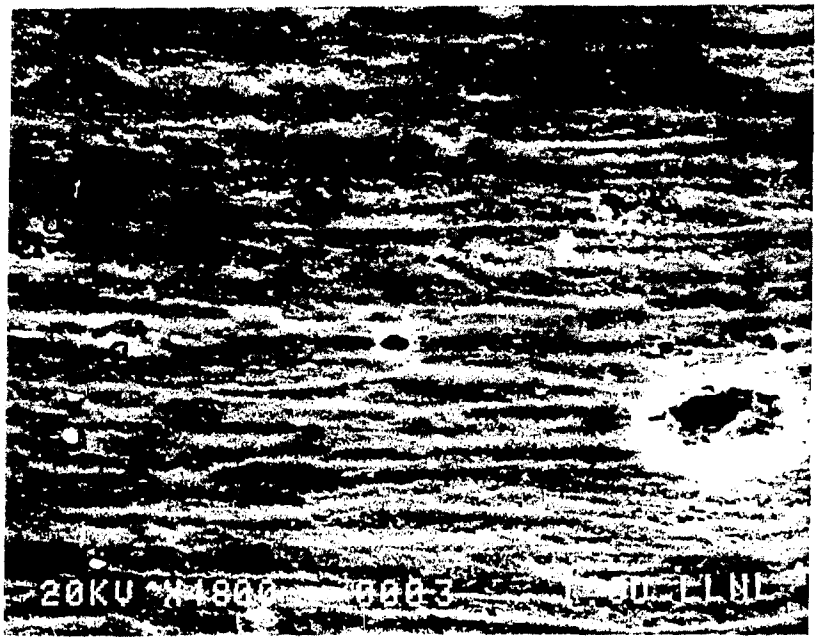

GL106

(a) Longitudinal

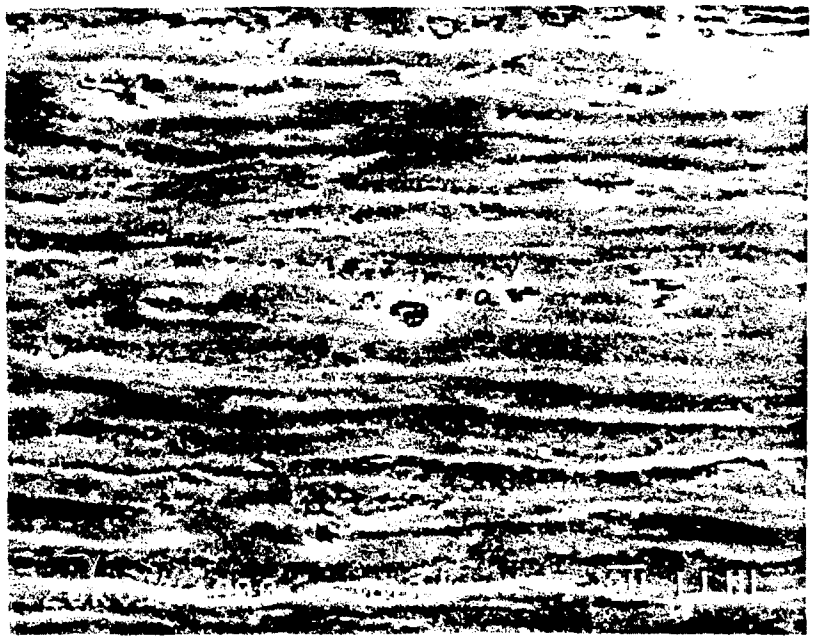

GT66

(b) Transverse

Fig. 43. Microstructure of Glid-Cop sheet given a 500 ^{o}C, 10 hour exposure. Note elongated grain structure (horizontal) and fine dispersion of particles (a).

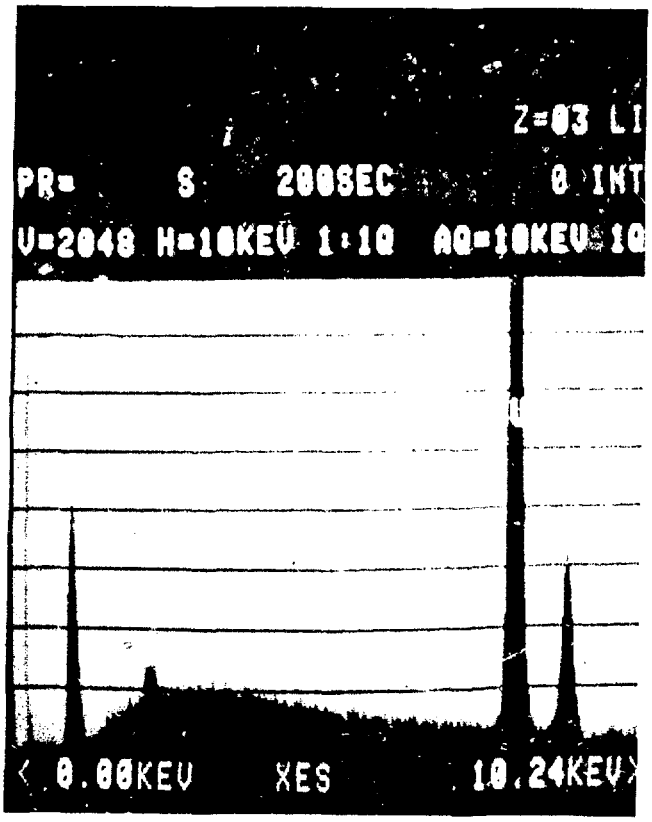

GL106 - Matrix

Longitudinal

Fig. 44. Edax spectrum from matrix of Glid-Cop sheet given an exposure of 500 °C, 10 hrs. Note copper lines and an Au line from the specimen holder.

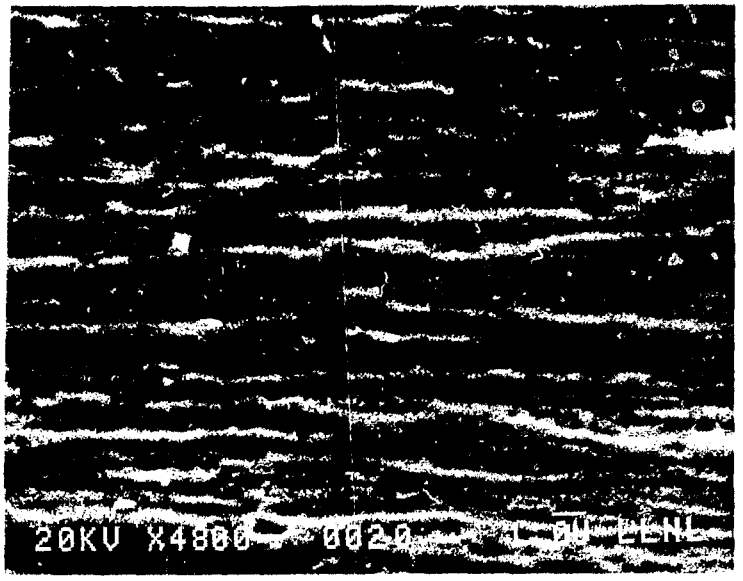

GL107

(a) Longitudinal

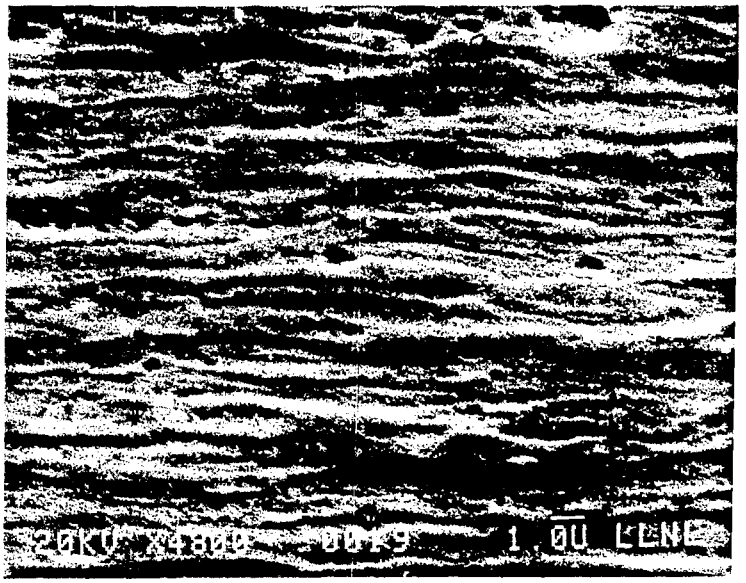

GT67

(b) Transverse

Fig. 45. Microstructure of Glid-Cop sheet given an exposure of 750 °C, 1 hour. Note elongated grain structure (horizontal) and a fine particle dispersion (a).

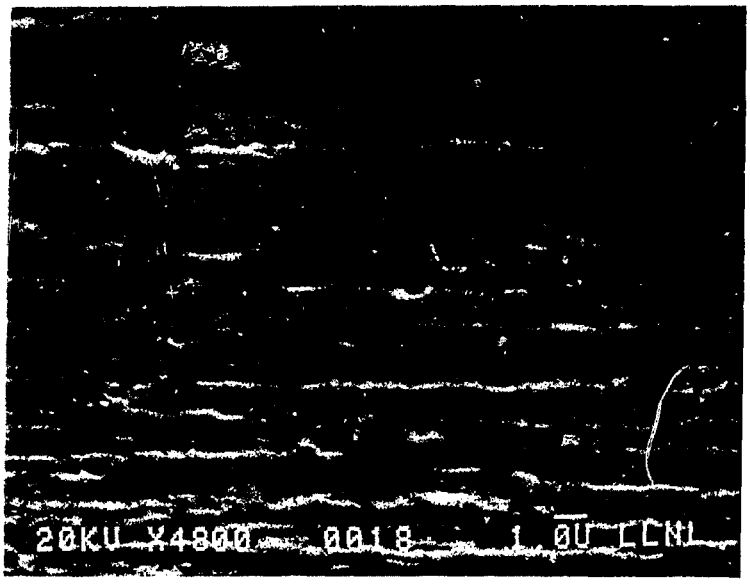

GL108

(a) Longitudinal

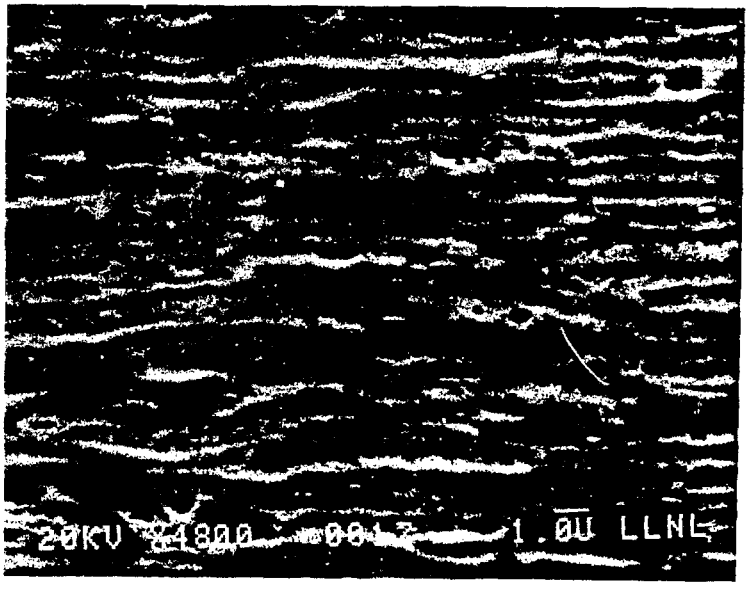

GT68

(b) Transverse

Fig. 46. Microstructure of Glid Cop sheet given an exposure of 800 °C, 1 hour. Note elongated grain structure (horizontal), and a fine particle dispersion (a).

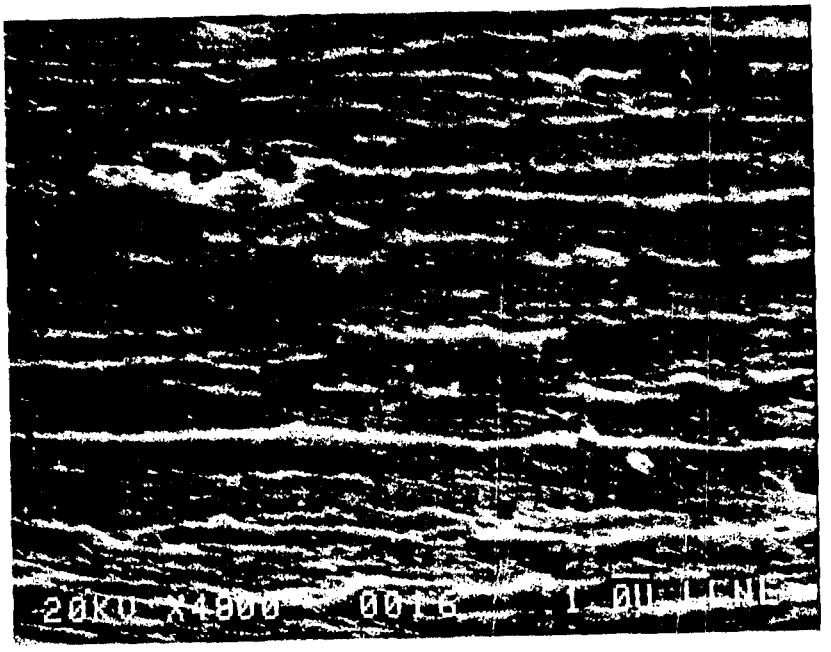

GL109

(a) Longitudinal

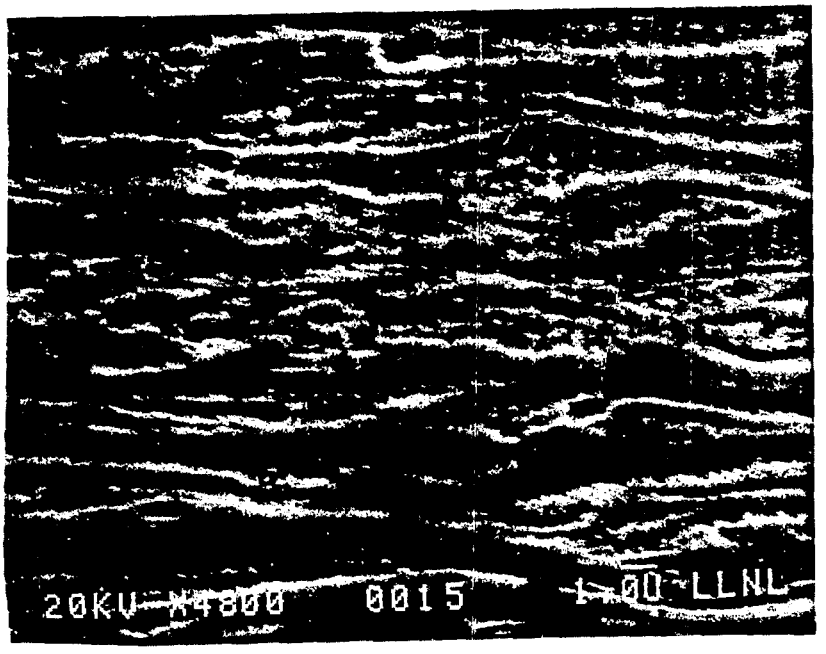

GT69

(b) Transverse

Fig. 47. Microstructure of Glid-Cop sheet given an exposure of 850 °C, 1 hour. Note elongated grain structure (horizontal) and a fine particle dispersion (a).

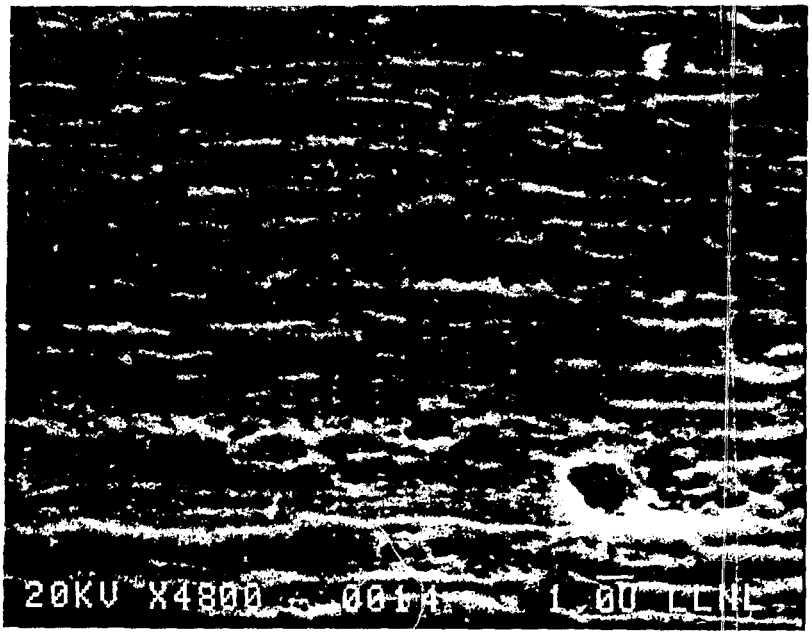

GL110

(a) Longitudinal

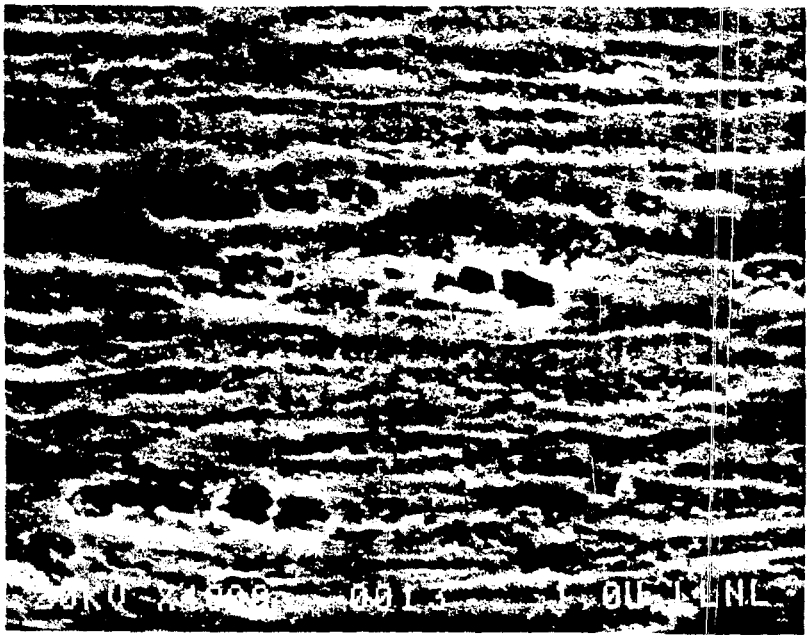

GT70

(b) Transverse

Fig. 48. Microstructure of Glid-Cop after an exposure of 900 ^{o}C for 1 hour. Note elongated grain structure (horizontal) and a fine particle dispersion (a).

COPPER ALLOYS FOR RIGGATRON APPLICATIONS

S. N. Rosenwasser

International Nuclear Energy Systems Company, Inc.

COPPER ALLOYS FOR RIGGATRON™ APPLICATIONS

S. N. ROSENWASSER

INESCO, INC.

The viability of the RIGGATRON tokamak design concept depends on the availability of high-strength, high-conductivity copper alloys. The RIGGATRON reactor is small (~3m wide x ~3m high) and requires normal conducting magnets which produce the high fields (~16T) necessary to confine the plasma. Both the density of the plasma and the first wall loading are about an order of magnitude higher than in the large, mainline super-conducting machines. Meeting the requirements for suitable copper alloys and fabrication methods used in the Toroidal Field Coils (TF), Central Ohmic Heating Coil (OH), and the First Wall/Vacuum Vessel presents a significant technological challenge.

The pressurized, water-cooled TF coil operates at temperatures below 150°C but is subjected to biaxial stresses in excess of 100 ksi. In addition electrical conductivity above 50% IACS is required for acceptable power consumption. A high-purity variant of a commercial CuBeNi alloy meeting these requirements has been developed and tested. Yield strength as high as 158 ksi at 55% IACS has been achieved at INESCO through special TMT processing. Considerable unirradiated mechanical property data has been developed at INESCO along with specialized fabrication methods such as solid-state bonding and E-B welding. The highly defected microstructure of this precipitation-hardened alloy and the relatively low operating temperature is favorable from a radiation damage standpoint, but data is required, particularly at the high lifetime damage levels (110 dpa) of commercial machines. Conductivity change from Ni,Zr transmutations is a concern.

The OH coil conductor is subjected to biaxial stresses of ~60 ksi, peak temperatures of 100°C, and even in commercial machines, modest lifetime radiation damage levels of 5 dpa. The more conductive, medium-strength alloys in the CuCrZr family have been selected, fabricated in the forms required and tested. The less severe thermal/structural and radiation environments of the outer PF coils and electrical leads enable the use of high-conductivity CuZr and OFHC Cu alloys respectively.

First Wall materials requirements are complex. The selection of structural material is based on a trade-off between electromagnetic loads and maximum allowable heat flux. Maximum heat fluxes in the "scrape-off" region or on limiters will be about 12 MW/m^2 resulting in maximum temperatures up to 250°C. The superposition of electromagnetic and thermally produced stresses may be in the 80-100 ksi range. Copper/beryllium alloys are being considered along with Ni-base alloys for this application.

TOKAMAK FUSION OPTIONS

RIGGATRON ™

NO MAGNET SHIELD REQUIRED
WATER–COOLED MAGNETS
BLANKET EXTERNAL TO SYSTEM

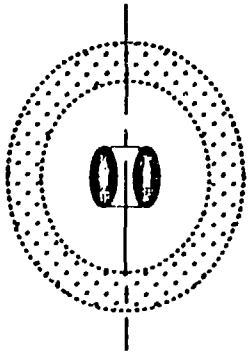

SMALL PLASMA
HIGH MAGNETIC FIELD
SMALL MACHINE SIZE

MAINLINE TOKAMAKS

RADIATION & HEAT SHIELD
SUPERCONDUCTING MAGNETS
BLANKET INTERNAL TO MAGNETS

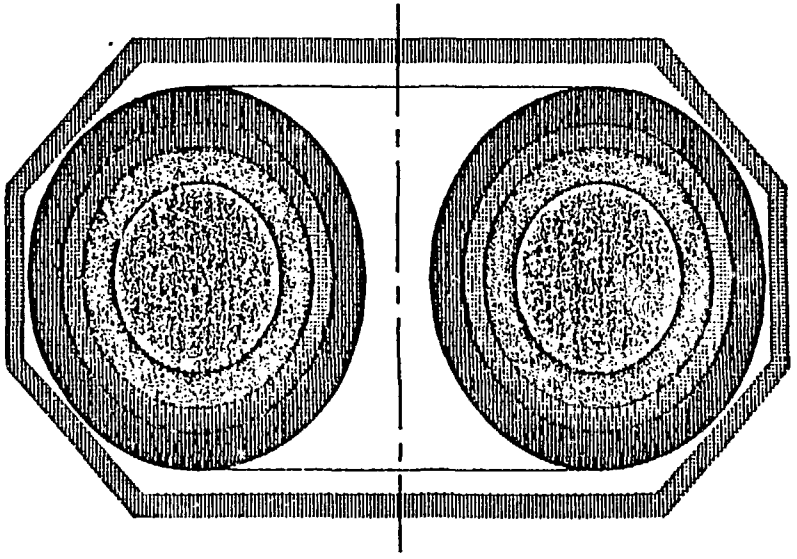

LARGE PLASMA
LOW MAGNETIC FIELD
LARGE MACHINE SIZE

INESCO, Inc.

RIGGATRON™
FUSION POWER CORE

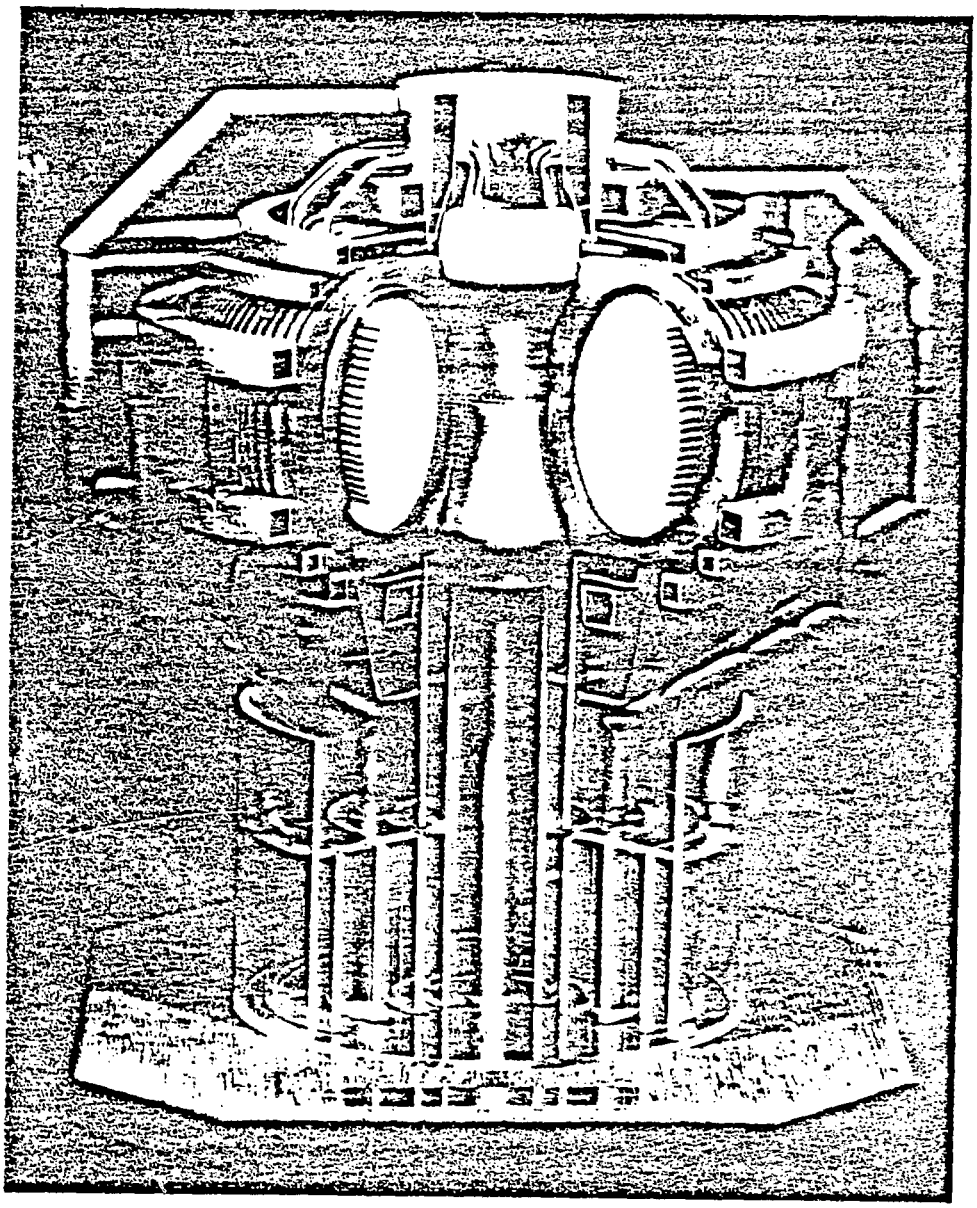

FDX-1 CONCEPTUAL ARRANGEMENT

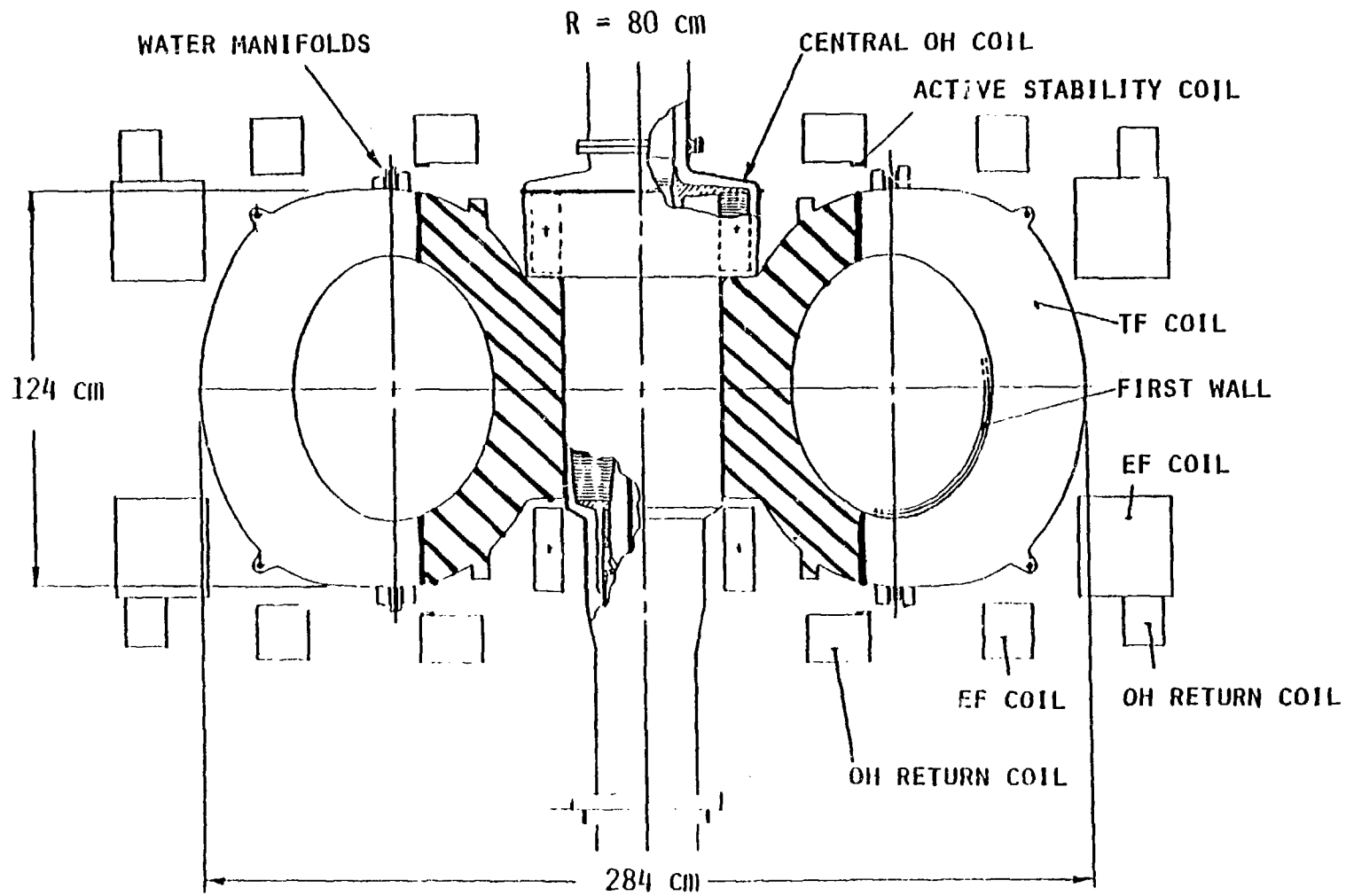

INESCO, Inc.

Typical Service Environments of Copper Alloy Components in RIGGATRON™ Tokamaks

Component	Maximum Average Stress (ksi)	Maximum Average Temperature (°C)	Maximum Neutron Damage (dpa) FDX	Commercial	Primary Alloy
TF Coil	100–130	130–150	1.0×10^{-3}	110	Cu–0.4Be–2Ni
Central OH Coil	55– 65	100	4.5×10^{-5}	5	CuCrZr (MZC)
Outer PF Coil	40– 60	100	2.0×10^{-4}	22	CuZr
First Wall	80–100	250	1.0×10^{-3}	110	Cu–0.4Be–2Ni
Bus Bars	~20	80	2.0×10^{-4}	22	OFHC Cu

INESCO, Inc.

STRESS DISTRIBUTION AT 16 TESLA IN A TYPICAL TF COIL

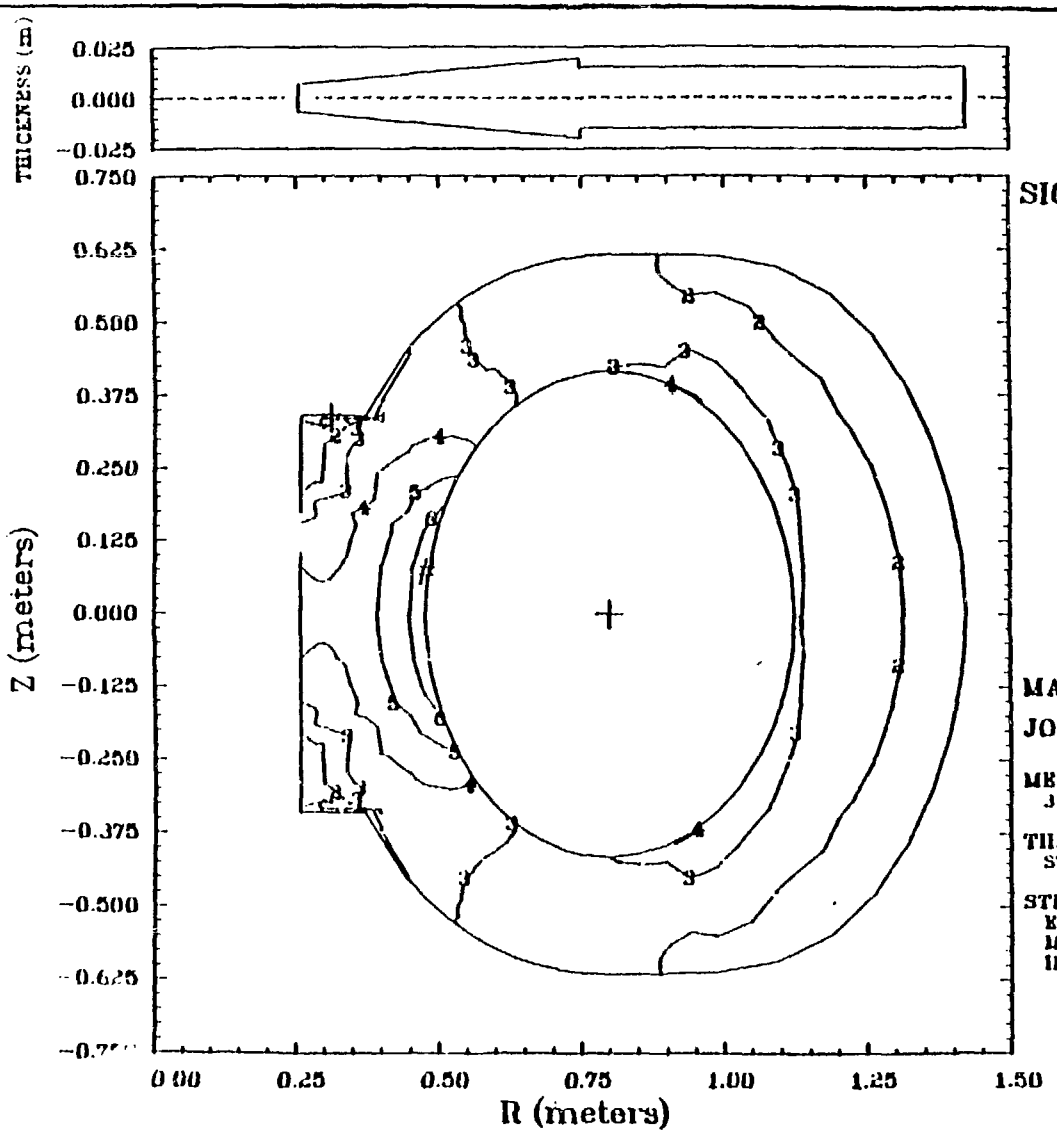

SIGMA MAX

(ksi)

+−9.40
1 0.00
2 20.00
3 40.00
4 60.00
5 80.00
6 100.00
112.11

MAGNETIC FIELD = 16.0 Tesla

JOULE HEATING = 618.2 MW

MESH:
30 x 8

THERMAL SOLUTION:
STEADY STATE

STRUCTURAL SOLUTION:
ELASTIC
MAGNETIC LOADING ONLY
INCLUDING COOLING CHANNELS

LOAD CARRYING CAPABILITY OF TF COIL DESIGN

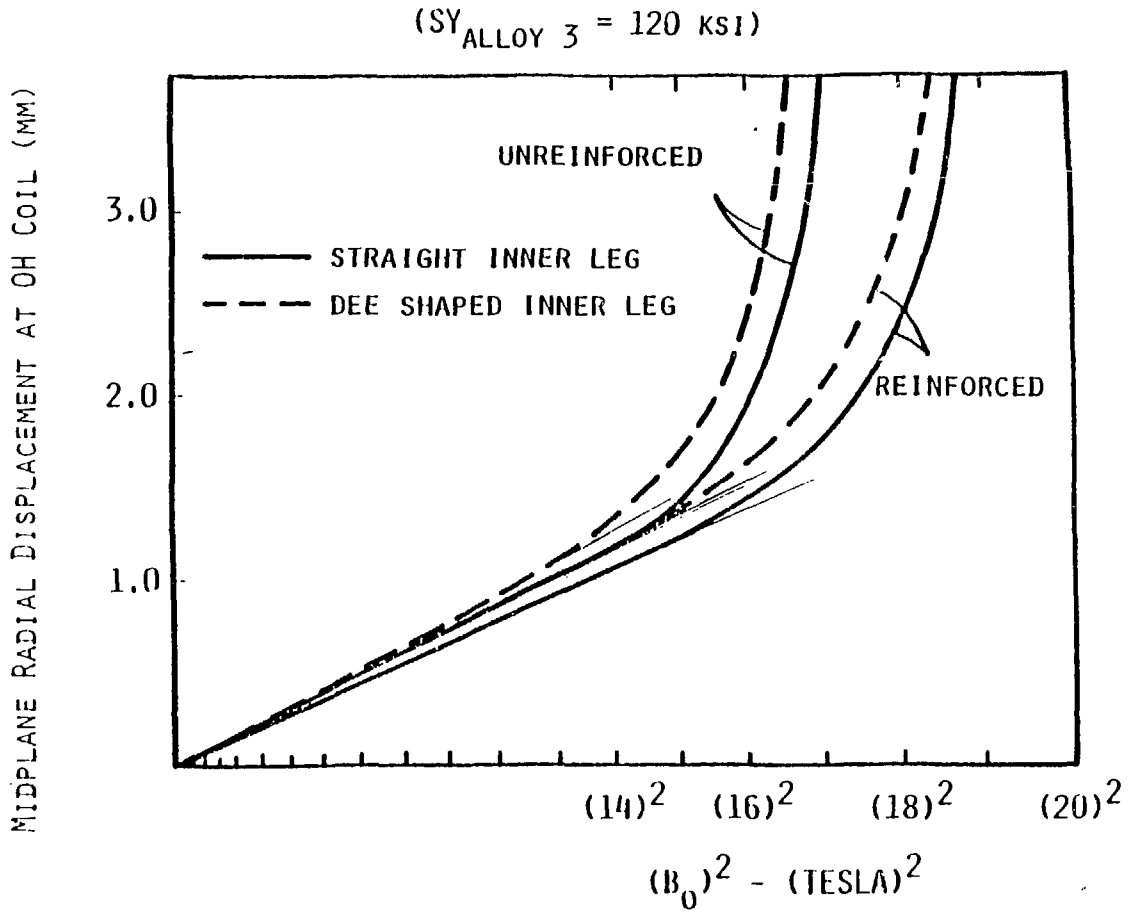

INESCO, Inc.

Mechanical and Electrical Properties of Possible Magnet Conductor Alloys

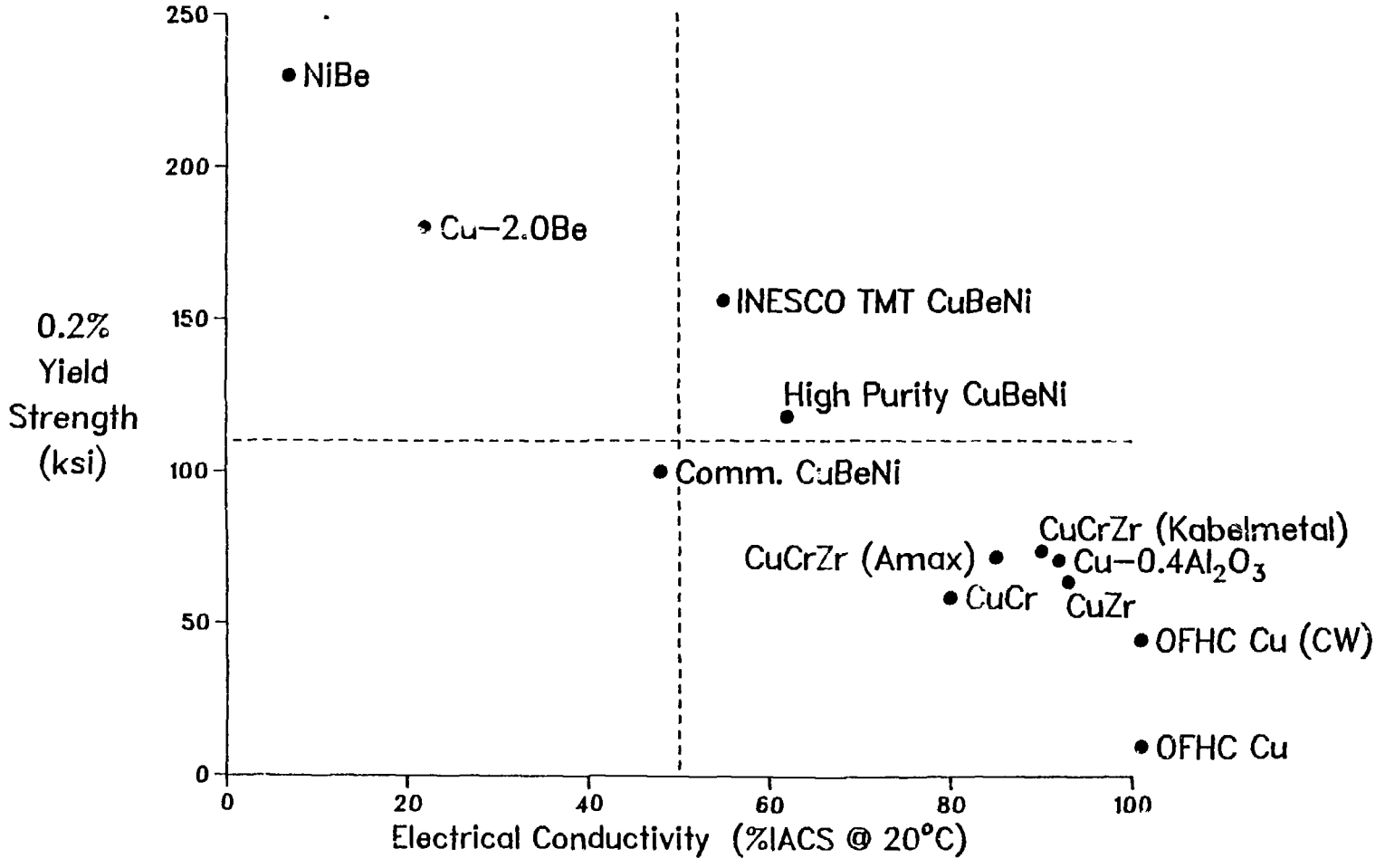

INESCO, Inc.

Electrical Conductivity vs Temperature

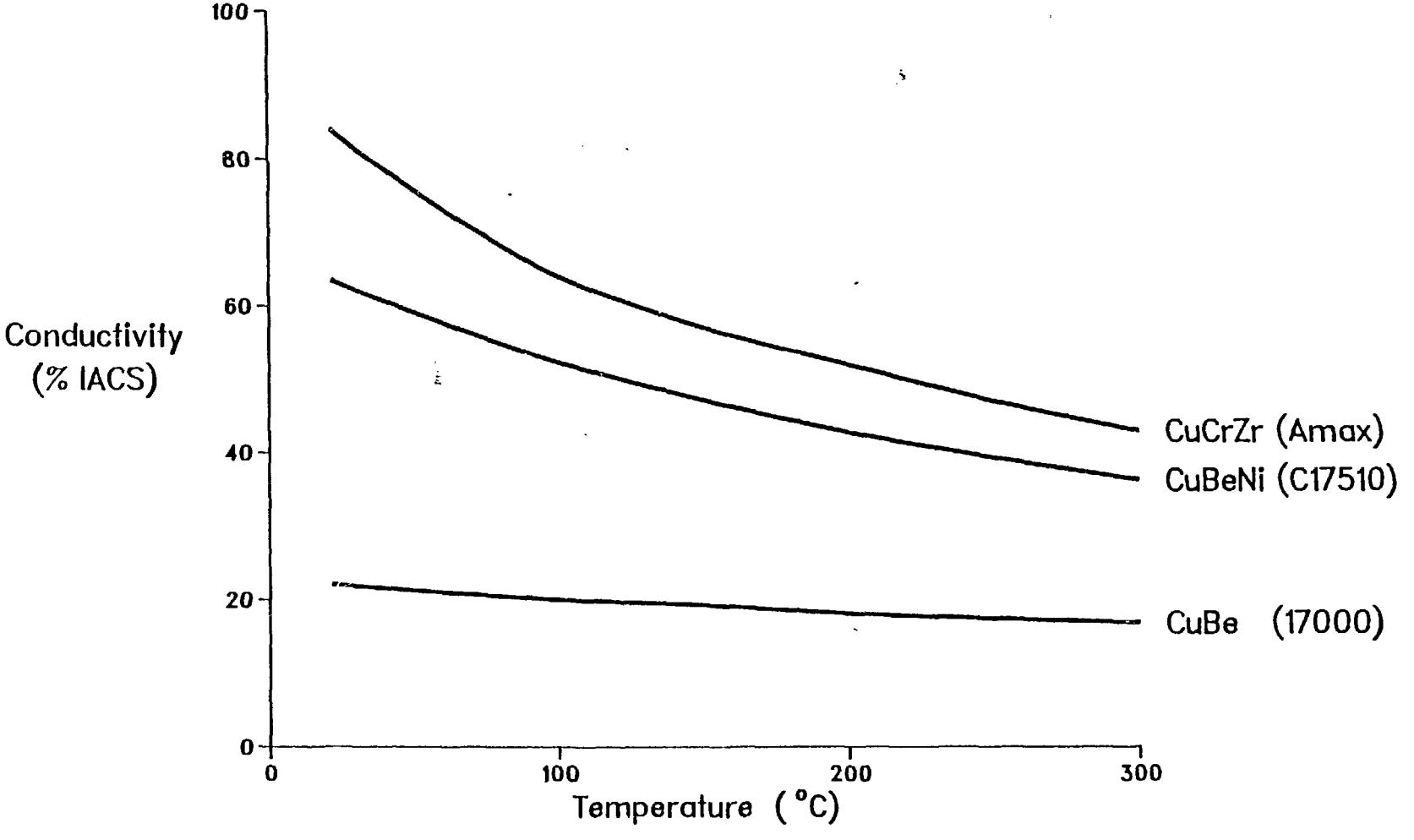

INESCO, Inc.

INESCO/INDUSTRY DEVELOPMENT OF Cu-0.4 Be-2Ni TF COIL CONDUCTOR ALLOY

	0.2% YIELD STRENGTH	% IACS	DATE
COMMERCIAL PRODUCT SPECIFICATION	100	48	2/15/81
CONTROLLED HEAT - 1750°F ST	119	61	8/1/81
IMPROVED AGING HEAT TREATMENT	124	58	10/30/81
IMPROVED THERMAL MECHANICAL TREATMENT #1	134	56	12/15/81
IMPROVED THERMAL MECHANICAL TREATMENT #2	150	52	1/15/82
IMPROVED THERMAL MECHANICAL TREATMENT #3	158	50	7/1/82
IMPROVED THERMAL MECHANICAL TREATMENT #4	~ 158	55	8/30/82

INESCO, Inc.

Tensile Properties of Conductor Alloy (Cu–0.4Be–2Ni) with INESCO Thermal Mechanical Treatment

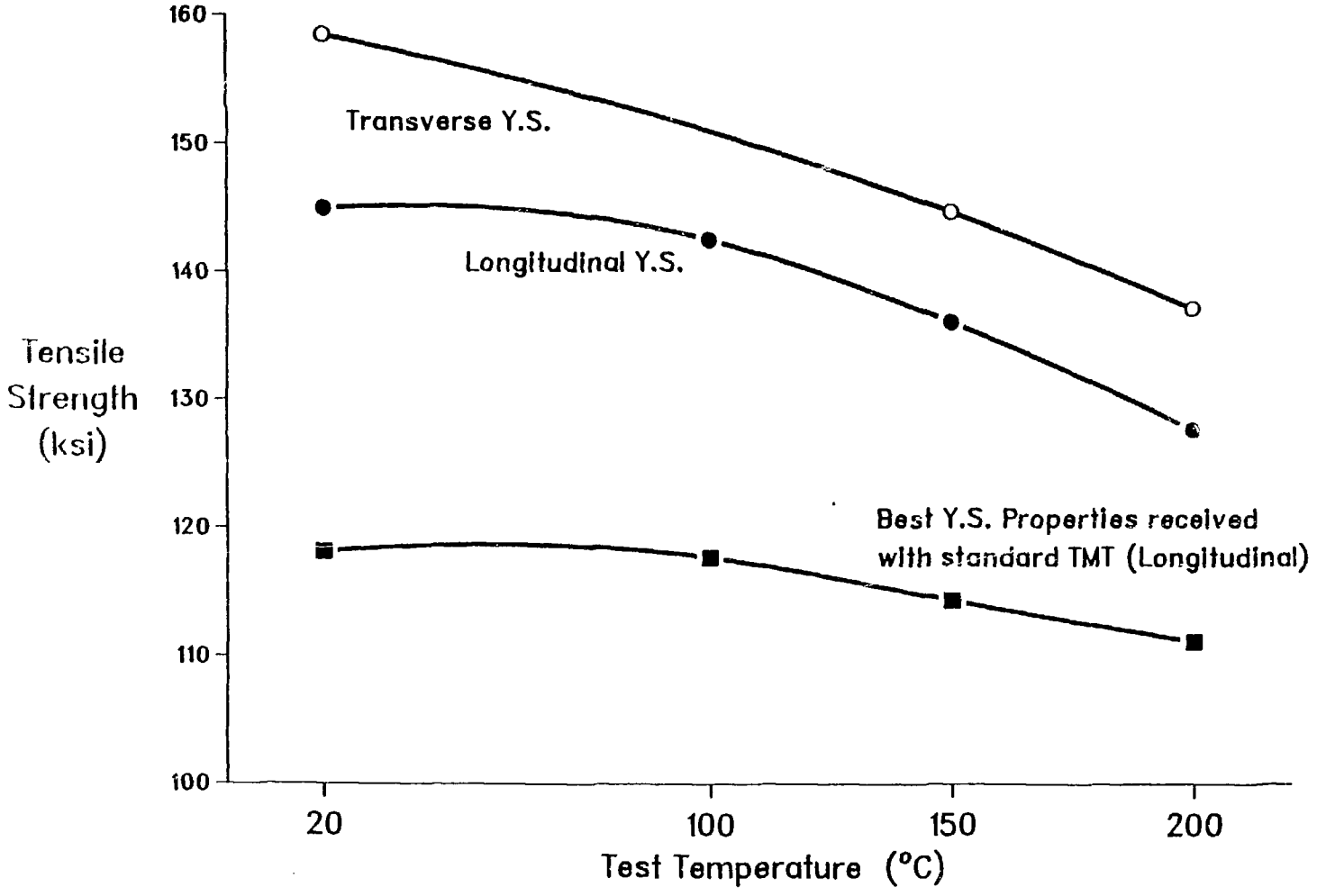

INESCO, Inc.

Stress vs Cycles to Failure for
Representative CuBeNi (Alloy C17510) Heat

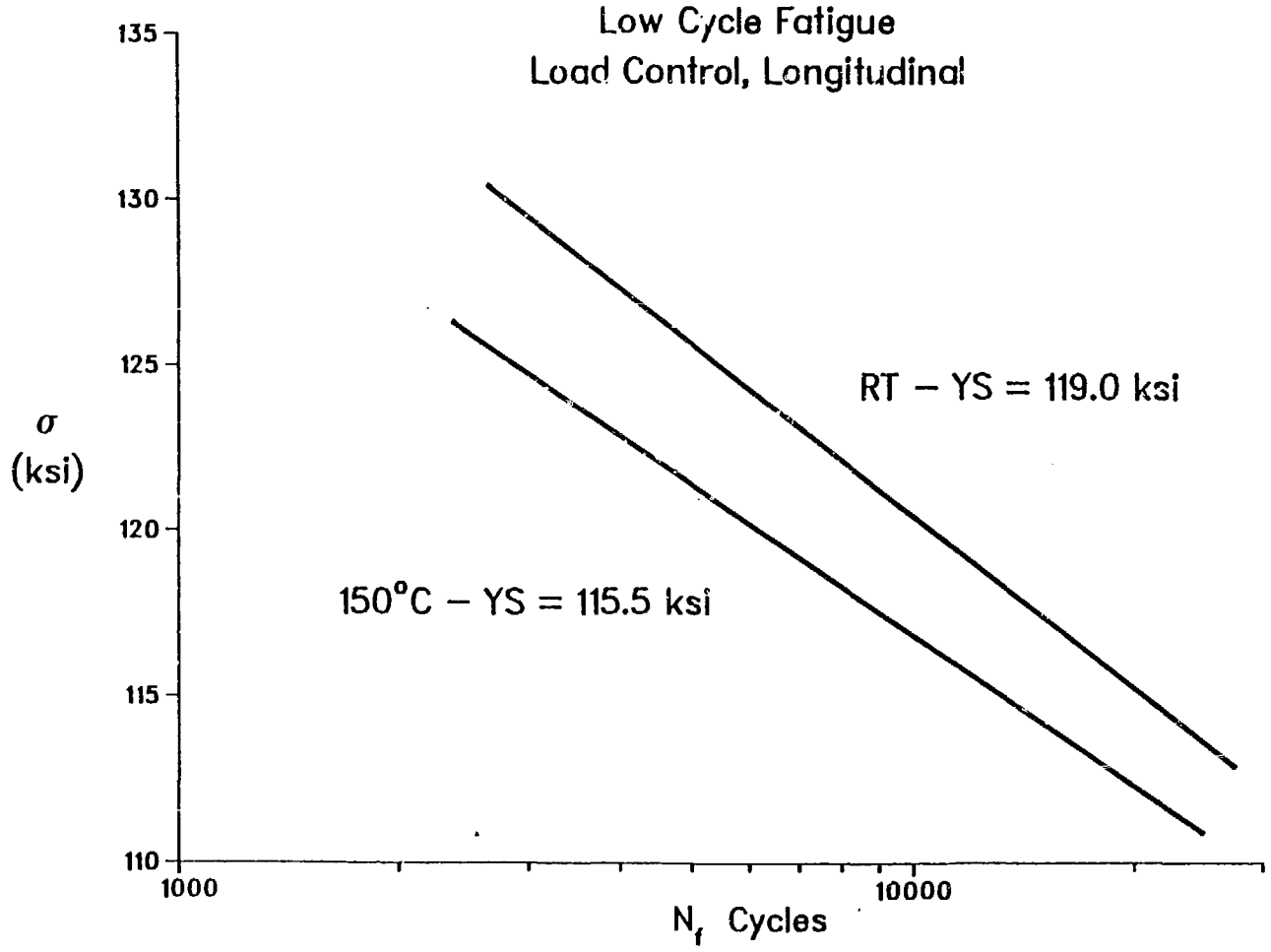

INESCO, Inc.

Radiation Damage
RIGGATRON™ Cu–0.4Be–2.0Ni Components

	Experimental Machines (FDX)	Commercial Machines
Maximum Neutron Fluence	1.3×10^{-4} (MW–y/m^2)	10 (MW–y/m^2)
Maximum Displacements	1.0×10^{-3} (dpa)	110 (dpa)
Helium Transmutation	4.0×10^{-3} (appm)	310 (appm)
Hydrogen Transmutation	1.2×10^{-2} (appm)	930 (appm)
Ni + Zn Transmutation	1.6×10^{-1} (appm)	1.2 %
Maximum Temperature	250°C First Wall 150°C Other Components	250°C First Wall 150°C Other Components
Expected Damage	Negligible	Mechanical Property and Swelling Unknown Favorable Microstructures Electrical Conductivity Decreases Due to Transmutations

CuBeNi Alloy

Electron Beam Welding:

2.0cm (0.8") Plate, welded in HT condition, then aged, transverse

Test Temperature (°C)	0.2% Yield Strength (ksi)	UTS (ksi)
RT	106.4	116.5
100	103.5	113.5
150	101.6	111.5
200	98.9	104.7

Solid State (Diffusion) Welding:

Test Temperature (°C)	Tensile Strength (ksi)	Shear Strength (ksi)
RT	65.1	26.5
150	55.2	18.9
250	43.0	

INESCO, Inc.

CENTRAL OH COIL COOLANT FLOW

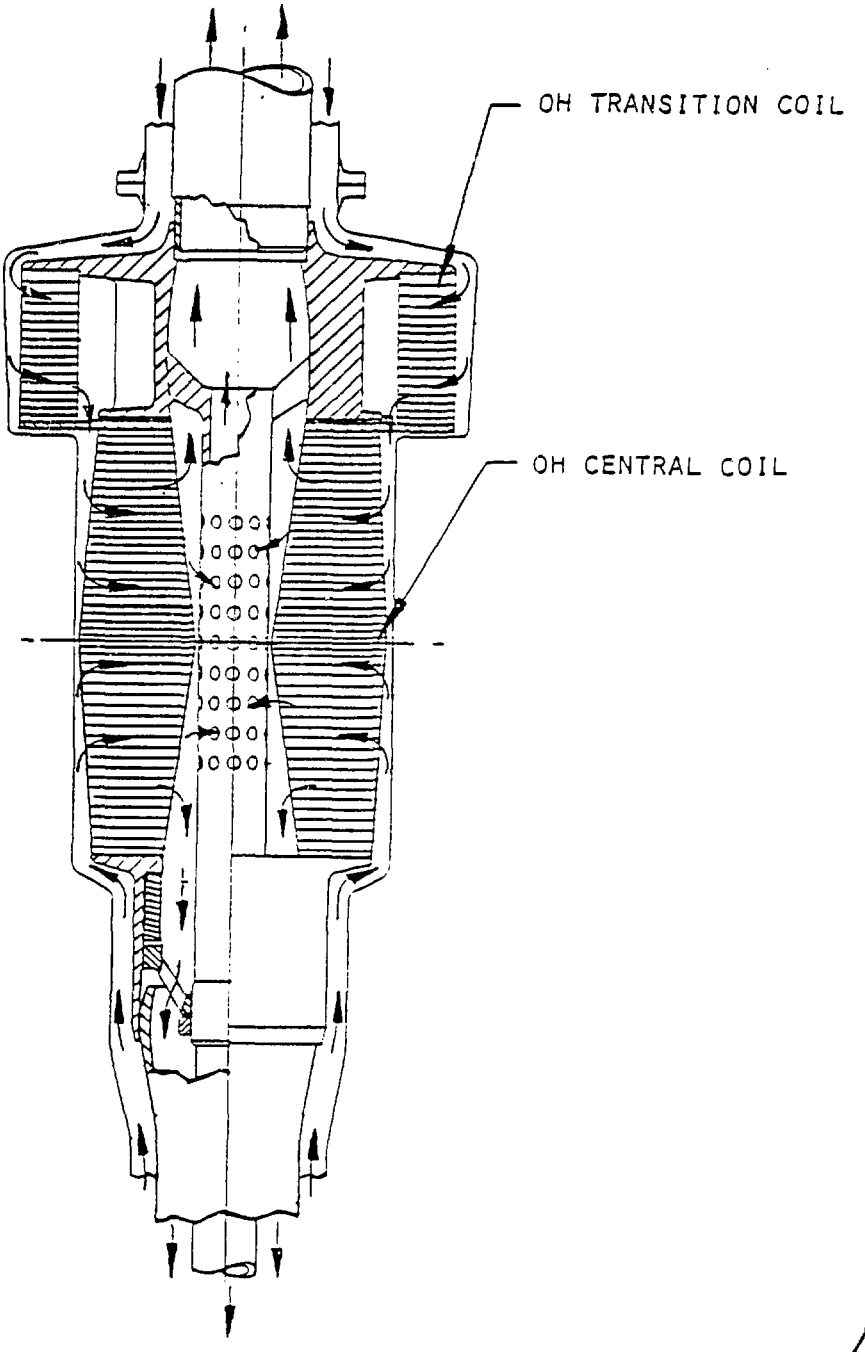

INESCO, Inc.

Yield Strength vs Temperature For Candidate OH Coil Alloys

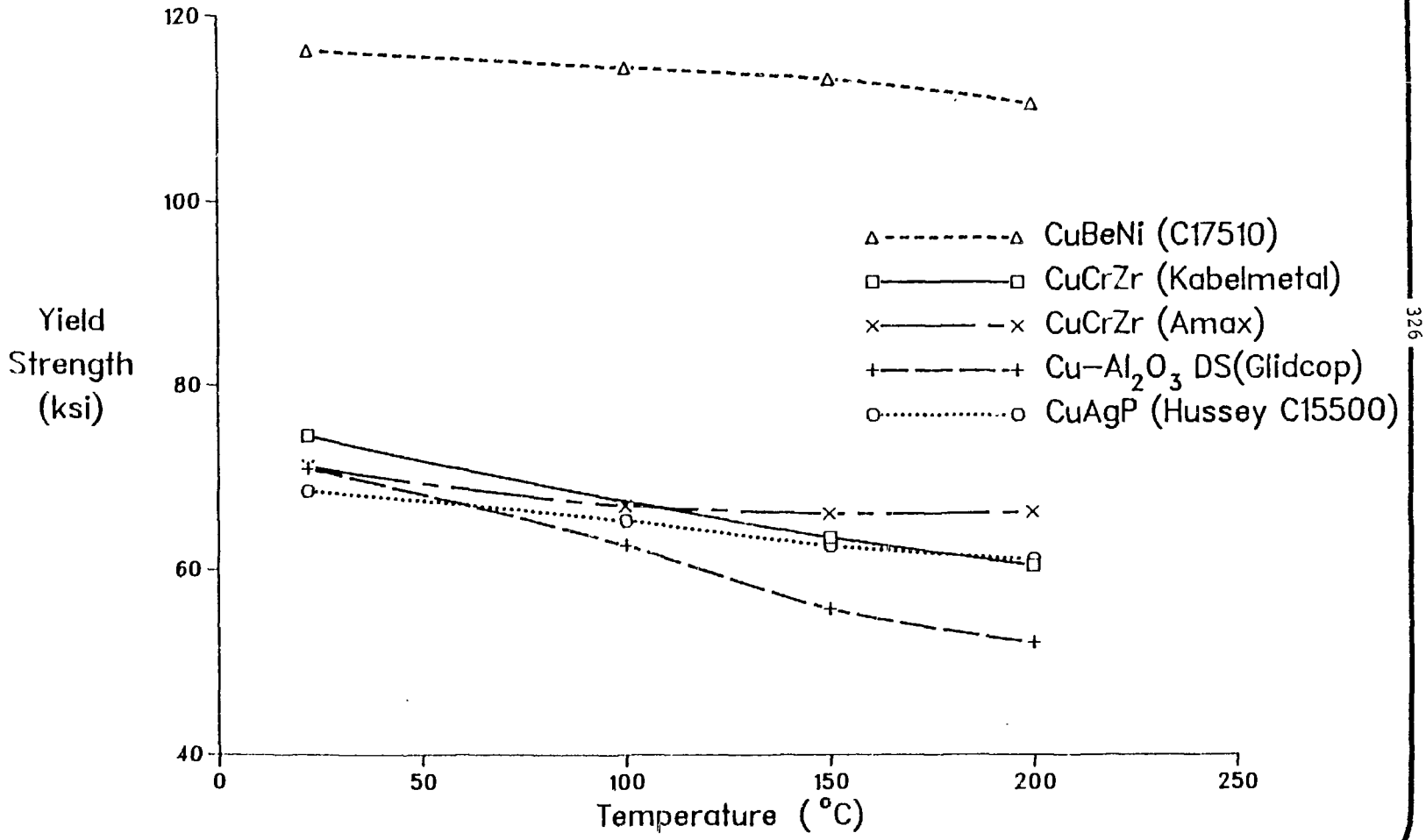

INESCO, Inc.

First Wall Stress Profile
(Restrained)

Plasma

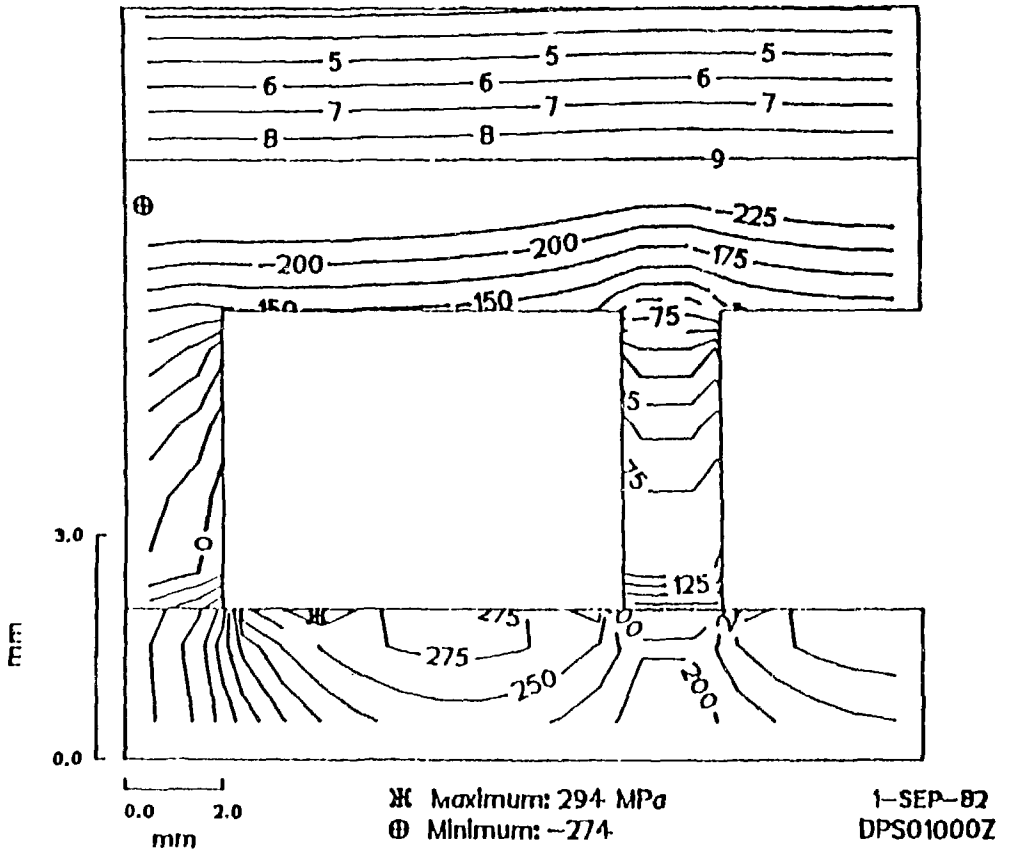

Out of Plane Stress

Compressive
Tensile

Surface Heat Flux: 12.1 MW/m²
Neutronic Heating: 300 MW/m³
Coolant Temperature: 72°C
Coolant Flow: 1.21 kg/s (13 m/s)
Coolant Pressure: 365 psig (2.5 MPa)

INESCO, Inc.

Thermal/Structural Comparison of Candidate First Wall Alloys

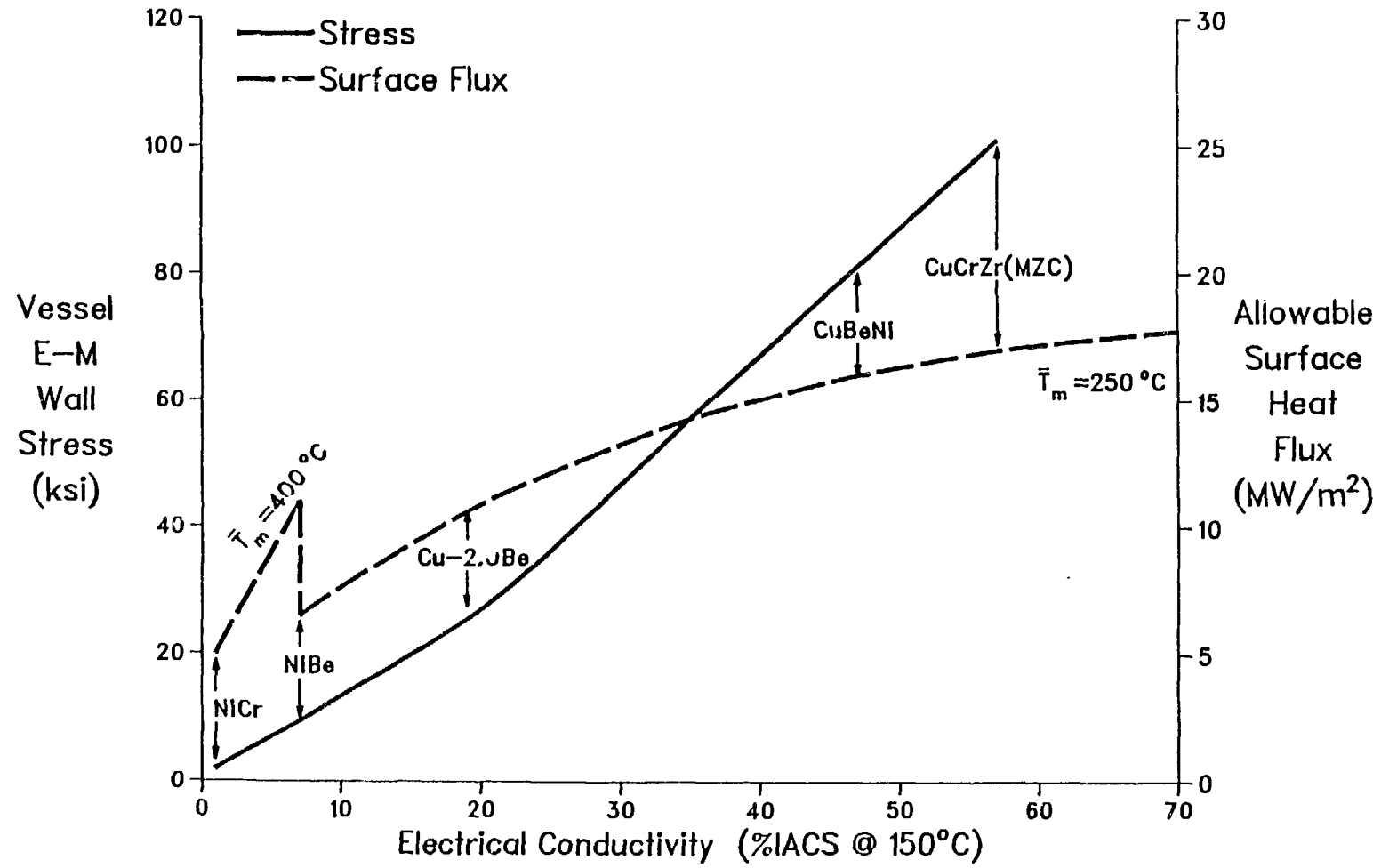

INESCO, Inc.

RIGGATRON™ Cu Alloy Development and Data Needs

- Irradiated Data Base
  - CuBeNi, CuBe, CuMgZrCr, CuCrZr, Cu–Al_2O_3, Cu
  - 20° – 300°C
  - ≤ 100 dpa (with transmutations)
  - Tensile Properties, Fatigue, Creep (some biaxial)
  - Swelling/Microstructure
  - Electrical/Thermal Conductivity

- Alloy and Product Form Development
  - Development of MZC, Cu–Al_2O_3 Flat and Extruded Product
  - Development of Alloys Based on CuMgZrCr, Cu–Al_2O_3 and Other Systems Capable of:
    - 90 – 100 ksi Y.S., 85 %IACS (20°C)
    - > 200 ksi Y.S., > 60 %IACS
    - Thermal/Irradiation Stability 300–400°C

A REVIEW OF MZC, Cu-Ni-Ti AND OD-Cu ALLOYS IN TERMS OF TENSILE PROPERTIES, ALLOY STABILITY AND HIGH-TEMPERATURE STRESS-RUPTURE BEHAVIOR

N. J. Grant

Massachusetts Institute of Technology

A Review of MZC, Cu-Ni-Ti and OD-Cu Alloys in Terms of Tensile Properties, Alloy Stability and High-Temperature Stress-Rupture Behavior

Nicholas J. Grant
Department of Materials Science and Engineering
Massachusetts Institute of Technology
Cambridge, Massachusetts

The MZC and Cu-Ni-Ti Alloys

Table I lists a number of MZC alloys, condition of the alloy, and tensile properties at room temperature. Conductivities generally are of the order of 80%-90% IACS, depending on total alloy content and specific thermomechanical treatments. For comparison purposes the properties of RS-PM Cu-Zr-Cr-Al, converted to fine flake by attrition grinding to introduce up to 1% Al_2O_3 and internally oxidized Cu-Al_2O_3 are shown in the as-extruded conditions. With higher Cr + Zr, still higher strength values are possible. Ductility values in all instances are excellent for these strength values.

Table II lists tensile properties of a relatively new alloy, the Cu - 5% Ni - 2 1/2% Ti alloy, at room temperature. Ingot material, RS-PM material, and RS-PM product attrition ground to fine flakes to produce up to about 1% TiO_2 are shown for a number of thermomechanical heat treatments. The best strength values are those for a number of thermomechanical heat treatments. The best are those for the RS-PM-Flake material after solution heat treating and aging at 575°C. Again ductility values are excellent, and these alloys (also true for the MZC alloys) can be extensively cold worked to further increase the strength values with small losses of conductivity.

The Cu-Ni-Ti alloy is based on the spinoidal alloy Cu - 2 to 5% Ti binary system which hardens on quenching from the solution heat treating temperature (see below). The binary alloy will

develop yield and ultimate strengths of about 200,000 psi, with only fair ductility and about 10% conductivity. The ternary system was developed to sharply decrease the amount of Ti left in solid solution by adding Ni. The ternary alloy (Table II) is significantly less strong than the binary alloy but has been shown to develop conductivity values near 50% IACS.

Figure 1 shows classical overaging of this fully heat treated (FHT) ingot MZC alloy (FHT involves solution, 65% cold work, and aging at 475°C). When the same alloy is produced as RS powder, and a -54μm size fraction is used, a small amount of ZrO_2 (and probably Cr_2O_3) forms on the surface (perhaps 0.1 to 0.2 wt. pct). Note the higher overaging temperature for the P/M hot extruded powder and its retention of hardness to high temperatures. If the RS powders are attrition milled to fine flake of thickness from 0.5 to about 1.5μm, the large increase in surface area introduces about 1 wt. pct. of refractory oxides producing an ODS MZC type alloy. This alloy can be heated up to 950°C without loss of hardness. See Table I for the attractive tensile properties in the as-extruded condition (no heat treatments used).

This alloy condition would permit the use of brazing temperatures and/or diffusion bonding temperatures up to 950°C without loss of properties.

In a similar way Fig. 2 shows comparable processing effects for the Cu - 5 Ni - 2 1/2 Ti alloy; however, this alloy has an additional attractive feature which doesn't exist for the MZC alloy. If one looks at the ingot curve, note that overaging begins between 400 and 450°C, but that on reaching an annealing temperature of about 800°C and higher, the alloy rehardens on quenching from the solution temperature. More hardening takes place for the air quenched condition (open squares) than on water quenching (solid squares). This behavior becomes very important when discussing the hot extruded flake-based alloy. In RS powder

form, softening due to overaging is delayed and higher levels of hardness are retained to about 900°C than for the ingot alloy. This is due to a small amount of TiO_2 which forms on the fine powders and produces an ODS effect. When the RS powders are attrition ground to fine flake (0.5 to about 1.5μm), about 1% TiO_2 forms and retains the deformational energy of extrusion. Note the extremely flat hardness curve out to 1000°C for one hour, at a hardness level higher than that for the fully heat treated ingot product.

Table III lists the tensile data for the three alloy conditions shown in Fig. 2.

The large degree of cold work necessary to optimize the tensile properties of the ingot alloy is not required either for the RS-PM or the flaked products. Even without such cold work the strength and ductility values are superior to those for the fully heat treated ingot product.

As with the flaked MZC alloy, brazing and/or diffusion bonding at temperatures as high as 1000°C do not diminish the strength of the Cu-Ni-Ti alloy, which requires only an aging treatment at 575°C to maintain its excellent strength. The cold working step is not required.

Copper-Al_2O_3 Alloys (ODS Copper)

Fine powders of Cu-Al alloys containing up to about 0.77% Al in solution can be internally oxidized, or first attrition ground to fine flake and internally oxidized to produce Cu-Al_2O_3 ODS alloys by hot extrusion of the powders or flakes. Figure 3 shows the remarkable stability of these alloys in terms of the room-temperature hardness after annealing for one hour at temperatures up to the melting point of copper (1083°C). As little as 0.4 vol. pct. of Al_2O_3, of proper particle size and dispersion, will prevent recrystallization of the very fine grained, highly

cold worked structure up to 1050°C. The 3.5 vol. pct. Al_2O_3 alloy resists recrystallization up to 1075°C (8°C below its melting point). Fine SiO_2 particles, also produced by internal oxidation (of Si in solution in Cu) are effective structural stabilizers, but clearly are not as effective as the more refractory, more stable Al_2O_3.

Figure 4 shows the stress-rupture behavior of the Cu-3.5% Al_2O_3 alloy, which has a 100-hour rupture life of 38,000 psi at 450°C. The extremely flat curves at 450°C and 650°C indicate that these slopes can be maintained out to 100,000 hours at 450°C. Even at 850°C this Cu-Al_2O_3 alloy is unusually strong since it will sustain a stress twice that of standard 18-8 stainless steel for a 100-hour life.

The 400°C Stress-Rupture Behavior of MZC and Cu-Ni-Ti Alloys

Figure 5 summarizes the stress-rupture behavior of a number of the MZC types of alloys at 400°C. The fully heat treated MZC alloy (with 0.13% Zr), ingot product, shows the highest short time strength values, but the slope is steep due to overaging in the long time tests. The RS-PM extruded alloys, variously processed, show lower strength values but with the typical flat slopes of ODS alloys. The flaked MZC alloy, with a small aluminum addition, has the most flat, stable slope and shows the best strength beyond about 2 or 3 thousand hours life.

Figure 6 shows a similar plot for the Cu-Ni-Ti alloys, also at 400°C. The ingot product properties are the poorest, and those of the RS-PM product, variously processed and heat treated, are only a little better. On the other hand, the RS-PM flaked and hot extruded alloy, in the as-extruded condition, has stress-rupture properties only a little lower than those shown by Cu - 3.5% Al_2O_3 (see Fig. 4). The extremely flat slope is a measure of the alloy stability at 400°C in long time tests.

Conductivity of Cu-Ni-Ti

Figure 6 shows the large changes in conductivity of the ingot-based Cu - 5% Ni - 2 1/2% Ti alloy in terms of the ratio of Ni:Ti. Cu and Ni form a complete range of solid solutions and thus show poor conductivity values with increasing Ni content. Titanium retains significant solid solubility to room temperature in Cu and therefore also results in poor conductivity. But in the combination of Ni + Ti, each element decreases the solid solubility of the other by forming precipitates of Ni_3Ti and $(Cu,Ni)_3Ti$. For maximum conductivity, processing and heat treatments must minimize the amounts of each element in solution. Figure 6 shows, for the fully heat treated condition, that maximum conductivity is achieved near the 2 to 1 ratio of Ni to Ti. Two alloys, one on each side of the 2:1 ratio, are being checked to see if the best values deviate from the 2:1 ratio. Values of conductivity for a number of other alloys are shown in Fig. 6. These values too can be shifted significantly for each alloy by other thermomechanical and heat treatments.

Table I. Properties of Representative MZC-TYPE Copper Alloys

MATERIAL	CONDITION	Y.S. KSI (MPA)	U.T.S. KSI (MPA)	EL %	RA %
.13 ZR MZC I/M	FHT	72 (496)	72 (496)	18	68
.23 ZR MZC P/M	AE	48 (330)	58 (399)	22	63
"	950°C WQ, 475°C AGED	40 (275)	54 (372)	17	64
"	950°C WQ, 54% CW, 475°C AGED	54 (372)	62 (427)	20	60
"	TMT	63 (434)	64 (441)	13	56
CU-ZR-CR-AL FLAKE	AE	69 (475)	75 (516)	9	31
CU-AL_2O_3	AE	65 (447)	76 (523)	13	31

Table II. Properties of a Cu - 5% Ni - 2 1/2% Ti Alloy Variously Processed

MATERIAL		CONDITION	Y.S. KSI (MPA)	U.T.S. KSI (MPA)	EL %	RA %
Cu-Ni-Ti	I/M	FHT	88 (606)	93 (640)	9	34
"	"	FHT + 950°C WQ 575°C AGED	67 (461)	93 (640)	20	49
"	"	FHT + 1000°C WQ 575°C AGED	73 (502)	97 (658)	19	46
"	P/M	AE	60 (413)	76 (523)	22	67
"	P/M	AE + 1000°C WQ 575°C AGED	88 (606)	103 (743)	18	65
"	FLAKE	AE	84 (578)	94 (647)	13	46
"	"	AE + 950°C WQ 575°C AGED	108 (743)	118 (812)	19	48
"	"	AE + 1000°C WQ 575°C AGED	97 (668)	109 (750)	14	45

Table III. Tensile Properties at 20°C for Various Processed Cu - 5 Ni - 2 1/2 Ti

Starting Material	Heat Treatment	Y.S. ksi	UTS ksi	Elong %
Ingot Bar Product	950°C Sol. + 65% CW + 575°C Age	85	93	13
RS-PM, Hot Extr.	1000°C Sol. + 575° Age	104	130	17
RS-PM, Flaked and Hot Extruded	950°C Sol. + 575° Age	108	120	19

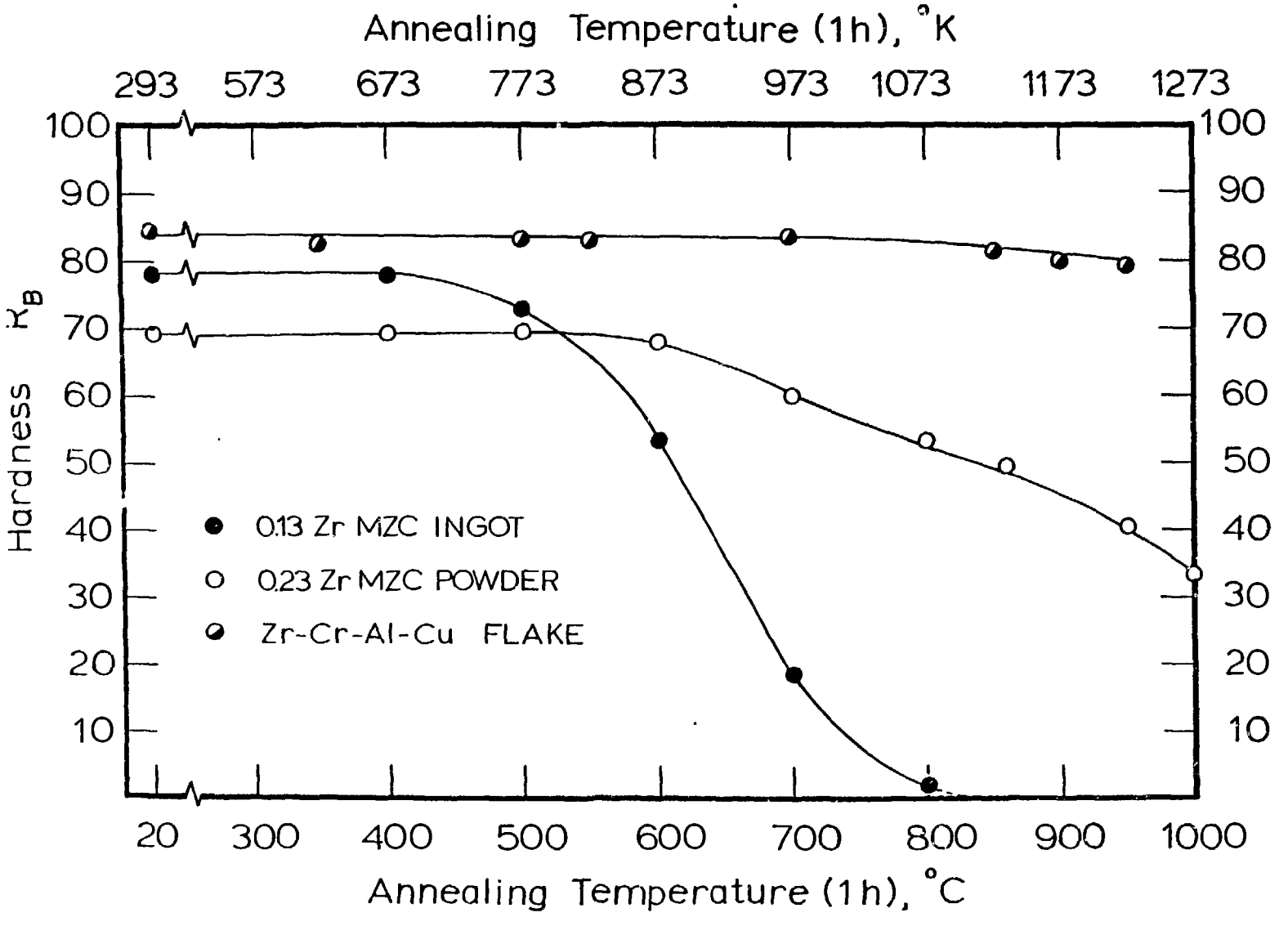

Fig. 1. Overaging and Solution Behavior of MZC Alloys in the Ingot, RS-PM, and RS-PM-Flake Conditions, Based on Room-Temperature Hardness. One Hour at Temperature.

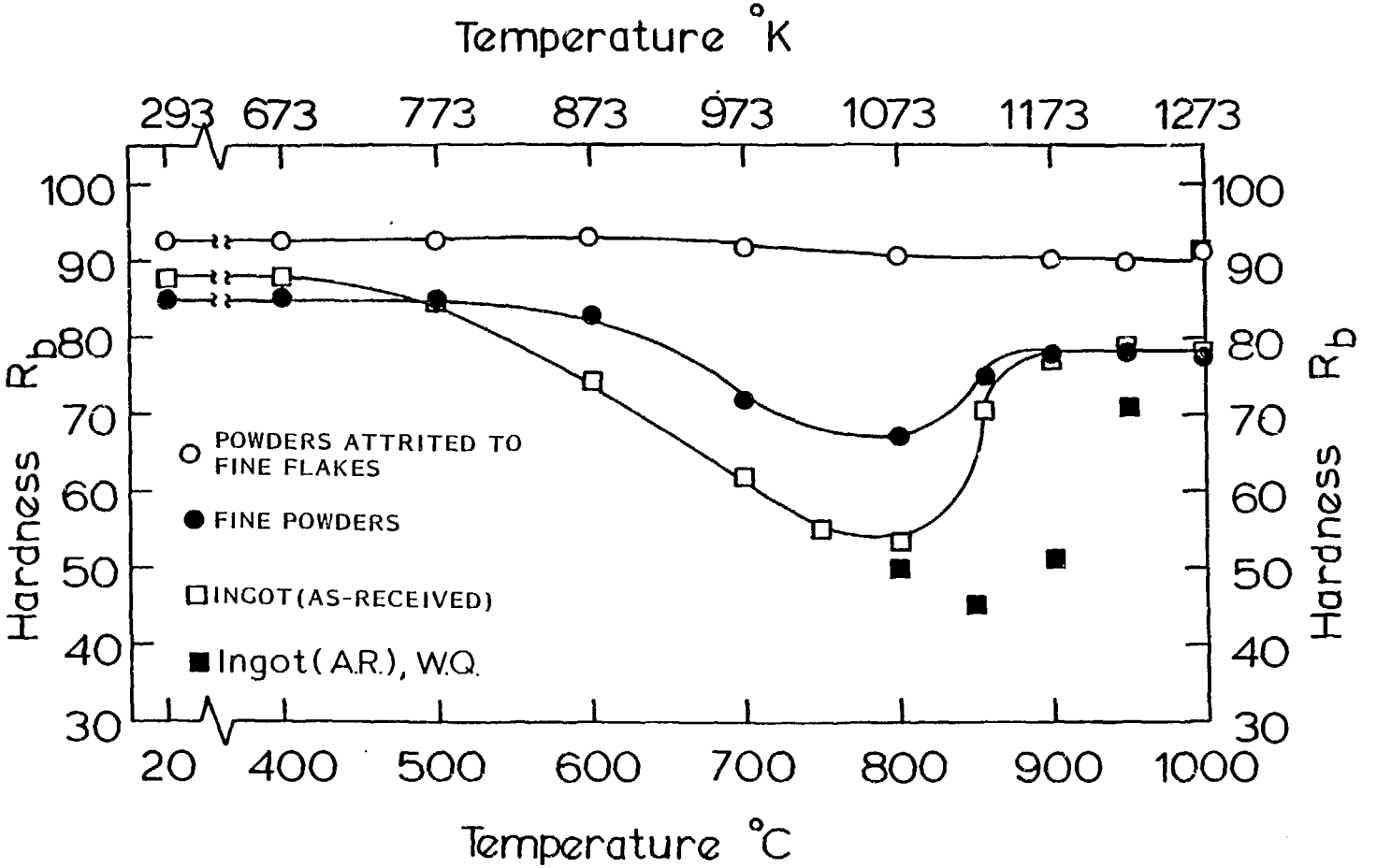

Fig. 2. Overaging and Solution Behavior of the Cu - 5 Ni - 2 1/2 Ti Alloy in the Ingot, RS-PM, and RS-PM-Flake Conditions, Based on Room-Temperature Hardness. One Hour at Temperature.

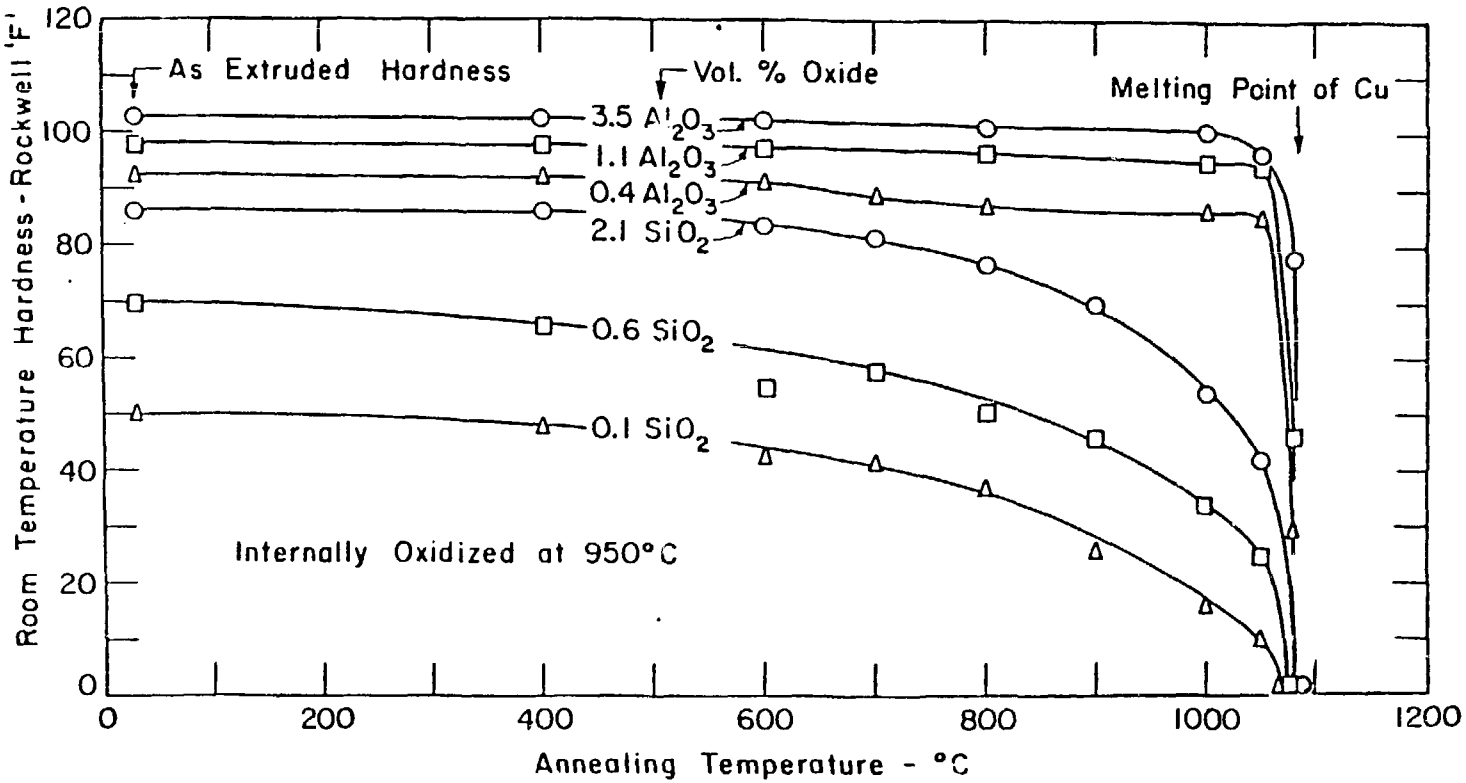

Fig. 3. Room-Temperature Hardness Versus a 1-Hour Annealing Temperature for Internally Oxidized and Hot-Extruded Cu-Al_2O_3 and Cu-SiO_2 Alloys.

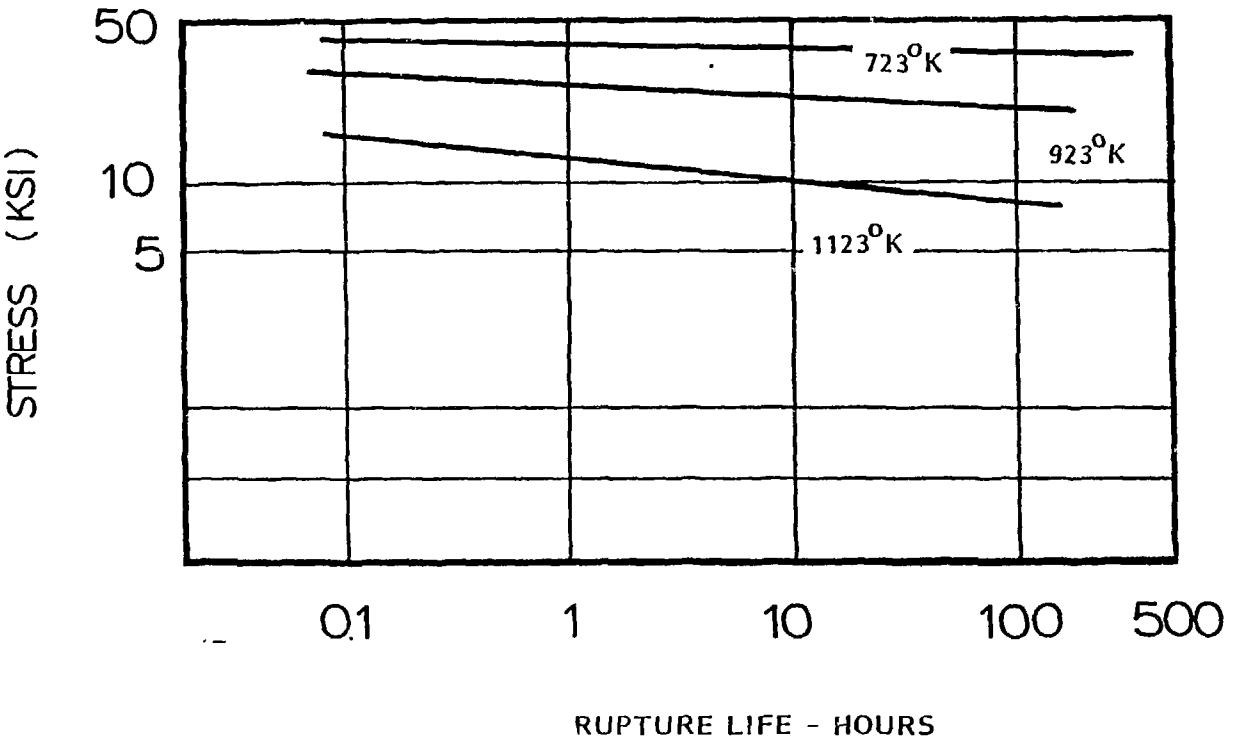

Fig. 4. Log Stress Versus Log Rupture Time for Internally Oxidized and Hot Extruded Cu - 3.5% Al_2O_3 Alloy at 450, 650, and 850°C.

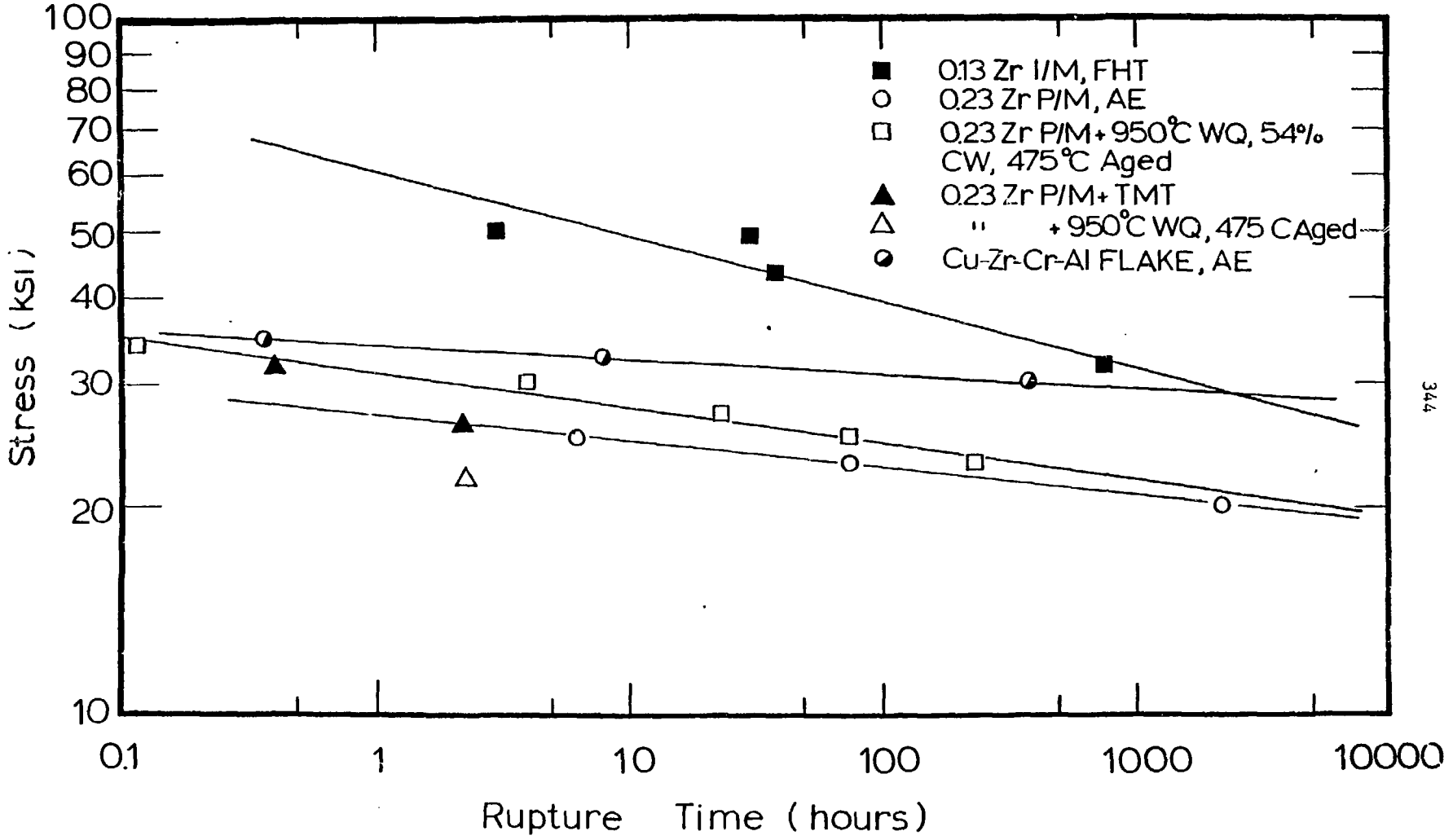

Fig. 5. Log Stress Versus Log Rupture Time at 400°C for Variously Processed MZC Alloys.

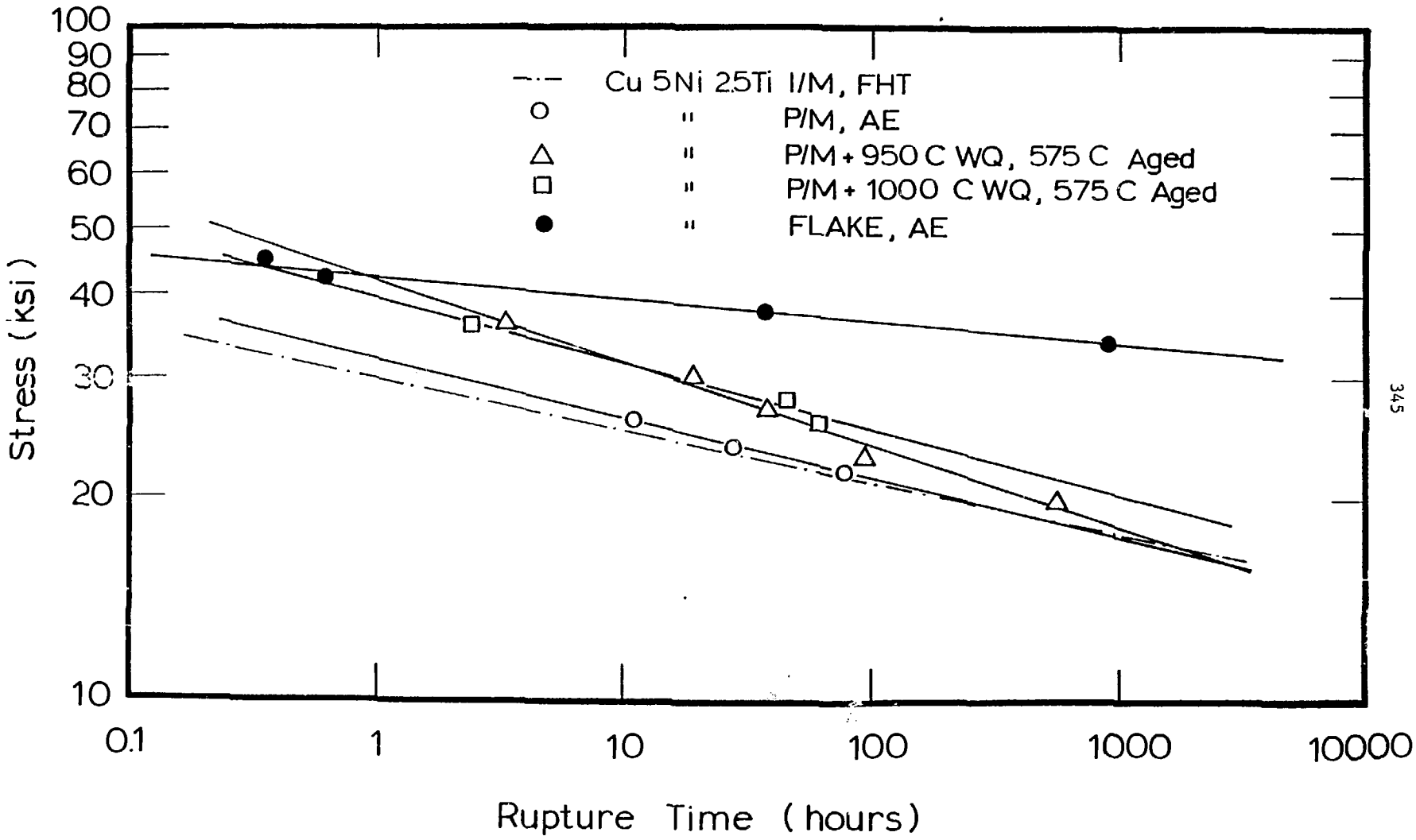

Fig. 6. Log Stress Versus Log Rupture Time at 400°C for Variously Processed Cu - 5 Ni - 2 1/2 Ti Alloy.

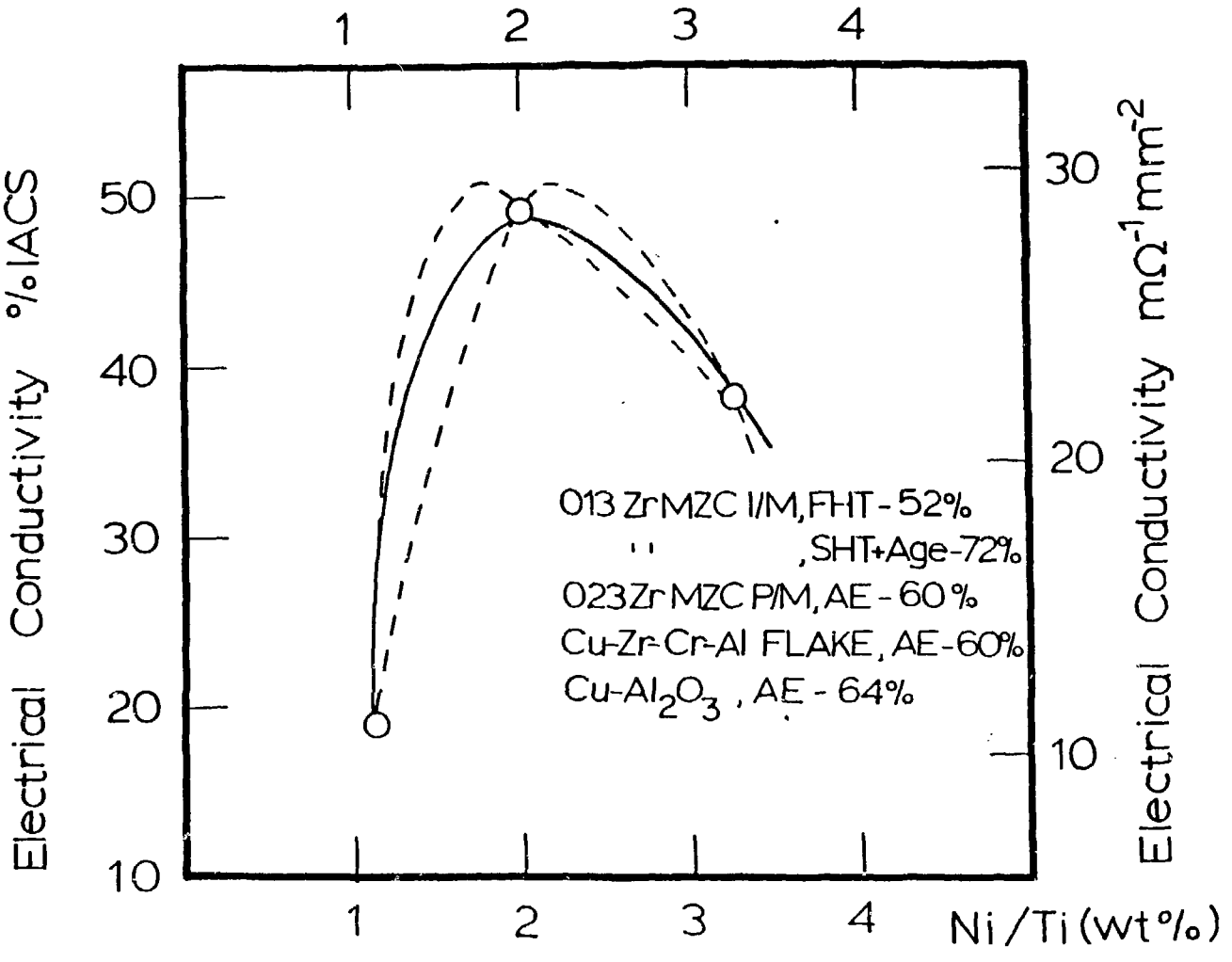

Fig. 7. Electrial Conductivity Versus the Ni:Ti Ratio (wt. pct.) for Cu-Ni-Ti Alloys.

COPPER ALLOY IRRADIATION STUDIES IN SUPPORT OF CRFPR FIRST WALL

F. W. Clinard, Jr.

Los Alamos National Laboratory

COPPER ALLOY IRRADIATION STUDIES IN SUPPORT OF CRFPR FIRST WALL*--F. W. Clinard, Jr., University of California, Los Alamos National Laboratory

The Compact Reversed-Field Pinch Reactor (CRFPR) design specifies a copper alloy first wall, with high thermal conductivity (to carry away the deposited heat) and good electrical conductivity (for wall stabilization of the plasma). Strength must be greater than that provided by unalloyed copper in order to resist combined thermal and pressure (coolant) stresses. Operating temperature will vary during the power cycle, peaking at ~400°C. Details of first-wall operating conditions are given in the paper by Hagenson in these proceedings.

The copper alloy first wall will be subjected to high neutron fluxes in this 17 MW/m^2 machine. Physical properties of concern include swelling, strength, ductility, and electrical and thermal conductivity. The data base for high-dose damage effects in copper and its alloys is poor, so that it is not possible at present to estimate degradation effects and lifetime for the first wall.

During the summer of 1982 we obtained sufficient internal funding to initiate an irradiation test of six copper-based materials (see vu-graph I), in order to begin an evaluation of damage response of these materials. The test, which is being piggybacked on another experiment in EBR-II, was originally intended to take place at ~450°C; however, revised thermal calculations indicate that somewhat lower temperatures are likely (vu-graph II). The results will thus be less appropriate to the CRFPR application than intended, but should nevertheless yield useful information on the role of temperature in damage response. Further, the data obtained will be directly applicable to other fusion applications such as limiters and beam dumps. Results from the unalloyed test materials should prove especially useful for those applications where high strength is not needed.

Irradiated samples will be tested for changes in the relevant physical properties mentioned earlier, and damage microstructure will be evaluated by TEM. We visualize that the latter studies will point the way to compositional and microstructural adjustments needed to optimize materials performance. Future plans (contingent on acquisition of funding to support this work) include the above post-irradiation evaluations of the EBR-II samples, lower-temperature irradiation tests in ORR, and irradiation studies of optimized materials.

*Work performed under the auspices of the U. S. Department of Energy.

I

MATERIALS UNDER STUDY

MZC COPPER -- Mg-Zr-Cr ALLOY, PRECIPITATION-HARDENABLE (COLD-ROLLED AND AGED)

AMZIRC COPPER -- Zr ALLOY, PRECIPITATION-HARDENABLE (COLD-ROLLED AND AGED)

AL-20 COPPER -- 0.4 WT.% Al_2O_3 PARTICLES, DISPERSION-STRENGTHENED (ANNEALED)

AL-60 COPPER -- 1.2 WT.% Al_2O_3 PARTICLES, DISPERSION-STRENGTHENED (ANNEALED)

OFHC COPPER -- HIGH PURITY, HIGH CONDUCTIVITY (ANNEALED)

99.999% COPPER -- HIGHEST PURITY, HIGH CONDUCTIVITY (COLD-ROLLED)

II

EBR-II IRRADIATION TEST CONDITIONS

	Low Dose	High Dose
Fluence, n/cm^2 >0.1 MeV	4 x 10^{21}	2 x 10^{22}
Temperature, ^{o}C	~385	~385
Schedule	Placed in reactor Sept. 1982; to be removed ~Sept. 1983.	

III

POST-IRRADIATION TESTS*

SWELLING

YIELD AND ULTIMATE TENSILE STRENGTH

ELONGATION

FRACTOGRAPHIC CHARACTERISTICS

ELECTRICAL CONDUCTIVITY

DAMAGE MICROSTRUCTURE (TEM)

---

*IRRADIATED AND CONTROL SAMPLES

IV

FUTURE PLANS*

EVALUATE SAMPLES FROM EBR-II IRRADIATION

CONDUCT IRRADIATIONS IN ORR AT LOWER TEMPERATURES

TEST MODIFIED MATERIALS SELECTED ON THE BASIS OF EARLIER STUDIES

---

*CONTINGENT ON FUNDING

THE M.I.T. NEUTRON IRRADIATION EFFECTS PROGRAM WITH COPPER ALLOYS

O. K. Harling and N. J. Grant

Massachusetts Institute of Technology

SUMMARY

Copper alloys have interesting properties for several applications in fusion. The potential application of copper alloys for first wall and other applications was reviewed in a recent paper.[1] Among those areas where existing data on copper alloys was inadequate, we identified neutron induced bulk radiation damage as a critical area. Little or no experimental information on irradiation performance is available for these materials at dose levels and temperatures relevant to the fusion application. A scoping experiment to provide the first such irradiation performance data was designed at M.I.T. and has been initiated with support of the International Copper Research Association.

In this presentation we will briefly provide some perspective and background to considerations related to the use of copper alloys for fusion. We will then outline the M.I.T. neutron irradiation effects program with copper alloys including our objectives, approach and the status of this research. Appendices include some more detail concerning the alloys placed in irradiation.

---

[1] O. K. Harling, G. P. Yu, N. J. Grant and J. E. Meyer, "Application of High Strength Copper Alloys for a Fusion Reactor First Wall," J. of Nucl. Mater. 103 & 104 (1981) 127-132.

HIGH PERFORMANCE COPPER ALLOYS FOR FUSION APPLICATIONS

O. K. HARLING, M.I.T.

1. CONTENTS OF PRESENTATION

- SOME CONSIDERATIONS RELATED TO THE USE OF COPPER ALLOYS FOR THE FUSION APPLICATION

- PROPOSED EXPERIMENTS TO SCOPE THE IRRADIATION PERFORMANCE OF COPPER ALLOYS AT SERVICE TEMPERATURES AND SIGNIFICANT NEUTRON DAMAGE

2. PROPERTIES OF HIGH STRENGTH RS COPPER-BASE ALLOYS

- COMPOSITIONS AND MECHANICAL BEHAVIOR

  This will be adequately covered in other presentations at this workshop.

- COMPATIBILITY OF Cu ALLOYS WITH CTR ENVIRONMENT

  COOLANTS

  He, H_2, ORGANICS AND H_2O -- GOOD

  LIQUID Li -- NOT COMPATIBLE

  SOLID BREEDERS

  Likely to be compatible with several Li compounds.

  MULTIPLIERS

  Be, BeO, Zr

- WELDING AND JOINING COPPER ALLOYS

  A range of appropriate techniques is available even for advanced RST alloys which have excellent high temperature performance.

- COST, RESOURCE BASE AND COMMERCIAL POTENTIAL

COSTS ARE AS LOW OR LOWER THAN SS.

AVAILABILITY IN USA IS EXCELLENT.

REDUCED USE OF STRATEGIC MATERIALS UNAVAILABLE IN USA.

COMMERCIAL PRODUCTION OF SOME OF THESE ALLOYS IS CURRENTLY DONE BY INGOT TECHNOLOGY. ADVANCED POWDER METALLURGICAL TECHNIQUES SUITED FOR HIGH PERFORMANCE ALLOYS ARE RELATIVELY NEW BUT INTERESTING ALLOYS HAVE BEEN PREPARED WITHOUT LIMITATIONS OR COMPLICATIONS.

3. STRUCTURAL DESIGN CONSIDERATIONS

- HIGH PERFORMANCE COPPER ALLOYS HAVE STRENGTHS SUPERIOR TO CONVENTIONALLY PRODUCED COPPER ALLOYS BUT LESS THAN MOST OTHER FIRST WALL CANDIDATE MATERIALS. THE THERMAL CONDUCTIVITIES ARE, ON THE OTHER HAND, MARKEDLY SUPERIOR TO THE CONDUCTIVITIES OF OTHER CANDIDATES.

- AN ESTIMATE OF THE NET WORTH OF RELATIVELY HIGH HEAT CONDUCTIVITY AND RELATIVELY LOWER STRENGTH IS MADE BY CALCULATING THE ALLOWABLE SURFACE HEAT LOADS FOR A SIMPLE GEOMETRY USING THE SIMPLEST TECHNIQUES SPECIFIED IN THE ASME CODE FOR PRESSURE VESSELS.

ALLOY	SURFACE HEAT DEPOSITION RATE (MW/m^2)
TZM	23
V ALLOY, V-25%Cr-0.8%Zr	12
Cu ALLOY, ZAC-2	11
HT-9	6.6
Nb ALLOY, D-43	3.6
Ti ALLOY, Ti-6%Al-4%V	2.5
316SS	1.4
SAP, sintered aluminum product	0.4

ASSUMPTIONS

MINIMUM WALL THICKNESS

A WALL EROSION ALLOWANCE MOVES Cu UP IN RANKING

T_h 400°C

10 yrs., DF 66%, 30 min. BURNS

4. NEUTRONICS AND RADIATION EFFECTS

- NEUTRONICS

COPPER ALLOYS ARE ROUGHLY COMPARABLE TO SS, Ti ALLOYS AND FERRITIC HT-9 FOR DAMAGE AND GAS PRODUCTION.

DAMAGE AND GAS PRODUCTION IN CANDIDATE FIRST WALL ALLOYS

MATERIAL	PER MWY/m^2		
	dpa	at ppm He	at ppm H
SAP	14	319	291
SS316	11	155	536
Ti-6Al-4V	15	115	169
HT-9	11	114	452
Copper Alloy (ZAC-1)	14	102	544
V-25Cr-0.8Zr	11	61	263
TZM	7	47	68
Nb-10W-1Zr-0.1C	6	28	95

σ(n, 2n) = 0.656 at 14 MeV for Cu compares favorably.

- SAFETY, OPERATIONAL AND RADWASTE CONSIDERATIONS

RADIOACTIVITY OF CTR BLANKETS AT SHUTDOWN

THE RADIOACTIVITY OF COPPER AT SHUTDOWN IS THE LARGEST OF THE CANDIDATE FIRST WALL MATERIALS. HOWEVER, WITHIN A FEW DAYS, THE ACTIVITY DECAYS BELOW THAT FOR 316SS; AND AFTER A YEAR, THE COPPER ACTIVITY IS BELOW THAT OF A12023. AFTER A FEW HUNDRED YEARS, ONLY VANADIUM HAS A LOWER RESIDUAL ACTIVITY. DEPENDING UPON WHICH MINOR ALLOYING CONSTITUENTS ARE CHOSEN FOR A COPPER ALLOY, THE LONG-TERM RADWASTE PROBLEM AND POSSIBLE REPROCESSING APPEAR RELATIVELY FAVORABLE.

LOSS OF COOLANT ACCIDENTS

COPPER'S EXCELLENT HEAT CONDUCTIVITY SHOULD ASSIST THE REACTOR DESIGNERS IN MITIGATING THE PROBLEMS FROM SOME TYPES OF LOSS OF COOLANT ACCIDENTS.

NOTE ADDED BY EDITORS:

MORE DETAILED CALCULATIONS HAVE SHOWN THAT ^{63}Ni PRODUCED FROM COPPER DURING SERVICE IN A FUSION REACTOR NEUTRON SPECTRUM WILL IMPOSE SEVERE LIMITS ON THE LONG-TERM RADWASTE HANDLING OF COPPER.

RADIOACTIVITY OF CTR BLANKETS AFTER SHUTDOWN

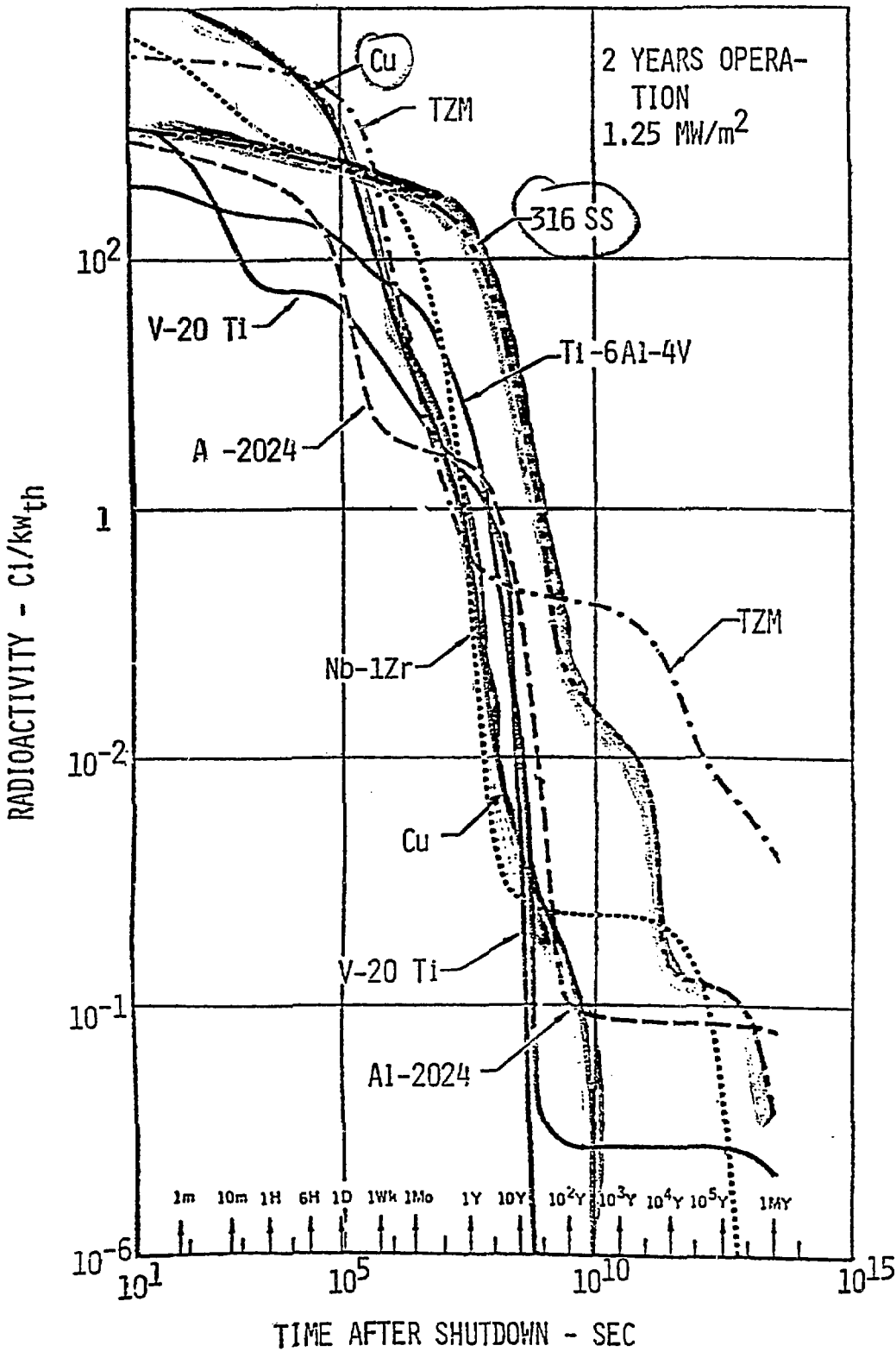

- BULK RADIATION EFFECTS

VERY LITTLE IS KNOWN ABOUT THE HIGH DOSE IRRADIATION PERFORMANCE OF COPPER ALLOYS. THEREFORE IT IS NOT POSSIBLE TO REACH INFORMED JUDGMENTS CONCERNING THE RELATIVE IRRADIATION PERFORMANCE OF COPPER ALLOYS AND OTHER CANDIDATE ALLOYS SUCH AS STAINLESS STEEL.

- SURFACE EFFECTS

SPUTTERING YIELDS OF COPPER ARE PROBABLY SEVERAL TIMES HIGHER THAN FOR STAINLESS STEEL. HOWEVER, IMPURITY GENERATION BY FIRST WALL EROSION IS PROBABLY UNACCEPTABLY HIGH FOR ALL CANDIDATE METAL ALLOYS UNLESS COATINGS AND DIVERTORS ARE USED. COPPER ALLOYS WOULD BE USED WITH LOW Z SURFACE LAYERS IF EXPOSED TO THE PLASMA LEAKAGE FLUX.

UNDER CONDITIONS WHERE HIGH SURFACE EROSION WILL INADVERTENTLY OCCUR, THE HIGH THERMAL CONDUCTIVITY OF COPPER ALLOYS WOULD ALLOW MUCH THICKER SECTIONS. FOR EXAMPLE, ESTIMATES INCLUDING SURFACE EROSION INDICATE THAT ALLOWABLE SURFACE HEAT LOADS WOULD BE ~10 TIMES HIGHER FOR COPPER ALLOYS THAN FOR AUSTENITIC STAINLESS STEEL.

COPPER ALLOYS SHOULD BE PARTICULARLY EFFECTIVE IN RESISTING THE EFFECTS OF PLASMA DISRUPTIONS AND FOR HIGH HEAT LOAD APPLICATIONS AS BEAM DUMPS OR LIMITERS. MELTING RESISTANCE (SEE TABLE) IS SUPERIOR TO MOST CANDIDATE ALLOYS.

MELTING RESISTANCE* $MW/m^2\text{-}S^{\frac{1}{2}}$

TMZ	Cu ZAC-2	Nb-1Zr	V-20Ti	HT-9	SS316	Ti-6Al-4V	Al 2219
56.8	20.3	19.9	12	10	8.2	6.8	5.5

* MELTING RESISTANCE

$$W_M = \frac{T_M - T_0}{2} (\pi \rho C_p k)^{\frac{1}{2}}$$

5. STATUS OF HIGH STRENGTH COPPER ALLOYS FOR CTR APPLICATION

- THERE DO NOT SEEM TO BE ANY A PRIORI REASONS TO RULE OUT COPPER FOR HIGH HEAT COMPONENTS OR EVEN FOR FIRST WALL STRUCTURAL APPLICATION.

- COMPARISON WITH OTHER CANDIDATE ALLOYS INDICATES THAT HIGH PERFORMANCE COPPER ALLOYS ARE SUFFICIENTLY ATTRACTIVE TO WARRANT FURTHER CONSIDERATION.

- MAJOR DATA GAPS INCLUDING IRRADIATION PERFORMANCE AT SERVICE TEMPERATURES AND COMPATIBILITY QUESTIONS NEED TO BE STUDIED.

6. PROPOSED EXPERIMENT TO SCOPE THE NEUTRON IRRADIATION PERFORMANCE OF COPPER ALLOYS

- OBJECTIVES
- ALLOYS
- IRRADIATION CONDITIONS
- ALLOY CHARACTERIZATIONS

- OBJECTIVES

SCOPE THE BULK FAST NEUTRON IRRADIATION PERFORMANCE OF A VARIETY OF READILY AVAILABLE ALLOYS.

OBTAIN SIGNIFICANT FAST NEUTRON DAMAGE LEVELS AT RELEVANT SERVICE TEMPERATURES.

CARRY OUT INITIAL IRRADIATION TESTS WITH A MINIMUM OF COST AND EFFORT.

- ALLOYS IN IRRADIATION*

14 EXPERIMENTAL ALLOYS PRODUCED FROM RS POWDERS, INGOT PRODUCT FOR COMPARISON

Cu-Al-Al_2O_3 (0.58-2.8 wt% Al), 4 alloys

MZC (0.02 Mg, 0.2 Zr, 0.6 Cr), 2 alloys

Cu-Ni-Ti (0.5 Ni, 2.5 Ti), 3 alloys

ZCA (0.57 Al, 0.27 Zr, 0.22 Cr), 2 alloys

ZAC (0.1-0.8 Zr, 0.32 Cr), 2 alloys

10 COMMERCIAL ALLOYS, VARIOUS TMT'S

AMZIRC (0.16 Zr)

110 ETP Cu

151 ETP Cu (1 Zr)

194 ETP Cu (0.03 P, 2.35 Fe, 0.12 Zn)

195 ETP Cu (0.1 P, 1.5 Fe, 0.8 Co, 0.6 Zn)

AMCROM (0.72 Cr)

SSC-155 (0.11 Mg, 0.034 Ag, 0.06 P), 2 alloys

Cu-Be (0.38 Be, 1.67 Ni)

OFHC

* Additional information on these alloys, e.g., the processing, is included in 2 tables which are in the handout.

- IRRADIATION CONDITIONS

FAST NEUTRON DOSE - EBR II FAST REACTOR

15 dpa, 30 dpa

~1 yr, ~2 yr

TEMPERATURE

~400°C

ONE TEMPERATURE TO MINIMIZE MAGNITUDE AND COST OF INITIAL EXPERIMENT. 400°C JUDGED A GOOD FIRST CHOICE FOR A SERVICE TEMPERATURE IRRADIATION IN EBR-II. LOWER NOT FEASIBLE IN THIS REACTOR. MUCH HIGHER PUSHES ALLOY CAPABILITIES.

SPECIMENS

3mm Φ X 0.010 in. PRECISION TEM DISKS

IN 4 GAS FILLED CAPSULES, ~300 DISKS

FUTURE IRRADIATIONS

SHOULD LOOK AT TRANSMUTATION AND DPA EFFECTS, e.g., H AND He + DPA

- ALLOY CHARACTERIZATION PRE- AND POST-IRRADIATION

MICROSTRUCTURES

OPTICAL, SEM, TEM and STEM MICROSCOPY

LIMITED ELECTRON MICROSCOPY FOR THIS FIRST EXPERIMENT

SELECT MOST INTERESTING MATERIALS

USE MECHANICAL TESTS TO HELP SELECT CANDIDATES FOR INITIAL EM WORK

MECHANICAL PROPERTIES

PRECISION 10 mil TEM DISKS WILL BE TESTED IN THE MIT-DEVELOPED MINIATURIZED DISK BEND TEST[2] TO OBTAIN TENSILE PROPERTIES AND, POTENTIALLY, INFORMATION ABOUT FATIGUE AND FRACTURE BEHAVIOR.

1. VIEWGRAPH SHOWING SCHEMATIC OF MINIATURIZED DISK BEND TEST AND DISK SAMPLES VERSUS STANDARD DOG BONE.

2. VIEWGRAPH OF IRRADIATED VERSUS UNIRRADIATED LOAD DEFLECTION CURVE FOR STAINLESS STEEL USING MDBT.

---

[2]Manahan, M. P., Argon, A. S., Harling, O. K., "The Development of a Miniaturized Disk Bend Test for the Determination of Mechanical Properties," Journal of Nuclear Materials, 103 and 104 (1981) 1545-1550 (copy attached), and Manahan, M. P., "The Development of a Miniaturized Disk Bend Test for the Determination of Post-Irradiation Mechanical Behavior," Ph.D. Thesis, M.I.T., May 1982.

M.I.T. MINIATURIZED DISK BEND TEST (MDBT) FOR DETERMINATION OF MECHANICAL PROPERTIES AFTER IRRADIATION

ONE SMALL CONVENTIONAL TENSILE SPECIMEN

OR

484 MINIATURIZED DISK BEND TEST SPECIMENS

OCCUPY SAME VOLUME

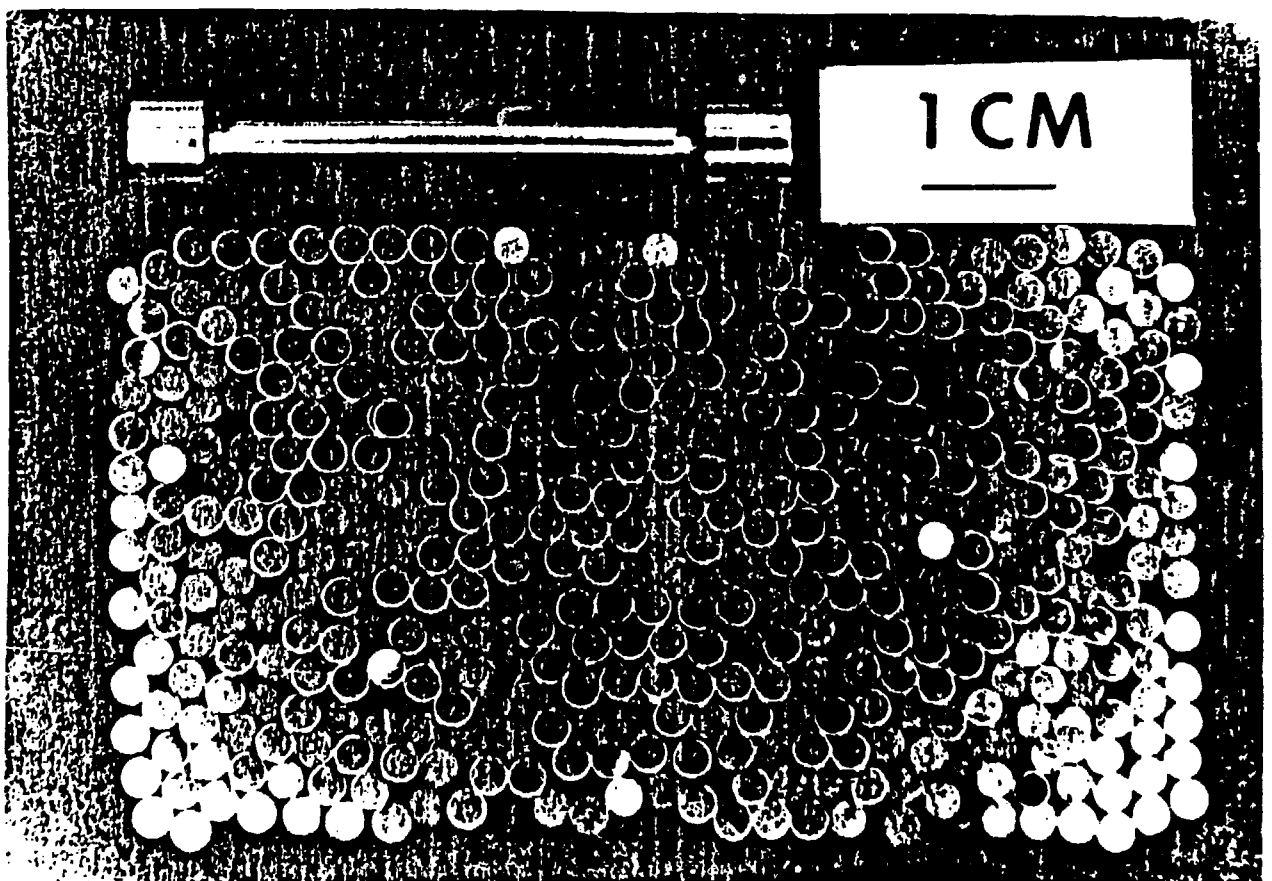

M.I.T. MINIATURIZED DISK BEND TEST APPARATUS

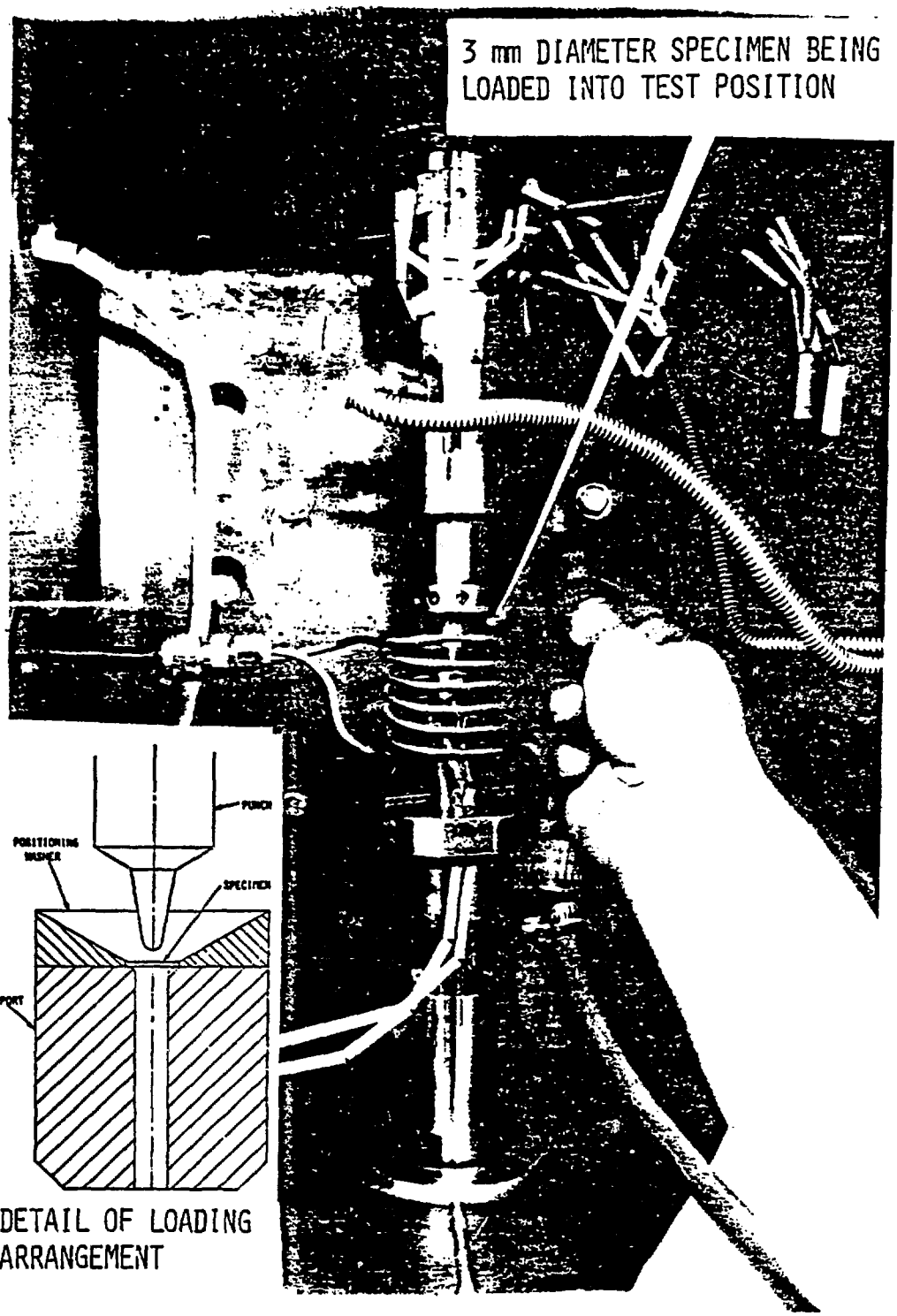

DETAIL OF LOADING ARRANGEMENT

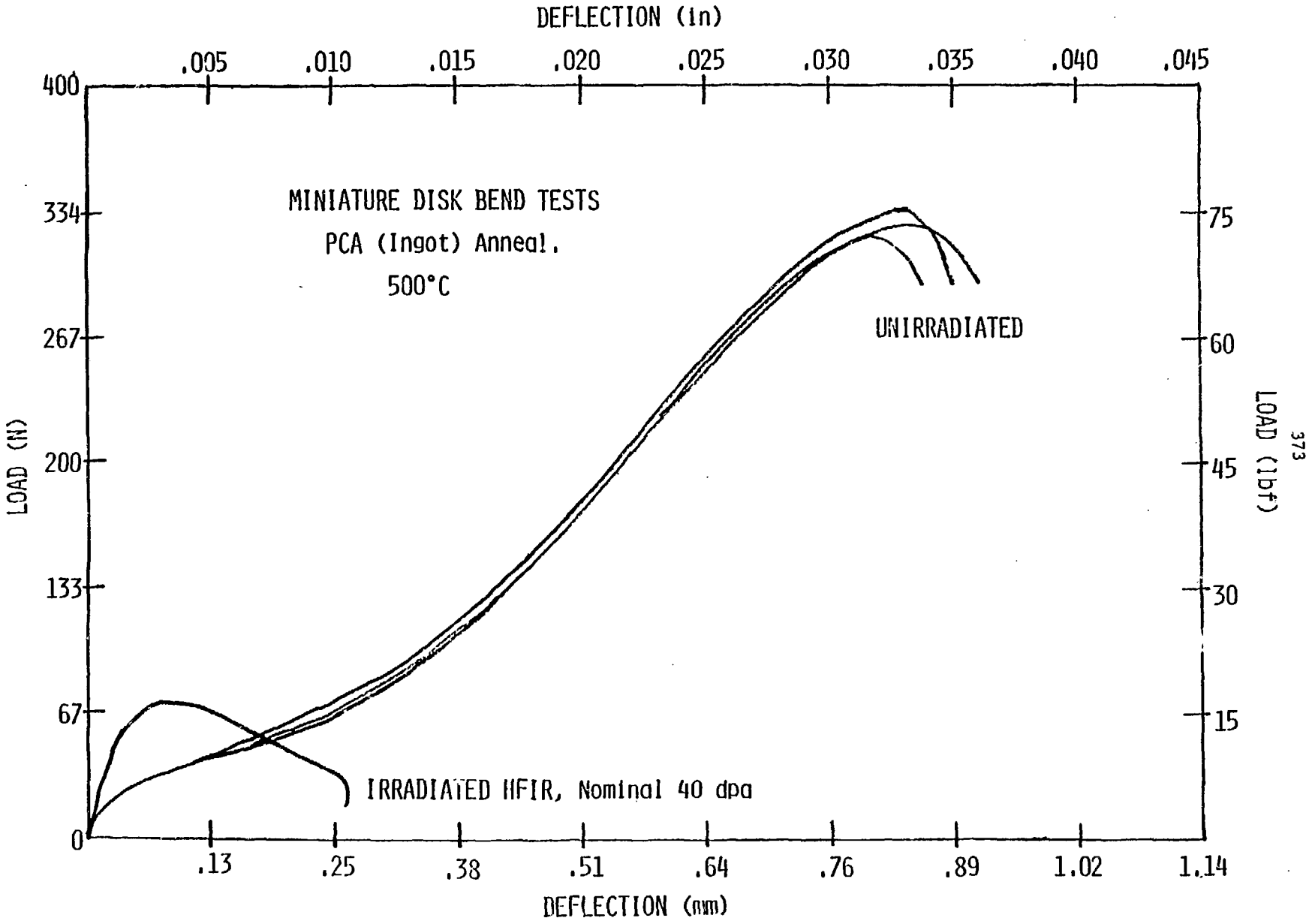
DEFLECTION (in)
.005
.010
.015
.020
.025
.030
.035
.040
.045
400
334
267
200
133
67
0
MINIATURE DISK BEND TESTS
PCA (Ingot) Anneal.
500°C
UNIRRADIATED
IRRADIATED HFIR, Nominal 40 dpa
LOAD (N)
75
60
45
30
15
LOAD (lbf)
.13
.25
.38
.51
.64
.76
.89
1.02
1.14
DEFLECTION (mm)

STATUS OF RESEARCH

300 TEM DISK SPECIMENS IN 4 GAS-FILLED CAPSULES ARE IN EBR-II.

CURRENTLY WE EXPECT TO BEGIN UNIRRADIATED MATERIAL CHARACTERIZATIONS THIS SUMMER AND PREPARATIONS FOR ANALYZING IRRADIATED SPECIMENS.

FIRST BATCH OF ~15 dpa IRRADIATED SPECIMENS SHOULD ARRIVE AT M.I.T. BY THIS FALL.

APPENDICES

1. DETAILED INFORMATION CONCERNING ALLOYS PLACED IN EBR-II BY M.I.T. - TABLE I AND TABLE II

2. "APPLICATION OF HIGH STRENGTH COPPER ALLOYS FOR A FUSION REACTOR FIRST WALL," BY O. K. HARLING, G. P. YU, N. J. GRANT AND J. E. MEYER, JOURNAL OF NUCLEAR MATERIALS 103 AND 104 (1981) 127-132.

3. "THE DEVELOPMENT OF A MINIATURIZED DISK BEND TEST FOR THE DETERMINATION OF POST-IRRADIATION MECHANICAL PROPERTIES," BY M. P. MANAHAN, A. S. ARGON AND O. K. HARLING, JOURNAL OF NUCLEAR MATERIALS 103 AND 104 (1981) 1545-1550.

TABLE I

ALLOY	TYPE AND TREATMENT		Chemical Analysis, wt%						
			Al	Mg	Zr	Cr	Ni	Ti	Be
Cu-Al-Al_2O_3[1]	A1:	gas-atomized Cu-Al powders, attrited, hydrogen reduced, cold compacted, hot extruded	0.65		--	--	--	--	--
	A2:	same as for A1	2.8	--	--	--	--	--	--
	B1:	gas-atomized Cu-Al powders, attrited, internally oxidized, reduced in hydrogen, cold compacted, hot extruded	0.58	--	--	--	--	--	--
	B2:	same as for B1	2.65	--	--	--	--	--	--
MZC[2]	Ingot:	hot rolled, soln ann, cold rolled, aged	--	0.02	0.2	0.6	--	--	--
	P/M:	gas-atomized powders of MZC, reduced in hydrogen, cold compacted, hot extruded	--	0.02	0.2	0.6	--	--	--
Cu-Ni-Ti[3]	Ingot:	hot rolled, soln ann, cold rolled, aged	--	--	--	--	5	2.5	--
	P/M:	gas-atomized powders of Cu-Ni-Ti, reduced in hydrogen, cold compacted, hot extruded	--	--	--	--	5	2.5	--
	Flake:	gas-atomized powders of Cu-Ni-Ti, attrited, reduced in hydrogen, cold compacted, hot extruded	--	--	--	--	5	2.5	--
ZTA[4]	Ingot:	cold rolled	0.57	--	0.27	0.22	--	--	--
	P/M:	gas-atomized powders, pre-aged, attrited, reduced in hydrogen, cold compacted, hot extruded	0.57	--	0.27	0.22	--	--	--
ZAC[5]	ZAC-1:	gas-atomized powders, reduced in hydrogen, cold compacted, hot extruded	--	--	0.1	0.32	--	--	--
	ZAC-2B:	gas-atomized powders, reduced in hydrogen, cold compacted, hot extruded	--	--	0.23	0.33	--	--	--
	ZA-8:	gas-atomized powders, cold compacted, hot extruded	--	--	0.8	--	--	--	--
Cu-Be[6]	Ingot:	hot rolled, soln ann, cold rolled, aged	--	--	--	--	2.67	--	0.39
OFHC[7]	Ingot:	ann	--	--	--	--	--	--	--
	Ingot:	cold worked	--	--	--	--	--	--	--

1. W. F. Schilling and N. J. Grant, "High Temperature Behavior of Cu-Al_2O_3 Alloys," Powder Met. Intern'l, 5, No. 3 (Aug. 1973), 117.
2. Commercial MZC bar and RS powder prepared in fine flake form (MIT INCRA Progress Report).
3. Commercial Cu-Ni-Ti bar and RS powders prepared in fine flake form.
4. MIT experimental alloy.
5. V. K. Sarin and N. J. Grant, "The Effect of Thermomechanical Treatments on Powder Metallurgical Cu-Zr and Cu-Zr-Cr Alloys," Powder Met. Intern'l, 11, No. 4 (Nov. 1979), 153.
6. INESCO
7. Commercial OFHC bar.

TABLE II

Commercial Cu Alloys

ALLOY	Chemical Analysis wt%												
	Al	Mg	Zr	Cr	Ni	Ti	Be	Ag	P	Fe	Zn	Co	Sn
110 ETP Cu, 75% CW	--	--	--	--	--	--	--						
151	--	--	1	--	--	--	--						
194									0.03	2.35	0.12		
195									0.1	1.5		0.8	0.6
OFHC (S), 50% CW	--	--	--	--	--	--	--						
AMZIRC, 80% CW aged 450°C 1 h			0.16										
AMCROM, 50% CW aged 425°C 1 h				0.72									
SSC-155, An		0.11						0.034	0.06				
SSC-155, CW		0.11						0.034	0.06				

THE HIGH HEAT FLUX COMPONENTS PROGRAM

J. B. Whitley

Sandia National Laboratories,
Albuquerque

The High Heat Flux Component Development Program (HHFCDP) has as its purpose the development of those technologies necessary to design, build and operate high heat flux components. These components include actively cooled limiters, divertor collector plates, R. F. antennas, mirror end cells, mirror halo collectors, direct convertor collectors, and neutral beam dumps. These components often interact directly with the plasma and require an integrated design that considers the plasma-materials interaction (PMI) issues, heat removal problems and materials issues (including possible low Z coatings and claddings). As a general definition, high heat flux components see heat fluxes ranging from 1 to 100 MW/m^2. The High Heat Flux program involves activities such as studies of fundamental heat transfer processes, determinations of critical heat flux levels in component-like test specimens, studies of the thermal fatigue behavior of candidate materials, and design and test activities directed toward components for both operating and planned fusion devices.

Suitable materials for use as base structural materials for high heat flux components are limited to those materials with high thermal conductivities and low thermal expansions. Copper and copper alloys are currently used extensively in high heat flux components due to their desirable thermal properties and compatibility with water coolant. Thermal fatigue tests have shown that copper components can successfully perform under severe thermal cycling conditions (i.e., > 10,000 cylces at 40 MW/m^2). Data is lacking, however, on the effects of neutron irradiation on most of the copper alloys, with the effect of neutron irradiation on crack propagation being of major importance in these highly fatigued components.

The High Heat Flux Program centered at Sandia National Laboratories has either in operation or under construction the facilities necessary to answer many of the engineering problems associated with these components. A vital part of this program is the interaction with users or potential users of this technology. Many of these interactions are currently in place and other programs with high heat flux problems are encouraged to contact Sandia to discuss potential collaboration in this area.

Scope

- HHF/HPF Components
- Steady State Operation → Active Cooling
- Fully Integrated with Reactor Materials Program
- Will Provide
  - > Data Base In HHF Technology
  - > Preliminary Design Packages

HIGH HEAT FLUX COMPONENT DEVELOPMENT PROGRAM

- FUNDAMENTAL HEAT REMOVAL STUDIES
- DEVELOPMENT AND TESTING OF ENGINEERING PROTOTYPES
- DESIGN AND TESTING OF SPECIFIC COMPONENTS, INCLUDING EXPERIMENTATION.

HIGH HEAT FLUX DEFINITION

	Range	
Areal Power Density	100 W/cm^2 to 10 kW/cm^2 1 MW/m^2 to 100 MW/m^2	
Pulse Duration	250 μsec (Off-Normal Operation)	to Steady State (Normal Operation)
Particle Energy Range	100 eV (Plasma Edge-H, He Isotopes)	to 1 MeV (Runaway Electrons)
Heat Source Character	Energetic Low Mass Particles (Electrons)	Energetic Atomic Species (Ions, Neutrals)
	Non-Penetrating Radiation	

GENERIC LIMITER DESIGN

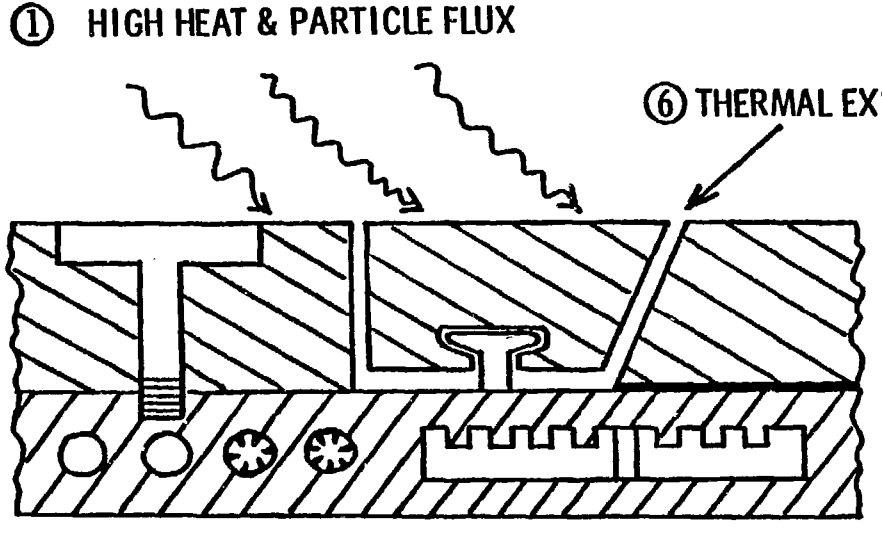

LIMITER DESIGN PROBLEMS

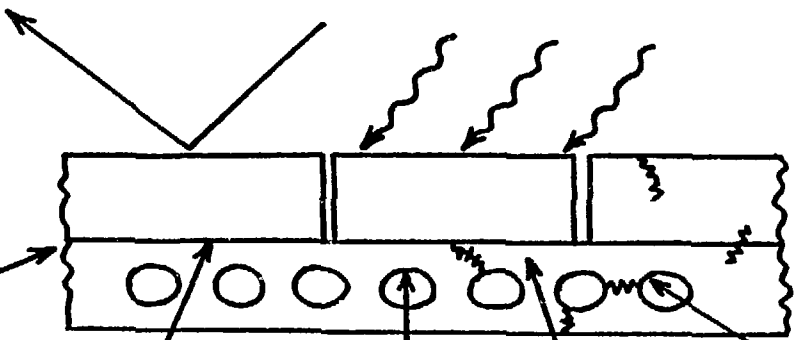

- EROSION [physical/chemical sputtering, arcing vaporization, & blistering]
- HIGH HEAT & PARTICLE FLUX [normal & disruptions]
- RADIATION DAMAGE [swelling & embrittlement]
- OUTGASSING
- RECYCLING
- FATIGUE CRACK INITIATION & GROWTH
- GAP THERMAL CONDUCTANCE
- DEBONDING
- BURNOUT
- CHANNEL EROSION / CORROSION / PLUGGING
- DIFFERENTIAL THERMAL EXPANSION
- EDDY CURRENTS & DISRUPTION FORCES
- CREEP RUPTURE
- TRITIUM PERMEATION
- THERMAL AGING
- PUMPING POWER
- FABRICABILITY
- COST
- NEUTRON ACTIVATION
- TRITIUM INVENTORY

LIMITERS OF NEXT-GENERATION TOKAMAKS AND FUTURE REACTORS

	HEATING POWER (MW)	PULSE LENGTH (s)	DESIGN LOAD ($MW\ m^{-2}$)	LIMITER AREA (m^2)	MATERIAL	COOLING
TFTR	4	1.5	5	2	Inconel, Stainless Steel	Inertial
	4	1.5	5	8.5	TiC-coated Graphite	Active between Shots
	33	0.1	5	20	Graphite	Active Between Shots
JET	5	20	4	2.5	Graphite	Inertial
	18	20	10	5	Ni on Cu	Active
JT-60	20	10	0.5	25	TiC on Mo	Inertial
INTOR	120	100	5	57	W on Cu	Active
STARFIRE ($1200\ MW_E$)	200	Steady State	2.3 average 4.0 Peak	58	Be on Cu	Active

MATERIAL REQUIREMENTS FOR HHF COMPONENTS

- HIGH THERMAL CONDUCTIVITY
- LOW THERMAL EXPANSION
- COMPATIBLE WITH HIGH VELOCITY WATER COOLING
- GOOD THERMAL FATIGUE RESISTANCE
- COMPATIBLE WITH HYDROGEN
- LOW TRITIUM PERMEATION RATES
- GOOD MECHANICAL PROPERTIES AFTER MODERATE NEUTRON FLUENCES
- LIMITED SWELLING
- IF NECESSARY, MUST BE COMPATIBLE WITH LOW Z COATING OR CLADDING
- LOW ACTIVATION IF POSSIBLE
- CAN BE FABRICATED

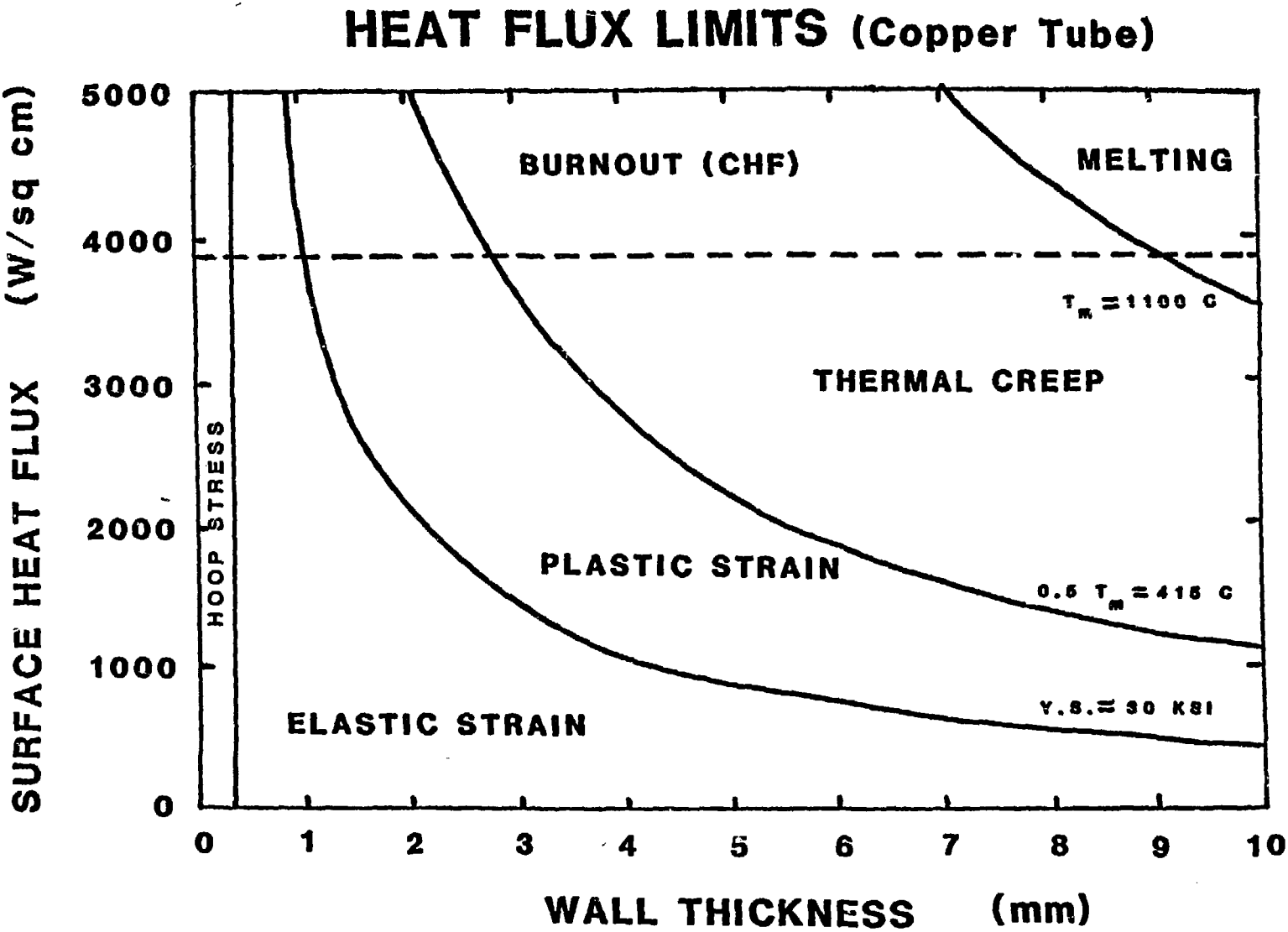
HEAT FLUX LIMITS (Copper Tube)
SURFACE HEAT FLUX (W/sq cm)
5000
4000
3000
2000
1000
0
BURNOUT (CHF)
MELTING
T_M = 1100 C
THERMAL CREEP
HOOP STRESS
PLASTIC STRAIN
0.5 T_M = 415 C
Y.S. = 30 KSI
ELASTIC STRAIN
0 1 2 3 4 5 6 7 8 9 10
WALL THICKNESS (mm)

HHF TESTING

- HHF Data Base
- Materials Response, Development
- Engineering Applications

Test Program (Design concept path):

- Small size, single channel

  (basic heat transfer, fluid behavior, erosion)

- Moderate size, multichannel or tube arrays

  (thermal stress-fatigue, size effects, coolant channel interaction, armor bonding)

- Large size, near full-scale

  (edge effects, life testing, size effects, attachment stress, off-normal operations)

- Generic component

  (model comparisons, attachments, compatability)

- In-device tests

  (actual operation, disruption response, instrumentation, integration)

ELECTRON BEAM TEST SYSTEM

- 30 kV, 1 Amp, rastered beam
- Pulse length 50 msec to continuous
- Area from 1 - 10cm in x and y
  ($1cm^2$ to $100cm^2$)
- Samples size up to 25 x 50 cm
- Computer control
- Low energy ion beam
- Diagnostics
  - Optical viewing, recording
  - Mass spectrometer
  - Pyrometer
  - Imbedded thermocouples
  - Acoustic emission

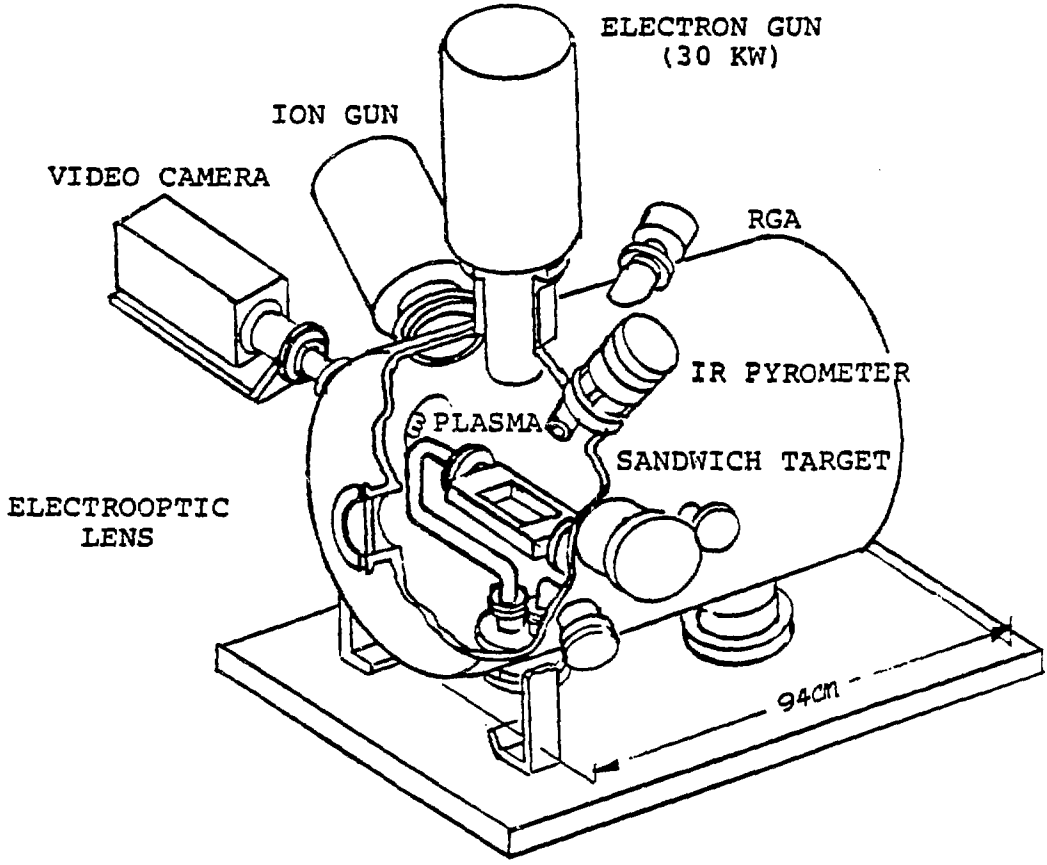
ELECTRON GUN
(30 KW)
ION GUN
VIDEO CAMERA
RGA
IR PYROMETER
PLASMA
SANDWICH TARGET
ELECTROOPTIC
LENS
94CM

HIGH HEAT FLUX TESTS

	Ion Beam	Electron Beam
Material	Cu	Cu
Wall Thickness	1.1 mm	4.0 mm
Coolant	H_2O	H_2O
Flow Rate	3.2 l/s (50 gpm)	0.6 l/s (10 gpm
Inlet Pressure	2 MPa (300 psi)	0.4 MPa (70 ps
Flow Velocity	37 m/s	7.3 m/s
Particle	D^+	e^-
Energy	160 keV	25 keV
Heat Flux	4 kW/cm^2 (6 peak)	2 kW/cm^2
Beam Area	10 cm^2	10 cm^2
Total Beam Time	5.0×10^5 sec (140 hr)	3.6×10^5 sec (100 hr)
Number Cycles	~300	36,000

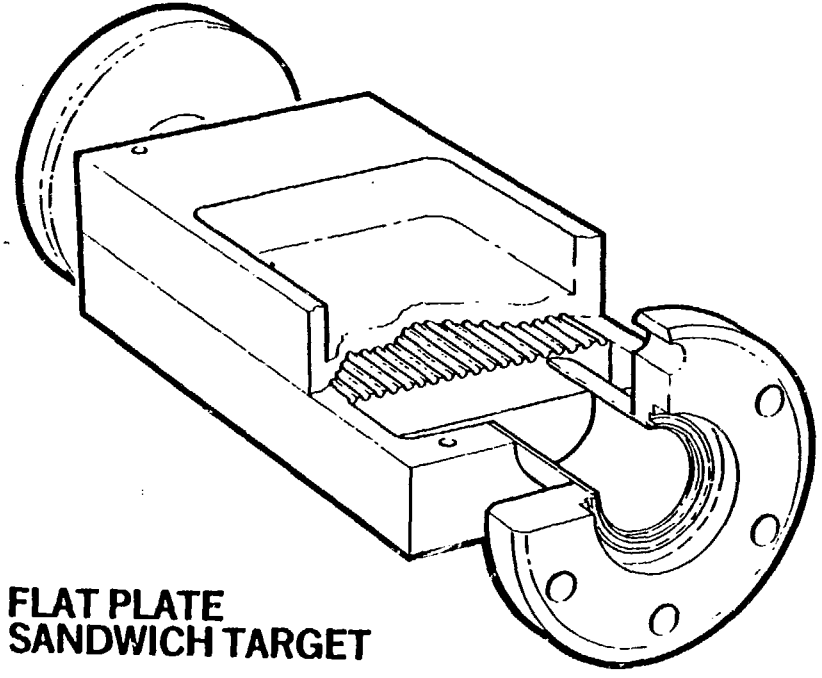

FLAT PLATE
SANDWICH TARGET

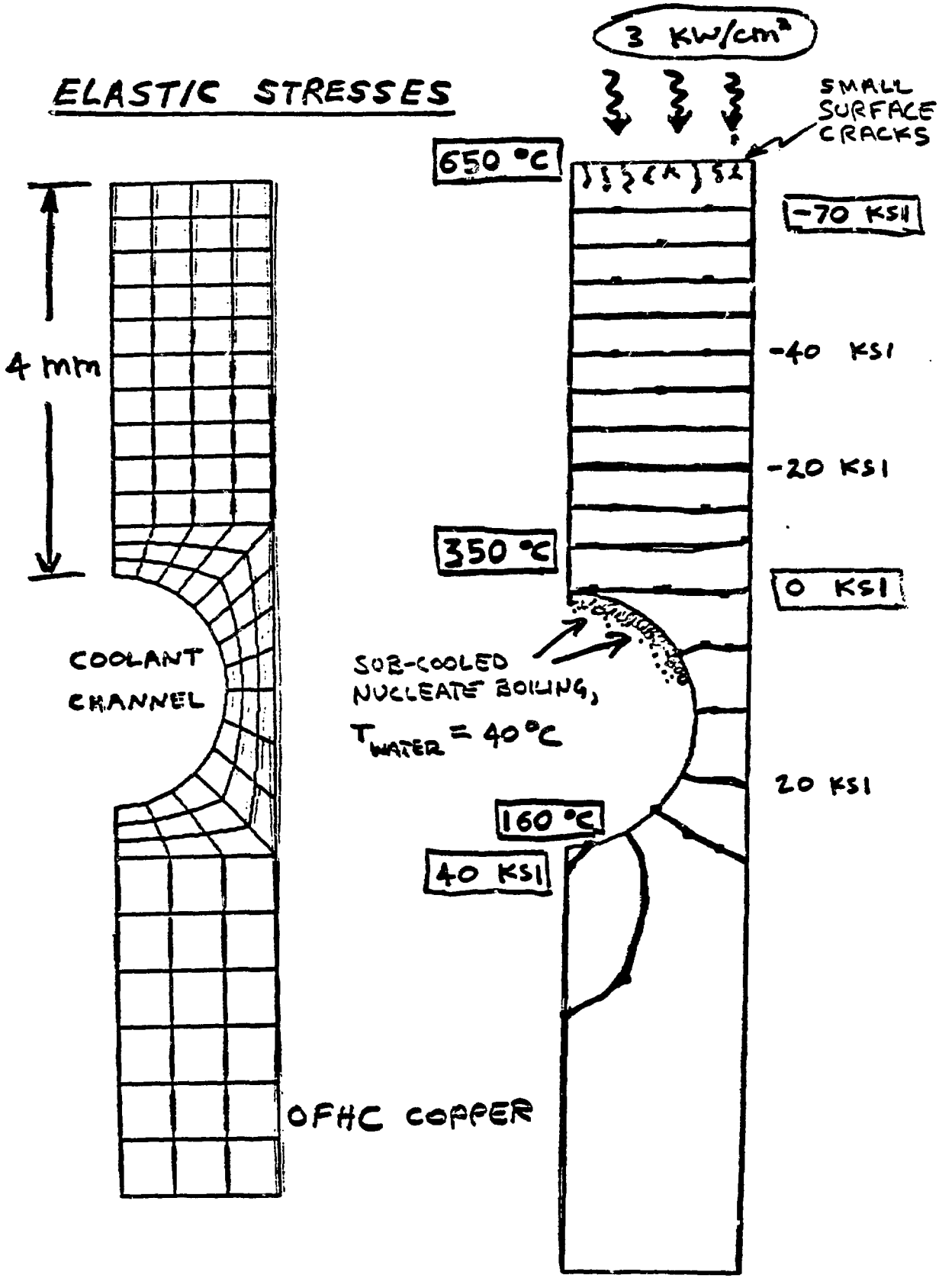
ELASTIC STRESSES
3 KW/cm²
SMALL SURFACE CRACKS
650 °C
-70 KSI
-40 KSI
-20 KSI
350 °C
0 KSI
4 mm
COOLANT CHANNEL
SUB-COOLED NUCLEATE BOILING,
T WATER = 40 °C
20 KSI
160 °C
40 KSI
OFHC COPPER

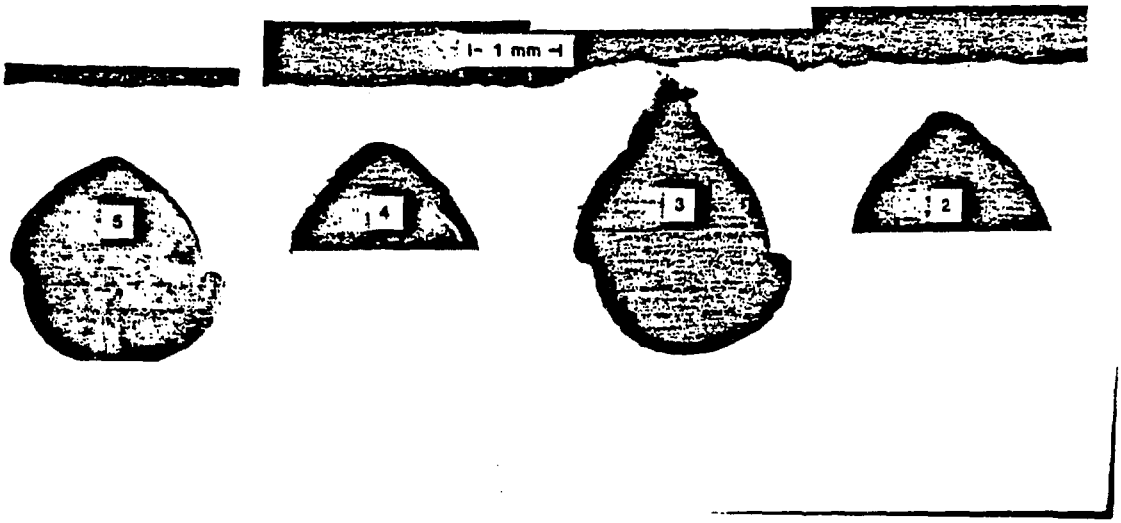

INTERNAL EROSION OF A WATER COOLED HIGH HEAT FLUX TARGET AFTER AN EXPOSURE OF 140 HR AT 4Kw/cm^2 WITH 300 PSI WATER AT 100 FT/SEC

THERMAL FATIGUE TEST SUMMARY FOR PLASMA SPRAYED COATINGS*

Coating/Substrate	Cycles to Failure** As Deposited	HIPPED†	Effect of HIPPING
Al_2O_3/Cu	9, 9		
B/Mo	8, 8		
B/Ta	9, 11		
B/Poco	8, 8	nf	↑
B 25V/Ta	nf, nf(2)		
TiB_2/Cu	nf(2)	356	----
TiB_2/SS	28, 28		
TiB_2/Mo	9, 9, 8, 8	nf	↑
TiB_2/Ta	8, 8, 8	nf	↑
TiB_2/Poco	10	61	----
TiC/Cu	nf(2), nf(2), 194	nf	----
TiC/SS	nf(2), 18, 29	9	----
TiC/Mo	nf(2), nf(4)	nf	----
TiC/Ta	nf(2), nf(4)	nf	----
TiC/Poco	7	2	----
TiC 25V/Mo	nf(3), 187, nf	176	----
TiC 25V/Ta	nf(3), nf(4), 194	22	↓
V/Cu		11	
VC/V/Cu	7, 6, 6	11	----
VC/Mo	nf(2), nf(4)	nf	----
VC/Ta	nf(2), nf(3), 356	119	↓
VC/Poco	7	nf	↑

*Coating thicknesses 100 to 200 μm.

**nf = no failure. No underline = 1 kW/cm^2, 1.5 second pulse to a maximum of 200 cycles. An underline = 1.5 kW/cm^2, 1.5 second pulse to a maximum of 500 cycles. (2) = number of samples which did not fail during testing.

†HIP = Hot Isostatic Pressing at 1500°C and 18 ksi for Mo, Ta, Poco substrates and 700°C at 15 ksi for Cu and SS substrates.

4 KW/cm² (Beam power)

2,000 CYCLES

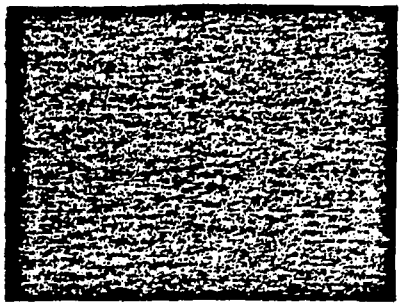

SURFACE CRACKS -6X

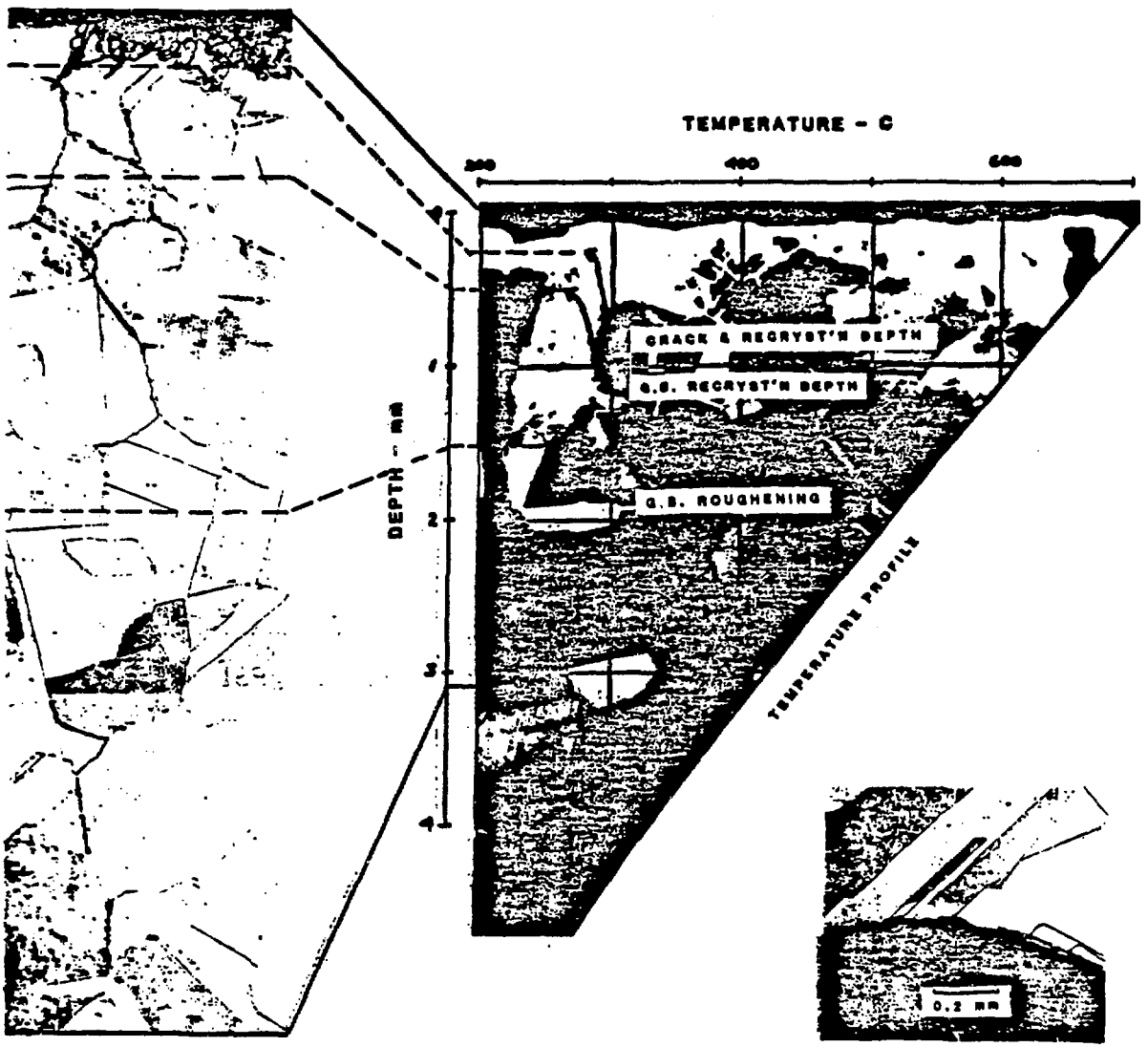

COOLING CHANNEL

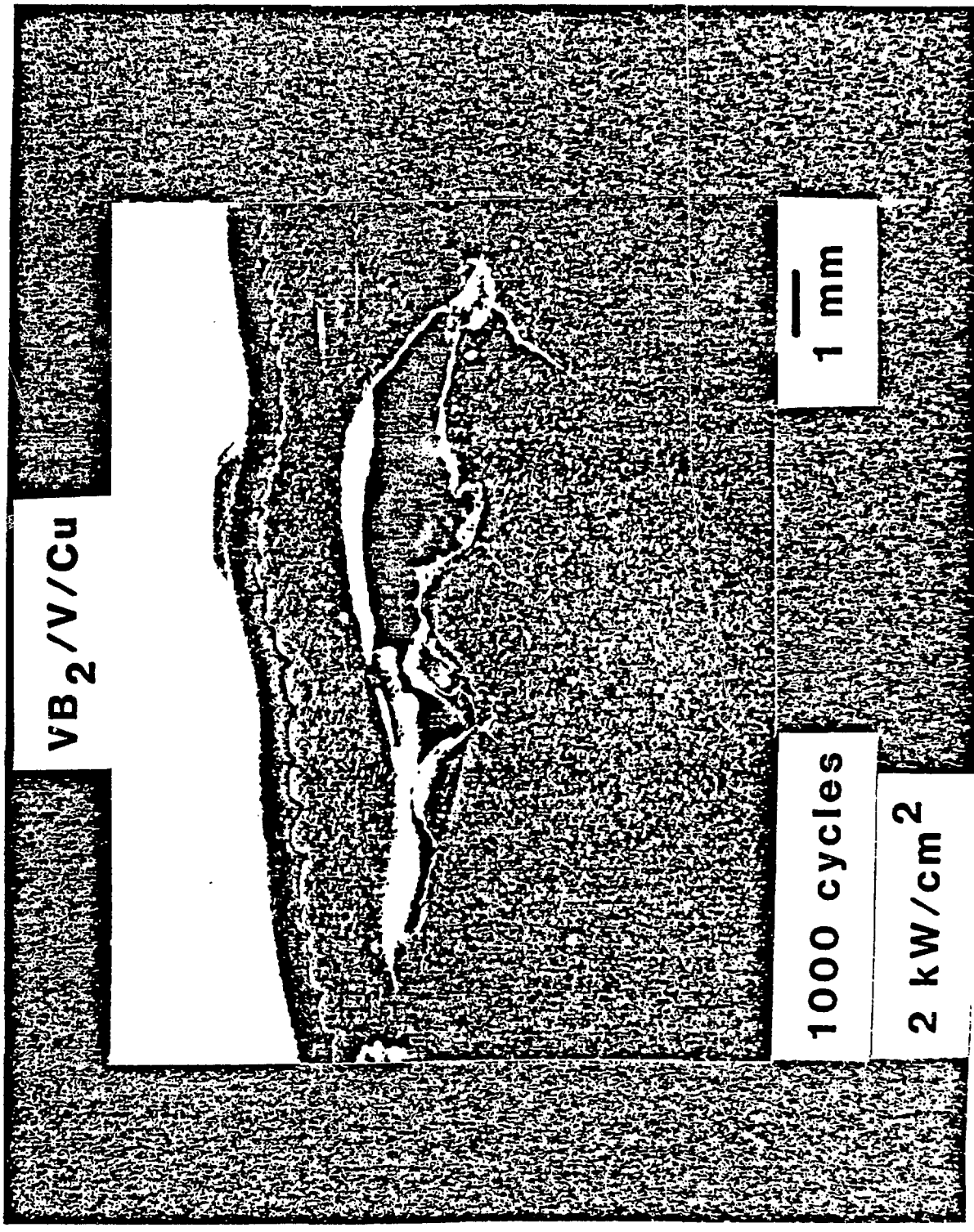
VB_2/V/Cu
1000 cycles
2 kW/cm^2
1 mm

PLASMA MATERIALS TEST FACILITY
(PMTF)

- DEDICATED MATERIALS AND HHF TEST FACILITY
- STEADY-STATE ION BEAM HEAT SOURCE
- CONTROLLED AND INSTRUMENTED COOLANT FLOW LOOP
  - CONTROL INLET TEMPERATURE
    PRESSURE
    FLOW RATE
    WATER CHEMISTRY
  - INSTRUMENTATION FOR COOLANT BEHAVIOR
    SURFACE EFFECTS
    STRUCTURAL RESPONSE
- SAMPLE SIZES UP TO 1 M x 1 M

PLASMA MATERIALS TEST FACILITY (PMTF)

NEUTRON IRRADIATION EFFECTS

- CAN COATINGS AND/OR BONDED OVERLAYS WITHSTAND HIGH ENERGY NEUTRON IRRADIATION?

FLUENCE LEVELS:

A) TFTR, JET

B) FED OR EQUIVALENT

C) DEMO, POWER REACTORS

POSSIBLE PROBLEM AREAS:

A) STRESSES FROM DIFFERENTIAL SWELLING

B) GAS BUILDUP AT INTERFACE;
INTERFACE DEGRADATION

C) LOSS OF DUCTILITY OF COATING

NEUTRON IRRADIATION STUDIES OF HIGH HEAT FLUX MATERIALS

COATINGS/SUBSTRATE	SAMPLES IN FFTF	SAMPLES IN FBR-II
Be/Cu (braze)	-	4
Be/Cu (PS)	2	-
SiC/C (CVD)	-	2
TiC/C (CVD)	4	4
TiB_2/C (CVD)	2	2
Mo/Cu (PS)	4	-
Mo/V/Cu (PS)	1	-
TiC/Mo (PS)	1	-
Be/304SS (PS)	2	-
TiB_2/304SS (PS)	1	-
V/TZM (EB)	2	-
TiC	2	-
TiB_2	2	-
TiB_2 + BN	2	-
SiC	4	-
SiC + (B+C)	2	-
	31	12
	2-3 DPA	6-12 DPA
	~450°C	~450°C

LAPS System

ADVANCED LIMITER PROGRAM
SANDIA/UCLA/KFA JÜLICH

GOAL: PERFORM LONG PULSE ADVANCED LIMITER EXPERIMENTS TO PROVIDE

- OPERATIONAL EXPERIENCE
- PHYSICS AND ENGINEERING DATA FOR REACTOR ADVANCED LIMITER DESIGNS.

KEY ISSUES:

- PARTICLE REMOVAL AND CONTROL
- IMPURITY CONTROL
- HELIUM REMOVAL
- HEAT LOADS
- MATERIALS AND STRUCTURAL RESPONSE

LONG PULSE IMPLICATIONS:

- STEADY-STATE WITH RESPECT TO HYDROGEN-WALL INTERACTION;
- IMPURITY ACCUMULATION RATES;
- PARTICLE AND IMPURITY CONTROL METHODS UNDER STEADY-STATE LIMITER LOADING CONDITIONS;
- EXPERIMENTAL TESTS OF ABOVE ISSUES.

ADVANCED LIMITER TEST II (ALT-II)

1983-85

TEXTOR: EXTENDED PERFORMANCE PHASE

- PULSE LENGTHS 5-10 SEC;
- LONG PULSE (3 SEC) NEUTRAL BEAM INJECTION, ION CYCLOTRON RESONANCE HEATING; TOTAL PLASMA POWER TO 5 MW;
- INCREASE OF TOROIDAL MAGNETIC FIELD FROM 2.0 TO 2.6 T.

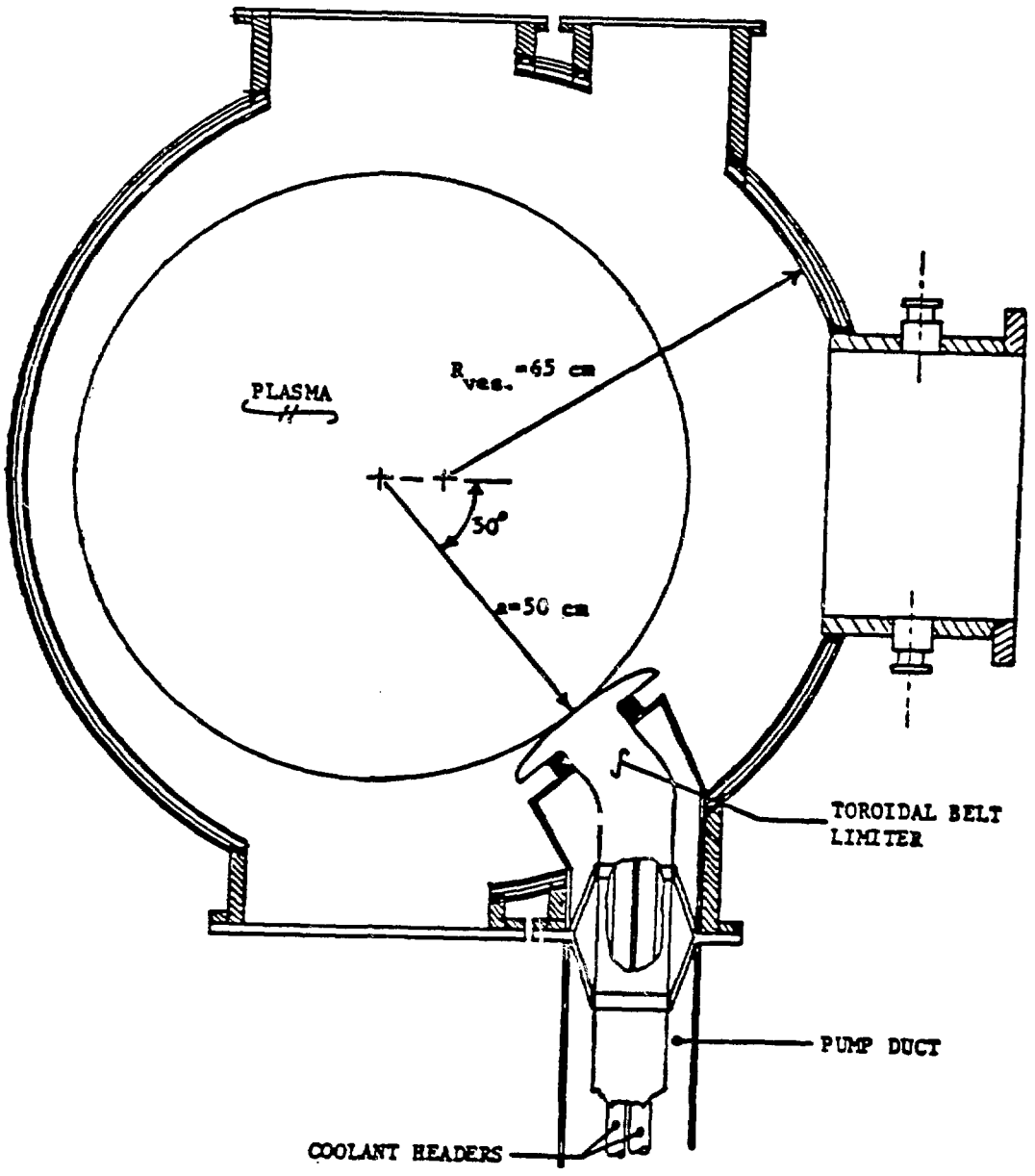

Figure 3-1. TEXTOR Vacuum Vessel with ALT-II Installed

SUMMARY

- Cu has several desirable features:
  1) high thermal conductivity, low thermal stress
  2) high strength, high thermal conductivity alloys exist
  3) compatible with water cooling
  4) has withstood several thermal fatigue tests successfully
  5) easily coated or bonded
  6) easily fabricated

- Potential problems with Cu
  1) neutron irradiation effects on mechanical properties are uncertain, especially on the alloys
  2) relatively low melting temperature (1100°C) will limit its use to low outlet water temperature
  3) potentially high swelling rate (.4 $T_M \approx$ 350-400°C)
  4) high activation
  5) possible erosion from intense boiling

FABRICATION OF COPPER ALLOY BEAM DUMPS

W. A. Rinehart

McDonnell Douglas Corporation

FABRICATION OF COPPER ALLOY BEAM DUMPS

W. A. Rinehart

An actively cooled, heat absorption panel was designed and fabricated for use as a calorimeter or beam dump. The panel was designed to withstand an average heating rate of 2 kW/cm^2 at angles to the beam of 4-90° for up to 25,000 beam pulses of 30 seconds duration. The design approach was to minimize panel and ancillary equipment cost such as the cooling water system while meeting all panel performance specifications. This involved performing a parametric study of several interdependent criteria such as material properties, thermal/mechanical stresses, water flow rates and pressures, boiling, flow passage design and fabrication techniques.

The criteria used in the panel material comparisons included strength, thermal, design, and manufacturing characteristics. In particular, material properties such as thermal conductivity, thermal expansion, strength and modulus of elasticity as a function of temperature, fatigue, sputtering, machinability, bonding, and cost were all involved in the parametric analysis. The materials considered in the analyses included copper, Amzirc (copper alloy), molybdenum, tantalum, niobium, tungsten, and nickel. Amzirc, an oxygen-free copper containing about 0.2% zirconium, was chosen because of its high thermal conductivity, good strength at elevated temperatures, machinability, availability, and reasonable cost.

Using Amzirc as the baseline material, a trade study was made to determine the effect of panel geometry on strength. Panel front and base plate thicknesses were optimized to minimize stress for various coolant passage configurations and coolant pressures. A fin parametric analysis was performed using a general heat transfer program. Special computer logic was developed to accommodate boiling heat transfer. The analysis showed the effect of fin geometry and flow passage design on core pressure loss, maximum external wall temperature, internal wall heat flux, and flow velocity.

Panel specifications limited the average water outlet temperature to 98°C with a maximum temperature rise through the panel of 55°C. The water system pressure requirement was minimized by allowing boiling in about 30% of the panel flow length. The panel only required a water inlet pressure of 220 psig. With an outlet pressure of 105 psig, the panel water flow rate was approximately 57 gpm.

The panel front plate was brazed to the base plate; the water headers were an integral part of the base plate. Exterior ribs were provided in the header areas for structural support, but the ribs did not significantly restrict panel expansion or edge rotation in order to meet the panel design life requirements. The panel was designed to allow edge rotation up to 2°. However, this panel curvature resulted in a significant increase in panel heat flux at small beam angles-of-incidence (design requirement was 4-90°). The base plate material between the header areas was reduced in thickness to provide panel flexibility. This prevented excessive compression loads on the front plate in the longitudinal direction and excessive bending loads on the edge ribs in the transverse direction.

Over 650 tests have been conducted on the prototype panel with beam pulses up to 0.7 sec at a peak flux of 2 kW/cm^2. Over 100 production panels have been built and delivered.

LAWRENCE BERKELEY LABORATORY
CONCEPTUAL NEUTRAL BEAM ENGINEERING TEST FACILITY (NBETF)

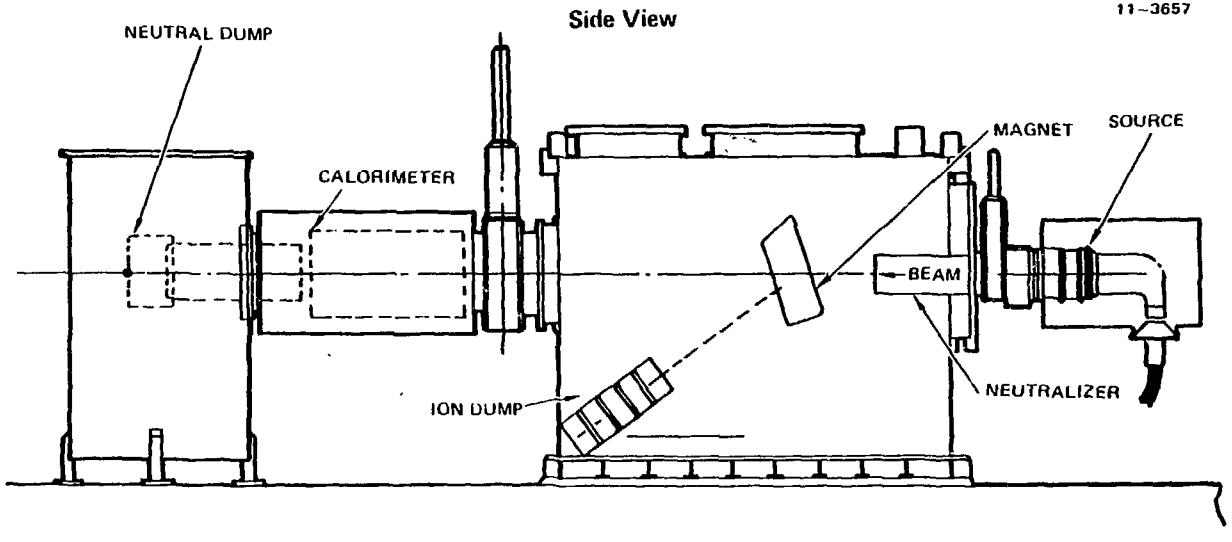

MCDONNELL DOUGLAS CORPORATION

NEUTRAL BEAM ENGINEERING TEST FACILITY (NBETF) ION DUMP

11–3732

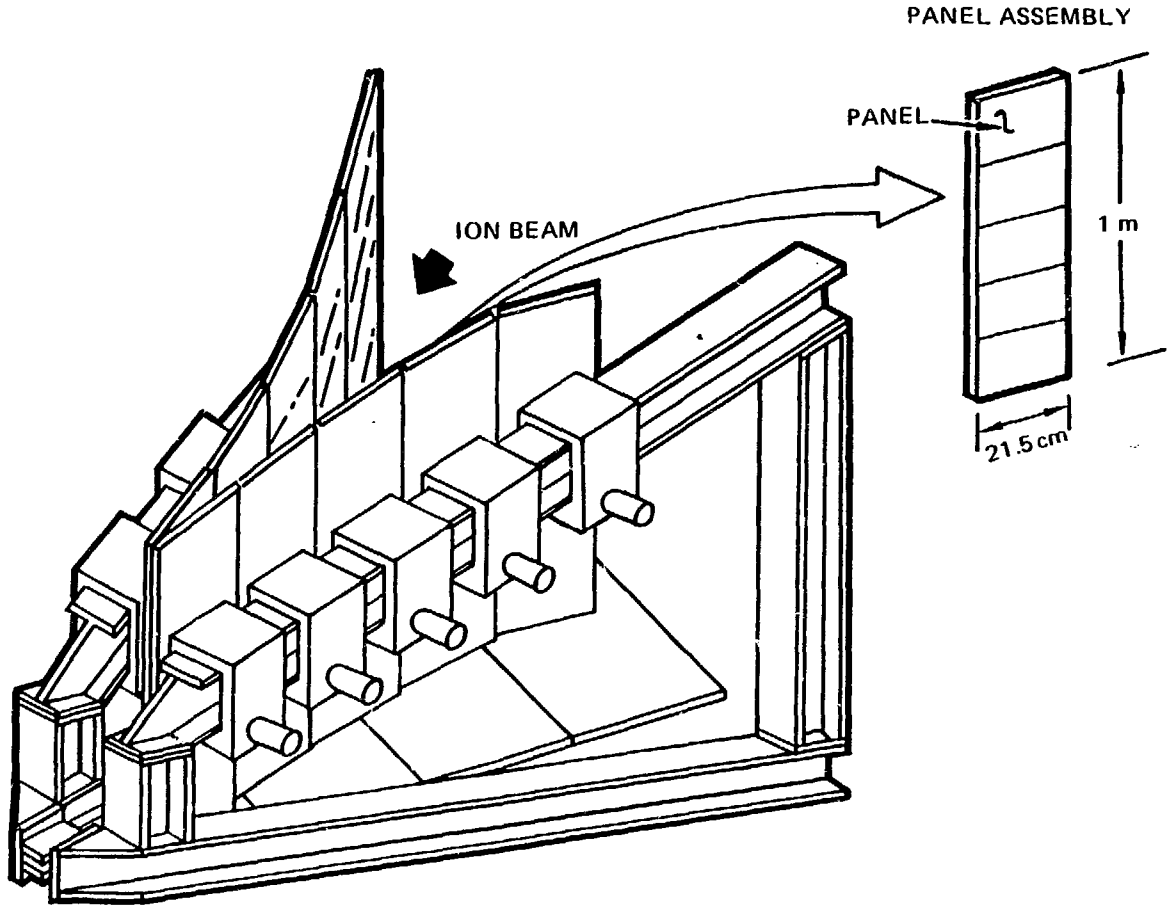

McDONNELL DOUGLAS CORPORATION

HEAT ABSORPTION PANEL

11-3658

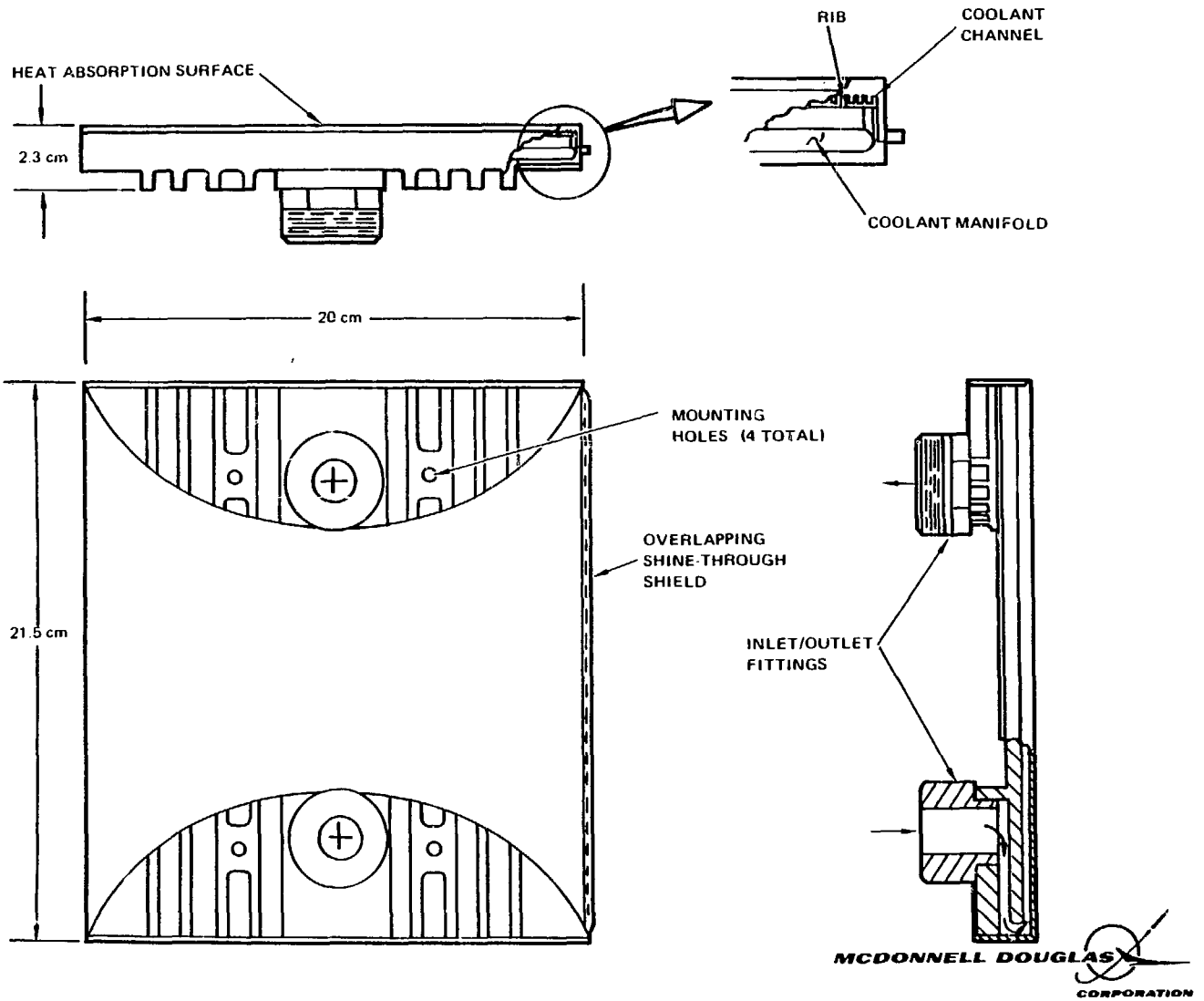

MCDONNELL DOUGLAS CORPORATION

EXPLODED VIEW OF HEAT ABSORPTION PANEL

11–4412

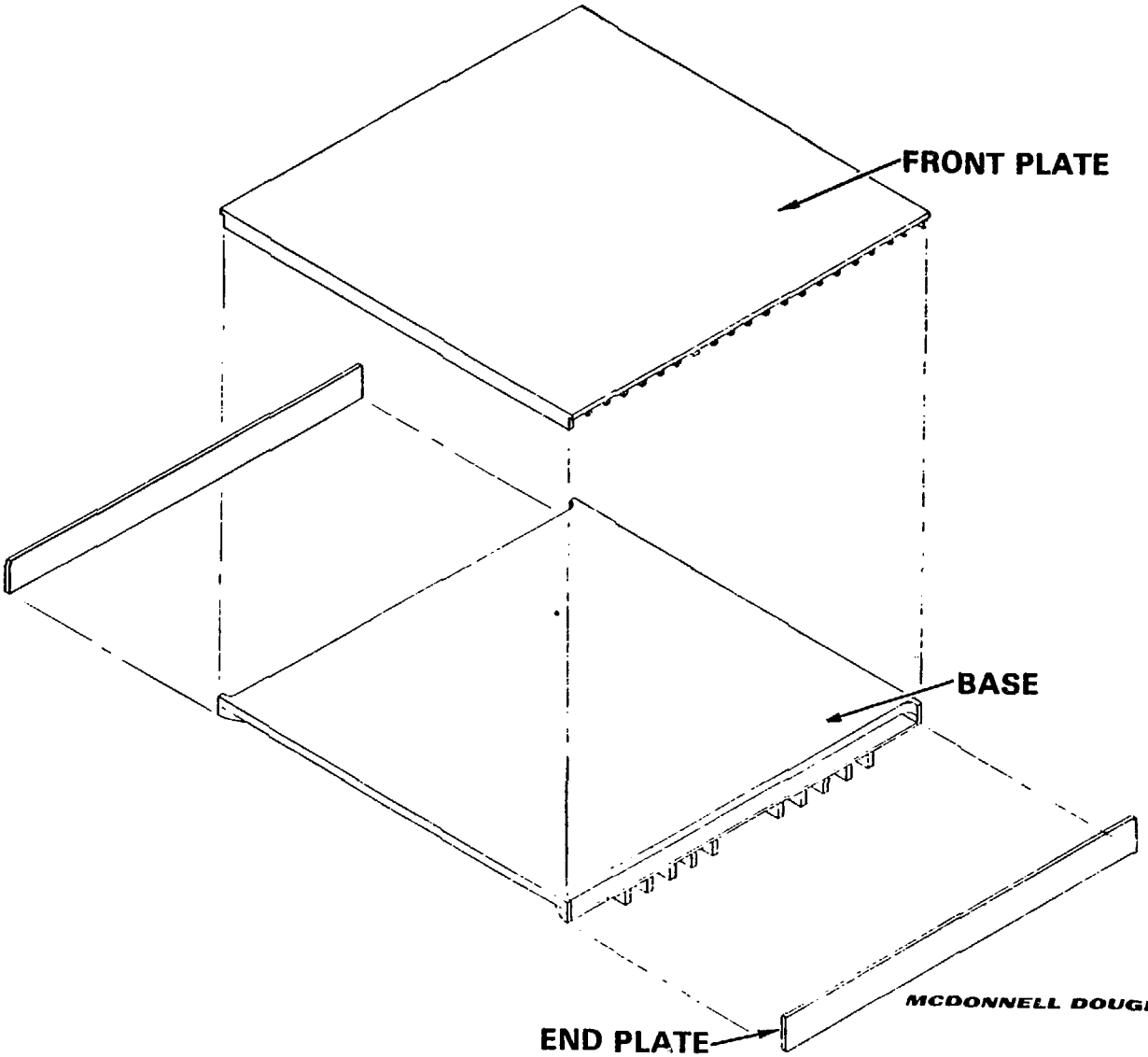

MCDONNELL DOUGLAS CORPORATION

HEAT ABSORPTION PANEL

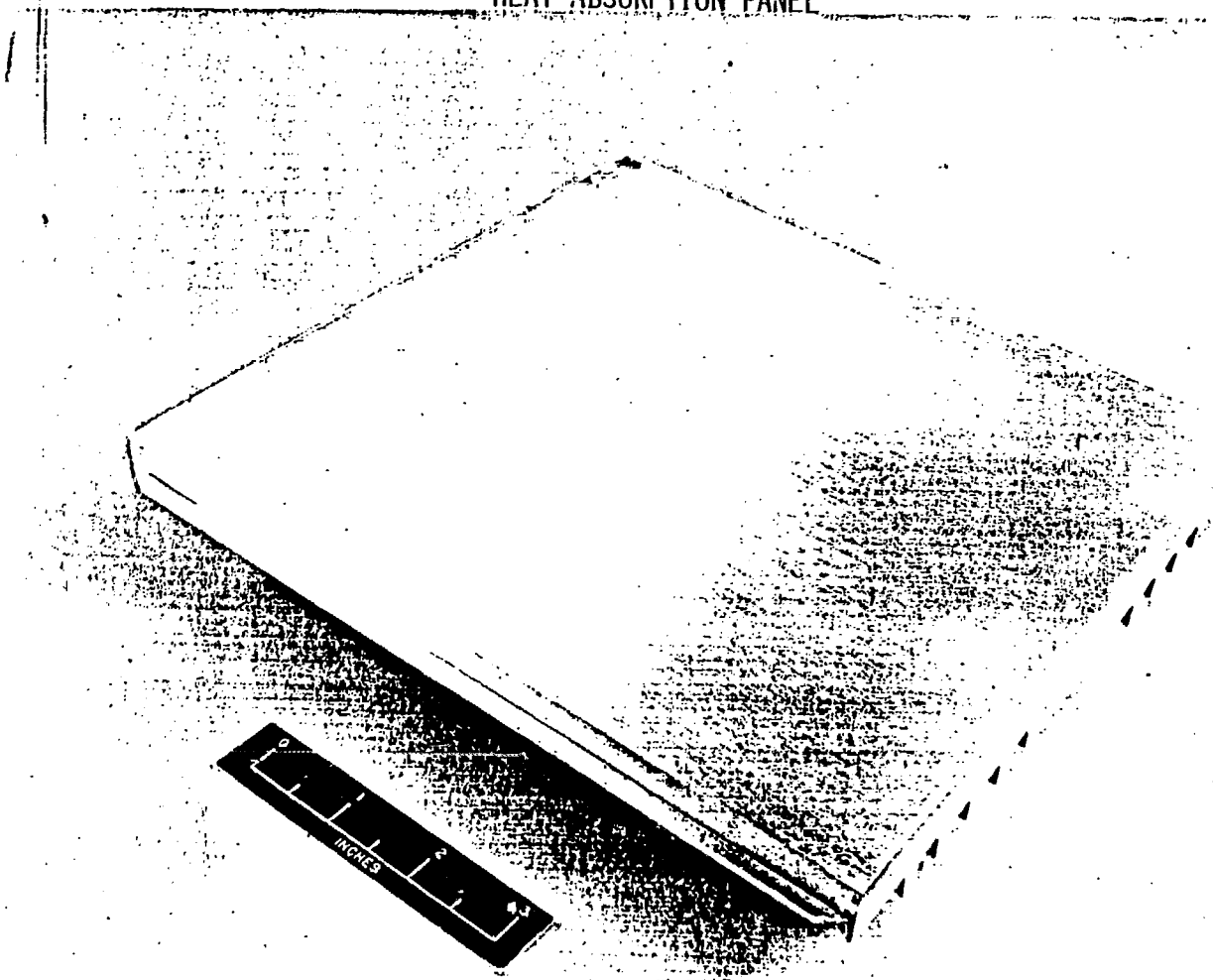

HEAT ABSORPTION PANEL

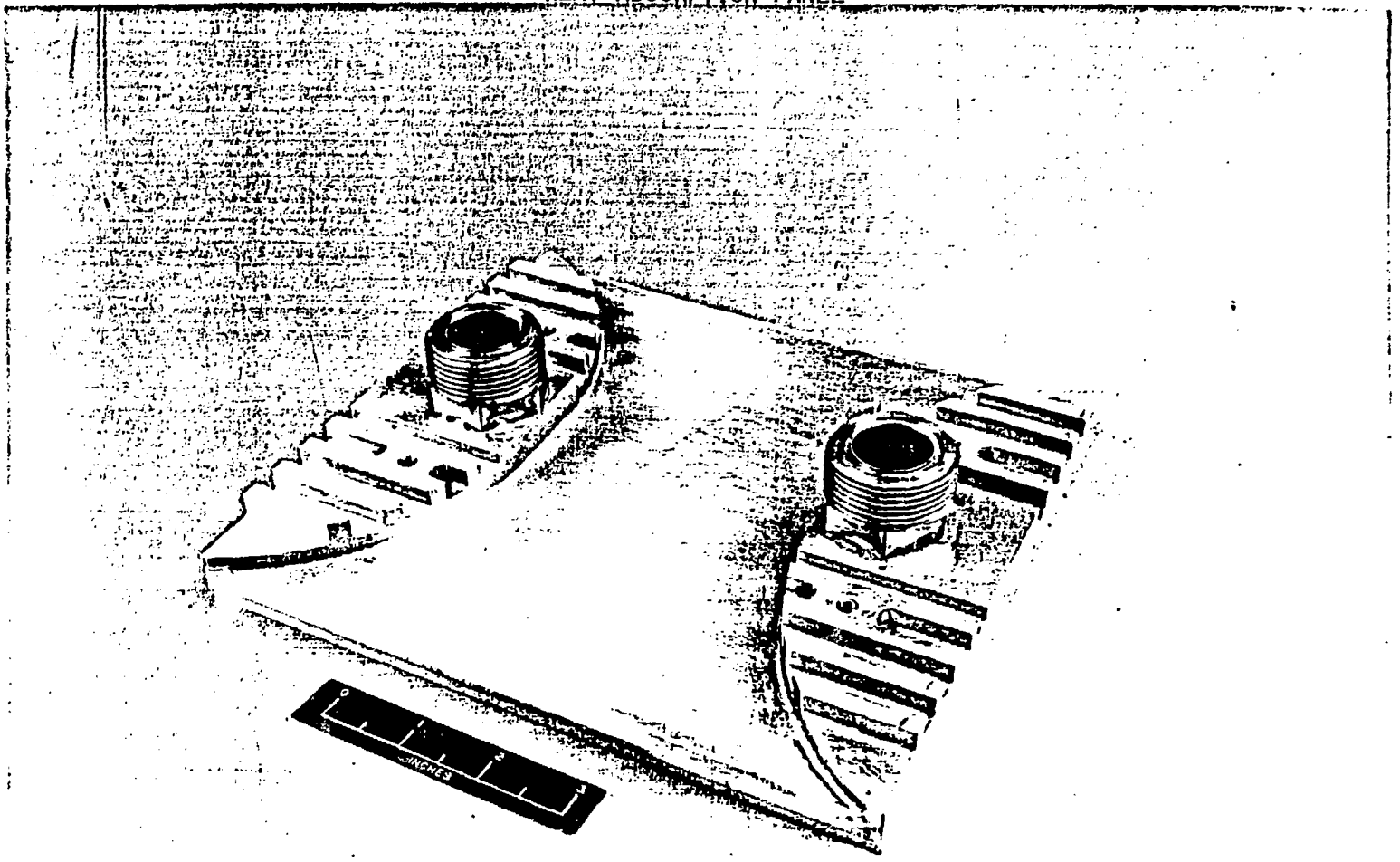

PANEL DESIGN SPECIFICATIONS

- DESIGN LIFE OF 25,000 CYCLES OF 30 SEC DURATION EACH
- DESIGN HEAT FLUX REQUIREMENT (2 kW/cm^2) IS FOR ALL BEAM INCIDENT ANGLES FROM 4 TO 90^{o}.
- DESIGN TO INCORPORATE A GIVEN SPUTTERING ALLOWANCE IN ACCORDANCE WITH THE MATERIAL CHOSEN
- NO HIGH VAPOR PRESSURE MATERIALS TO BE USED
- ALL PANEL JOINTS TO BE LEAK TIGHT WITH LEAK RATE LESS THAN 1×10^{-8} STD CC/SEC
- MINIMIZE COOLING WATER SYSTEM COST.
- MAXIMUM PANEL EXIT WATER TEMPERATURE EQUAL TO $98^{o}C$
- MAXIMUM WATER TEMPERATURE RISE IN PANEL EQUAL TO $55^{o}C$

HEAT ABSORPTION PANEL CANDIDATE MATERIALS

- OXYGEN FREE HIGH CONDUCTIVITY (OFHC) COPPER
  - ANNEALED
  - 50% COLD WORK
- OFHC COPPER WITH 0.2% ZIRCONIUM (AMZIRC)
  - ANNEALED
  - 30% COLD WORK
- TUNGSTEN
- MOLYBDENUM
- TANTALUM
- NIOBIUM
- NICKEL

MATERIAL RANKING PARAMETERS

- YIELD STRENGTH
- FATIGUE STRENGTH
- THERMAL LOAD (E α)
- THERMAL CONDUCTIVITY
- RAW MATERIAL COST
- BRAZING DIFFICULTY
- MACHINABILITY

MCDONNELL DOUGLAS CORPORATION

ULTIMATE TENSILE STRENGTH OF COPPER AND COPPER ALLOYS

11–2685A

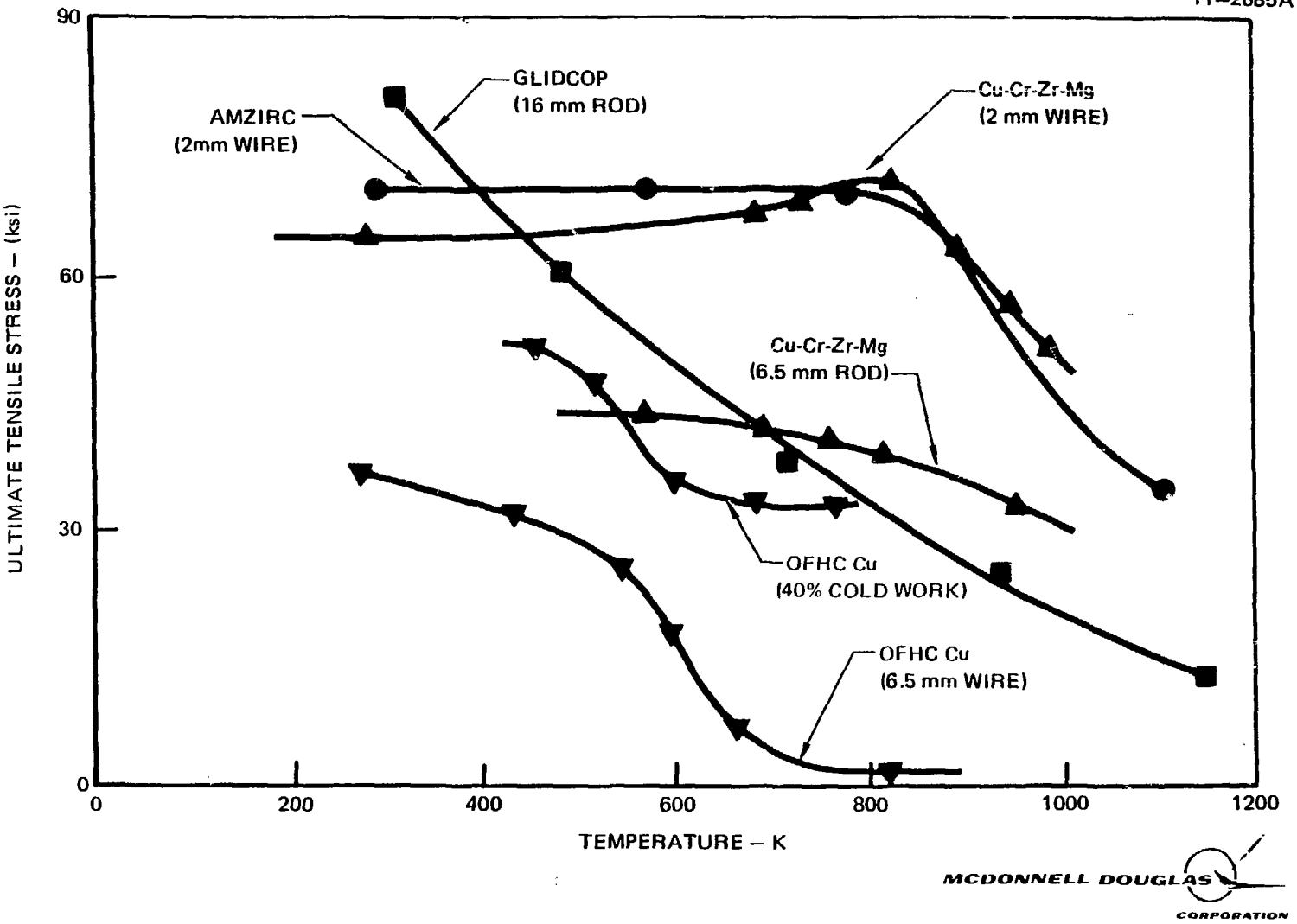

MCDONNELL DOUGLAS CORPORATION

THERMAL CONDUCTIVITY OF COPPER ALLOY MATERIALS

11-2688

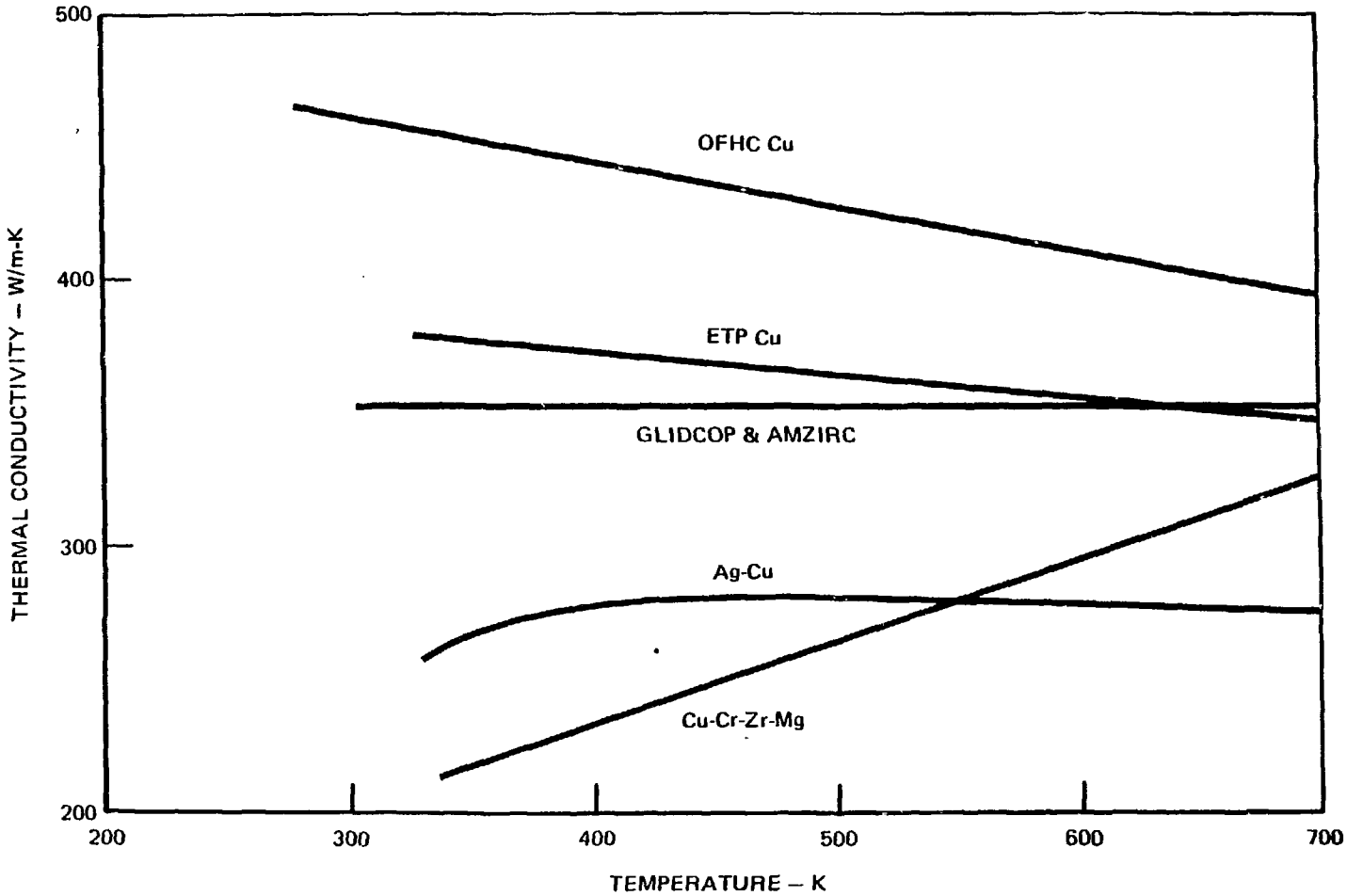

MCDONNELL DOUGLAS CORPORATION

THERMAL DESIGN STUDIES

- NON-BOILING ANALYSIS
- BOILING ANALYSIS
- WATER SYSTEM REQUIREMENTS

PANEL EDGE THERMAL MODEL

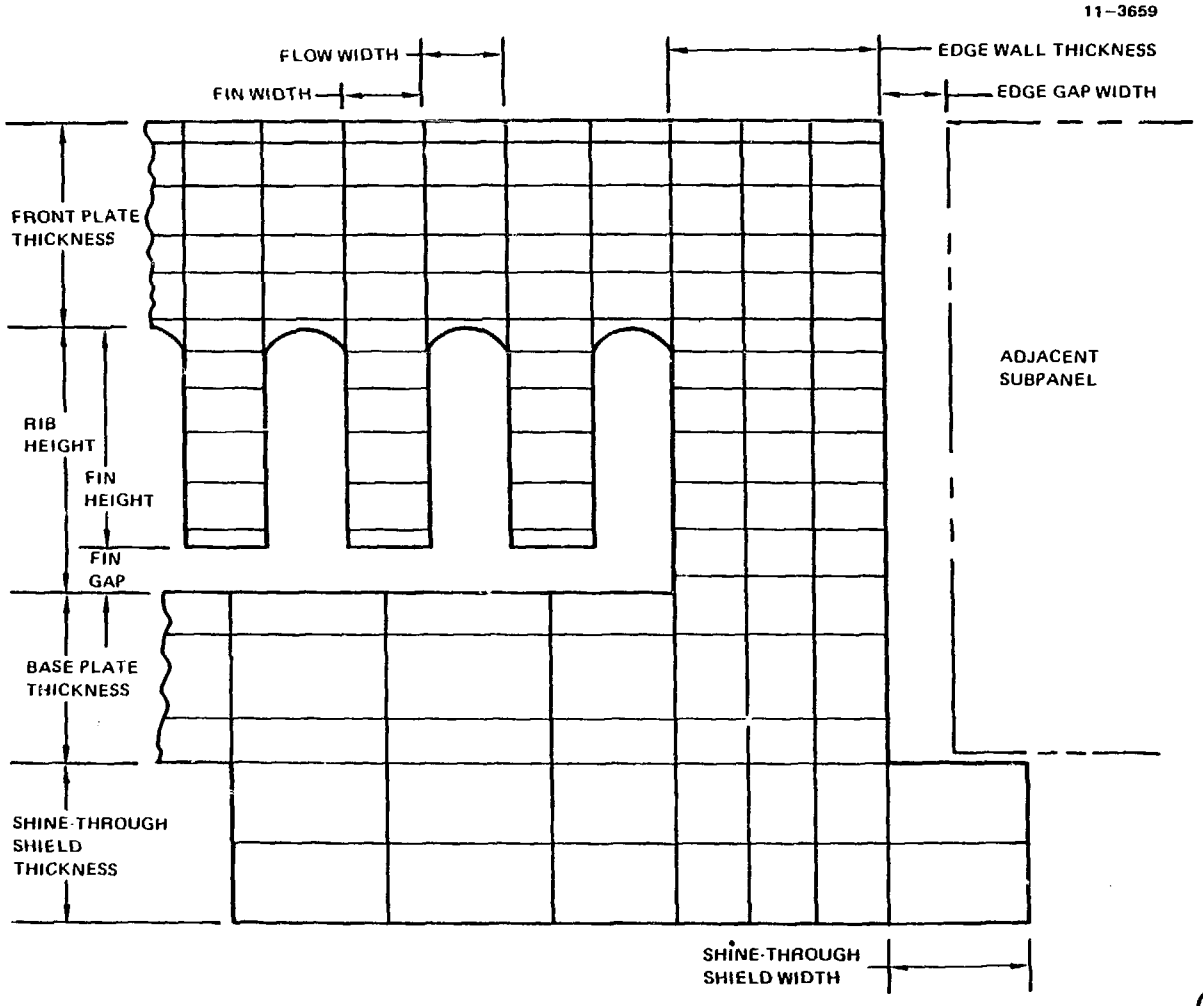

MCDONNELL DOUGLAS CORPORATION

FIN GEOMETRY PARAMETRIC DATA

(NON-BOILING)

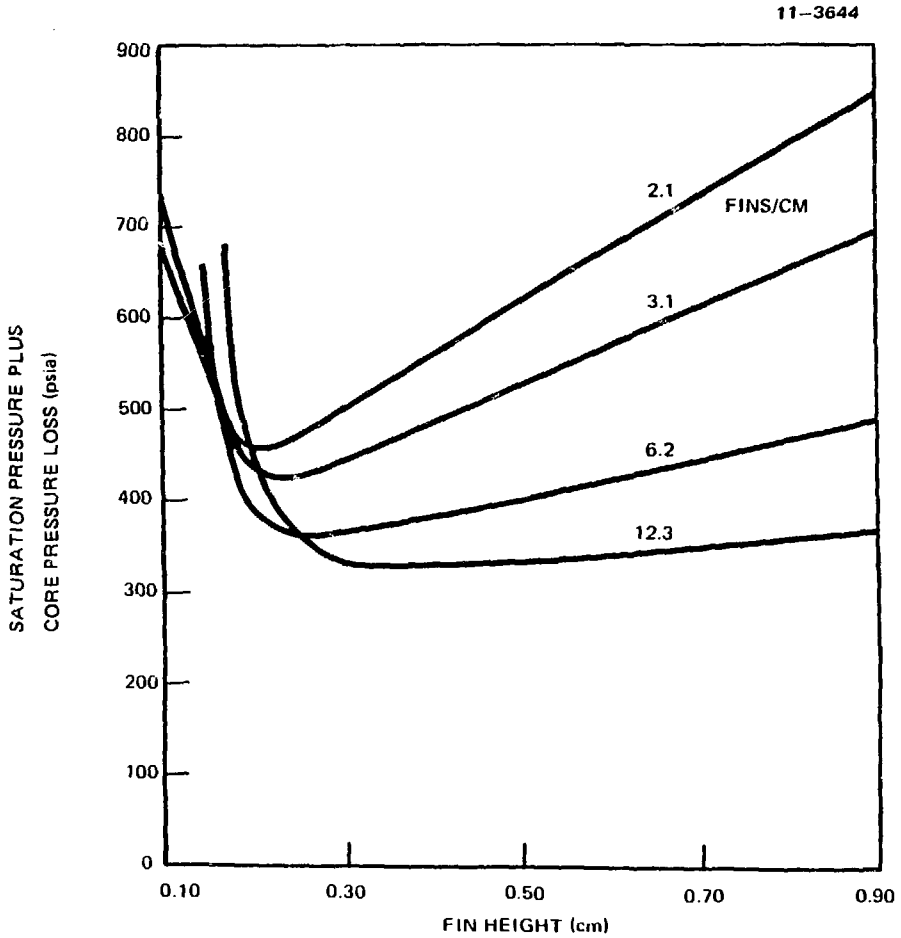

MCDONNELL DOUGLAS CORPORATION

SYSTEM PRESSURE REQUIREMENTS BASED ON CRITICAL HEAT FLUX CRITERIA

(BOILING)

11-3645

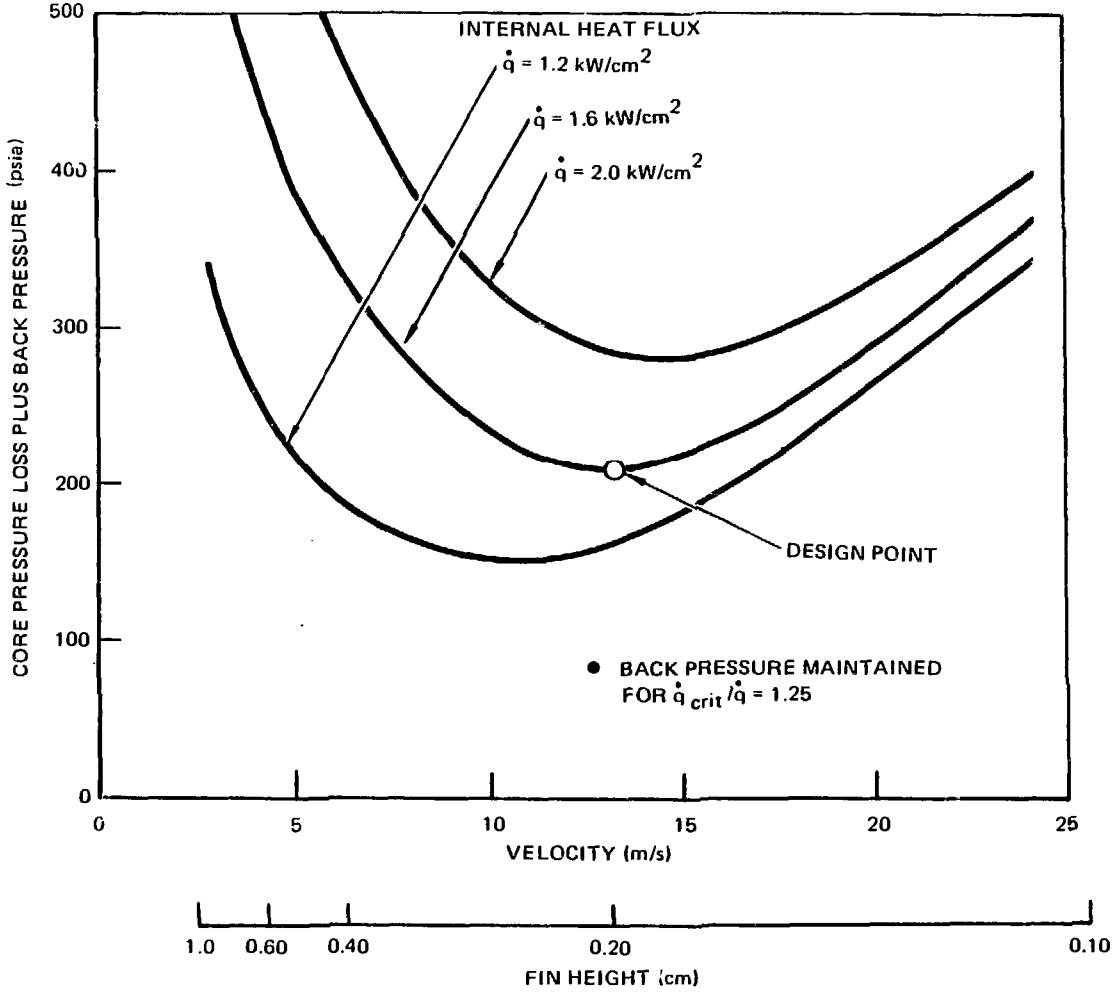

MCDONNELL DOUGLAS CORPORATION

427

STRUCTURAL DESIGN CRITERIA

- NO DETRIMENTAL DEFORMATION UNDER COMBINED THERMAL AND LIMIT MECHANICAL LOAD
- NO FAILURE UNDER PROOF PRESSURE AT ROOM TEMPERATURE
  PROOF PRESSURE = 1.5 x LIMIT LOAD
- AMZIRC YIELD STRENGTH = 20 ksi AT ROOM TEMPERATURE
- DESIGN LIFE = 25,000 CYCLES
- LIMIT PLATE ROTATION TO 2^{o}
- PERMIT ONE RIB BRAZE SEPARATION

DESIGN LIFE SUMMARY

11–3656

LOCATION AND ORIENTATION		LOAD		FATIGUE LIFE WITHOUT FLAW (cycles)	FLAW SIZE AT 25,000 CYCLES*		FATIGUE LIFE WITH FLAW (cycles)
		STRESS RANGE (psi)	TEMP (^{o}C)		FLAW DEPTH** (mm)	FLAW HALF WIDTH (mm)	
LONGITUDINAL	FRONT PLATE	24,200	314	230,000	1.34 (0.61)	2.5	35,000
	RIB	16,000	114	$> 10^7$	0.43	2.0	88,000
	BASE PLATE	13,900	100	$> 10^7$	0.38	1.9	340,000
TRANSVERSE	FRONT PLATE	8,700	198	$>10^7$	0.41 (0.00)	2.0	170,000
	RIB	21,800	200	1.9×10^6	0.64	2.0	46,000
	BASE PLATE	18,100	100	10^7	0.48	2.0	200,000
LONGITUDINAL – FRONT PLATE (3 kW/cm^2)		30,800	400	85×10^3	(0.828)	2.0	38,000

*INITIAL FLAW SIZE 0.254 mm x 1.905 mm

**NUMBERS IN PARENTHESES ACCOUNT FOR SPUTTERING ALLOWANCE

McDONNELL DOUGLAS CORPORATION

SUMMARY

11–3814A

- A PROTOTYPE HEAT ABSORPTION PANEL WAS DESIGNED AND FABRICATED TO WITHSTAND A HEAT FLUX OF 2 kW/cm^2 FOR 25,000 HEAT PULSES OF 30 SEC DURATION EACH.
- THE WATER COOLED PANEL IS 20 x 21.5 cm (HEATED SURFACE) AND IS MADE OF A HIGH STRENGTH COPPER ALLOY (AMZIRC).
- THE PANEL HAS ONE INELT AND ONE OUTLET, UTILIZES FINNED FLOW PASSAGES, AND REQURES ONLY 220 PSI COOLING WATER.
- BOILING OCCURS IN A PORTION OF THE FLOW PASSAGES, BUT THE CRITICAL HEAT FLUX IS AT LEAST 40% HIGHER THAN THE MAXIMUM INTERNAL HEAT FLUX IN WORST CASE.
- CONSERVATIVE ASSUMPTIONS WERE USED IN BOTH THE THERMAL AND STRUCTURAL DESIGN ANALYSES.
- OVER 100 PRODUCTION PANELS HAVE BEEN BUILT AND DELIVERED.

MCDONNELL DOUGLAS CORPORATION

PARTICIPANTS IN THE WORKSHOP ON COPPER AND COPPER ALLOYS

FOR FUSION REACTOR APPLICATIONS

PARTICIPANTS

Name	Affiliation
F. W. Clinard, Jr.	Los Alamos National Laboratory
E.N.C. Dalder	Lawrence Livermore National Laboratory
J. W. Davis	McDonnell Douglas Astronautics Company
F. R. Ficket	National Bureau of Standards
R. E. Gold	Westinghouse Advanced Energy Systems Division
N. J. Grant	Massachusetts Institute of Technology
M. W. Guinan	Lawrence Livermore National Laboratory
G. M. Haas	Department of Energy, Office of Fusion Energy
R. L. Hagenson	Technology International/Los Alamos National Laboratory
O. K. Harling	Massachusetts Institute of Technology
J. J. Holmes	Westinghouse Hanford Company
B. L. Hunter	Fusion Engineering Design Center
R. Kostoff	Department of Energy/ERAB - Materials Panel
L. J. Perkins	Lawrence Livermore National Laboratory
T. C. Reuther, Jr.	Department of Energy, Office of Fusion Energy
W. A. Rinehart	McDonnell Douglas Astronautics Company
S. N. Rosenwasser	INESCO, Inc.
L. M. Schetky	International Copper Research Association
D. L. Smith	Argonne National Laboratory
W. D. Spiegelburg	Brush Wellman, Inc.
P. W. Taubenblatt	AMAX - Base Metals Research & Development
J. M. Vitek	Oak Ridge National Laboratory
R. J. Weggel	Francis Bitter National Magnet Laboratory
J. B. Whitley	Sandia National Laboratories - Albuquerque
C. I. Whitman	SCM Corporation
F. W. Wiffen	Oak Ridge National Laboratory

DISTRIBUTION

1. AMAX, Base Metals Research and Development, Carteret, NJ 07008

   Pierre Taubenblatt

2–3. Argonne National Laboratory, 9700 South Cass Avenue, Argonne, IL 60439

   R. F. Mattas
   D. L. Smith

4. Brush Wellman, Inc., Beryllium Products Group, 17876 St. Clair Ave., Cleveland, OH 44110

   W. D. Spiegelburg, Director of Alloy Marketing

5. Copper Development Association, Greenwich Office Park 2, Box 1840, Greenwich, CT 06836

   S. Lyman

6–32. Department of Energy, Technical Information Center, Office of Information Services, P.O. Box 62, Oak Ridge, TN 37830

33–39. Department of Energy, Office of Fusion Energy, Washington, DC 20545

   M. M. Cohen
   G. M. Haas
   T. C. Reuther, Jr. (5 copies)

40. Department of Energy, Oak Ridge Operations Office, P.O. Box E, Oak Ridge, TN 37830

   Office of Assistant Manager for Energy Research and Development

41. GA Technologies, Inc., P.O. Box 81608, San Diego, CA 92138

   K. R. Schultz

42. General Dynamics, Convair Division, P.O. Box 85357, San Diego, CA 92138

   R. Baldi

43. INESCO, Inc., 11077 N. Torrey Pines Road, La Jolla, CA 92037

S. N. Rosenwasser

44. International Copper Research Association, 708 Third Avenue, New York, NY 10017

Technical Director

45–47. Lawrence Livermore National Laboratory, P.O. Box 808, Livermore, CA 94550

E.N.C. Dalder
M. Guinan
L. J. Perkins

48. Los Alamos National Laboratory, Mail Stop H809, Los Alamos, NM 87545

F. W. Clinard, Jr.

49. Massachusetts Institute of Technology, 138 Albany Street, Cambridge, MA 02139

O. K. Harling

50. Massachusetts Institute of Technology, 77 Massachusetts Ave., Cambridge, MA 02139

N. J. Grant

51. Massachusetts Institute of Technology, Cambridge, MA 02139
Plasma Fusion Center, Headquarters (Building NW 16)

B. J. Weggel

52–53. McDonnell Douglas Astronautics Company, East, P.O. Box 516, St. Louis, MO 63166

J. W. Davis
W. A. Rinehart

54. Memory Metals, Inc., Box 2518, 652 Glenbrook, Stamford, CT 06906

L. M. Schetky

55. National Bureau of Standards, Boulder, CO 80302

F. R. Fickett

56. Naval Research Laboratory, Washington, DC 20375

J. A. Sprague

57–73. Oak Ridge National Laboratory, P.O. Box X, Oak Ridge, TN 37831

Central Research Library (1 copy)
Document Reference Section
Laboratory Records Department (2 copies)
Laboratory Records Department, RC
E. E. Bloom
M. J. Saltmarsh
J. L. Scott
P. T. Thornton (3 copies)
J. M. Vitek
F. W. Wiffen (5 copies)

74. Oak Ridge National Laboratory, Fusion Engineering Design Center, P.O. Box Y, Oak Ridge, TN 37831

J. R. Haines

75–76. Princeton University, Plasma Physics Laboratory, P.O. Box 451, Princeton, NJ 08544

G. V. Sheffield
P. Heitzenroeder

77. SCM Corporation, 11000 Cedar Ave., Cleveland, OH 44106

C. I. Whitman, Director of Research and Development

78. Sandia National Laboratories, Albuquerque, NM 87185

J. B. Whitley

79. Technology International, 2515 Elwood, Suite 102, Ames, Iowa 50010

R. L. Hagenson

80. University of California, Department of Chemical, Nuclear, and Thermal Engineering, Los Angeles, CA 90024

M. A. Abdou

81. University of Wisconsin, 1500 Johnson Drive, Madison, WI 53706

G. L. Kulcinski

82. Westinghouse Electric Company, Steam Generator Technology Division, P.O. Box 355, Pittsburgh, PA 15230

R. E. Gold

83–84. Westinghouse Hanford Company, P.O. Box 1970, Richland, WA 99352

H. R. Brager
J. J. Holmes